AD_____

Award Number: **W81XWH-11-1-0313**

TITLE: **Novel Functions of NF-kappaB2/p52 in Androgen Receptor Signaling in CRPC**

PRINCIPAL INVESTIGATOR: **Nagalakshmi Nadiminty, PhD**

CONTRACTING ORGANIZATION: **Regents of the University of California, Davis Davis, CA 95618-6134**

REPORT DATE: **September 2015**

TYPE OF REPORT: **Addendum to Final**

PREPARED FOR: **U.S. Army Medical Research and Materiel Command**
Fort Detrick, Maryland 21702-5012

DISTRIBUTION STATEMENT: **Approved for Public Release;**
Distribution Unlimited

The views, opinions and/or findings contained in this report are those of the author(s) and should not be construed as an official Department of the Army position, policy or decision unless so designated by other documentation.

REPORT DOCUMENTATION PAGE

Form Approved
OMB No. 0704-0188

1. REPORT DATE	2. REPORT TYPE	3. DATES COVERED
September 2015	Addendum to Final	07/01/2011 to 06/30/2015

4. TITLE AND SUBTITLE

Novel Functions of NF-kappaB2/p52 in Androgen Receptor Signaling in CRPC

5a. CONTRACT NUMBER
W81XWH-11-1-0313

5b. GRANT NUMBER

5c. PROGRAM ELEMENT NUMBER

6. AUTHOR(S)

Nagalakshmi Nadiminty, PhD

E-Mail:nnadiminty@ucdavis.edu

5d. PROJECT NUMBER

5e. TASK NUMBER

5f. WORK UNIT NUMBER

7. PERFORMING ORGANIZATION NAME(S) AND ADDRESS(ES)

University of California, Davis
1850 Research Park Drive, Ste 300
Davis, Ca 9568-6134

8. PERFORMING ORGANIZATION REPORT NUMBER

9. SPONSORING / MONITORING AGENCY NAME(S) AND ADDRESS(ES)

U.S. Army Medical Research and Materiel Command
Fort Detrick, Maryland 21702-5012

10. SPONSOR/MONITOR'S ACRONYM(S)

11. SPONSOR/MONITOR'S REPORT NUMBER(S)

12. DISTRIBUTION / AVAILABILITY STATEMENT

Approved for Public Release; Distribution Unlimited

13. SUPPLEMENTARY NOTES

14. ABSTRACT

Purpose: Prostate cancer is one of the leading causes of cancer-related mortality in men in the United States. Androgen receptor signaling remains active in castration-resistant prostate cancer (CRPC). Here we show that NF-kappaB2/p52 activates the androgen receptor in the absence of ligand, via modulation of microRNA such as let-7c and via activation of intratumoral steroidogenesis by induction of higher levels of steroidogenic enzymes. We also show that NF-kappaB2/p52 induces resistance to anti-androgen therapies by inducing alternative splicing of the androgen receptor to increase levels of constitutively active variants.

Scope: The identification of the pathway leading to androgen receptor activation by NF-κB2/p52 may have implications for therapeutic applications against CRPC. The finding that p52 induces resistance to anti-androgenic therapies may have implications in the choice of treatment regimen in CRPC.

Major Findings: We showed that: Downregulation of p52 reduces intracrine androgen synthesis; p52 regulates expression of steroidogenic enzymes; p52 induces expression of AR splice variants and thereby enhances resistance of prostate cancer cells to anti-androgens; p52 regulates expression of miR-let-7c; miR-let-7c reduces expression of AR; and that the NF-kappaB2/p52:c-Myc:let-7c:Lin28 axis plays a major role in the development of castration resistance.

Significance: Current research efforts focus primarily on targeting the androgen receptor in CRPC. But the persistent activation of AR has been suggested to be one of the mechanisms of development of resistance to AR-targeted therapies. Our findings show that p52 plays a significant role in the development of castration and therapy resistance.

15. SUBJECT TERMS

CRPC, intracrine androgens, steroidogenic enzymes, NF-kappaB2/p52, Androgen receptor, miR-let-7c, Lin28, c-Myc, AR-V7, hnRNP

16. SECURITY CLASSIFICATION OF:			17. LIMITATION OF ABSTRACT	18. NUMBER OF PAGES	19a. NAME OF RESPONSIBLE PERSON
a. REPORT	b. ABSTRACT	c. THIS PAGE			USAMRMC
U	U	U	UU	223	19b. TELEPHONE NUMBER *(include area code)*

Standard Form 298 (Rev. 8-98)
Prescribed by ANSI Std. Z39.18

Table of Contents

Introduction: Prostate cancer is one of the leading causes of cancer-related mortality in men in the United States. Androgen receptor signaling remains active in castration-resistant prostate cancer (CRPC). Several mechanisms were postulated to result in the persistent androgen receptor (AR) signaling seen in CRPC, of which the most intriguing are the overexpression of the AR and the ability of prostate cancer cells to synthesize intracellular androgens. Even though recent efforts to target these mechanisms have made significant progress, development of resistance has become a common problem. Our preliminary data indicated that NF-kappaB2/p52 regulates expression of steroidogenic enzymes and microRNA let-7c which inhibits AR expression. Generation of constitutively active splice variants of the AR, which lack the C-terminal ligand-binding domain and are hence resistant to AR-targeted therapies has been suggested as one of the mechanisms of development of drug resistance. The most abundant splice variant, AR-V7, has been postulated to drive CRPC progression under androgen deprivation. AR-Vs confer resistance to not only AR targeted therapies [1, 2] but to conventional chemotherapeutics such as taxanes used as first line therapies against CRPC [3]. The mechanisms mediating increased expression of aberrant AR-Vs in PCa are still largely unknown. One possible cause of defective splicing is the genomic rearrangement and/or intragenic deletions of the *AR* locus in CRPC [4]. Alternatively, aberrant expression of specific splicing factors in PCa cells may also contribute to unbalanced splicing and aberrant recognition of cryptic exons in the *AR* gene. Alternative splicing modulates the generation of protein isoforms with distinct structural and functional properties or affects mRNA stability, by the insertion of premature stop codons, and translatability, by altering microRNA target sites [5]. Two nuclear RNA-binding protein families, heterogeneous nuclear ribonucleoproteins (hnRNP) and serine/arginine-rich proteins (SR), play pivotal roles in regulation of alternative splicing. The hnRNP family consists of ~20 members which bind to splicing silencers located in exons or introns to promote exon exclusion and act as splicing repressors [5]. The best characterized proteins of this group are hnRNPA1 and hnRNPA2, which share a high degree of sequence and functional homology [6]. HnRNPA1 and hnRNPA2 are over-expressed in various kinds of tumors and serve as early tumor biomarkers [7-9]. Our results show that NF-kB2/p52 regulates expression of hnRNPA1 via c-Myc and thereby contributes to aberrant splicing of AR.

Keywords: Prostate Cancer, Androgen Receptor, NF-kB2/p52, c-Myc, Lin28, miR-let-7c, hnRNPA1, Castration resistance, Enzalutamide, Therapy Resistance

Overall Project Summary for the Years 01 July 2011 to 30 June 2015

We have made significant progress in Task 2.

2a. Analyze whether p52 regulates the transcription of steroidogenic enzymes

Total RNA from LNCaP cells stably expressing p52 was analyzed by qRT-PCR using specific primers to test the expression levels of a wide panel of steroidogenic enzymes as shown in Fig. 1A. The expression levels of CYP17A1, HSD3B2, HSD17B2, HSD17B3, AKR1C3, AKR1C1C1, SRD5A1 and RND3 were enhanced by expression of p52 in LNCaP cells. These results were confirmed by Western analysis. Specific antibodies against some of the steroidogenic enzymes were used to analyze lysates from LNCaP cells stably expressing p52. As shown in Fig. 1B, protein levels of CYP17A1, HSD3B2, AKR1C3, CYP11A1 and SRD5A1 were increased by expression of p52 in LNCaP cells. In addition, we transfected p52 into PZ-HPV7 cells (normal prostate epithelial cell line) and analyzed expression levels of CYP11A1,

CYP17A1, HSD3B2, AKR1C3 and SRD5A1 by qRT-PCR. As shown in Fig. 1C, expression levels of these enzymes were enhanced with overexpression of p52 in PZ-HPV7 cells. These findings collectively show that p52 promotes expression of enzymes involved in intracrine androgen synthesis in prostate cells.

2b. Determine the mechanisms of transcriptional regulation of steroidogenic enzymes by p52

To determine whether activation of steroidogenic enzymes by p52 is by a transcriptional mechanism, we cloned promoter regions of HSD3B2, AKR1C3, HSD3B1 and SRD5A1 into luciferase reporter vectors and transfected them into LNCaP cells stably expressing p52. As shown in Fig. 1D, luciferase activities of the reporter vectors were enhanced in LNCaP cells expressing p52, indicating that p52 increases transcription of steroidogenic enzymes in PCa cells.

We have made significant progress in Task 3.

3a. Determine whether p52 induces androgen synthesis *in vitro*

To determine whether p52 induces intracellular androgen synthesis in prostate cells in vitro, we transfected either empty vector or p52 into PZ-HPV7 normal prostate epithelial cells and analyzed the cell lysates by Enzyme Immunoassay (EIA) using Testosterone EIA kit (Cayman Chemicals) according to the manufacturer's instructions. Briefly, $5x10^7$ cells were collected by centrifugation and homogenized in EIA buffer. The homogenates were extracted twice with 1:1 (v/v) ethyl acetate and the organic phase retained. The organic phase containing steroids was evaporated under vacuum and the resultant steroids were dissolved in EIA buffer for testosterone estimation by EIA. As shown in Fig. 2A, overexpression of p52 induced significantly higher levels of intracellular testosterone synthesis in PZ-HPV7 normal prostate epithelial cells. These results were confirmed in LNCaP cells stably expressing p52 (Fig. 2B). In addition, we also analyzed intracellular testosterone levels after induction of p52 expression by doxycycline (DOX) in LNCaP cells inducibly expressing p52. As shown in Fig. 2C, induction of p52 expression by DOX enhanced intracellular testosterone synthesis by 2-fold in these cells. Collectively, these findings show that p52 enhances intracrine androgen synthesis in vitro in PCa cells.

To determine whether downregulation of p52 reduces intracellular androgen synthesis in prostate cells in vitro, we transfected shRNA against p52 into C4-2B, LN-IL6 and DU145 cells and analyzed the cell lysates by Enzyme Immunoassay (EIA) using Testosterone EIA kit (Cayman Chemicals) according to the manufacturer's instructions. As shown in Fig. 3A, downregulation of p52 expression significantly abrogated the levels of intracellular testosterone synthesis in all cell lines tested. In addition, we also analyzed expression levels of steroidogenic enzymes in these cells by qRT-PCR. The results showed that downregulation of p52 expression reduced the expression levels of steroidogenic enzymes significantly (Fig. 3B). We also generated C4-2B, LN-IL6 and DU145 stable cell lines expressing shRNA against p52 and analyzed the intracellular androgen levels as detailed above. Steroidogenic enzyme expression levels were also analyzed. The results demonstrated that downregulation of p52 expression abrogated intracrine androgen synthesis in vitro (Fig. 3C and 3D). Collectively, these findings show that p52 regulates intracrine androgen synthesis in vitro in PCa cells.

3b. Determine whether p52 induces androgen synthesis *in vivo.*

To determine whether p52 regulates androgen synthesis in vivo, we generated xenografts of C4-2B cells in nude mice by injecting $2x10^6$ cells/flank sub-cutaneously. After the tumors reached 0.5 cm^3, retroviruses encoding either control shRNA against EGFP or shRNA against p52 were injected intratumorally into the xenografts and tumor growth was monitored. At the end of the experiments, tumors were harvested and intracellular testosterone levels were analyzed by EIA as described above. As shown in Fig. 4A, downregulation of p52 expression by shRNA reduced growth of C4-2B tumor xenografts significantly. In addition, as shown in Fig. 4B, levels of intracellular androgens were reduced drastically in xenografts injected with shRNA against p52. We also analyzed expression levels of steroidogenic enzymes in the tumor xenografts and found that steroidogenic enzyme expression was downregulated by reduction in expression of p52 (Fig. 4C). These findings demonstrate that downregulation of p52 expression reduces synthesis of intracrine androgens in vivo.

PCa cells with stable knock-down of p52 synthesize lower levels of intracrine androgens

The above experiments showed that retroviral-induced knock-down of p52 expression in C4-2B xenografts reduced tumor growth and levels of steroidogenic enzymes. In order to rule out the possibility of off-target effects of the retroviruses in reducing tumor growth, we generated C4-2B and DU145 cells stably expressing specific shRNA against p52. C4-2B-shp52 and C4-2B-shEGFP control cells were injected orthotopically into the prostates of SCID mice and tumor growth was measured using serum PSA levels as a surrogate for tumor volume. At the end of the experiment, tumors were collected and weighed. Tumor weights in the C4-2B-shp52 group were significantly lower than in the C4-2B-shEGFP group indicating that downregulation of p52 expression reduced the tumorigenic ability of C4-2B cells (Fig. 5A). We also measured intracrine testosterone levels using EIA (Cayman Chemicals) in the tumor tissues. Our results showed that synthesis of intra-tumoral testosterone was diminished in xenografts from C4-2B-shp52 cells (Fig. 5B). These results were confirmed using Mass Spectrometry. Tumor tissues resulting from orthotopic injection of C4-2B-shEGFP and C4-2B-shp52 cells were analyzed for their steroid profile using Mass Spectrometry. As shown in Fig. 5C, intra-tumoral testosterone levels as well as 5α-Dihydrotestosterone (DHT) levels were diminished in xenografts from C4-2B-shp52 cells compared to C4-2B-shEGFP cells. These findings conclusively attest to the importance of p52 expression in the upregulation of intracrine androgen synthesis by CRPC cells. Total RNAs were extracted from the tumor tissues and levels of steroidogenic enzymes were measured using qPCR. As shown in Fig. 5D, levels of most steroidogenic enzymes measured were reduced in C4-2B-shp52 xenografts.

In order to confirm these results, DU145 cells stably expressing shRNA against p52, DU145-shp52 and DU145-shEGFP control cells were injected orthotopically into the prostates of SCID mice and the resultant tumor tissues were collected and weighed. Tumor weights (Fig. 6A), levels of intra-tumoral testosterone (Fig. 6B) and expression levels of steroidogenic enzymes (Fig. 6C) were diminished in DU145-shp52 xenografts, demonstrating that downregulation of p52 reduces the ability of PCa cells to synthesize intracellular androgens in vivo. These findings clearly demonstrate that expression of p52 is critical for maintenance of intracrine androgen synthesis in PCa cells.

We have made significant progress in Task 4.

4a. Generate C4-2B cells stably expressing EGFP-tagged let-7c. Generate LNCaP cells stably expressing Lin28B.

We subcloned the ORF of Lin28 from pLOC-Lin28 (Open Biosystems) into pCDNA3.1 and verified the directionality by restriction digestion and sequencing. The pCDNA3.1-Lin28 vector thus generated was transfected into LNCaP cells and clones stably expressing Lin28 were selected by neomycin selection. Expression of Lin28 in the stable clones is shown in Fig. 7A. In addition, we have generated LNCaP cells inducibly expressing Lin28 using a Tet-inducible ViraPower lentiviral expression system (Invitrogen). The expression of Lin28 in LNCaP cells inducibly expressing Lin28 is shown in Fig. 7B. We also generated C4-2B cells stably expressing EGFP tagged-let-7c using the let-7c lentivector from System Biosciences. The expression of EGFP-tagged let-7c in C4-2B cells is shown in Fig. 7C.

Determine the mechanisms by which p52 regulates let-7c expression.

Our preliminary data showed that p52 regulates expression of let-7c. To determine whether this regulation occurs at the level of transcription, we analyzed the putative promoter region of let-7c using MatInspector and found that the promoter region contains putative NF-κB binding sites. Analysis of the NF-κB binding sites by Chromatin Immunoprecipitation (ChIP) assays revealed that p52 does not bind to the putative NF-κB binding sites. In addition, the precursor form of let-7c was found to be not affected by p52. These results led to the conclusion that the regulation of let-7c expression by p52 is not at the level of transcription. Next, we tested whether p52 regulates let-7c via regulation of expression of Lin28 and c-Myc. We analyzed expression levels of Lin28 and c-Myc in LN-neo (control) and LN-p52 (stably expressing p52) cells by qPCR (right panel)and Western blotting (left panel) (Fig. 8A) and found that expression levels of both Lin28 and c-Myc were higher in LN-p52 cells. Next, we tested whether p52 regulates expression of Lin28 by binding to its promoter region. We performed ChIP assays using specific primers to amplify putative p52-binding sites in Lin28 promoter and found that recruitment of p52 to Lin28 promoter was higher in LN-p52 cells compared to LN-neo cells (Fig. 8B). These results demonstrated that p52 regulates let-7c via its regulation of Lin28 and c-Myc.

4b. Analyze whether let-7c inhibits AR expression directly or indirectly. Analyze transcription factors which regulate AR expression. (and)

4c. Analyze whether downregulation of let-7c expression leads to activation of the AR and enhances proliferation of prostate cancer cells.

Let-7c decreases expression of AR

Our preliminary data showed that the levels of let-7c were lower in castration-resistant cell lines, C4-2B, LNCaP-s17 (overexpressing IL-6) and LN-IL6+ (LNCaP chronically treated with IL-6) that express higher levels of AR compared to parental LNCaP cells that express lower levels of AR, indicating an inverse relationship between AR and let-7c. Hence, we tested whether let-7c affects AR expression in PCa cells. Anti-sense oligonucleotides against let-7c (Ambion) were transfected into LNCaP cells which express high levels of let-7c and the expression level of AR was analyzed by qRT-PCR. Downregulation of let-7c enhanced AR mRNA level ~3.5-fold (Fig. 9A). To confirm that the increase in AR mRNA results in an increase in AR protein, we analyzed whole cell lysates from LNCaP cells transfected with let-7c anti-sense oligos by Western blotting. AR protein level was increased ~70% when let-7c was downregulated (Fig. 9B). These findings were further confirmed in LN-IL6+ cells which express higher levels of AR, but lower levels of let-7c compared to LNCaP cells. Overexpression of let-7c in LNCaP-IL6+ cells reduced the levels of AR mRNA (Fig. 9C) and protein expression (Fig. 9D). These results suggested that let-7c inhibits AR expression in PCa cells. Since the above

results were obtained by transient overexpression of let-7c and to test whether stable expression of let-7c would exhibit similar effects, we generated LNCaP and C4-2B cells stably expressing let-7c and LNCaP cells stably expressing Lin28. Western blotting was performed to analyze protein levels of AR and Lin28. The results demonstrated that levels of AR were downregulated in both LNCaP and C4-2B cells stably expressing let-7c, while AR expression was enhanced in LNCaP cells expressing Lin28 (Fig. 9E, F & G). Collectively, these data demonstrate that let-7c represses AR expression in prostate cancer cells.

Let-7c reduces AR activity

We next examined whether the reduction in expression of AR by let-7c results in inhibition of transcriptional activity of AR. LNCaP cells were co-transfected with pGL3-PSA6.0-Luc reporter containing the enhancer and promoter regions of PSA gene and plasmids expressing let-7c. As shown in Fig. 10A, transcriptional activity of the AR in activating reporter gene expression was reduced by ~60% in the presence of let-7c. These results were confirmed by analysis of PSA mRNA and protein expression by qRT-PCR and ELISA respectively. LNCaP cells were transfected with let-7c or let-7c anti-sense oligonucleotides and PSA mRNA levels were analyzed. Downregulation of let-7c expression by let-7c anti-sense oligonucleotides led to a >4-fold increase in PSA expression, whereas overexpression of let-7c reduced PSA expression by ~50% (Fig. 10B). In addition to PSA, downregulation of let-7c expression by let-7c antisense increased, while overexpression of let-7c reduced NKX3.1 (another typical androgen regulated gene) mRNA expression (Fig. 10B). Similarly, PSA levels in the supernatants of LNCaP cells transfected with let-7c anti-sense were found to be upregulated by ~40% (Fig. 10C). These results were also confirmed in LNCaP and C4-2B cells stably expressing let-7c. Stable expression of let-7c decreased while stable expression of Lin28 increased transactivation of reporter activity by AR (Fig. 10D) and secretion of PSA by LNCaP cells (Fig. 10E). To determine whether expression of let-7c affects the recruitment of AR to PSA and NKX3.1 promoters, ChIP assays were performed. Overexpression of let-7c in LNCaP cells reduced binding of AR to PSA (Fig. 10F) and NKX3.1 (Fig. 10G) promoters, whereas expression of Lin28, a repressor of let-7c, increased AR binding to these promoters. Collectively, these results demonstrate that the suppression of AR expression by let-7c leads to decrease in the transactivation potential of AR, while increased AR expression by let-7c anti-sense or Lin28 leads to an increase in the transactivation potential of AR and expression of its target genes.

Repression of AR by let-7c is mediated by Myc

MiRNAs target several genes by binding to consensus binding sites in the 3'-UTR of the transcript, leading to degradation of the mRNA via the RISC complex. Therefore, we analyzed whether let-7c binding sites exist in the 3'-UTR of the AR mRNA, using algorithms from miRBase, TargetScan, Pictar and Microcosm. Analysis of the 3'-UTR of AR failed to detect the presence of let-7c binding sites. To confirm whether let-7c leads to degradation of the AR mRNA, we analyzed the stability of AR mRNA in LNCaP cells expressing high levels of let-7c. LNCaP cells were transfected with plasmids expressing let-7c, were treated with vehicle or 50 μM Actinomycin D (to inhibit *de novo* RNA synthesis) and total RNAs were isolated. Northern blotting (Fig. 11A) and qRT-PCR (Fig. 11B) were performed with a probe specifically against AR mRNA and primers amplifying AR mRNA respectively. As shown in Fig. 11A & 11B, the half-life of AR mRNA in LNCaP cells was ~3.5 h in the presence of androgen, which was not altered when let-7c was overexpressed in LNCaP cells. These results suggested that let-7c does

not enhance the degradation of AR mRNA, implying that a mechanism other than direct mRNA degradation may be involved in let-7c-mediated AR inhibition. Next, we examined whether let-7c affects transcription of AR. Let-7c or let-7c anti-sense oligos were co-transfected with a luciferase reporter driven by the full-length (~6 kb) promoter of AR gene into LNCaP cells and luciferase assays were performed. Downregulation of let-7c expression by let-7c anti-sense increased, whereas overexpression of let-7 decreased the activation of AR promoter (Fig. 11C), suggesting that suppression of AR expression by let-7c may be at the level of transcription.

Since our results showed that suppression of AR expression and activity by let-7c is not through typical miRNA-mediated mRNA degradation, but at the level of transcription, we hypothesized that a let-7c target gene may function as a transcriptional regulator of AR. We analyzed whether any of the transcription factors binding to AR promoter was a target of let-7c using MatInspector (http://www.genomatix.de/matinspector.html) and miRBase (http://www.mirbase.org/) and found that Myc, which activates AR transcription by binding to a consensus element in the AR promoter [10], was one of the targets of let-7c. LNCaP cells overexpressing let-7c were analyzed by Western blotting to confirm whether let-7c reduces Myc expression. Results showed that Myc expression was downregulated in LNCaP cells expressing let-7c (Fig. 12A). Similarly, we found an increase in Myc expression in LNCaP cells transfected with let-7c anti-sense oligos (Fig. 12B). In addition, the levels of Myc are correlated with AR expression (Fig. 12B). Downregulation of Myc by Myc shRNA reduced AR promoter activity (Fig. 12C) and AR mRNA expression (Fig. 12D), while overexpression of Myc enhanced AR promoter activity (Fig. 12C) and AR mRNA expression (Fig. 12D). Downregulation of Myc also reduced the levels of PSA and NKX3.1 mRNA, while overexpression of Myc enhanced the levels of PSA and NKX3.1 mRNA (Fig. 12E).

To determine whether reduced expression of Myc is responsible for let-7c-mediated AR suppression, we co-transfected let-7c with Myc in LNCaP cells expressing a luciferase reporter driven by the full-length AR promoter. The results showed that let-7c suppressed AR promoter activity, which was reversed by overexpression of Myc (Fig. 12F). ChIP assays were performed using primers spanning the consensus binding site for Myc in AR promoter to determine whether let-7c affects the recruitment of Myc to the promoter of AR gene. Overexpression of let-7c reduced, while overexpression of Lin28 increased the recruitment of Myc to AR promoter (Fig. 12G). Collectively, these results demonstrate that AR suppression by let-7c is mediated by direct down regulation of Myc.

Let-7c suppresses growth of PCa cells in vitro

To determine whether let-7c affects the growth of PCa cells, LNCaP, C4-2B, DU145, LNCaP-S17 and LN-IL6+ cells were transfected with plasmids encoding let-7c or empty vector and cell numbers were counted after 24 and 48 h. Cell numbers of all PCa cell lines overexpressing let-7c were reduced by ~40% at 48 h (Fig. 13A-E). Insets show the levels of expression of let-7c plasmid in these cells. To determine whether the observed decrease in cell growth was due to apoptotic cell death, DNA fragmentation was analyzed by Cell Death Detection ELISA. As shown in Fig. 13F, apoptosis in cells overexpressing let-7c was enhanced compared to the controls, suggesting that the inhibition in cell growth induced by let-7c is partly due to increased apoptotic cell death.

In addition, we tested whether downregulation of let-7c would enhance the ability of androgen-sensitive PCa cells to grow in androgen-deprived conditions. We transfected anti-sense oligos against let-7c or control scrambled oligos into LNCaP cells supplemented with either FBS or charcoal-stripped FBS (CS-FBS) and monitored cell growth. The results demonstrated that downregulation of let-7c by anti-sense promoted androgen-dependent LNCaP cell growth in conditions of androgen deprivation (Fig. 13G). These findings suggested that castration-resistant growth of PCa may be characterized by downregulation of let-7c expression.

We also analyzed clonogenic ability of PCa cells expressing let-7c in both anchorage-dependent and anchorage-independent conditions. LNCaP-S17 and C4-2B cells were transfected with let-7c or empty vector and colony formation assays were performed. Both clonogenic (Fig. 14A) and soft agar colony (Fig. 14B) formation abilities of LNCaP-S17 and C4-2B cells were suppressed by overexpression of let-7c. The number of colonies formed on substrata by LNCaP-S17 cells was reduced from 142±15 to 46±10 and the number of colonies formed by C4-2B cells was reduced from 122±10 to 34±7 (Fig. 14A). Similarly, the number of colonies formed in soft agar by LNCaP-S17 cells was reduced from 82±4 to 15±2 and the number of colonies formed by C4-2B cells was reduced from 61±5 to 21±5 (Fig. 14B) by overexpression of let-7c. Furthermore, the size of colonies formed by control-transfected cells was larger compared to the colonies formed by let-7c-transfected cells (Fig. 14C&D). These results suggest that let-7c may inhibit PCa cell growth in anchorage-dependent as well as –independent conditions. These findings were also confirmed with clonogenic assay in C4-2B cells stably expressing let-7c (Fig. 14E).

Let-7c inhibits tumor growth of human PCa cell xenografts

We generated lentiviruses encoding GFP-tagged let-7c precursor using the Lentivector Expression System (System Biosciences). To determine whether let-7c exhibits anti-proliferative effects on PCa xenografts *in vivo*, we injected $2x10^6$ C4-2B or PC346C (both cell lines are AR-positive) cells s.c. into both flanks of male nude mice and monitored tumor development. Once tumors reached the size of 0.5 cm^3, mice were randomized into two groups. The experimental mice received a single intratumoral injection of lentivirally encoded let-7c, while control mice received lentiviruses expressing GFP. Tumor growth was monitored over 3 weeks, with tumor measurements twice weekly. At the end of 3 weeks, tumors were excised, RNAs prepared and qRT-PCR performed to assess levels of let-7c in the xenografts. The results showed that tumor growth of C4-2B (Fig. 15A) and PC346C (Fig. 15B) xenografts was inhibited significantly in mice injected with let-7c-containing lentiviruses compared to mice injected with control lentiviruses. In addition, we also tested whether let-7c can suppress tumor growth of AR-negative xenografts. We injected $1x10^6$ DU145 cells/flank s.c. into male nude mice and performed similar experiments with half the mice receiving a single intratumoral injection of lentiviruses encoding let-7c and the other half receiving lentiviruses encoding the empty vector. The results showed that let-7c was successful in suppressing tumor growth of DU145 xenografts similar to C4-2B or PC346C xenografts (Fig. 15C). Levels of PSA, a classic target gene of AR, secreted by the AR-positive xenografts were measured in the mouse sera using a human-specific PSA ELISA kit and were normalized to tumor weights. Results showed that injection of let-7c-expressing lentiviruses reduced the secretion of PSA by the tumor xenografts of C4-2B and PC346C compared to control lentiviruses (Fig. 15D). qRT-PCR showed that let-7c levels were enhanced in the tumors injected with let-7c-encoding lentiviruses, while levels of Lin28 were reduced (Fig. 15E&F). These findings suggest that overexpression of let-7c suppresses prostate

tumor growth, and that reconstitution of let-7c levels may present an attractive therapeutic strategy against human PCa.

Expression of let-7c suppresses AR, Lin28 and Myc in PCa xenografts

To determine whether let-7c suppresses AR expression in xenografts of PCa cells *in vivo*, we analyzed the tumors from xenografts injected with let-7c lentiviruses. Tumors were excised, RNAs prepared and levels of let-7c, AR, Lin28 and Myc were analyzed by qRT-PCR. As shown in Fig. 16, expression of let-7c suppressed AR, Lin28 and Myc levels in the xenograft tissues.

Let-7c expression is downregulated in human PCa

To determine whether the levels of let-7c expression are downregulated in clinical PCa, we analyzed RNAs from 10 paired benign and tumor human PCa specimens by quantitative RT-PCR. RNAs were isolated from human tissues, reverse transcribed and subjected to qRT-PCR using LNA-conjugated let-7c primers (Exiqon). The levels of let-7c were significantly decreased in 8/10 tumors compared to their matched benign prostate tissues (Fig. 17A). We also analyzed two tissue microarrays containing benign and cancerous prostate biopsies respectively by *in situ* hybridization using LNA-conjugated mature let-7c-specific probe (Exiqon). Our results showed that let-7c was highly expressed in benign PCa, while its expression was downregulated in the cancerous prostate (Fig. 17B). Collectively, these results suggest that loss of let-7c expression may be associated with prostate tumorigenesis.

Since Lin28 is a key regulator of let-7c expression, we examined Lin28 expression in the 10 paired benign and tumor prostate samples by qRT-PCR using primers which amplify Lin28 mRNA specifically. Expression levels of Lin28 were found to be significantly elevated in 9/10 pairs of matched benign and tumor prostate specimens (Fig. 17C). Expression of Lin28 was correlated inversely with expression of let-7c with a correlation coefficient of -0.4, suggesting that let-7c expression is regulated primarily by Lin28 in human PCa.

Let-7c and AR are negatively correlated in human PCa

We have demonstrated that let-7c represses AR expression and the levels of let-7c are inversely correlated with AR in cell culture and xenografts of PCa mouse models. To determine whether a correlation exists between expression levels of let-7c and AR in clinical PCa, we analyzed RNAs from 22 human PCa specimens by quantitative RT-PCR. RNAs were isolated from human tissues, reverse transcribed and subjected to qRT-PCR using LNA-conjugated let-7c primers (Exiqon). This was followed by measurement of expression levels of AR using primers specifically amplifying AR mRNA. The levels of let-7c and AR were negatively correlated, with a correlation coefficient of -0.52 using two tailed t-test in Microsoft Excel Tools (Fig. 18A&B). Expression levels of Lin28 and Myc were also examined in these specimens and are correlated negatively with expression levels of let-7c with correlation coefficients of -0.1765 and -0.3354 respectively using two-tailed t-test in Microsoft Excel Tools (Fig. 18C&D). The correlation coefficients do not show perfect negative correlation between expression levels of the respective genes but demonstrate a trend towards negative correlation, which should be validated with larger numbers of samples.

As Lin28 is a key regulator of let-7c expression, we examined Lin28 expression in 42 archival matched pairs of benign and cancerous human prostate samples and 20 samples of normal prostate by Western blotting using an antibody specifically against Lin28 (AbCam). The levels of Lin28 protein expression were higher in most of the tumors compared to the matched

benign prostates (Fig. 18E). We found that 86% of tumor tissues were positive for Lin28, while only 47% of benign and 40% of normal tissues exhibited Lin28 expression. We also analyzed expression levels of AR in these samples by Western blotting and the results show that AR levels correlate with Lin28 levels (Fig. 18E). Collectively, these data suggest that expression levels of let-7c and AR are negatively correlated with each other, and that Lin28 is overexpressed in prostate cancer vs benign prostate and is correlated positively with AR.

Expression levels of AR, Lin28 and Myc are increased in human PCa

To validate our above results from clinical PCa specimens, Gene expression analysis was performed using public domain datasets deposited in the Gene Expression Omnibus of the NCBI and in Oncomine. The former utilized datasets generated by Affymetrix human genome microarrays of well-described human tissues, while the latter utilized the Oncomine cancer transcriptome data. Analysis of Affymetrix human gene arrays demonstrated that expression levels of AR, Lin28 and Myc were enhanced ($P \leq 0.05$) in primary and metastatic prostate cancer specimens compared to benign prostate specimens (Fig. 19A&B). Similarly, significant ($P \leq 0.001$) increases were observed in expression levels of AR, Lin28 and Myc in prostate cancer specimens compared to their normal counterparts and were positively correlated with each other (Fig. 19C). These results imply that Lin28 and Myc play important roles in the regulation of AR expression in human PCa. Downregulation of expression of let-7c in human PCa may lead to higher levels of expression of Lin28 and Myc, which in turn enhance the expression of AR, which is an important survival factor for PCa cells.

Lin28 is overexpressed in clinical prostate cancer specimens

To determine the relative levels of expression of Lin28 in human CaP compared to benign prostates, we examined RNAs from 10 paired benign and tumor human CaP samples by qRT-PCR. Expression levels of Lin28 were found to be significantly elevated in 9/10 pairs of matched benign and tumor prostate specimens (Fig. 20A). Extracts from archived human clinical prostatectomy specimens were also examined for expression of Lin28 by Western blotting. The dataset contains 42 matched benign and cancer specimens and expression levels of Lin28 were higher in cancer tissues (86% positive and 14% negative) compared to benign prostate tissues (47% positive and 53% negative) (Fig. 20B). Immunohistochemistry was performed in FFPE prostate clinical specimens in a TMA PROS-006 (UC Davis Cancer Center Biorepository) with Lin28 antibody (Ab-71415) and staining intensity was scored over a scale of 0-3 (0 = negative, 1 = weak, 2 = strong and 3 = very strong). Documentation of staining specificity for IHC is presented in Suppl. Fig. 1. Expression of Lin28 was higher in CaP compared to benign prostates, with no significant differences in the pattern of expression with increasing Gleason grade (Fig. 20C). We observed strong nuclear staining of Lin28 in benign prostate tissues almost exclusively in the basal cell layer, with no staining in the luminal epithelial compartment. This can be explained by the following: 1) Lin28 is highly expressed in progenitor cells and 2) the basal cell compartment is generally considered to harbor putative "prostate stem cells". Thus, it is conceivable that the benign prostate gland exhibits high expression of Lin28 in the basal cell layer. It is interesting to note that an apparent shift from exclusively nuclear localization to a nuclear+cytoplasmic or exclusively cytoplasmic localization appears to occur in CaP, which would have to be confirmed by further studies. Collectively, these results indicate that Lin28 is overexpressed in human CaP.

Lin28 enhances growth of prostate cancer cells

To test whether Lin28 activates a pro-survival mechanism in CaP cells, we transfected Lin28 into a panel of CaP cell lines: LNCaP, C4-2B, DU145, LNCaP-S17 and LNCaP-IL6 and into PZ-HPV7, a non-tumorigenic prostate epithelial cell line. Lin28 enhanced the growth rate of all CaP cell lines tested (Fig. 21A). To confirm these results, LNCaP and C4-2B cells stably expressing Lin28 (LN-Lin28 and C4-2B-Lin28) were generated and growth characteristics examined. Compared to control LNCaP cells expressing the empty vector (LN-neo and C4-2B-neo), LN-Lin28 and C4-2B-Lin28 cells exhibited faster growth rates (Fig. 21B&C), suggesting that Lin28 promotes growth of prostate cancer cells *in vitro*. To examine the effects of downregulation of Lin28 on CaP growth, lentiviral vector-driven shRNA against Lin28 (Open Biosystems) was transfected into C4-2B cells and cell growth was monitored. Compared to cells transfected with the EGFP shRNA, C4-2B cells transfected with Lin28 shRNA exhibited lower rates of growth (Fig. 21D). Downregulation of Lin28 was confirmed by Western blotting. These data demonstrated that downregulation of Lin28 reduces proliferation of CaP cells.

Lin28 increases clonogenic ability of LNCaP cells

To test whether Lin28 influences the ability of CaP cells to form colonies in anchorage-dependent and independent conditions, we performed clonogenic assays by transiently transfecting Lin28 into C4-2B and LNCaP-S17 cells. The results showed that the number of colonies formed by C4-2B cells expressing Lin28 was 356±14, whereas the number of colonies formed by control C4-2B cells was 182±10 (Fig. 22A, left panel). Similarly, the number of colonies formed by LNCaP-S17 cells expressing Lin28 was 392±19, whereas the number of colonies formed by control LNCaP-S17 cells was 212±15 (Fig. 22A, right panel). These experiments were confirmed using LN-Lin28 cells (LNCaP cells stably expressing Lin28), which exhibited a 3.4-fold increase in colony forming ability compared to LN-neo cells (228±21 vs. 67±13 colonies) (Fig. 22B, left panel). These results were also confirmed using LN/TR/Lin28 cells (LNCaP cells expressing tet-inducible Lin28), which exhibited higher clonogenic ability compared to control LN/TR/Con cells upon doxycycline induction (Fig. 22B, right panel). Collectively, these findings suggest that Lin28 enhances the ability of prostate cancer cells to form colonies in anchorage-dependent conditions.

To further test whether Lin28 regulates anchorage-independent growth of CaP cells, we performed soft agar colony formation assays with C4-2B and LNCaP-S17 cells transfected with Lin28 as described in Methods. The results showed that Lin28 promoted the growth of both C4-2B (Fig. 11C, left panel) and LNCaP-S17 (Fig. 22C, right panel) cells in soft agar, compared to control C4-2B or LNCaP-S17 cells transfected with the empty vector. Similarly, LN-Lin28 cells exhibited significantly better ability to grow in soft agar, whereas control LN-neo cells failed to grow in soft agar (Fig. 22D, left panel), demonstrating that Lin28 confers soft agar colony forming ability on CaP cells.

Lin28 increases invasiveness of LNCaP cells

To test whether Lin28 regulates the ability of CaP cells to invade through matrigel *in vitro*, we performed Boyden chamber invasion assays using LN-Lin28 and control LN-neo cells. Cells were plated on matrigel in the upper compartment of the Boyden chamber and allowed to invade towards the lower compartment filled with complete medium containing complete FBS or

CS-FBS. The number of LN-Lin28 cells invading through matrigel in FBS-containing medium was 118±10, while the number of control cells invading through matrigel was 60±5 (Fig. 22D, right panel). Similarly, the number of LN-Lin28 cells invading through matrigel in CS-FBS-containing medium was 54±6, while the number of control cells was 4±2 (Fig. 22D, right panel), indicating that Lin28 induces invasion of CaP cells through basement membrane *in vitro*.

Lin28 promotes tumorigenicity of CaP cells in vivo

To test whether the growth-promoting effect of Lin28 can be recapitulated *in vivo*, we injected $2x10^6$ LN-Lin28 cells or control LN-neo cells s.c into each flank of male nude mice and monitored their tumorigenic ability. Tumors were measured twice weekly and sera were collected at the end of the experiment to confirm that the tumor cells secreted PSA. We found that mice injected with LN-Lin28 cells exhibited significantly higher rates of incidence and growth of tumors compared to control LN-neo cells, which formed very slow-growing tumors (Fig. 23A). Higher levels of secretion of PSA were observed in mice bearing tumors expressing Lin28 compared to mice bearing control tumors (Fig. 23B), indicating that higher expression of Lin28 enhances expression of AR and promotes tumor growth of LNCaP human CaP cells *in vivo*.

Lin28 activates androgen receptor signaling axis

Since we reported previously that hsa-let-7c, a miRNA regulated by Lin28, suppressed expression of the AR, we examined whether Lin28 regulates expression of the AR. We transfected a luciferase reporter vector driven by the full length promoter of AR (pGL4-AR-Prom-Luc) into LN-neo and LN-Lin28 cells and performed luciferase assays. LN-Lin28 cells exhibited higher levels of activation of AR promoter compared to control cells (Fig. 24A, left panel), indicating that Lin28 may activate the transcription of AR gene. Next, we analyzed the mRNA levels of AR in LN-neo and LN-Lin28 cells and found that LN-Lin28 cells exhibited significantly higher levels of AR mRNA (Fig. 24A, right panel). These results were confirmed by Western blotting (Fig. 24B, left panel). To determine whether downregulation of Lin28 affects the expression of AR, we transfected shRNA against Lin28 into C4-2B cells and analyzed the protein levels of AR by Western blotting. The results showed that downregulation of Lin28 led to a decrease in protein levels of AR (Fig. 24B, right panel), suggesting that Lin28 expression is necessary for maintenance of AR expression in CaP cells.

To determine whether Lin28 regulates androgen receptor-dependent signaling, we analyzed the expression levels of PSA and NKX3.1, two typical androgen receptor target genes, in LN-neo and LN-Lin28 cells by qRT-PCR. The results showed that expression levels of PSA and NKX3.1 were enhanced in LN-Lin28 cells (Fig. 24C). We analyzed the effect of Lin28 on transactivating ability of AR using luciferase assays. A luciferase reporter vector driven by the full length promoter of PSA (PSA-E/P-Luc) was transfected into LN-neo and LN-Lin28 cells and luciferase assays were performed. The results showed that Lin28 induced activity of PSA promoter (Fig. 24D, left panel), indicating that Lin28 may contribute to increased transcription of AR-dependent genes by activating the AR. To confirm these findings, we analyzed levels of PSA in supernatants of LN-neo and LN-Lin28 cells by ELISA and found that secretion of PSA by LN-Lin28 cells was higher compared to LN-neo cells (Fig. 24D, right panel). We also examined

the effect of Lin28 on recruitment of AR to the promoters of PSA and NKX3.1 genes by ChIP assays. The results showed that recruitment of AR to ARE I/II and ARE III regions in PSA (Fig. 24E, left panel) as well as ARE in NKX3.1 (Fig. 24E, right panel) promoters was enhanced in Lin28 expressing cells compared to controls. Taken together, these results demonstrate that Lin28 activates the AR signaling axis.

Lin28 induces resistance to AR-targeted therapies in PCa cells

As the above studies indicated that NF-κB2/p52 regulates the let-7c/Lin28 axis, we tested whether overexpression of Lin28 confers resistance to anti-androgens such as enzalutamide and bicalutamide as well as to the CYP17A1 inhibitor, abiraterone. LN-Lin28 cells stably expressing Lin28 and LN-neo control cells were treated with different concentrations of enzalutamide, abiraterone or bicalutamide and cell growth was analyzed. As shown in Fig. 25A, survival rates of LN-Lin28 cells were higher when treated with enzalutamide, abiraterone or bicalutamide compared to LN-neo control cells. Fig. 25B shows the expression of Lin28 in LN-Lin28 cells treated with enzalutamide, abiraterone or bicalutamide. These results were further confirmed with anchorage-dependent clonogenic assays after treatment with enzalutamide, abiraterone or bicalutamide. As shown in Fig. 25C & D, numbers of colonies formed by LN-neo control cells were reduced by ~50% when treated with enzalutamide, abiraterone or bicalutamide, while numbers of colonies formed by LN-Lin28 cells were only reduced by ~5-10%. Similarly, we performed anchorage-independent soft agar assays to test the ability of LN-Lin28 cells to form colonies in soft agar after treatment with enzalutamide, abiraterone or bicalutamide. As shown in Fig. 25E & F, ability of LN-neo control cells to form colonies in soft agar was significantly diminished by treatment, while the ability of LN-Lin28 cells to form colonies in soft agar was not affected significantly. We also tested AR nuclear translocation using immunoblots with specific antibodies against AR (Fig. 26A), recruitment to AREs using ChIP assays (Fig. 26B) and expression of AR target genes using qPCR and ELISA (Fig. 26C, D & E) to confirm that cells expressing Lin28 maintain activation of the AR even when treated with enzalutamide, abiraterone or bicalutamide, rendering the cells resistant to apoptosis induced by these drugs. These results collectively demonstrate that Lin28 enhances the resistance of PCa cells to AR-targeted therapeutics. Alternative splicing of the AR has been implicated as one of the mechanisms mediating resistance to anti-androgens in PCa cells. To further dissect the mechanism through which cells expressing Lin28 acquire resistance to anti-androgens, we analyzed the levels of AR splice variants as well as levels of hnRNP proteins in LN-neo and LN-Lin28 cells. Our results showed that LN-Lin28 cells express significantly higher levels of both AR-V7 and hnRNPA1 (Fig. 27A & B). Therefore, we examined whether higher expression levels of AR-V7 and hnRNPA1 are relevant for the acquired resistance of LN-Lin28 cells to anti-androgens. siRNAs against either full length AR or AR-V7 were transfected into LN-neo and LN-Lin28 cells and it was found that while downregulation of either AR or AR-V7 did not affect the viability of LN-Lin28 cells treated with vehicle, downregulation of either full length AR or AR-V7 enhanced the sensitivity of LN-Lin28 cells to enzalutamide (Fig. 27C). Similarly, downregulation of hnRNPA1 or hnRNPA2 resensitized LN-Lin28 cells to enzalutamide, abiraterone or bicalutamide (Fig. 27D). Next, we tested whether downregulation or overexpression of hnRNPA1 affects expression of AR-V7 in LN-Lin28 cells. As shown in Fig. 27E & F, downregulation of hnRNPA1 reduced AR-V7 levels, while overexpression of hnRNPA1 increased AR-V7 levels in LN-Lin28 cells. These results collectively demonstrate that

alternative splicing of AR leading to higher expression of AR-V7 which is mediated by hnRNPA1 plays a major role in acquired resistance of PCa cells expressing Lin28.

Next, we tested whether Lin28 mediates the acquired resistance of LN-p52 cells to enzalutamide. Specific shRNA against Lin28 was transfected into LN-neo control and LN-p52 cells and the cells were subjected to enzalutamide treatment. As shown in Fig. 28A, downregulation of Lin28 enhanced the sensitivity of LN-p52 cells to enzalutamide. LN-p52 cells transfected with shRNA against Lin28 exhibited a ~40-50% reduction in cell survival compared to LN-p52 cells transfected with the control shRNA when treated with enzalutamide. Fig. 28A right panel shows the confirmation of downregulation of Lin28 by shRNA. Knocking down Lin28 expression reduced expression levels of most alternative splicing forms of AR (Fig. 28B, C, D, E, F & G). These results indicate that Lin28 may mediate the acquisition of resistance to enzalutamide in PCa cells.

CaP cells expressing NF-κB2/p52 are resistant to Enzalutamide and Bicalutamide

Next, we tested whether regulation of AR expression by the p52-Lin28-Myc-let-7c axis plays a role in development of drug resistance. LN-neo (LNcaP cells expressing the empty vector) and LN-p52 cells (LNCaP cells stably expressing p52) were treated with 0, and 20 μM Enzalutamide or Bicalutamide in media containing either complete FBS or charcoal-stripped FBS and cell growth was examined after 48 h. DMSO was used as the vehicle control. As shown in Fig. 29A, cells stably expressing p52 exhibited better cell survival ability when exposed to Enzalutamide or Bicalutamide compared to control LN-neo cells. To confirm these experiments, we treated LN-neo or LN-p52 cells with 0, 20 and 40 μM Enzalutamide or Bicalutamide and performed clonogenic assays. As shown in Fig. 29B, LN-neo cells were highly sensitive to both Enzalutamide and Bicalutamide and formed fewer colonies, whereas the number of colonies formed by cells expressing p52 was significantly higher, indicating that NF-κB2/p52 may induce resistance to Enzalutamide and Bicalutamide in CaP cells. These results collectively demonstrate that CaP cells expressing higher levels of NF-κB2/p52 are more resistant to Enzalutamide and Bicalutamide compared to cells which do not express p52.

CaP cells chronically treated with Enzalutamide exhibit higher levels of NF-κB2/p52

To test whether CaP cells resistant to Enzalutamide exhibit higher levels of p52, we treated CWR22Rv1 cells with 5-10 μM Enzalutamide chronically for >10 months. The resultant cells showed higher cell survival rates when treated with Enzalutamide. We examined the expression levels of NF-κB2/p52 in these cells by qRT-PCR and by Western blotting. As shown in Fig. 30A, CWR22Rv1 cells treated chronically with Enzalutamide exhibited higher levels of both precursor p100 as well as p52, indicating that CaP cells resistant to Enzalutamide may upregulate the endogenous levels of NF-κB2/p52. To test whether downregulation of p52 resensitizes these cells to Enzalutamide, we transfected shRNAs specific to p52 into CWR22Rv1 cells treated chronically with Enzalutamide (expressing higher levels of p52) and examined cell growth after 24 and 48 h. Downregulation of p52 after transfection was confirmed by qRT-PCR. As shown in Fig. 30B, cells transfected with p52 shRNA were increasingly sensitive to Enzalutamide compared to control CWR22Rv1-Enza-R cells, indicating that expression of p52 may be necessary for the survival of cells treated chronically with Enzalutamide. These results collectively demonstrate that NF-κB2/p52 may regulate the induction of resistance to Enzalutamide in CaP cells.

NF-κB2/p52 enhances expression of AR splice variants

It has been shown that higher levels of AR splice variants may be responsible for the resistance to Enzalutamide in CaP, hence we tested whether NF-κB2/p52 regulates the expression of AR splice variants. Total RNAs from LNCaP and C4-2B cells transfected with either empty vector or p52 in media containing either complete or charcoal-stripped FBS (CS-FBS) were analyzed by qRT-PCR for the expression levels of full length AR as well as the major splice variant AR-V7. As shown in Fig. 31A, expression of p52 enhanced the expression levels of the splice variant AR-V7 in both FBS and CS-FBS, while expression of full length AR remained unchanged in LNCaP cells (left panel). These results were confirmed by Western blotting using antibodies specific for full length AR and AR-V7 (right panel). Similar results were observed in C4-2B cells, in which expression of p52 enhanced the expression levels of AR-V7 while expression levels of full length AR were unaffected (Fig. 31B). To substantiate these results, we examined expression levels of full length AR and AR-V7 in LN-neo and LN-p52 cells by qRT-PCR and Western blotting and found that expression levels of AR-V7 were elevated in LN-p52 cells compared to LN-neo cells (Fig. 31C). These findings demonstrate that NF-κB2/p52 may induce upregulation of the expression of AR-V7.

Downregulation of NF-κB2/p52 abrogates expression of AR splice variants

Next, we tested whether NF-κB2/p52 was necessary for the enhanced expression of AR splice variants. VCaP and CWR22Rv1 CaP cells express endogenous levels of AR splice variants, AR-V1, AR-V5, AR-V7, AR-1/2/2b and AR-1/2/3/2b. We transfected shRNA specific to p52 into VCaP and CWR22Rv1 cells and examined the expression levels of these splice variants by qRT-PCR using specific primers. As shown in Fig. 32A and B (left panels), downregulation of p52 reduced the expression levels of most of the splice variants significantly, while levels of full length AR remained unaffected. These results were confirmed for AR-V7 expression by Western blotting using antibodies specific against AR-V7 and FL AR in VCaP and CWR22Rv1 cells (Fig. 32A and B, right panels), indicating that expression of p52 may be necessary for the synthesis of AR splice variants.

Downregulation of full length AR and AR-V7 increase sensitivity of p52-expressing CaP cells to Enzalutamide

LNCaP cells stably expressing p52 (LN-p52) exhibit higher levels of AR-V7. To test whether full length AR or AR-V7 play a role in the p52-induced resistance to Enzalutamide, we transfected siRNAs specific against either full length AR or AR-V7 into LN-neo and LN-p52 cells and monitored cell growth in response to Enzalutamide. As shown in Fig. 33A, downregulation of either FL AR or AR-V7 reduced growth of control LN-neo cells by ~20%, and enzalutamide itself reduced growth of LN-neo cells by ~50%. No additional reduction of growth was observed in LN-neo cells when FL AR or AR-V7 was downregulated in the presence of enzalutamide, showing that inhibition of either FL AR or AR-V7 had no effect on the sensitivity of LN-neo cells to Enzalutamide. In LN-p52 cells which express higher levels of AR-V7, downregulation of either FL AR or AR-V7 reduced growth by ~50% in the presence of Enzalutamide, thus resensitizing LN-p52 cells to Enzalutamide. These results suggest that resistance of LN-p52 cells to Enzalutamide is mediated by alterations in the AR signaling pathway and demonstrate that activation of the AR axis by p52 plays an important role in the p52-induced resistance to Enzalutamide. To confirm these results and test whether downregulation of full length AR or AR-V7 modulates p52-induced AR activation, we co-

transfected a luciferase reporter containing the enhancer and promoter regions of PSA (PSA-E/P-Luc) along with p52 and siRNAs against full length AR or AR-V7 into VCaP and CWR22Rv1 cells. The cells were treated with either vehicle or 20 μM Enzalutamide and luciferase assays performed. As shown in Fig. 33B, p52-induces activation of AR-mediated target gene transcription, which was abolished by downregulation of either FL AR or AR-V7. p52-induced activation of AR was unaffected by Enzalutamide treatment. Treatment with Enzalutamide further enhanced the suppressive effect of siRNAs against FL AR or AR-V7 on p52-induced AR-mediated target gene transcription. These results demonstrate that activation of AR signaling is necessary for the p52-induced resistance against Enzalutamide. Similar results were obtained in CWR22Rv1 cells (Fig. 33C), demonstrating that the interplay between full length AR, AR-V7 and NF-κB2/p52 may be critical in the development of resistance to Enzalutamide in CaP cells. These results implicate the activation of the AR signaling axis by p52 via full length AR and its splice variants as being responsible for the induction of resistance against enzalutamide.

HnRNPA1 regulates the expression of AR variants

It is known that AR variants are generated by alternative splicing of the precursor AR mRNA, and that splicing factors are involved in the process. To test whether generation of AR variants by alternative splicing is dependent upon expression of hnRNPs in PCa cells which express endogenous levels of AR variants, we transfected siRNAs specific against hnRNPA1 and hnRNPA2 into 22Rv1 and VCaP prostate cancer cells which express detectable levels of AR splice variants and tested whether expression levels of full length AR as well as of variants such as AR-V7, AR-V1, AR-V5, AR-1/2/2b and AR-1/2/3/2b are affected by downregulation of hnRNPs using qRT-PCR. As shown in Fig. 34A and B, downregulation of hnRNPA1 and hnRNPA2 decreased the expression levels of AR variants in both 22Rv1 and VCaP prostate cancer cells. Insets in Fig. 34A and B confirm the downregulation of hnRNPA1 and hnRNPA2 by specific siRNAs. The downregulation of hnRNPA1 and the resultant suppression of AR-V7 protein levels were confirmed by Western blot analysis (Fig. 34C). The protein levels of the AR-V7 variant were decreased in both 22Rv1 and VCaP cells transfected with hnRNPA1 siRNA, using either specific antibodies against AR-V7 or monoclonal antibodies against AR (AR-441) which detect all forms of AR. These results indicate that hnRNPA1 may regulate the generation of AR splice variants in prostate cancer cells.

Next, we tested whether overexpression of hnRNPA1 affects the expression levels of AR splice variants in LNCaP prostate cancer cells. LNCaP cells were transfected with plasmids expressing the full length hnRNPA1 cDNA and levels of AR variants were analyzed by Western blotting and qRT-PCR. As shown in Fig. 34D, overexpression of hnRNPA1 enhanced AR-V7 protein levels in LNCaP cells which possess undetectable endogenous levels of AR-V7 protein. qRT-PCR confirmed that overexpression of hnRNPA1 significantly enhanced the mRNA levels of AR-V7, AR-V5, AR-1/2/2b and AR-1/2/3/2b variants in LNCaP cells (Fig. 34E). Inset in Fig. 34E confirms the overexpression of hnRNPA1 after transfection in LNCaP cells. These results using downregulation as well as overexpression of hnRNPA1 suggest that hnRNPA1 plays an important role in the generation of AR splice variants.

Association of hnRNPA1 with splice variant mRNAs is increased in enzalutamide- resistant cells

We analyzed the hnRNP binding sites (UAGGGA) in AR mRNA using sequence analysis and the ESE finder program and found that hnRNPA1 and hnRNPA2 binding sites exist

in the full length AR mRNA. In order to determine whether hnRNPA1 is associated with AR splice variant mRNAs, we performed RNA Immunoprecipitation (RIP) assays using specific antibodies against hnRNPA1 and hnRNPA2 in 22Rv1 vs. 22Rv1-Enza-R and C4-2B vs. C4-2B-Enza-R cell lines. The 22Rv1-Enza-R and C4-2B-Enza-R cell lines were generated by chronic exposure to enzalutamide and display resistance to enzalutamide [11, 12]. As shown in Fig. 35A&B, the degree of association between AR-V7 transcript and hnRNPA1 was significantly higher in 22Rv1-Enza-R cells compared to parental 22Rv1 cells, indicating that hnRNPA1 may promote generation of AR-V7 splice variant in PCa cells resistant to enzalutamide. Even though the association of hnRNPA2 with AR-V7 mRNA was also enhanced in 22Rv1-Enza-R cells compared to 22Rv1 cells, the degree of association was much higher in the case of hnRNPA1 than with hnRNPA2 (Fig. 35A&B). We also analyzed association between other splice variants such as AR-V1, AR-V5, AR-1/2/2b and AR-1/2/3/2b and hnRNPA1. As shown in Suppl. Fig. 1A & B, association between hnRNPA1 and AR-1/2/2b transcript alone was significantly higher in 22Rv1-Enza-R cells, indicating that hnRNPA1 may play a selective role in generation of AR splice variants. In addition, we analyzed the association of hnRNPA2 with AR splice variants other than AR-V7. As shown in Suppl. Fig. 1A & B, association of hnRNPA2 with AR-1/2/3/2b was significantly enhanced in 22Rv1-Enza-R cells. These results imply that different splicing factors may function co-operatively to promote generation of AR splice variants in enzalutamide-resistant PCa cells. These results also confirm that hnRNP proteins physically associate with AR splice variant mRNAs with the degree of association increasing in PCa cells resistant to enzalutamide, indicating that hnRNP proteins may drive the generation of AR splice variants leading to enzalutamide resistance.

When the C4-2B vs. C4-2B-Enza-R cell line pair was analyzed, we found that association of hnRNPA1 with AR-V7, AR-V5, AR-1/2/2b and AR-1/2/2b mRNAs was significantly enhanced in C4-2B-Enza-R cells compared to parental C4-2B cells, while association of hnRNPA2 with AR-V7, AR-1/2/2b and AR-1/2/3/2b mRNAs was significantly enhanced in C4-2B-Enza-R cells compared to parental C4-2B cells (Fig. 35C&D and Suppl. Fig. 1C & D). In all cases, the fold enrichment of association of hnRNPA1 with AR splice variants was much higher compared to hnRNPA2, indicating that hnRNPA1 may play a more central role in promoting the expression of AR splice variants. These results collectively demonstrate that different splicing factors may play context- and cell type-dependent roles in PCa cells in alternative splicing of the AR transcript.

Expression levels of hnRNPA1 are elevated in PCa tissues

To determine whether increased expression of splicing factors and AR variants is associated with prostate cancer, we examined the expression levels of hnRNPA1 and hnRNPA2 by Western blotting in lysates from 27 archived paired benign and tumor PCa clinical samples. As shown in Fig. 36A and Suppl. Fig. 2A, levels of hnRNPA1 and hnRNPA2 were elevated in ~44% of the tumor tissues examined compared to their matched benign tissues. These results were correlated well with the protein expression levels of AR-V7, which were enhanced in ~ 48% of the tumor tissues examined, compared to their benign counterparts (Fig. 36B and Suppl. Fig. 2A). In addition, expression levels of hnRNPA1 were low or undetectable in 9/12 of donor prostates, while expression levels of hnRNPA2 were low or undetectable in 6/12 of donor prostates. These observations were also correlated with expression levels of AR-V7 in donor tissues which were low or undetectable in 8/12 tissues (Fig. 36B and Suppl. Fig. 2A).

To confirm these findings in another sample set, we analyzed the mRNA expression levels of hnRNPA1, hnRNPA2 and AR-V7 in archival total RNAs extracted from 10 pairs of matched benign and tumor clinical PCa samples described previously [13, 14]. As shown in Fig. 36C, transcript levels of hnRNPA1 were elevated in 5/10 of tumor tissues compared to their matched benign tissues with no appreciable differences between tumor and benign being observed in the other 5/10 of samples. Transcript levels of AR-V7 were elevated in 6/10 tumor tissues compared to their matched benign counterparts (Fig. 36D), demonstrating that expression of hnRNPA1 and AR-V7 may be positively correlated with each other in human PCa specimens. No significant differences were observed in mRNA levels of hnRNPA2 between matched tumor and benign prostate tissues (Suppl. Fig. 2B).

To further confirm our findings, we analyzed expression levels of hnRNPA1 and hnRNPA2 in clinical prostate cancer tissues using publicly available datasets from Gene Expression Omnibus (GEO) and Oncomine. As shown in Fig. 36E&F and Suppl. Fig. 2C, results from an analysis of Oncomine datasets revealed that expression levels of hnRNPA1 and hnRNPA2 are significantly elevated in prostate tumor tissues compared to benign prostates in 17/21 and 15/21 datasets respectively. An analysis of GEO revealed that expression levels of hnRNPA1 and hnRNPA2 were elevated in primary as well as metastatic PCa compared to benign prostates (Fig. 36G&H and Suppl. Fig. 2D). Data regarding expression levels of AR splice variants were not available in these datasets, but nonetheless, these results indicate that elevated levels of hnRNPA1 may contribute to PCa development and progression. Our findings correlate well with studies showing that expression levels of AR-V7 are elevated in ~40% of CRPC tissues [15, 16], indicating that elevated expression of hnRNPA1 in prostate tumors may contribute to generation of higher levels of AR variants.

Expression of hnRNPA1 is regulated by c-Myc

Next, we examined the mechanisms involved in the elevated expression of hnRNPA1 in PCa cells. Previous studies indicated that hnRNPA1 and c-Myc exhibit positive reciprocal regulation [17]. C-Myc enhances hnRNPA1 expression transcriptionally, while hnRNPA1 regulates c-Myc via alternative splicing. To determine whether this mutual regulation holds true in PCa, we analyzed the status of c-Myc or hnRNPA1 when the expression of either was downregulated in PCa cells. 22Rv1 and VCaP cells were transfected with shRNA against c-Myc and the resultant cell lysates were subjected to Western blotting using specific antibodies against hnRNPA1. Downregulation of c-Myc reduced protein levels of hnRNPA1 significantly (Fig. 37A). Similarly, LNCaP, 22Rv1 and VCaP prostate cancer cells were transfected with siRNA against hnRNPA1 and the cell lysates were subjected to Western blotting using specific antibodies against c-Myc. Downregulation of hnRNPA1 reduced protein levels of c-Myc (Fig. 37B). These results confirm that hnRNPA1 and c-Myc exhibit reciprocal regulation in PCa cells. We also analyzed whether reduction in hnRNPA1 levels by c-Myc shRNA affects expression of AR splice variants in 22Rv1 and VCaP cells which exhibit endogenous levels of AR splice variants. As shown in Fig. 37B, C and D, Western blotting and qRT-PCR analyses showed that levels of AR variants, including that of AR-V7, were abrogated due to depletion of hnRNPA1 caused by downregulation of c-Myc. These findings support an important role for c-Myc in the generation of AR splice variants.

NF-kappaB2/p52 regulates AR-V7 expression via hnRNPA1 and c-Myc

Our previous studies demonstrated that activation of NF-κB2/p52 promotes progression to CRPC and enzalutamide resistance via the generation of AR variants, specifically AR-V7 [11, 18, 19]. Our previous findings also indicated that NF-κB2/p52 may regulate c-Myc expression (Nadiminty et al., unpublished observations). Hence, we examined whether NF-κB2/p52 plays a role in the elevated expression of hnRNPA1 and c-Myc in PCa. We examined lysates from LNCaP cells stably expressing p52 (LN-p52) by Western blotting to determine the expression levels of AR-V7, hnRNPA1, hnRNPA2 and c-Myc. As shown in Fig. 38A left panel, protein levels of AR-V7, hnRNPA1 and c-Myc were elevated in cells expressing p52, while no appreciable differences were found in the expression of hnRNPA2. These results were confirmed using LNCaP cells expressing p52 under the control of a Tet-inducible promoter (LN/TR/p52). As shown in Fig. 38A right panel, induction of p52 expression by doxycycline, led to increases in expression levels of AR-V7, hnRNPA1 and c-Myc, indicating that upregulation of AR-V7 by p52 may be mediated by hnRNPA1 and c-Myc. To examine the association between hnRNPA1, c-Myc and AR-V7 in LN-p52 cells, we transfected siRNAs against either hnRNPA1 or hnRNPA2 into LN-p52 cells and analyzed levels of AR-V7 by Western blotting. As shown in Fig. 38B left panel, downregulation of hnRNPA1 by siRNA abrogated the expression of AR-V7 in LN-p52 cells, while downregulation of hnRNPA2 did not have an appreciable effect on AR-V7 protein levels. Protein levels of c-Myc were also downregulated, keeping in line with earlier findings that hnRNPA1 and c-Myc regulate each other [17]. Expression levels of other AR splice variants also showed a decrease when hnRNPA1 was downregulated (Suppl. Fig. 3A). In addition, we transfected shRNA against c-Myc into LN-p52 cells and found that expression of hnRNPA1 and AR-V7 were abolished as a result of downregulation of c-Myc expression (Fig. 38B middle panel). Expression levels of other AR splice variants were also decreased when c-Myc was downregulated (Suppl. Fig. 3B).

In order to confirm these findings in a cell line with constitutive expression of both p52 and AR-V7, we transfected shRNA against p52 into 22Rv1 cells and analyzed expression levels of AR-V7, hnRNPA1 and c-Myc by immunoblotting. As shown in Fig. 38B right panel, downregulation of p52 in 22Rv1 cells abrogated expression of AR-V7, hnRNPA1 and c-Myc. These results demonstrate that NF-κB2/p52 may modulate generation of AR splice variants by regulation of hnRNPA1 and c-Myc.

PCa cells resistant to enzalutamide exhibit higher levels of splicing factors

As our results demonstrate that expression of hnRNPA1 and AR variants may be positively correlated with each other in PCa cells, and AR-V7 expression has been shown to be involved in the acquisition of resistance to enzalutamide [11, 20], we tested the correlation between levels of AR variants and hnRNPA1 using Western blotting in PCa cells that have acquired resistance to enzalutamide. Whole cell lysates from enzalutamide-resistant 22Rv1-Enza-R and C4-2B-Enza-R cells were analyzed by Western blotting using specific antibodies against AR-V7 and hnRNPA1. As shown in Fig. 38C, both PCa cell lines exhibited higher levels of AR-V7 as well as of hnRNPA1, indicating that expression of hnRNPA1 may be positively correlated with expression of AR splice variants. Furthermore, expression levels of c-Myc and NF-κB2/p52 were also elevated in enzalutamide-resistant cells, confirming the importance of the NF-κB2/p52:c-Myc:hnRNPA1:AR-V7 axis in enzalutamide resistance. We also tested the expression levels of hnRNPA2 in PCa cells that have acquired resistance to enzalutamide. Whole cell lysates from 22Rv1-Enza-R and C4-2B-Enza-R cells were analyzed by Western blotting using specific antibodies against hnRNPA2. No significant differences were observed in the

expression of hnRNPA2 (Fig. 38C right and middle panels). To confirm these results *in vivo*, we analyzed extracts from xenograft tumors derived from C4-2B and C4-2B-Enza-R cells by Western blotting using antibodies against AR-V7 and hnRNPA1. As shown in Fig. 38C right panel, higher levels of AR-V7 were observed in xenografts derived from C4-2B-Enza-R cells, which was correlated well with higher levels of hnRNPA1 and c-Myc, confirming our observations that expression of AR splice variants is positively correlated with expression of hnRNPA1 in PCa cell lines resistant to enzalutamide.

Next, we tested whether downregulation of hnRNPA1 affects endogenous levels of AR splice variants in 22Rv1-Enza-R cells. As shown in Fig. 38D left panel, transfection of siRNA against hnRNPA1 abrogated levels of AR-V7 in 22Rv1-Enza-R cells. Similarly, downregulation of c-Myc by specific shRNA reduced expression levels of AR-V7 and hnRNPA1 in 22Rv1 and 22Rv1-Enza-R cells (Fig. 38D right panel), confirming the c-Myc: hnRNPA1: AR-V7 axis in PCa cells.

To confirm the importance of the link between NF-κB2/p52, c-Myc, hnRNPA1 and AR-V7 in PCa, we analyzed the correlation between their expression levels at mRNA and protein levels in paired benign and tumor prostate clinical samples. As shown in Fig. 38E, mRNA (left panel) and protein (right panel) levels of NF-κB2/p52, c-Myc, hnRNPA1 and AR-V7 were positively correlated with each other, demonstrating that the NF-κB2/p52:c-Myc:hnRNPA1:AR-V7 axis plays a vital role in PCa and in the development of castration and therapy resistance.

Suppression of hnRNPA1 resensitizes enzalutamide-resistant PCa cells to enzalutamide

As the expression of AR-V7 has been shown to be required for the development of resistance to enzalutamide [2], and to examine the functional relevance of regulation of AR alternative splicing by hnRNPA1, we tested whether downregulation of hnRNPA1 resulting in decreased levels of AR-V7 resensitizes enzalutamide-resistant 22Rv1-Enza-R cells to enzalutamide. We treated 22Rv1 and 22Rv1-Enza-R cells transfected with siRNAs against hnRNPA1 and hnRNPA2 with 0 and 20 μM enzalutamide for 24 h and examined cell survival. As shown in Fig. 39A left panel, reduced expression of hnRNPA1 enhanced the sensitivity of enzalutamide-resistant 22Rv1-Enza-R cells to enzalutamide, indicating that upregulation of AR-V7 expression by hnRNPA1 may be required to sustain the acquired resistance of 22Rv1-Enza-R cells to enzalutamide. Fig. 39A right panel shows Western blots to confirm the downregulation of hnRNPA1, hnRNPA2 and AR-V7 in the cell lysates from 22Rv1 and 22Rv1-Enza-R cells treated with vehicle and enzalutamide. Next, to confirm these results in another cell line resistant to enzalutamide, we transfected siRNAs against hnRNPA1 and hnRNPA2 into LN-neo and LN-p52 cells and subjected them to 20 μM enzalutamide to analyze their sensitivity to enzalutamide. Our previous studies showed that LN-p52 cells exhibit resistance to enzalutamide via generation of higher levels of AR splice variants [11]. As shown in Fig. 39B left panel, downregulation of hnRNPA1 and hnRNPA2 enhanced the sensitivity of these cells to enzalutamide. Suppression of hnRNPA1 expression reduced cell survival by ~40-50% when enzalutamide-resistant LN-p52 cells were treated with enzalutamide. Fig. 39B right panel shows Western blots to confirm the downregulation of hnRNPA1, hnRNPA2 and AR-V7 in LN-neo and LN-p52 cells treated with vehicle or enzalutamide. Interestingly, suppression of hnRNPA1 expression also reduced survival of VCaP cells when treated with enzalutamide (Fig. 39C left panel), confirming the essential nature of AR variants in these cells, which is in line with earlier reports. Fig. 39C right panel shows Western blots to confirm the downregulation of hnRNPA1, hnRNPA2 and AR-V7 in VCaP cells treated with vehicle or enzalutamide.

Our findings collectively demonstrate that hnRNPA1 plays a major role in the generation of splice variants of the androgen receptor. Expression of hnRNPA1 is modulated by NF-κB2/p52 via c-Myc. Our results point to the enhanced expression of hnRNPA1 in prostate tumors being instrumental in inducing alternative splicing of the precursor AR mRNA and thereby contributing to resistance to AR-targeted therapies.

We have made significant progress in Task 5.

Steroidogenic enzymes mediate p52-induced intracrine androgen synthesis

We generated LN-p52 stable clones with stable knockdown of AKR1C3 and CYP17A1 using specific shRNAs against AKR1C3 and CYP17A1. Expression levels of AKR1C3 and CYP17A1 were analyzed by Western blotting in the stable clones and were found to be reduced by >70% in the stable clones compared to the LN-p52-shEGFP control cells. Cellular extracts from LN-p52-shEGFP, LN-p52-shAKR1C3 and LN-p52-shCYP17A1 cells were analyzed by Mass Spectrometry for their steroid profiles. Briefly, $50x10^6$ cells were homogenized, and the resulting homogenate was cooled on ice. The precipitated material was removed by centrifuging at high speed for 5 minutes, and the supernatant was removed and evaporated in a SpeedVac (Labconco) followed by lyophilizer (Labconco). The residue was suspended in 150 µL of CH3OH/H2O (1:1), filtered through a 0.2 µm ultracentrifuge filter (Millipore) and subjected to UPLC/MS-MS analysis. Samples were run in duplicate during UPLC/MS-MS analysis. Samples were placed in an Acquity sample manager, which was cooled to 8°C to preserve the analytes. Pure standards were used to optimize the UPLC/MS-MS conditions before sample analysis. Also, the standard mixture was run before the first sample to prevent errors due to matrix effect and day-to-day instrument variations. In addition, immediately after the initial standard and before the first sample, two spiked samples were run to calibrate for the drift in the retention time of all analytes due to the matrix effect. After standard and spiked sample runs, blank was injected to wash the injector and remove carry over effect. All experiments were performed on a Waters Xevo-TQ triple quadruple mass spectrometer (Milford) and MS and MS-MS spectra were recorded using Electro Spray Ionization (ESI) in positive ion (PI) and negative ion (NI) mode, capillary voltage of 3.0 kV, extractor cone voltage of 3 V, and detector voltage of 650 V. Cone gas flow was set at 50 L/h and desolvation gas flow was maintained at 600 L/h. Source temperature and desolvation temperatures were set at 150°C and 350°C, respectively. The collision energy was varied to optimize daughter ions. The acquisition range was 20 to 500 Da. Analytic separations were conducted on the UPLC system using an Acquity UPLC HSS T3 1.8 µm 1 × 150-mm analytic column kept at 50°C and at a flow rate of 0.15 mL/min. The gradient started with 100% A (0.1% formic acid in H2O) and 0% B (0.1% formic acid in CH3CN), after 2 minutes, changed to 80% A over 2 minutes, then 45% A over 5 minutes, followed by 20% A in 2 minutes. Finally, it was changed over 1 minute to original 100% A, resulting in a total separation time of 15 minutes. The eluates from the UPLC column were introduced to the mass spectrometer and resulting data were analyzed and processed using MassLynx 4.1 software. Results showed that intracellular levels of both testosterone as well as DHT were greatly reduced in LN-p52 cells with stable knockdown of AKR1C3 (Fig. 40A) or CYP17A1 (Fig. 40B), indicating that the increase in intracrine androgen synthesis induced by p52 is mediated by activation of steroidogenic enzymes such as AKR1C3 or CYP17A1. Conversely, mass spectrometric analysis of LNCaP cells stably overexpressing AKR1C3 showed that intracellular levels of testosterone were greatly enhanced

(Fig. 40C), indicating that higher expression of AKR1C3 may be sufficient for induction of intracrine androgen synthesis in vitro.

Steroidogenic enzymes mediate induction of castration resistance by p52

We tested whether castration resistance exhibited by p52-expressing CaP cells is mediated by steroidogenic enzymes, using LN-p52 cells with stable knockdown of AKR1C3 or CYP17A1. Cell survival of LN-p52-shEGFP and LN-p52-shAKR1C3 or LN-p52-shCYP17A1 cells in media containing CS-FBS were analyzed by growth assays. Results showed that suppression of expression of either AKR1C3 or CYP17A1 reduced the ability of LN-p52 cells to survive in androgen-depleted media (Fig. 41A). These findings point to the ability of CaP cells expressing p52 to upregulate intracellular androgen synthesis, thus evading cell cycle suppression due to androgen withdrawal. Conversely, LNCaP cells stably overexpressing AKR1C3 exhibit greatly enhanced ability to survive in androgen depleted media (Fig. 41B), indicating that upregulation of intracellular androgen synthesis after androgen withdrawal may be one of the principal mechanisms driving the development of castration resistance.

Let-7c modulates induction of castration resistance by p52

We tested whether reconstitution of let-7c expression reduces survival of LN-p52 cells under androgen-depleted conditions. LN-p52 cells were infected with lentiviruses encoding let-7c and cell survival was analyzed in media containing CS-FBS. Results showed that LN-p52 cells exhibited resistance to growth suppression by androgen withdrawal which was abolished by reconstitution of let-7c expression (Fig. 42A). These results were confirmed by overexpression of let-7c in C4-2B cells which are castration resistant and express higher levels of p52. C4-2B cells stably expressing let-7c exhibited lower rates of survival under androgen depleted conditions compared to their parental control cells, showing that let-7c may modulate castration resistance of CaP cells (Fig. 42B).

Key Research Accomplishments:

We have:

- demonstrated that NF-kB2/p52 regulates transcription of key steroidogenic enzymes
- demonstrated that p52 induces intracellular androgen synthesis in prostate cancer cells
- shown that let-7c regulates AR expression via its regulation of Myc
- demonstrated that downregulation of let-7c expression relieves its repression of AR and enhances proliferation of prostate cancer cells
- generated prostate cancer cell lines stably expressing shRNAs/genes of interest (as outlined below).
- demonstrated that p52 induces resistance to newly approved anti-androgens such as enzalutamide by enhancing generation of AR splice variants

- shown that Lin28 regulates CaP cell growth by enhancing AR expression
- demonstrated that p52 regulates expression levels of Lin28 and c-Myc and thereby contributes to increased activation of the AR
- demonstrated that NF-κB2/p52 regulates expression of hnRNPA1 via c-Myc
- demonstrated that p52-induced resistance to anti-androgens such as enzalutamide is mediated by hnRNPA1
- shown that Lin28 enhances CaP cell resistance to AR-targeted therapies
- demonstrated that orthotopic xenografts from CaP cells stably expressing p52 shRNA exhibit lower rates of growth
- demonstrated that orthotopic xenografts from CaP cells stably expressing p52 shRNA exhibit lower expression of steroidogenic enzymes and consequently synthesize lower levels of intracrine androgens

Conclusions:

- We demonstrated that NF-kB2/p52 regulates expression of steroidogenic enzymes in PCa cells.
- We demonstrated that NF-kB2/p52 regulates intracellular androgen synthesis in vitro and in vivo in PCa cells.
- We demonstrated that miR-let-7c regulates AR expression and proliferation of PCa cells.
- We demonstrated that Lin28 regulates AR expression and proliferation of PCa cells.
- We showed that decrease in miR-let-7c promotes castration-resistant growth of PCa cells.
- We showed that Lin28 and Myc are involved in the regulation of AR expression by miR-let-7c.
- We showed that p52 regulates Lin28 and Myc and thereby enhances CaP cell proliferation.
- We showed that p52 promotes the generation of constitutively active AR splice variants that are resistant to AR-targeted therapies.
- We demonstrated that p52 and Lin28 enhance CaP cell resistance to second-generation anti-androgens such as enzalutamide.
- We demonstrated that NF-κB2/p52 regulates expression of hnRNPA1 via c-Myc in CaP cells.
- We demonstrated that p52-induced resistance to enzalutamide is mediated by hnRNPA1.

Our results implicate NF-kB2/p52 in the development of resistance to castration by promoting intracrine androgen synthesis and by promoting alternative splicing of AR. In addition, we provide evidence for the existence of the NF-kB2/p52:Lin28:c-Myc:let-7c:AR pathway and for the NF-κB2/p52:c-Myc:hnRNPA1 axis and their role in AR alternative splicing and enzalutamide resistance. Our results underscore the importance of NF-κB2/p52 in CaP cells resistance to currently used anti-androgen therapeutics.

"So What" Section: Our findings provide conclusive evidence for the importance of the p52-Lin28-Myc-let-7c-AR pathway in PCa. Our most recent findings also implicate p52 in the development of resistance to newly approved drugs such as enzalutamide and in the generation of constitutively active AR splice variants such as AR-V7. Since the current focus of research in CRPC therapy is to target the androgen receptor, our findings are very relevant to the recent advancements in the field.

Publications, Abstracts and Presentations:

Publications:

Nadiminty N, Tummala R, Liu C, Lou W, Evans CP, Gao AC (2015) NF-kappaB2/p52:c-Myc:hnRNPA1 pathway regulates expression of androgen receptor splice variants and enzalutamide sensitivity in prostate cancer. *Mol Cancer Ther* 2015 Jun 8. [Epub ahead of print] PMID: 26056150

Liu C, Lou W, Zhu Y, Yang JC, Nadiminty N, Gaikwad NW, Evans CP, Gao AC (2015) Intracrine Androgens and AKR1C3 Activation Confer Resistance to Enzalutamide in Prostate Cancer. *Cancer Research* 75(7):1413-22. PMID: 25649766

Cui Y, Nadiminty N, Liu C, Lou W, Schwartz CT, Gao AC (2014) Upregulation of glucose metabolism by NF-κB2/p52 mediates enzalutamide resistance in castration-resistant prostate cancer cells. *Endocr Relat Cancer* 21(3):435-42. PMID: 24659479

Liu C, Lou W, Zhu Y, Nadiminty N, Schwartz CT, Evans CP, Gao AC (2014) Niclosamide inhibits androgen receptor variants expression and overcomes enzalutamide resistance in castration-resistant prostate cancer. *Clin Cancer Res* 20(12):3198-210. PMID: 24740322

Zhu Y, Liu C, Cui Y, Nadiminty N, Lou W, Gao AC (2014) Interleukin-6 induces neuroendocrine differentiation (NED) through suppression of RE-1 silencing transcription factor (REST). *Prostate* 74(11):1086-94. PMID: 24819501

Nadiminty N, Tummala R, Liu C, Yang J, Lou W, Evans CP, Gao AC (2013) NF-κB2/p52 induces resistance to enzalutamide in prostate cancer: role of androgen receptor and its variants. *Mol Cancer Ther* 12(8):1629-37. PMID: 23699654

Tummala R, Nadiminty N, Lou W, Zhu Y, Gandour-Edwards R, Chen HW, Evans CP, Gao AC (2013) Lin28 promotes growth of prostate cancer cells and activates the androgen receptor. *Am J Pathol* 183(1):288-95 PMID: 23790802

Zhu Y, Liu C, Tummala R, Nadiminty N, Lou W, Gao AC (2013) RhoGDIα downregulates androgen receptor signaling in prostate cancer cells. *Prostate* 73(15):1614-22. PMID: 23922223

Nadiminty N, Tummala R, Lou W, Zhu Y, Zhang J, Chen X, eVere White RW, Kung HJ, Evans CP, Gao AC (2012) MicroRNA let-7c suppresses androgen receptor expression and activity via

regulation of Myc expression in prostate cancer cells. *J Biol Chem* 287(2):1527-37 PMID: 22128178

Nadiminty N, Tummala R, Lou W, Zhu Y, Shi XB, Zou JX, Chen H, Zhang J, Chen X, Luo J, deVere White RW, Kung HJ, Evans CP, Gao AC (2012) MicroRNA let-7c is downregulated in prostate cancer and suppresses prostate cancer growth. *PLoS One* 7(3):e32832 PMID: 22479342

Nadiminty N, Gao AC (2012) Mechanisms of persistent activation of the androgen receptor in CRPC: recent advances and future perspectives. *World J Urol* 30(3):287-95. PMID: 22009116

Zhu Y, Tummala R, Liu C, Nadiminty N, Lou W, Evans CP, Zhou Q, Gao AC (2012) RhoGDIα suppresses growth and survival of prostate cancer cells. *Prostate* 72(4):392-8. PMID: 21681778

Abstracts and Presentations:

Nadiminty N, Tummala R, Lou W, Yang JC, Evans CP, Gao AC. NF-kappaB2/p52 induces resistance to enzalutamide possibly by upregulation of AR-V7. *AACR Annual Meeting, 2013, Washington DC*.

Nadiminty N, Tummala R, Lou W, Evans CP, Gao AC. NF-κB2/p52 induces expression of inflammatory mediators in prostate cancer in vivo. *AACR Annual Meeting 2013, Washington DC*.

Nadiminty N, Tummala R, Lou W, Yang JC, Evans CP, Gao AC. NF-κB2/p52 induces resistance to enzalutamide possibly by upregulation of AR-V7. *AUA Annual Meeting 2013, San Diego, CA*.

Nadiminty N, Zhu Y, Tummala R, Lou W, de vere White R, Evans CP, Gao AC. miR-let-7c axis regulates androgen signaling and the growth of prostate cancer cells. *AUA Annual Meeting 2013, San Diego, CA*.

Tummala R, Nadiminty N, Zhu Y, Lou W, Evans CP, Gao AC. Lin28 promotes growth of prostate cancer cells and activates the androgen receptor**.** *AUA Annual Meeting 2013, San Diego, CA.*

Nadiminty N, Tummala R, Liu C, Yang J, Lou W, Evans CP, Gao AC . NF-kappaB2/p52 induces resistance to enzalutamide in Prostate Cancer: Role of androgen receptor and its variants. *AUA Annual Meeting 2014, Orlando, FL*.

Nadiminty N, Tummala R, Lou W, Evans CP, Gao AC. miR-Let-7c/Lin28 axis regulates the sensitivity of prostate cancer cells to anti-androgens via AR variants. *SBUR Annual Meeting 2014, Dallas, TX.*

Nadiminty N, Tummala R, Liu C, Lou W, Evans CP, Gao AC. NF-kappaB2/p52:c-Myc:hnRNPA1 regulatory pathway controls expression of androgen receptor splice

variants and enzalutamide sensitivity in prostate cancer. *AUA Annual Meeting 2015, New Orleans, LA*.

Inventions, patents and licenses:

None to report.

Reportable Outcomes:

Cell lines generated:

- C4-2B, LN-IL6 and DU145 cells stably expressing p52 shRNA
- C4-2B, LN-IL6 and DU145 cells stably expressing Lin28 shRNA
- PZ-HPV7, LAPC-4 and LNCaP cells stably expressing p52
- LNCaP cells stably and inducibly expressing p52
- LNCaP, C4-2B and DU145 cells stably expressing let-7c
- LNCaP cells stably expressing Lin28
- LNCaP cells inducibly expressing Lin28
- LN-p52 cells stably expressing AKR1C3 shRNA
- LN-p52 cells stably expressing CYP17A1 shRNA
- LN-p52 cells stably expressing HSD3B2 shRNA
- PZ-HPV7 cells stably expressing Lin28

Other Achievements:
Grants applied for:
NIH/NCI-2014 R21 (Exploratory/Developmental Grant)-Novel Targets in Androgen Receptor Signaling in Prostate Cancer

NIH/NCI-2014 RO3 (Small Grant)-Alteration of the miR-let-7c:Lin28 ratio as a potential predictor of therapy resistance in Prostate Cancer

NIH/NCI-2015 R21 (Exploratory/Developmental Grant)-MicroRNAs modulate therapy resistance in Prostate Cancer

References

1. Mostaghel, E.A., et al., *Resistance to CYP17A1 Inhibition with Abiraterone in Castration-Resistant Prostate Cancer: Induction of Steroidogenesis and Androgen Receptor Splice Variants.* Clinical Cancer Research, 2011. 17(18): p. 5913-5925.
2. Li, Y., et al., *Androgen Receptor Splice Variants Mediate Enzalutamide Resistance in Castration-Resistant Prostate Cancer Cell Lines.* Cancer Research, 2013. 73(2): p. 483-489.
3. Thadani-Mulero, M., et al., *Androgen Receptor Splice Variants Determine Taxane Sensitivity in Prostate Cancer.* Cancer Research, 2014. 74(8): p. 2270-2282.
4. Li, Y., et al., *AR intragenic deletions linked to androgen receptor splice variant expression and activity in models of prostate cancer progression.* Oncogene, 2012. 31(45): p. 4759-4767.
5. Thiery, J.P., et al., *Epithelial-Mesenchymal Transitions in Development and Disease.* Cell, 2009. 139(5): p. 871-890.
6. Blanchette, M., et al., *Genome-wide Analysis of Alternative Pre-mRNA Splicing and RNA-Binding Specificities of the Drosophila hnRNP A/B Family Members.* Molecular Cell, 2009. 33(4): p. 438-449.
7. Golan-Gerstl, R., et al., *Splicing Factor hnRNP A2/B1 Regulates Tumor Suppressor Gene Splicing and Is an Oncogenic Driver in Glioblastoma.* Cancer Research, 2011. 71(13): p. 4464-4472.
8. Mayeda, A., D.M. Helfman, and A.R. Krainer, *Modulation of exon skipping and inclusion by heterogeneous nuclear ribonucleoprotein A1 and pre-mRNA splicing factor SF2/ASF.* Molecular and Cellular Biology, 1993. 13(5): p. 2993-3001.
9. Tauler, J., et al., *hnRNP A2/B1 Modulates Epithelial-Mesenchymal Transition in Lung Cancer Cell Lines.* Cancer Research, 2010. 70(18): p. 7137-7147.
10. Kumar, M.S., et al., *Impaired microRNA processing enhances cellular transformation and tumorigenesis.* Nat Genet, 2007. 39(5): p. 673-677.
11. Nadiminty, N., et al., *NF-κB2/p52 Induces Resistance to Enzalutamide in Prostate Cancer: Role of Androgen Receptor and Its Variants.* Molecular Cancer Therapeutics, 2013. 12(8): p. 1629-1637.
12. Liu, C., et al., *Niclosamide Inhibits Androgen Receptor Variants Expression and Overcomes Enzalutamide Resistance in Castration-Resistant Prostate Cancer.* Clinical Cancer Research, 2014. 20: p. 3198-3210.
13. Nadiminty, N., et al., *MicroRNA let-7c Is Downregulated in Prostate Cancer and Suppresses Prostate Cancer Growth.* PLoS ONE, 2012. 7(3): p. e32832.
14. Nadiminty, N., et al., *MicroRNA let-7c Suppresses Androgen Receptor Expression and Activity via Regulation of Myc Expression in Prostate Cancer Cells.* Journal of Biological Chemistry, 2012. 287(2): p. 1527-1537.
15. Guo, Z., et al., *A Novel Androgen Receptor Splice Variant Is Up-regulated during Prostate Cancer Progression and Promotes Androgen Depletion–Resistant Growth.* Cancer Research, 2009. 69(6): p. 2305-2313.
16. Hu, R., et al., *Ligand-Independent Androgen Receptor Variants Derived from Splicing of Cryptic Exons Signify Hormone-Refractory Prostate Cancer.* Cancer Research, 2009. 69(1): p. 16-22.
17. David, C.J., et al., *HnRNP proteins controlled by c-Myc deregulate pyruvate kinase mRNA splicing in cancer.* Nature, 2010. 463(7279): p. 364-368.

18. Nadiminty, N., et al., *NF-κB2/p52 enhances androgen-independent growth of human LNCaP cells via protection from apoptotic cell death and cell cycle arrest induced by androgen-deprivation.* The Prostate, 2008. 68(16): p. 1725-1733.
19. Nadiminty, N., et al., *Aberrant Activation of the Androgen Receptor by NF-kB2/p52 in Prostate Cancer Cells.* Cancer Research, 2010. 70(8): p. 3309-3319.
20. Cao, B., et al., *Androgen receptor splice variants activating the full-length receptor in mediating resistance to androgen-directed therapy*. 2014. Vol. 5. 2014.
21. Varambally, S., et al., *Integrative genomic and proteomic analysis of prostate cancer reveals signatures of metastatic progression.* Cancer Cell, 2005. 8(5): p. 393-406.
22. Chandran, U., et al., *Gene expression profiles of prostate cancer reveal involvement of multiple molecular pathways in the metastatic process.* BMC Cancer, 2007. 7(1): p. 64.

Figure Legends

Figure 1: p52 enhances expression of enzymes involved in intracrine androgen synthesis. **A)** qRT-PCR of steroidogenic enzymes in LNCaP cells stably expressing p52. **B)** Western analysis of expression levels of steroidogenic enzymes in LNCaP cells stably expressing p52. **C)** qRT-PCR analysis of steroidogenic enzymes expression in normal epithelial PZ-HPV7 cells. **D)** Luciferase assay showing increased activation of promoters of steroidogenic enzymes in LNCaP cells stably expressing p52.

Figure 2: p52 induces intracellular androgen synthesis. **A)** PZ-HPV7 normal prostate epithelial cells overexpressing p52 were analyzed by EIA for intracellular testosterone levels. **B)** LNCaP cells stably expressing p52 were analyzed by EIA for intracellular testosterone levels. **C)** LNCaP cells inducibly expressing p52 (after addition of DOX) were analyzed by EIA for intracellular testosterone levels. In all cases p52 induced significantly higher levels of testosterone compared to controls.

Figure 3: Downregulation of p52 reduces intracrine androgen synthesis in vitro. **A)** C4-2B, LN-IL6 and DU145 cells were transiently transfected with shRNA against p52 and intracellular testosterone levels were measured by EIA. Knock down of p52 reduced intracellular testosterone levels in all cell lines tested. **B)** Expression levels of steroidogenic enzymes were measured by qRT-PCR in C4-2B, LN-IL6 and DU145 cells transfected with shRNA against p52. Expression levels of all enzymes tested were downregulated by p52 knock down. **C)** C4-2B, LN-IL6 and DU145 cells stably expressing p52 shRNA were generated and intracellular testosterone levels were measured by EIA. **D)** Expression levels of steroidogenic enzymes were measured by qRT-PCR in C4-2B, LN-IL6 and DU145 cells stably expressing p52 shRNA.

Figure 4: Downregulation of p52 reduces intracrine androgen synthesis in vivo. **A)** C4-2B xenografts were injected with control retroviruses or retroviruses encoding shRNA against p52 and tumor volumes were measured. Downregulation of p52 led to decreased tumor growth. **B)** Intratumoral testosterone levels were measured by EIA in C4-2B xenografts injected with control retroviruses or retroviruses encoding p52 shRNA. Intracellular testosterone levels were reduced significantly with downregulation of p52. **C)** Expression levels of steroidogenic enzymes were measured by qRT-PCR in the above xenograft tissues. Expression levels of all enzymes tested were reduced by downregulation of p52.

Figure 5: Downregulation of NF-kB2/p52 abolishes intracrine androgen synthesis. A) C4-2B-shp52 and C4-2B-shEGFP control cells were injected orthotopically into the prostates of SCID mice and tumor weights were analyzed. Weights of tumors formed by C4-2B-shp52 cells were significantly lower than weights of tumors formed by C4-2B-shEGFP control cells. B) Intratumoral testosterone levels were analyzed using EIA according to manufacturer's instructions (Cayman Chemicals) in the xenograft tumors from C4-2B-shp52 and C4-2B-shEGFP cells. Intracrine testosterone levels were significantly diminished in C4-2B-shp52 tumors compared to control C4-2B-shEGFP tumors. C) Intratumoral testosterone, Dihydrotestosterone and DHEA levels were analyzed by LC-MS analysis in xenograft tumors from C4-2B-shEGFP and C4-2B-shp52 cells. Levels of all three steroids were diminished in C4-2B-shp52 tumors compared to control tumors. D) Expression levels of steroidogenic enzymes were analyzed by qPCR using total RNAs extracted from the above tumor tissues. Expression levels of most steroidogenic enzymes were suppressed by downregulation of p52 in C4-2B-shp52 tumors. Results are presented as means ± SD of 3 experiments performed in triplicate.

Figure 6: Downregulation of NF-kB2/p52 abolishes intracrine androgen synthesis. A) DU145-shp52 and DU145-shEGFP control cells were injected orthotopically into the prostates of SCID mice and tumor weights were analyzed Weights of tumors formed by DU145-shp52 cells were significantly lower than weights of tumors formed by DU145-shEGFP control cells. B) Intratumoral testosterone levels were analyzed using EIA according to manufacturer's instructions (Cayman Chemicals) in the xenografts tumors from DU145-shp52 and DU145-shEGFP cells. Intracrine testosterone levels were significantly diminished in DU145-shp52 tumors compared to control DU145-shEGFP tumors. C) Expression levels of steroidogenic enzymes were analyzed by qPCR using total RNAs extracted from the above tumor tissues. Expression levels of most steroidogenic enzymes were suppressed by downregulation of p52 in DU145-shp52 tumors. Results are presented as means ± SD of 3 experiments performed in triplicate.

Figure 7: A) Western analysis of expression of Lin28 in LNCaP cells stably expressing Lin28. **B)** Western analysis of expression of Lin28 in the absence and presence of Doxycycline in LNCaP cells inducibly expressing Lin28. **C)** Expression of let-7c in LNCaP cells expressing EGFP-tagged let-7c.

Figure 8: p52 regulates expression of Lin28 and c-Myc. **A)** Relative expression of Lin28 and c-Myc in LN-neo and LN-Lin28 cells was measured by Western blotting (left panel) and qPCR (right panel). **B)** ChIP assays were performed to assess the recruitment of p52 to the promoter region of Lin28. Recruitment of p52 to Lin28 promoter was higher in LN-p52 cells compared to LN-neo cells.

Figure 9: A) LNCaP cells were transfected with let-7c anti-sense oligonucleotides and AR mRNA levels were analyzed by qRT-PCR. Results are presented as relative fold change compared to expression levels in LNCaP cells transfected with control oligonucleotides. **B)** Western blot showing the increase in AR expression in LNCaP cells transfected with let-7c anti-sense. **C)** LN-IL6+ cells were transfected with let-7c and AR mRNA levels were analyzed by qRT-PCR. **D)** Western blot showing the downregulation of AR expression in LN-IL6+ cells transfected with let-7c. **E & F)** AR levels were analyzed in LNCaP and C4-2B cells stably

expressing let-7c by Western blotting. **G)** Protein levels of AR were analyzed in LNCaP cells stably expressing Lin28 by Western blotting.

Figure 10: A) LNCaP cells were co-transfected with let-7c and pGL3-PSA6.0-Luc reporter and luciferase activities were analyzed. **B)** LNCaP cells were transfected with control or let-7c or let-7c anti-sense and levels of PSA and NKX3.1 mRNAs were analyzed by qRT-PCR. Results are presented as relative fold change compared to expression levels in LNCaP cells transfected with control oligonucleotides. **C)** PSA secretion in LNCaP cells was enhanced when let-7c expression was downregulated. **D)** LNCaP cells stably expressing control, let-7c or Lin28 were transfected with pGL3-PSA6.0-Luc reporter and luciferase activities were assayed. **E)** Secretion of PSA by LNCaP cells stably expressing let-7c or Lin28 was analyzed by ELISA. Recruitment of AR to AREs in PSA **(F)** and NKX3.1 **(G)** promoters was analyzed by ChIP in LNCaP cells transfected with let-7c or Lin28.

Figure 11: LNCaP cells were transfected with control or let-7c in the presence or absence of actinomycin D and AR mRNA levels were analyzed by Northern blotting **(A)** or qRT-PCR **(B)**. **C)** LNCaP cells were co-transfected with control or let-7c or with let-7c anti-sense oligos along with pGL4-AR-Prom-Luc reporter.

Figure 12: Expression levels of AR and c-Myc were analyzed by Western blotting in LNCaP cells transfected with let-7c **(A)** or let-7c anti-sense oligos **(B)**. **C)** LNCaP cells were transfected with plasmids expressing Myc or shRNA against Myc along with the pGL4-AR prom-Luc reporter and luciferase assays were performed. **D & E)** mRNA levels of AR, PSA and NKX3.1 were measured by qRT-PCR in LNCaP cells transfected with Myc or shRNA against Myc. **F)** LNCaP cells were transfected with let-7c and Myc alone or together along with the pGL4-AR prom-Luc reporter. **G)** Recruitment of Myc to the Myc binding site in AR promoter was analyzed by ChIP assays.

Figure 13: Let-7c inhibits growth of human PCa cells *in vitro*. LNCaP **(A)**, C4-2B **(B)**, DU145 **(C)**, LN-IL6+ **(D)** and LNCaP-S17 **(E)** cells were transfected with let-7c or empty vector (Con) and cell numbers were determined after 24 and 48 h. **F)** Cell death was analyzed in LNCaP, DU145, LNCaP-S17 and LN-IL6+ cells transfected with let-7c or empty vector (Con). **G)** LNCaP cells transfected with anti-sense oligos against let-7c or scrambled oligos (Con) were grown in FBS and CS-FBS and cell numbers determined. LNCaP cells with downregulated expression of let-7c exhibited faster growth in CS-FBS compared to controls. Error bars denote ± SD (*$p < 0.05$).

Figure 14: Let-7c inhibits colony forming abilities of human PCa cells. Clonogenic **(A)** and soft agar colony forming **(B)** abilities of LNCaP-S17 and C4-2B cells transfected with let-7c or empty vector (Con) were assayed. **C)** Clonogenic assay-Upper and lower panels represent colony sizes of C4-2B and LNCaP-S17 cells expressing control (empty vector) or let-7c respectively. **D)** Soft agar assay-Upper and lower panels represent colony sizes of C4-2B and LNCaP-S17 cells expressing control (empty vector) or let-7c respectively. **E)** Number of colonies formed in clonogenic assay by C4-2B cells stably expressing let-7c. Let-7c decreased the number of colonies formed by the PCa cells. Data points represent mean ± SD of triplicate samples from two independent experiments. Error bars denote ± SD (*$p < 0.05$).

Figure 15: Let-7c suppresses tumor growth of human PCa xenografts *in vivo*. C4-2B **(A)**, PC346C **(B)** and DU145 **(C)** cells were injected into both flanks of nude mice and the tumors received a single intratumoral injection of lentiviruses expressing either GFP (control) or let-7c. Tumor growth was monitored twice weekly over 3 weeks. Data points represent mean ± SD of tumor volume (mm^3) of all mice at the indicated time points. **D)** Secretion of PSA by C4-2B and PC346C xenografts was measured in mouse sera by ELISA. Reconstitution of let-7c in the tumors reduced secretion of PSA by the xenografts. At the end of the experiments, tumor tissues were excised, total RNAs prepared and subjected to qRT-PCR to assess mRNA levels of let-7c **(E)** and Lin28 **(F)**. Error bars denote ± SD (*$p < 0.05$).

Figure 16: Relative expression levels of let-7c, AR, Lin28 and Myc were analyzed by qRT-PCR in PCa xenografts injected intratumorally with let-7c expressing lentiviruses. Data points represent mean ± SD of triplicate samples from two independent experiments. Error bars denote ± SD ($p \leq 0.05$).

Figure 17: A) Relative expression levels of let-7c were measured by qRT-PCR in total RNAs extracted from 10 paired benign and tumor human prostate samples. **B)** Let-7c levels were measured using *in situ* hybridization in TMAs containing 160 cores each from unmatched benign and cancerous prostate biopsies. Representative images are shown for benign and cancer cores. **C)** Relative expression levels of Lin28 in the 10 paired benign and tumor human prostate samples. Expression levels of Lin28 were correlated inversely with those of let-7c. Error bars denote ± SD (*$p < 0.05$).

Figure 18: A) Relative expression levels of let-7c and AR were measured by qRT-PCR in total RNAs extracted from 22 human prostate cancer samples. p=0.015 by two-tailed t-Test. Plots showing the negative correlation between levels of **B)** let-7c and AR, **C)** let-7c and Lin28 and **D)** let-7c and Myc mRNAs in the above samples. **E)** Western blot showing protein levels of Lin28 and AR in extracts from normal, benign (B) and adjacent tumor (T)–containing human prostate samples.

Figure 19: A) Comparison of AR, Lin28 and Myc expression in the dataset GDS1439 [21]. Benign, n=6; primary prostate cancer, n=7 and metastatic prostate cancer, n=6. **B)** Comparison of AR, Lin28 and Myc levels in GDS2547 [22]. Normal prostate tissue, n=18; normal tissue adjacent to tumor, n=16; primary prostate cancer, n=65 and metastatic prostate cancer, n=25. Data are expressed as means ±SEM (in percentages) of the maximum single channel count determined in each dataset. **C)** Gene expression analysis using Oncomine database showing the relative expression levels of AR, Lin28 and Myc in 3 datasets comparing normal prostate tissue and prostate cancer. Wallace_prostate: normal, n=20, cancer, n=69; Yu_prostate: normal, n=23, cancer, n=64 and Vanaja_prostate: normal, n=8, cancer, n=32. Data presented as means ± SEM of normalized expression units, as per Oncomine output.

Figure 20: Lin28 is overexpressed in human prostate cancer. **A)** qRT-PCR analysis of Lin28 expression in 10 paired benign and tumor CaP tissues. Data are presented as mean±SD of 2 experiments performed in triplicate. Lin28 mRNA expression levels were higher in cancer tissues compared to matched benign tissues. **B)** Western blot analysis of Lin28 expression in 42

paired benign and tumor samples. Representative Western blot is shown. The table summarizes the results of Lin28 protein expression levels in the dataset. **C)** Immunohistochemical analysis of Lin28 expression in benign and cancer CaP tissues. Brown staining represents positive staining for expression of Lin28. Images are presented at 200X magnification.

Figure 21: Lin28 promotes growth of CaP cells. **A)** LNCaP, PZ-HPV7, C4-2B, DU145, LNCaP-S17 and LNCaP-IL6 cells were transfected with empty vector or pLKO.1-Lin28 and growth was monitored at 0, 24 and 48 h. Lin28 enhanced growth rates of all cell lines tested. **B)** LNCaP cells stably expressing Lin28 (LN-Lin28) and control LN-neo cells were plated in media containing complete FBS and growth was monitored at 0, 24, 48 and 72h. Lin28 enhanced the growth of LNCaP cells. Right panel shows the expression levels of Lin28 in LN-Lin28 and LN-neo cells. **C)** C4-2B cells stably expressing Lin28 (C42-B-Lin28) and control C4-2B-neo cells were plated in media containing complete FBS and growth was monitored at 0, 24, 48 and 72 h. Right panel shows the expression levels of Lin28 in C4-2B-Lin28 and C4-2B-neo cells. Data are presented as mean±SD of 3 experiments performed in triplicate. **D)** Downregulation of endogenous Lin28 suppresses CaP cell growth. C4-2B cells were transfected with shRNA against Lin28 and growth was measured in media containing complete FBS. Growth of C4-2B cells was abrogated with downregulation of Lin28. Right panel shows the reduced expression of Lin28 protein after transfection with shRNA. Data are presented as mean±SD of 3 experiments performed in triplicate.

Figure 22: Lin28 promotes clonogenic ability of CaP cells. **A)** C4-2B (left panel) and LNCaP-S17 (right panel) cells were transfected with empty vector or pLKO.1-Lin28 and anchorage-dependent clonogenic assays were performed. Lin28 enhanced the colony forming ability of both C4-2B and LNCaP-S17 cells. **B)** Left panel, LN-Lin28 and control LN-neo cells were subjected to clonogenic assays. Lin28-expressing LNCaP cells exhibited higher clonogenic ability compared to control cells. Right panel, LN/TR/Lin28 (LNCaP cells expressing Lin28 under a Tet-inducible promoter) and LN/TR/Con cells were subjected to clonogenic assays in media containing either complete FBS or CS-FBS. Induction of Lin28 expression by doxycycline (DOX) enhanced colony formation of LN/TR/Lin28 cells compared to control cells. **C)** C4-2B and LNCaP-S17 cells were transfected with empty vector or pLKO.1-Lin28 and subjected to anchorage-independent soft agar colony formation assays. Lin28 expression increased the number of colonies formed in soft agar by both cell lines. **D)** Left panel, LN-Lin28 and control LN-neo cells were subjected to soft agar assays. LN-Lin28 cells were able to form larger number of colonies in soft agar compared to LN-neo cells. Right panel, Lin28 increases invasiveness of CaP cells. LN-Lin28 and LN-neo cells were subjected to Boyden chamber Invasion Assays. Inset picture shows representative images of invading cells. Data are presented as mean±SD of 3 experiments performed in triplicate.

Figure 23: Lin28 promotes tumor growth of CaP xenografts. **A)** $2x10^6$ cells/flank LN-Lin28 or LN-neo cells were injected s.c into both flanks of male nude mice and tumor growth was monitored. **B)** Secretion of PSA by the CaP xenografts was measured in the mouse sera. Tumors expressing Lin28 secreted higher levels of PSA compared to the control tumors.

Figure 24: Lin28 enhances expression and activation of the AR. **A)** Left panel, LN-Lin28 and LN-neo cells were transfected with pGL4-AR-Prom-Luc and luciferase activities were measured.

Activity of the full length promoter of AR was increased in Lin28-expressing cells. Right panel, qRT-PCR assays showing the increase in AR mRNA expression in Lin28-expressing LNCaP cells. **B)** Left panel, Western blot showing the increase in AR protein expression in LN-Lin28 cells compared to LN-neo cells. Right panel, C4-2B cells were transfected with shRNA against Lin28 and protein expression of AR was analyzed. Downregulation of Lin28 by shRNA reduced the expression of AR. **C)** Expression levels of AR target genes PSA and NKX3.1 were measured by qRT-PCR in LN-neo and LN-Lin28 cells. mRNA levels of both genes were increased in Lin28-expressing cells compared to control cells. **D)** Left panel, LN-Lin28 and LN-neo cells were transfected with PSA-E/P-Luc and luciferase activities were measured. Activation of PSA promoter was enhanced in Lin28-expressing cells compared to control cells. Right panel, secretion of PSA by LN-Lin28 and LN-neo cells was measured by ELISA. Levels of PSA secreted by Lin28-expressing cells were higher than control cells. Data are presented as mean±SD of 3 experiments performed in triplicate. **E)** Recruitment of AR to the ARE I/II and ARE III regions of PSA promoter (left panel) and ARE in NKX3.1 promoter (right panel) was analyzed by ChIP assays. Expression of Lin28 enhanced recruitment of AR to AREs in target gene promoters.

Figure 25: Lin28 induces resistance to AR-targeted therapeutics. **A)** LN-Lin28 and LN-neo control cells were treated with 0, 20 or 40 μM concentrations of enzalutamide, abiraterone or bicalutamide for 24 h and cell survival was analyzed. LN-Lin28 cells were not significantly affected by treatment while cell survival of LN-neo control cells was diminished by treatment. **B)** Western blot showing expression of Lin28 in lysates from cells treated with enzalutamide, abiraterone or bicalutamide. **C)** Anchorage-dependent clonogenic assay was performed using LN-Lin28 and LN-neo cells treated with enzalutamide, abiraterone or bicalutamide. Representative images from 3 independent experiments are shown. **D)** Numbers of colonies formed by LN-Lin28 and LN-neo cells were counted. Numbers of colonies formed by LN-neo cells were reduced by ~50% while numbers of colonies formed by LN-Lin28 cells were not reduced significantly. **E)** Anchorage-independent soft agar colony formation assays were performed using LN-Lin28 and LN-neo cells treated with enzalutamide, abiraterone or bicalutamide. Representative images from 3 independent experiments are shown. **F)** Numbers of colonies formed by LN-Lin28 and LN-neo cells in soft agar were counted. Numbers of colonies formed by LN-neo cells were reduced drastically, while numbers of colonies formed by LN-Lin28 cells were not reduced significantly. Results are presented as means ± SD of 3 experiments performed in triplicate.

Figure 26: Lin28 expressing cells maintain activation of the AR during treatment with enzalutamide, abiraterone or bicalutamide. **A)** Nuclear translocation of the AR was examined by Western blotting using specific antibodies against AR in LN-neo and LN-Lin28 cells treated with enzalutamide, abiraterone or bicalutamide. AR nuclear translocation was inhibited by the drugs in LN-neo cells, while nuclear translocation of AR was not affected in LN-Lin28 cells. **B)** Recruitment of the AR to AREs in PSA promoter was analyzed by ChIP assays in LN-neo and LN-Lin28 cells treated with enzalutamide, abiraterone or bicalutamide. Recruitment of AR to ARE in PSA promoter was not affected significantly in LN-Lin28 cells by treatment. Expression levels of classic AR target genes, PSA **(C)** and NKX3.1 **(D)** were examined by qPCR in LN-neo and LN-Lin28 cells treated with enzalutamide, abiraterone or bicalutamide. AR-activated expression of PSA and NKX3.1 was not affected significantly in LN-Lin28 cells. **E)** Secretion of

PSA by LN-Lin28 and LN-neo cells treated with enzalutamide, abiraterone or bicalutamide was analyzed by ELISA. Treatment with the drugs diminished secretion of PSA by LN-neo cells while PSA secretion was not affected in LN-Lin28 cells. Results are presented as means ± SD of 3 experiments performed in triplicate.

Figure 27: Alternative splicing of AR mediates resistance to AR-targeted therapeutics in Lin28 expressing cells. **A)** Relative mRNA levels of full length (FL) AR and AR-V7 were measured using qPCR in LN-neo and LN-Lin28 cells. LN-Lin28 cells express significantly higher levels of both FL AR and AR-V7. **B)** LN-Lin28 cells express higher levels of hnRNPA1 compared to LN-neo cells as analyzed by Western blotting. **C)** LN-neo and LN-Lin28 cells were treated with enzalutamide after transfection with siRNAs against either FL AR or AR-V7. Downregulation of either FL AR or AR-V7 resensitizes LN-Lin28 cells to treatment with enzalutamide. **D)** Specific siRNAs against hnRNPA1 or hnRNPA2 were transfected into LN-neo and LN-Lin28 cells which were subsequently subjected to treatment with enzalutamide, abiraterone or bicalutamide. Downregulation of either hnRNPA1 or hnRNPA2 enhanced the sensitivity of LN-Lin28 cells to treatment. Results are presented as means ± SD of 3 experiments performed in triplicate. **E)** Whole cell lysates from LN-neo and LN-Lin28 cells transfected with siRNAs against hnRNPA1 or hnRNPA2 were analyzed by Western blotting to assess levels of AR-V7. Downregulation of hnRNPA1 reduced expression levels of AR-V7. **F)** LN-neo and LN-Lin28 cells were transfected with plasmids encoding full length hnRNPA1 cDNA and the resultant lysates were analyzed by Western blotting for the expression of AR-V7. Overexpression of hnRNPA1 enhanced expression of AR-V7.

Figure 28: Lin28 mediates enzalutamide resistance in p52-expressing PCa cells. **A)** Specific shRNAs against Lin28 were transfected into LN-neo and LN-p52 cells in media containing either complete or charcoal-stripped (CS) FBS. The cells were then treated with 20 μM enzalutamide. Downregulation of Lin28 reduced the ability of LN-p52 cells to survive in media containing enzalutamide. Right panel confirms reduction in mRNA levels of Lin28 after transfection with shRNA. **B-G)** Expression levels of AR splice variants were examined by qPCR in total RNAs extracted from LN-neo and LN-p52 cells transfected with shRNAs against Lin28. Expression levels of most AR splice variants were reduced upon downregulation of Lin28. Results are presented as means ± SD of 3 experiments performed in triplicate.

Figure 29: NF-kB2/p52-expressing CaP cells are resistant to Enzalutamide. **A)** LNCaP cells stably expressing p52 (LN-p52) and control LNCaP cells (LN-neo) were treated with 0 and 20 μM Enzalutamide or Bicalutamide in media containing either FBS or CS-FBS and cell numbers were counted after 48 h. Results are presented as means±SD of 3 experiments performed in triplicate. LN-p52 cells exhibited higher survival rates when treated with Enzalutamide or Bicalutamide compared to LN-neo cells. **B)** LN-neo and LN-p52 cells were treated with 0, 20 or 40 μM Enzalutamide or Bicalutamide and clonogenic assays were performed. Results are presented as means±SD of 2 experiments performed in triplicate. LN-p52 cells formed higher numbers of colonies compared to LN-neo cells when treated with Enzalutamide or Bicalutamide.

Figure 30: CaP cells treated chronically with Enzalutamide upregulate the expression of NF-kB2/p52. **A)** CWR22Rv1 cells treated chronically with Enzalutamide exhibit higher endogenous levels of both p100 and p52. **B)** CWR22Rv1 cells treated chronically with Enzalutamide were

transfected with either control shRNA or shRNA against NF-kB2/p52 and were treated with 0, 20 or 40 μM Enzalutamide. Cell numbers were counted after 24 and 48 h. Results are presented as means±SD of 2 experiments performed in triplicate. * denotes $P \leq 0.05$. Cells transfected with shRNA against p52 exhibited lower cell survival when treated with Enzalutamide.

Figure 31: NF-kB2/p52 induces higher expression of AR splice variants. Total RNAs from LNCaP **(A)** and C4-2B **(B)** cells transfected with empty vector or p52 were analyzed by qRT-PCR for the expression of FL AR and AR-V7 in media containing either FBS or CS-FBS. Expression of p52 enhanced the levels of AR-V7 while levels of FL AR remained unchanged. *Right panels*, immunoblotting of above lysates with antibodies specific against either FL AR or AR-V7. **C)** Total RNAs from LN-p52 and LN-neo cells were analyzed by qRT-PCR for the expression levels of FL AR or AR-V7. LN-p52 cells showed higher levels of expression of AR-V7 compared to LN-neo cells, while FL AR levels were unaffected. *Right panel*, immunoblotting of above lysates with antibodies against FL AR or AR-V7. Results are presented as means±SD of 2 experiments performed in triplicate. * denotes $P \leq 0.05$.

Figure 32: Downregulation of NF-kB2/p52 in CaP cells reduces expression of AR splice variants. VCaP **(A)** and CWR22Rv1 **(B)** cells were transfected with either control shRNA or shRNA against p52 and expression levels of the indicated AR splice variants were analyzed by qRT-PCR. Downregulation of p52 led to a decrease in synthesis of AR splice variants while expression levels of FL AR remained unchanged. Right panels show immunoblots of above lysates with antibodies against FL AR or AR-V7. Results are presented as means±SD of 3 experiments performed in triplicate. * denotes $P \leq 0.05$.

Figure 33: Downregulation of FL AR and AR-V7 increase sensitivity of p52-expressing CaP cells to Enzalutamide. **A)** LN-p52 and LN-neo cells were transfected with siRNAs specific to either FL AR or AR-V7 and were treated with 0 or 20 μM Enzalutamide. Cell numbers were counted after 48 h. Results are presented as means±SD of 3 experiments performed in triplicate. Downregulation of either FL AR or AR-V7 increased sensitivity of LN-p52 cells to Enzalutamide. VCaP **(B)** and CWR22Rv1 **(C)** cells were transfected with PSA-E/P-Luc reporter, empty vector or p52 together with siRNAs against FL AR or AR-V7. Cells were treated with 0 or 40 μM Enzalutamide and luciferase assays were performed after 48 h. Results are presented as means±SD of 2 experiments performed in triplicate. * denotes $P \leq 0.05$. Downregulation of either FL AR or AR-V7 suppressed p52-induced activation of AR in both VCaP and CWR22Rv1 cells.

Figure 34: HnRNPA1 promotes generation of AR splice variants. **A)** 22Rv1 and **B)** VCaP cells were transfected with specific siRNAs against hnRNPA1 or hnRNPA2 and the total RNAs were subjected to real-time qPCR analysis to determine the expression levels of AR splice variants. Downregulation of hnRNPA1 suppressed expression of most AR splice variants. Results are presented as means ± SD of 3 experiments performed in triplicate. **C)** Whole cell extracts from 22Rv1 and VCaP cells transfected with siRNAs against hnRNPA1 or hnRNPA2 were subjected to Western analysis with indicated antibodies. Downregulation of hnRNPA1 suppressed protein expression levels of AR-V7 specifically. Results are presented as representative images from 3 experiments performed in duplicate. **D)** LNCaP cells were transfected with plasmids encoding hnRNPA1 and the resulting whole cell extracts were subjected to Western blotting with the indicated antibodies. Overexpression of hnRNPA1 enhanced protein levels of AR-V7 in LNCaP

cells which express undetectable levels of AR-V7 protein. Results are presented as representative images from 3 experiments. **E)** Total RNAs from LNCaP cells transfected with plasmids encoding hnRNPA1 were subjected to qPCR analysis to determine the levels of AR splice variants. Overexpression of hnRNPA1 enhanced expression of most AR splice variants. Results are presented as means ± SD of 3 experiments performed in triplicate. * denotes $p \leq 0.05$.

Figure 35: Association between hnRNPA1 and AR-V7 is enhanced in enzalutamide-resistant PCa cells. **A)** 22Rv1 vs. 22Rv1-Enza-R and **C)** C4-2B vs. C4-2B-Enza-R cells were analyzed by RNA Immunoprecipitation (RIP) assays to determine the degree of association between hnRNPA1 protein and AR-V7 mRNA. Higher levels of AR-V7 mRNAs were associated with hnRNPA1 protein in both 22Rv1 and C4-2B cells resistant to enzalutamide. **B)** 22Rv1 vs. 22Rv1-Enza-R and **D)** C4-2B vs. C4-2B-Enza-R cells were analyzed by RIP assays to determine the association between hnRNPA1 and full length AR mRNA. No significant differences were observed in association between hnRNPA1 and FL AR mRNA. Results are presented as means ± SD of 2 experiments performed in duplicate. * denotes $p \leq 0.05$.

Figure 36: Expression levels of hnRNPA1 and AR-V7 are positively correlated with each other. **A)** Whole cell lysates from 27 paired benign and tumor patient samples were analyzed by Western blotting to examine the expression levels of hnRNPA1, hnRNPA2 and AR-V7. A representative immunoblot is shown. **B)** Table showing the summary of results from the western analysis of 27 paired benign and tumor clinical prostate samples. Expression levels of hnRNPA1, AR-V7 and hnRNPA2 were higher in tumor tissues in 44%, 48% and 44% of the samples respectively. qRT-PCR of mRNA levels of hnRNPA1 **(C)** and AR-V7 **(D)** in 10 paired normal and tumor clinical prostate samples. Expression levels of hnRNPA1 and AR-V7 were higher in tumor tissues compared to normal counterparts and were positively correlated with each other. Results are presented as means ± SD of 2 experiments performed in triplicate. * denotes $p \leq 0.05$. Relative expression levels of hnRNPA1 **(E)** and hnRNPA2 **(F)** in a GEO dataset were analyzed. Expression levels of both proteins increased progressively from primary PCa to metastatic PCa compared to benign prostate tissue. Relative expression levels of hnRNPA1 **(G)** and hnRNPA2 **(H)** were analyzed in the Singh_prostate (n=102) dataset using Oncomine database. Expression levels of both proteins were higher in PCa compared to normal prostate tissue.

Figure 37: Reciprocal regulation between c-Myc and hnRNPA1 is responsible for the generation of AR splice variants. **A)** Expression levels of hnRNPA1 and AR-V7 were analyzed by immunoblotting in 22Rv1 and VCaP cells transfected with shRNAs against c-Myc. Downregulation of c-Myc expression resulted in downregulation of AR-V7 and hnRNPA1 expression. Results are shown as representative images from 2 experiments performed in duplicate. **B)** Expression of c-Myc was analyzed by Western blotting in LNCaP, 22Rv1 and VCaP cells transfected with siRNAs against either hnRNPA1 or hnRNPA2. Protein levels of c-Myc were downregulated when hnRNPA1 expression was suppressed in all cell lines tested. Results are shown as representative images from 2 experiments performed in duplicate. mRNA levels of full length AR and AR splice variants were analyzed by qRT-PCR in 22Rv1 **(C)** and VCaP **(D)** cells transfected with shRNA against c-Myc. Downregulation of c-Myc resulted in suppression of AR splice variant expression in both cell lines which express AR splice variants endogenously. Insets show the relative expression of c-Myc mRNA in cells transfected with

control shRNA or shRNA against c-Myc. Results are presented as means ± SD of 2 experiments performed in triplicate. * denotes $p \leq 0.05$.

Figure 38: NF-kB2/p52 regulates expression of c-Myc and hnRNPA1. **A)** *Left panel*, Western analysis showed that LNCaP cells stably expressing p52 (LN-p52) express higher levels of hnRNPA1, c-Myc and AR-V7. *Right panel*, Induction of p52 expression by doxycycline (DOX) in LNCaP cells expressing p52 under the control of a tetracycline-inducible promoter (LN/TR/p52) induced the expression of hnRNPA1, c-Myc and AR-V7. **B)** *Left panel*, Western blotting revealed that downregulation of hnRNPA1 using siRNA abolished the protein levels of AR-V7 in LN-p52 cells. *Middle panel*, Downregulation of c-Myc using shRNA abolished the expression of AR-V7 and hnRNPA1 in LN-p52 cells. *Right panel*, Downregulation of p52 using shRNA suppressed expression of AR-V7, hnRNPA1 and c-Myc in 22Rv1 cells which express endogenous levels of p52. **C)** *Left panel*, 22Rv1 cells resistant to enzalutamide (22Rv1-Enza-R) express higher levels of AR-V7, hnRNPA1, c-Myc and NF-kB2/p52. *Middle panel*, C4-2B cells resistant to enzalutamide (C4-2B-Enza-R) also express higher levels of hnRNPA1, AR-V7, c-Myc and NF-kB2/p52. *Right panel*, Xenografts generated from C4-2B-Enza-R cells also exhibit higher levels of AR-V7, hnRNPA1 and c-Myc. **D)** *Left panel*, Downregulation of hnRNPA1 using siRNA abolished the expression of AR-V7 in 22Rv1-Enza-R cells. *Right panel*, Downregulation of c-Myc using shRNA abolished the expression of AR-V7 and hnRNPA1 in 22Rv1-Enza-R cells. All results are shown as representative images from 2 experiments performed in duplicate. **E)** *Left panel*, Chart depicting the positive correlation between relative mRNA levels of NF-kB2/p52, c-Myc, hnRNPA1 and AR-V7 in 10 paired benign and tumor prostate clinical samples from Fig. 3B. *Right panel*, Chart depicting the correlation between relative protein levels of NF-kB2/p52, c-Myc, hnRNPA1 and AR-V7 in 27 paired benign and tumor prostate clinical samples from Fig. 3A. Band intensities in immunoblots were quantified using ImageJ software and plotted as arbitrary units output by ImageJ.

Figure 39: Suppression of hnRNPA1 restores enzalutamide sensitivity of enzalutamide-resistant prostate cancer cells. **A)** *Left panel*, 22Rv1-Enza-R cells were transfected with siRNAs against either hnRNPA1 or hnRNPA2 and subjected to treatment with vehicle or 20 μM enzalutamide. Cell numbers were counted after 48 h. Downregulation of hnRNPA1 resensitized 22Rv1-Enza-R cells to enzalutamide. *Right panel*, immunoblots confirm the downregulation of hnRNPA1 or hnRNPA2 and of AR-V7. **B)** *Left panel*, LN-p52 cells (resistant to enzalutamide) were transfected with siRNAs against either hnRNPA1 or hnRNPA2 and subjected to treatment with vehicle or 20 μM enzalutamide. Cell numbers were counted after 48 h. Downregulation of hnRNPA1 resensitized LN-p52 cells to enzalutamide. *Right panel*, immunoblots confirm the downregulation of hnRNPA1 or hnRNPA2 and of AR-V7. **C)** *Left panel*, VCaP cells (resistant to enzalutamide) were transfected with siRNAs against either hnRNPA1 or hnRNPA2 and subjected to treatment with vehicle or 20 μM enzalutamide. Cell numbers were counted after 48 h. Downregulation of hnRNPA1 resensitized VCaP cells to enzalutamide. Results are presented as means ± SD of 3 experiments performed in triplicate. * denotes $p \leq 0.05$. *Right panel*, immunoblots confirm the downregulation of hnRNPA1 or hnRNPA2 and of AR-V7. **D)** Pictorial representation of role of the NF-kB2/p52:c-Myc:hnRNPA1:AR-V7 axis in castration and drug resistance in PCa.

Figure 40: Suppression of steroidogenic enzymes reduces intracrine androgen levels in p52-expressing cells. Levels of intracellular testosterone **(A)** and dihydrotestosterone **(B)** were measured by LC-MS analysis in LN-p52 cells stably expressing shRNAs against either AKR1C3 or CYP17A1. Intracellular testosterone as well as dihydrotestosterone levels were reduced significantly in LN-p52-shAKR1C3 and LN-p52-shCYP17A1 cells compared to control LN-p52-shEGFP cells. **C)** Levels of intracellular testosterone were measured by LC-MS analysis in LNCaP cells stably overexpressing AKR1C3. LNCaP-AKR1C3 cells synthesized higher levels of testosterone compared to control LNCaP-Empty Vector cells.

Figure 41: Steroidogenic enzymes modulate castration-resistant growth of CaP cells. **A)** LN-p52-shEGFP, LN-p52-shAKR1C3 and LN-p52-shCYP17A1 cells were subjected to growth in media containing CS-FBS and cell numbers were monitored at 0, 24, 48 and 72 h. Downregulation of either AKR1C3 or CYP17A1 by shRNA diminished the ability of LN-p52 cells to survive in androgen-depleted media. **B)** LNCaP-neo control and LNCaP-AKR1C3 cells were subjected to growth in media containing CS-FBS and cell numbers were monitored at 0, 24, 48 and 72 h. LNCaP cells stably overexpressing AKR1C3 exhibited higher survival and growth rate in androgen-depleted media.

Figure 42: Let-7c modulates castration-resistant growth of CaP cells. **A)** LN-p52 cells infected with lentiviruses encoding either empty vector or let-7c were subjected to growth in media containing CS-FBS and cell numbers were monitored at 0, 24, 48 and 72 h. LN-p52 cells infected with let-7c exhibited lower rates of survival in androgen depleted media. **B)** C4-2B cells stably expressing let-7c and C4-2B parental control cells were subjected to growth in androgen depleted media. Ability of castration resistant C4-2B cells to survive and grow in androgen-depleted media was diminished by overexpression of let-7c.

Supplementary Figure Legends

Supplementary Figure 1 (related to Fig. 35). Association of hnRNPA1 and hnRNPA2 with the minor AR splice variants AR-V1 (A), AR-V5 (B), AR-1/2/2b (C) and AR-1/2/3/2b (D) was analyzed after RNA immunoprecipitation assays by qRT-PCR in 22Rv1 and 22Rv1-Enza-R cells. Association of hnRNPA1 and hnRNPA2 with the minor AR splice variants AR-V1 (E), AR-V5 (F), AR-1/2/2b (G) and AR-1/2/3/2b (H) was analyzed after RNA immunoprecipitation assays by qRT-PCR in C4-2B and C4-2B-Enza-R cells. * denotes $p \leq 0.05$.

Supplementary Figure 2 (related to Fig. 36). A) Immunoblots showing relative expression levels of hnRNPA1, AR-V7 and hnRNPA2 in 27 paired benign and tumor clinical prostate samples. B) qRT-PCR analysis showing relative mRNA levels of hnRNPA2 in 10 paired benign and tumor clinical prostate samples. C) Summary of analyses of expression levels of hnRNPA1 and hnRNPA2 in 21 datasets from Oncomine. D) Relative expression levels of hnRNPA2 in GDS2545 and GDS1439 datasets from GEO.

Supplementary Figure 3 (related to Fig. 38). A) qRT-PCR showing the relative expression levels of full length AR and AR splice variants in LN-p52 cells transfected with siRNA against hnRNPA1. B) qRT-PCR showing the relative expression levels of full length AR and AR splice variants in LN-p52 cells transfected with shRNA against c-Myc. Inset shows the downregulation of c-Myc expression by shRNA.

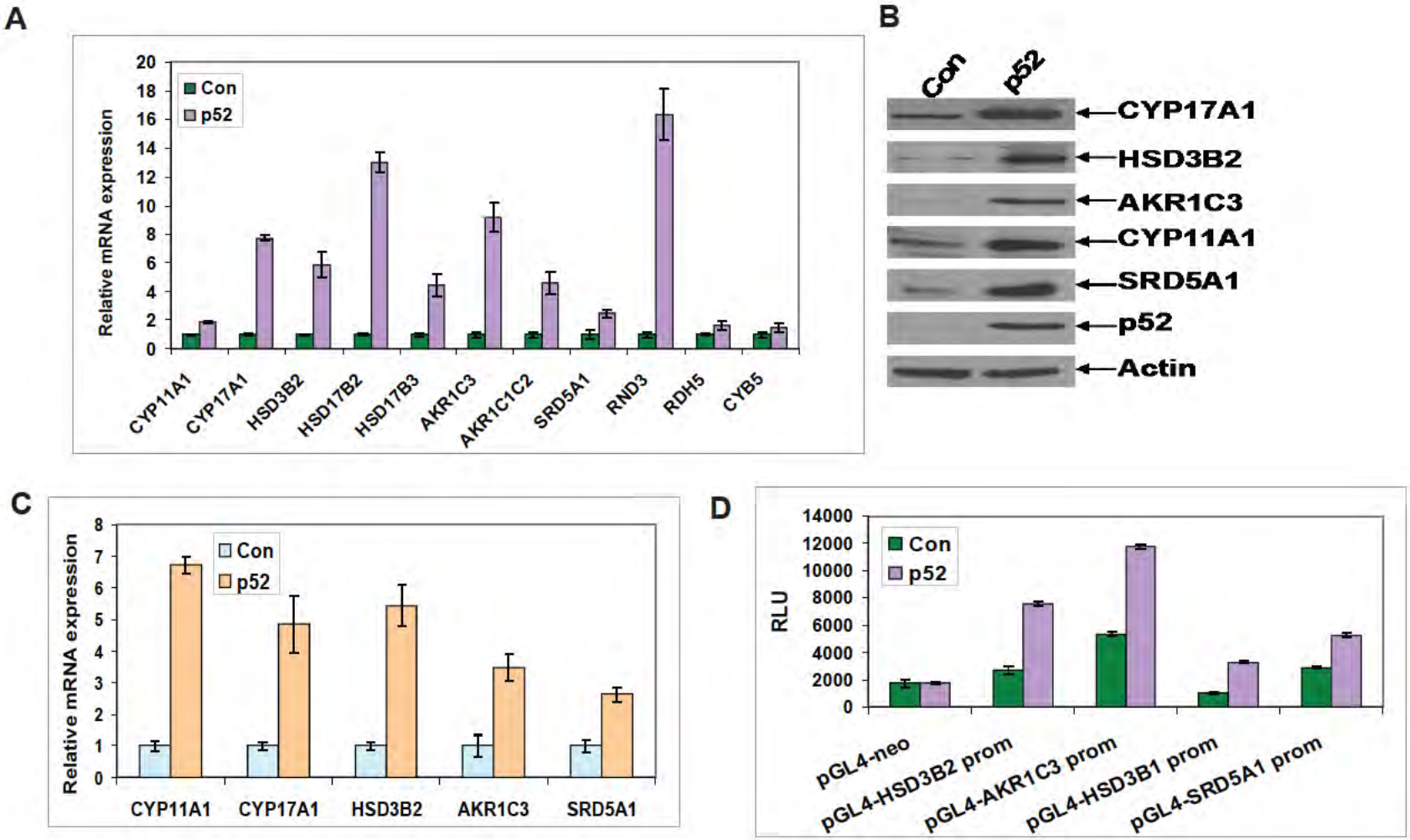
A
Relative mRNA expression
Con
p52
CYP11A1
CYP17A1
HSD3B2
HSD17B2
HSD17B3
AKR1C3
AKR1C1C2
SRD5A1
RND3
RDH5
CYB5
B
Con
p52
CYP17A1
HSD3B2
AKR1C3
CYP11A1
SRD5A1
p52
Actin
C
Relative mRNA expression
Con
p52
CYP11A1
CYP17A1
HSD3B2
AKR1C3
SRD5A1
D
RLU
Con
p52
pGL4-neo
pGL4-HSD3B2 prom
pGL4-AKR1C3 prom
pGL4-HSD3B1 prom
pGL4-SRD5A1 prom

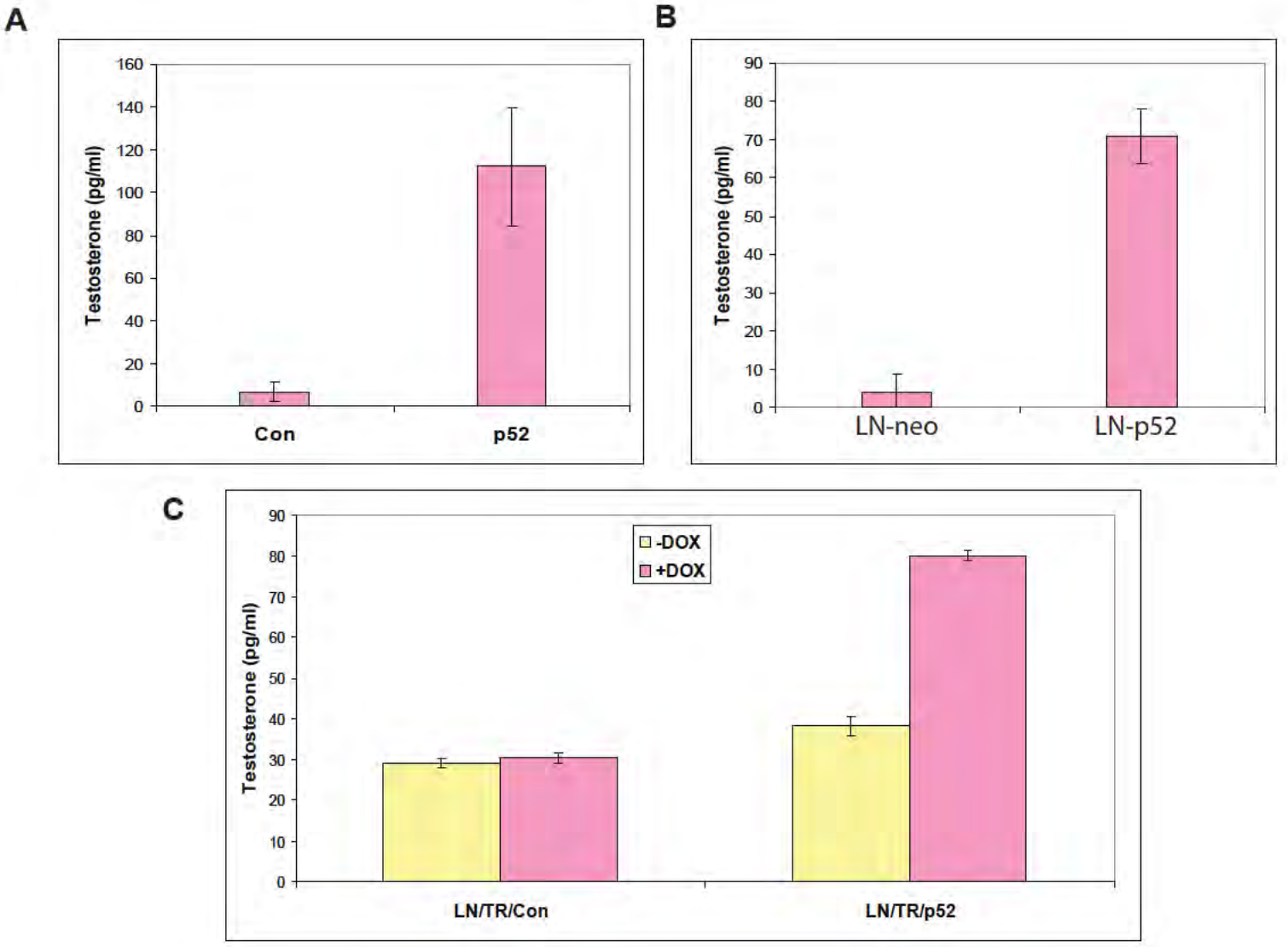
A
Testosterone (pg/ml)
160
140
120
100
80
60
40
20
0
Con
p52
B
Testosterone (pg/ml)
90
80
70
60
50
40
30
20
10
0
LN-neo
LN-p52
C
Testosterone (pg/ml)
90
80
70
60
50
40
30
20
10
0
-DOX
+DOX
LN/TR/Con
LN/TR/p52

FIGURE 3

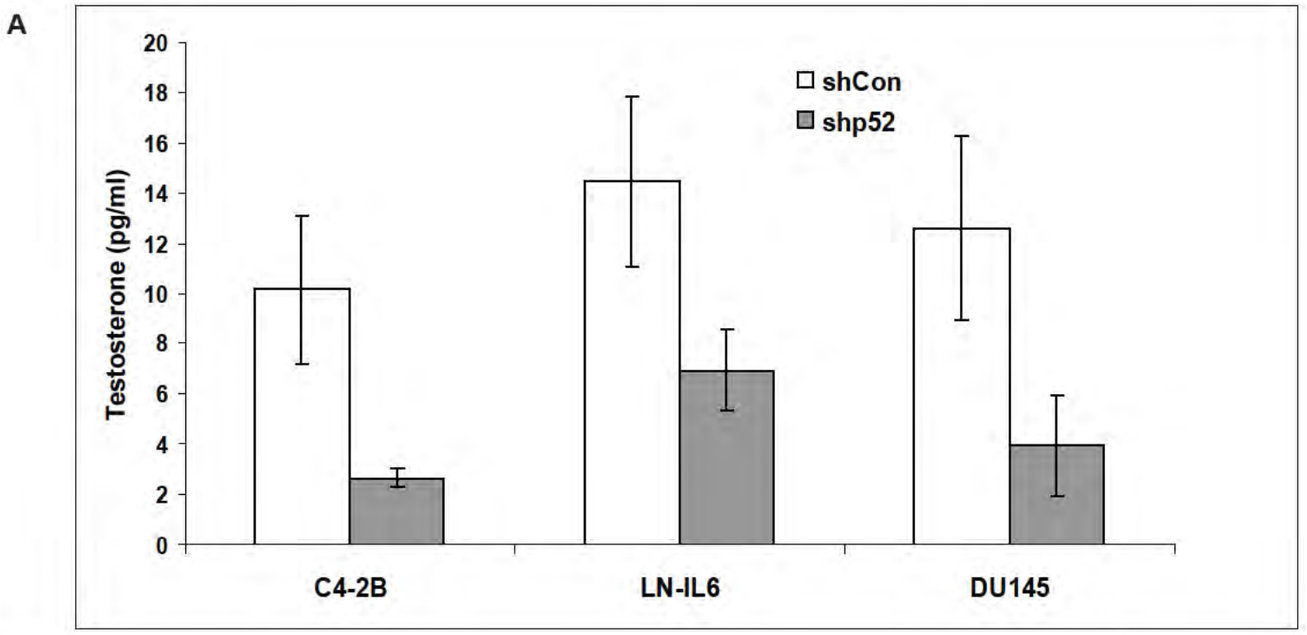
A
Testosterone (pg/ml)
shCon
shp52
C4-2B
LN-IL6
DU145

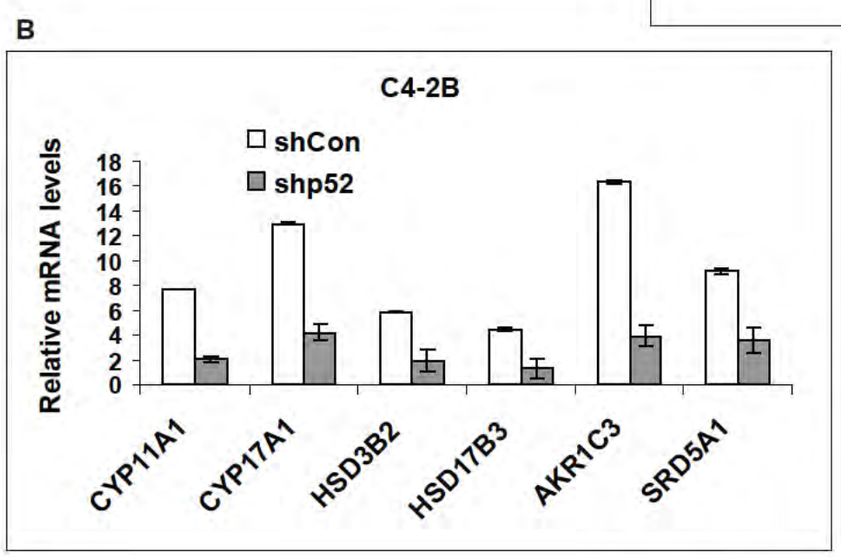
B
C4-2B
Relative mRNA levels
shCon
shp52
CYP11A1
CYP17A1
HSD3B2
HSD17B3
AKR1C3
SRD5A1

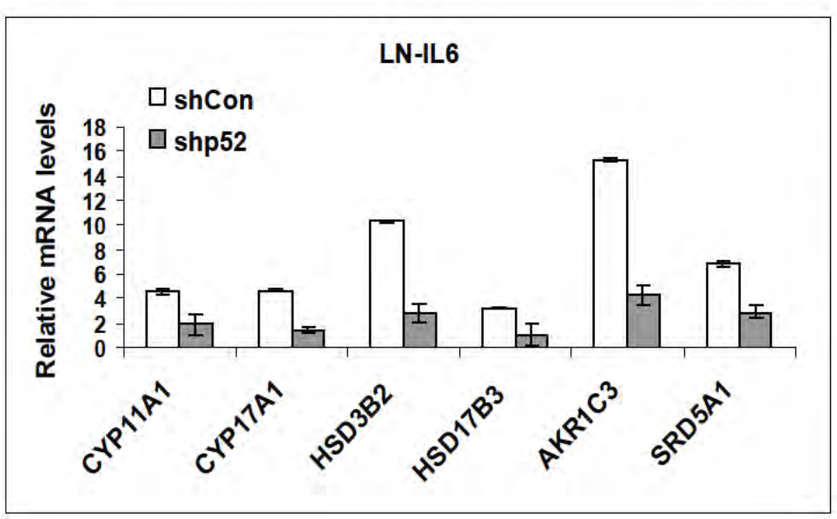
LN-IL6
Relative mRNA levels
shCon
shp52
CYP11A1
CYP17A1
HSD3B2
HSD17B3
AKR1C3
SRD5A1

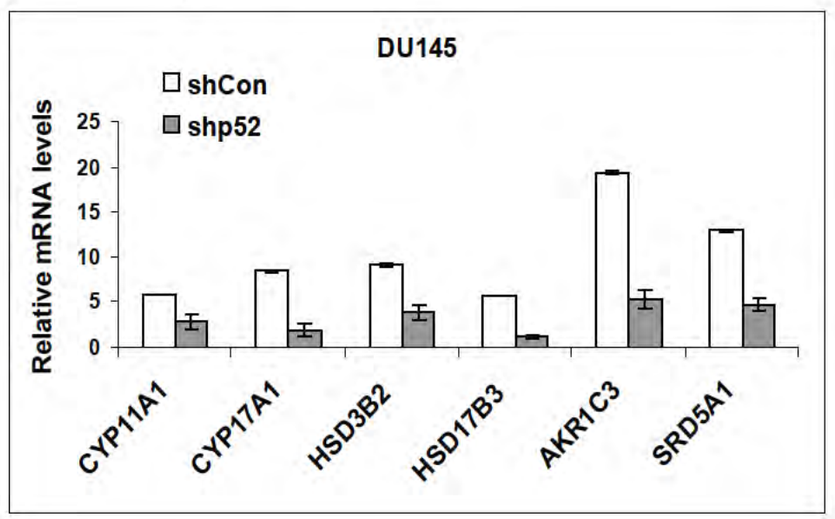
DU145
Relative mRNA levels
shCon
shp52
CYP11A1
CYP17A1
HSD3B2
HSD17B3
AKR1C3
SRD5A1

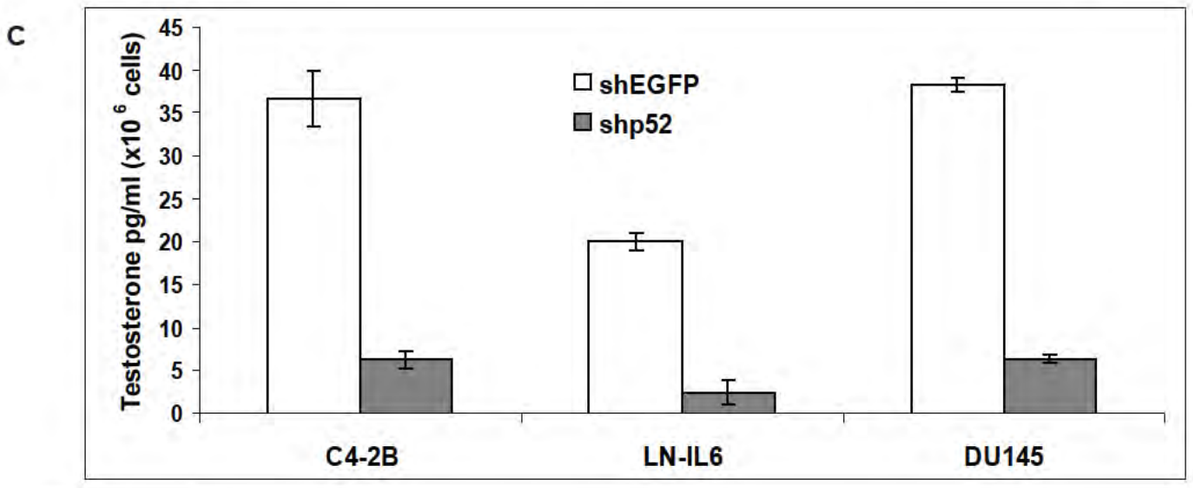
C
Testosterone pg/ml (x10 6 cells)
shEGFP
shp52
C4-2B
LN-IL6
DU145

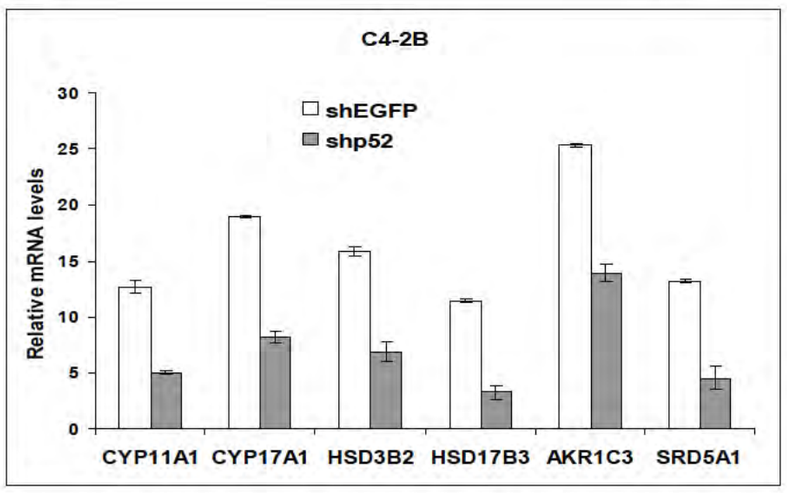
D
C4-2B
Relative mRNA levels
shEGFP
shp52
CYP11A1
CYP17A1
HSD3B2
HSD17B3
AKR1C3
SRD5A1

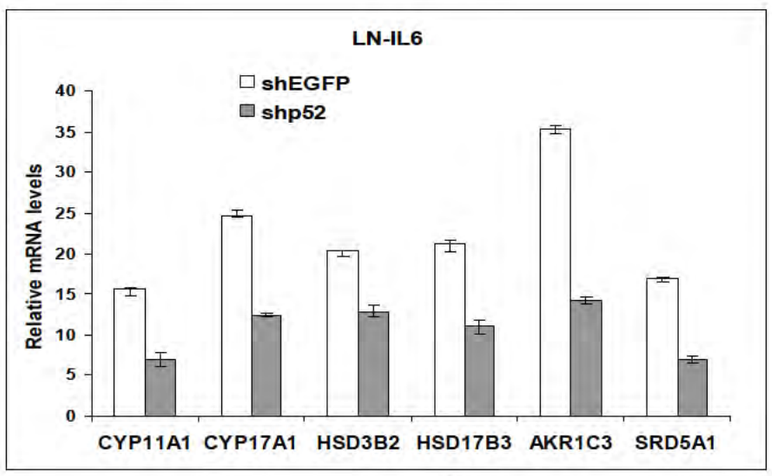
LN-IL6
Relative mRNA levels
shEGFP
shp52
CYP11A1
CYP17A1
HSD3B2
HSD17B3
AKR1C3
SRD5A1

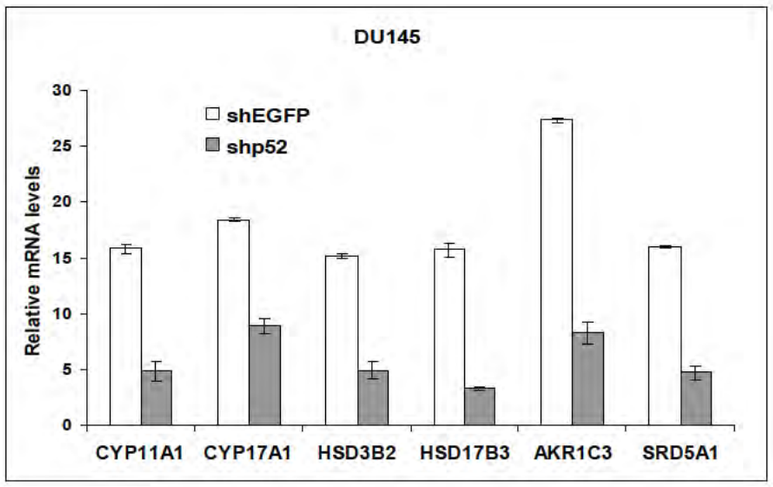
DU145
Relative mRNA levels
shEGFP
shp52
CYP11A1
CYP17A1
HSD3B2
HSD17B3
AKR1C3
SRD5A1

FIGURE 4

A

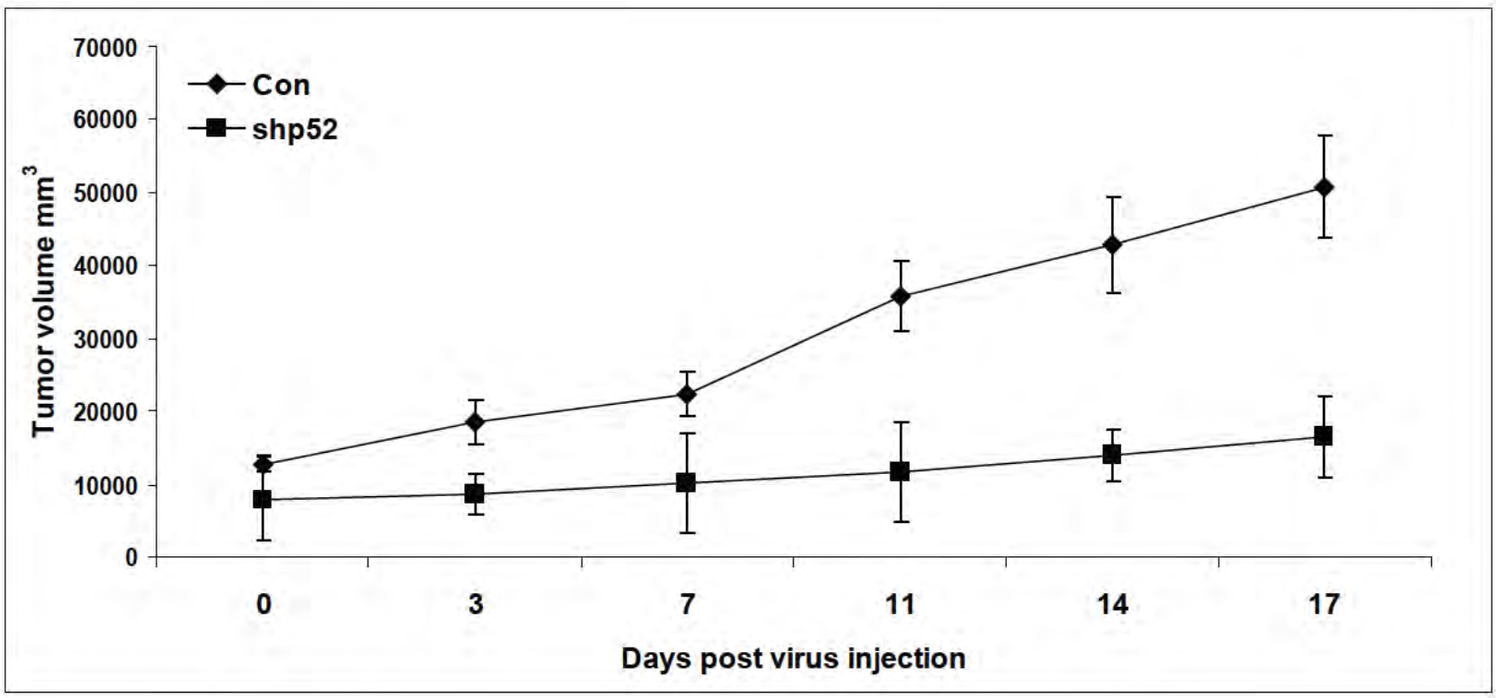
70000
60000
50000
40000
30000
20000
10000
0
Con
shp52
Tumor volume mm3
0
3
7
11
14
17
Days post virus injection

B

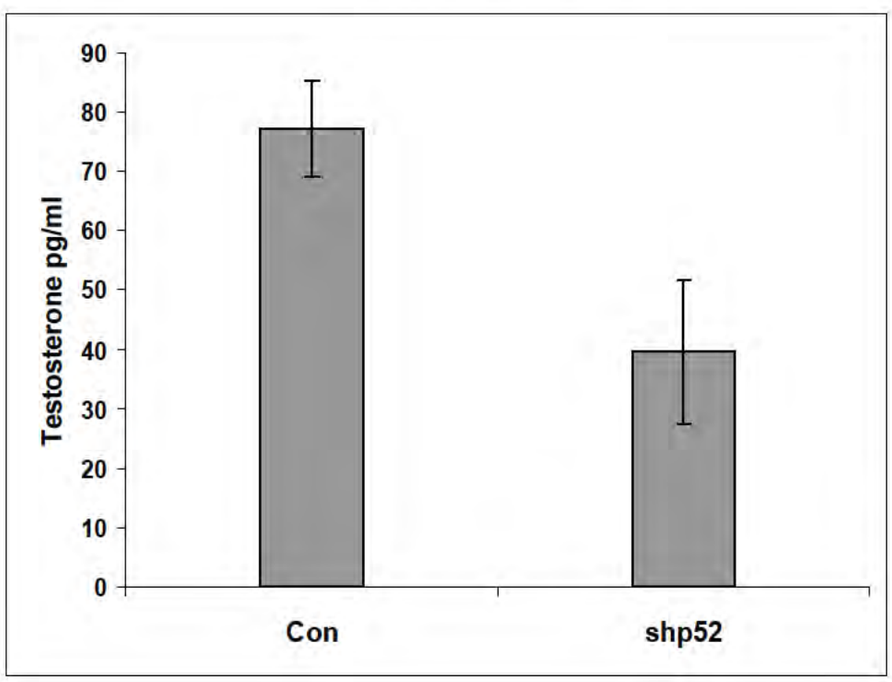
90
80
70
60
50
40
30
20
10
0
Testosterone pg/ml
Con
shp52

C

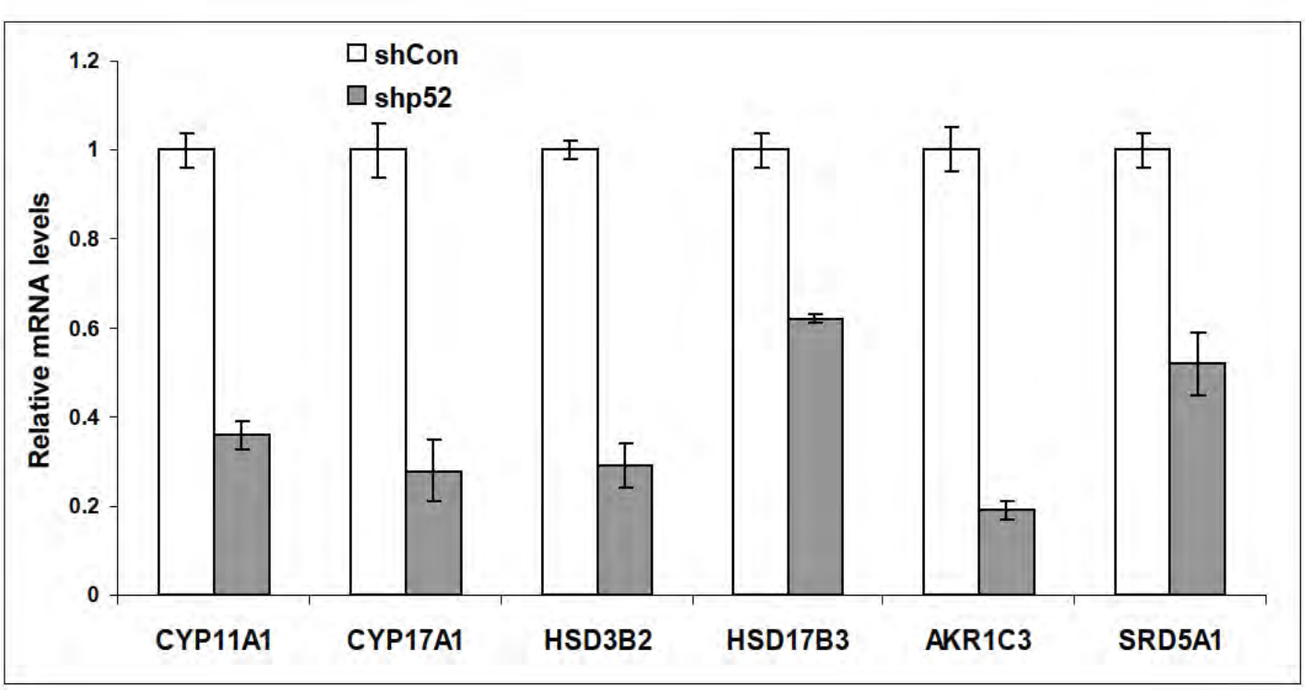
shCon
shp52
1.2
1
0.8
0.6
0.4
0.2
0
Relative mRNA levels
CYP11A1
CYP17A1
HSD3B2
HSD17B3
AKR1C3
SRD5A1

Figure 5

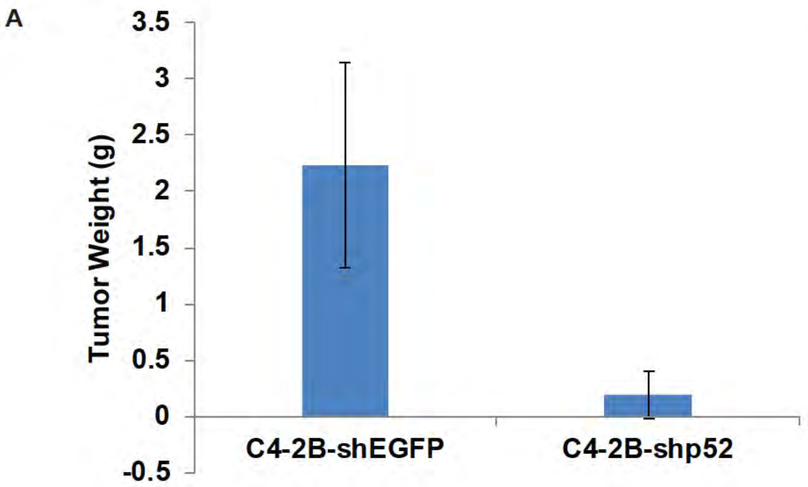
A
Tumor Weight (g)
3.5
3
2.5
2
1.5
1
0.5
0
-0.5
C4-2B-shEGFP
C4-2B-shp52

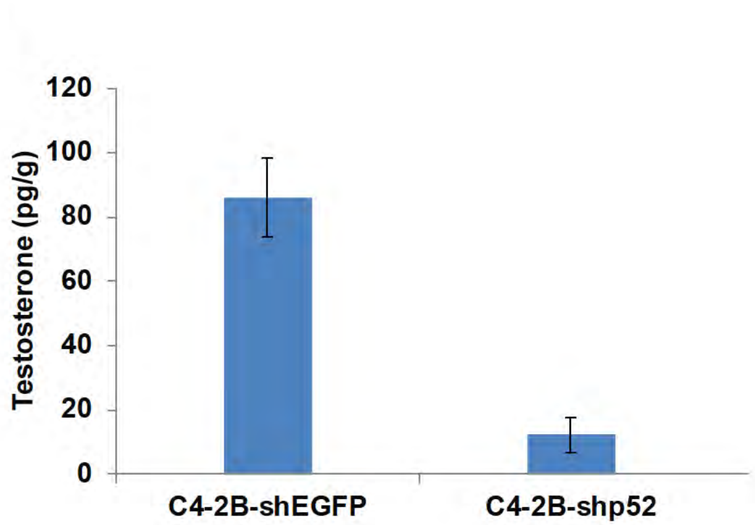
B
Testosterone (pg/g)
120
100
80
60
40
20
0
C4-2B-shEGFP
C4-2B-shp52

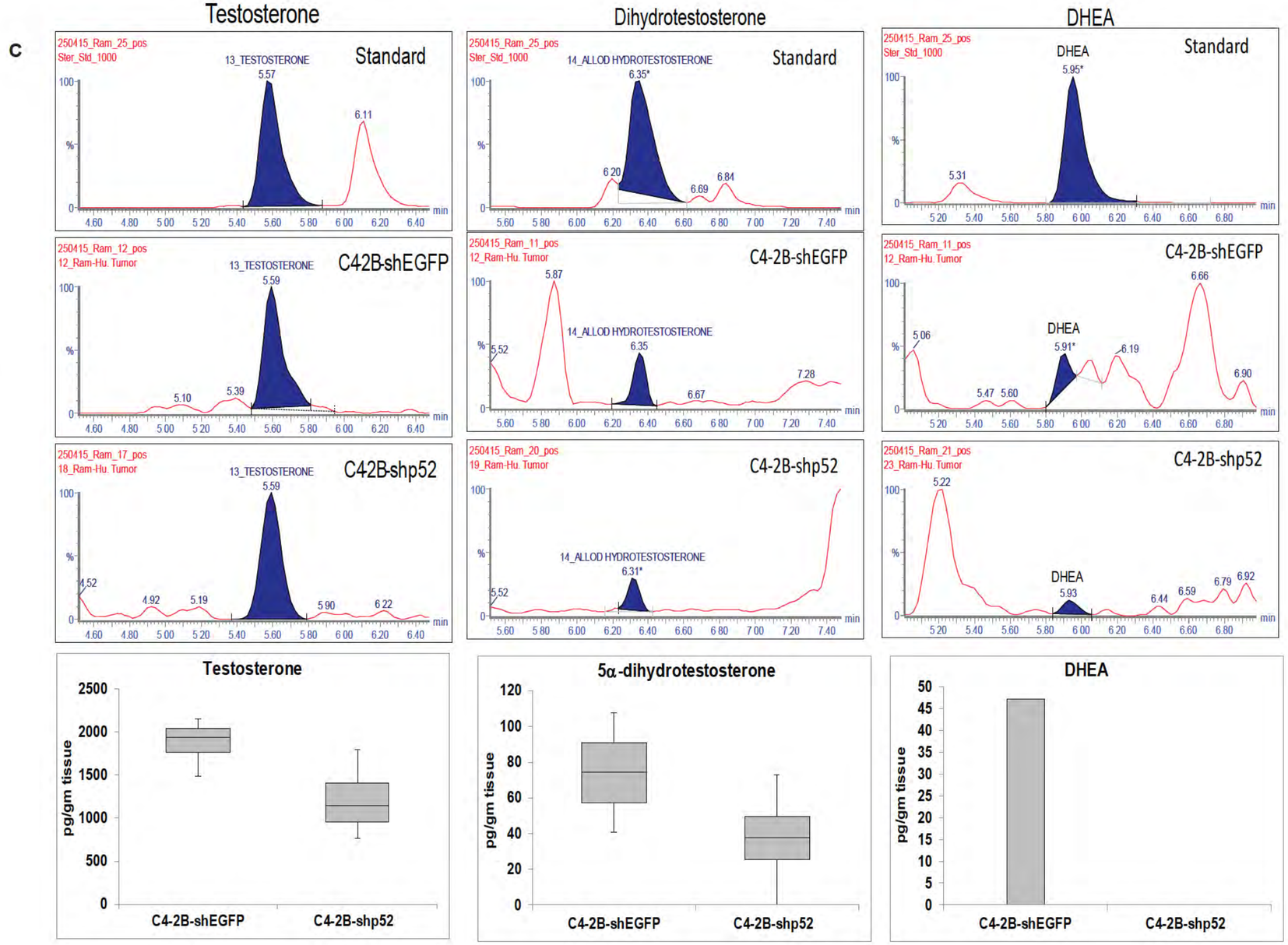
C
Testosterone
Dihydrotestosterone
DHEA
250415_Ram_25_pos
Ster_Std_1000
13_TESTOSTERONE
Standard
14_ALLOD HYDROTESTOSTERONE
DHEA
250415_Ram_12_pos
12_Ram-Hu. Tumor
C42B-shEGFP
C4-2B-shEGFP
250415_Ram_11_pos
250415_Ram_17_pos
18_Ram-Hu. Tumor
C42B-shp52
C4-2B-shp52
250415_Ram_20_pos
19_Ram-Hu. Tumor
250415_Ram_21_pos
23_Ram-Hu. Tumor
min

Testosterone
pg/gm tissue
2500
2000
1500
1000
500
0
C4-2B-shEGFP
C4-2B-shp52

5α-dihydrotestosterone
pg/gm tissue
120
100
80
60
40
20
0
C4-2B-shEGFP
C4-2B-shp52

DHEA
pg/gm tissue
50
45
40
35
30
25
20
15
10
5
0
C4-2B-shEGFP
C4-2B-shp52

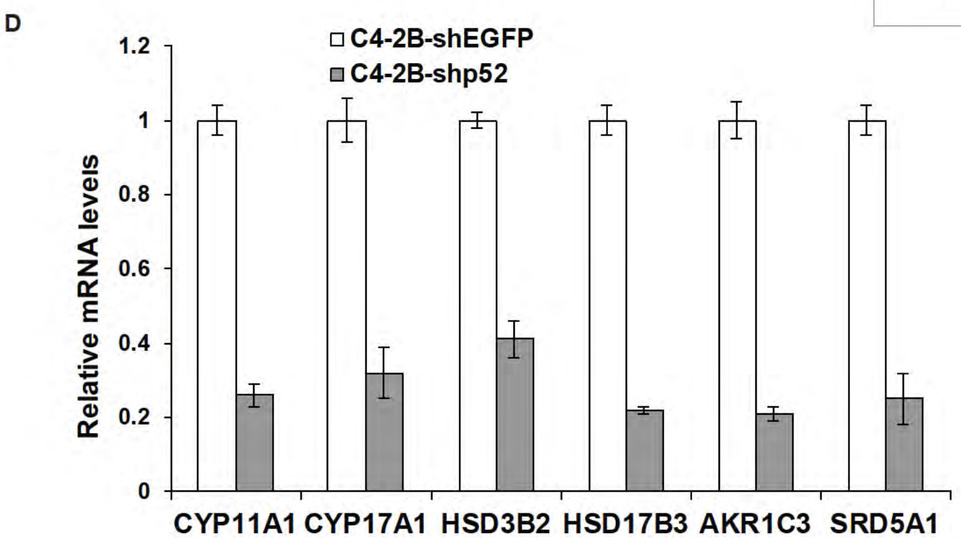
D
C4-2B-shEGFP
C4-2B-shp52
Relative mRNA levels
1.2
1
0.8
0.6
0.4
0.2
0
CYP11A1
CYP17A1
HSD3B2
HSD17B3
AKR1C3
SRD5A1

Figure 6

A

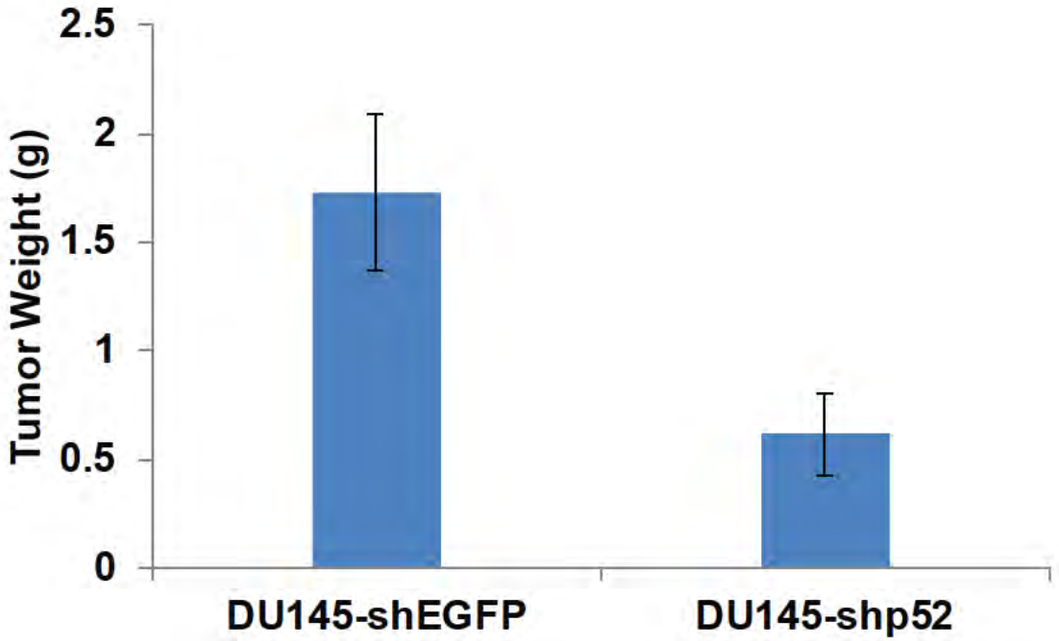
Tumor Weight (g)
2.5
2
1.5
1
0.5
0
DU145-shEGFP
DU145-shp52

B

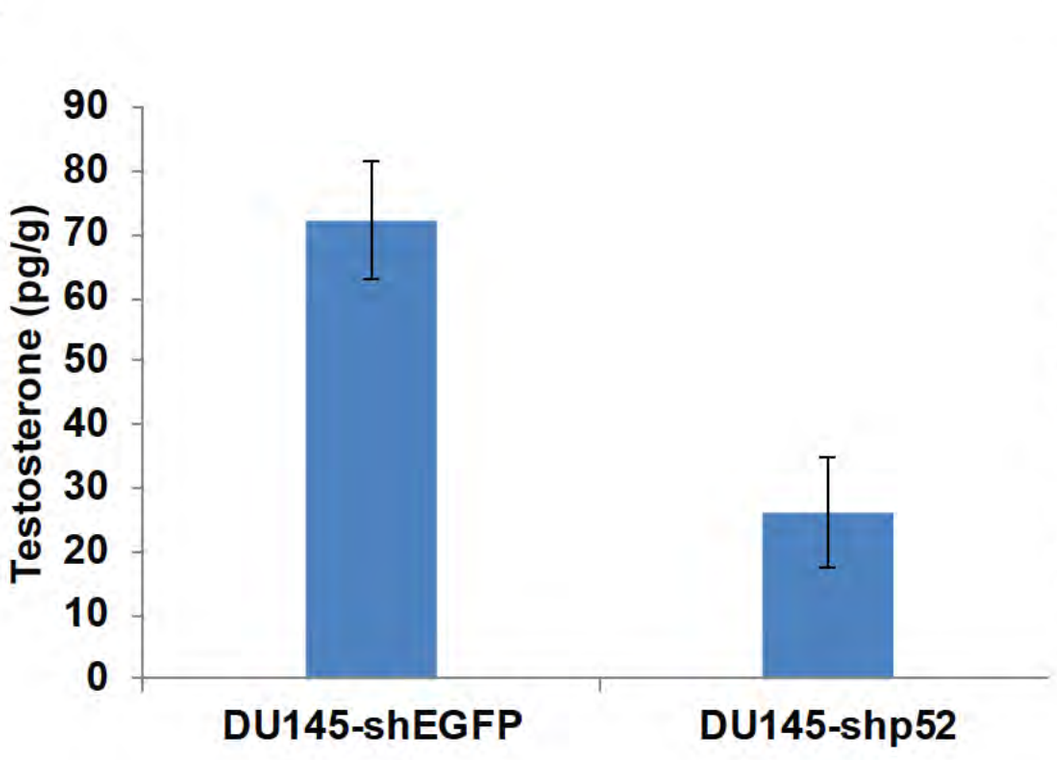
Testosterone (pg/g)
90
80
70
60
50
40
30
20
10
0
DU145-shEGFP
DU145-shp52

C

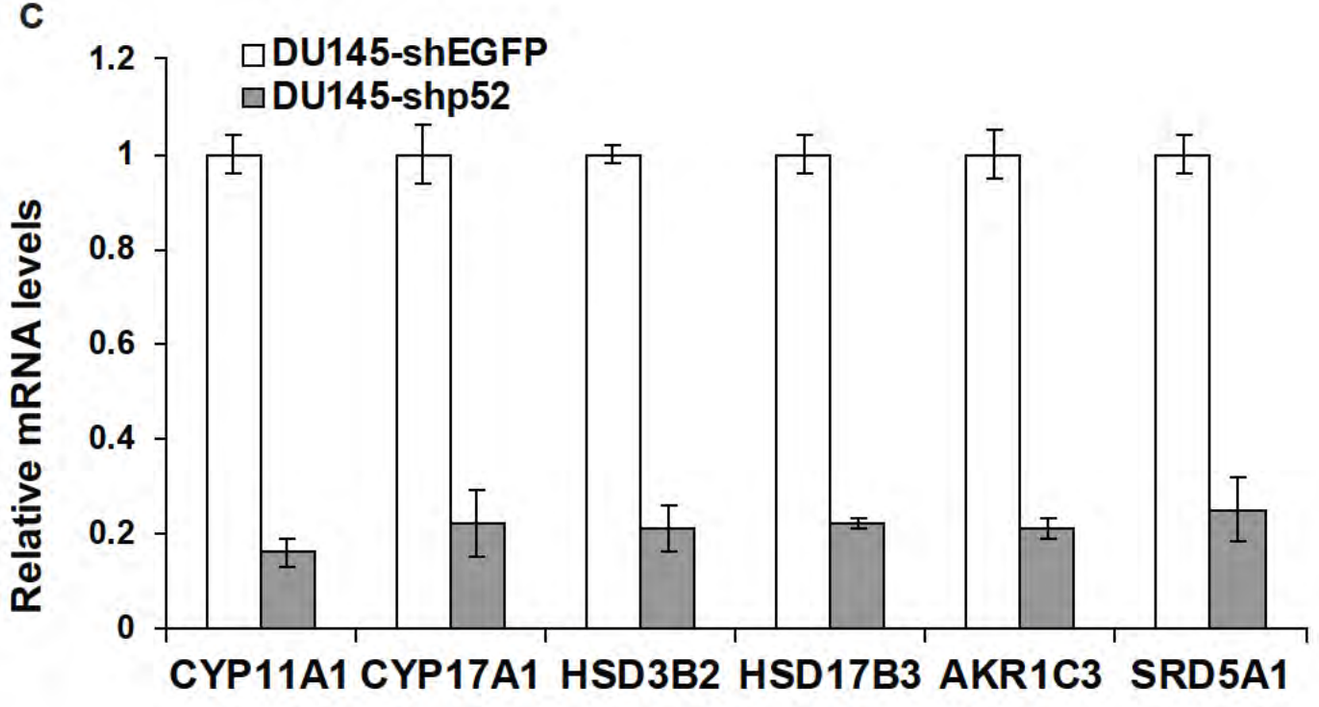
DU145-shEGFP
DU145-shp52
Relative mRNA levels
1.2
1
0.8
0.6
0.4
0.2
0
CYP11A1
CYP17A1
HSD3B2
HSD17B3
AKR1C3
SRD5A1

Figure 7

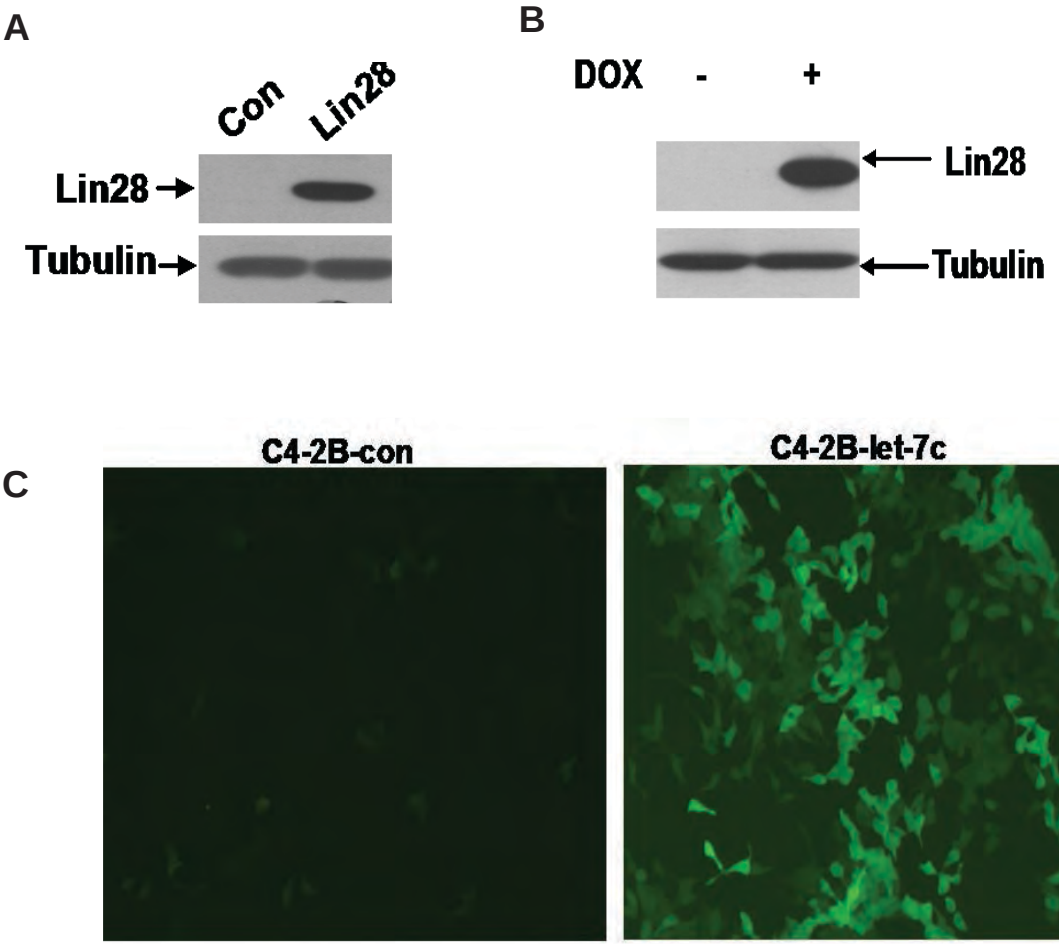
A
Con
Lin28
Lin28
Tubulin
B
DOX
-
+
Lin28
Tubulin
C
C4-2B-con
C4-2B-let-7c

FIGURE 8

A

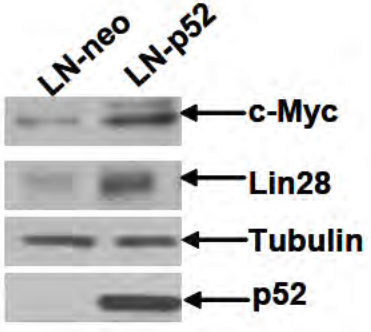
LN-neo
LN-p52
c-Myc
Lin28
Tubulin
p52

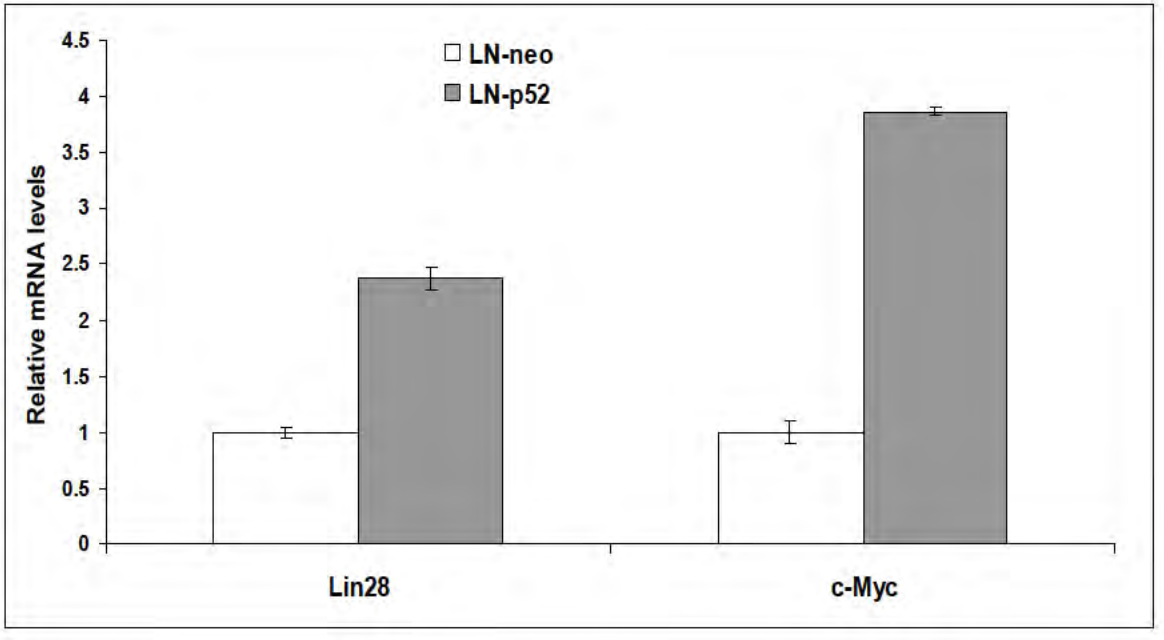
LN-neo
LN-p52
Relative mRNA levels
4.5
4
3.5
3
2.5
2
1.5
1
0.5
0
Lin28
c-Myc

B

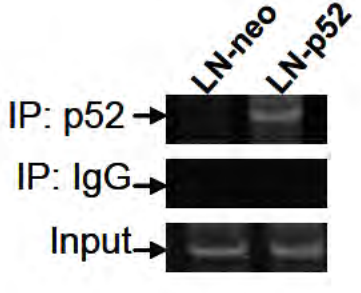
LN-neo
LN-p52
IP: p52
IP: IgG
Input

Figure 9

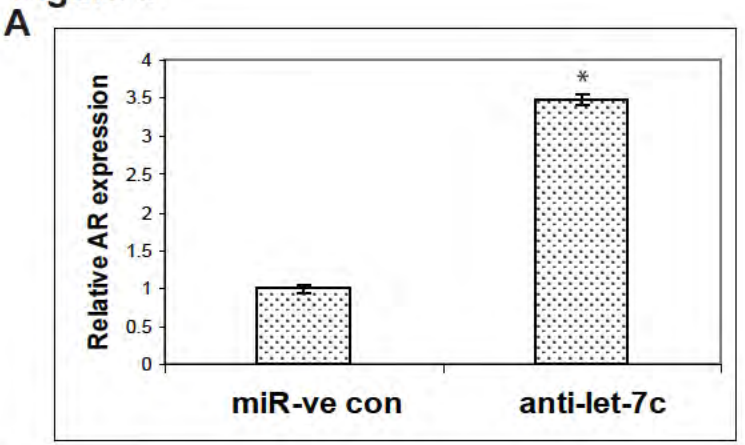
A
Relative AR expression
4
3.5
3
2.5
2
1.5
1
0.5
0
*
miR-ve con
anti-let-7c

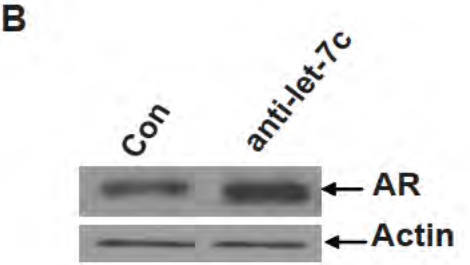
B
Con
anti-let-7c
AR
Actin

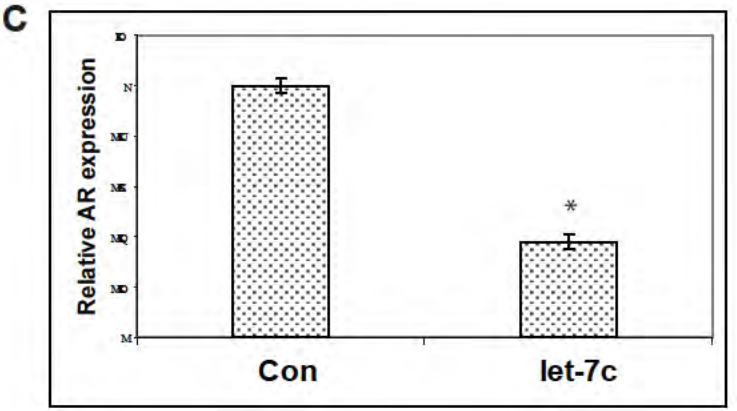
C
Relative AR expression
*
Con
let-7c

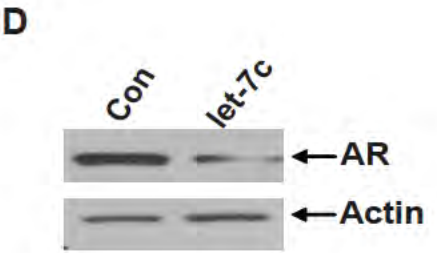
D
Con
let-7c
AR
Actin

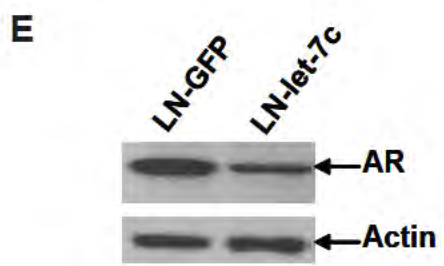
E
LN-GFP
LN-let-7c
AR
Actin

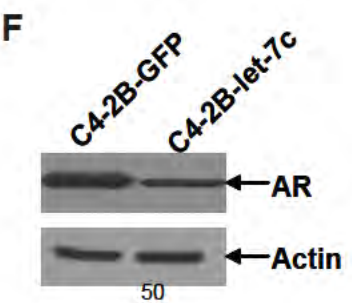
F
C4-2B-GFP
C4-2B-let-7c
AR
Actin

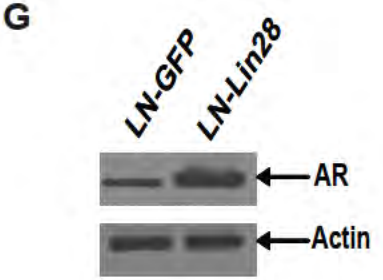
G
LN-GFP
LN-Lin28
AR
Actin

Figure 10

A

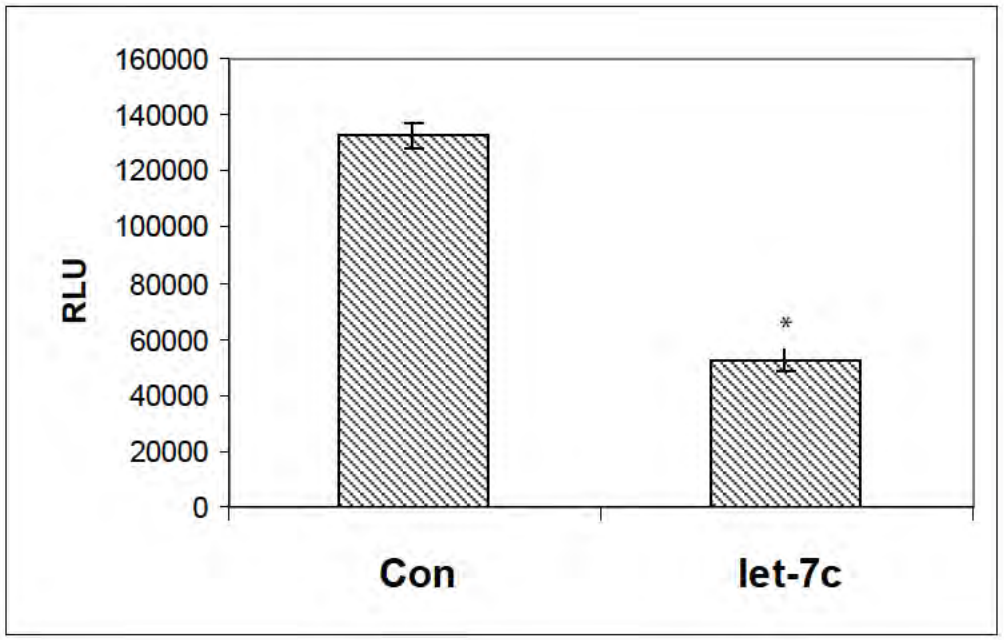

B

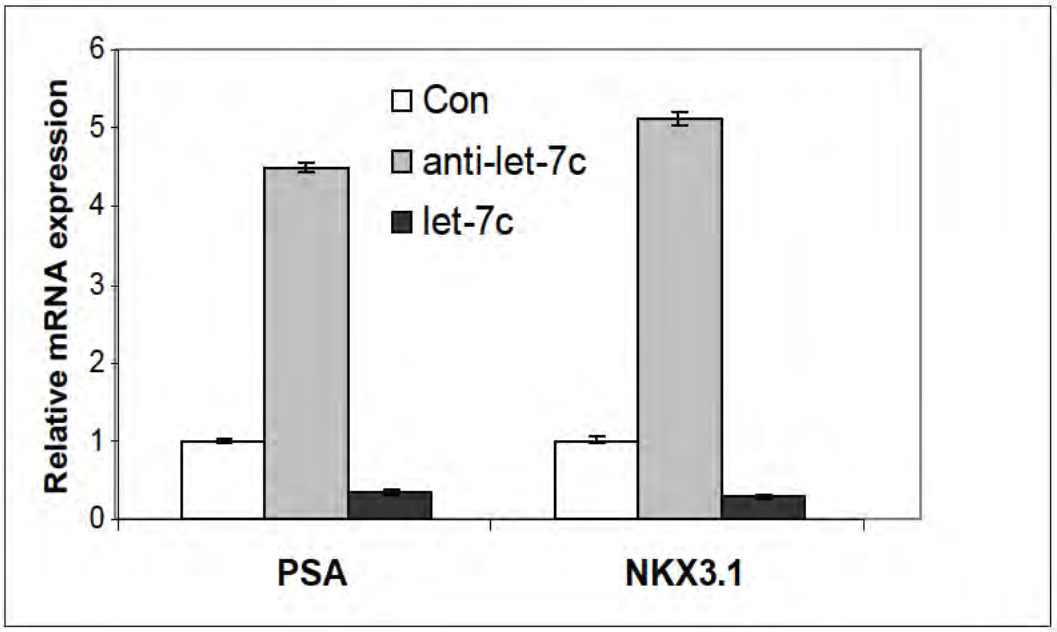

C

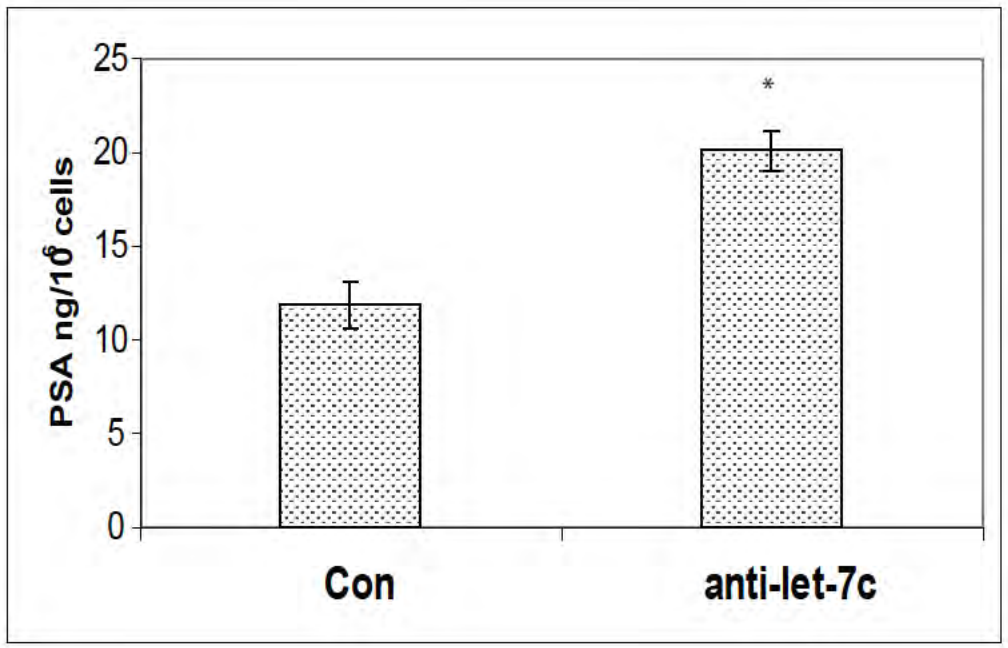

D

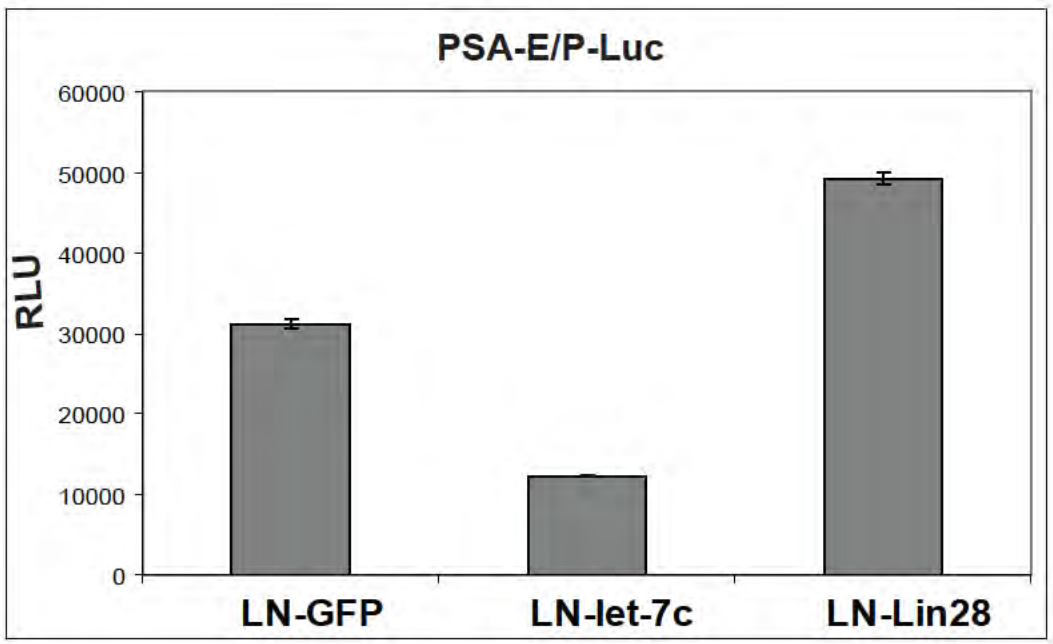

E

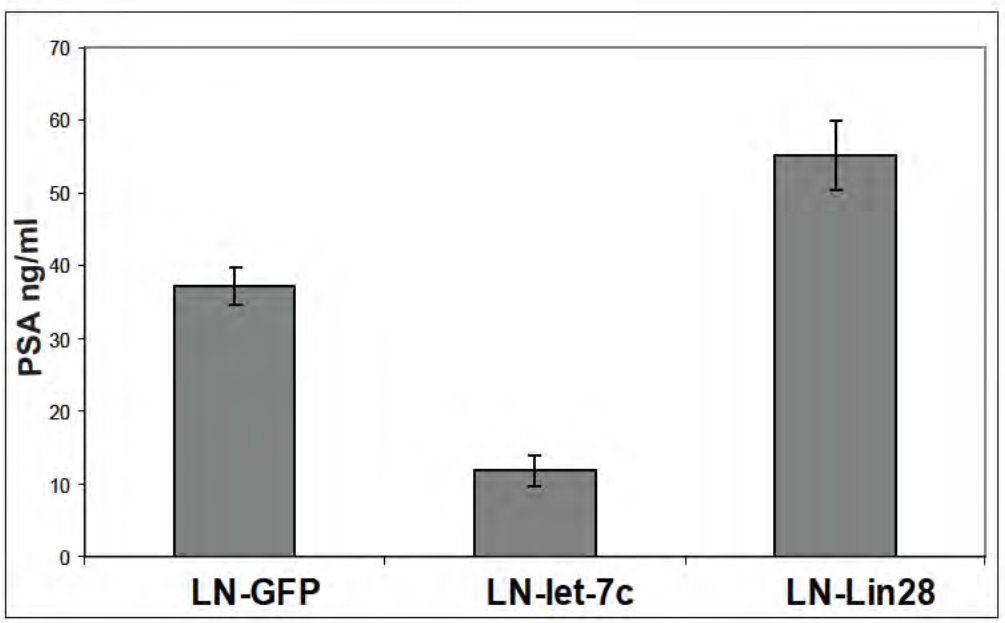

F

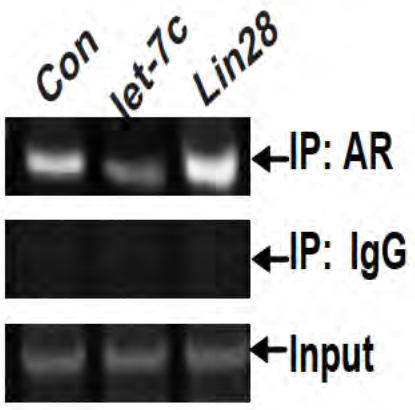

G

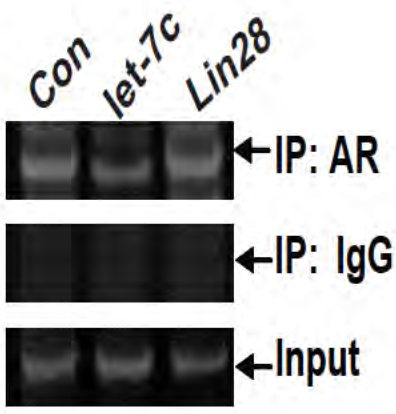

Figure 11

A

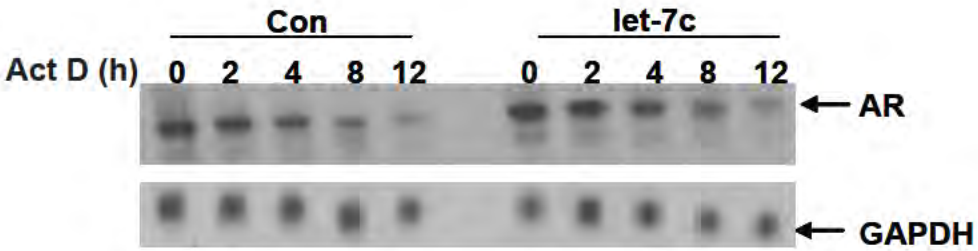

B

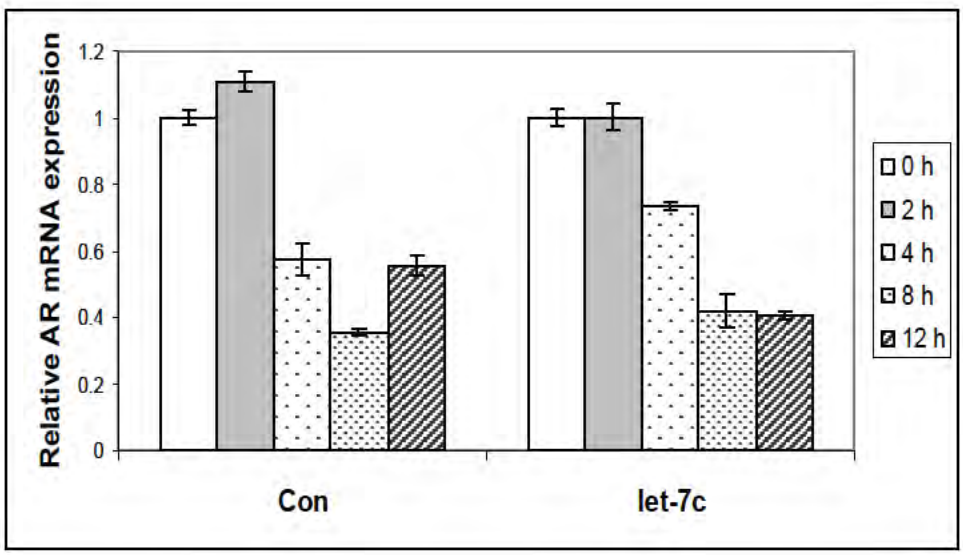

C

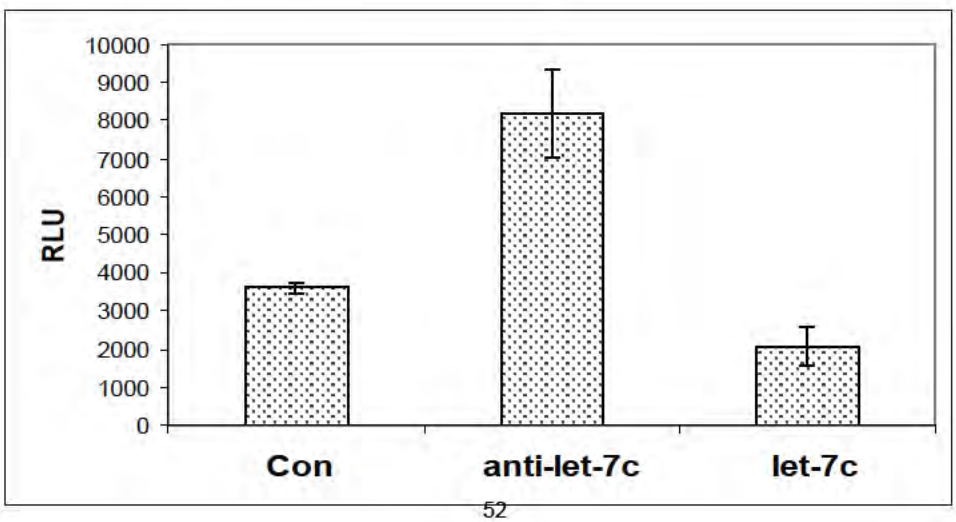

Figure 12

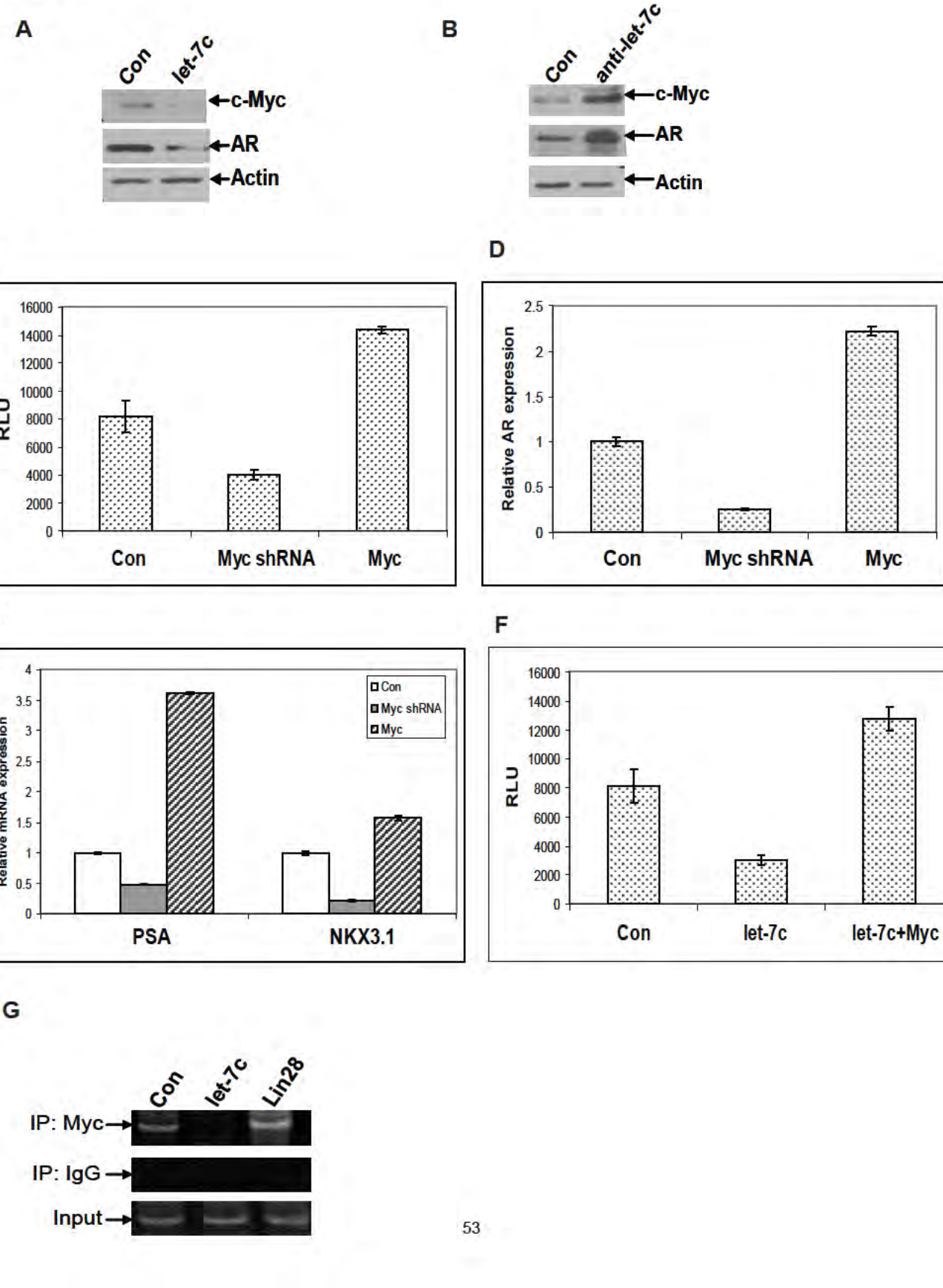
A
Con
let-7c
c-Myc
AR
Actin
B
Con
anti-let-7c
c-Myc
AR
Actin
C
RLU
16000
14000
12000
10000
8000
6000
4000
2000
0
Con
Myc shRNA
Myc
D
Relative AR expression
2.5
2
1.5
1
0.5
0
Con
Myc shRNA
Myc
E
Relative mRNA expression
4
3.5
3
2.5
2
1.5
1
0.5
0
Con
Myc shRNA
Myc
PSA
NKX3.1
F
RLU
16000
14000
12000
10000
8000
6000
4000
2000
0
Con
let-7c
let-7c+Myc
G
Con
let-7c
Lin28
IP: Myc
IP: IgG
Input

Figure 13

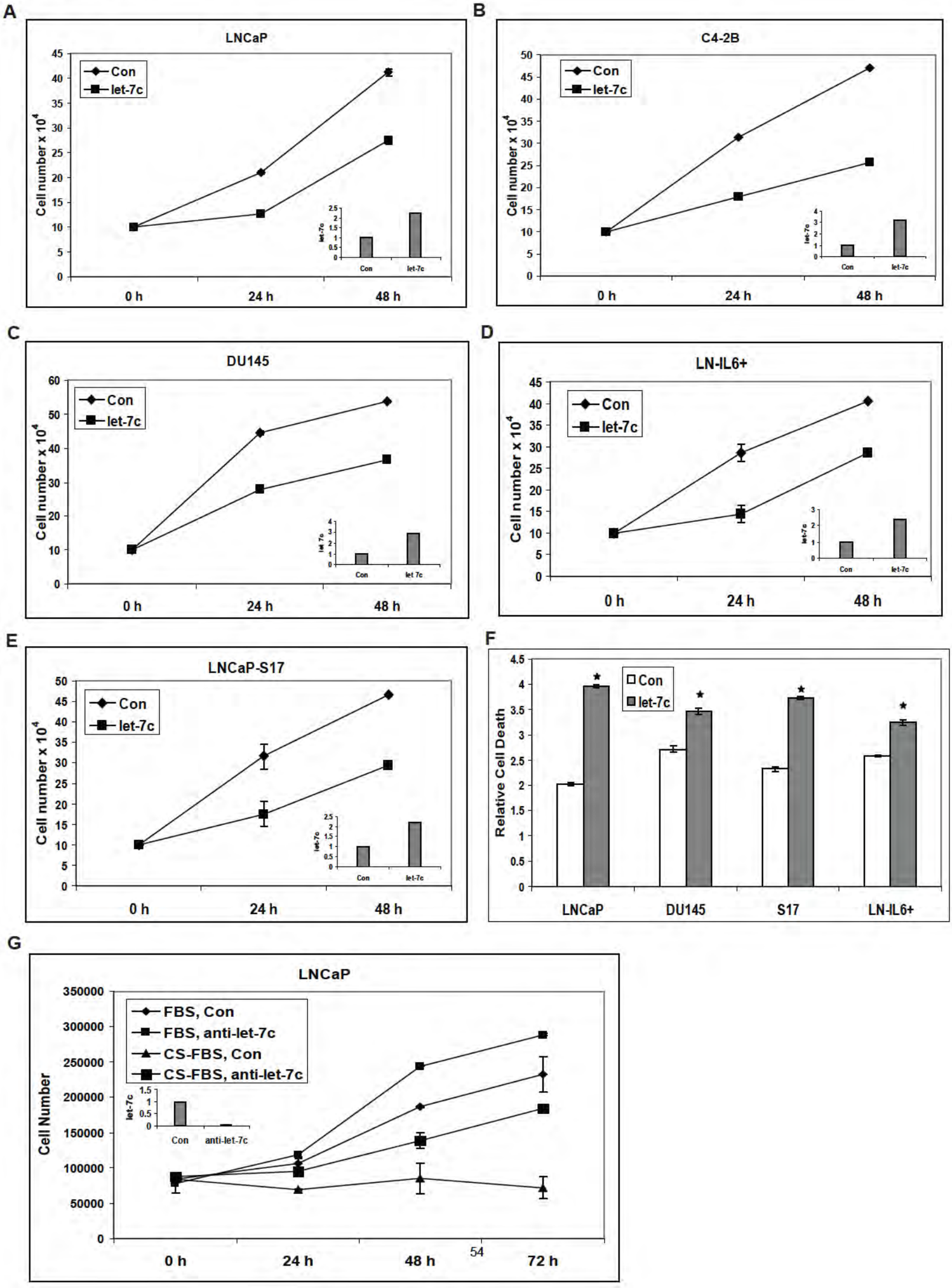
A
LNCaP
Con
let-7c
Cell number x 10^4
0 h
24 h
48 h
B
C4-2B
C
DU145
D
LN-IL6+
E
LNCaP-S17
F
Relative Cell Death
LNCaP
DU145
S17
LN-IL6+
G
LNCaP
FBS, Con
FBS, anti-let-7c
CS-FBS, Con
CS-FBS, anti-let-7c
Cell Number
anti-let-7c
72 h

Figure 14

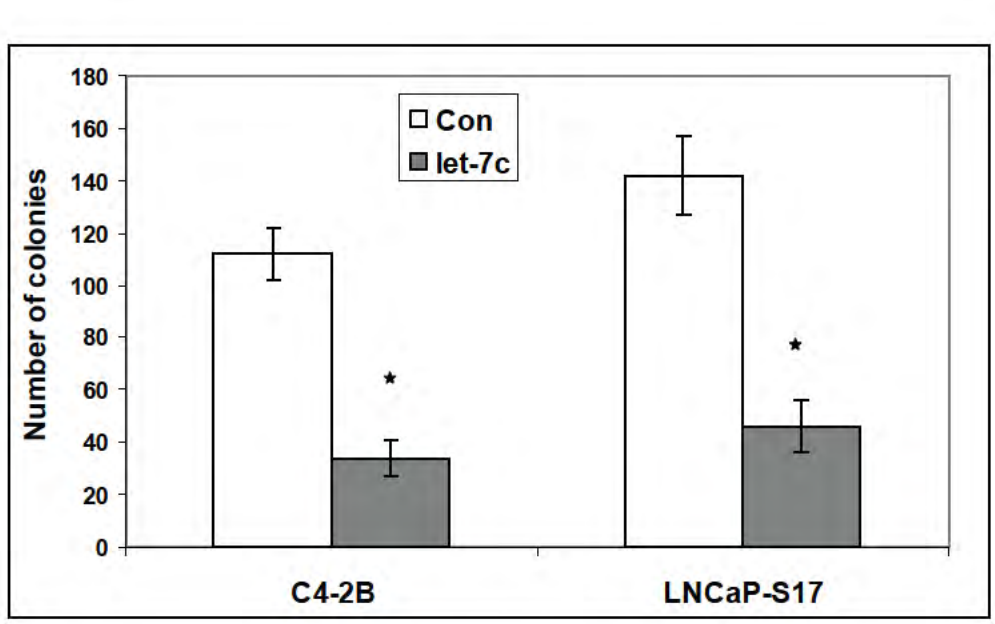
A
Number of colonies
Con
let-7c
C4-2B
LNCaP-S17

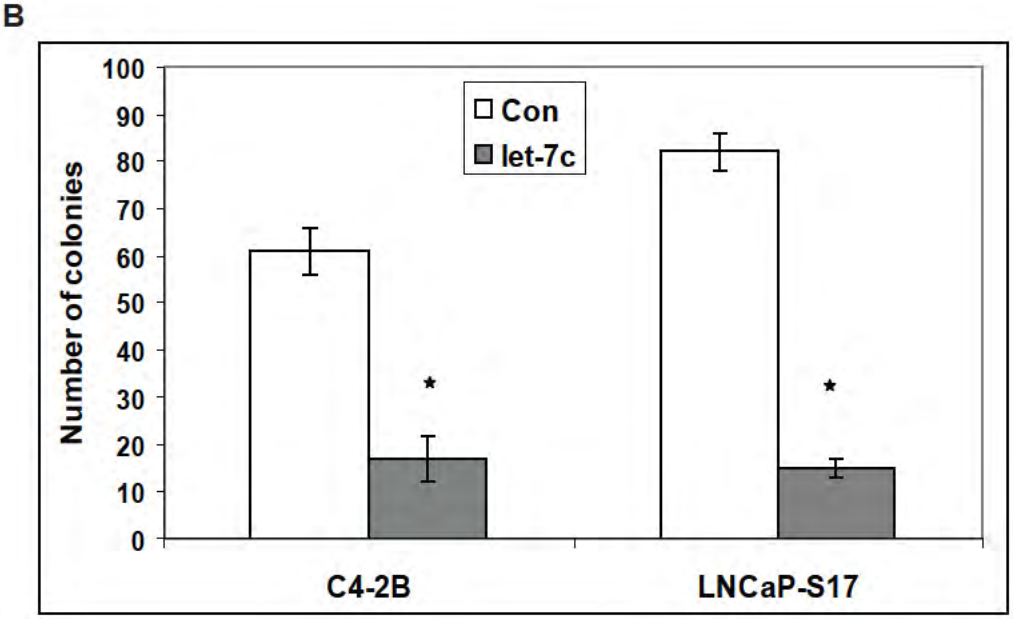
B
Number of colonies
Con
let-7c
C4-2B
LNCaP-S17

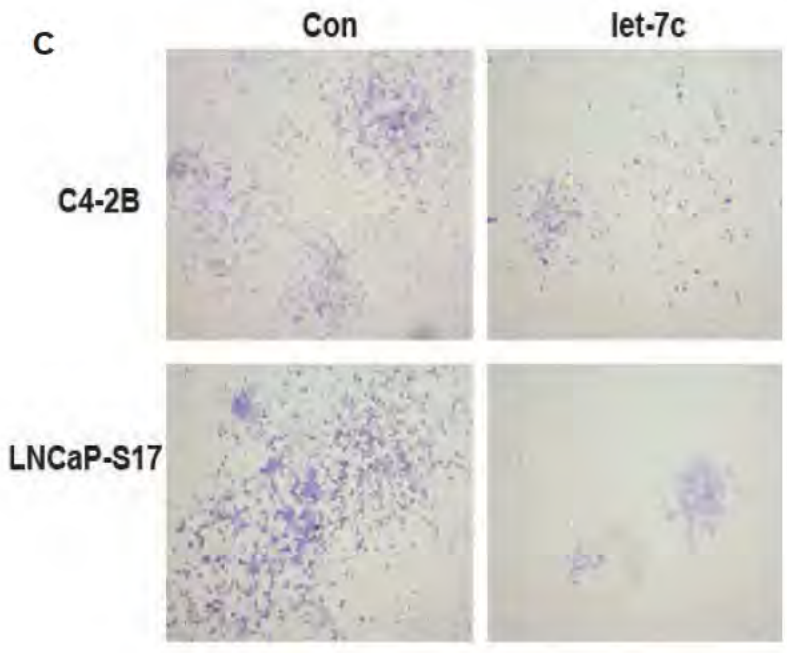
C
Con
let-7c
C4-2B
LNCaP-S17

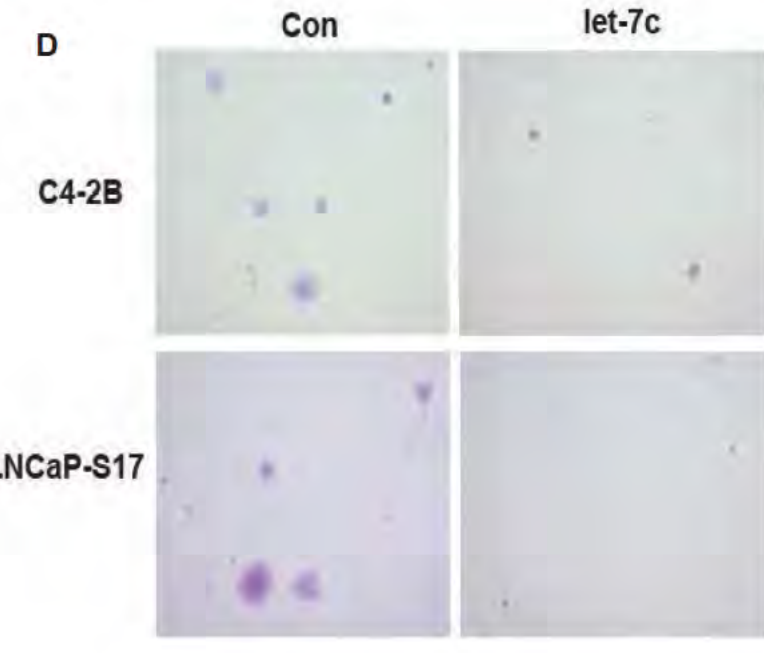
D
Con
let-7c
C4-2B
LNCaP-S17

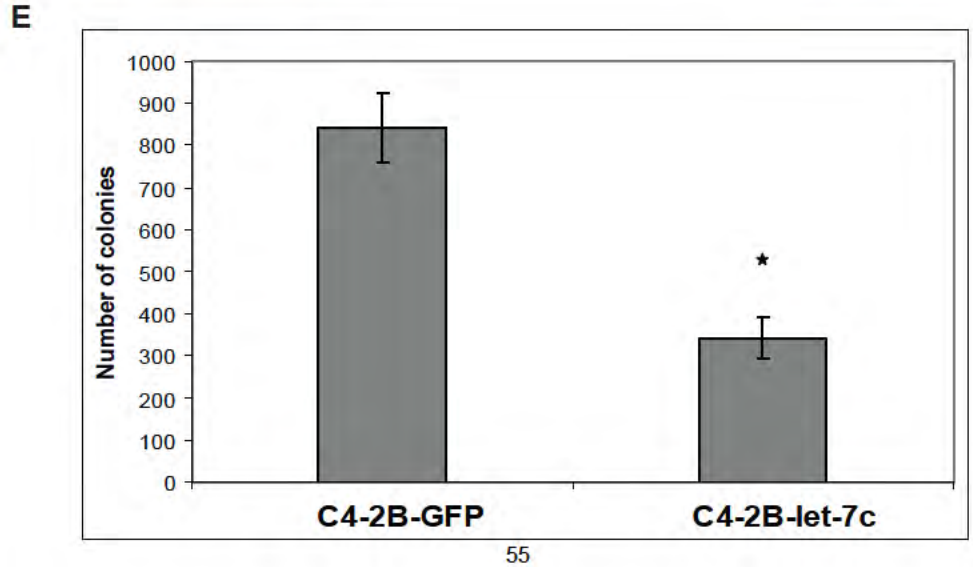
E
Number of colonies
C4-2B-GFP
C4-2B-let-7c

Figure 15

A

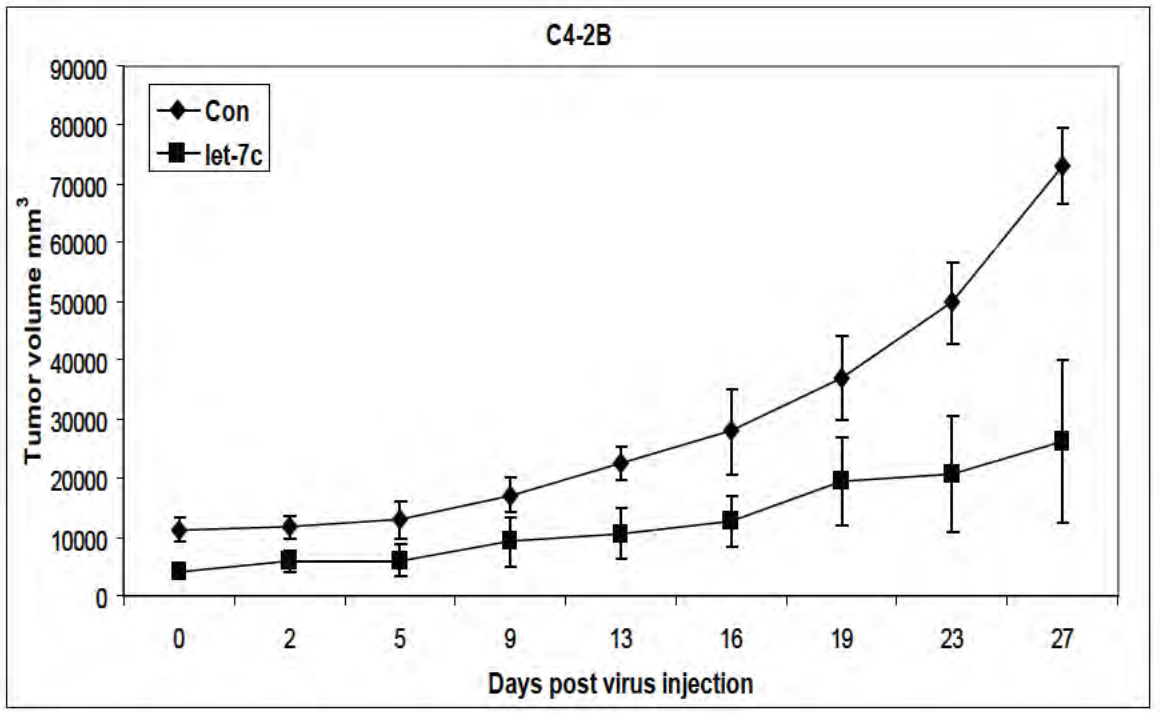

B

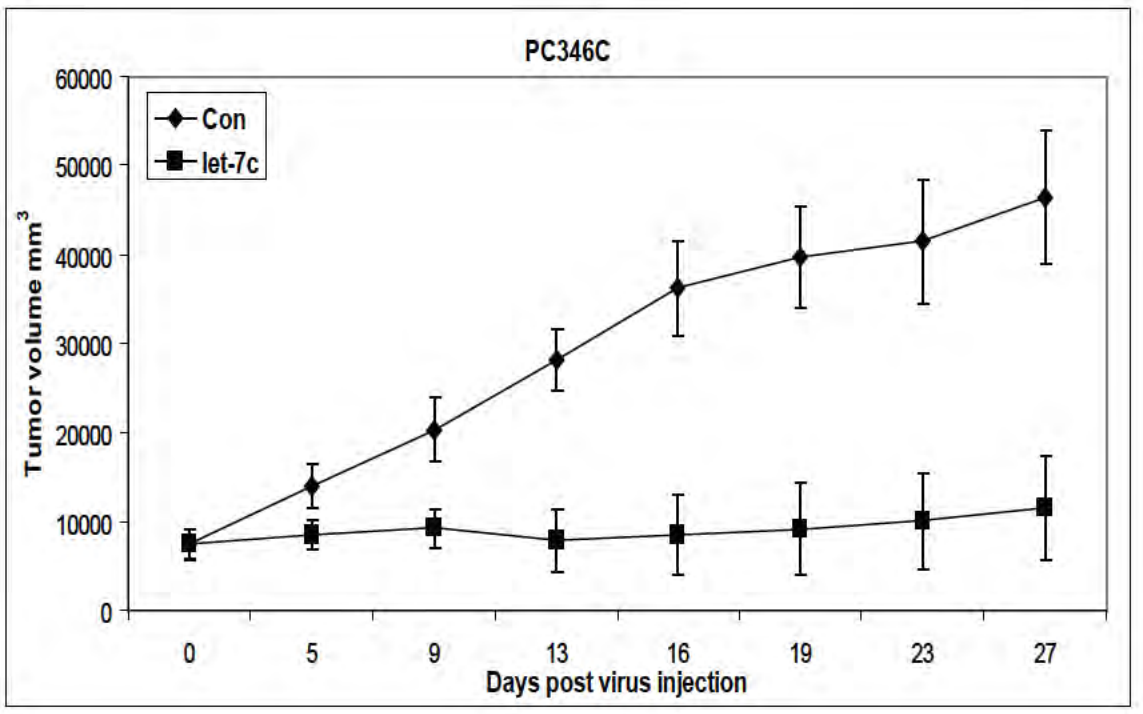

C

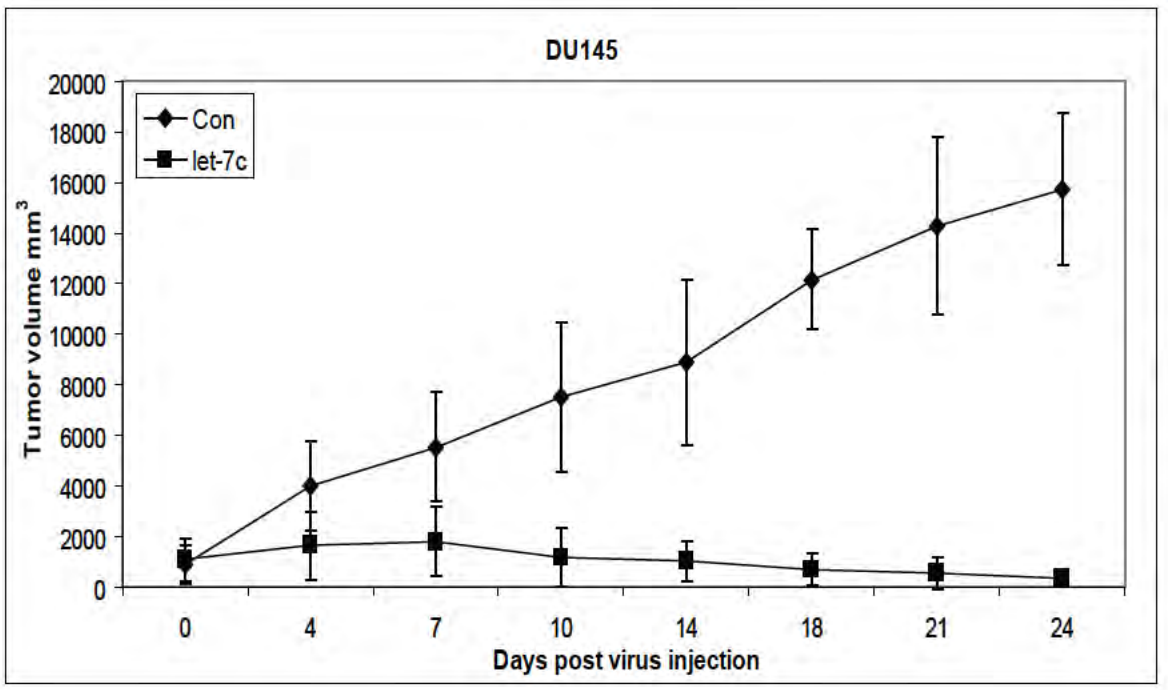

D

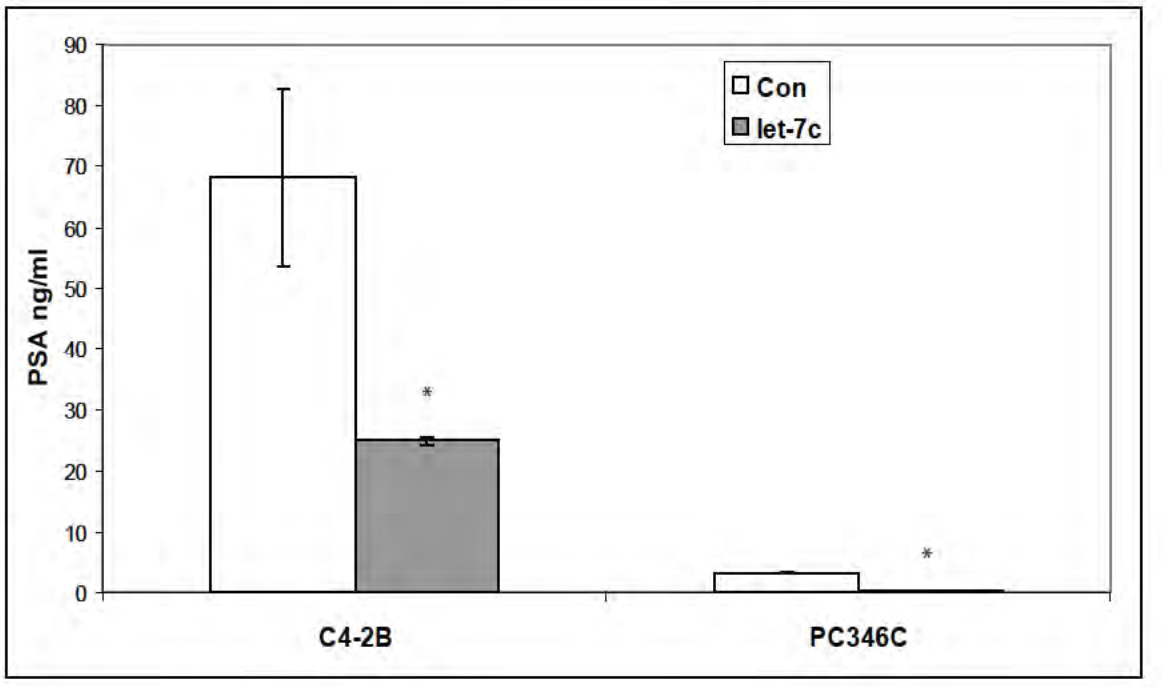

E

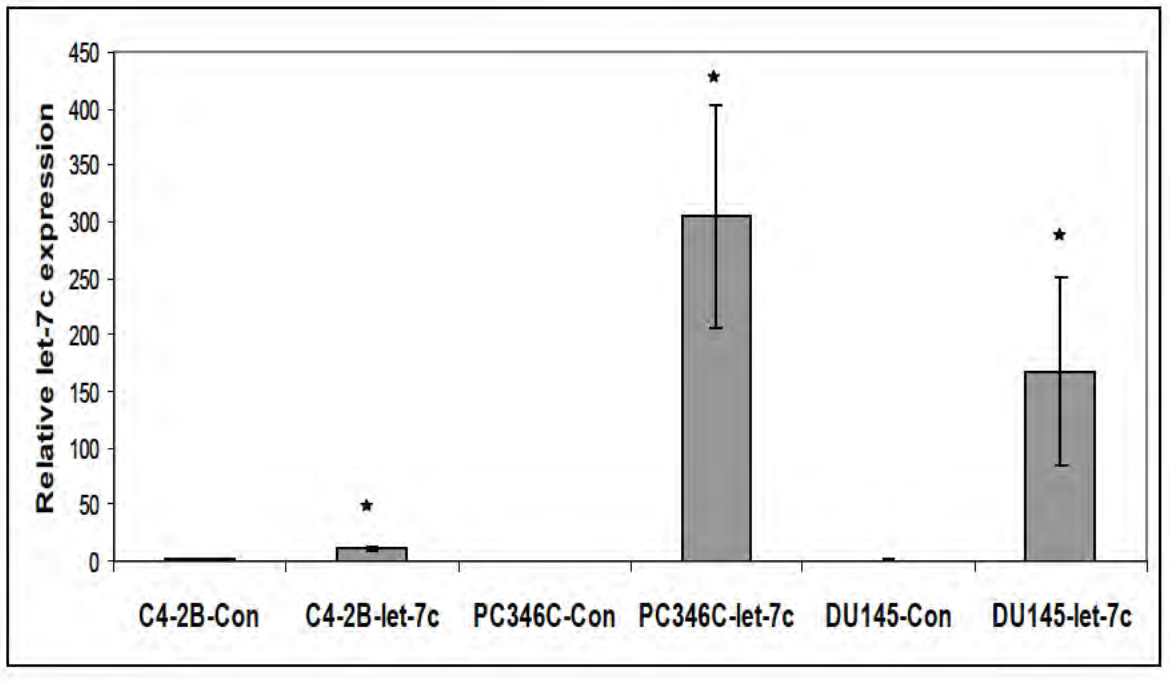

F

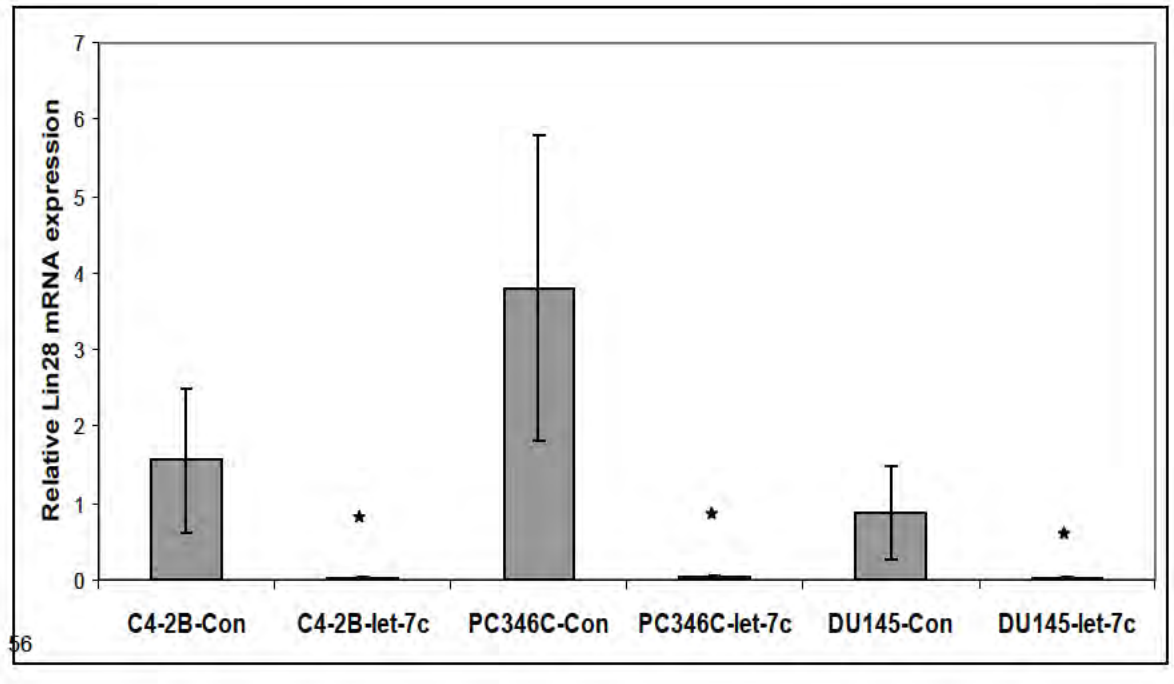

Figure 16

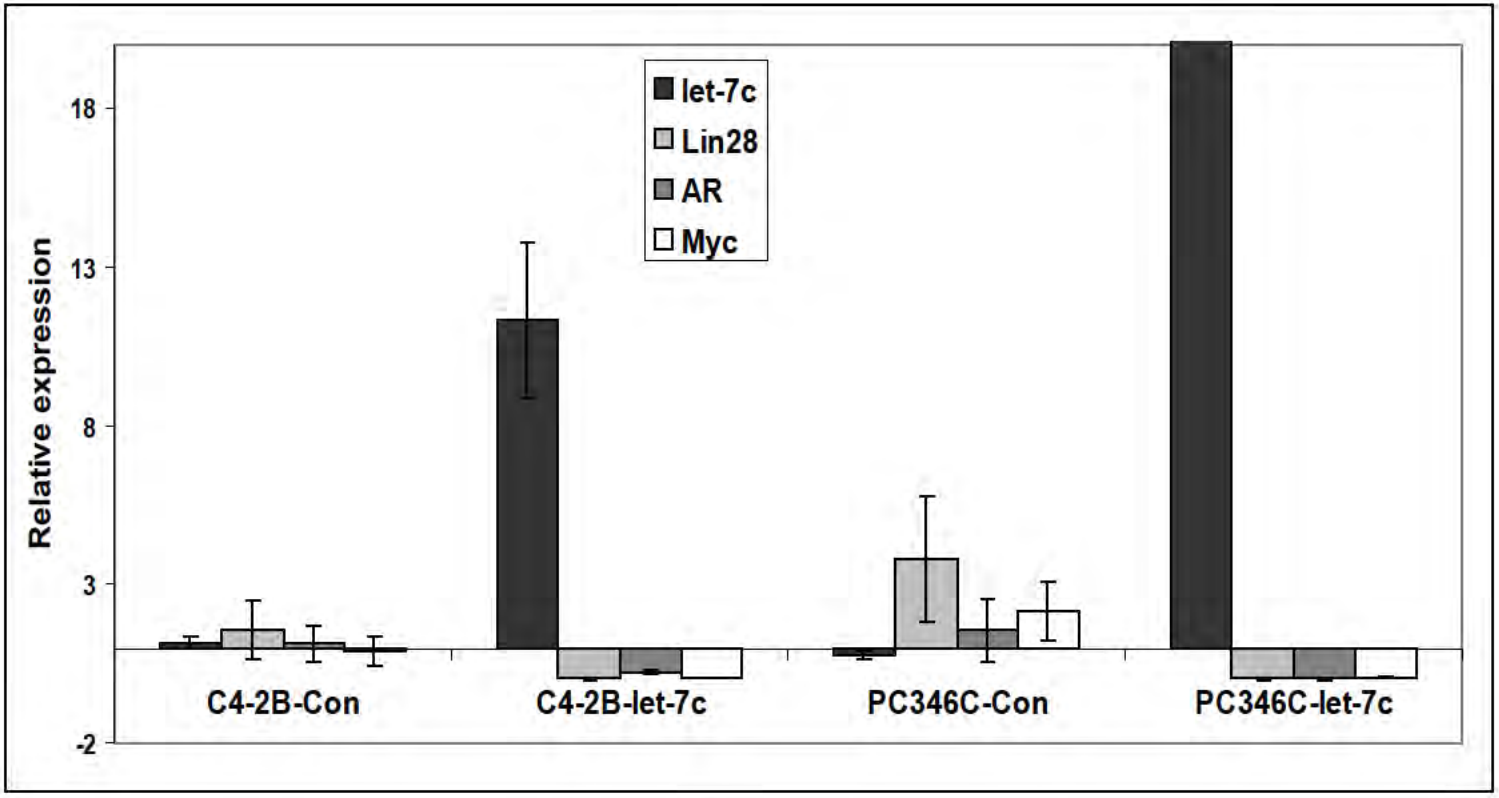
let-7c
Lin28
AR
Myc
Relative expression
18
13
8
3
-2
C4-2B-Con
C4-2B-let-7c
PC346C-Con
PC346C-let-7c

Figure 17

A

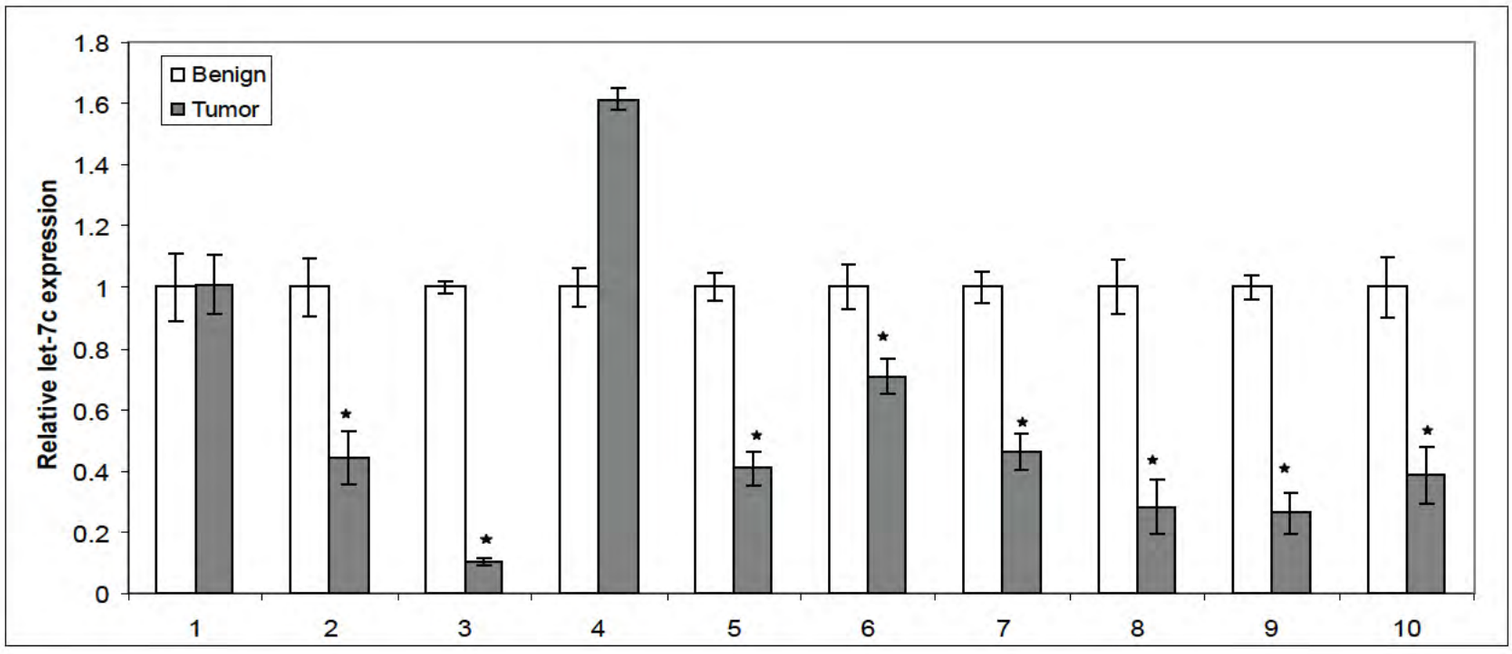

B

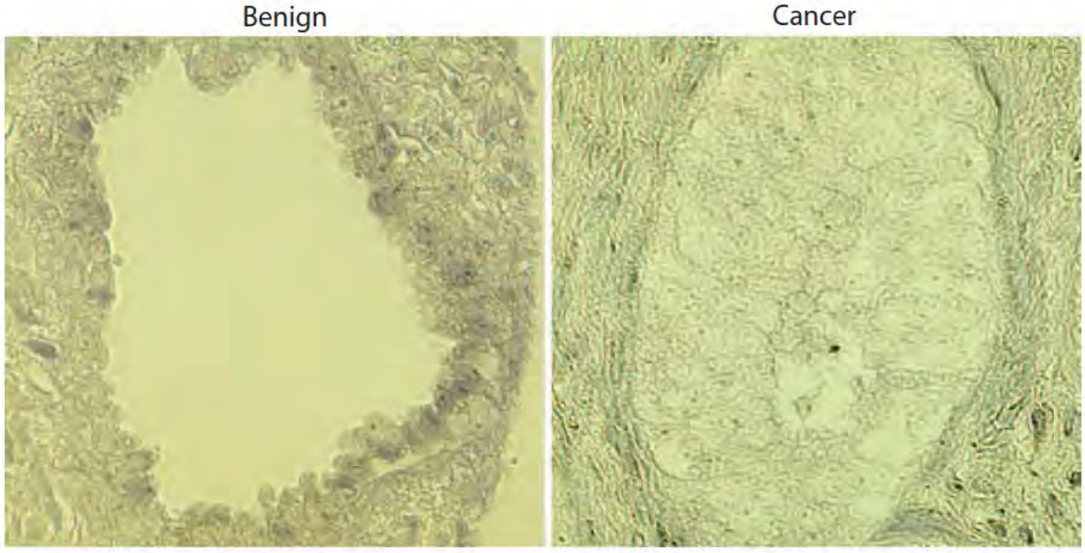

C

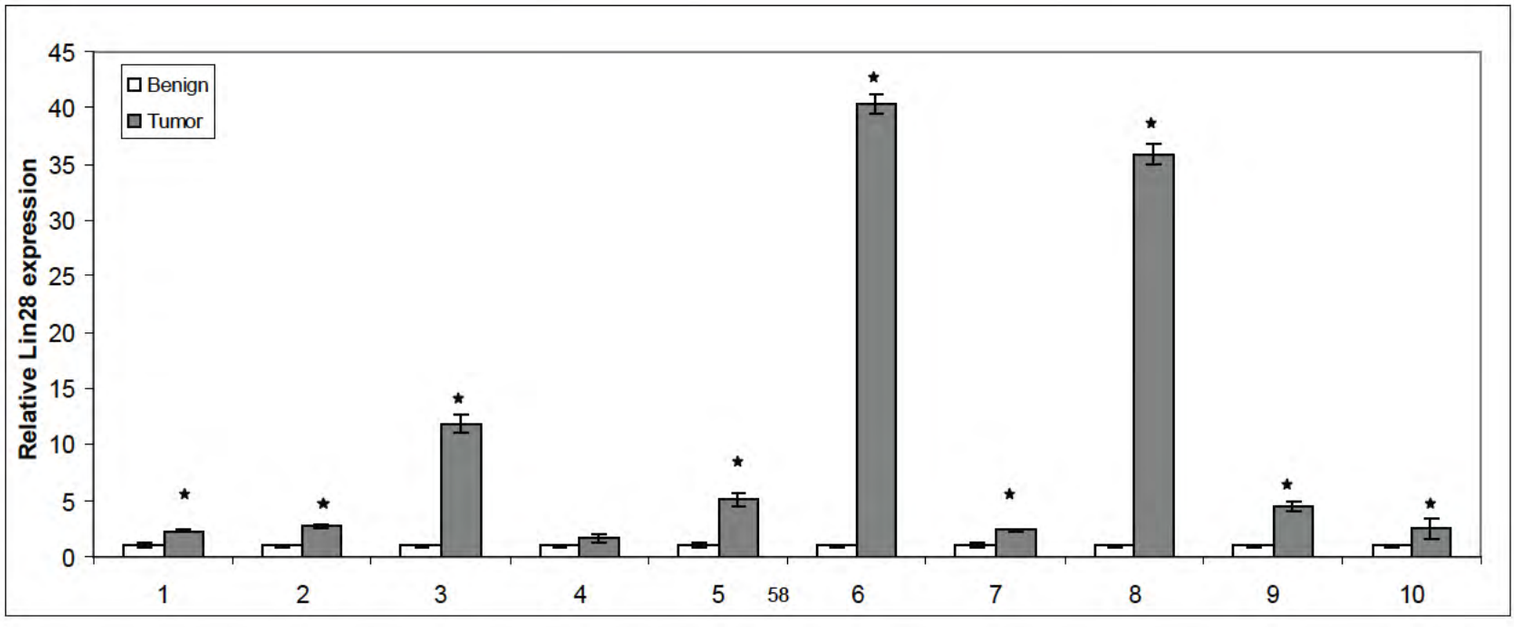

Figure 18

A

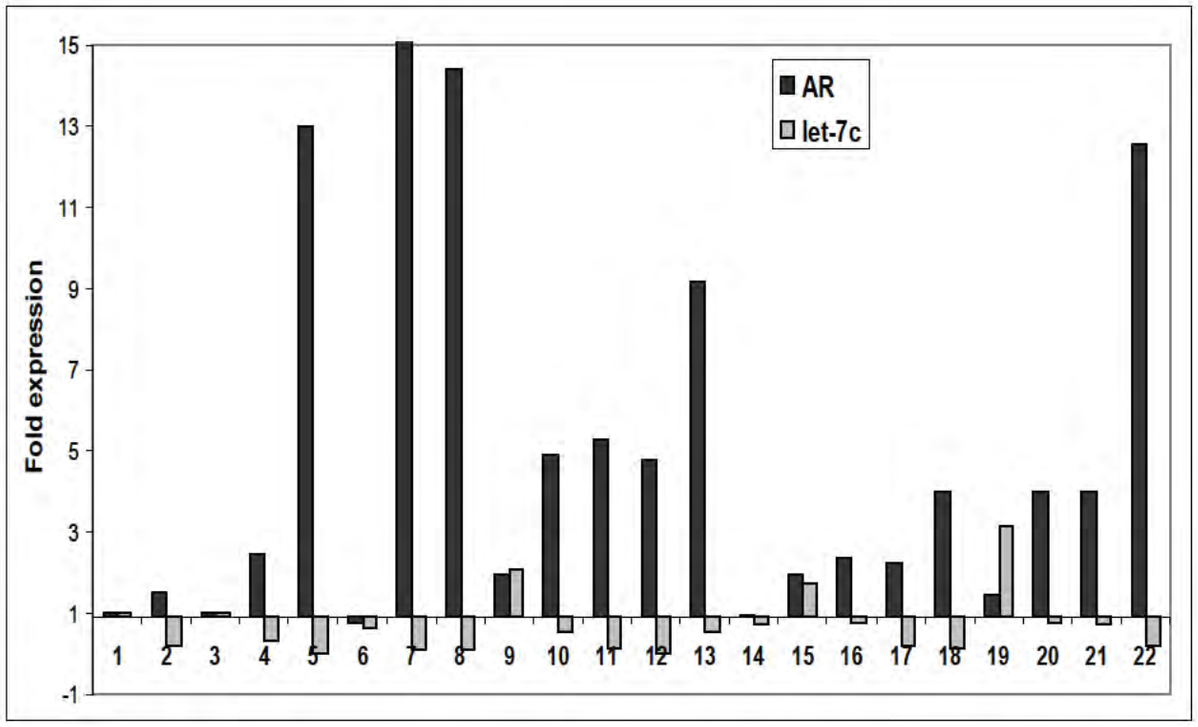

B

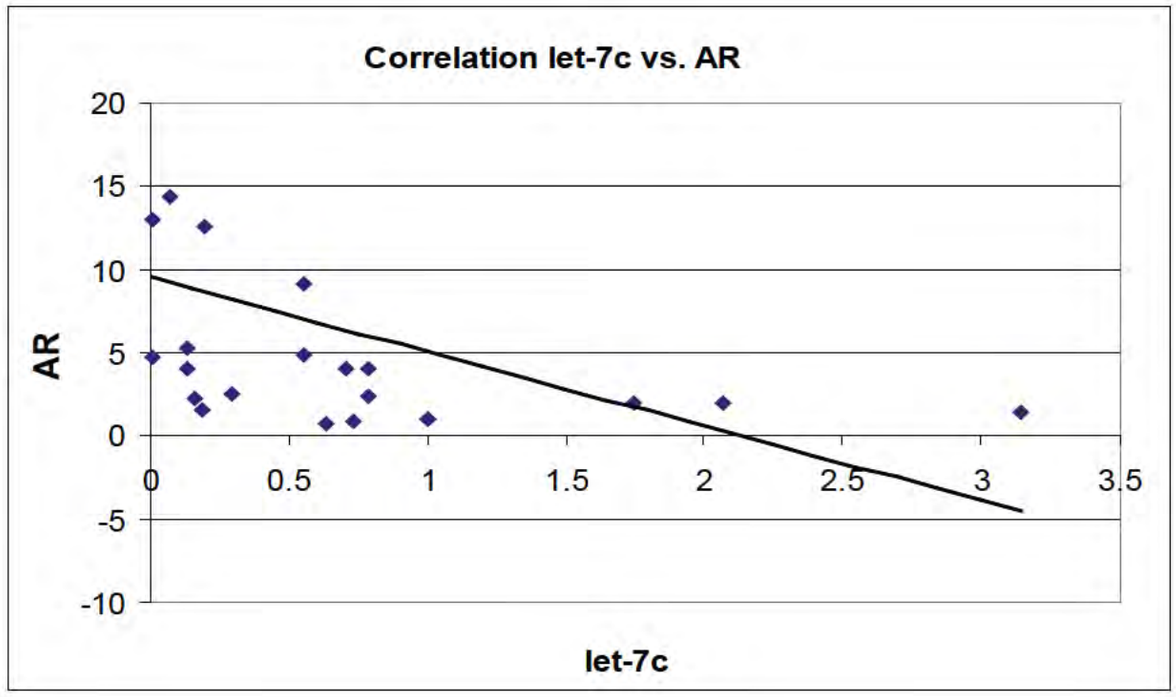

C

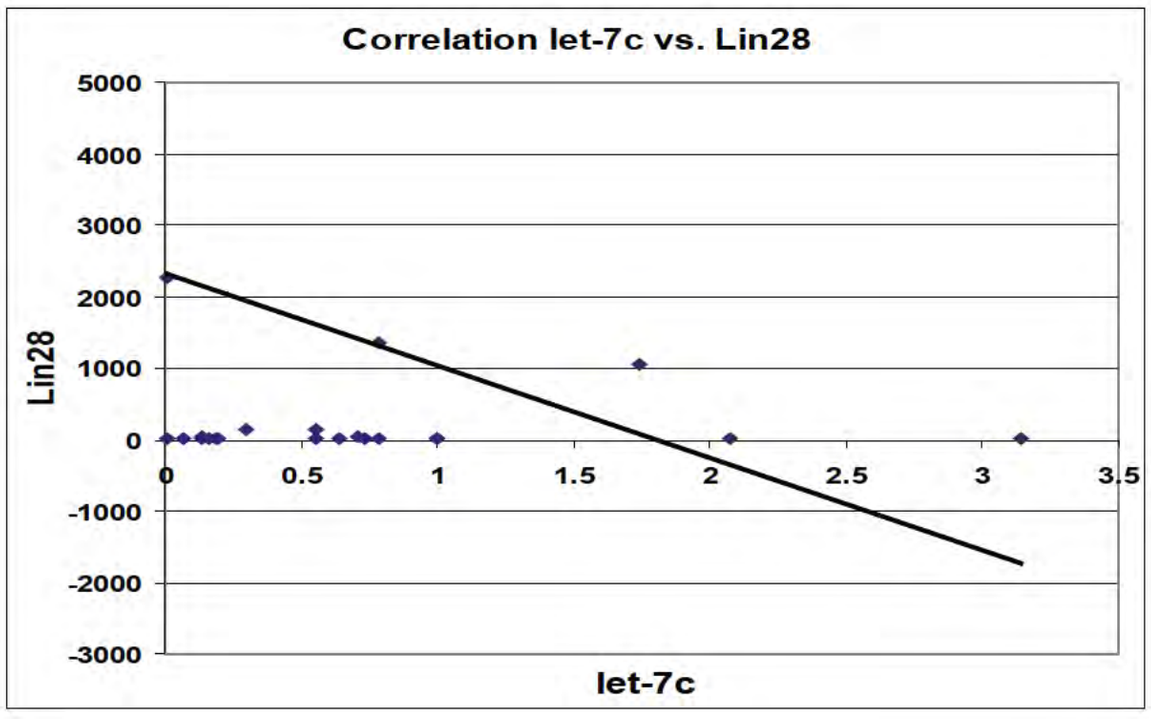

D

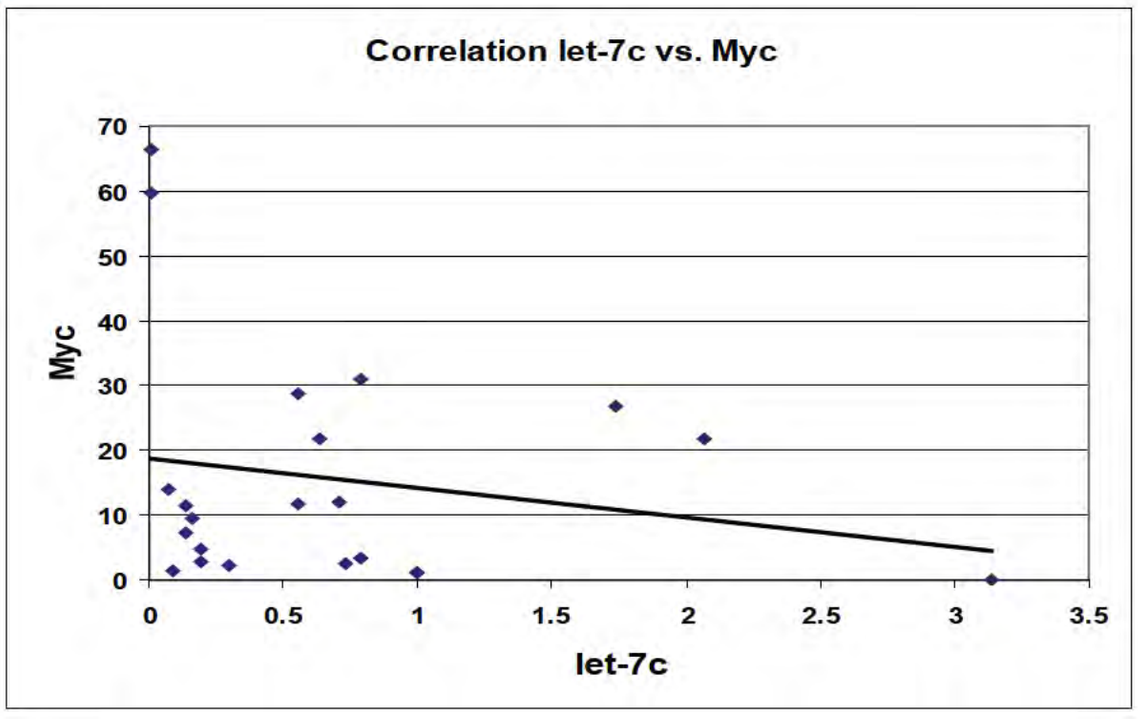

E

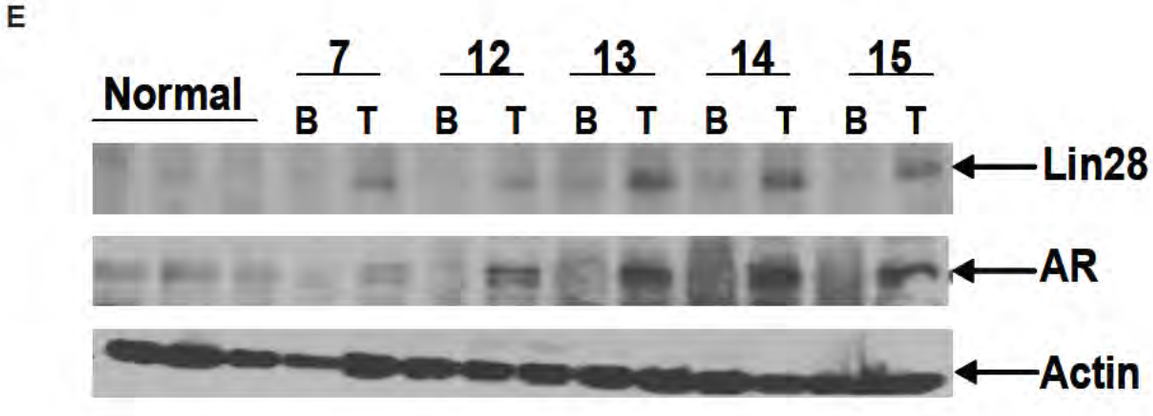

Figure 19

A

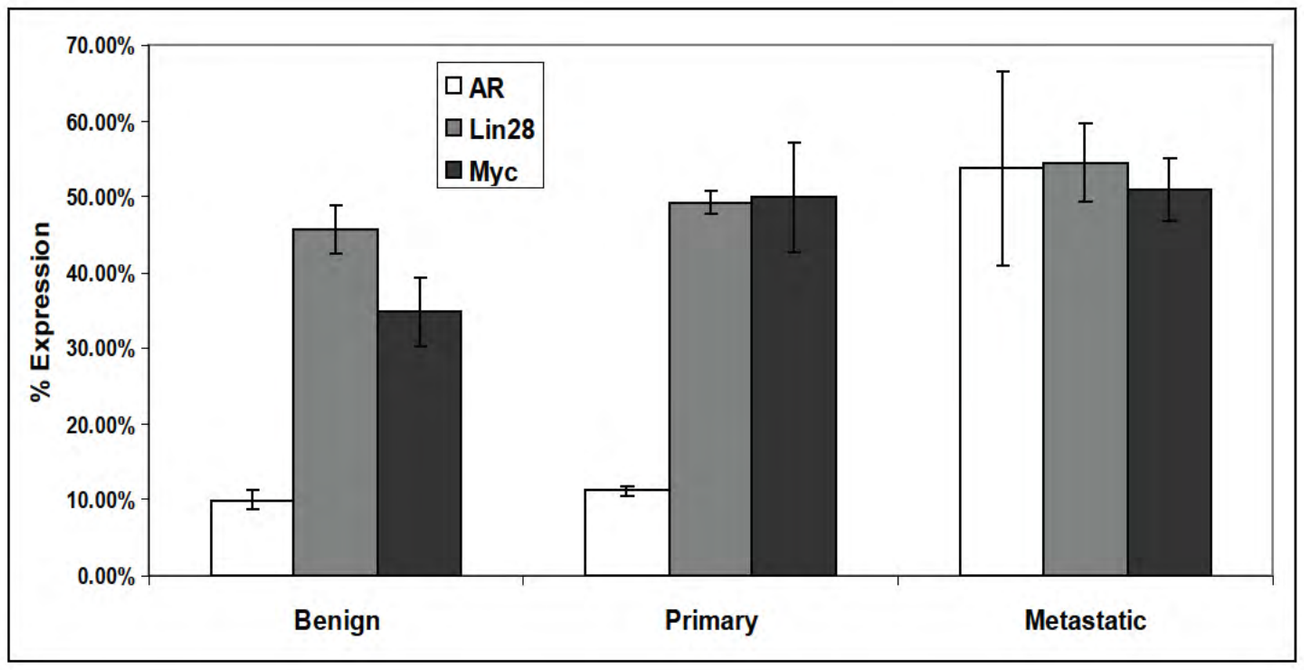

B

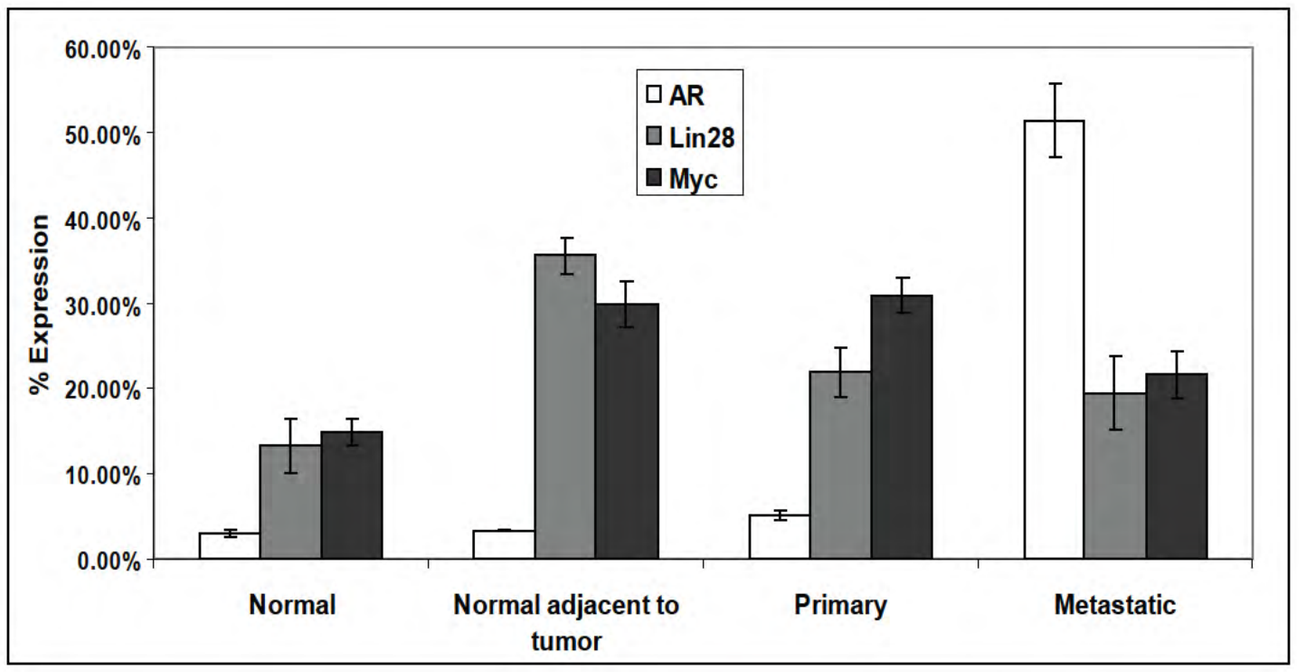

C

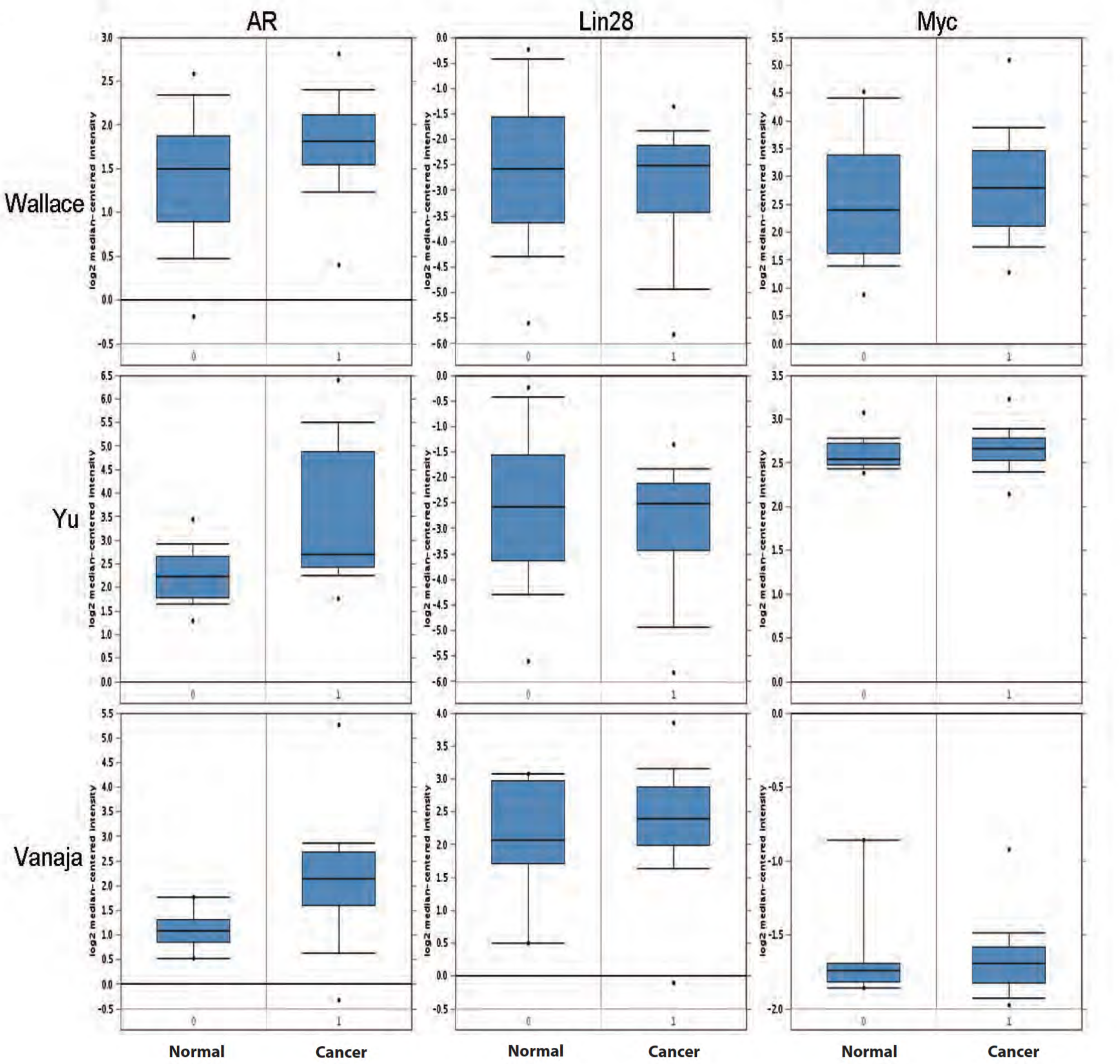

FIGURE 20

A

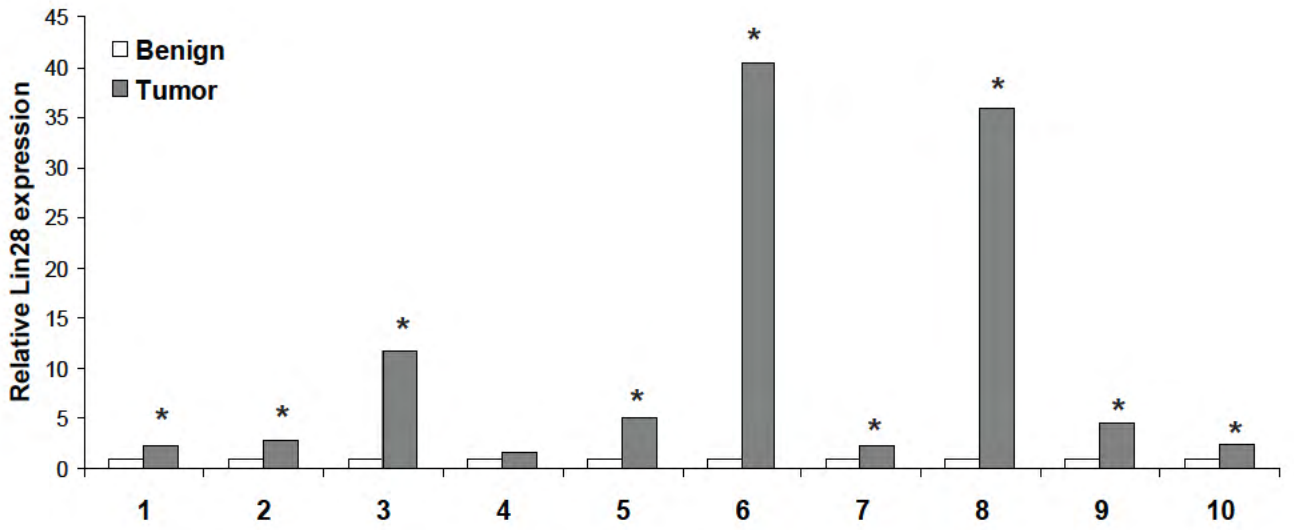

B

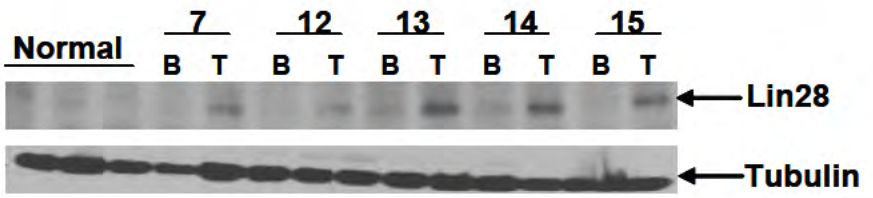

N=42	Normal	Benign	Tumor
Positive	40%	47%	86%
Negative	60%	53%	14%

C

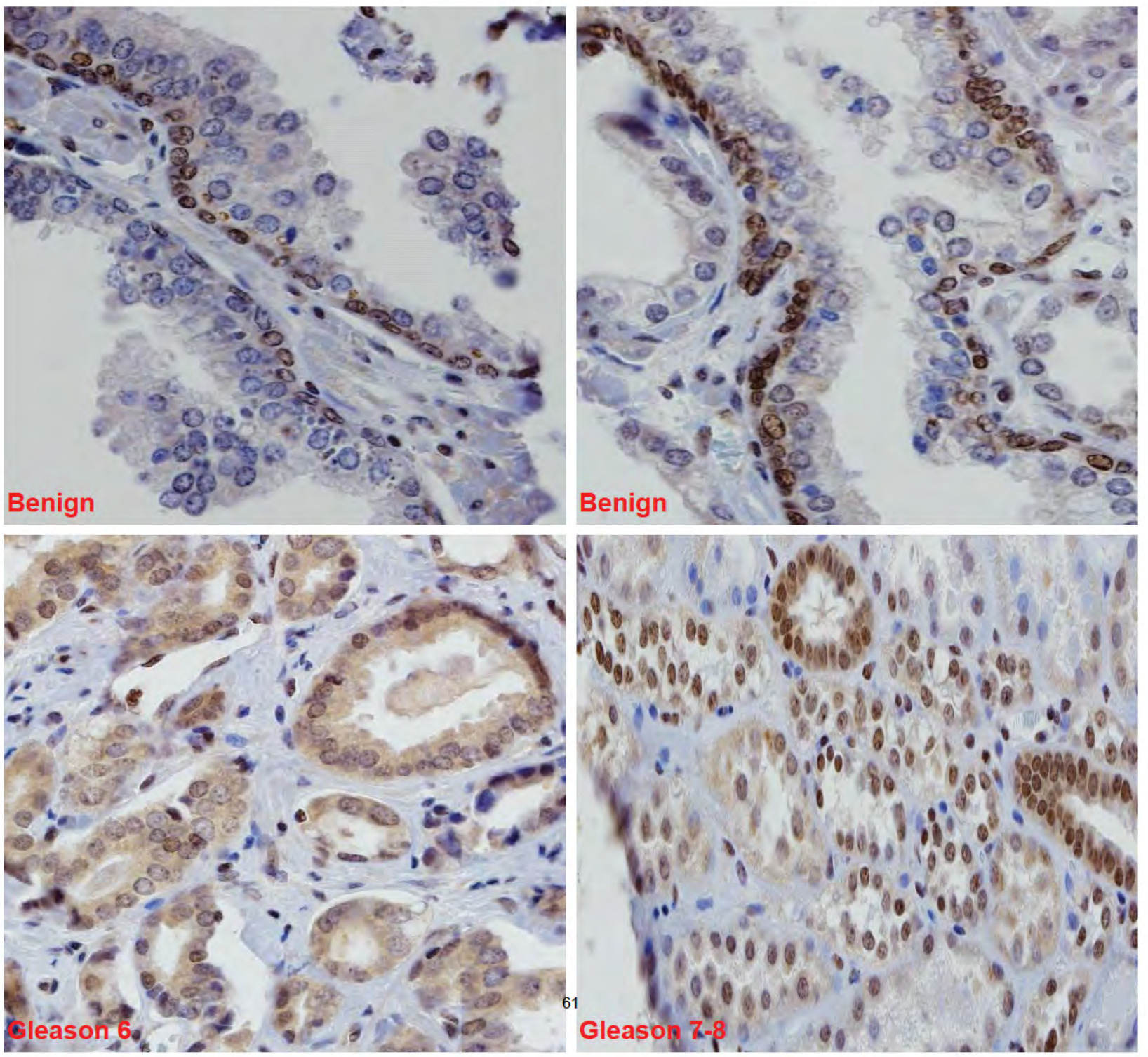

FIGURE 21

A

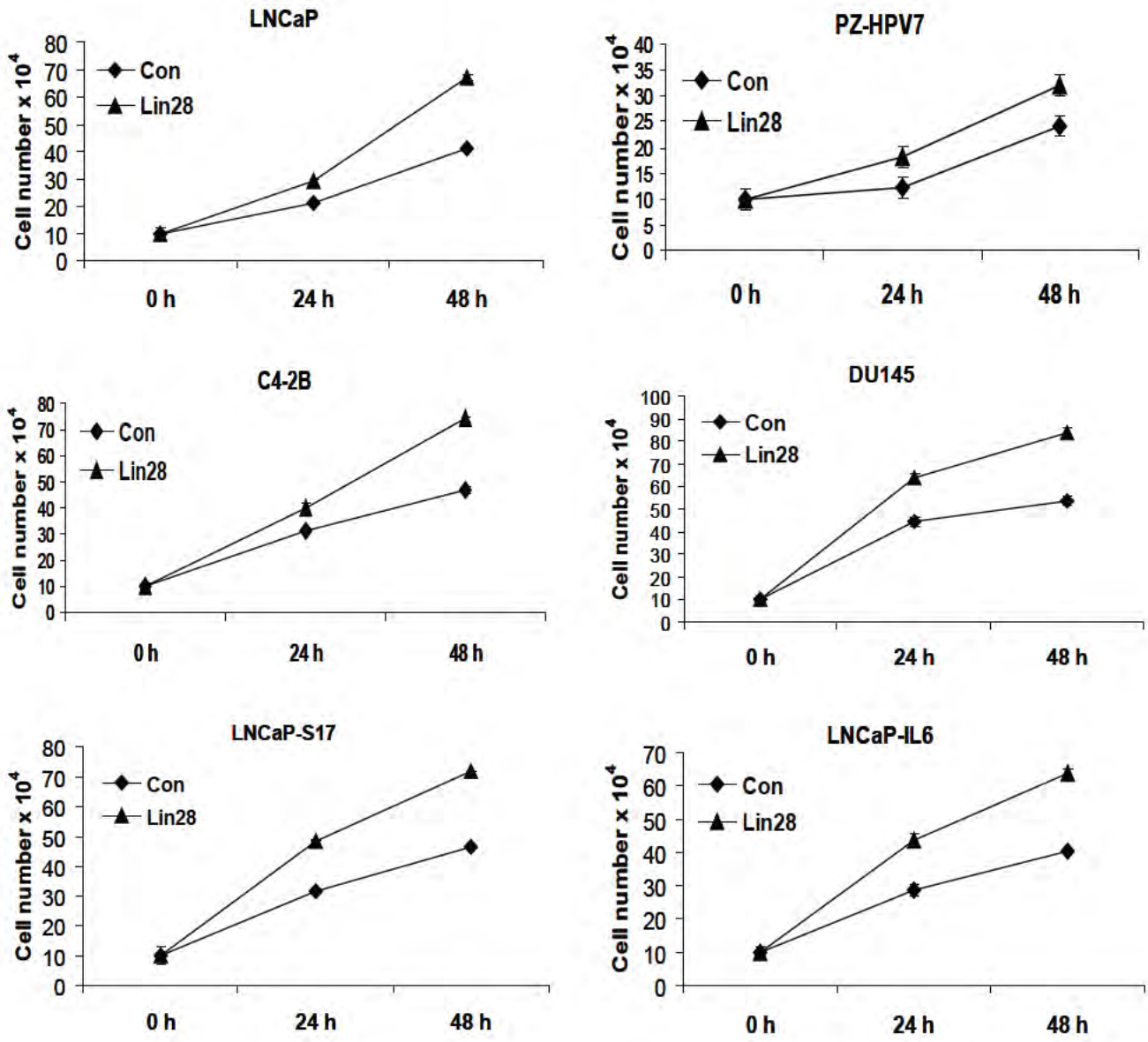

B

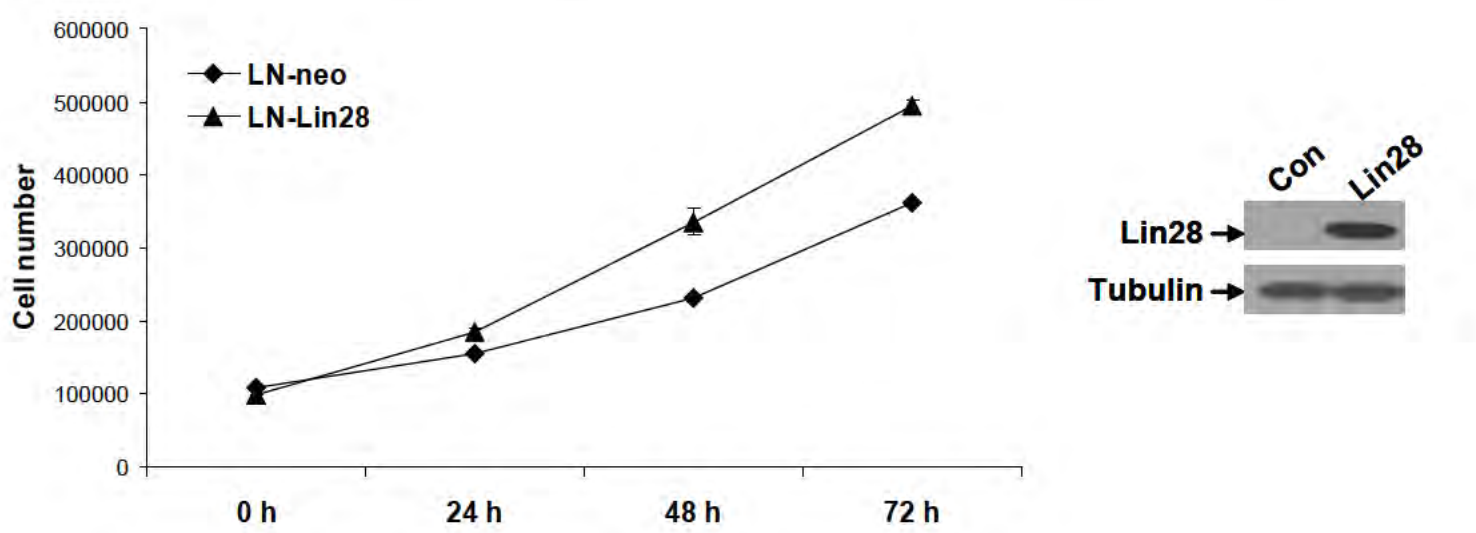

C

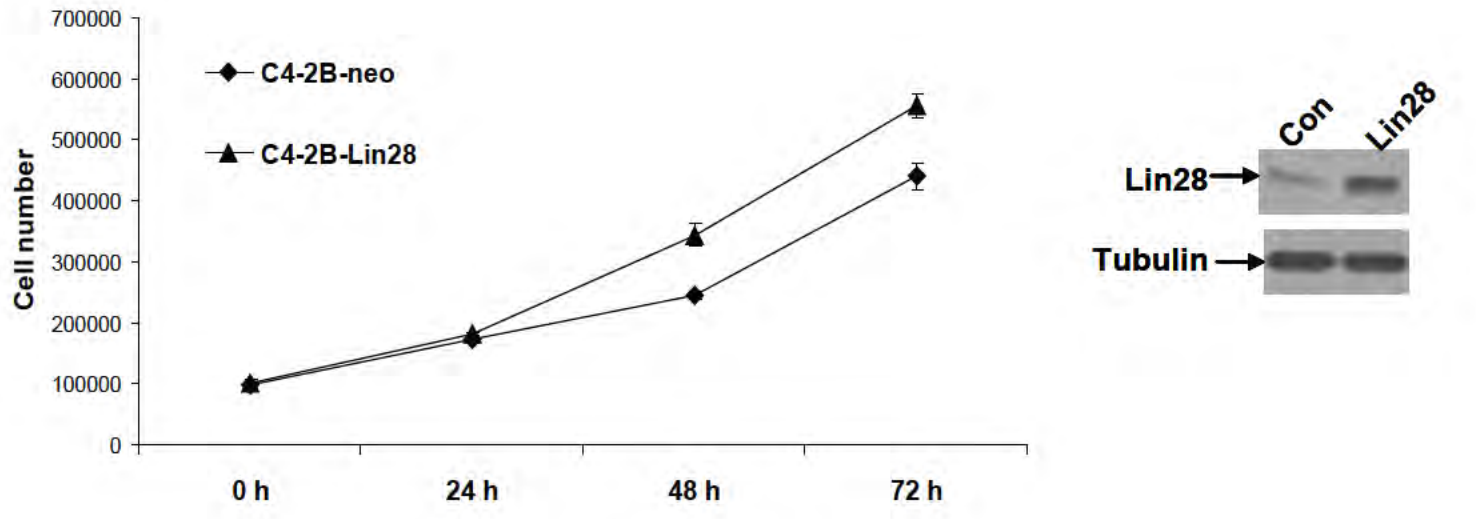

D

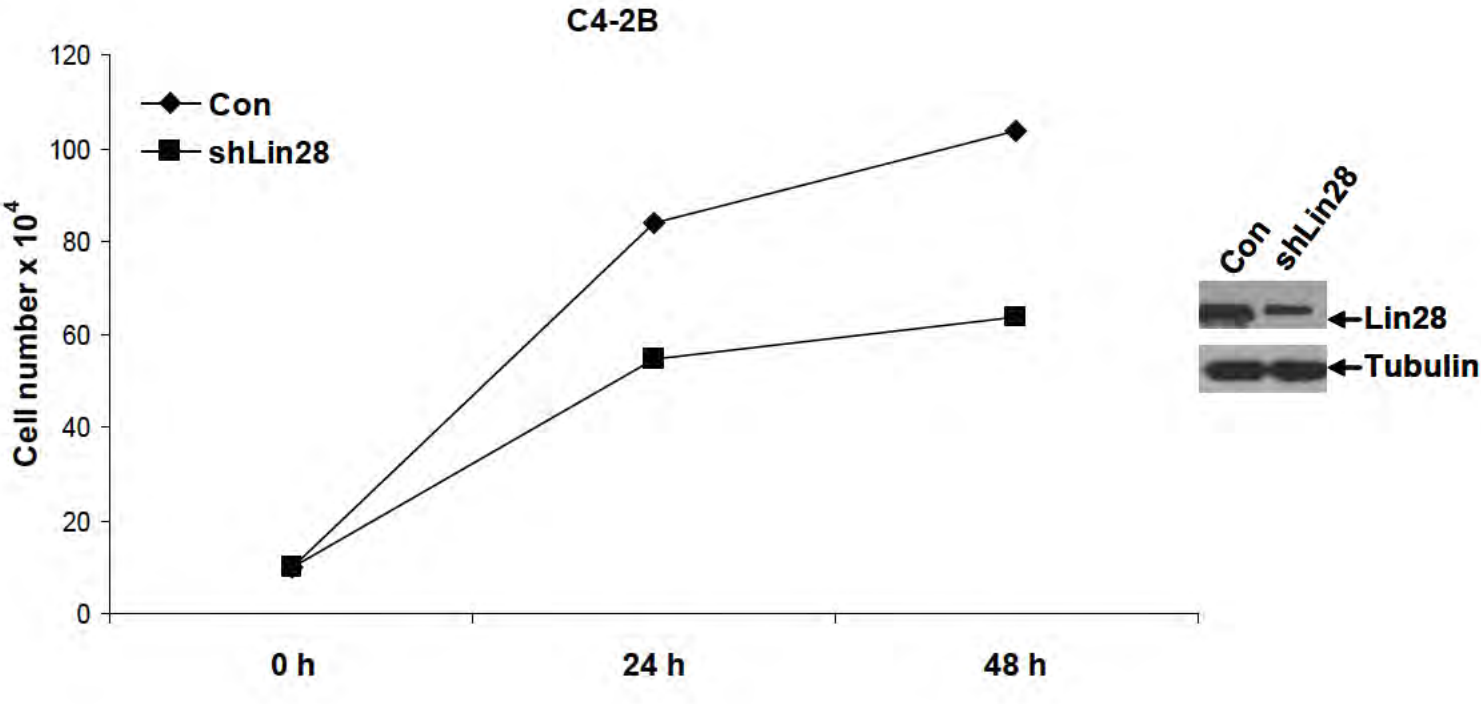

FIGURE 22

A

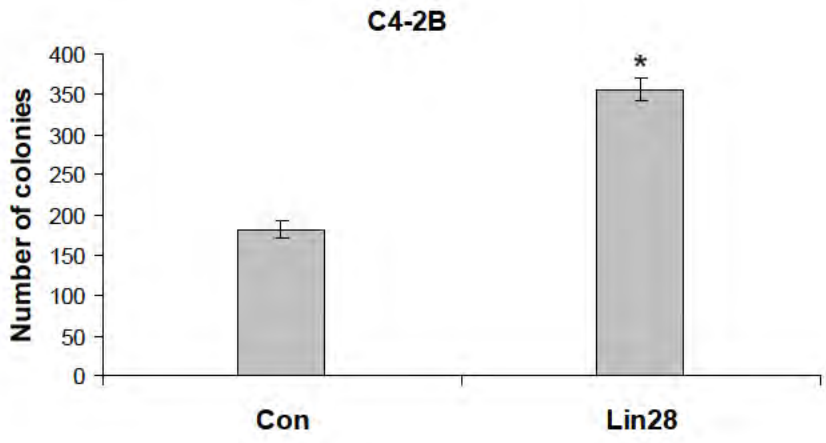

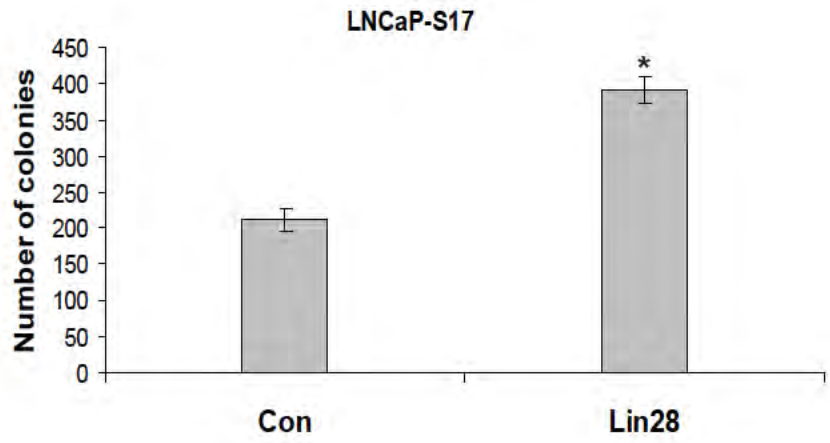

B

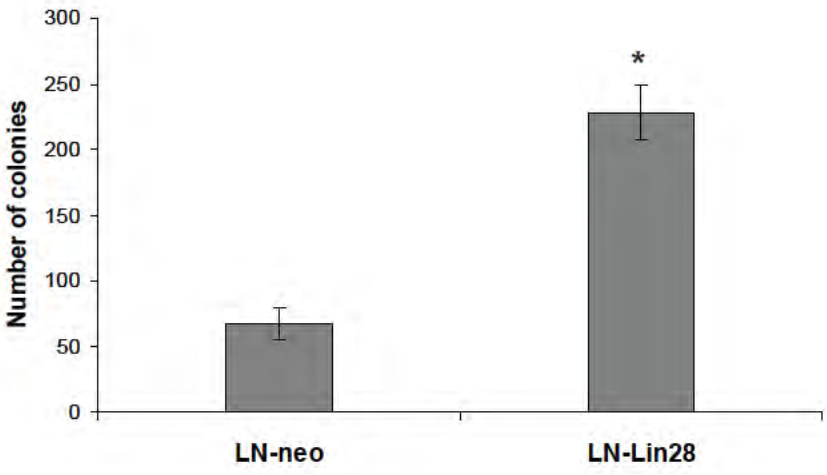

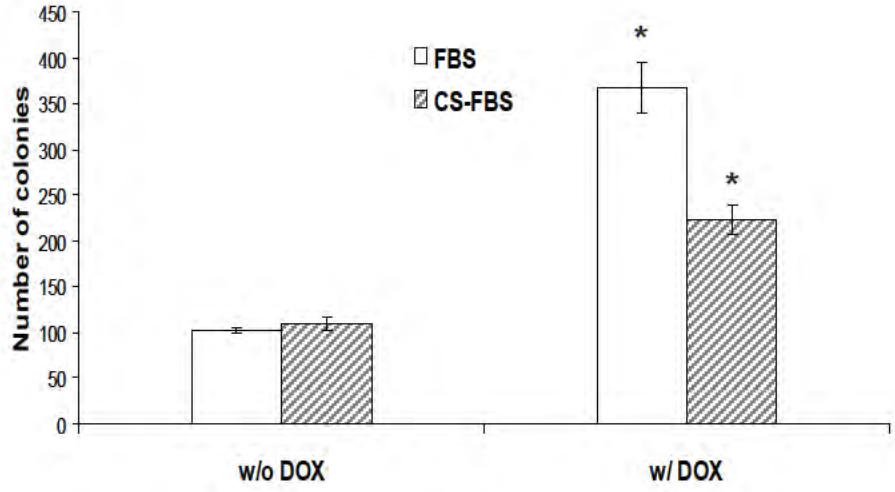

C

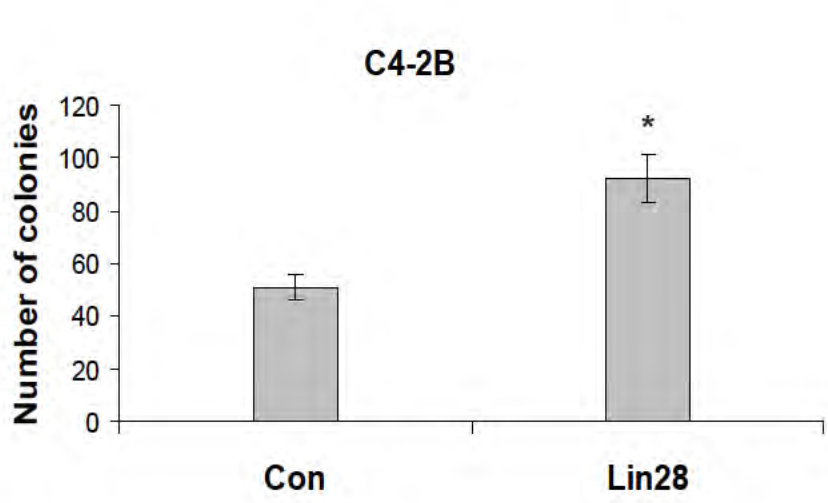

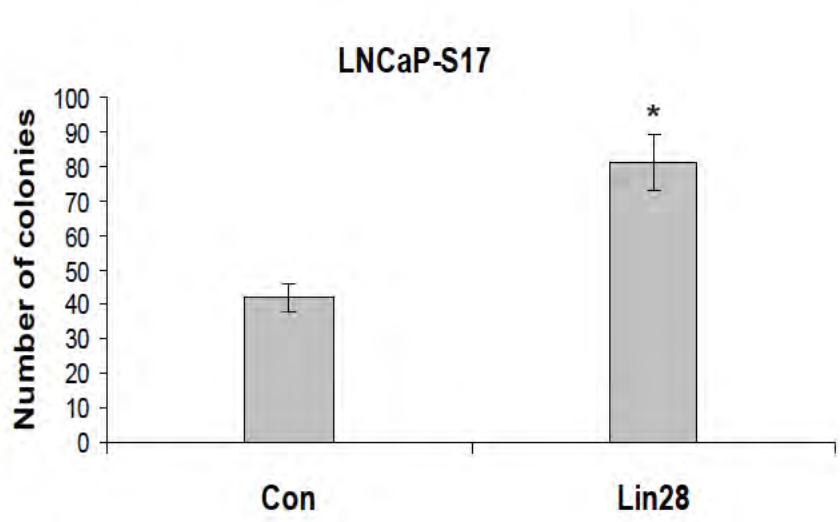

D

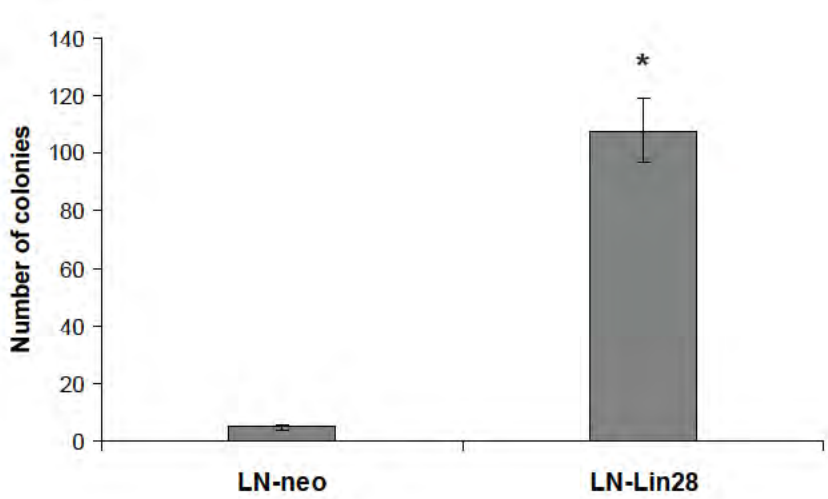

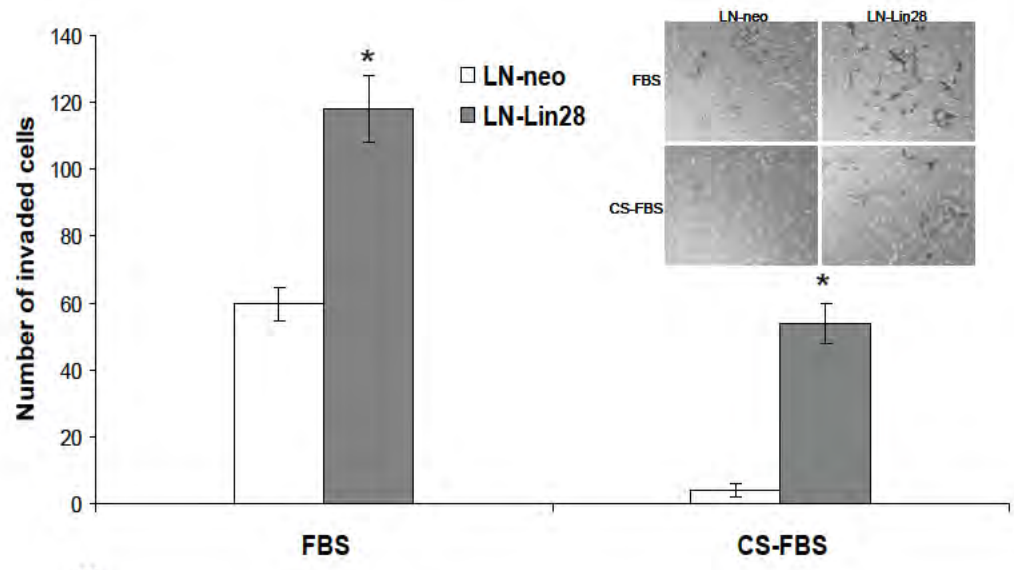

FIGURE 23

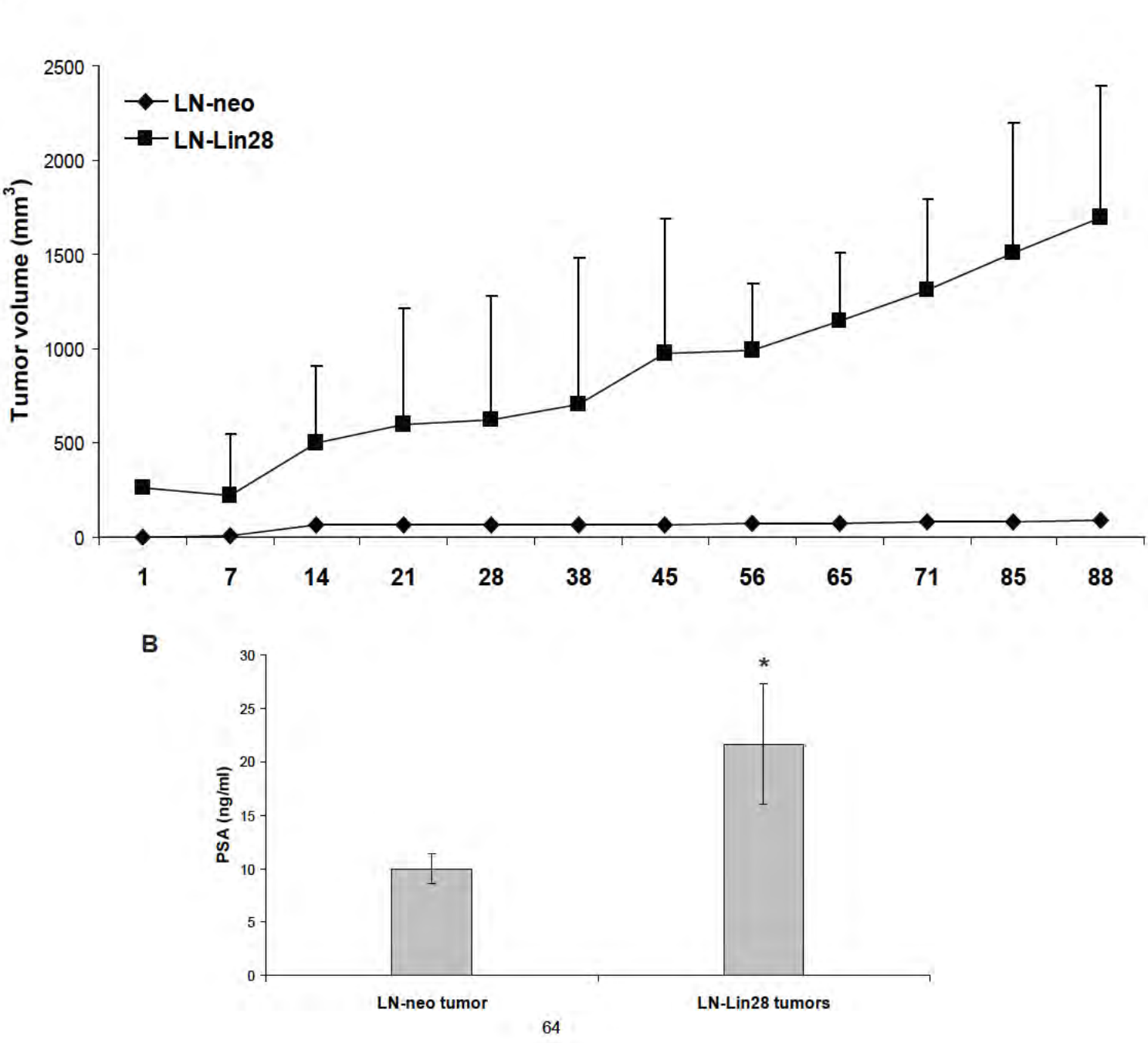
A
LN-neo
LN-Lin28
Tumor volume (mm3)
2500
2000
1500
1000
500
0
1
7
14
21
28
38
45
56
65
71
85
88
B
PSA (ng/ml)
30
25
20
15
10
5
0
*
LN-neo tumor
LN-Lin28 tumors

FIGURE 24

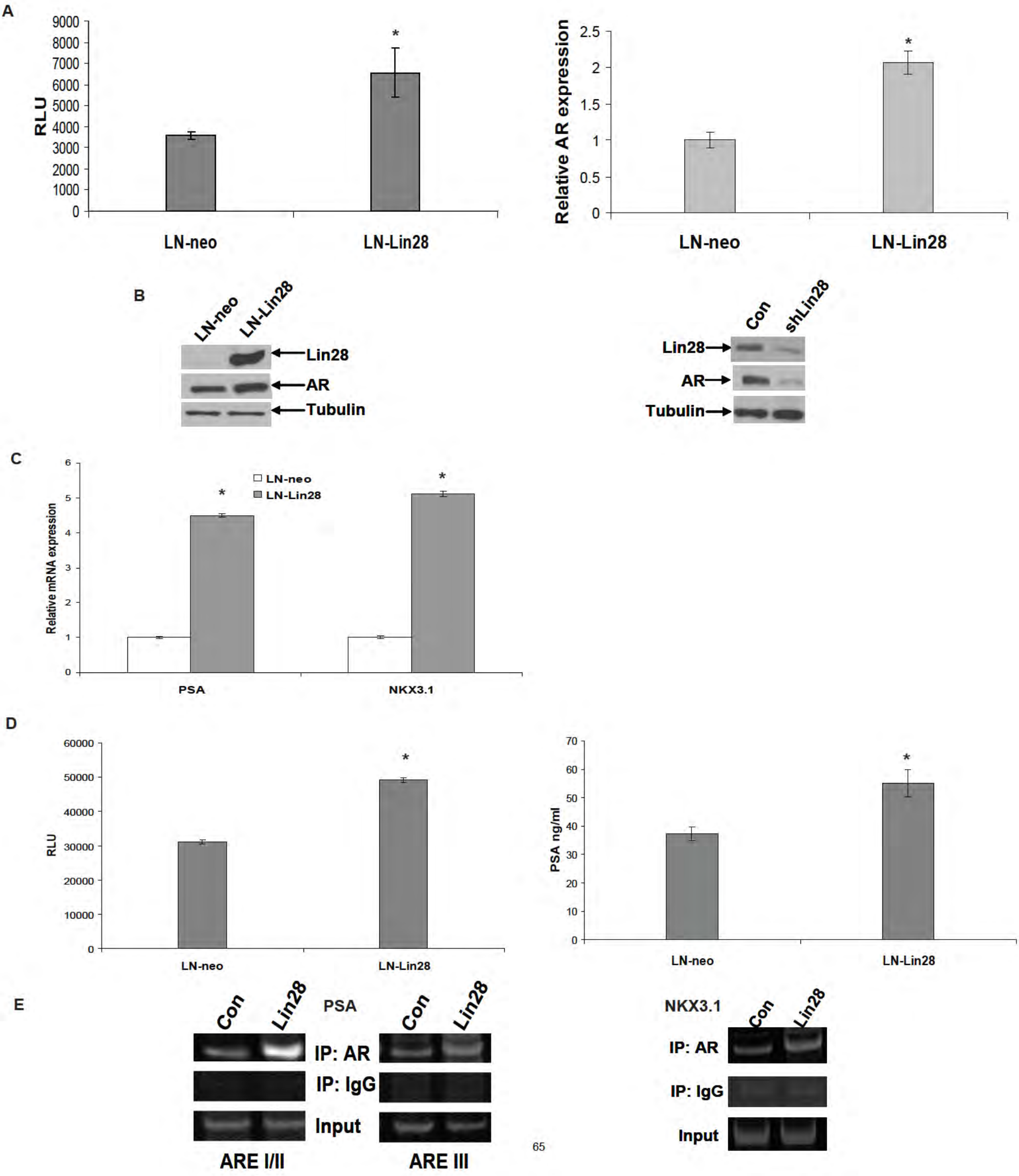
A
RLU
9000
8000
7000
6000
5000
4000
3000
2000
1000
0
*
LN-neo
LN-Lin28
Relative AR expression
2.5
2
1.5
1
0.5
0
*
LN-neo
LN-Lin28
B
LN-neo
LN-Lin28
Lin28
AR
Tubulin
Con
shLin28
Lin28
AR
Tubulin
C
Relative mRNA expression
6
5
4
3
2
1
0
LN-neo
LN-Lin28
*
*
PSA
NKX3.1
D
RLU
60000
50000
40000
30000
20000
10000
0
*
LN-neo
LN-Lin28
PSA ng/ml
70
60
50
40
30
20
10
0
*
LN-neo
LN-Lin28
E
Con
Lin28
PSA
Con
Lin28
IP: AR
IP: IgG
Input
ARE I/II
ARE III
NKX3.1
Con
Lin28
IP: AR
IP: IgG
Input

Figure 25

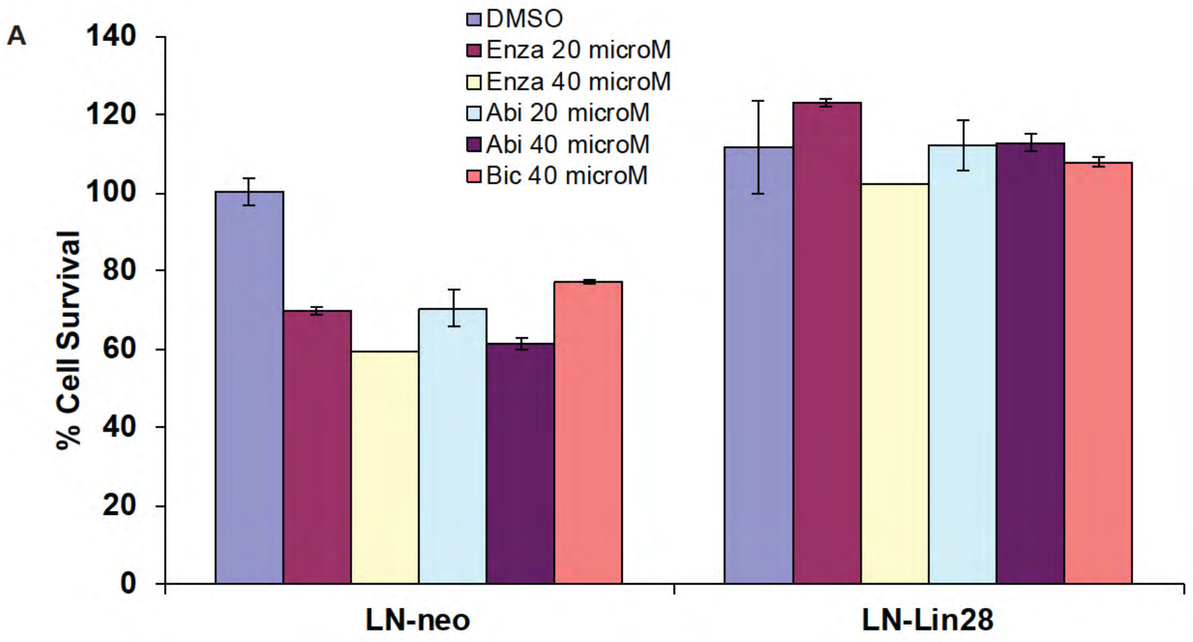
A
DMSO
Enza 20 microM
Enza 40 microM
Abi 20 microM
Abi 40 microM
Bic 40 microM
% Cell Survival
140
120
100
80
60
40
20
0
LN-neo
LN-Lin28

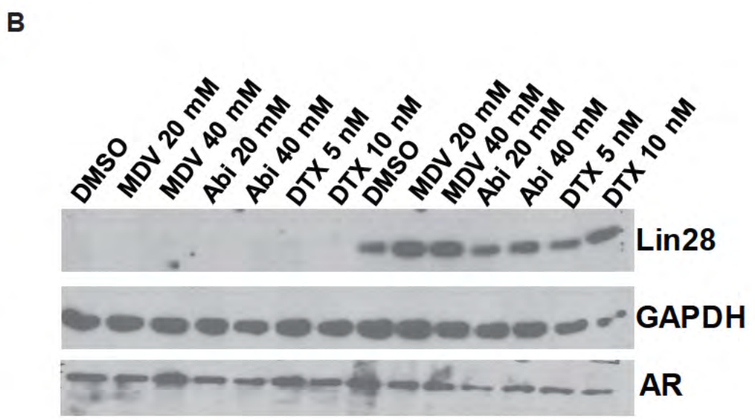
B
DMSO
MDV 20 mM
MDV 40 mM
Abi 20 mM
Abi 40 mM
DTX 5 nM
DTX 10 nM
DMSO
MDV 20 mM
MDV 40 mM
Abi 20 mM
Abi 40 mM
DTX 5 nM
DTX 10 nM
Lin28
GAPDH
AR

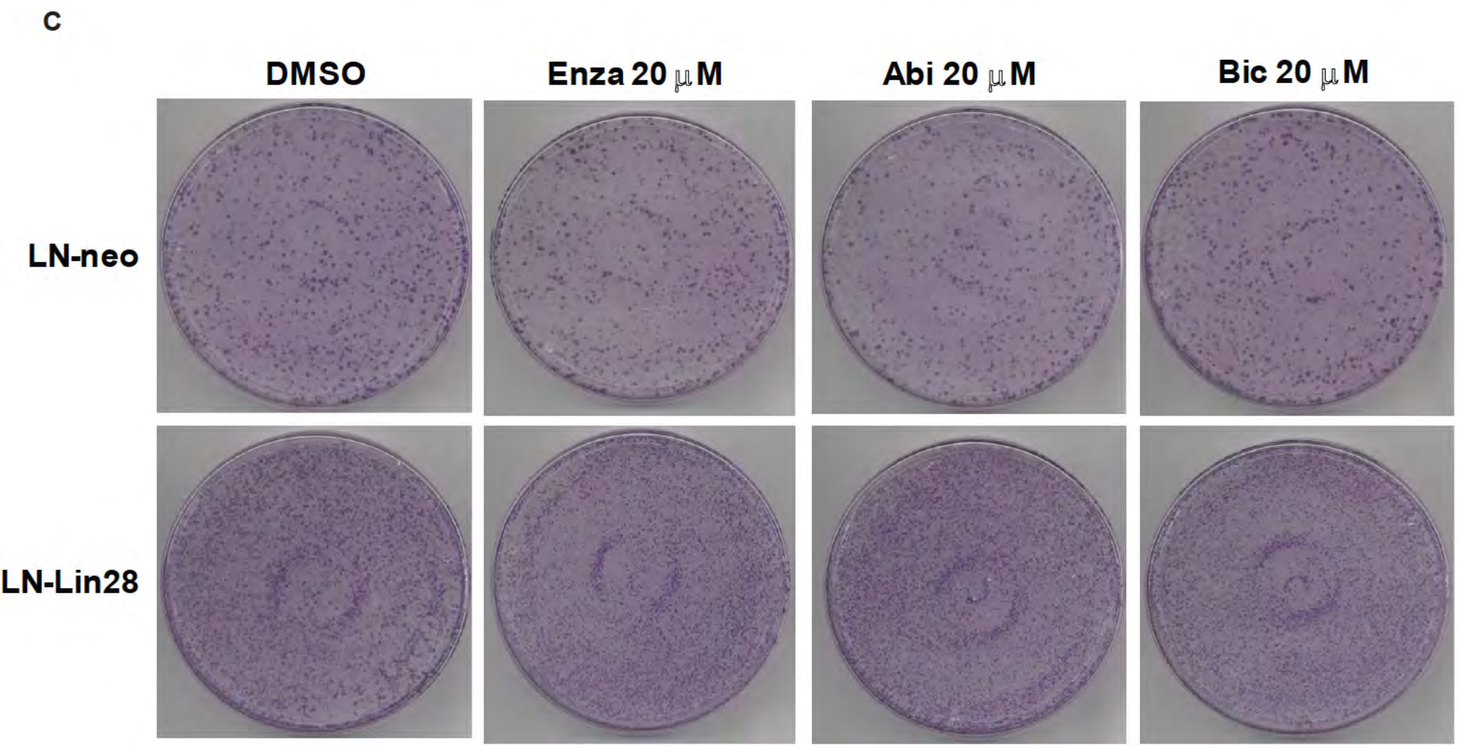
C
DMSO
Enza 20 μM
Abi 20 μM
Bic 20 μM
LN-neo
LN-Lin28

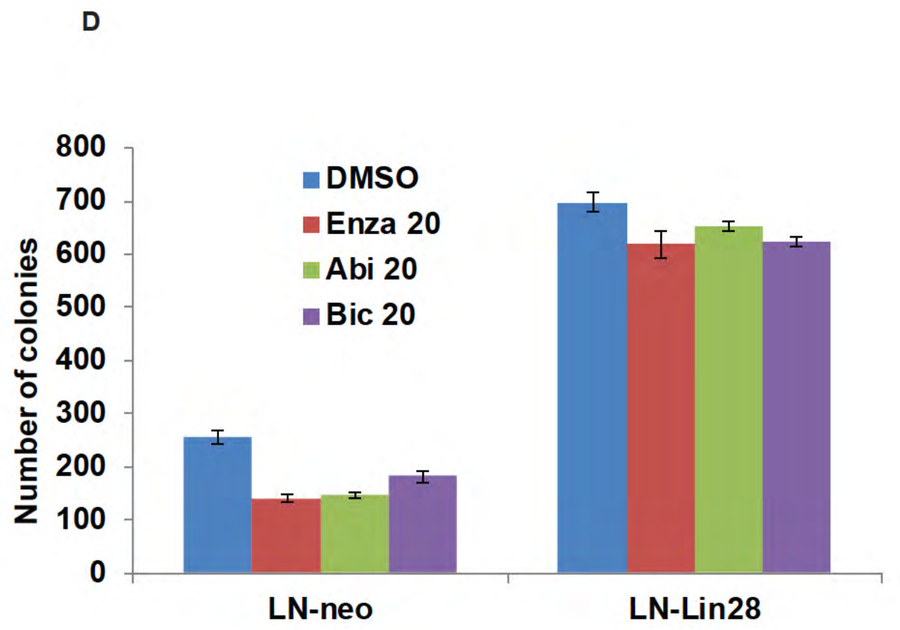
D
DMSO
Enza 20
Abi 20
Bic 20
Number of colonies
800
700
600
500
400
300
200
100
0
LN-neo
LN-Lin28

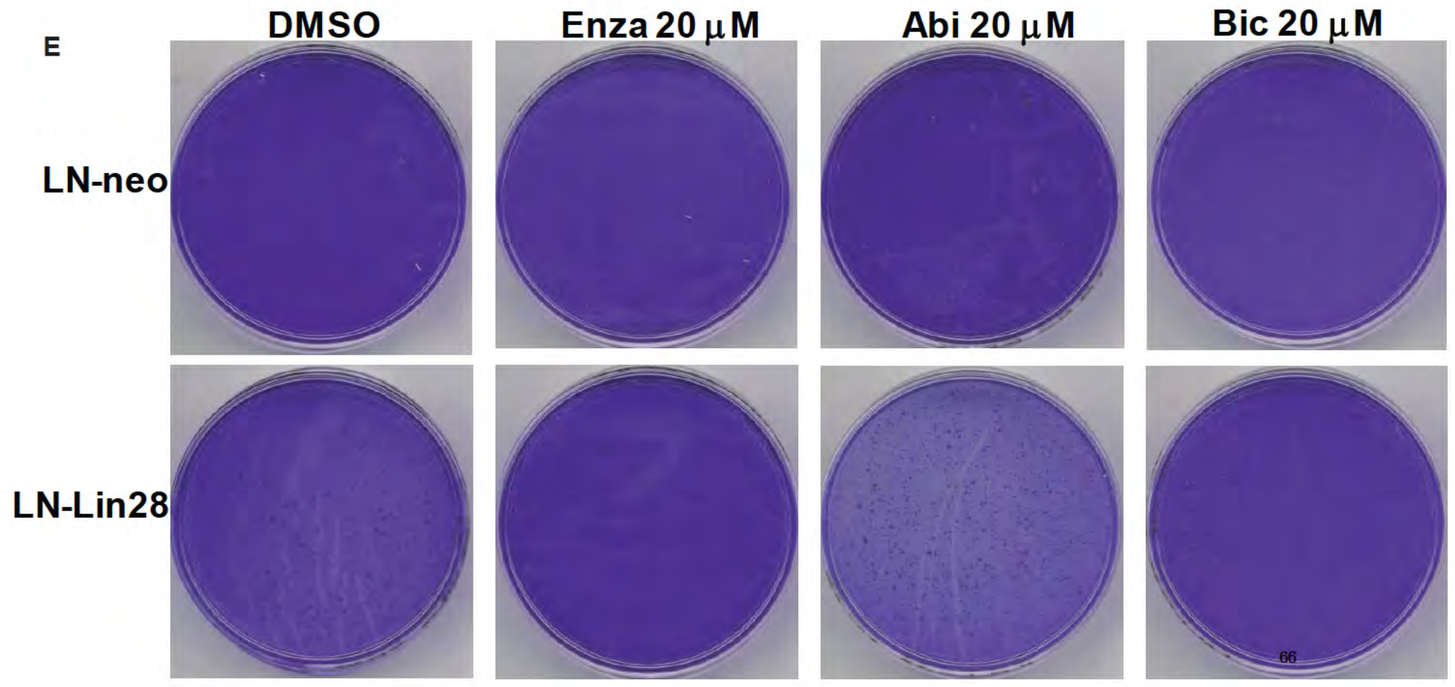
E
DMSO
Enza 20 μM
Abi 20 μM
Bic 20 μM
LN-neo
LN-Lin28

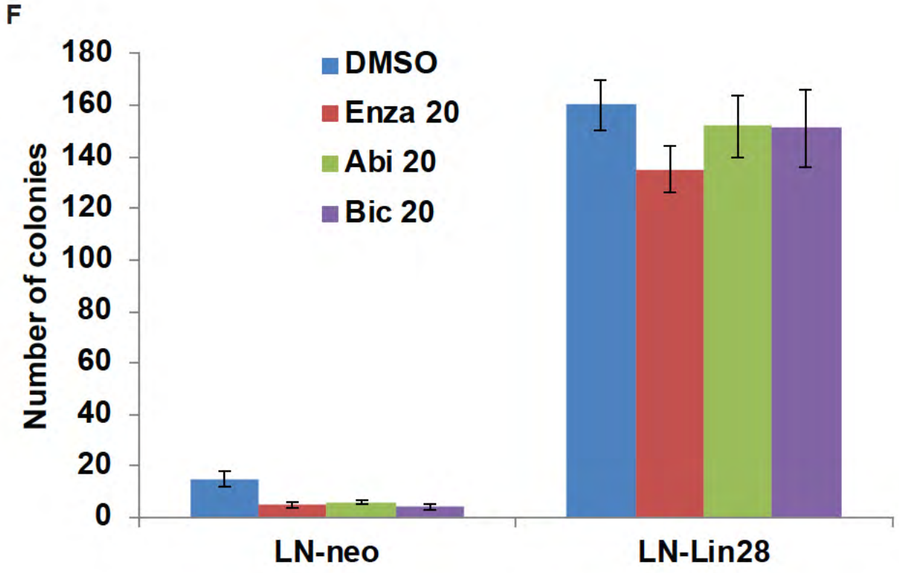
F
DMSO
Enza 20
Abi 20
Bic 20
Number of colonies
180
160
140
120
100
80
60
40
20
0
LN-neo
LN-Lin28

C

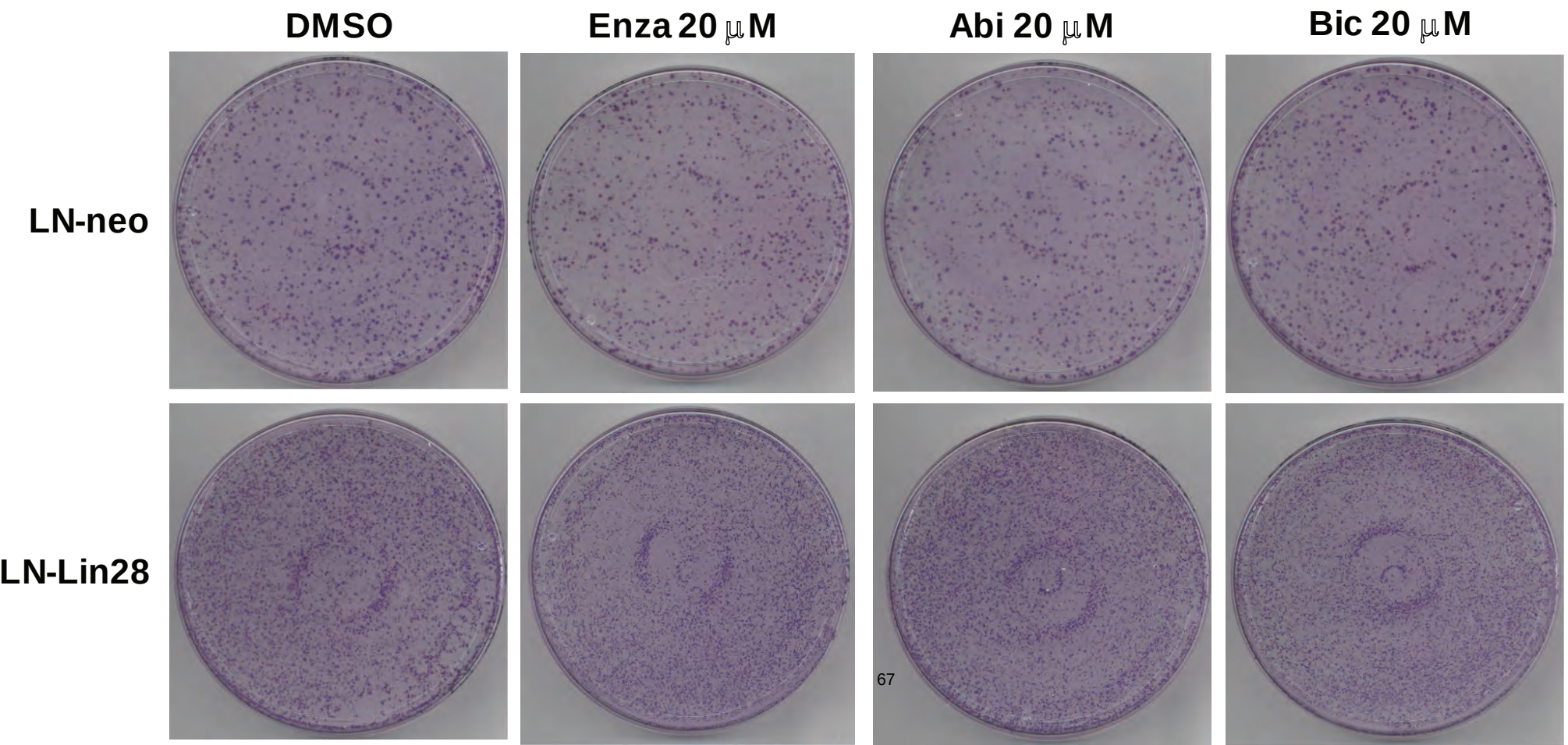

Figure 26

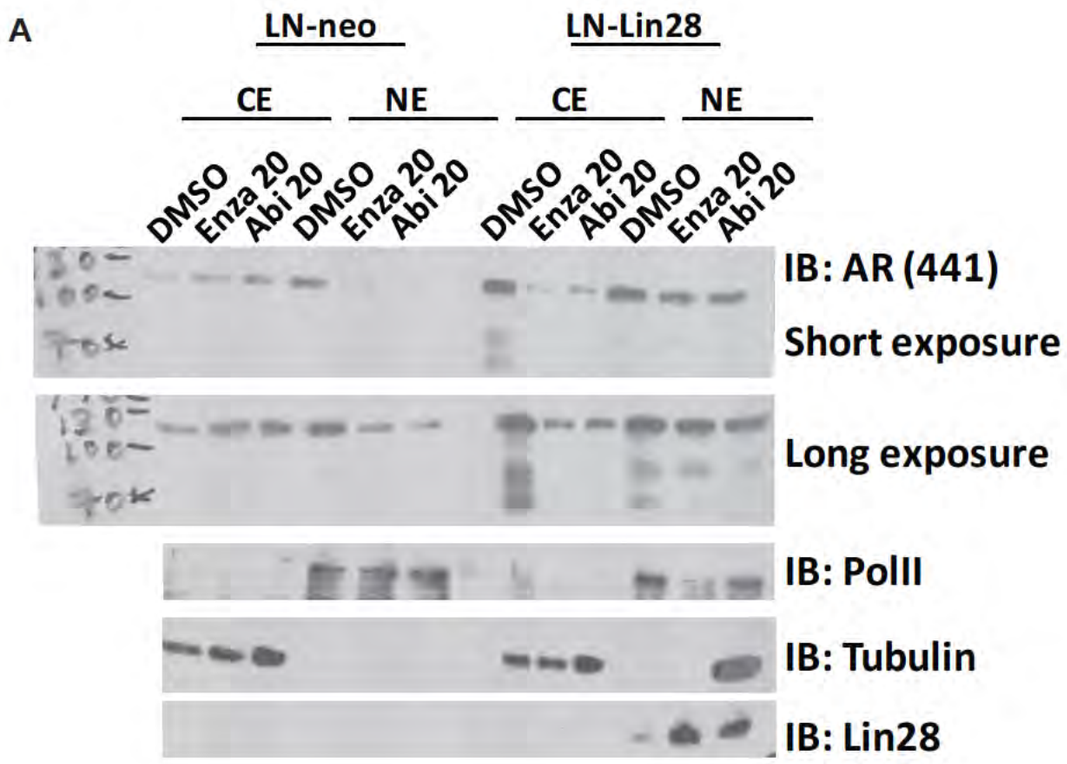
A
LN-neo
LN-Lin28
CE
NE
CE
NE
DMSO
Enza 20
Abi 20
DMSO
Enza 20
Abi 20
DMSO
Enza 20
Abi 20
DMSO
Enza 20
Abi 20
IB: AR (441)
Short exposure
Long exposure
IB: PolII
IB: Tubulin
IB: Lin28

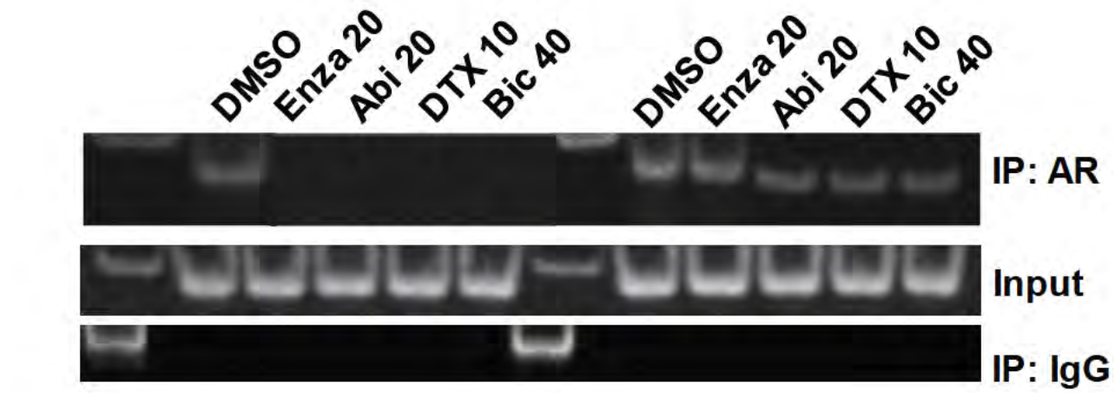
B
DMSO
Enza 20
Abi 20
DTX 10
Bic 40
DMSO
Enza 20
Abi 20
DTX 10
Bic 40
IP: AR
Input
IP: IgG

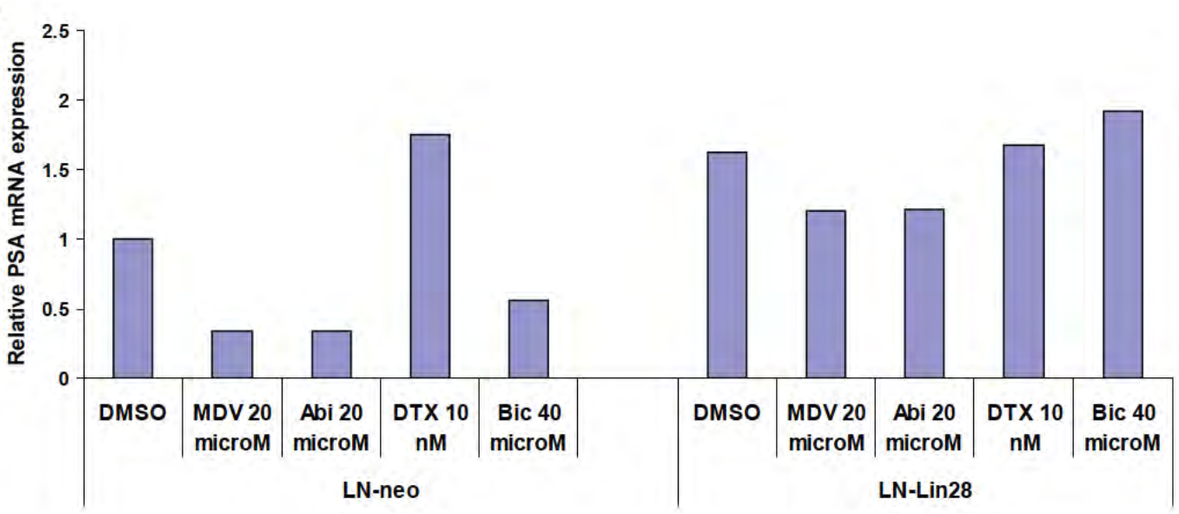
C
Relative PSA mRNA expression
2.5
2
1.5
1
0.5
0
DMSO
MDV 20 microM
Abi 20 microM
DTX 10 nM
Bic 40 microM
DMSO
MDV 20 microM
Abi 20 microM
DTX 10 nM
Bic 40 microM
LN-neo
LN-Lin28

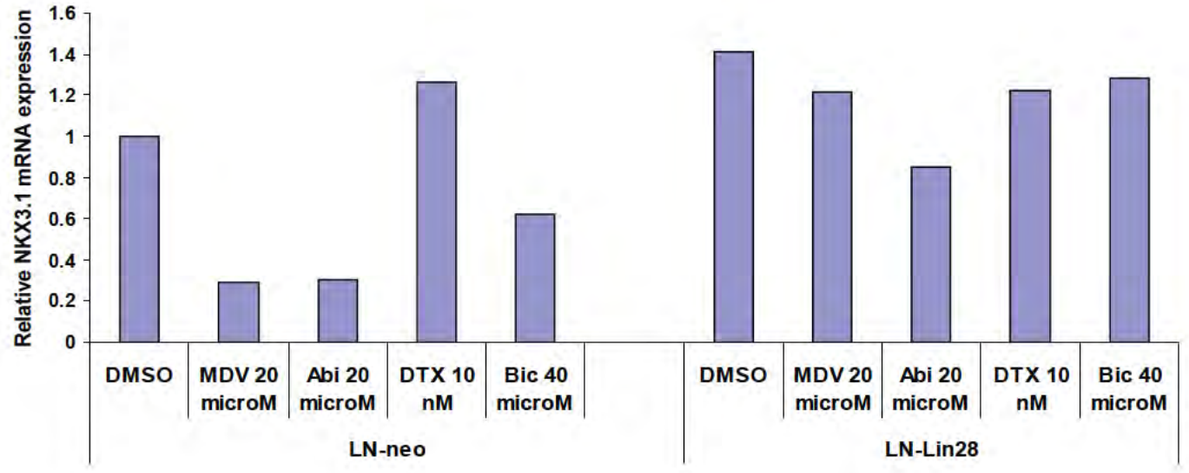
D
Relative NKX3.1 mRNA expression
1.6
1.4
1.2
1
0.8
0.6
0.4
0.2
0
DMSO
MDV 20 microM
Abi 20 microM
DTX 10 nM
Bic 40 microM
DMSO
MDV 20 microM
Abi 20 microM
DTX 10 nM
Bic 40 microM
LN-neo
LN-Lin28

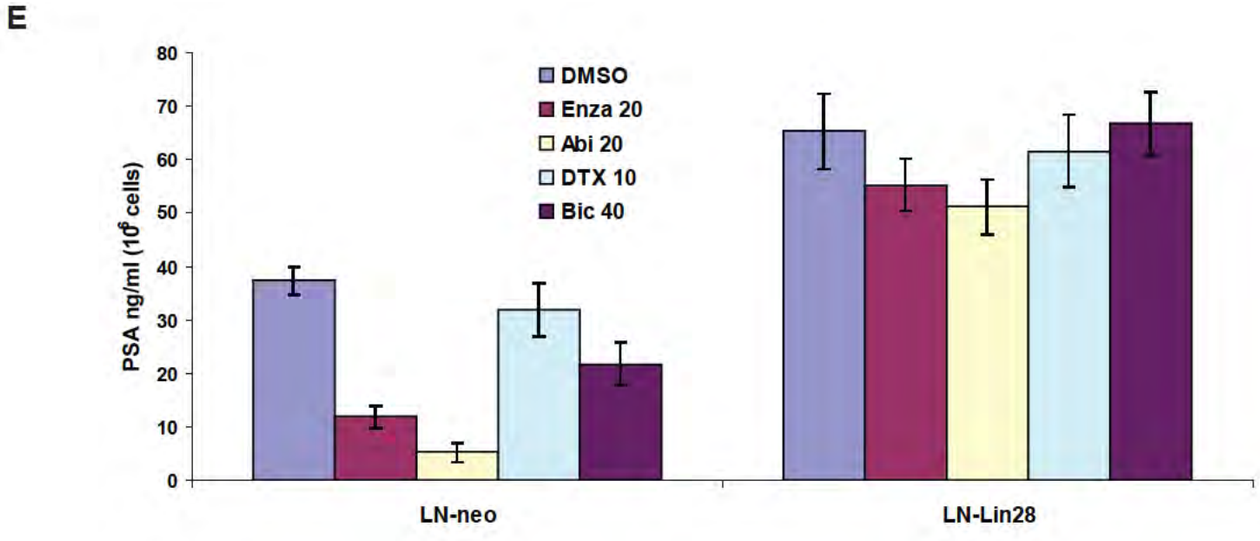
E
PSA ng/ml (10^6 cells)
80
70
60
50
40
30
20
10
0
DMSO
Enza 20
Abi 20
DTX 10
Bic 40
LN-neo
LN-Lin28

Figure 27

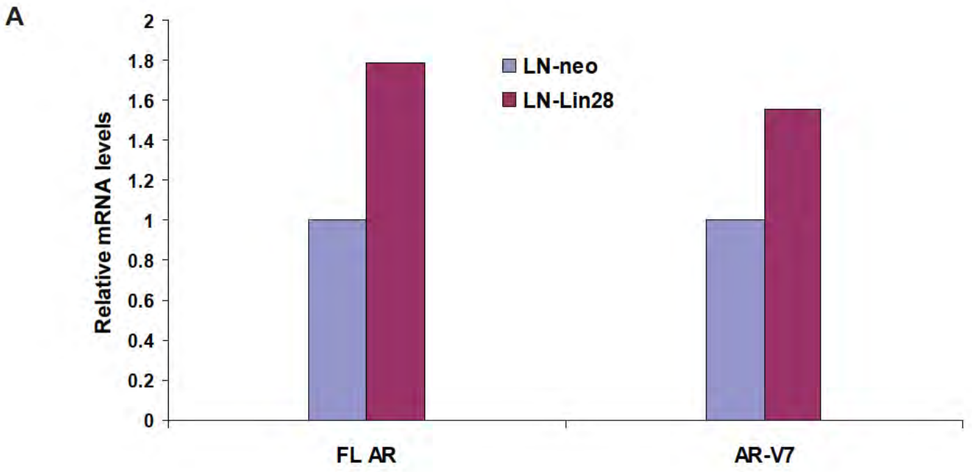
A
Relative mRNA levels
2
1.8
1.6
1.4
1.2
1
0.8
0.6
0.4
0.2
0
LN-neo
LN-Lin28
FL AR
AR-V7

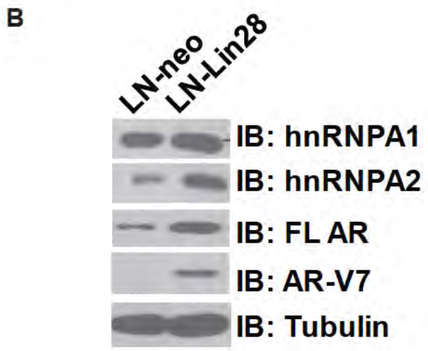
B
LN-neo
LN-Lin28
IB: hnRNPA1
IB: hnRNPA2
IB: FL AR
IB: AR-V7
IB: Tubulin

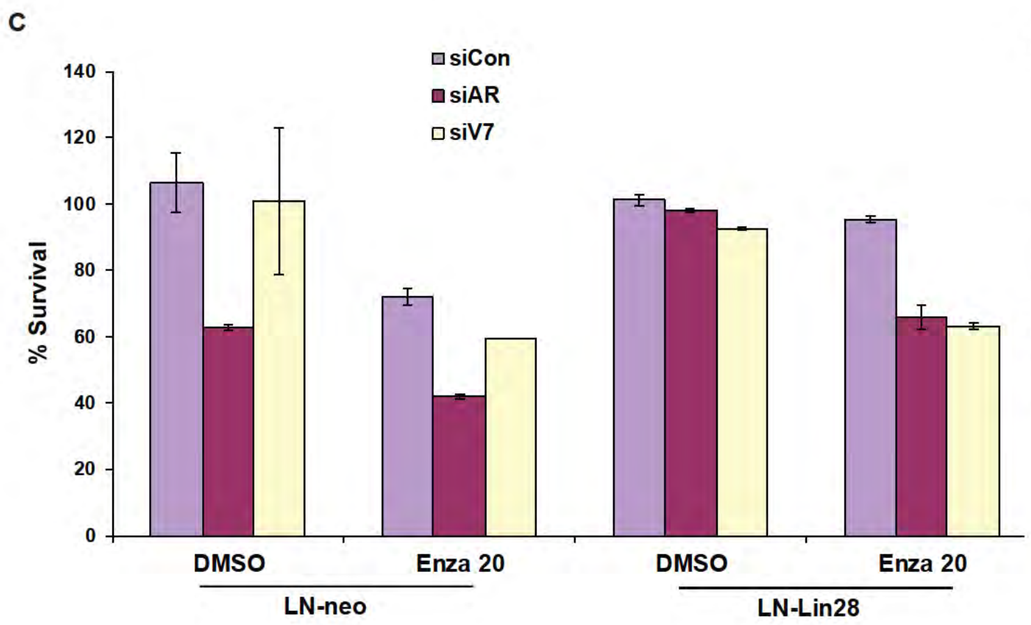
C
% Survival
140
120
100
80
60
40
20
0
siCon
siAR
siV7
DMSO
Enza 20
DMSO
Enza 20
LN-neo
LN-Lin28

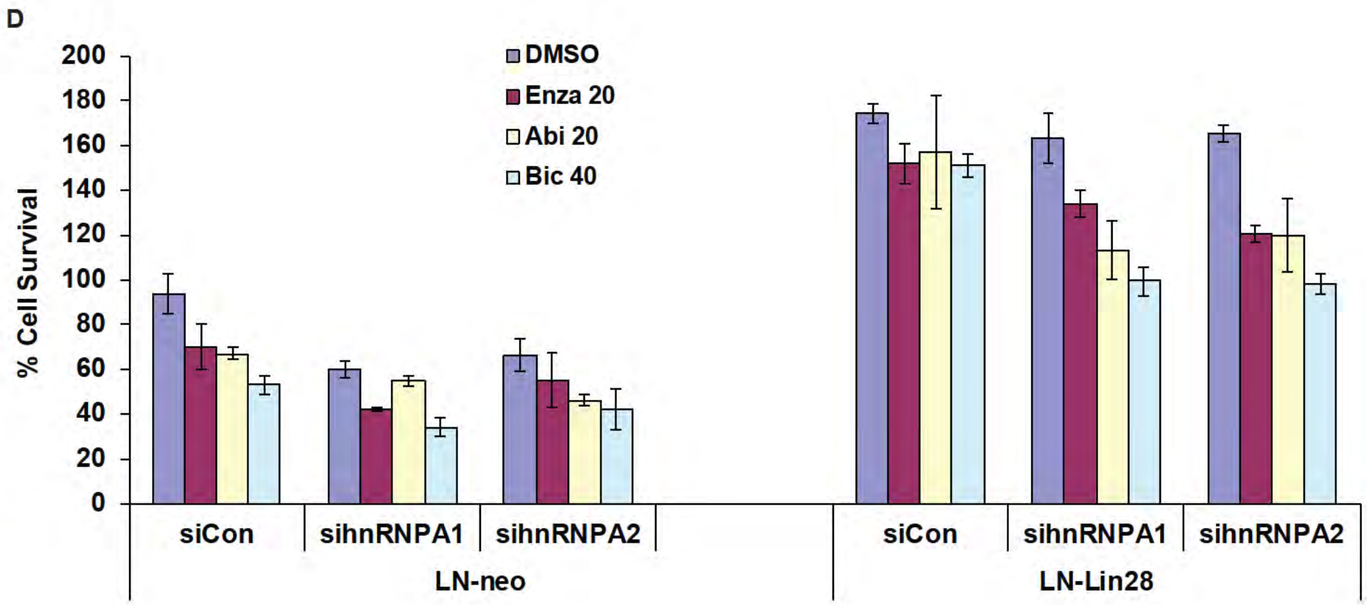
D
% Cell Survival
200
180
160
140
120
100
80
60
40
20
0
DMSO
Enza 20
Abi 20
Bic 40
siCon
sihnRNPA1
sihnRNPA2
siCon
sihnRNPA1
sihnRNPA2
LN-neo
LN-Lin28

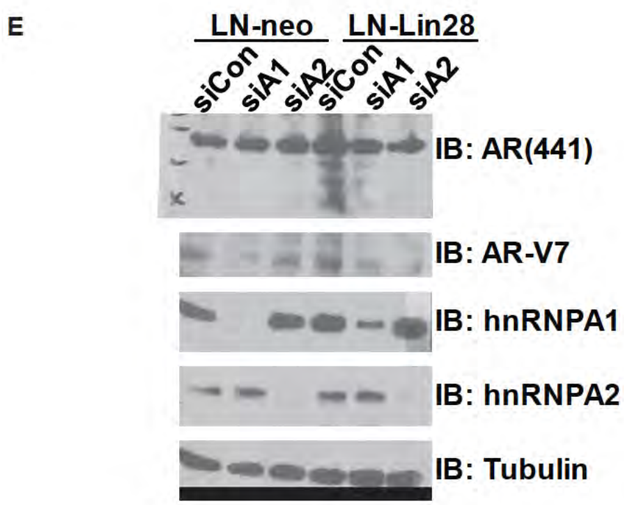
E
LN-neo
LN-Lin28
siCon
siA1
siA2
siCon
siA1
siA2
IB: AR(441)
IB: AR-V7
IB: hnRNPA1
IB: hnRNPA2
IB: Tubulin

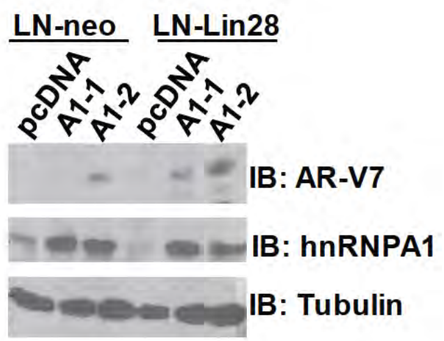
F
LN-neo
LN-Lin28
pcDNA
A1-1
A1-2
pcDNA
A1-1
A1-2
IB: AR-V7
IB: hnRNPA1
IB: Tubulin

Figure 28

A

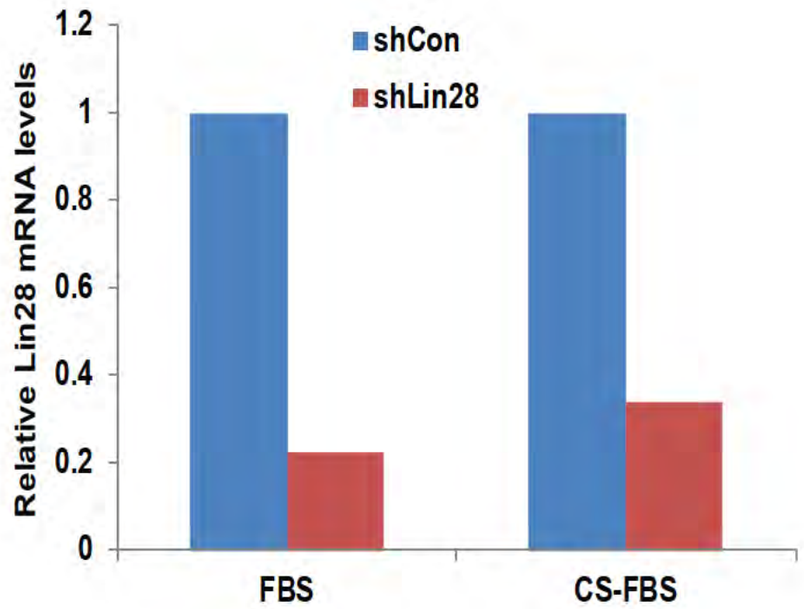

B

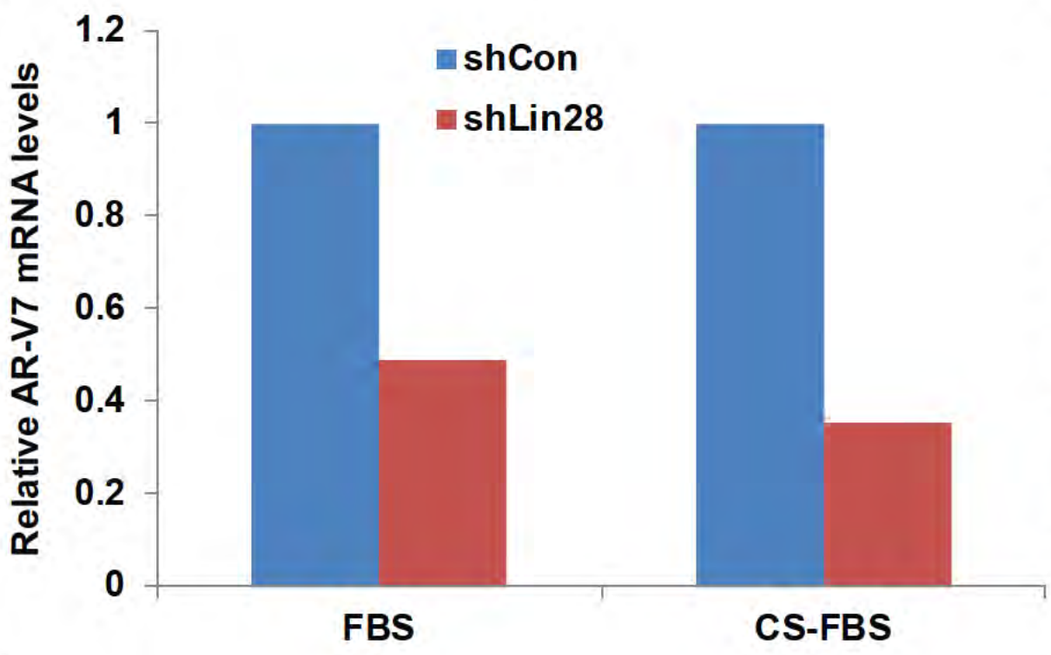

C

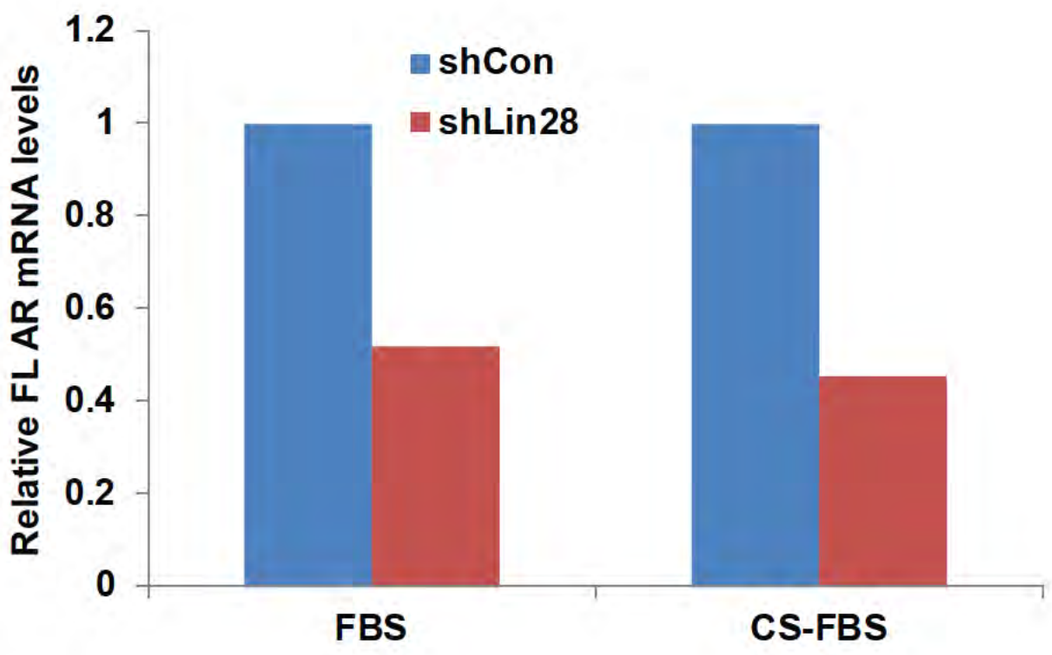

D

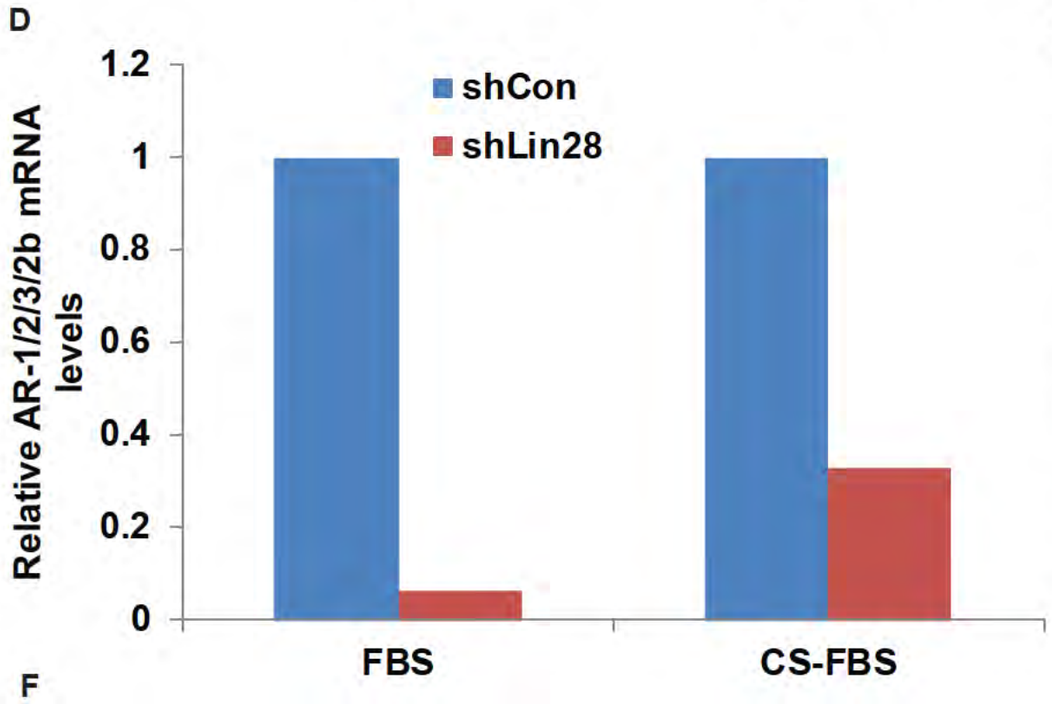

E

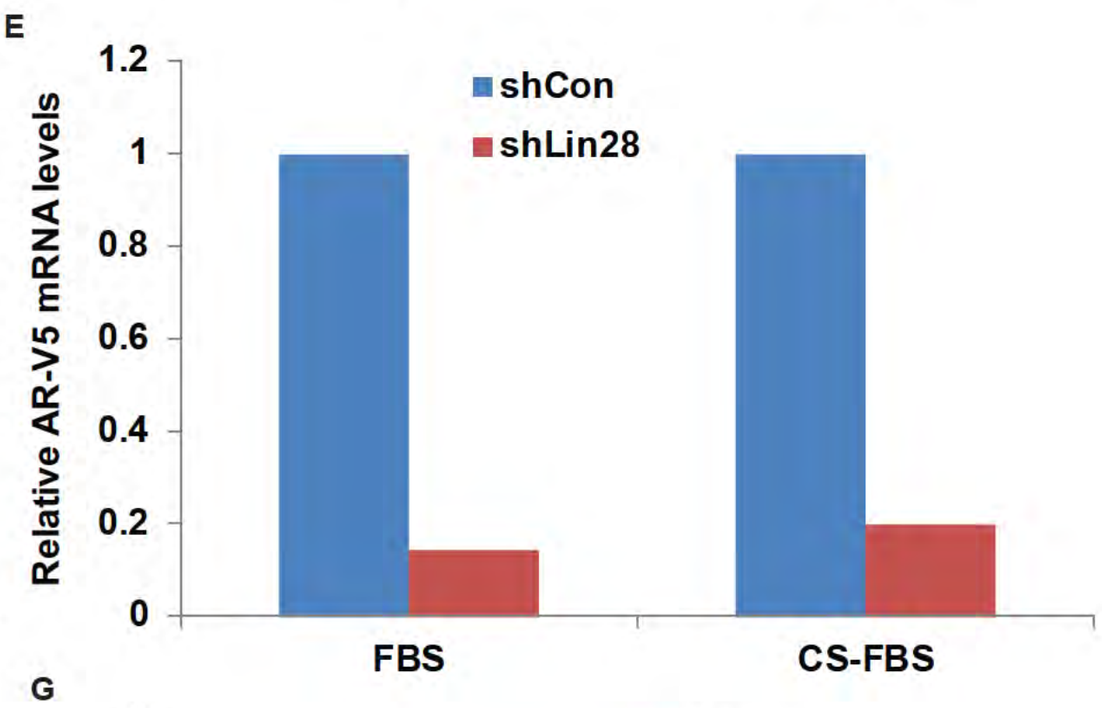

F

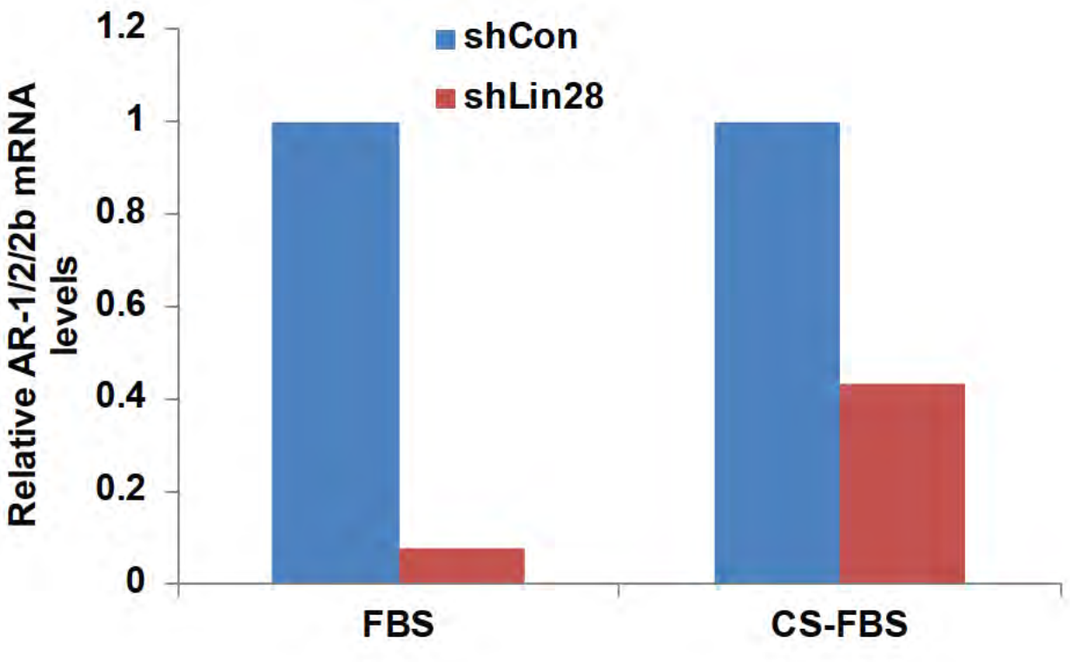

G

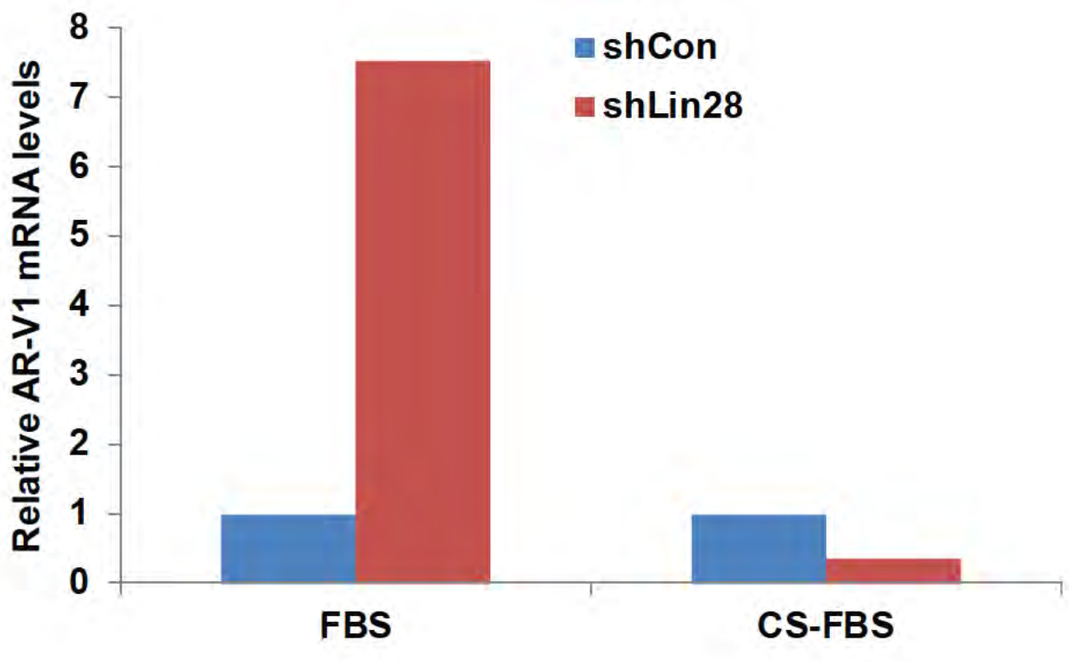

Figure 29

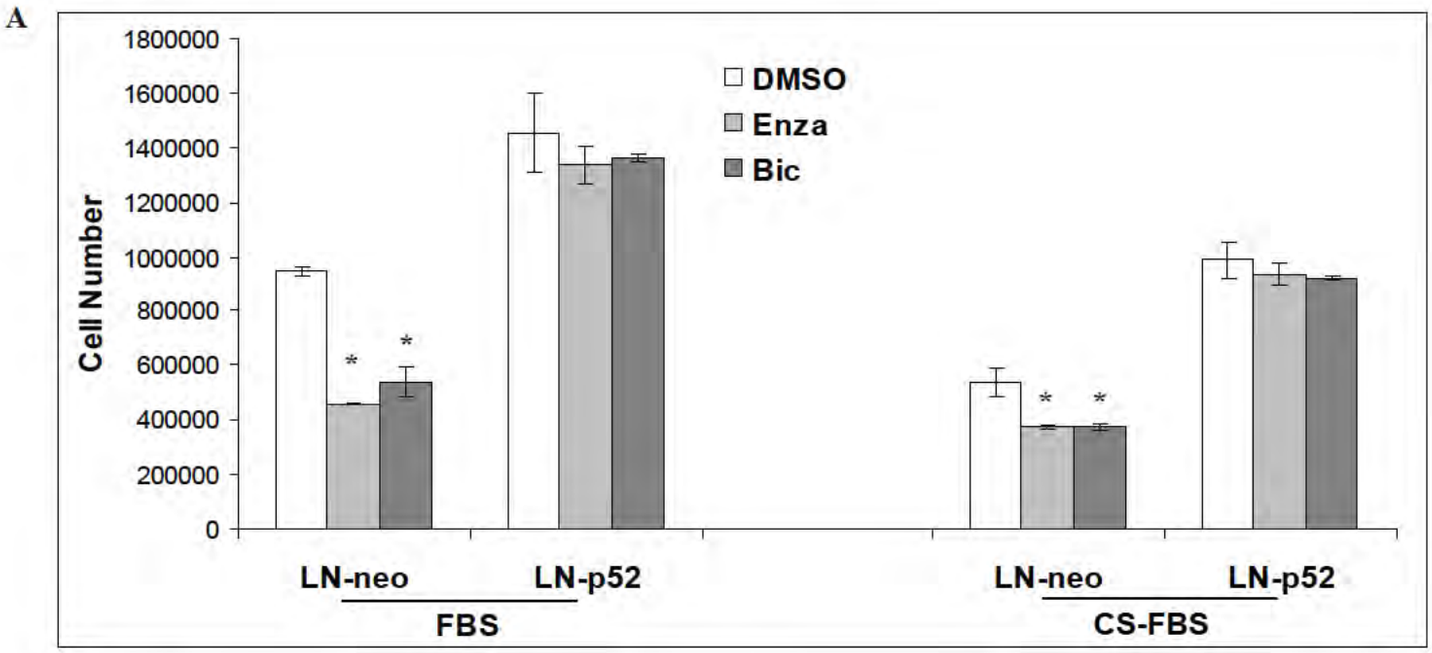
A
1800000
1600000
1400000
1200000
1000000
800000
600000
400000
200000
0
Cell Number
DMSO
Enza
Bic
*
LN-neo
LN-p52
FBS
CS-FBS

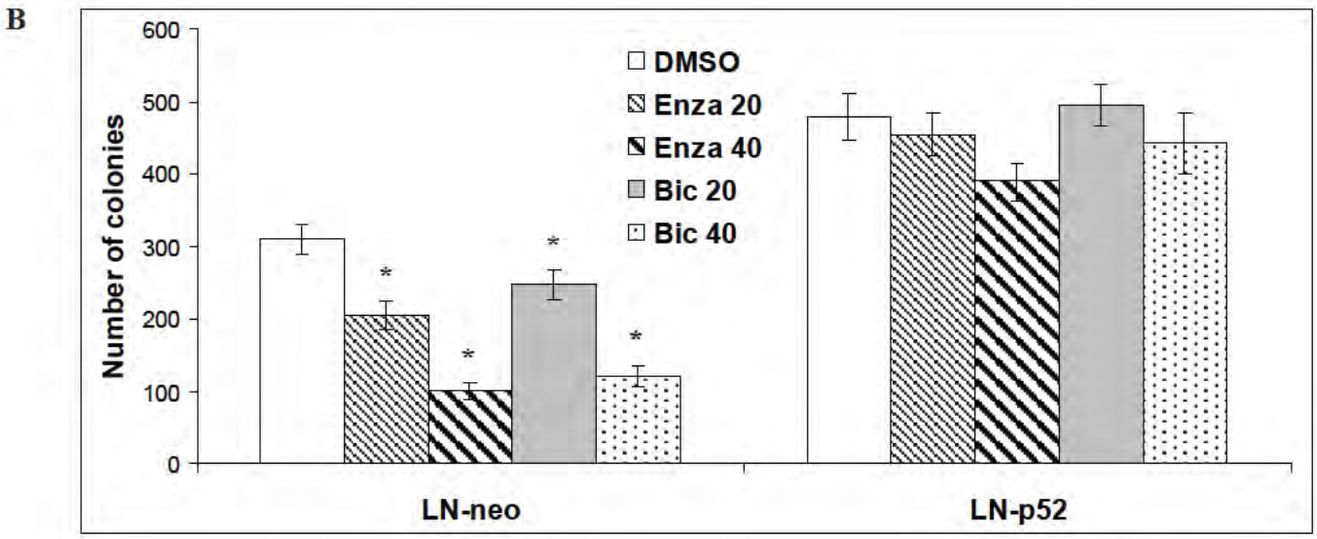
B
600
500
400
300
200
100
0
Number of colonies
DMSO
Enza 20
Enza 40
Bic 20
Bic 40
*
LN-neo
LN-p52

Figure 30

A

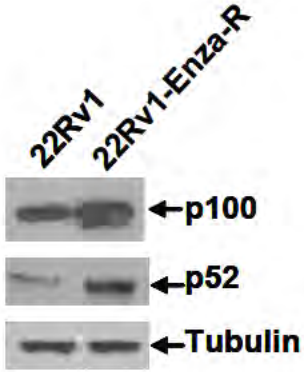
22Rv1
22Rv1-Enza-R
p100
p52
Tubulin

B

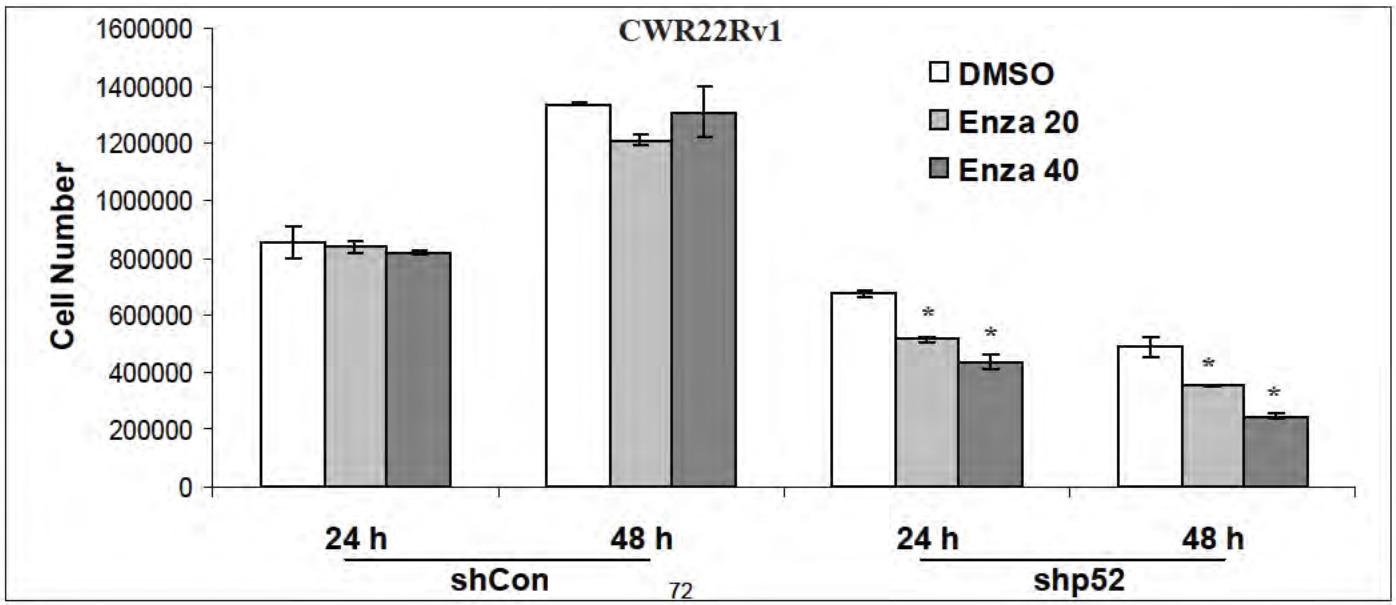
CWR22Rv1
Cell Number
1600000
1400000
1200000
1000000
800000
600000
400000
200000
0
DMSO
Enza 20
Enza 40
*
24 h
48 h
24 h
48 h
shCon
shp52

Figure 31

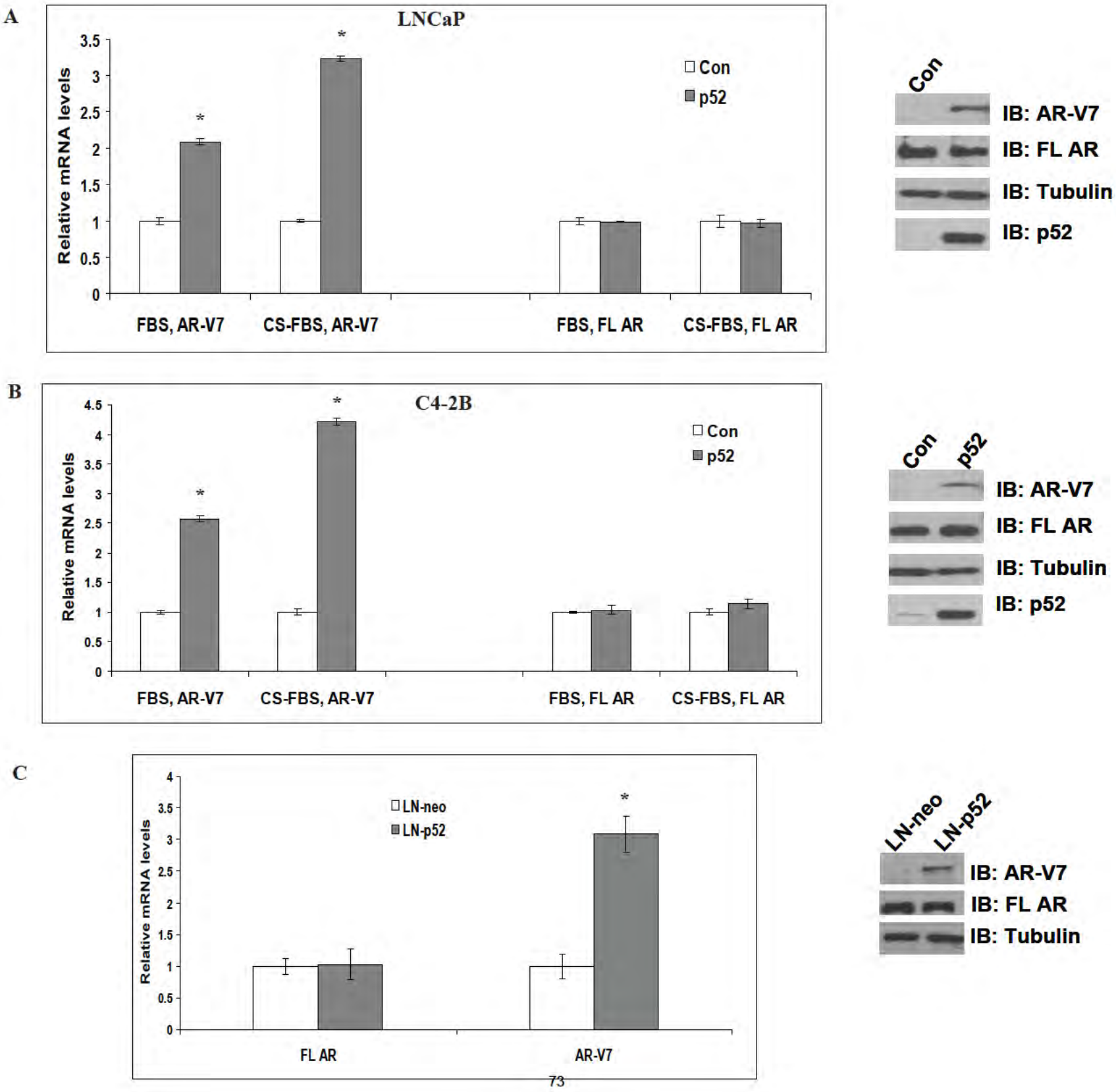
A
LNCaP
Relative mRNA levels
3.5
3
2.5
2
1.5
1
0.5
0
*
*
Con
p52
FBS, AR-V7
CS-FBS, AR-V7
FBS, FL AR
CS-FBS, FL AR
Con
IB: AR-V7
IB: FL AR
IB: Tubulin
IB: p52
B
C4-2B
Relative mRNA levels
4.5
4
3.5
3
2.5
2
1.5
1
0.5
0
*
*
Con
p52
FBS, AR-V7
CS-FBS, AR-V7
FBS, FL AR
CS-FBS, FL AR
Con
p52
IB: AR-V7
IB: FL AR
IB: Tubulin
IB: p52
C
Relative mRNA levels
4
3.5
3
2.5
2
1.5
1
0.5
0
*
LN-neo
LN-p52
FL AR
AR-V7
LN-neo
LN-p52
IB: AR-V7
IB: FL AR
IB: Tubulin

Figure 32

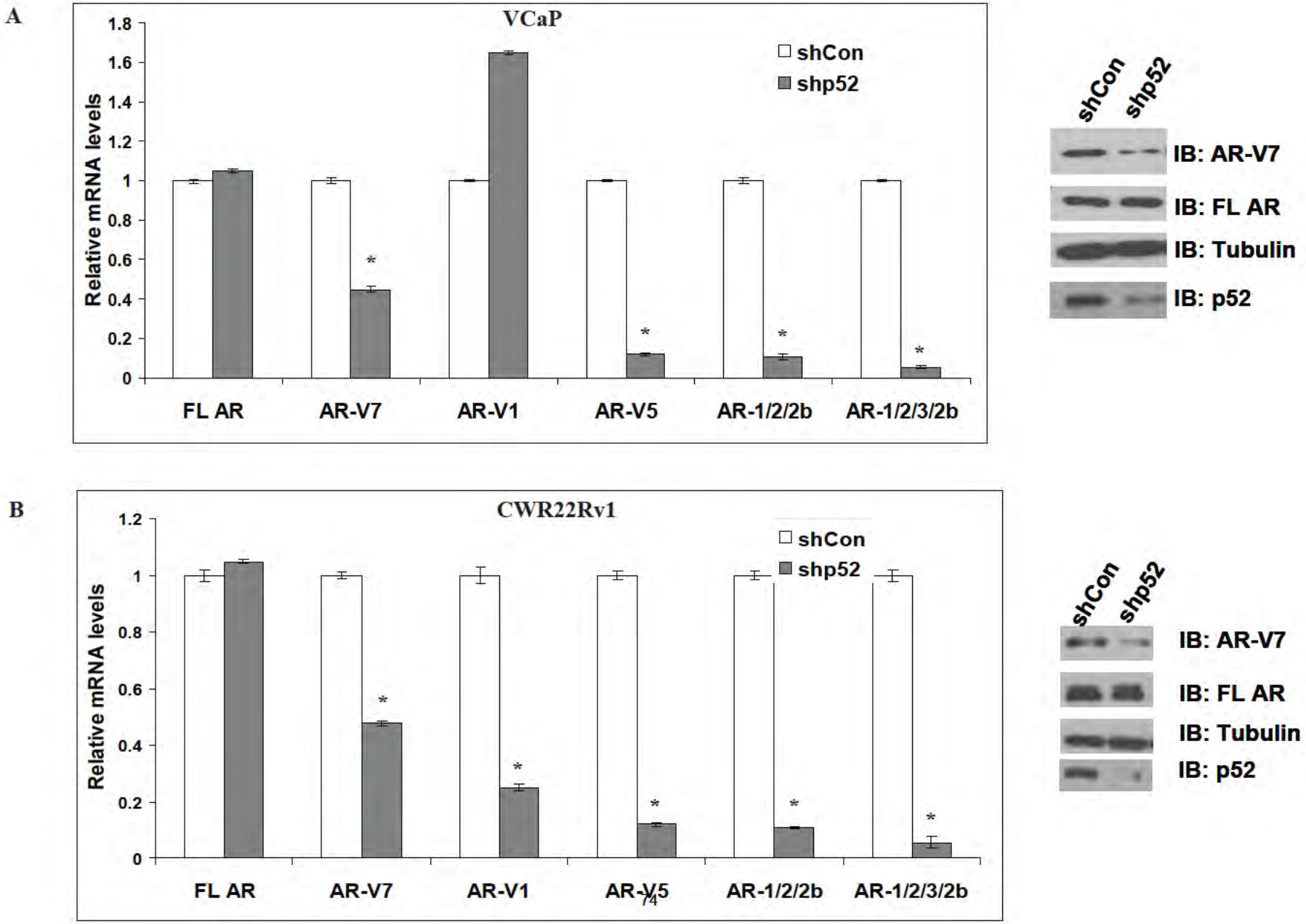
A
VCaP
Relative mRNA levels
1.8
1.6
1.4
1.2
1
0.8
0.6
0.4
0.2
0
shCon
shp52
*
FL AR
AR-V7
AR-V1
AR-V5
AR-1/2/2b
AR-1/2/3/2b
shCon
shp52
IB: AR-V7
IB: FL AR
IB: Tubulin
IB: p52
B
CWR22Rv1
Relative mRNA levels
1.2
1
0.8
0.6
0.4
0.2
0
shCon
shp52
*
FL AR
AR-V7
AR-V1
AR-V5
AR-1/2/2b
AR-1/2/3/2b
shCon
shp52
IB: AR-V7
IB: FL AR
IB: Tubulin
IB: p52

Figure 33

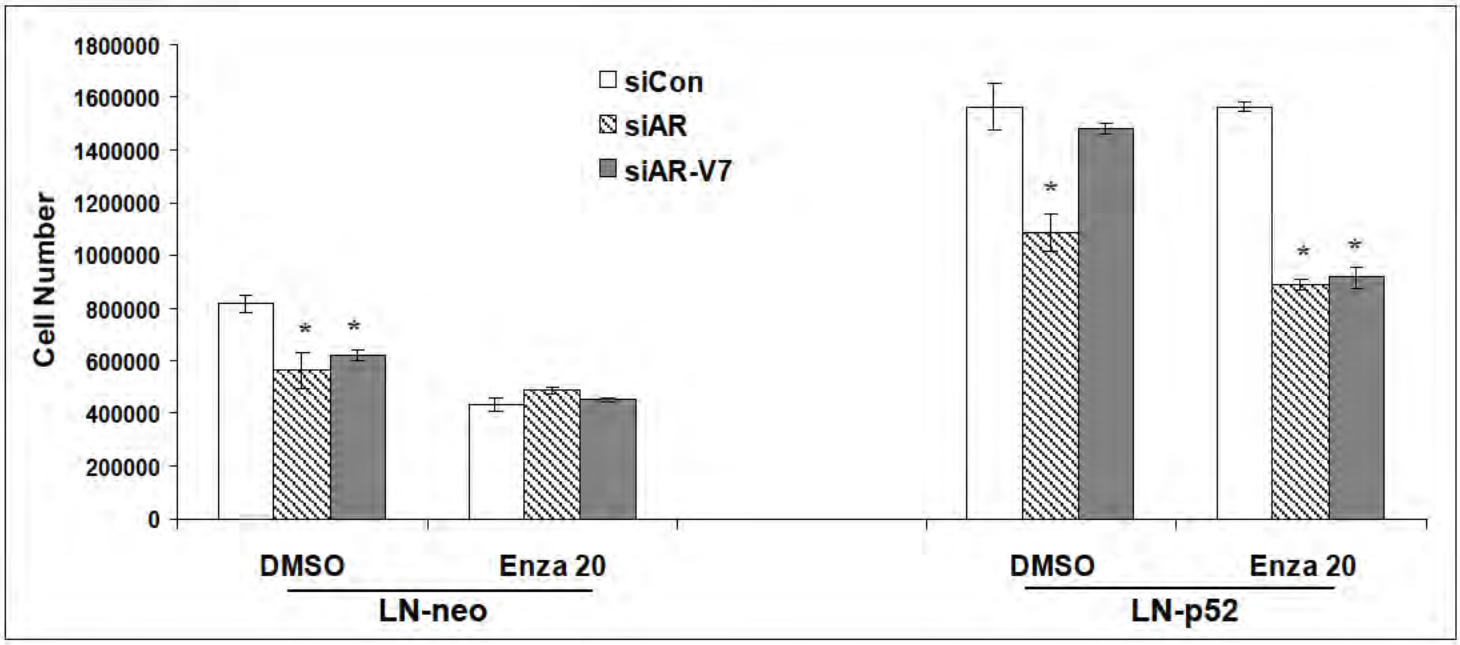
A
1800000
1600000
1400000
1200000
1000000
800000
600000
400000
200000
0
Cell Number
siCon
siAR
siAR-V7
*
DMSO
Enza 20
LN-neo
LN-p52

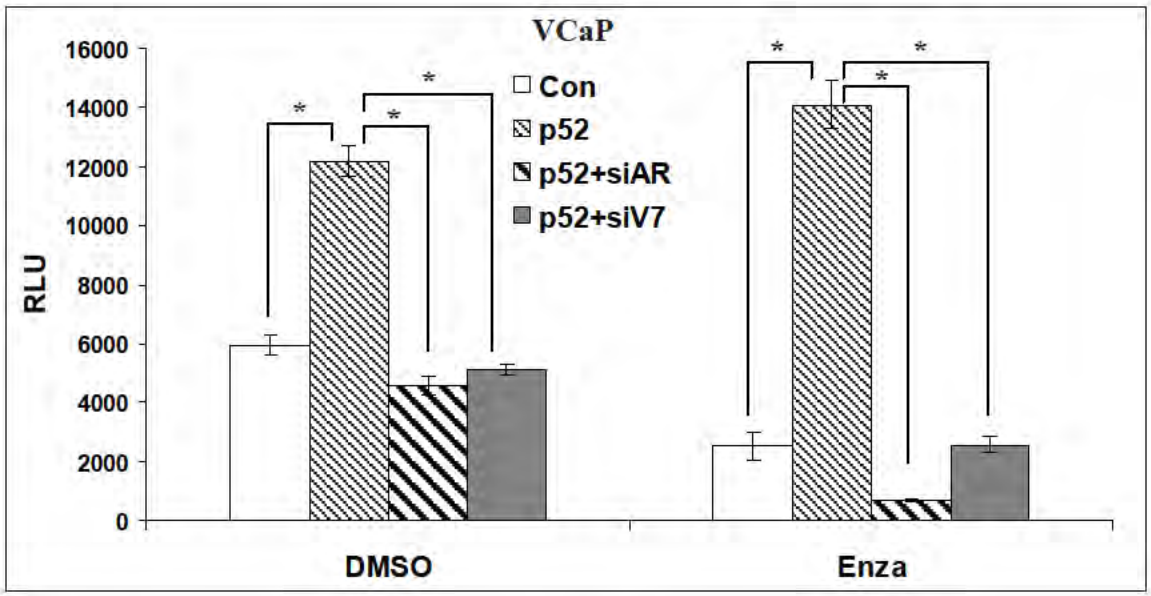
B
VCaP
16000
14000
12000
10000
8000
6000
4000
2000
0
RLU
Con
p52
p52+siAR
p52+siV7
*
DMSO
Enza

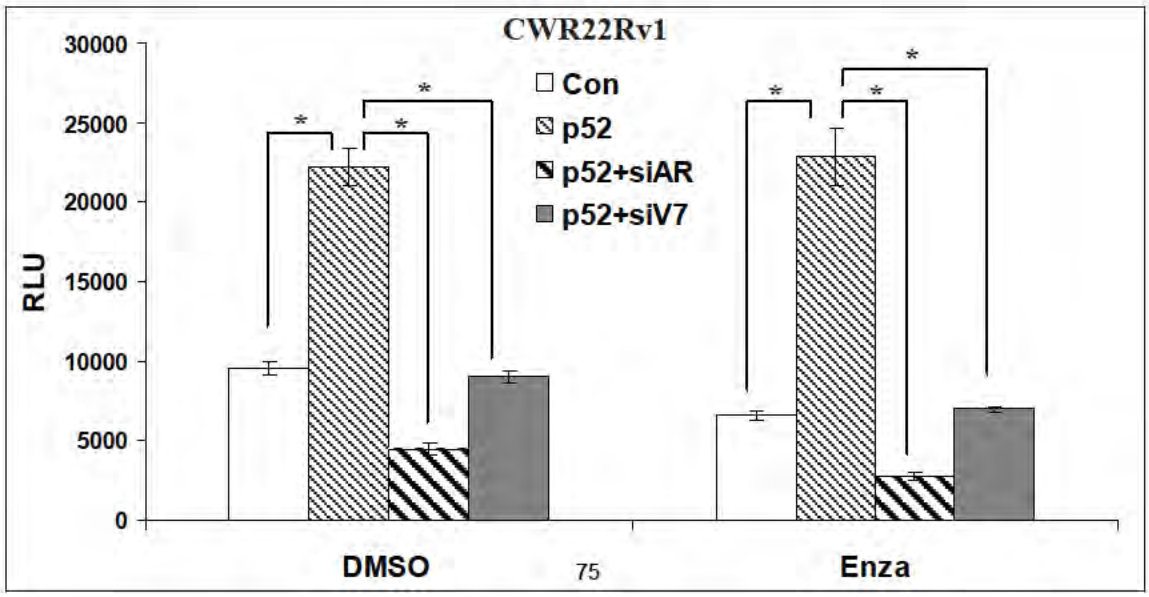
C
CWR22Rv1
30000
25000
20000
15000
10000
5000
0
RLU
Con
p52
p52+siAR
p52+siV7
*
DMSO
Enza

Figure 34

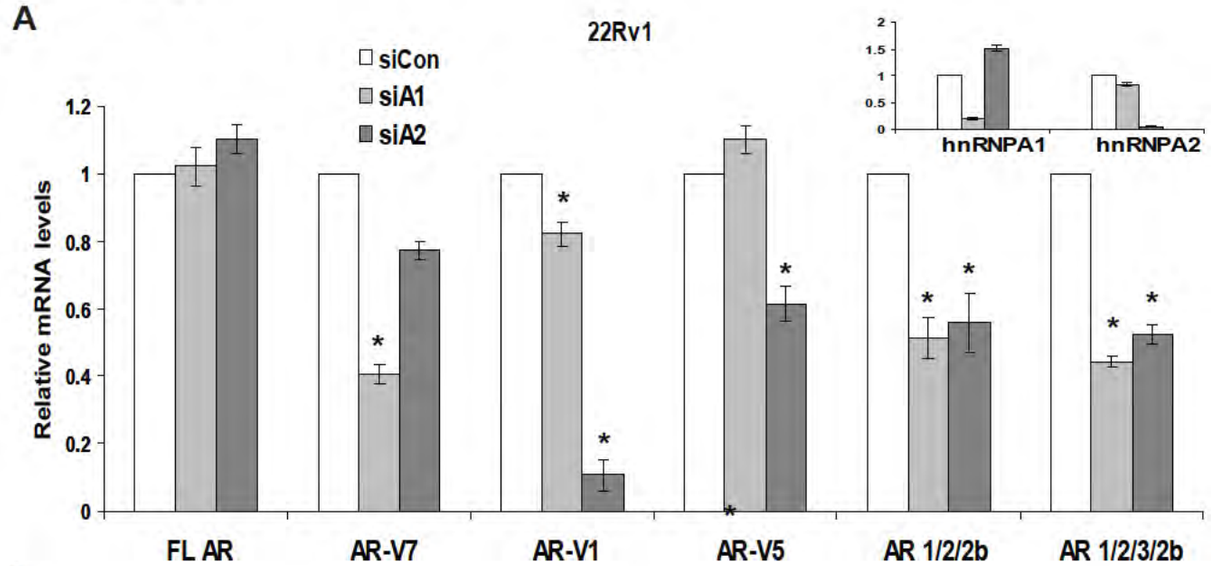
A
22Rv1
siCon
siA1
siA2
Relative mRNA levels
hnRNPA1
hnRNPA2
FL AR
AR-V7
AR-V1
AR-V5
AR 1/2/2b
AR 1/2/3/2b

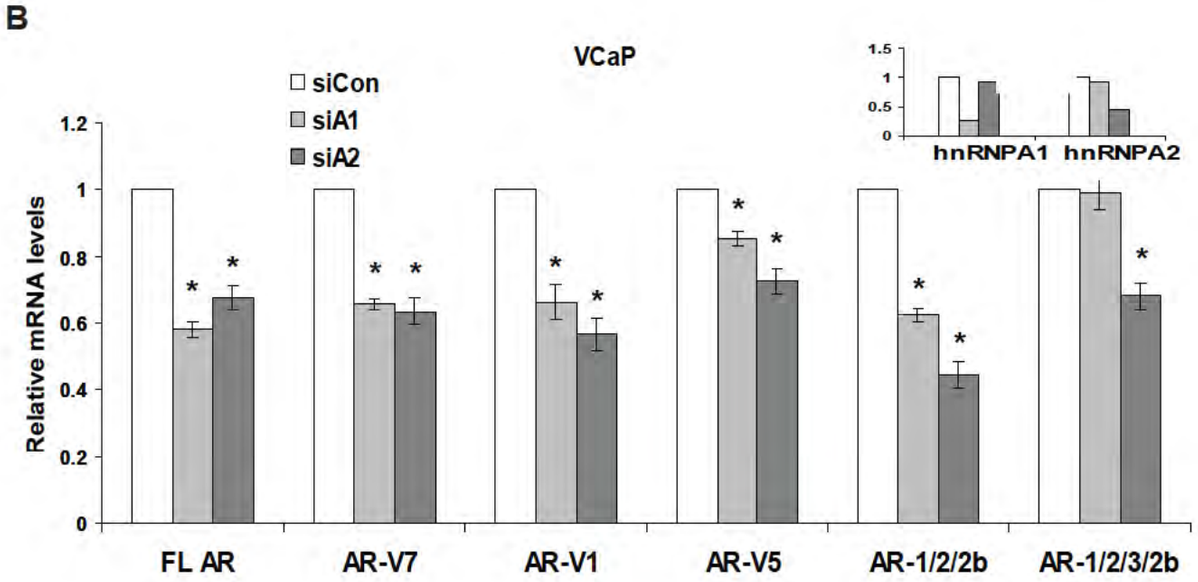
B
VCaP
siCon
siA1
siA2
Relative mRNA levels
hnRNPA1
hnRNPA2
FL AR
AR-V7
AR-V1
AR-V5
AR-1/2/2b
AR-1/2/3/2b

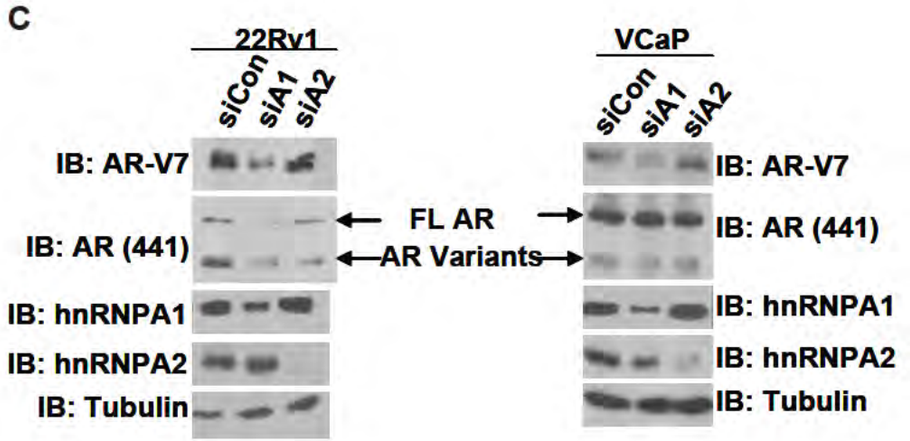
C
22Rv1
VCaP
siCon
siA1
siA2
IB: AR-V7
IB: AR (441)
IB: hnRNPA1
IB: hnRNPA2
IB: Tubulin
FL AR
AR Variants

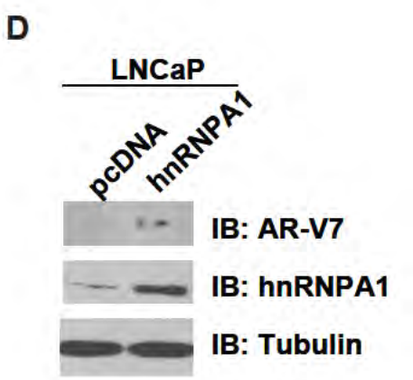
D
LNCaP
pcDNA
hnRNPA1
IB: AR-V7
IB: hnRNPA1
IB: Tubulin

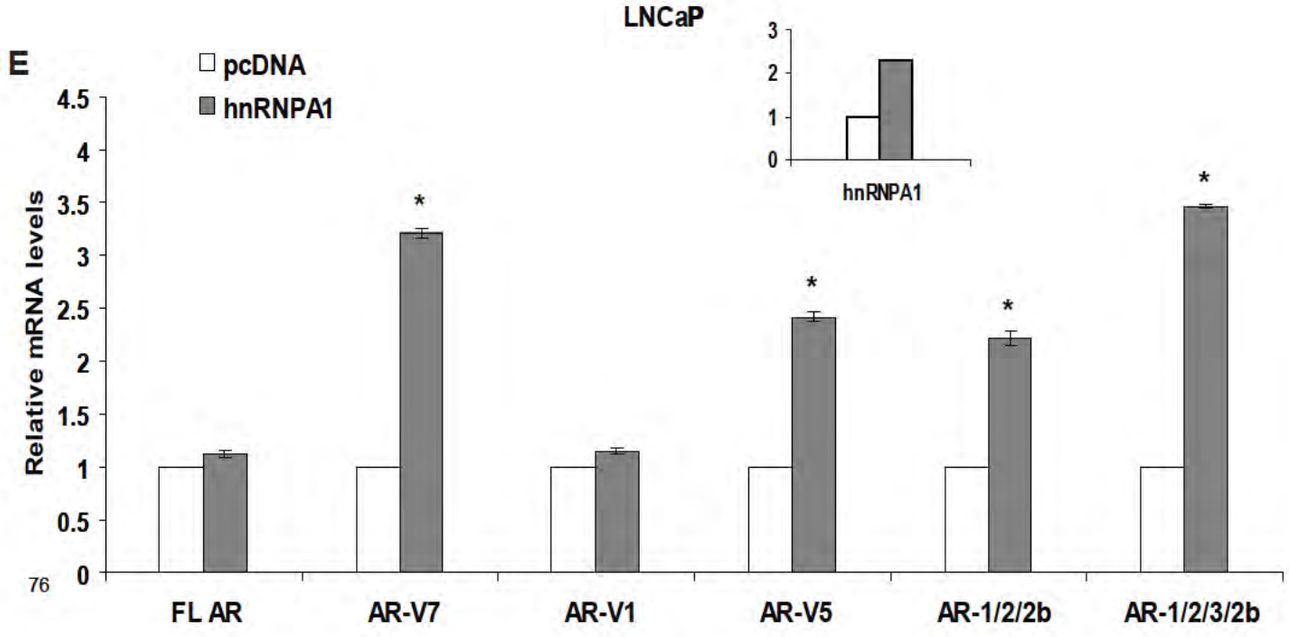
E
LNCaP
pcDNA
hnRNPA1
Relative mRNA levels
FL AR
AR-V7
AR-V1
AR-V5
AR-1/2/2b
AR-1/2/3/2b

Figure 35

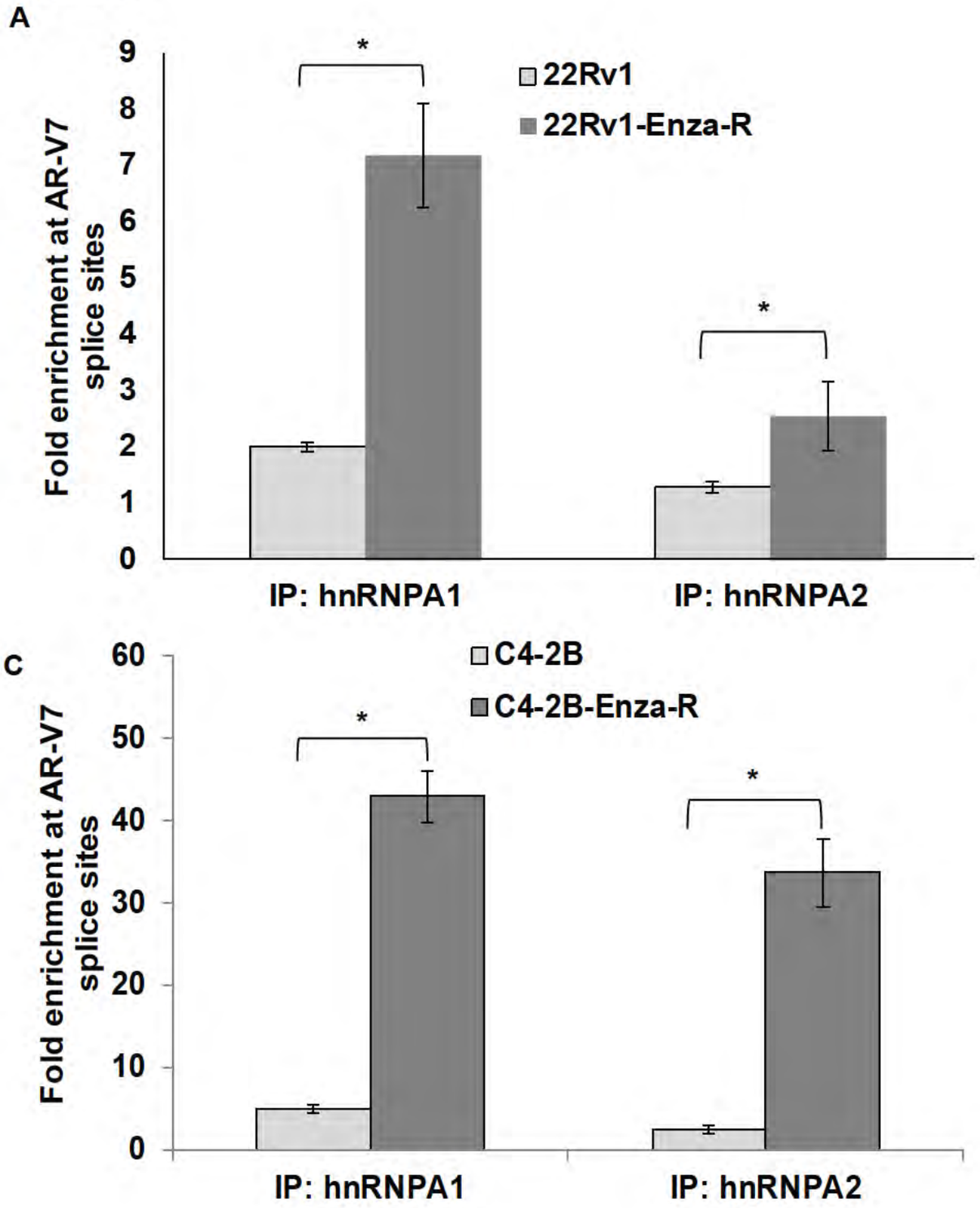
A
Fold enrichment at AR-V7 splice sites
0
1
2
3
4
5
6
7
8
9
22Rv1
22Rv1-Enza-R
*
*
IP: hnRNPA1
IP: hnRNPA2

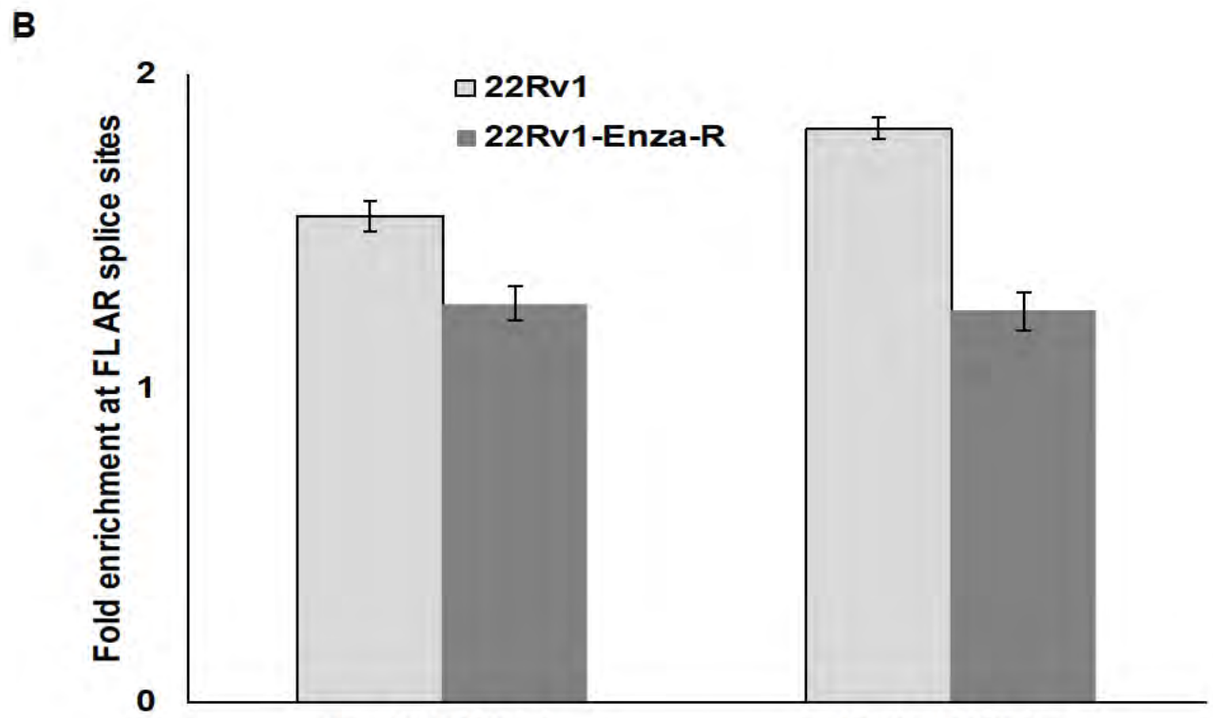
B
Fold enrichment at FL AR splice sites
0
1
2
22Rv1
22Rv1-Enza-R
IP: hnRNPA1
IP: hnRNPA2

C
Fold enrichment at AR-V7 splice sites
0
10
20
30
40
50
60
C4-2B
C4-2B-Enza-R
*
*
IP: hnRNPA1
IP: hnRNPA2

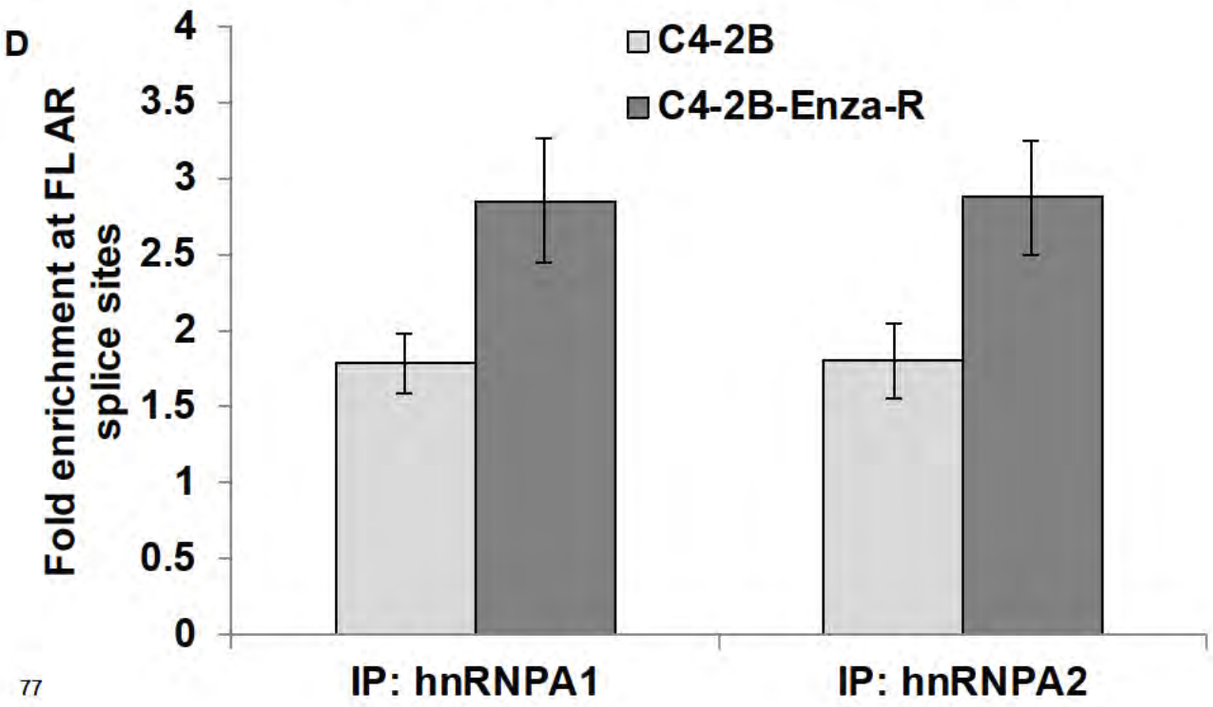
D
Fold enrichment at FL AR splice sites
0
0.5
1
1.5
2
2.5
3
3.5
4
C4-2B
C4-2B-Enza-R
IP: hnRNPA1
IP: hnRNPA2

Figure 36

A

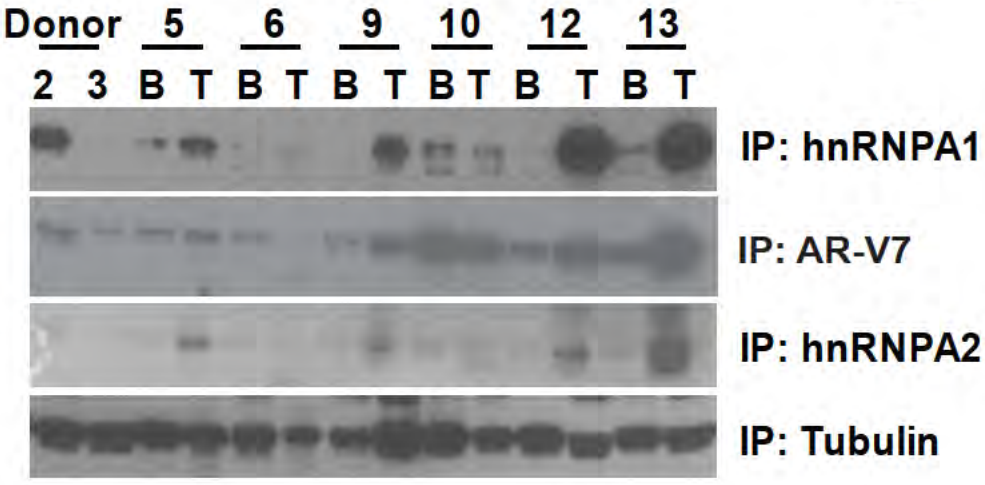

B

Gene	T>B	T<B	T=B	High in donor	Low in donor
hnRNPA1	12 (44%)	8 (29%)	7 (26%)	3/12	9/12
ARV7	13 (48%)	7 (25%)	7 (26%)	4/12	8/12
hnRNPA2	12 (44%)	8 (29%)	7 (26%)	6/12	6/12

C

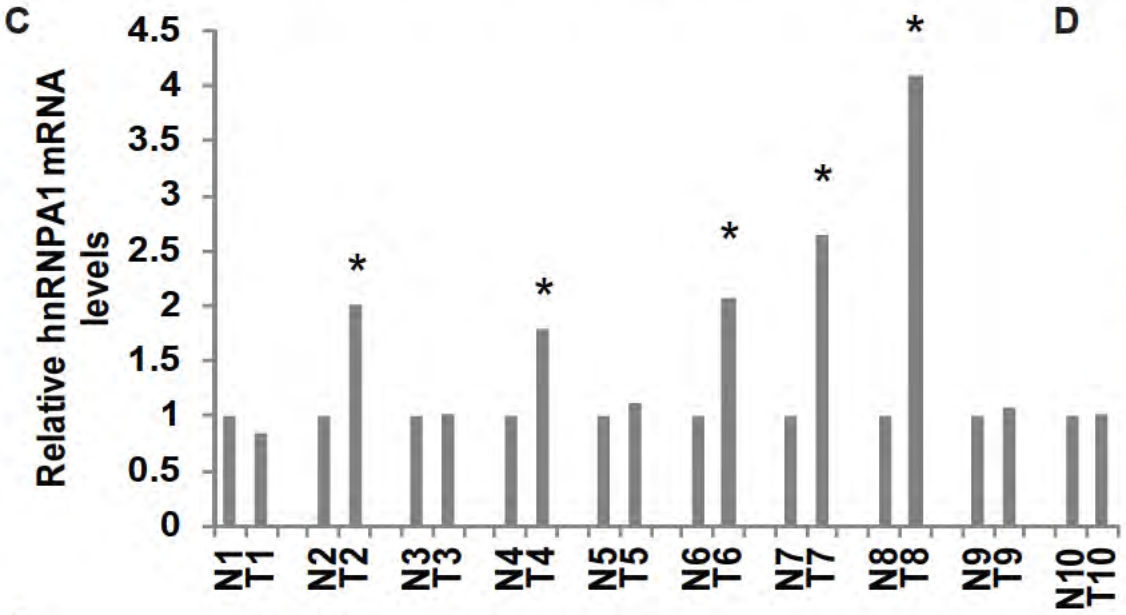

D

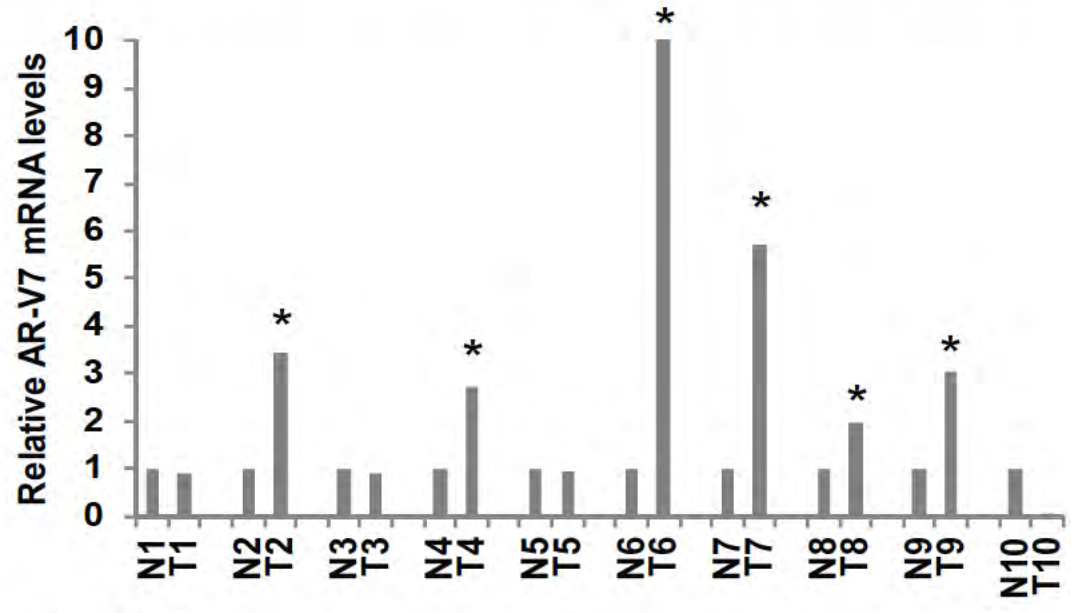

E

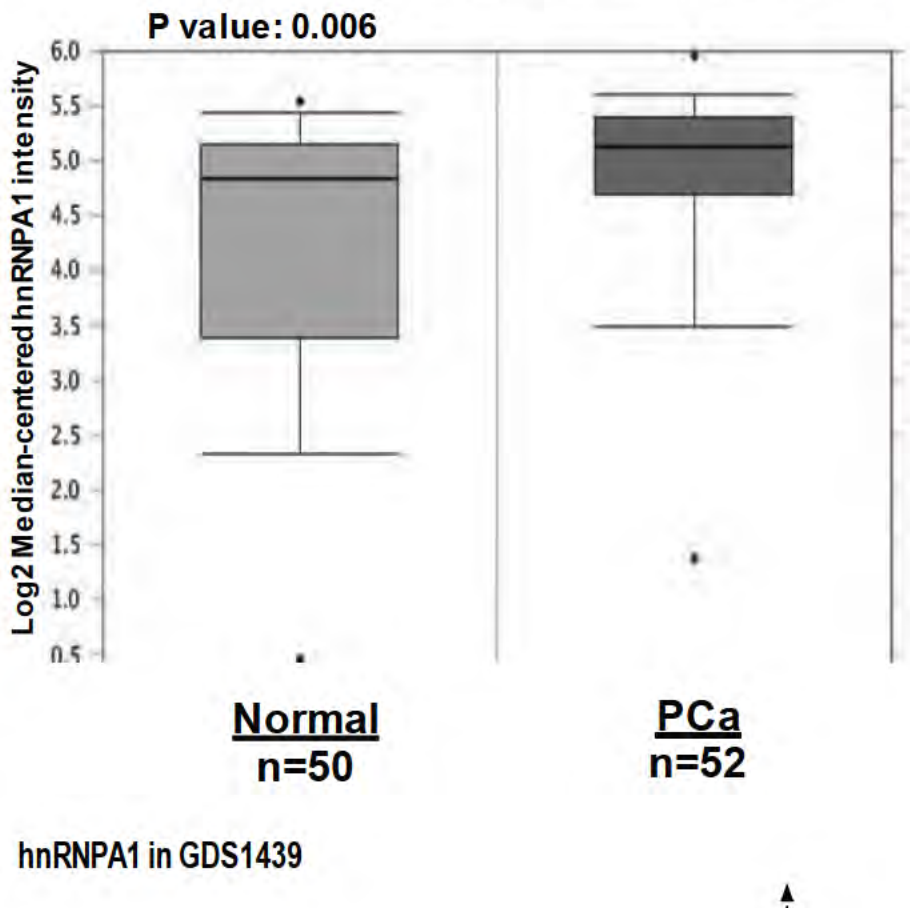

F

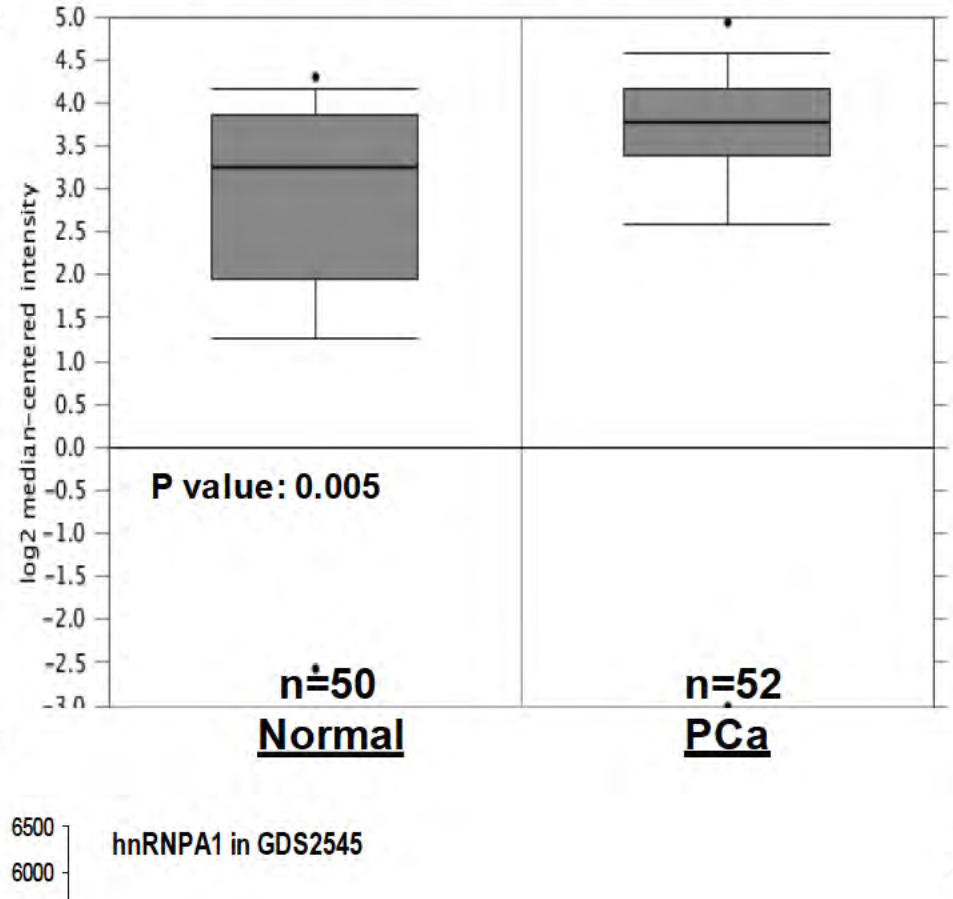

G

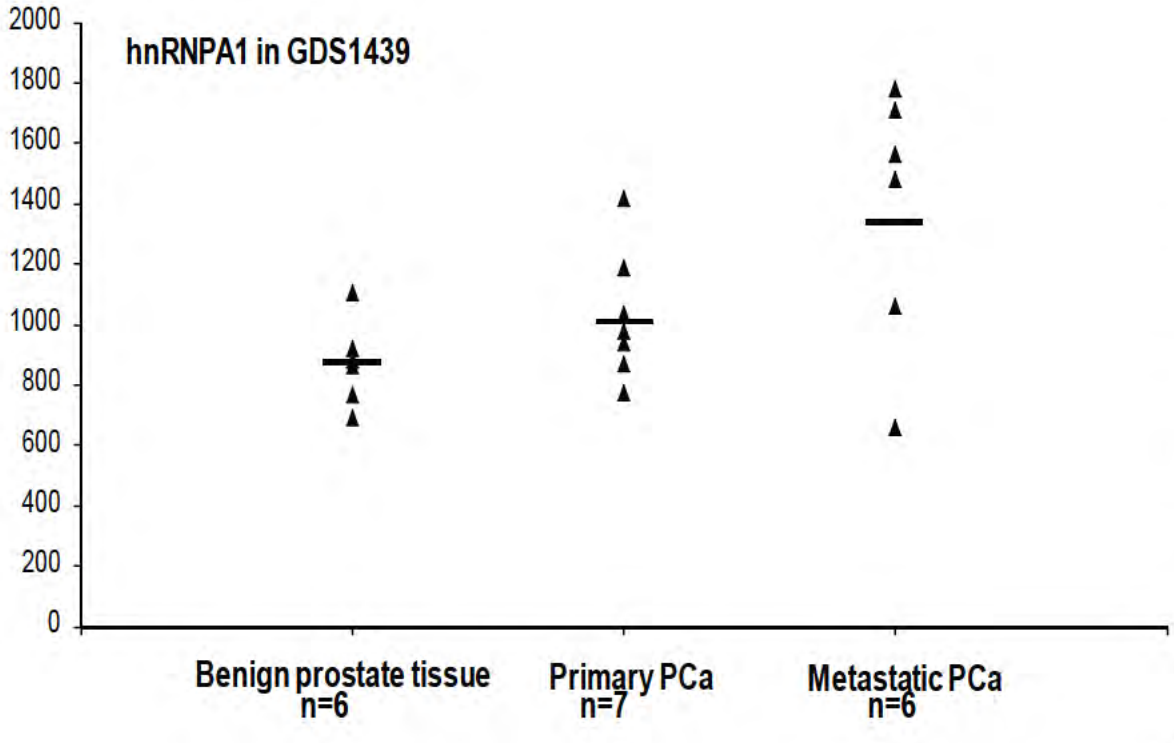

H

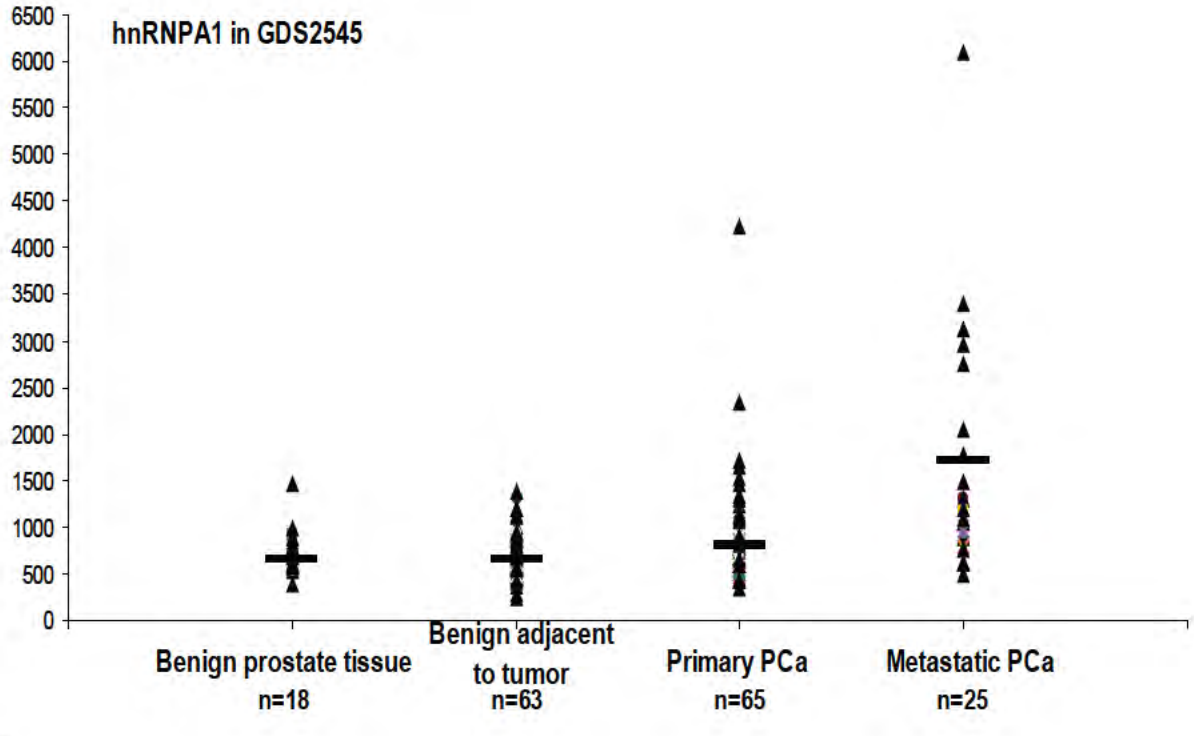

Figure 37

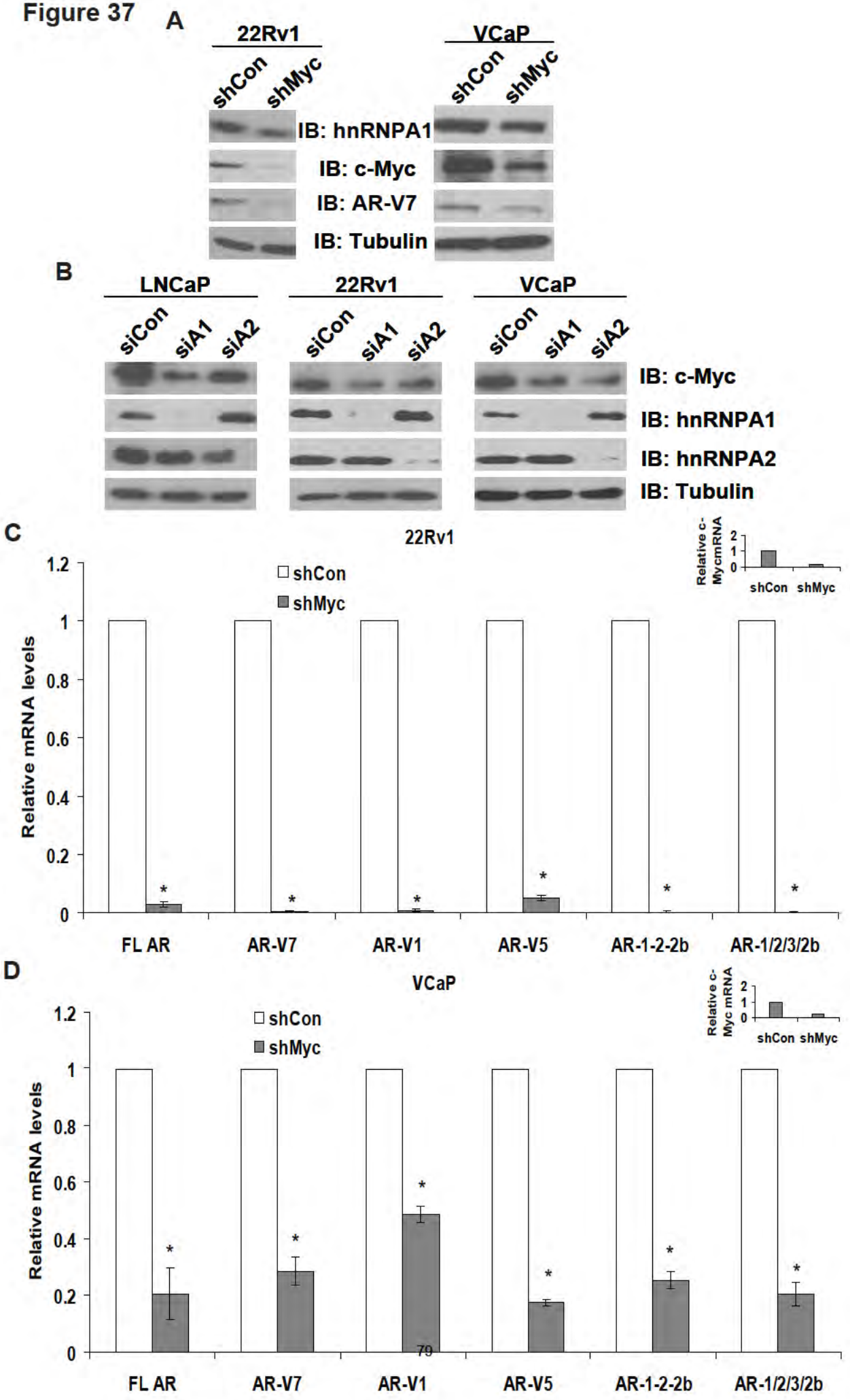
A
22Rv1
VCaP
shCon
shMyc
shCon
shMyc
IB: hnRNPA1
IB: c-Myc
IB: AR-V7
IB: Tubulin
B
LNCaP
22Rv1
VCaP
siCon
siA1
siA2
siCon
siA1
siA2
siCon
siA1
siA2
IB: c-Myc
IB: hnRNPA1
IB: hnRNPA2
IB: Tubulin
C
22Rv1
shCon
shMyc
Relative mRNA levels
1.2
1
0.8
0.6
0.4
0.2
0
FL AR
AR-V7
AR-V1
AR-V5
AR-1-2-2b
AR-1/2/3/2b
Relative c-Mycm RNA
2
1
0
shCon
shMyc
D
VCaP
shCon
shMyc
Relative mRNA levels
1.2
1
0.8
0.6
0.4
0.2
0
FL AR
AR-V7
AR-V1
AR-V5
AR-1-2-2b
AR-1/2/3/2b
Relative c-Myc mRNA
2
1
0
shCon
shMyc

Figure 38

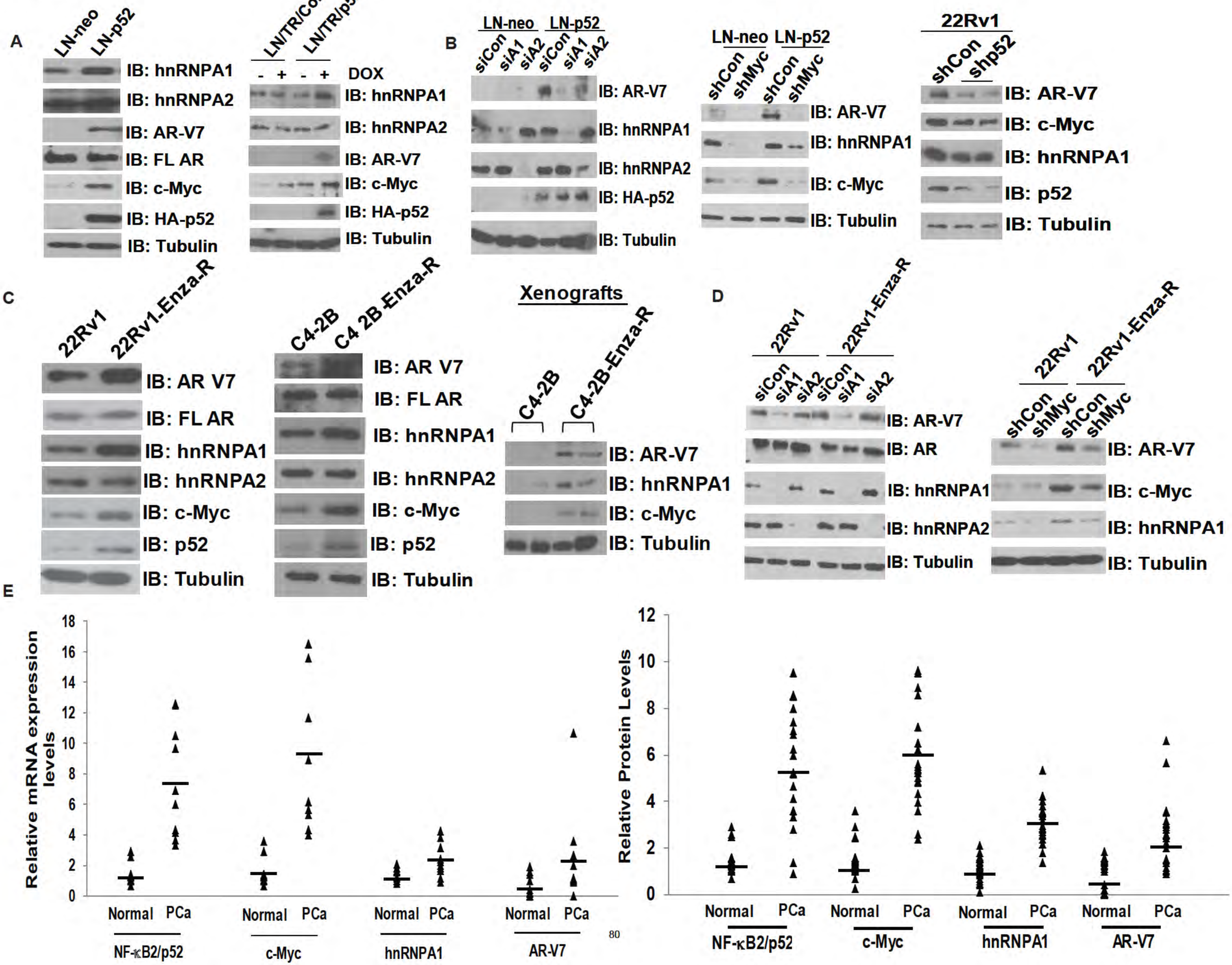
A
LN-neo
LN-p52
IB: hnRNPA1
IB: hnRNPA2
IB: AR-V7
IB: FL AR
IB: c-Myc
IB: HA-p52
IB: Tubulin
LN/TR/Con
LN/TR/p52
- + - +
DOX
IB: hnRNPA1
IB: hnRNPA2
IB: AR-V7
IB: c-Myc
IB: HA-p52
IB: Tubulin
B
LN-neo
LN-p52
siCon
siA1
siA2
siCon
siA1
siA2
IB: AR-V7
IB: hnRNPA1
IB: hnRNPA2
IB: HA-p52
IB: Tubulin
LN-neo
LN-p52
shCon
shMyc
shCon
shMyc
IB: AR-V7
IB: hnRNPA1
IB: c-Myc
IB: Tubulin
22Rv1
shCon
shp52
IB: AR-V7
IB: c-Myc
IB: hnRNPA1
IB: p52
IB: Tubulin
C
22Rv1
22Rv1-Enza-R
IB: AR V7
IB: FL AR
IB: hnRNPA1
IB: hnRNPA2
IB: c-Myc
IB: p52
IB: Tubulin
C4-2B
C4 2B-Enza-R
IB: AR V7
IB: FL AR
IB: hnRNPA1
IB: hnRNPA2
IB: c-Myc
IB: p52
IB: Tubulin
Xenografts
C4-2B
C4-2B-Enza-R
IB: AR-V7
IB: hnRNPA1
IB: c-Myc
IB: Tubulin
D
22Rv1
22Rv1-Enza-R
siCon
siA1
siA2
siCon
siA1
siA2
IB: AR-V7
IB: AR
IB: hnRNPA1
IB: hnRNPA2
IB: Tubulin
22Rv1
22Rv1-Enza-R
shCon
shMyc
shCon
shMyc
IB: AR-V7
IB: c-Myc
IB: hnRNPA1
IB: Tubulin
E
Relative mRNA expression levels
Normal
PCa
NF-κB2/p52
c-Myc
hnRNPA1
AR-V7
Relative Protein Levels
Normal
PCa
NF-κB2/p52
c-Myc
hnRNPA1
AR-V7

Figure 39

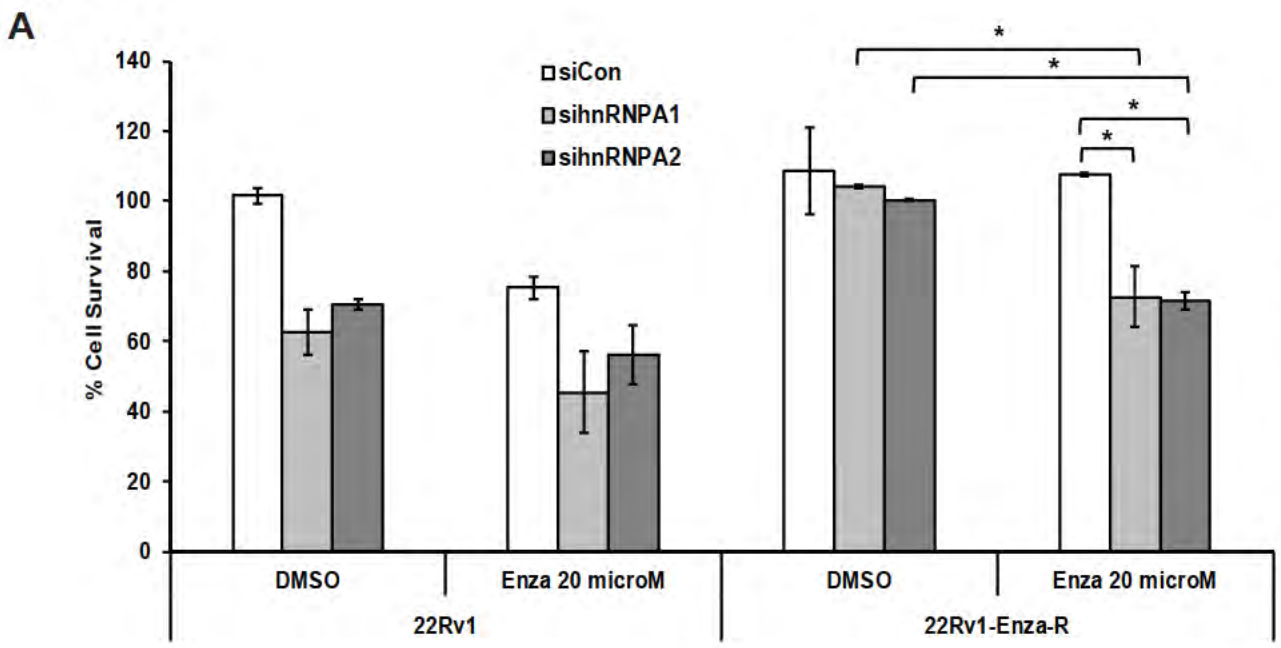
A
% Cell Survival
siCon
sihnRNPA1
sihnRNPA2
DMSO
Enza 20 microM
22Rv1
22Rv1-Enza-R

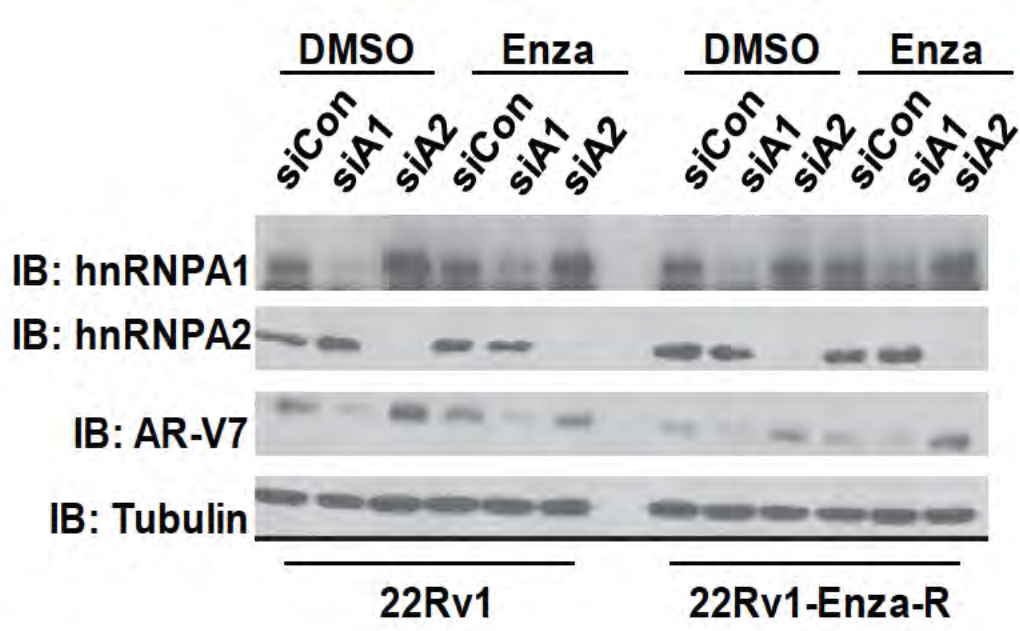
DMSO
Enza
siCon
siA1
siA2
IB: hnRNPA1
IB: hnRNPA2
IB: AR-V7
IB: Tubulin
22Rv1
22Rv1-Enza-R

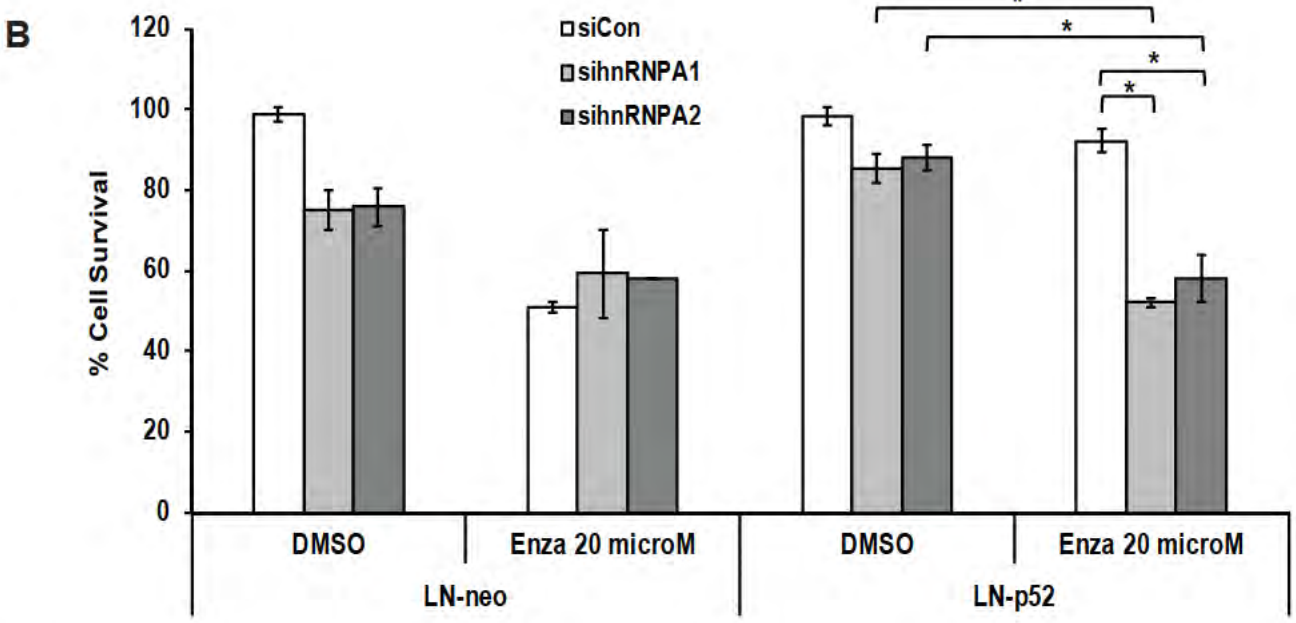
B
% Cell Survival
siCon
sihnRNPA1
sihnRNPA2
DMSO
Enza 20 microM
LN-neo
LN-p52

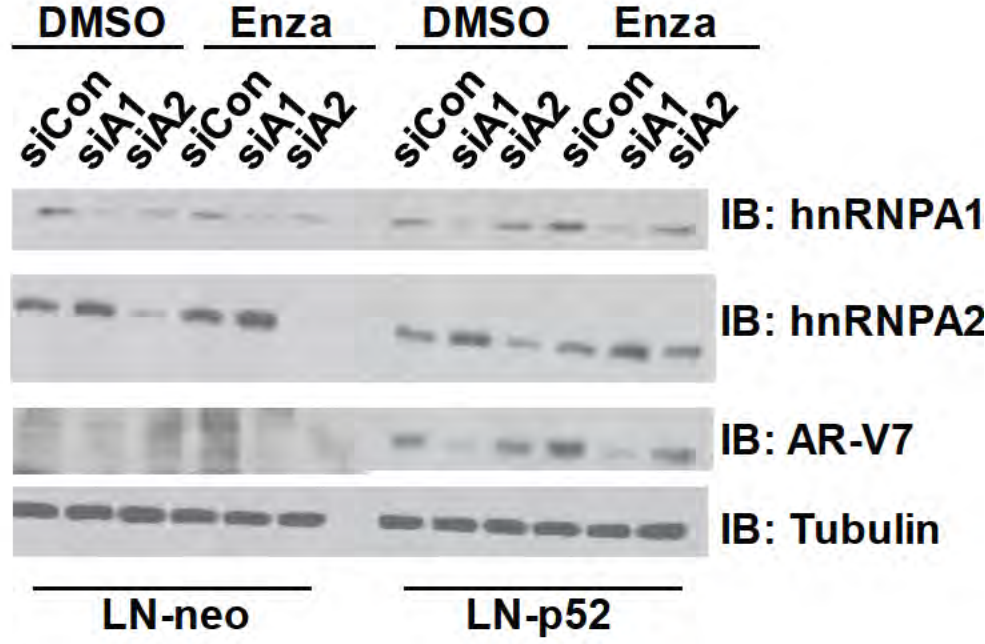
DMSO
Enza
siCon
siA1
siA2
IB: hnRNPA1
IB: hnRNPA2
IB: AR-V7
IB: Tubulin
LN-neo
LN-p52

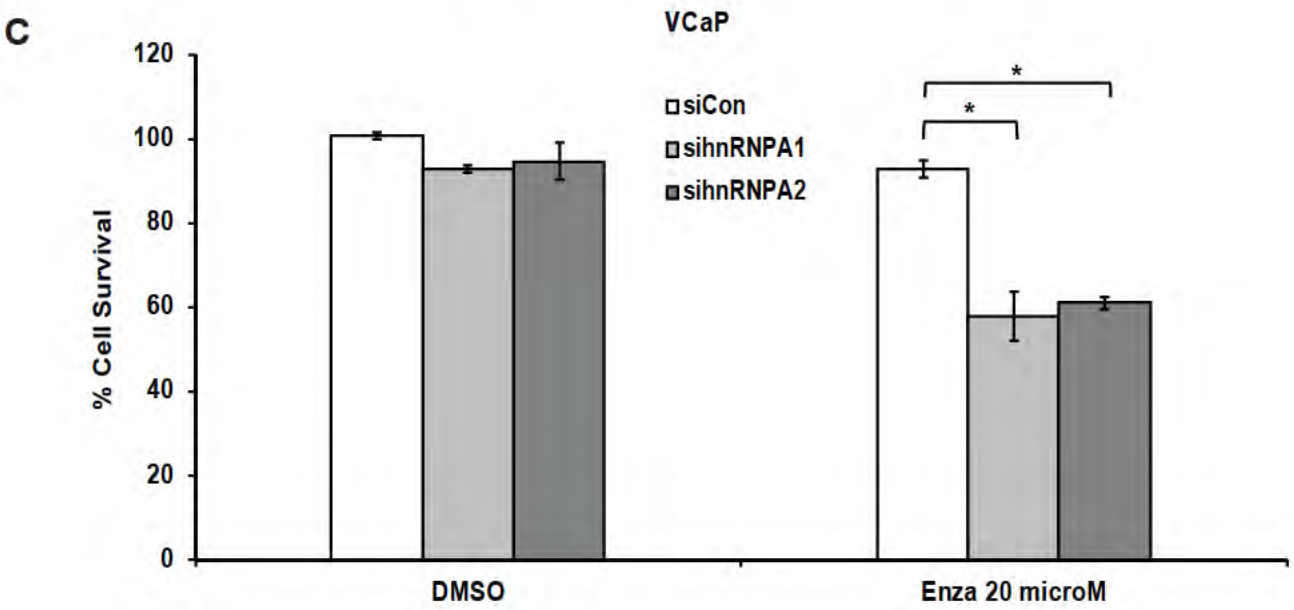
C
VCaP
% Cell Survival
siCon
sihnRNPA1
sihnRNPA2
DMSO
Enza 20 microM

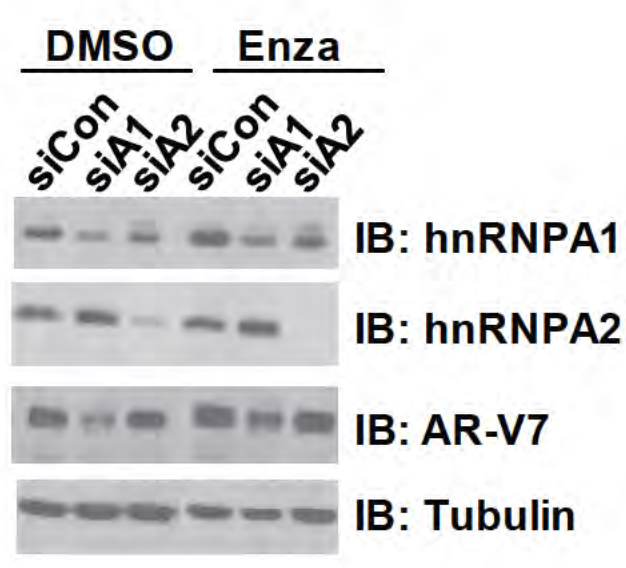
DMSO
Enza
siCon
siA1
siA2
IB: hnRNPA1
IB: hnRNPA2
IB: AR-V7
IB: Tubulin

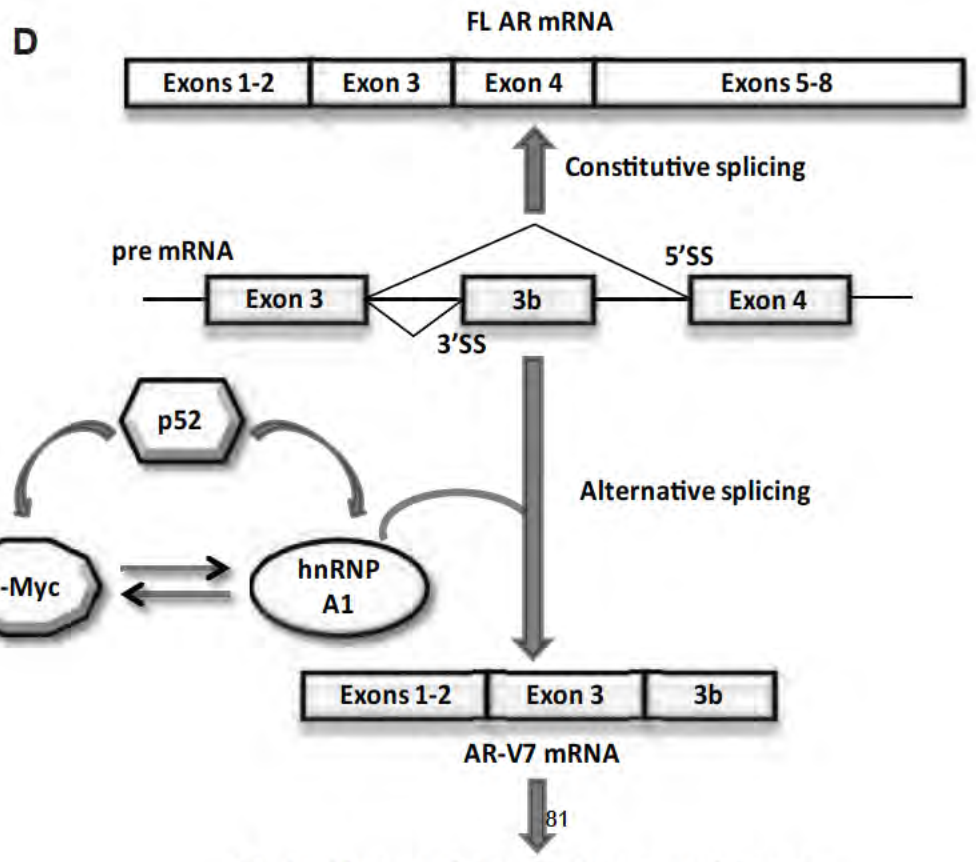
D
FL AR mRNA
Exons 1-2
Exon 3
Exon 4
Exons 5-8
Constitutive splicing
pre mRNA
5'SS
Exon 3
3b
Exon 4
3'SS
p52
c-Myc
hnRNP
A1
Alternative splicing
Exons 1-2
Exon 3
3b
AR-V7 mRNA
Castration resistance, Drug resistance

Figure 40

A

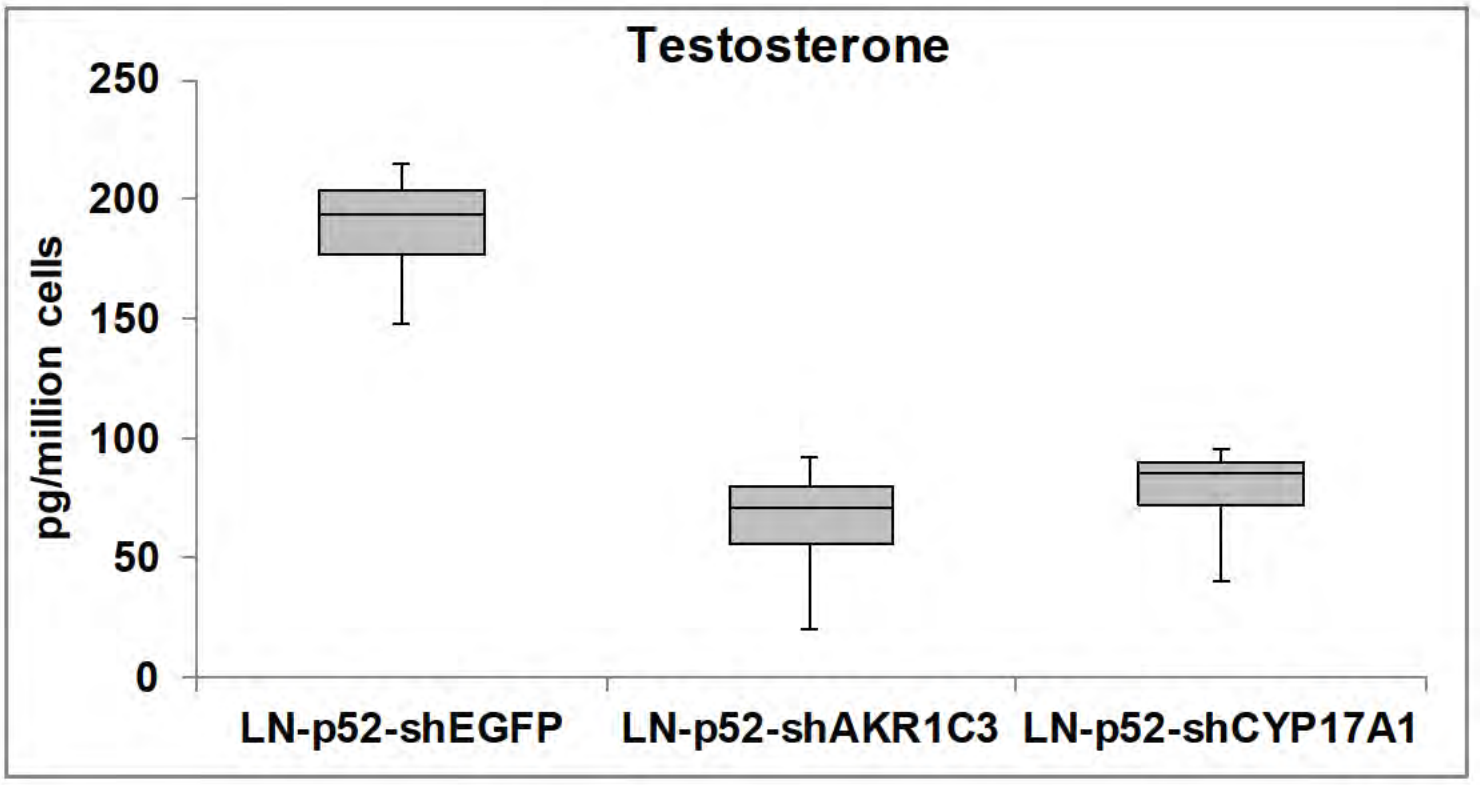

B

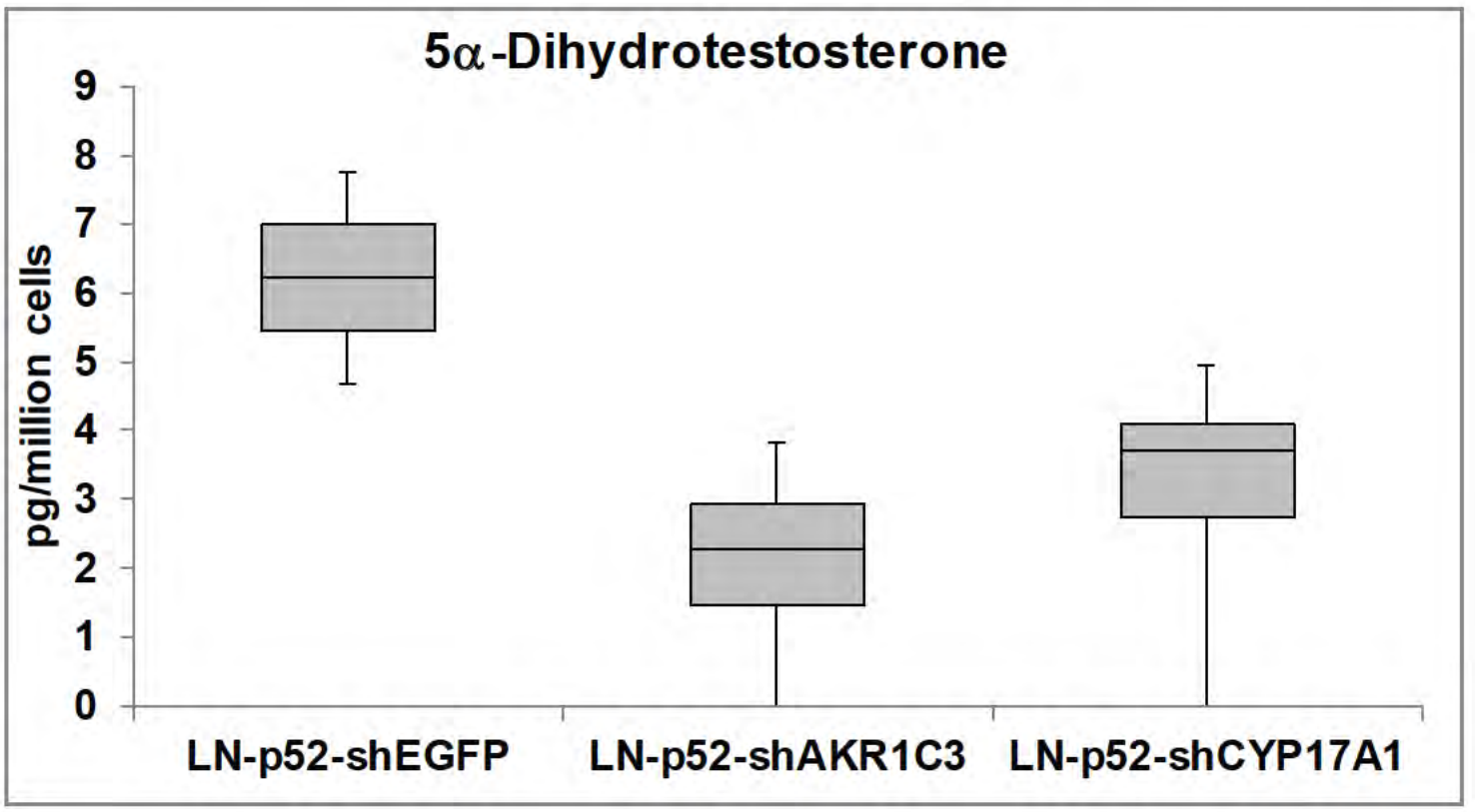

C

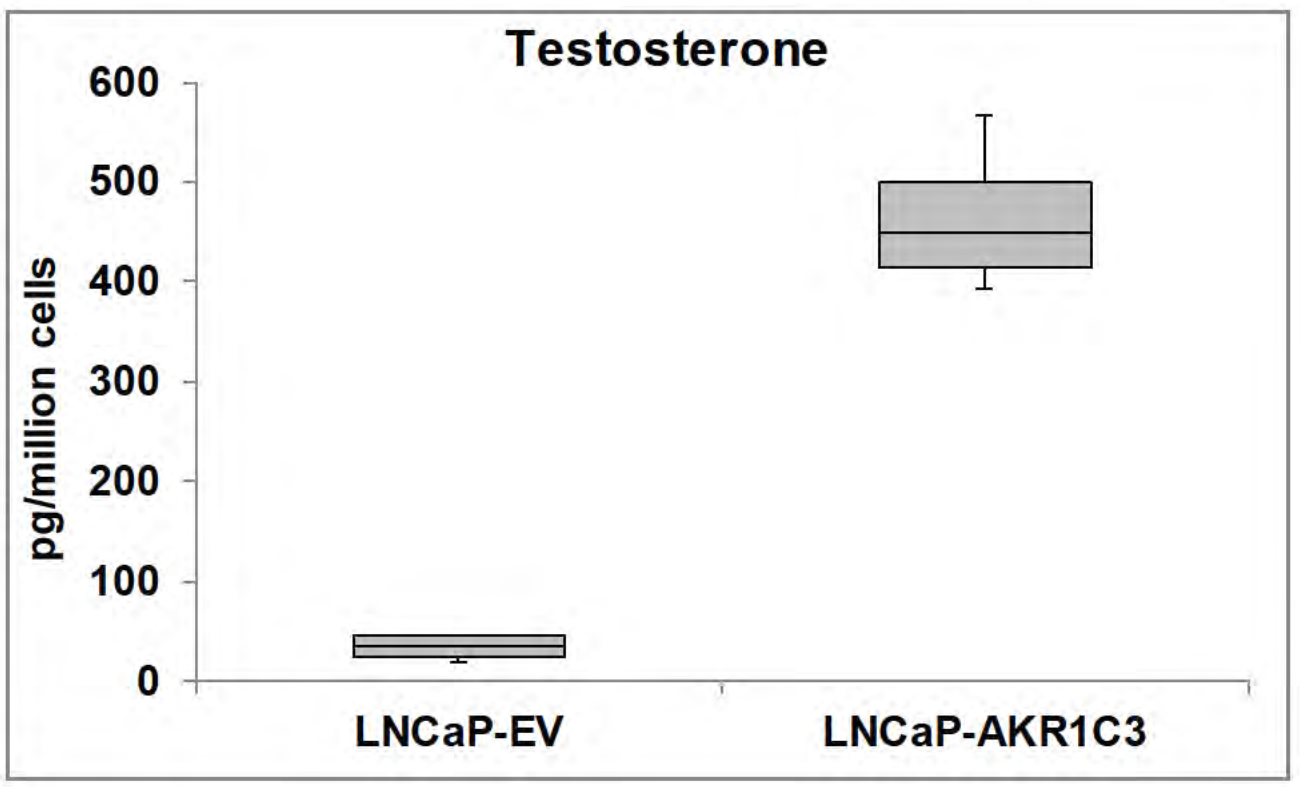

Figure 41

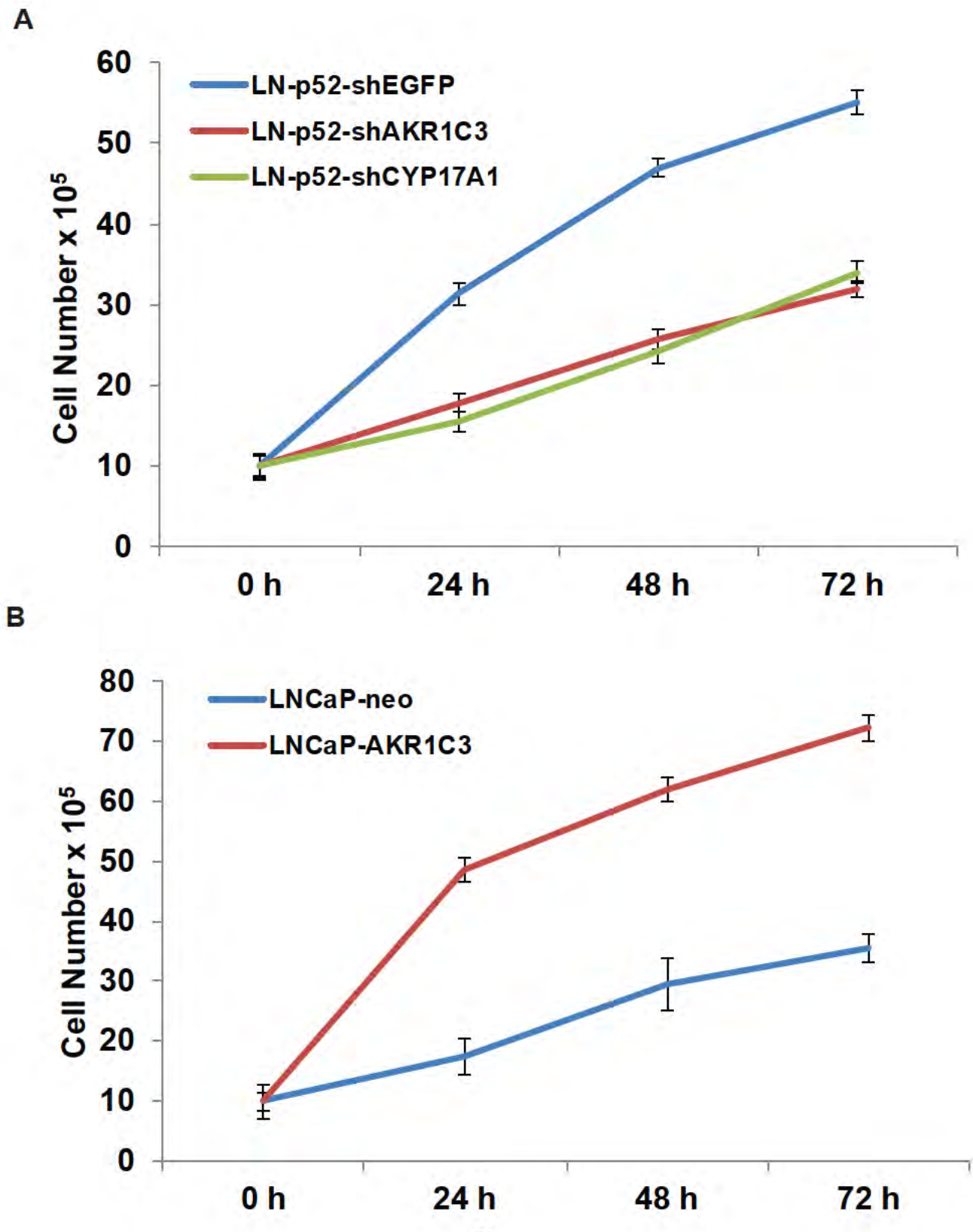
A
LN-p52-shEGFP
LN-p52-shAKR1C3
LN-p52-shCYP17A1
Cell Number x 10^5
60
50
40
30
20
10
0
0 h
24 h
48 h
72 h
B
LNCaP-neo
LNCaP-AKR1C3
Cell Number x 10^5
80
70
60
50
40
30
20
10
0
0 h
24 h
48 h
72 h

Figure 42

A

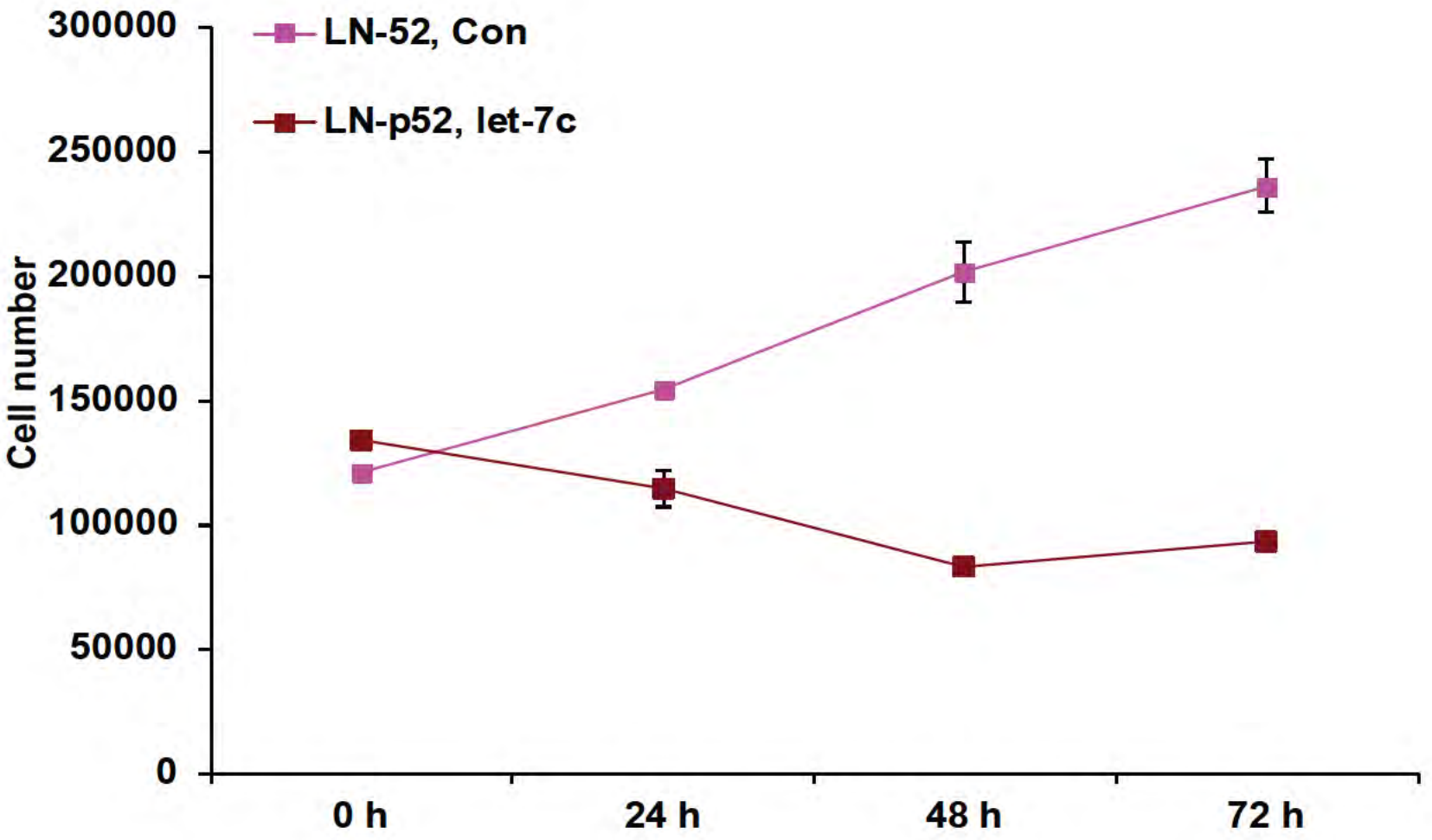
LN-52, Con
LN-p52, let-7c
Cell number
300000
250000
200000
150000
100000
50000
0
0 h
24 h
48 h
72 h

B

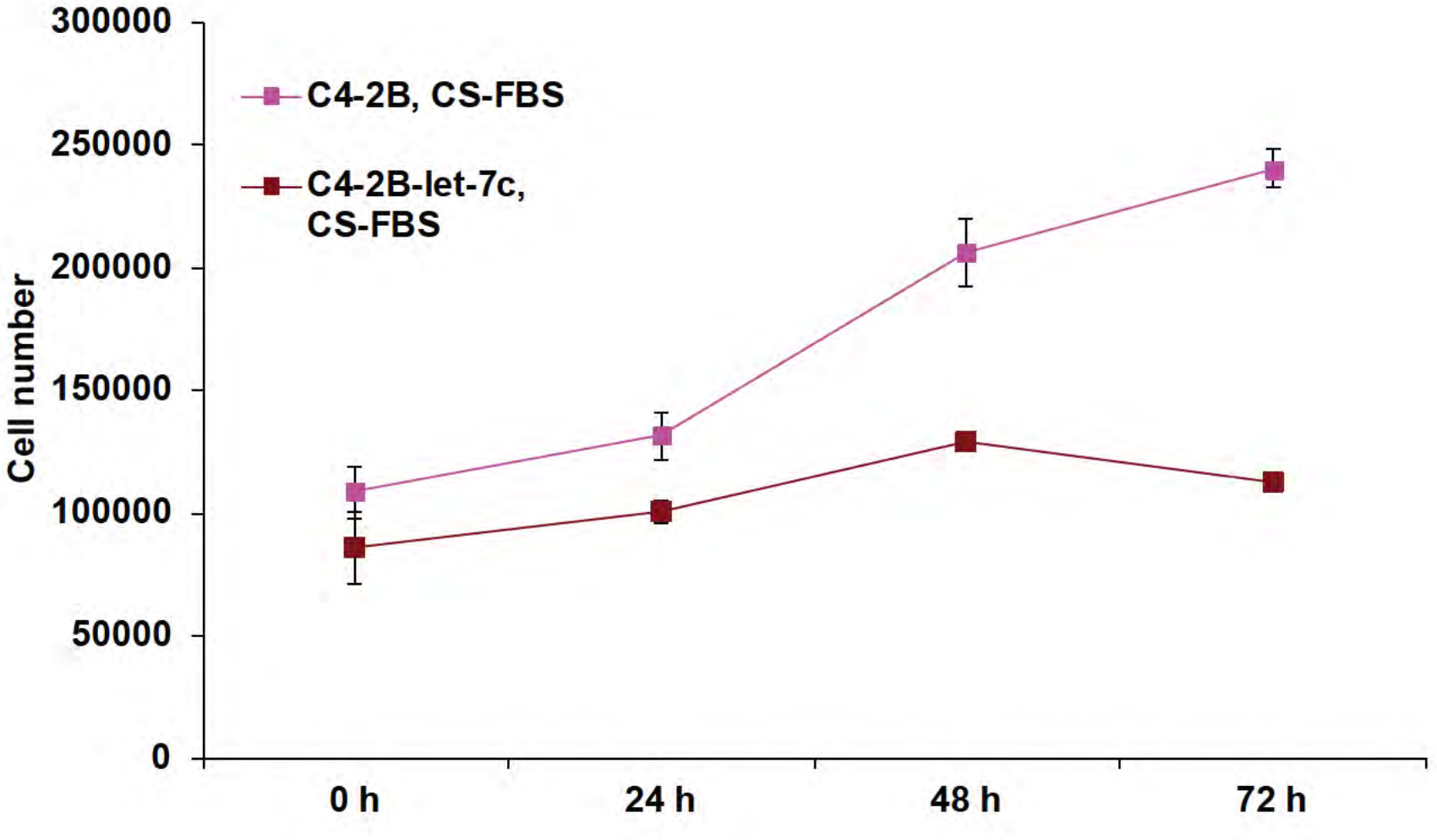
C4-2B, CS-FBS
C4-2B-let-7c, CS-FBS
Cell number
300000
250000
200000
150000
100000
50000
0
0 h
24 h
48 h
72 h

Supplementary Figure 1

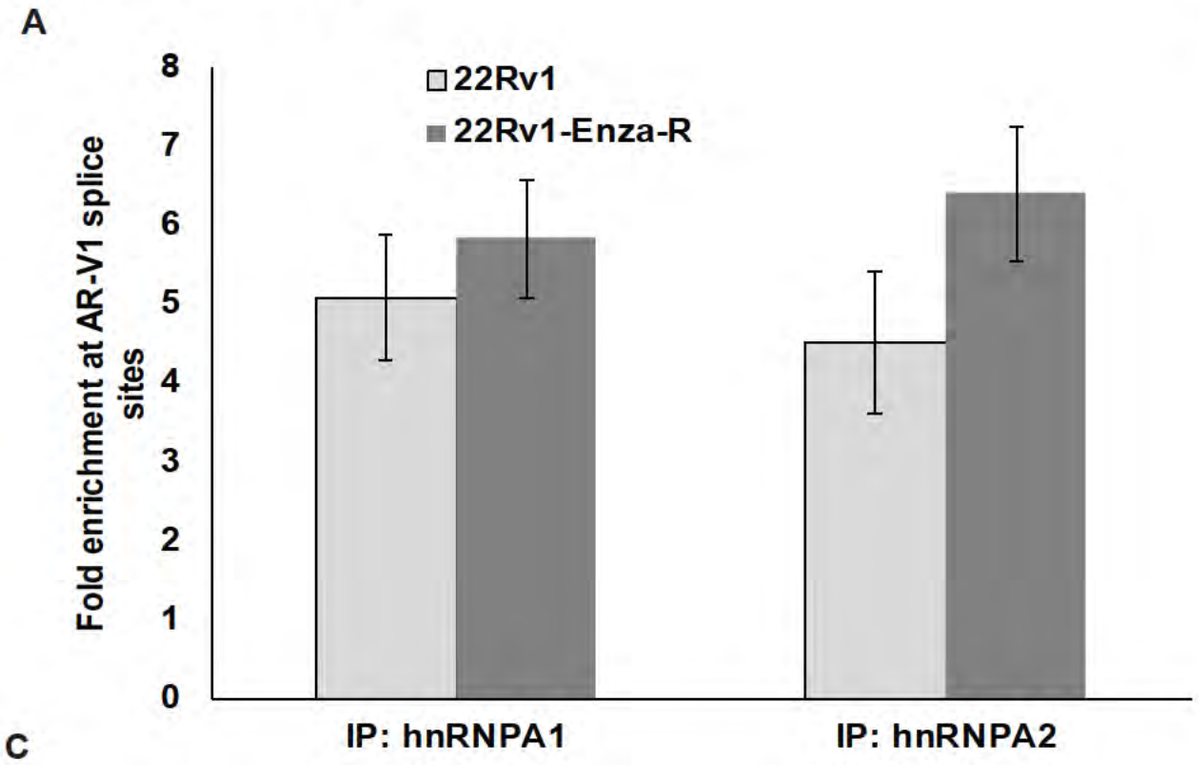

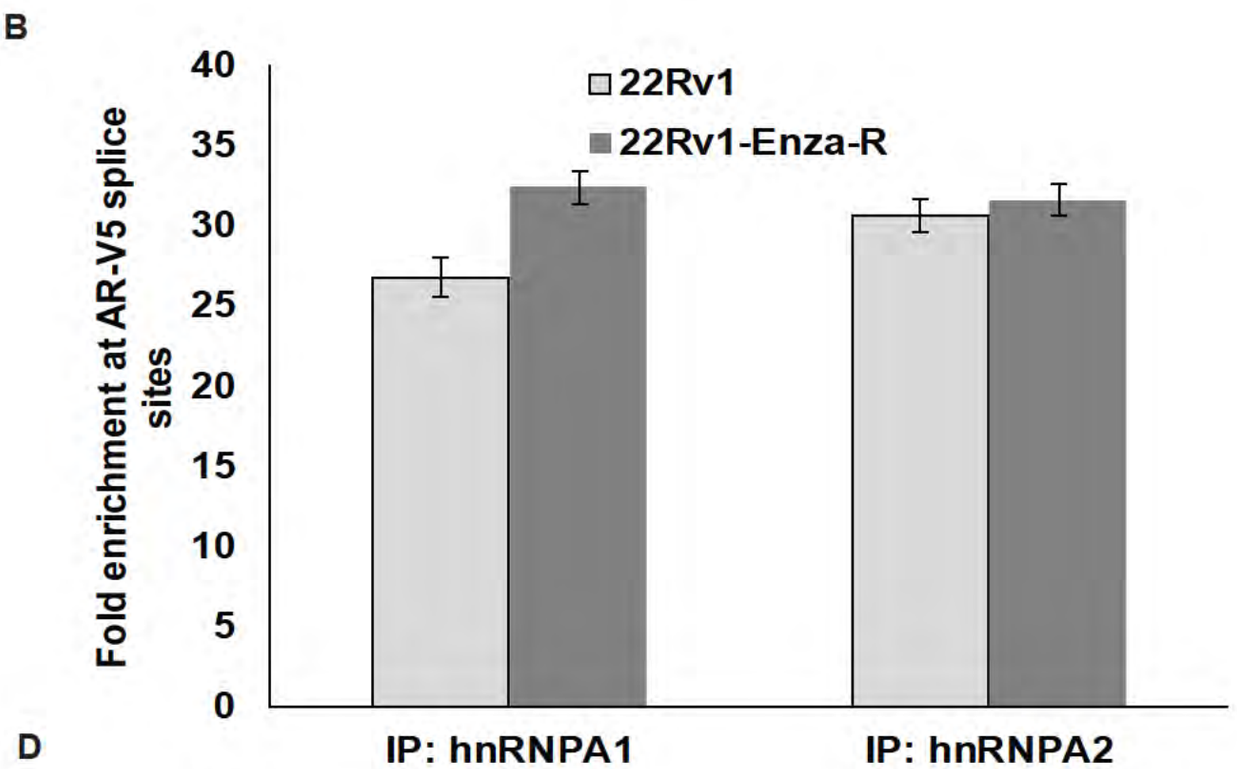

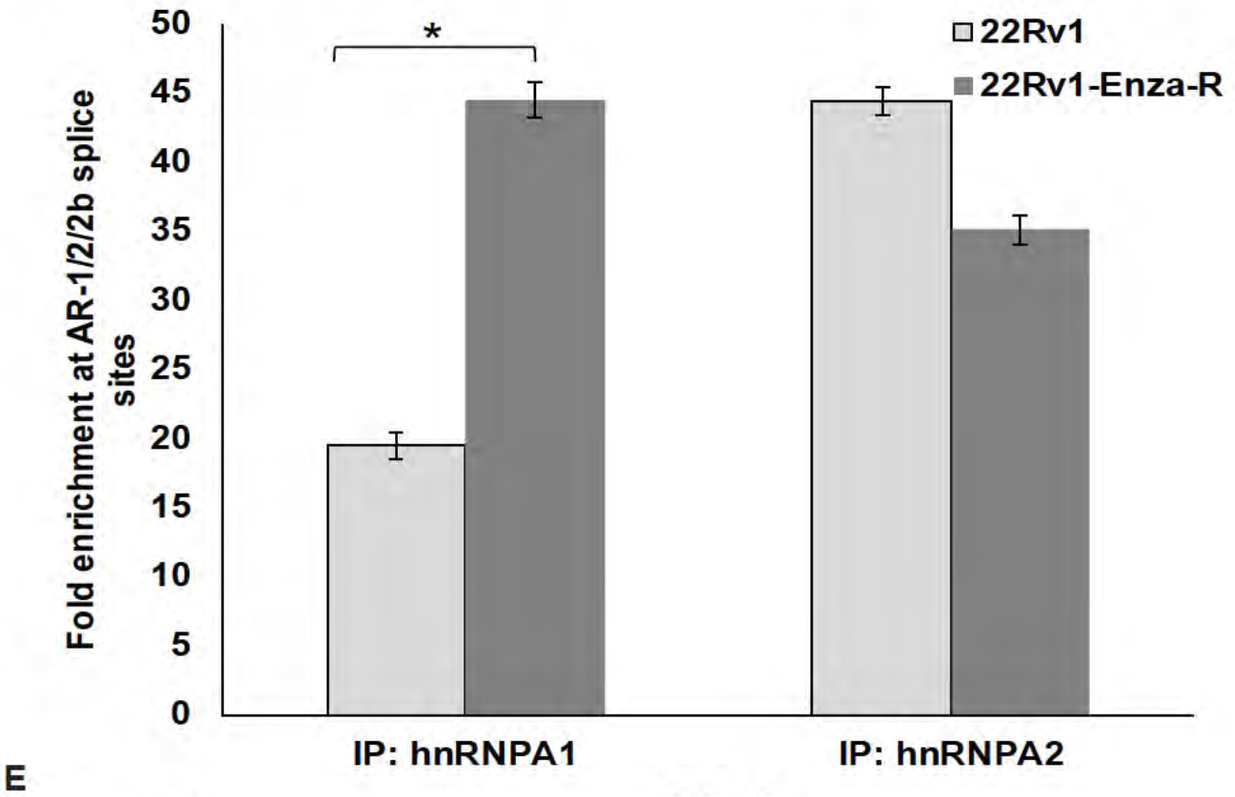

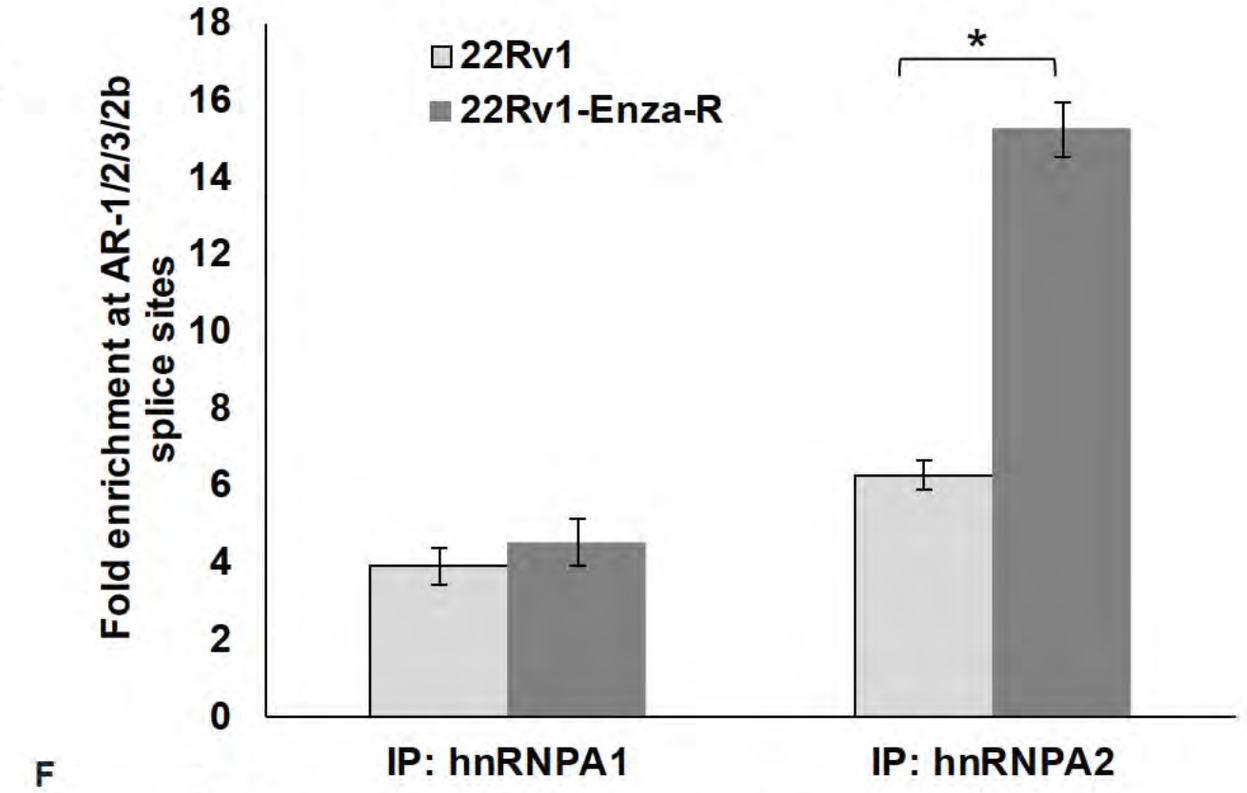

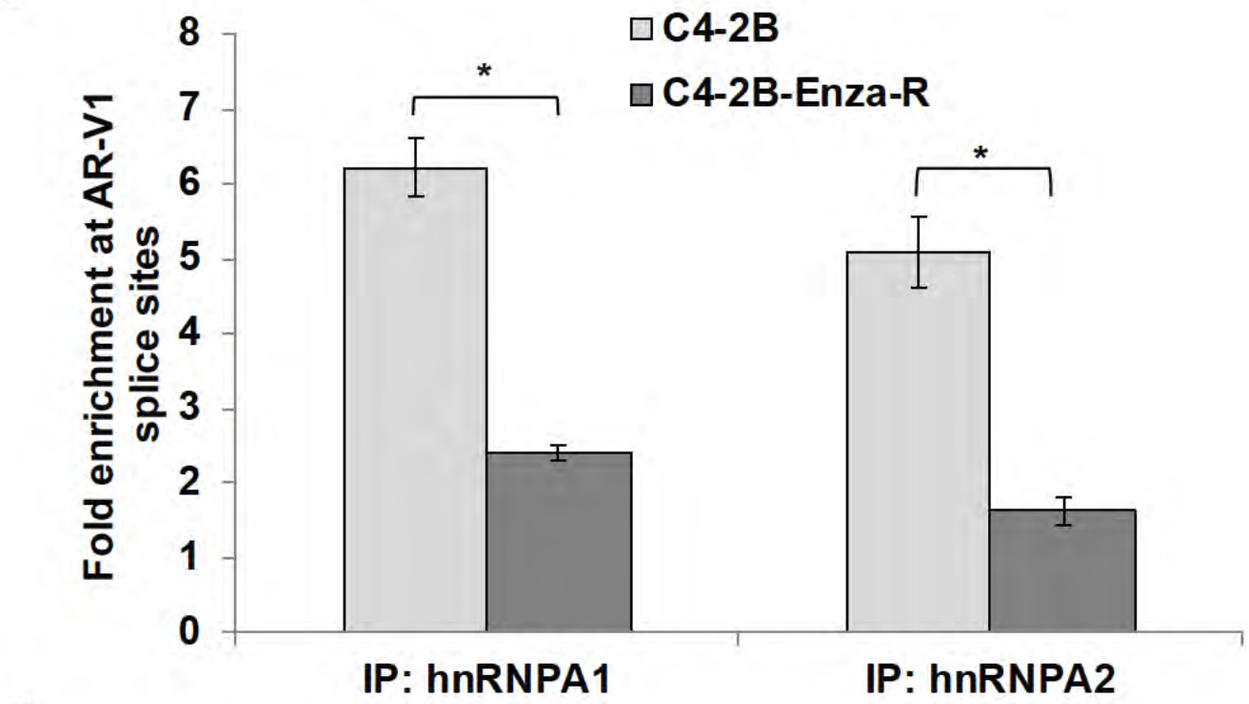

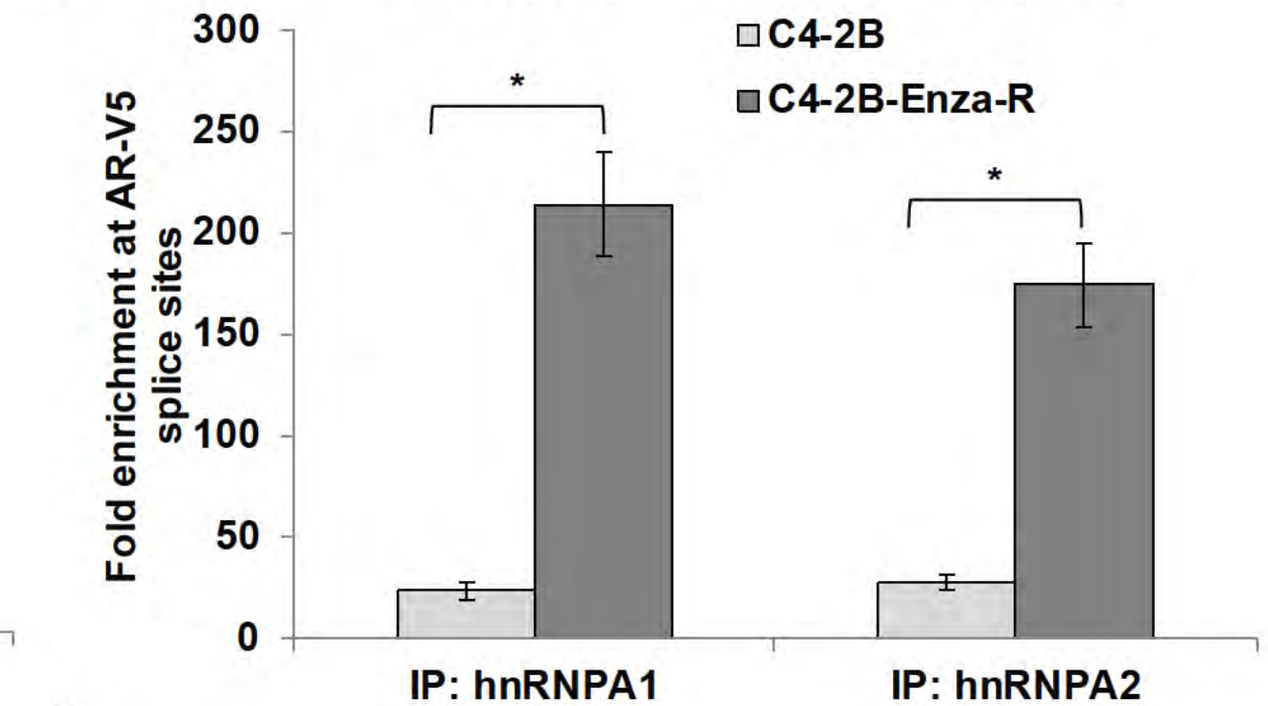

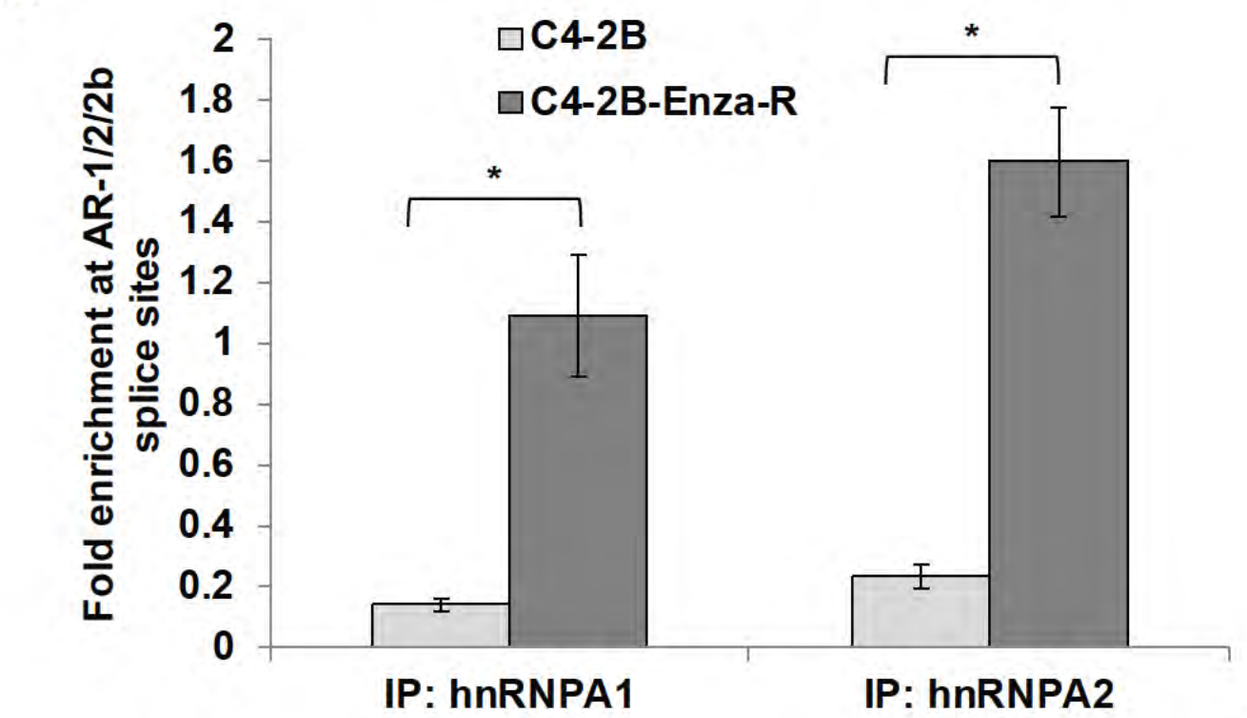

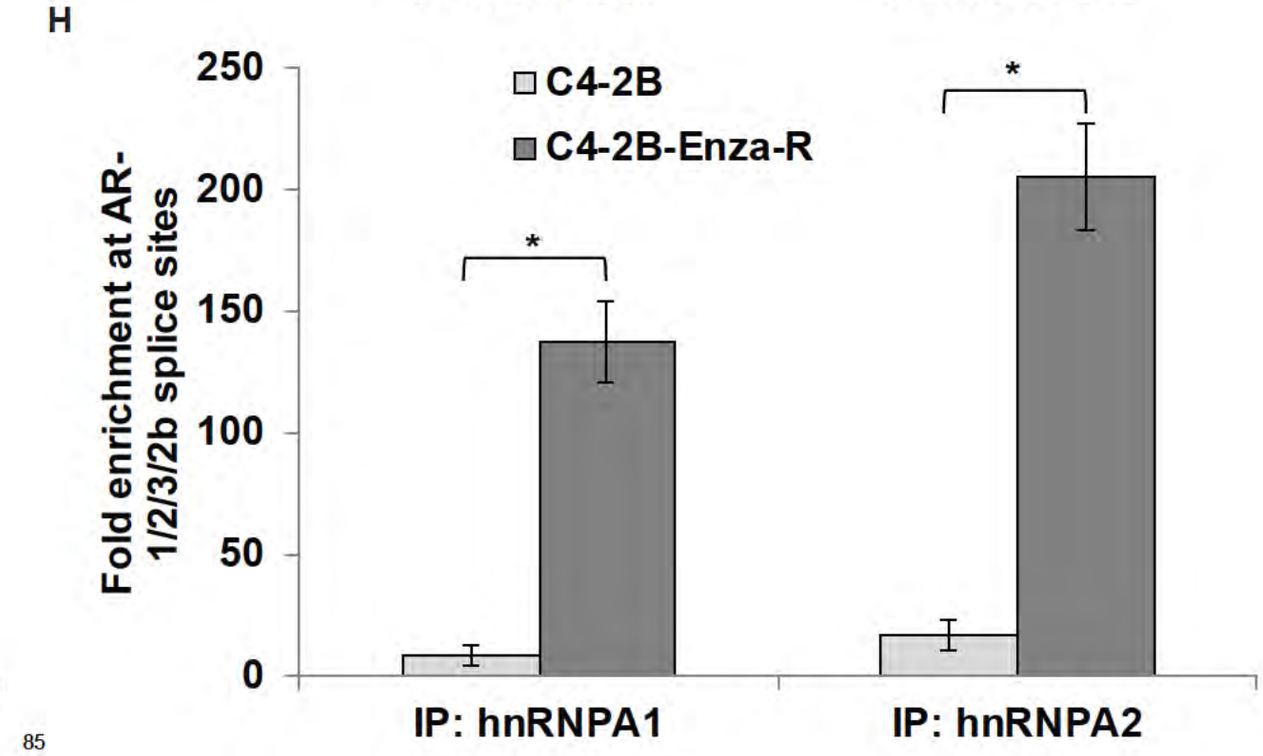

Supplementary Figure 2

A

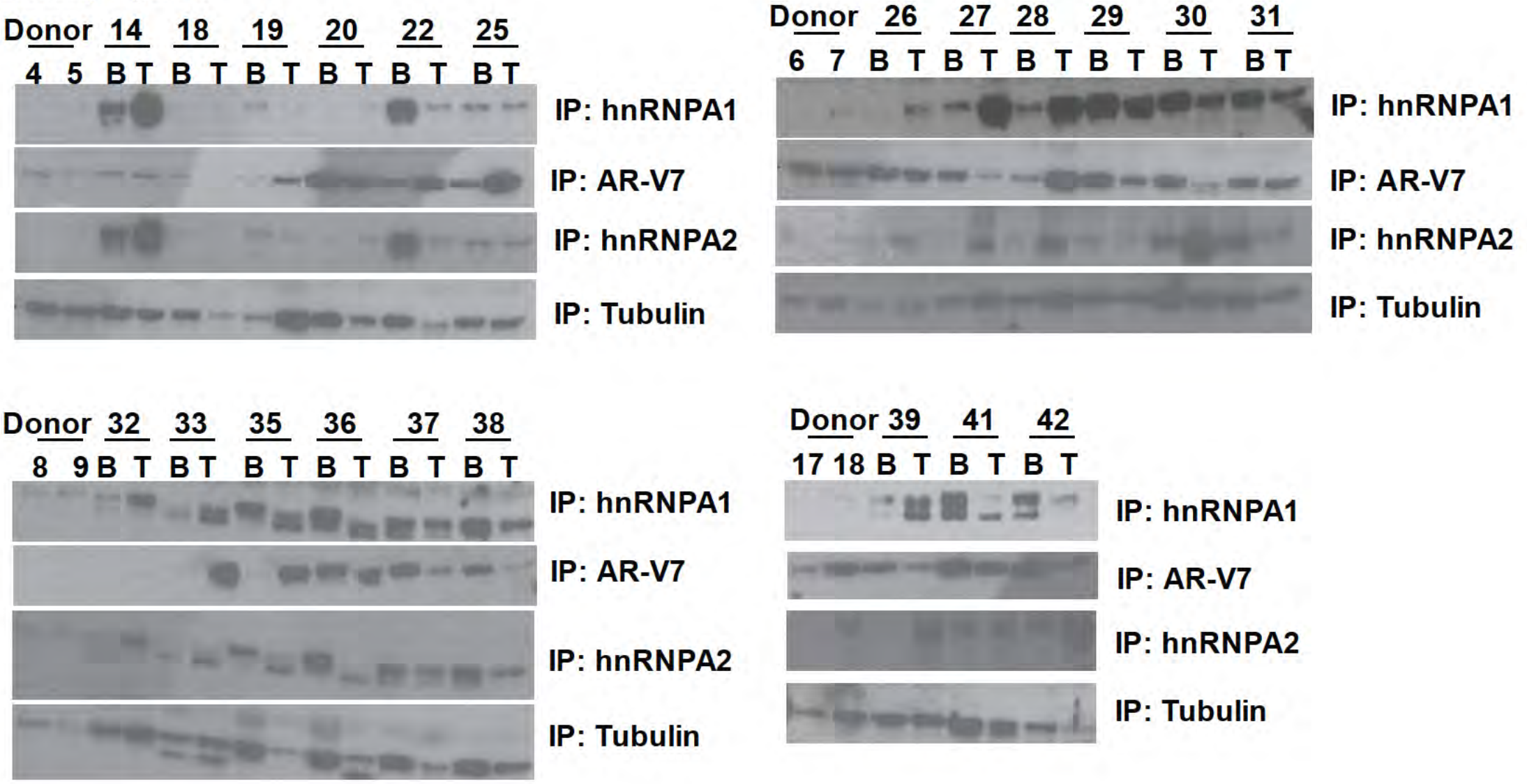

B

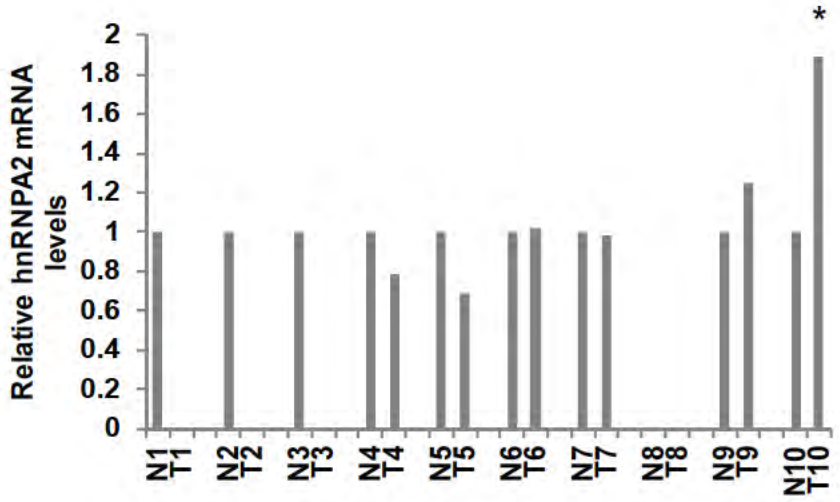

C

Gene	# of datasets	Up	Down	# of sites on AR mRNA
hnRNPA1	21	17	4	3
hnRNPA2	21	15	6	3

D

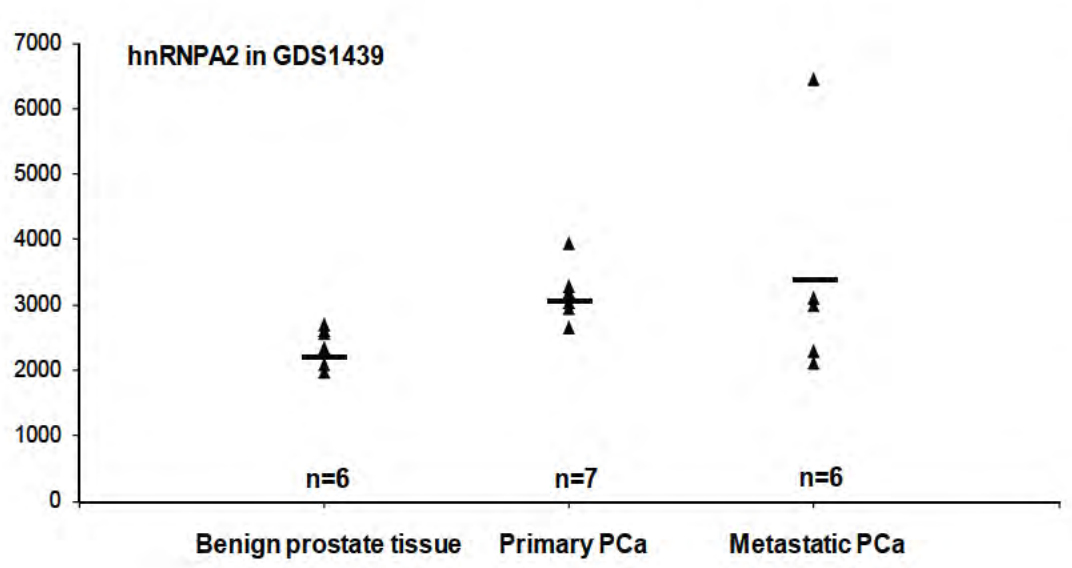

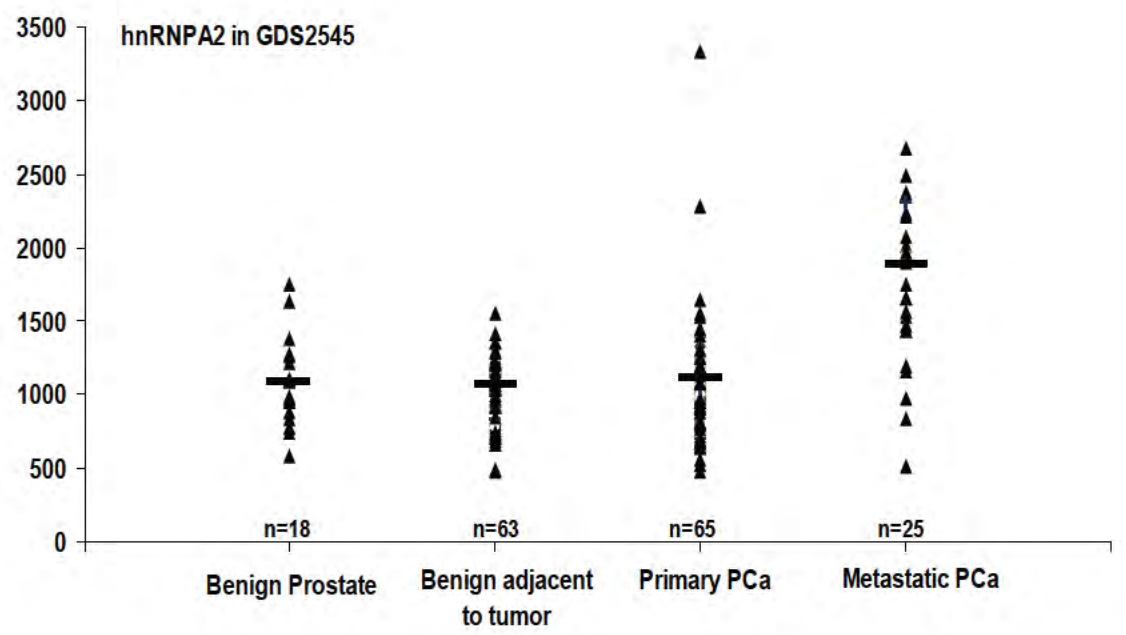

Supplementary Figure 3

A

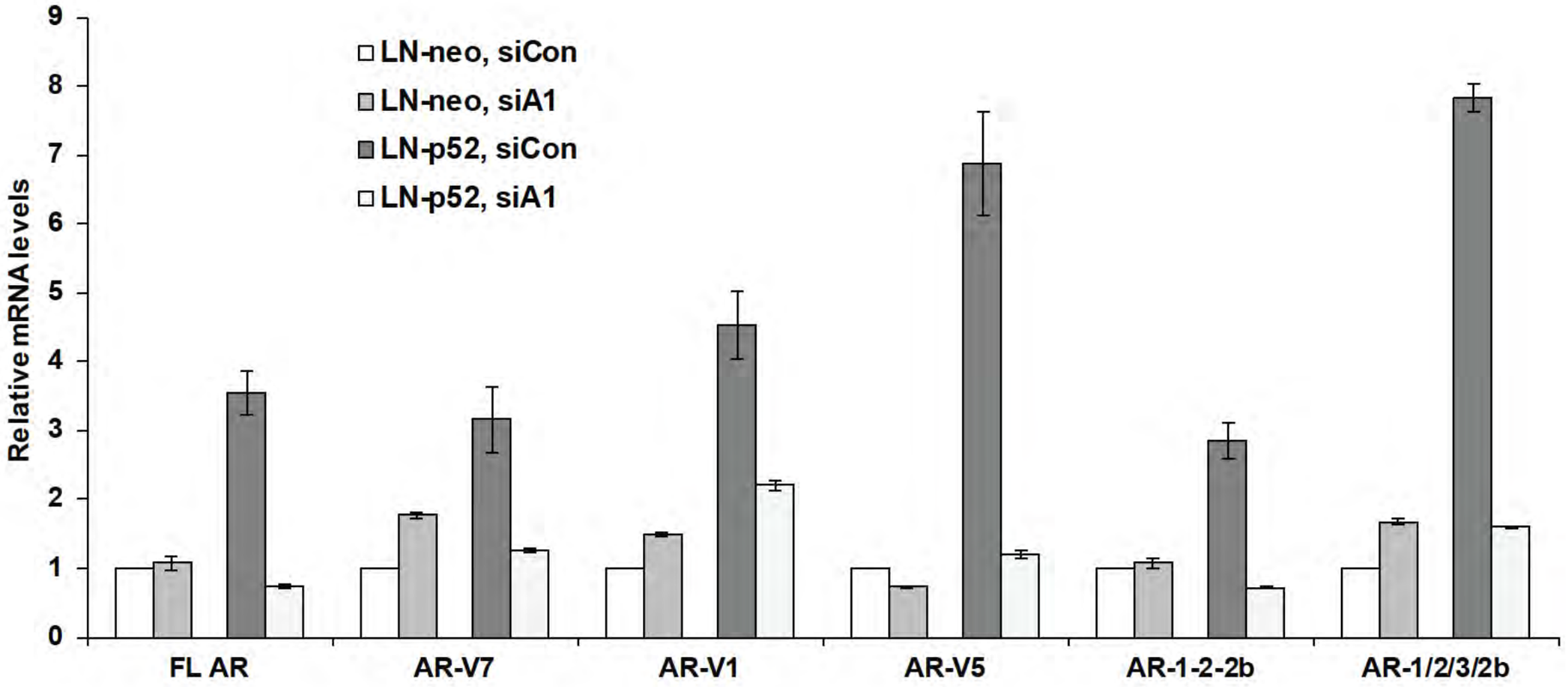

B

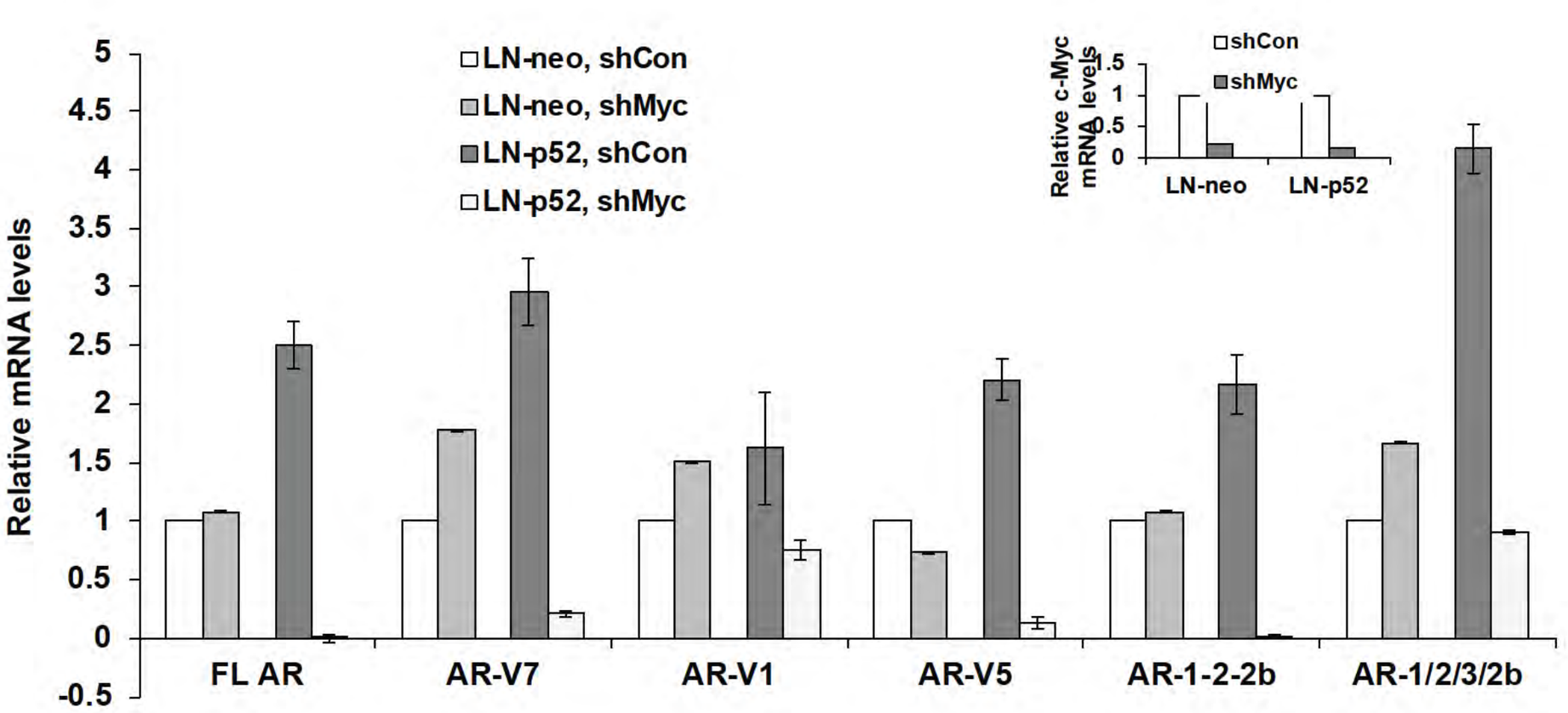

NF-kappaB2/p52:c-Myc:hnRNPA1 pathway regulates expression of androgen receptor splice variants and enzalutamide sensitivity in prostate cancer

Nagalakshmi Nadiminty[1¶], Ramakumar Tummala[1], Chengfei Liu[1], Wei Lou[1], Christopher P. Evans[1,2] and Allen C. Gao[1,2¶]

Authors' Affiliations: [1]Department of Urology, [2] Comprehensive Cancer Center, University of California at Davis, Sacramento, CA 95817

[¶]To whom correspondence should be addressed: Department of Urology, University of California Davis Medical Center, 4645 2nd Ave, Research III, Suite 1300, Sacramento, CA 95817. Email: acgao@ucdavis.edu, nnadiminty@ucdavis.edu

Running title: HnRNPA1 regulates alternative splicing of androgen receptor

Key words: hnRNPA1, AR-V7, c-Myc, Enzalutamide, Androgen Receptor

Financial Support

This work was supported by grants NIH/NCI CA140468, CA168601, CA179970 (A.C. Gao), DOD PC100502 (N. Nadiminty), and US Department of Veterans Affairs, ORD VA Merits I01 BX000526 (A.C. Gao), and by a Stand Up To Cancer Prostate Cancer Foundation-Prostate Dream Team Translational Cancer Research Grant SU2C-AACR-PCF DT0812, made possible by the generous support of the Movember Foundation. Stand Up To Cancer is a program of the Entertainment Industry Foundation administered by the American Association for Cancer research.

Conflicts of interest: The authors declare no conflicts of interest.

Word count: 5033

Figures: 6

Abstract

Castration resistant prostate cancer (CRPC) remains dependent on androgen receptor (AR) signaling. Alternative splicing of the AR to generate constitutively active, ligand-independent variants is one of the principal mechanisms that promote the development of resistance to next-generation anti-androgens such as enzalutamide. Here, we demonstrate that the splicing factor heterogeneous nuclear RNA-binding protein A1 (hnRNPA1) plays a pivotal role in the generation of AR splice variants such as AR-V7. HnRNPA1 is overexpressed in prostate tumors compared to benign prostates and its expression is regulated by NF-kappaB2/p52 and c-Myc. CRPC cells resistant to enzalutamide exhibit higher levels of NF-kappaB2/p52, c-Myc, hnRNPA1, and AR-V7. Levels of hnRNPA1 and of AR-V7 are positively correlated with each other in PCa. The regulatory circuit involving NF-kappaB2/p52, c-Myc and hnRNPA1 plays a central role in the generation of AR splice variants. Downregulation of hnRNPA1 and consequently of AR-V7 resensitizes enzalutamide-resistant cells to enzalutamide, indicating that enhanced expression of hnRNPA1 may confer resistance to AR-targeted therapies by promoting the generation of splice variants. These findings may provide a rationale for co-targeting these pathways to achieve better efficacy through AR blockade.

Introduction

Prostate cancer (PCa) remains the 2nd most lethal disease for males in western countries. The development of abiraterone and enzalutamide marked the continuing success of androgen deprivation therapy (ADT) practiced for over 70 years, reinforcing the concept that androgen receptor (AR) is the key factor for metastatic castration-resistant PCa (CRPC) progression and lethality. However, like earlier ADT, these new therapies have a short efficacy due to primary or acquired resistance. A major form of ADT-resistance in PCa is the generation of AR splicing variants that lack the ligand-binding-domain, thus evading binding of anti-androgens such as Bicalutamide and Enzalutamide. Several reports have documented the expression of alternatively spliced AR-Vs lacking the C-terminal ligand binding domain in PCa cells, which are constitutively nuclear and active even in the absence of androgens, thus indicating their potential role in the acquisition of the CRPC phenotype. Expression of these variants arises from the inclusion of cryptic exons located in intron 2 and 3 of the *AR* gene, which inserts premature stop codons and termination sites, yielding shorter AR proteins of 75 80 kDa lacking the androgen-binding domain (1, 2). Truncated AR-Vs such as AR-V7 (AR3) and AR^{v567es} can function independently of full-length AR and their selective knockdown can suppress androgen-independent growth of CRPC cells. Alternatively, AR-Vs may play important roles in activating the full length AR in a ligand-independent manner (3). AR-Vs confer resistance to not only AR targeted therapies (4, 5) but to conventional chemotherapeutics such as taxanes used as first line therapies against CRPC (6). These splice variants are rapidly induced after androgen deprivation and are suppressed after restoration of androgen supply (7). The mechanisms mediating increased expression of aberrant AR-Vs in PCa are still largely unknown. One possible cause of defective splicing is the genomic rearrangement and/or intragenic deletions of the *AR* locus in

CRPC (8). Alternatively, aberrant expression of specific splicing factors in PCa cells may also contribute to unbalanced splicing and aberrant recognition of cryptic exons in the *AR* gene. Understanding the molecular mechanism of AR-Vs production will facilitate the design of mechanism-based inhibitors, extending the efficacy of current ADT, and possibly treating progression of CRPC and prolonging patient survival.

The importance of alternative messenger RNA splicing in regulatory circuits is underscored by the fact that >90% of human genes encode transcripts that undergo at least one alternative splicing event with a frequency higher than 10% (9, 10). Alternative splicing plays important roles in development, physiology, and disease and is often disturbed in inflammatory disorders and cancers (11, 12). Alternative splicing modulates the generation of protein isoforms with distinct structural and functional properties or affects mRNA stability, by the insertion of premature stop codons, and translatability, by altering microRNA target sites (13). Two nuclear RNA-binding protein families, heterogeneous nuclear ribonucleoproteins (hnRNP) and serine/arginine-rich proteins (SR), play pivotal roles in regulation of alternative splicing. The hnRNP family consists of ~20 members which bind to splicing silencers located in exons or introns to promote exon exclusion and act as splicing repressors (13). The best characterized proteins of this group are hnRNPA1 and hnRNPA2, which share a high degree of sequence and functional homology (14). HnRNPA1 and hnRNPA2 are over-expressed in various kinds of tumors and serve as early tumor biomarkers (15-17). The SR family includes >20 members which bind to splicing enhancers and predominantly function to counterbalance the activity of hnRNP proteins (18). Splicing factor 2/alternative splicing factor (SF2/ASF), the best characterized member of the SR family, is up-regulated in multiple human cancers, including lung and cervical cancers, and plays important roles in the establishment and maintenance of

cellular transformation (19). During tumor progression, stimuli from the tumor microenvironment may affect the expression and/or activity of splicing regulatory factors, thus perturbing the physiological splicing program of genes involved in cellular processes. An increasing body of evidence indicates that splicing variants of many cancer-related genes can directly contribute to the oncogenic phenotype and to the acquisition of resistance to therapeutic treatments (11, 12, 20). Hence, understanding the functional role(s) of cancer-associated alternative splicing variants and the mechanisms underlying their production offers the potential to develop novel diagnostic, prognostic and more specific anticancer therapies.

In the present study, we investigated the mechanisms involved in aberrant splicing of AR transcripts in a constitutively occurring setting as well as in response to chronic treatment with enzalutamide. Our results show that the splicing factor hnRNPA1 plays a major role in generation of AR-Vs. We also demonstrate that enhanced expression of hnRNPA1 may be mediated by c-Myc and NF-kappaB2/p52, thus paving the way for increase in transcript numbers of constitutively active splice variants and contributing to CRPC therapy resistance.

Materials and Methods

Cell lines and reagents

LNCaP, CWR22Rv1 and VCaP cells were obtained in 2001 from the American Type Culture Collection (ATCC, Manassas, VA) and were cultured in RPMI containing 10% complete FBS and penicillin/streptomycin. ATCC uses Short Tandem Repeat (STR) profiling for testing and authentication of cell lines. C4-2B cells were kindly provided and authenticated by Dr. Leland Chung, Cedars-Sinai Medical Center, Los Angeles, CA in 2006. All experiments with these cell lines were performed within 6 months of resuscitation after cryopreservation. LNCaP cells stably expressing NF-kappaB2/p52 were generated by stable transfection of LNCaP cells

with plasmids expressing NF-kappaB2/p52 as described previously (21) and were not authenticated further. 22Rv1 and C4-2B cells resistant to enzalutamide (22Rv1-Enza-R and C4-2B-Enza-R) were generated by chronic culture of 22Rv1 and C4-2B cells in enzalutamide as described previously (22, 23) and were not authenticated further. Antibodies against NF-kappaB2/p52 (K-27), AR (441; mouse monoclonal), HA, Tubulin, U2AF65 and ASF/SF2 were from Santa Cruz Biotechnologies. Antibodies against splicing factors hnRNPA1 (9H10) and hnRNPA2B1 (DP3B3) were from Sigma-Aldrich and AbCam respectively. Sso Fast™ Eva Green qPCR Supermix was from Bio-Rad. All other reagents were of analytical grade and obtained from local suppliers.

Cell growth assays

Plasmid transfections were performed using Attractene transfection reagent (Qiagen). Oligonucleotide siRNA transfections were performed using Lipofectamine 2000 transfection reagent (Invitrogen). Viable cell numbers were determined using a Coulter cell counter (Beckman Coulter).

Western Blot Analysis

Cells were lysed in high salt buffer containing 50 mM Hepes pH 7.9, 250 mM NaCl, 1 mM EDTA, 1% NP-40, 1 mM PMSF, 1 mM Na Vanadate, 1 mM NaF and protease inhibitor cocktail (Roche). Total protein was estimated using the Coomassie Protein Assay Reagent (Pierce). Equal amounts of protein were loaded on 10% SDS PAGE and transferred to nitrocellulose membranes. The membranes were blocked with 5% nonfat milk in PBST (1x PBS+0.1% Tween-20) and probed with indicated primary antibodies in 1% BSA. The signal was detected by ECL (Millipore) after incubation with the appropriate HRP-conjugated secondary antibodies.

Real-Time quantitative RT-PCR

Total RNAs were extracted using TriZOL reagent (Invitrogen). 1 μg of total RNAs were subjected to digestion with RNase-free RQ1 DNase (Promega) and cDNAs were prepared using ImProm^{II} Reverse Transcriptase (Promega) according to manufacturer's instructions. The cDNAs were analyzed by real-time reverse transcription-PCR (RT-PCR) using Sso Fast^{TM} Eva Green Supermix (Bio-Rad) as described previously (24). Each reaction was normalized by co-amplification of actin. Triplicates of samples were run on a Bio-Rad CFX-96 real-time cycler.

RNA Immunoprecipitation Assay (RIP)

RIP assays were performed as described earlier (25). RNA-protein complexes were crosslinked using 1% formaldehyde. Nuclear extracts were immunoprecipitated with antibodies against indicated RNA-binding splicing factors. Isotype-matched IgG was used as control. Bound RNAs were purified, reverse transcribed and the levels of indicated transcripts were analyzed by qPCR. Splice sites in the full length AR pre-mRNA were detected using ESRsearch and ESEFinder programs (Suppl. Fig. 1).

Human clinical specimens

Paired benign and tumor prostate tissue extracts were described previously (26). Total RNAs from human clinical specimens used for measurement of splicing factor transcript levels were described previously (27).

Gene Expression Omnibus Analysis

Two separate datasets from NCBI GEO were screened independently for expression levels of hnRNPA1, hnRNPA2, U2AF65 and SF2/ASF. GDS1439 (28) compared specimens of benign prostatic hyperplasia with clinically localized primary PCa and metastatic PCa. GDS2545 (29) compared normal prostate specimens without any pathology, normal prostate adjacent to

tumor, primary prostate tumor, and metastatic PCa. Significant differences between groups were determined using Microsoft Excel Tools.

Oncomine Analysis

Data sets generated from four comparisons of normal prostate tissue with prostate carcinoma: Lapointe_prostate (30), Wallace_prostate (31), Singh_prostate (32) and Yu_prostate (33) were analyzed using the differential expression function of Oncomine.

Statistical Analyses

Data are shown as means ± SD. Multiple group comparison was performed by one-way ANOVA followed by the Scheffe procedure for comparison of means. $P \leq 0.05$ was considered significant.

Results

HnRNPA1 regulates the expression of AR variants

To test whether generation of AR variants by alternative splicing is dependent upon expression of hnRNPs, we analyzed expression levels of full length AR and of variants such as AR-V7, AR-V1, AR-V5, AR-1/2/2b and AR-1/2/3/2b using qRT-PCR in 22Rv1 and VCaP PCa cells transfected with siRNAs against hnRNPA1 and hnRNPA2. Downregulation of hnRNPA1 and hnRNPA2 decreased the expression levels of AR variants in 22Rv1 and VCaP cells (Fig. 1A, 1B & Suppl. Fig. 2A, 2B). Insets in Fig. 1A and B confirm the downregulation of hnRNPA1 and hnRNPA2 by specific siRNAs. The downregulation of hnRNPA1 and the resultant suppression of AR-V7 protein levels were confirmed by Western blot analysis (Fig. 1C). The protein levels of AR-V7 variant were decreased in both 22Rv1 and VCaP cells transfected with hnRNPA1 siRNA. These results indicate that hnRNPA1 may regulate the generation of AR-Vs in PCa cells.

Next, we tested whether overexpression of hnRNPA1 affects the expression levels of AR-Vs. LNCaP cells were transfected with full length hnRNPA1 cDNA and levels of AR-Vs were analyzed by Western blotting and qRT-PCR. Overexpression of hnRNPA1 enhanced AR-V7 protein levels in LNCaP cells which possess undetectable endogenous levels of AR-V7 protein (Fig. 1D). qRT-PCR confirmed that overexpression of hnRNPA1 significantly enhanced the mRNA levels of AR-V7, AR-V5, AR-1/2/2b and AR-1/2/3/2b variants in LNCaP cells (Fig. 1E & Suppl. Fig. 2C). Inset in Fig. 1E confirms the overexpression of hnRNPA1 after transfection in LNCaP cells. These results using downregulation as well as overexpression of hnRNPA1 suggest that hnRNPA1 plays an important role in the generation of AR splice variants.

Recruitment of hnRNPA1 to splice sites in AR pre-mRNA is increased in enzalutamide-resistant cells

We found hnRNP binding sites (UAGGGA) in the full length AR mRNA using sequence analysis and ESRSearch program (Suppl. Fig. 1). To determine whether hnRNPA1 is recruited to splice sites in the AR pre-mRNA, we performed RNA Immunoprecipitation (RIP) assays using specific antibodies against hnRNPA1 and hnRNPA2 in 22Rv1 vs. 22Rv1-Enza-R and C4-2B vs. C4-2B-Enza-R cell lines. The 22Rv1-Enza-R and C4-2B-Enza-R cell lines were generated by chronic exposure to enzalutamide and display resistance to enzalutamide (22, 23). The degree of recruitment of hnRNPA1 to AR-V7 splice sites was significantly higher in 22Rv1-Enza-R cells compared to parental 22Rv1 cells (Fig. 2A), indicating that hnRNPA1 may promote generation of AR-V7 in PCa cells resistant to enzalutamide. Even though the recruitment of hnRNPA2 to AR-V7 splice sites was also enhanced in 22Rv1-Enza-R cells compared to 22Rv1 cells, the recruitment of hnRNPA1 was several fold higher than that of hnRNPA2 (Fig. 2A). No

significant differences were observed in the recruitment of either hnRNPA1 or hnRNPA2 to FL AR splice sites between 22Rv1 parental and 22Rv1-Enza-R cells (Fig. 2B). We also analyzed recruitment of hnRNPA1 and hnRNPA2 to splice sites for other AR-Vs such as AR-V1, AR-V5, AR-1/2/2b and AR-1/2/3/2b (Suppl. Fig. 3A, B, C & D). Recruitment of hnRNPA1 to AR-1/2/2b splice sites was significantly higher in 22Rv1-Enza-R cells (Suppl. Fig. 3C), indicating that hnRNPA1 may play a selective role in generation of AR splice variants. In addition, recruitment of hnRNPA2 to AR-1/2/3/2b splice sites was significantly enhanced in 22Rv1-Enza-R cells (Suppl. Fig. 3D). These results imply that different splicing factors may function co-operatively to promote generation of AR-Vs in enzalutamide-resistant PCa cells. These results also confirm that hnRNP proteins are physically recruited to splice sites in the AR pre-mRNA with the degree of recruitment increasing in PCa cells resistant to enzalutamide, indicating that hnRNP proteins may drive the generation of AR splice variants leading to enzalutamide resistance.

To confirm the above results in another enzalutamide-resistant cell line, we analyzed the C4-2B vs. C4-2B-Enza-R cell line pair. Our results showed that recruitment of hnRNPA1 and hnRNPA2 to AR-V7 splice sites was significantly enhanced in C4-2B-Enza-R cells compared to parental C4-2B cells (Fig. 2C), while, similar to 22Rv1-Enza-R cells, recruitment of either hnRNPA1 or hnRNPA2 to FL AR splice sites was not altered significantly in C4-2B-Enza-R cells compared to parental C4-2B cells (Fig. 2D). In all cases, the fold enrichment of hnRNPA1 at splice sites on AR pre-mRNA was much higher compared to hnRNPA2, indicating that hnRNPA1 may play a more central role in promoting the expression of AR-Vs (Suppl. Fig. 3E, F, G & H). These results collectively demonstrate that different splicing factors may play context- and cell type-dependent roles in PCa cells in alternative splicing of the AR.

Expression levels of hnRNPA1 are elevated in PCa tissues

To determine whether increased expression of splicing factors and AR-Vs is associated with PCa, we examined the expression levels of hnRNPA1 and hnRNPA2 by immunoblotting in lysates from 27 archived paired benign and tumor PCa clinical samples. Levels of hnRNPA1 and hnRNPA2 were elevated in ~44% of tumor tissues compared to matched benign tissues (Fig. 3A and Suppl. Fig. 4A). These results were correlated positively with the protein expression levels of AR-V7, which were enhanced in ~ 48% of tumor tissues compared to their benign counterparts (Fig. 3A and Suppl. Fig. 4A). In addition, expression levels of hnRNPA1 and hnRNPA2 were low or undetectable in 9/12 and 6/12 of donor prostates respectively. These observations were also correlated with expression levels of AR-V7 which were low or undetectable in 8/12 donor tissues (Table 1).

We also analyzed the mRNA levels of hnRNPA1, hnRNPA2 and AR-V7 in archival total RNAs extracted from 10 pairs of matched benign and tumor clinical PCa specimens (27, 34). Transcript levels of hnRNPA1 were elevated in 5/10 of tumor tissues compared to matched benign tissues with no appreciable differences between tumor and benign being observed in the other 5/10 of samples (Fig. 3B). Transcript levels of AR-V7 were elevated in 6/10 tumor tissues compared to their matched benign counterparts (Fig. 3C), demonstrating that expression of hnRNPA1 and AR-V7 may be positively correlated with each other in human PCa. No significant differences were observed in mRNA levels of hnRNPA2 between matched tumor and benign prostate tissues (Suppl. Fig. 4B).

To further confirm our findings, we analyzed expression levels of hnRNPA1 and hnRNPA2 in clinical PCa tissues using publicly available datasets from Gene Expression Omnibus (GEO) and Oncomine. Results from an analysis of Oncomine datasets revealed that expression levels of hnRNPA1 and hnRNPA2 are significantly elevated in prostate tumor tissues

compared to benign prostates in 17/21 and 15/21 datasets respectively (Suppl. Fig. 4C). Results from a representative dataset, Singh_prostate (n 102) from Oncomine are shown (Fig. 3D & E). An analysis of GEO revealed that expression levels of hnRNPA1 and hnRNPA2 were elevated in primary as well as metastatic PCa compared to benign prostates (Fig. 3F & G and Suppl. Fig. 4D). Data regarding expression levels of AR-Vs were not available in these datasets, but nonetheless, these results indicate that elevated levels of hnRNPA1 may contribute to PCa development and progression. Our findings correlate well with studies showing that expression levels of AR-V7 are elevated in ~40% of CRPC tissues (2, 35), indicating that elevated expression of hnRNPA1 in prostate tumors may contribute to generation of higher levels of AR-Vs.

Expression of hnRNPA1 is regulated by c-Myc

Previous studies indicated that hnRNPA1 and c-Myc exhibit positive reciprocal regulation (36). C-Myc enhances hnRNPA1 expression transcriptionally, while hnRNPA1 regulates c-Myc via alternative splicing. Previous studies also showed that c-Myc is one of the transcription factors which regulate transcription of the AR (37). Hence, we analyzed the status of c-Myc or hnRNPA1 when the expression of either was downregulated in PCa cells. Lysates from 22Rv1 and VCaP cells transfected with shRNA against c-Myc were analyzed using specific antibodies against hnRNPA1. Downregulation of c-Myc reduced protein levels of hnRNPA1 significantly (Fig. 4A). Similarly, lysates from LNCaP, 22Rv1 and VCaP cells transfected with siRNA against hnRNPA1 were examined by immunoblotting using specific antibodies against c-Myc. Downregulation of hnRNPA1 reduced protein levels of c-Myc (Fig. 4B). These results confirm that hnRNPA1 and c-Myc exhibit reciprocal regulation in PCa cells. We also analyzed whether reduction in hnRNPA1 levels by c-Myc shRNA affects expression of AR-Vs in 22Rv1

and VCaP cells. Western blotting and qRT-PCR analyses showed that levels of AR-Vs, including that of AR-V7, were abrogated due to depletion of hnRNPA1 caused by downregulation of c-Myc (Fig. 4A, C & D and Suppl. Fig. 5). These findings support an important role for c-Myc in the generation of AR splice variants.

In order to analyze whether overexpression of hnRNPA1 can overcome the effects of downregulation of Myc, we suppressed expression of c-Myc using shRNA in 22Rv1 cells followed by overexpression of hnRNPA1. The results showed that even though suppression of c-Myc reduced mRNA as well as protein levels of both FL AR and AR-V7, subsequent overexpression of hnRNPA1 restored the expression of AR-V7 fully while having minimal effect on FL AR (Fig. 4E & F). These results indicate that hnRNPA1 primarily regulates generation of alternative splice variants of the AR and not the generation of the FL AR.

NF-kappaB2/p52 regulates AR-V7 expression via hnRNPA1 and c-Myc

We reported earlier that activation of NF-kappaB2/p52 promotes progression to CRPC and enzalutamide resistance via the generation of AR variants, specifically AR-V7 (21, 23, 24). Our previous findings also indicated that NF-kappaB2/p52 may regulate c-Myc expression. Hence, we examined whether NF-kappaB2/p52 plays a role in the elevated expression of hnRNPA1 and c-Myc in PCa using lysates from LNCaP cells stably expressing p52 (LN-p52). Protein levels of AR-V7, hnRNPA1 and c-Myc were elevated in LN-p52 cells, while no appreciable differences were found in the expression of hnRNPA2 (Fig. 5A, left panel). These results were confirmed using LNCaP cells expressing p52 under the control of a Tet-inducible promoter (LN/TR/p52). Induction of p52 expression led to increases in expression levels of AR-V7, hnRNPA1 and c-Myc (Fig. 5A, right panel), indicating that upregulation of AR-V7 by p52 may be mediated by hnRNPA1 and c-Myc. To examine the relationship between hnRNPA1, c-

Myc and AR-V7 in LN-p52 cells, we analyzed levels of AR-V7 by Western blotting in LN-p52 cells transfected with hnRNPA1 or hnRNPA2 siRNAs. Downregulation of hnRNPA1 abrogated the expression of AR-V7 in LN-p52 cells, while downregulation of hnRNPA2 did not have an appreciable effect on AR-V7 protein levels (Fig. 5B, left panel). Protein levels of c-Myc were also downregulated, keeping in line with earlier findings that hnRNPA1 and c-Myc regulate each other (36). In addition, expression of hnRNPA1 and AR-V7 were abolished as a result of downregulation of c-Myc expression in LN-p52 cells transfected with c-Myc shRNA (Fig. 5B, middle panel).

To confirm these findings in a cell line with constitutive expression of both p52 and AR-V7, we analyzed levels of AR-V7, hnRNPA1 and c-Myc by immunoblotting in 22Rv1 cells transfected with p52 shRNA. Downregulation of p52 in 22Rv1 cells abrogated expression of AR-V7, hnRNPA1 and c-Myc (Fig. 5B, right panel). These results demonstrate that NF-kappaB2/p52 may modulate generation of AR-Vs by regulation of hnRNPA1 and c-Myc.

PCa cells resistant to enzalutamide exhibit higher levels of splicing factors

As our results demonstrate that expression of hnRNPA1 and AR variants may be positively correlated with each other in PCa cells, and AR-V7 expression has been shown to be involved in the acquisition of resistance to enzalutamide (3, 23), we tested the correlation between levels of AR variants and hnRNPA1 in PCa cells that have acquired resistance to enzalutamide. 22Rv1-Enza-R and C4-2B-Enza-R cell lines exhibited higher levels of AR-V7 and hnRNPA1 (Fig. 5C), indicating that expression of hnRNPA1 may be positively correlated with expression of AR-Vs. Furthermore, expression levels of c-Myc and NF-kappaB2/p52 were also elevated in enzalutamide-resistant cells, confirming the importance of the NF-kappaB2/p52:c-Myc:hnRNPA1:AR-V7 axis in enzalutamide resistance. No significant differences were

observed in the expression of hnRNPA2 in 22Rv1-Enza-R and C4-2B-Enza-R cells compared to their parental cells (Fig. 5C right & middle panels). To confirm these results *in vivo*, we analyzed extracts from xenograft tumors derived from C4-2B and C4-2B-Enza-R cells using antibodies against AR-V7 and hnRNPA1. Higher levels of AR-V7 were observed in xenografts derived from C4-2B-Enza-R cells, which was correlated well with higher levels of hnRNPA1 and c-Myc (Fig. 5C right panel), confirming our observations that expression of AR-Vs is positively correlated with expression of hnRNPA1 in PCa cell lines resistant to enzalutamide.

Next, we tested whether downregulation of hnRNPA1 affects endogenous levels of AR-Vs in 22Rv1-Enza-R cells. Transfection of hnRNPA1 siRNA abrogated levels of AR-V7 in 22Rv1-Enza-R cells (Fig. 5D left panel). Similarly, downregulation of c-Myc by specific shRNA reduced expression levels of AR-V7 and hnRNPA1 in 22Rv1 and 22Rv1-Enza-R cells (Fig. 5D right panel), confirming the c-Myc: hnRNPA1: AR-V7 axis in PCa cells.

To confirm the importance of the link between NF-kappaB2/p52, c-Myc, hnRNPA1 and AR-V7 in PCa, we analyzed the correlation between their expression levels at mRNA and protein levels in paired benign and tumor prostate clinical samples from Fig. 3. Transcript (left panel) and protein (right panel) levels of NF-kappaB2/p52, c-Myc, hnRNPA1 and AR-V7 were positively correlated with each other (Fig. 5E), demonstrating that the NF-kappaB2/p52:c-Myc:hnRNPA1:AR-V7 axis plays a vital role in PCa and in the development of castration and therapy resistance.

Suppression of hnRNPA1 resensitizes enzalutamide-resistant PCa cells to enzalutamide

To examine the functional relevance of regulation of AR alternative splicing by hnRNPA1, we tested whether downregulation of hnRNPA1 resulting in decreased levels of AR-V7 resensitizes enzalutamide-resistant cells to enzalutamide. We examined cell survival in

22Rv1 and 22Rv1-Enza-R cells transfected with hnRNPA1 or hnRNPA2 siRNAs and treated with 0 and 20 μM enzalutamide for 24 h. Reduced expression of hnRNPA1 enhanced the sensitivity of enzalutamide-resistant 22Rv1-Enza-R cells to enzalutamide (Fig. 6A), indicating that upregulation of AR-V7 expression by hnRNPA1 may be required to sustain the acquired resistance of 22Rv1-Enza-R cells to enzalutamide. Downregulation of hnRNPA1 and hnRNPA2 also enhanced the sensitivity of LN-neo and LN-p52 cells transfected with hnRNPA1 or hnRNPA2 siRNAs and treated with 20 μM enzalutamide to enzalutamide (Fig. 6B). Suppression of hnRNPA1 expression reduced cell survival by ~40-50% when enzalutamide-resistant LN-p52 cells were treated with enzalutamide. Suppression of hnRNPA1 expression also reduced survival of VCaP cells when treated with enzalutamide (Fig. 6C), confirming the essential nature of AR variants in these cells.

Our findings collectively demonstrate that hnRNPA1 plays a major role in the generation of AR splice variants. Expression of hnRNPA1 is modulated by NF-kappaB2/p52 via c-Myc (Fig. 6D). Our results point to the enhanced expression of hnRNPA1 in prostate tumors being instrumental in inducing alternative splicing of the precursor AR mRNA.

Discussion

A large number of previous studies have shown that C-terminally truncated AR-Vs are expressed in PCa cells and even in normal prostate epithelial cells (35, 38) and promote CRPC progression under androgen deprivation (39, 40). In addition, enhanced expression of AR-V7 confers resistance to next generation therapeutics such as enzalutamide and abiraterone (4, 5). These studies attest to the importance of AR-Vs in CRPC and co-targeting the mechanisms which contribute to their generation may increase the efficacy of currently used AR-targeted

therapies and prolong time to development of resistance. Our findings in this study demonstrate that the splicing factor hnRNPA1 plays a major role in the alternative splicing of AR mRNA.

HnRNPA1 is a multifunctional RNA-binding protein involved in the regulation of RNA biogenesis. HnRNPA1 is under the transcriptional control of the c-Myc proto-oncogene and modulates the splicing of PKM2, activating the metabolic switch to aerobic glycolysis that is a hallmark of cancer cells (11, 36). HnRNPA1 also regulates alternative splicing of genes involved in invasion and metastasis such as Rac1 and Ron (11). Increased expression of hnRNPA1 has been documented in proliferating and transformed cells (20) and in lung, breast, colon, renal cell carcinomas and gliomas (41-46). HnRNPs co-operate with other splicing factors to generate pro-oncogenic and pro-inflammatory molecules in cancers (41, 47). Silencing of hnRNPA1 and A2 promotes apoptosis in human and mouse cancer cell lines, while having no effect on normal epithelial and fibroblastic cell lines (48).

In this study, hnRNPA1 binding sites (UAGGGA) were identified in AR mRNA using sequence analysis and ESRSearch program. Downregulation of hnRNPA1 significantly reduced the expression of AR-Vs such as AR-V7, while not affecting full length AR. HnRNPA1 binding sites were not detected at full length AR splice sites in the AR pre-mRNA. Moreover, the slight decrease seen in either full length AR mRNA or protein levels in VCaP or 22Rv1 cells respectively (Fig. 1) was not observed consistently in all experiments. In consideration of these observations, we concluded that hnRNPA1 does not play a significant role in splicing of full length AR from AR pre-mRNA. RNA-binding assays revealed that hnRNPA1 is recruited to splice sites for AR splice variants. Enhanced expression of hnRNPA1 was observed in PCa tissues compared to their benign counterparts, which was correlated positively with expression of AR-V7. Increased expression of hnRNPA1 was also correlated with higher levels of AR-V7 in

PCa cells with acquired resistance to enzalutamide. Exploration of the mechanisms revealed that c-Myc and NF-kappaB2/p52 contribute to the development of therapy resistance in PCa cells by inducing hnRNPA1 expression and thereby ligand-independent AR-Vs. Downregulation of hnRNPA1 resensitized enzalutamide-resistant cells to enzalutamide, indicating that suppression of hnRNPA1 resulting in suppression of AR-Vs reversed the acquired resistance to enzalutamide. These data led us to conclude that hnRNPA1 is the central player in a splicing regulatory circuit involving c-Myc, NF-kappaB2/p52 and AR.

Our study demonstrates that elevated levels of splicing factors such as hnRNPA1 promote expression of alternative splice forms of AR. Relative amounts of splicing factors have been proposed to determine alternative splicing (45). A recent study by Liu et al (49) showed that recruitment, and not expression, of splicing factors SF2/ASF and U2AF65 determines the generation of AR splice variants in enzalutamide resistance. We found higher levels of hnRNPA1 in PCa clinical samples compared to SF2/ASF (data not shown), indicating that higher expression of a splicing factor, and not simply its recruitment to splice sites under certain conditions, may determine the levels of alternative splice forms. These results are supported by previous studies which showed that the relative levels of hnRNPA1 expression increased to a greater extent than those of SF2/ASF in lung tumors (44). Of note, analysis of expression levels of U2AF65 and SF2/ASF in PCa tissues using GEO and Oncomine datasets revealed that expression levels of both splicing factors are elevated in PCa tissues compared to benign counterparts (Suppl. Fig. 6), lending credence to our observations that enhanced expression of splicing factors may be one of the principal mechanisms driving generation of AR-Vs. Elevated levels of hnRNPA1 may conceivably change the splicing milieu of a broad spectrum of proteins in addition to that of the AR, with splicing of CD44 being an example. But splice variants of AR

have been demonstrated to play major roles in resistance to enzalutamide, underlining the importance of our results in splicing regulation of the AR. Furthermore, earlier studies indicated that the splice variant AR-1/2/3/2b is also generated by intragenic genomic rearrangement of the AR gene due to duplication of exon 3 (1). Our studies consistently found transcripts corresponding to this splice variant in LNCaP, C4-2B and VCaP cells, albeit at extremely low levels. These observations warrant further exploration of the mechanisms involved in generation of this splice variant and further validation.

In summary, we demonstrated that hnRNPA1, in concert with NF-kappaB2/p52 and c-Myc, regulates the generation of AR-Vs in PCa cells and that the NF-kappaB2/p52:c-Myc:hnRNPA1:AR-V7 axis (Fig. 6D) plays a pivotal role in the development and maintenance of resistance to androgen blockade. These findings may have important implications in targeting AR-Vs and the splicing factors responsible to overcome acquired enzalutamide resistance in PCa.

References

1. Dehm SM, Schmidt LJ, Heemers HV, Vessella RL, Tindall DJ. Splicing of a Novel Androgen Receptor Exon Generates a Constitutively Active Androgen Receptor that Mediates Prostate Cancer Therapy Resistance. Cancer Research. 2008;68:5469-77.
2. Hu R, Dunn TA, Wei S, Isharwal S, Veltri RW, Humphreys E, et al. Ligand-Independent Androgen Receptor Variants Derived from Splicing of Cryptic Exons Signify Hormone-Refractory Prostate Cancer. Cancer Research. 2009;69:16-22.
3. Cao B, Qi Y, Zhang G, Xu D, Zhan Y, Alvarez X, et al. Androgen receptor splice variants activating the full-length receptor in mediating resistance to androgen-directed therapy. Oncotarget. 2014;5:1646-56.
4. Mostaghel EA, Marck BT, Plymate SR, Vessella RL, Balk S, Matsumoto AM, et al. Resistance to CYP17A1 Inhibition with Abiraterone in Castration-Resistant Prostate Cancer: Induction of Steroidogenesis and Androgen Receptor Splice Variants. Clinical Cancer Research. 2011;17:5913-25.
5. Li Y, Chan SC, Brand LJ, Hwang TH, Silverstein KAT, Dehm SM. Androgen Receptor Splice Variants Mediate Enzalutamide Resistance in Castration-Resistant Prostate Cancer Cell Lines. Cancer Research. 2013;73:483-9.
6. Thadani-Mulero M, Portella L, Sun S, Sung M, Matov A, Vessella RL, et al. Androgen Receptor Splice Variants Determine Taxane Sensitivity in Prostate Cancer. Cancer Research. 2014;74:2270-82.

7. Yu Z, Chen S, Sowalsky AG, Voznesensky OS, Mostaghel EA, Nelson PS, et al. Rapid Induction of Androgen Receptor Splice Variants by Androgen Deprivation in Prostate Cancer. Clinical Cancer Research. 2014;20:1590-600.
8. Li Y, Hwang TH, Oseth LA, Hauge A, Vessella RL, Schmechel SC, et al. AR intragenic deletions linked to androgen receptor splice variant expression and activity in models of prostate cancer progression. Oncogene. 2012;31:4759-67.
9. Bonomi S, di Matteo A, Buratti E, Cabianca DS, Baralle FE, Ghigna C, et al. HnRNP A1 controls a splicing regulatory circuit promoting mesenchymal-to-epithelial transition. Nucleic Acids Research. 2013;41:8665-79.
10. Pan Q, Shai O, Lee LJ, Frey BJ, Blencowe BJ. Deep surveying of alternative splicing complexity in the human transcriptome by high-throughput sequencing. Nat Genet. 2008;40:1413-5.
11. David CJ, Manley JL. Alternative pre-mRNA splicing regulation in cancer: pathways and programs unhinged. Genes & Development. 2010;24:2343-64.
12. Ghigna C., Valacca C., Biamonti G. Alternative splicing and tumor progression. Curr Genomics. 2008;9:556-70.
13. Thiery JP, Acloque H, Huang RYJ, Nieto MA. Epithelial-Mesenchymal Transitions in Development and Disease. Cell. 2009;139:871-90.
14. Blanchette M, Green RE, MacArthur S, Brooks AN, Brenner SE, Eisen MB, et al. Genome-wide Analysis of Alternative Pre-mRNA Splicing and RNA-Binding Specificities of the Drosophila hnRNP A/B Family Members. Molecular Cell. 2009;33:438-49.
15. Golan-Gerstl R, Cohen M, Shilo A, Suh S-S, Bakàcs A, Coppola L, et al. Splicing Factor hnRNP A2/B1 Regulates Tumor Suppressor Gene Splicing and Is an Oncogenic Driver in Glioblastoma. Cancer Research. 2011;71:4464-72.
16. Mayeda A, Helfman DM, Krainer AR. Modulation of exon skipping and inclusion by heterogeneous nuclear ribonucleoprotein A1 and pre-mRNA splicing factor SF2/ASF. Molecular and Cellular Biology. 1993;13:2993-3001.
17. Tauler J, Zudaire E, Liu H, Shih J, Mulshine JL. hnRNP A2/B1 Modulates Epithelial-Mesenchymal Transition in Lung Cancer Cell Lines. Cancer Research. 2010;70:7137-47.
18. Liu H-X, Zhang M, Krainer AR. Identification of functional exonic splicing enhancer motifs recognized by individual SR proteins. Genes & Development. 1998;12:1998-2012.
19. Karni R, de Stanchina E, Lowe SW, Sinha R, Mu D, Krainer AR. The gene encoding the splicing factor SF2/ASF is a proto-oncogene. Nat Struct Mol Biol. 2007;14:185-93.
20. Biamonti G, Bonomi S, Gallo S, Ghigna C. Making alternative splicing decisions during epithelial-to-mesenchymal transition (EMT). Cell Mol Life Sci. 2012;69:2515-26.
21. Nadiminty N, Chun JY, Lou W, Lin X, Gao AC. NF-κB2/p52 enhances androgen-independent growth of human LNCaP cells via protection from apoptotic cell death and cell cycle arrest induced by androgen-deprivation. The Prostate. 2008;68:1725-33.
22. Liu C, Lou W, Zhu Y, Nadiminty N, Schwartz CT, Evans CP, et al. Niclosamide Inhibits Androgen Receptor Variants Expression and Overcomes Enzalutamide Resistance in Castration-Resistant Prostate Cancer. Clinical Cancer Research. 2014;20:3198-210.
23. Nadiminty N, Tummala R, Liu C, Yang J, Lou W, Evans CP, et al. NF-κB2/p52 Induces Resistance to Enzalutamide in Prostate Cancer: Role of Androgen Receptor and Its Variants. Molecular Cancer Therapeutics. 2013;12:1629-37.

24. Nadiminty N, Lou W, Sun M, Chen J, Yue J, Kung H-J, et al. Aberrant Activation of the Androgen Receptor by NF-kB2/p52 in Prostate Cancer Cells. Cancer Research. 2010;70:3309-19.
25. Selth LA, Close P, Svejstrup JQ. Studying RNA-protein interactions In vivo by RNA immunoprecipitation. Methods in Molecular Biology. 2011;791:253-64.
26. Dhir R, Ni Z, Lou W, DeMiguel F, Grandis JR, Gao AC. Stat3 activation in prostatic carcinomas. The Prostate. 2002;51:241-6.
27. Nadiminty N, Tummala R, Lou W, Zhu Y, Shi X-B, Zou JX, et al. MicroRNA let-7c Is Downregulated in Prostate Cancer and Suppresses Prostate Cancer Growth. PLoS ONE. 2012;7:e32832.
28. Varambally S, Yu J, Laxman B, Rhodes DR, Mehra R, Tomlins SA, et al. Integrative genomic and proteomic analysis of prostate cancer reveals signatures of metastatic progression. Cancer Cell. 2005;8:393-406.
29. Chandran U, Ma C, Dhir R, Bisceglia M, Lyons-Weiler M, Liang W, et al. Gene expression profiles of prostate cancer reveal involvement of multiple molecular pathways in the metastatic process. BMC Cancer. 2007;7:64.
30. Lapointe J, Li C, Higgins JP, van de Rijn M, Bair E, Montgomery K, et al. Gene expression profiling identifies clinically relevant subtypes of prostate cancer. Proceedings of the National Academy of Sciences of the United States of America. 2004;101:811-6.
31. Wallace TA, Prueitt RL, Yi M, Howe TM, Gillespie JW, Yfantis HG, et al. Tumor Immunobiological Differences in Prostate Cancer between African-American and European-American Men. Cancer Research. 2008;68:927-36.
32. Singh D, Febbo PG, Ross K, Jackson DG, Manola J, Ladd C, et al. Gene expression correlates of clinical prostate cancer behavior. Cancer Cell. 2002;1:203-9.
33. Yu YP, Landsittel D, Jing L, Nelson J, Ren B, Liu L, et al. Gene Expression Alterations in Prostate Cancer Predicting Tumor Aggression and Preceding Development of Malignancy. Journal of Clinical Oncology. 2004;22:2790-9.
34. Nadiminty N, Tummala R, Lou W, Zhu Y, Zhang J, Chen X, et al. MicroRNA let-7c Suppresses Androgen Receptor Expression and Activity via Regulation of Myc Expression in Prostate Cancer Cells. Journal of Biological Chemistry. 2012;287:1527-37.
35. Guo Z, Yang X, Sun F, Jiang R, Linn DE, Chen H, et al. A Novel Androgen Receptor Splice Variant Is Up-regulated during Prostate Cancer Progression and Promotes Androgen Depletion Resistant Growth. Cancer Research. 2009;69:2305-13.
36. David CJ, Chen M, Assanah M, Canoll P, Manley JL. HnRNP proteins controlled by c-Myc deregulate pyruvate kinase mRNA splicing in cancer. Nature. 2010;463:364-8.
37. Ni M, Chen Y, Fei T, Li D, Lim E, Liu XS, et al. Amplitude modulation of androgen signaling by c-MYC. Genes & Development. 2013;27:734-48.
38. Sun S, Sprenger CCT, Vessella RL, Haugk K, Soriano K, Mostaghel EA, et al. Castration resistance in human prostate cancer is conferred by a frequently occurring androgen receptor splice variant. The Journal of Clinical Investigation. 2010;120:2715-30.
39. Mostaghel EA, Plymate SR, Montgomery B. Molecular Pathways: Targeting Resistance in the Androgen Receptor for Therapeutic Benefit. Clinical Cancer Research. 2014;20:791-8.
40. Liu G, Sprenger C, Sun S, Epilepsia KS, Haugk K, Zhang X, et al. AR Variant ARv567es Induces Carcinogenesis in a Novel Transgenic Mouse Model of Prostate Cancer. Neoplasia. 2013;15:1009 17.

41. Guo R, Li Y, Ning J, Sun D, Lin L, Liu X. HnRNP A1/A2 and SF2/ASF Regulate Alternative Splicing of Interferon Regulatory Factor-3 and Affect Immunomodulatory Functions in Human Non-Small Cell Lung Cancer Cells. PLoS ONE. 2013;8:e62729.
42. LeFave CV, Squatrito M, Vorlova S, Rocco GL, Brennan CW, Holland EC, et al. Splicing factor hnRNPH drives an oncogenic splicing switch in gliomas. The EMBO Journal. 2011;30:4084-97.
43. Zhou J, Allred DC, Avis I, Martinez A, Vos MD, Smith L, et al. Differential expression of the early lung cancer detection marker, heterogeneous nuclear ribonucleoprotein-A2/B1 (hnRNP-A2/B1) in normal breast and neoplastic breast cancer. Breast Cancer Res Treat. 2001;66:217-24.
44. Zerbe LK, Pino I, Pio R, Cosper PF, Dwyer-Nield LD, Meyer AM, et al. Relative amounts of antagonistic splicing factors, hnRNP A1 and ASF/SF2, change during neoplastic lung growth: Implications for pre-mRNA processing. Molecular Carcinogenesis. 2004;41:187-96.
45. Piekielko-Witkowska A, Wiszomirska H, Wojcicka A, Poplawski P, Boguslawska J, Tanski Z, et al. Disturbed Expression of Splicing Factors in Renal Cancer Affects Alternative Splicing of Apoptosis Regulators, Oncogenes, and Tumor Suppressors. PLoS ONE. 2010;5:e13690.
46. Boukakis G, Patrinou-Georgoula M, Lekarakou M, Valavanis C, Guialis A. Deregulated expression of hnRNP A/B proteins in human non-small cell lung cancer: parallel assessment of protein and mRNA levels in paired tumour/non-tumour tissues. BMC Cancer. 2010;10:434.
47. Mole S, McFarlane M, Chuen-Im T, Milligan SG, Millan D, Graham SV. RNA splicing factors regulated by HPV16 during cervical tumour progression. The Journal of Pathology. 2009;219:383-91.
48. Patry C, Bouchard L, Labrecque P, Gendron D, Lemieux B, Toutant J, et al. Small Interfering RNA-Mediated Reduction in Heterogeneous Nuclear Ribonucleoparticule A1/A2 Proteins Induces Apoptosis in Human Cancer Cells but not in Normal Mortal Cell Lines. Cancer Research. 2003;63:7679-88.
49. Liu LL, Xie N, Sun S, Plymate S, Mostaghel E, Dong X. Mechanisms of the androgen receptor splicing in prostate cancer cells. Oncogene. 2013;33:3140-50.

Table 1: Summary of the Western analysis of levels of hnRNPA1, hnRNPA2 and AR-V7 in 27 paired benign and tumor prostate clinical samples.

Gene	T>B	T<B	T B	High in donor	Low in donor
hnRNPA1	**12 (44%)**	**8 (29%)**	**7 (26%)**	**3/12**	**9/12**
AR-V7	**13 (48%)**	**7 (25%)**	**7 (26%)**	**4/12**	**8/12**
hnRNPA2	**12 (44%)**	**8 (29%)**	**7 (26%)**	**6/12**	**6/12**

Figure Legends

Figure 1. HnRNPA1 promotes generation of AR splice variants. qPCR to determine the expression levels of AR-V7 and FL AR in **A)** 22Rv1 and **B)** VCaP cells transfected with hnRNPA1 or hnRNPA2 siRNAs. **C)** Western analysis in 22Rv1 and VCaP cells transfected with hnRNPA1 or hnRNPA2 siRNAs. **D)** Western blotting for AR-V7 in LNCaP cells transfected with hnRNPA1 cDNA. **E)** qPCR analysis in LNCaP cells transfected with hnRNPA1 cDNA. Results are presented as means ± SD of 3 experiments performed in triplicate. * denotes $p \leq 0.05$.

Figure 2. Recruitment of hnRNPA1 and hnRNPA2 to splice sites in AR pre-mRNA is enhanced in 22Rv1-Enza-R and C4-2B-Enza-R enzalutamide-resistant PCa cells compared to 22Rv1 and C4-2B parental cells respectively. RIP assays for splice sites of **A)** AR-V7, **B)** AR in 22Rv1-Enza-R compared to 22Rv1 and **C)** AR-V7, **D)** AR in C4-2B-Enza-R compared to C4-2B. Results are presented as means ± SD of 2 experiments performed in duplicate. * denotes $p \leq 0.05$.

Figure 3. Expression levels of hnRNPA1 and AR-V7 are positively correlated with each other. **A)** Representative immunoblot for hnRNPA1, hnRNPA2 and AR-V7 in lysates from 27 paired benign and tumor patient samples. qRT-PCR of mRNA levels of **(B)** hnRNPA1 and **(C)** AR-V7 in 10 paired normal and tumor clinical prostate samples. Results are presented as means ± SD of 2 experiments performed in triplicate. * denotes $p \leq 0.05$. Relative expression levels of hnRNPA1 **(D)** and hnRNPA2 **(E)** in the representative Singh_prostate (n 102) dataset from Oncomine. Relative expression levels of hnRNPA1 in GDS1439 dataset **(F)** and in GDS2545 dataset **(G)** from GEO.

Figure 4. Reciprocal regulation between c-Myc and hnRNPA1 is responsible for the generation of AR splice variants. **A)** Immunoblotting for hnRNPA1 and AR-V7 in 22Rv1 and VCaP cells transfected with c-Myc shRNA. **B)** Immunoblotting for c-Myc in LNCaP, 22Rv1 and VCaP cells

transfected with hnRNPA1 or hnRNPA2 siRNAs. qRT-PCR for mRNA levels of full length AR and AR-V7 in 22Rv1 **(C)** and VCaP **(D)** cells transfected with c-Myc shRNA. Insets show the expression of c-Myc mRNA in cells transfected with c-Myc shRNA. **(E)** Protein and **(F)** mRNA levels of AR-V7, FL AR, c-Myc and hnRNPA1 in 22Rv1 cells transfected with c-Myc shRNA with or without overexpression of hnRNPA1. Results are presented as means ± SD of 2 experiments performed in triplicate. * denotes $p \leq 0.05$.

Figure 5. NF-kappaB2/p52 regulates expression of c-Myc and hnRNPA1. **A)** *Left panel*, Immunoblotting for hnRNPA1, c-Myc and AR-V7 in LN-p52 cells. *Right panel*, Immunoblotting for hnRNPA1, c-Myc and AR-V7 in LN/TR/p52 cells. **B)** *Left panel*, Western blotting for AR-V7 in LN-p52 cells transfected with hnRNPA1 siRNA. *Middle panel*, Immunoblotting for AR-V7 and hnRNPA1 in LN-p52 cells transfected with c-Myc shRNA. *Right panel*, Immunoblotting for AR-V7, hnRNPA1 and c-Myc in 22Rv1 cells transfected with p52 shRNA. **C)** *Left panel*, 22Rv1 cells resistant to enzalutamide (22Rv1-Enza-R) express higher levels of AR-V7, hnRNPA1, c-Myc and NF-kappaB2/p52. *Middle panel*, C4-2B cells resistant to enzalutamide (C4-2B-Enza-R) express higher levels of hnRNPA1, AR-V7, c-Myc and NF-kappaB2/p52. *Right panel*, Xenografts from C4-2B-Enza-R cells exhibit higher levels of AR-V7, hnRNPA1 and c-Myc. **D)** *Left panel*, Western analysis of AR-V7 in 22Rv1-Enza-R cells transfected with hnRNPA1 siRNA. *Right panel*, Expression of AR-V7 and hnRNPA1 in 22Rv1-Enza-R cells transfected with c-Myc shRNA. All results are shown as representative images from 2 experiments performed in duplicate. **E)** *Left panel*, Chart depicting the positive correlation between mRNA levels of NF-kappaB2/p52, c-Myc, hnRNPA1 and AR-V7 in 10 paired benign and tumor prostate clinical samples. *Right panel*, Chart depicting the correlation between relative protein levels of NF-kappaB2/p52, c-Myc, hnRNPA1 and AR-V7 in 27 paired benign and tumor

prostate clinical samples. Band intensities in immunoblots were quantified using ImageJ software and plotted as arbitrary units. The horizontal lines represent the median of each series.

Figure 6. Suppression of hnRNPA1 restores enzalutamide sensitivity of enzalutamide-resistant PCa cells. **A)** *Left panel*, Cell survival in 22Rv1-Enza-R cells transfected with hnRNPA1 or hnRNPA2 siRNAs and treated with vehicle or 20 μM enzalutamide. Cell numbers were counted after 48 h. *Right panel*, immunoblots confirm the downregulation of hnRNPA1 or hnRNPA2 and of AR-V7. **B)** *Left panel*, Cell survival in LN-p52 cells transfected with hnRNPA1 or hnRNPA2 siRNAs and treated with vehicle or 20 μM enzalutamide. Cell numbers were counted after 48 h. *Right panel*, immunoblots confirm the downregulation of hnRNPA1 or hnRNPA2 and AR-V7. **C)** *Left panel*, Cell survival in VCaP cells transfected with hnRNPA1 or hnRNPA2 siRNAs and treated with vehicle or 20 μM enzalutamide. Cell numbers were counted after 48 h. *Right panel*, immunoblots confirm the downregulation of hnRNPA1 or hnRNPA2 and of AR-V7. Results are presented as means ± SD of 3 experiments performed in triplicate. * denotes $p \leq 0.05$. **D)** Schematic representation of the alternative splicing of AR mRNA regulated by the NF-kappaB2:c-Myc:hnRNPA1 axis.

Figure 1

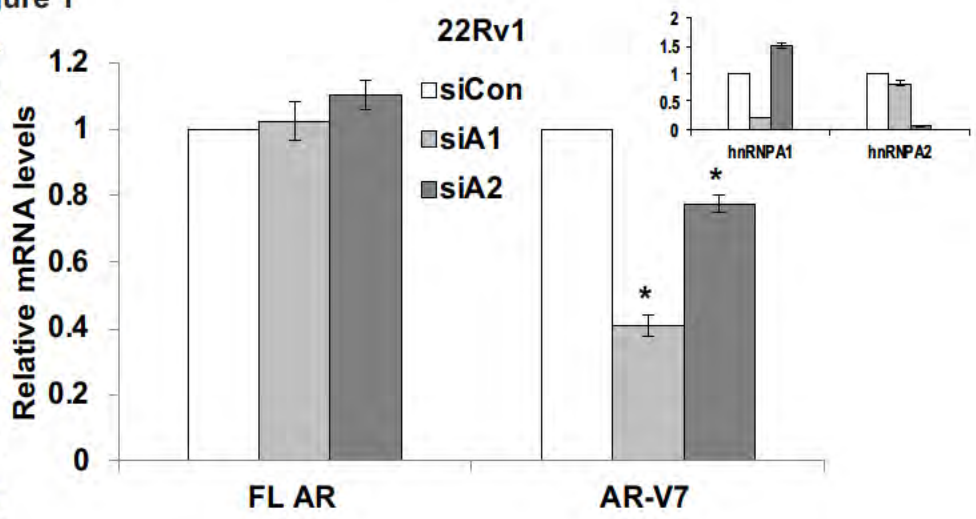

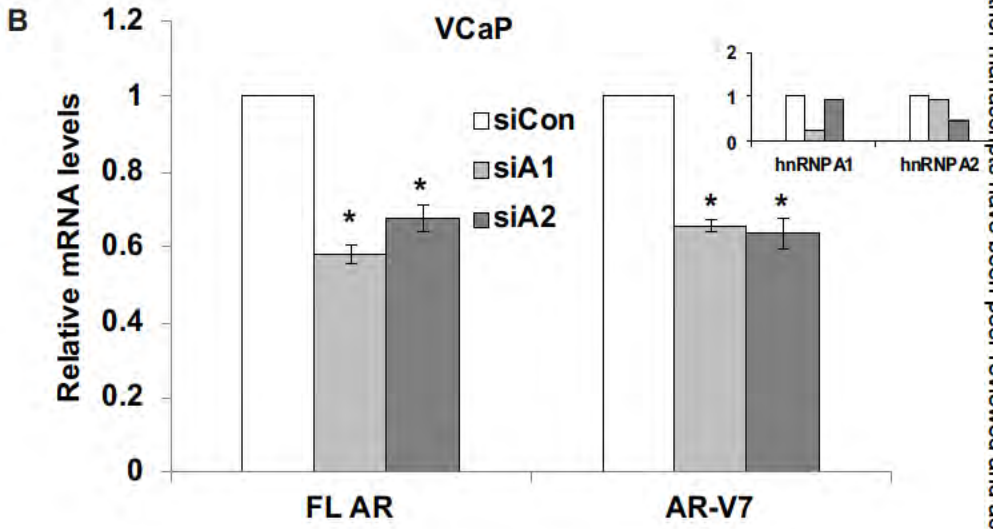

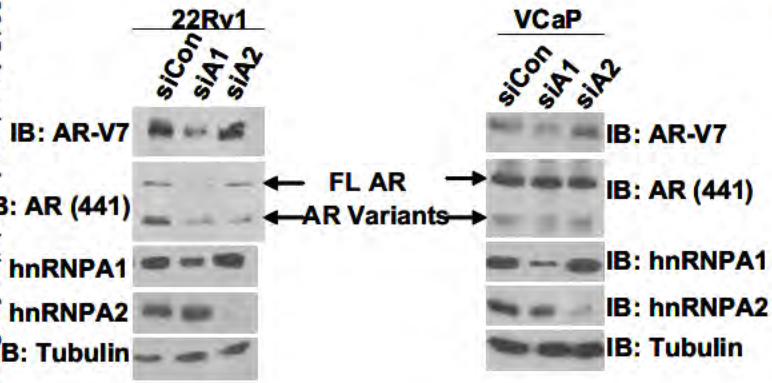

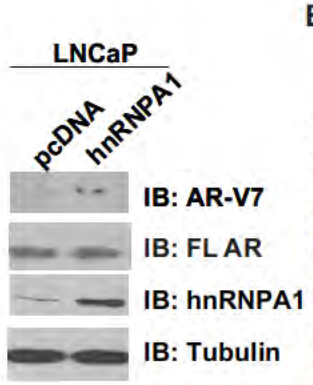

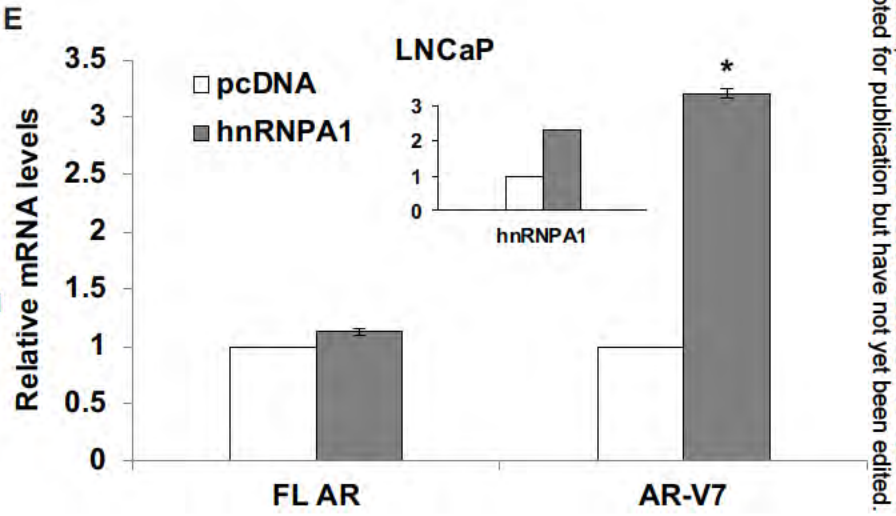

Figure 2

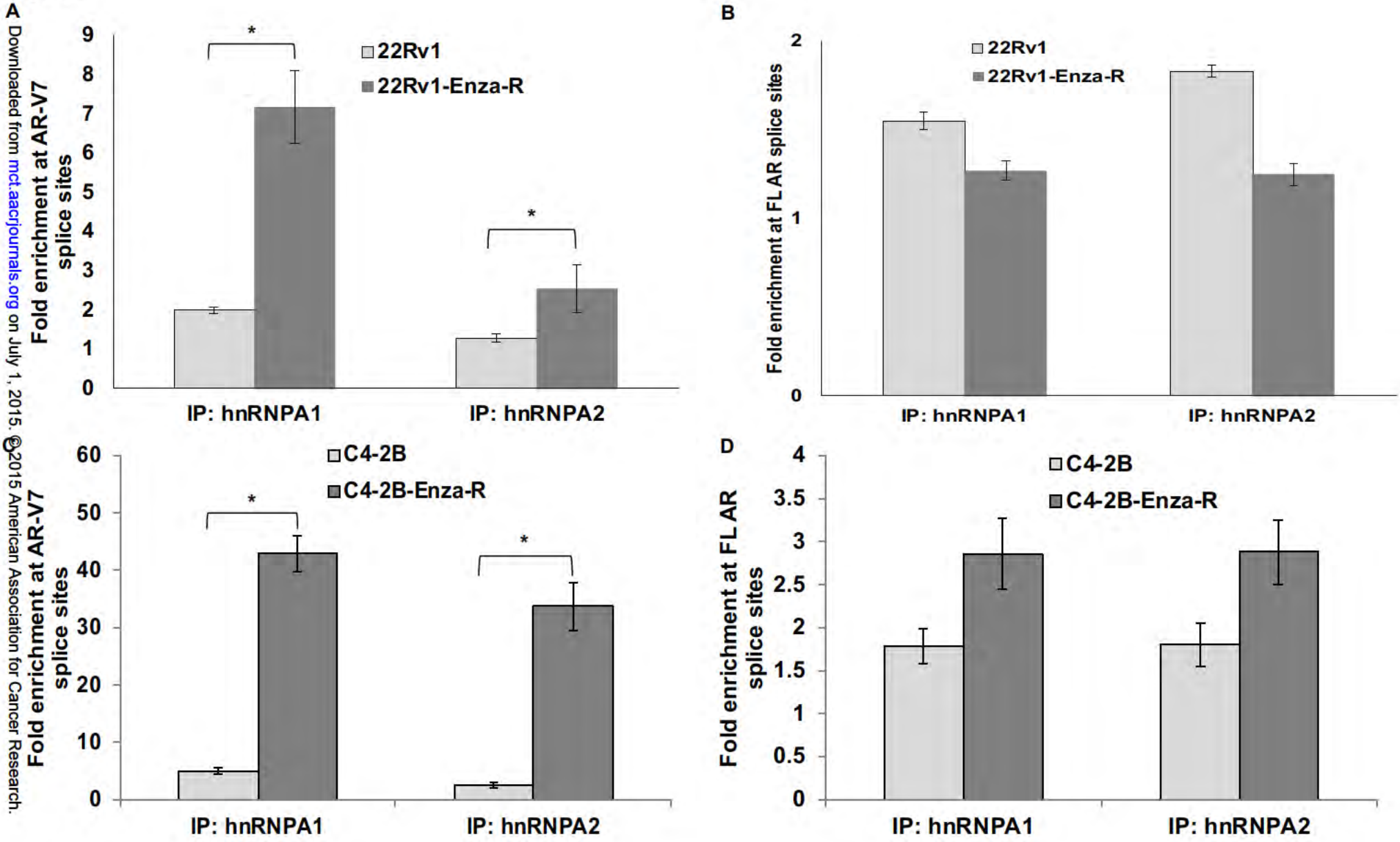

Author Manuscript Published OnlineFirst on June 8, 2015; DOI: 10.1158/1535-7163.MCT-14-1057
Author manuscripts have been peer reviewed and accepted for publication but have not yet been edited.

Figure 3

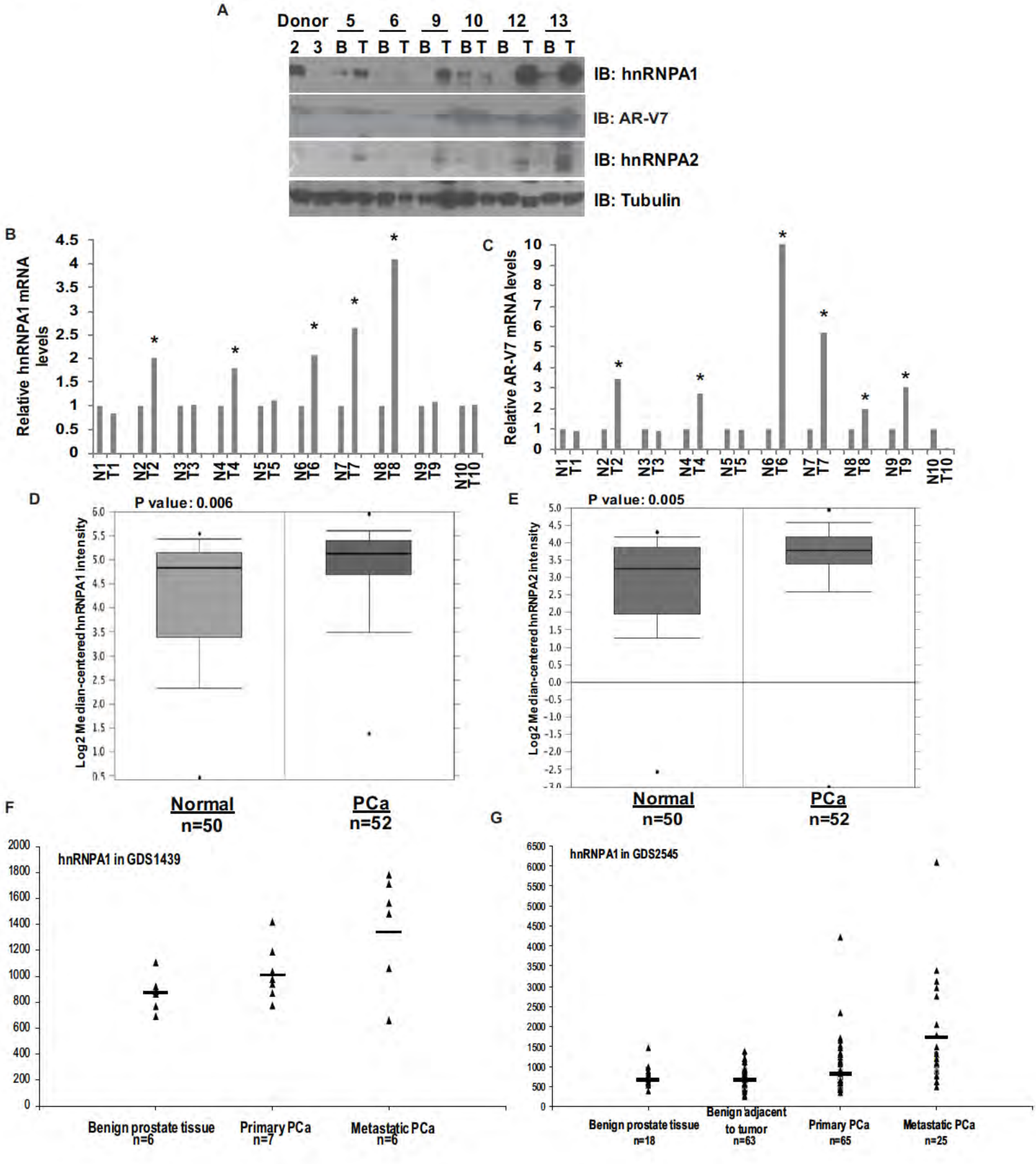

Figure 4

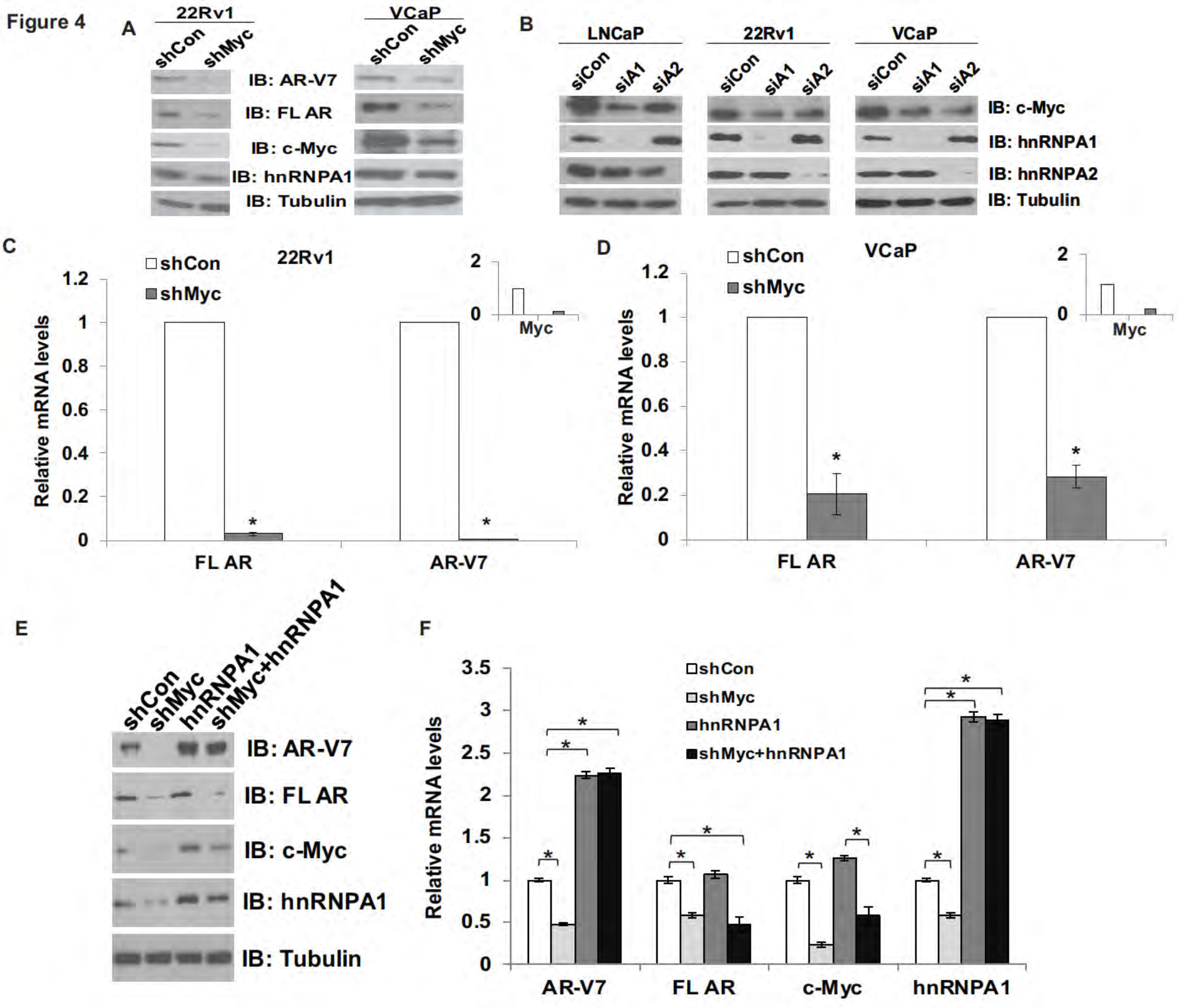

Figure 5

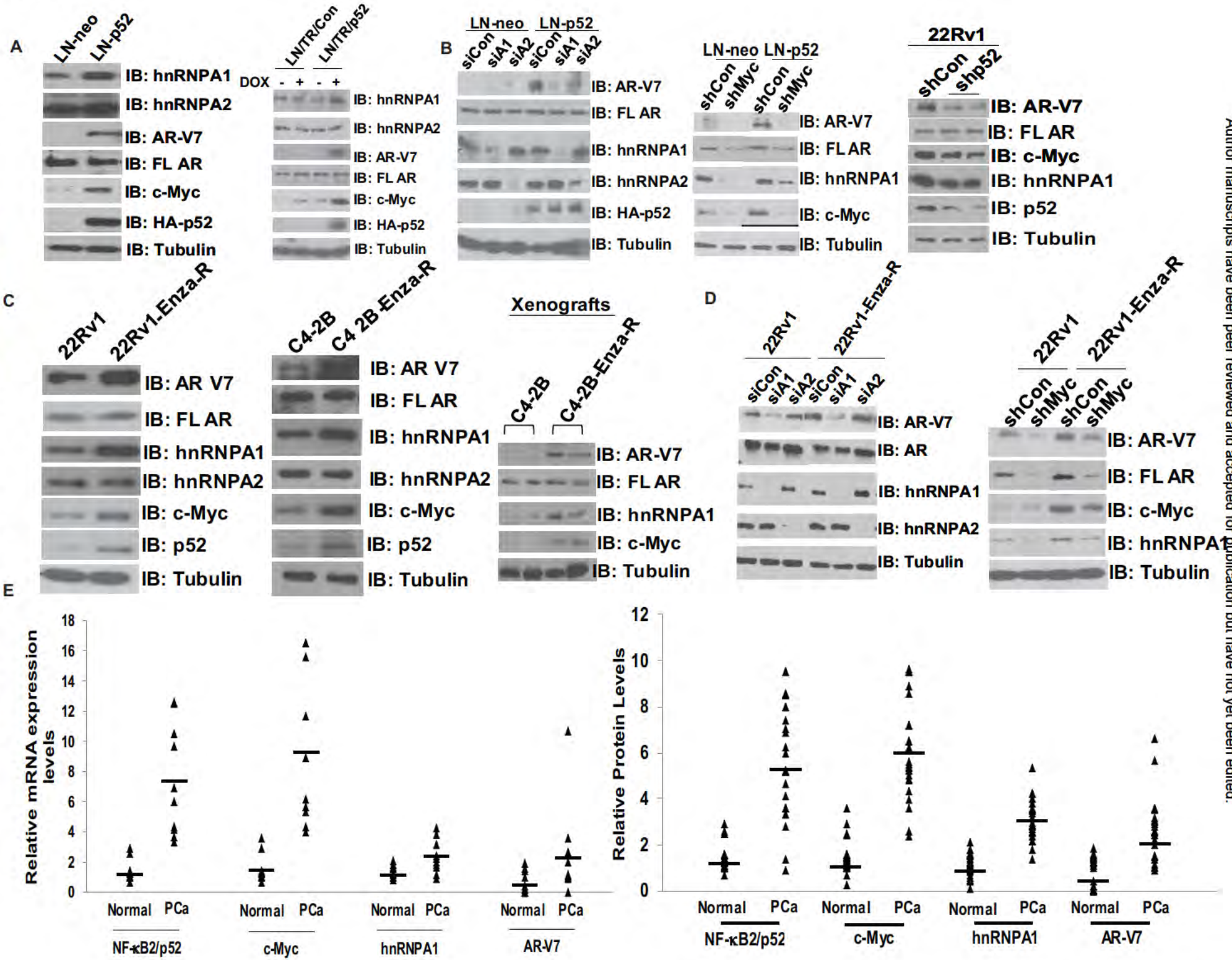

Author Manuscript Published OnlineFirst on June 8, 2015; DOI: 10.1158/1535-7163.MCT-14-1057

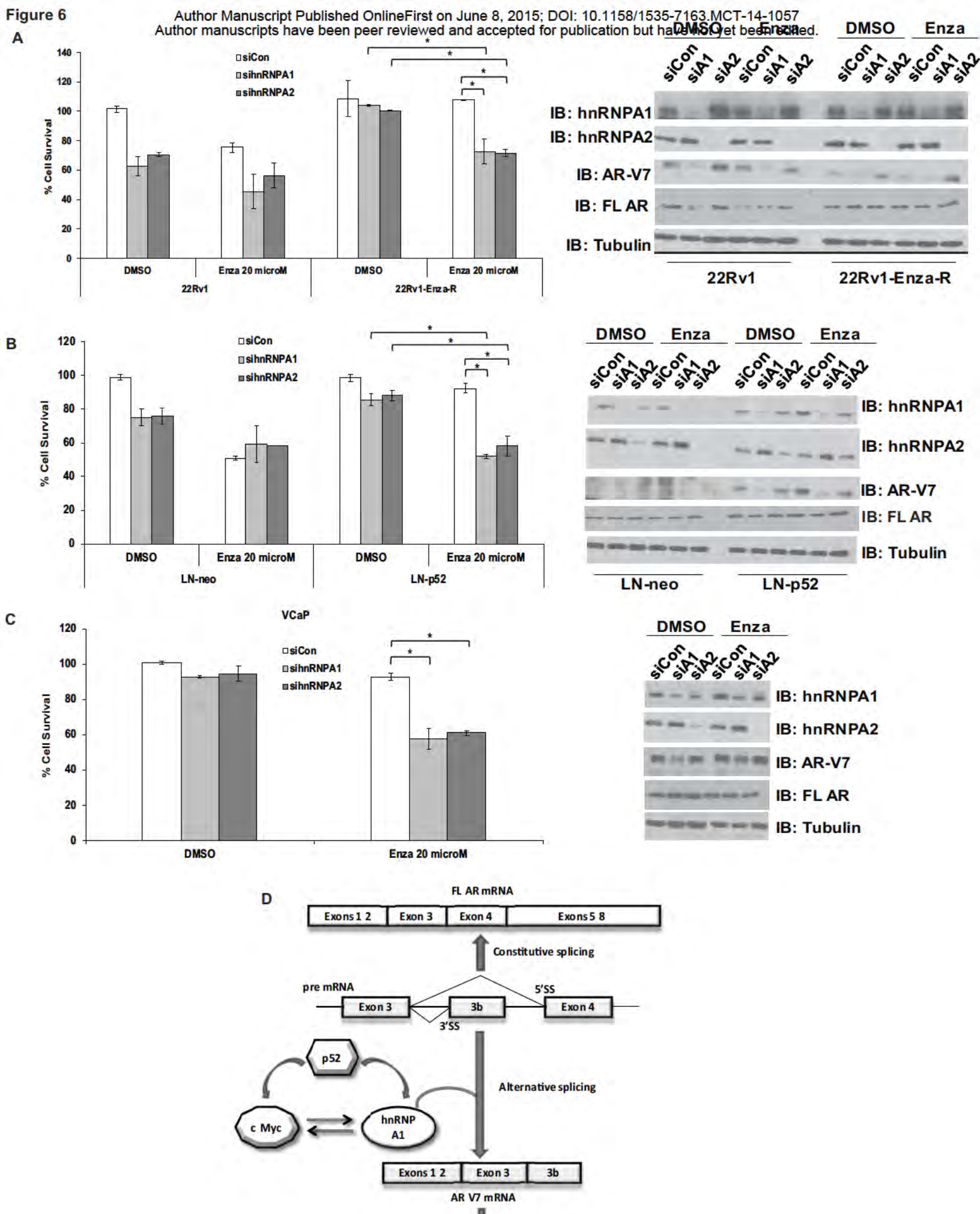

AACR American Association for Cancer Research

Molecular Cancer Therapeutics

NF-kappaB2/p52:c-Myc:hnRNPA1 pathway regulates expression of androgen receptor splice variants and enzalutamide sensitivity in prostate cancer

Nagalakshmi Nadiminty, Ramakumar Tummala, Chengfei Liu, et al.

Mol Cancer Ther Published OnlineFirst June 8, 2015.

Published OnlineFirst February 3, 2015; DOI: 10.1158/0008-5472.CAN-14-3080

Therapeutics, Targets, and Chemical Biology

Cancer Research

Intracrine Androgens and AKR1C3 Activation Confer Resistance to Enzalutamide in Prostate Cancer

Chengfei Liu[1], Wei Lou[1], Yezi Zhu[1,2], Joy C. Yang[1], Nagalakshmi Nadiminty[1], Nilesh W. Gaikwad[3], Christopher P. Evans[1,4], and Allen C. Gao[1,2,4]

Abstract

The introduction of enzalutamide and abiraterone has led to improvement in the treatment of metastatic castration resistant prostate cancer. However, acquired resistance to enzalutamide and abiraterone therapies frequently develops within a short period in many patients. In the present study, we developed enzalutamide resistant prostate cancer cells in an effort to understand the mechanisms of resistance. Global gene expression analysis showed that the steroid biosynthesis pathway is activated in enzalutamide resistant prostate cancer cells. One of the crucial steroidogenic enzymes, AKR1C3, was significantly elevated in enzalutamide resistant cells. In addition, AKR1C3 is highly expressed in metastatic and recurrent prostate cancer and in enzalutamide resistant prostate xenograft tumors. LC/MS analysis of the steroid metabolites revealed that androgen precursors such as cholesterol, DHEA and progesterone, as well as androgens are highly upregulated in enzalutamide resistant prostate cancer cells compared to the parental cells. Knockdown of AKR1C3 expression by shRNA or inhibition of AKR1C3 enzymatic activity by indomethacin resensitized enzalutamide resistant prostate cancer cells to enzalutamide treatment both in *vitro* and *in vivo*. In contrast, overexpression of AKR1C3 confers resistance to enzalutamide. Furthermore, the combination of indomethacin and enzalutamide resulted in significant inhibition of enzalutamide resistant tumor growth. These results suggest that AKR1C3 activation is a critical resistance mechanism associated with enzalutamide resistance; targeting intracrine androgens and AKR1C3 will overcome enzalutamide resistance and improve survival of advanced prostate cancer patients. *Cancer Res; 75(7); 1413 22. ©2015 AACR.*

Introduction

Targeting androgen signaling via androgen deprivation therapy has been the mainstay of clinical interventions in prostate cancer. Although initially effective, the majority of men experience only transient benefit and relapse with castration resistant prostate cancer (CRPC), which is currently incurable. Enzalutamide, a second generation antiandrogen, was recently approved for the treatment of CRPC in patients. Despite these advances that provide temporary respite, resistance to enzalutamide occurs frequently, and the mechanisms that contribute to resistance are still rudimentary and are under intense investigation. Several potential mechanisms of resistance have been revealed such as androgen receptor (AR) variants expression (1 3) , IL6 Stat3 AR axis activation (4), AR F876L mutation (5, 6), and glucocorticoid receptor (GR) overexpression (7, 8).

Intratumoral androgen biosynthesis has been well characterized as a mechanism of CRPC (9 12), but its role in enzalutamide resistance is yet to be understood. Clinical reports have shown that patients treated with enzalutamide have elevated testosterone levels in the bone marrow (13, 14). A cascade of enzymes is involved in the biosynthesis of intratumoral androgens, including CYP17A1, HSD3B and AKR1C3. A gain of function mutation in HSD3B1 (N367T) has been identified in CRPC patients recently, and was postulated to confer resistance to enzalutamide (15, 16). Aldo keto reductase family 1 member C3 (AKR1C3) is a multifunctional enzyme and is one of the most important genes involved in androgen synthesis and metabolism. AKR1C3 facilitates the conversion of weak androgens androstenedione (A′ dione) and 5 α androstanedione (5α dione) to the more active androgens testosterone and DHT, respectively (17, 18). It catalyzes conversion of steroids and modulates transactivation of steroid receptors. Elevated expression of AKR1C3 has been associated with prostate cancer progression and aggressiveness (19, 20). The role of AKR1C3 in enzalutamide resistant prostate cancer is unknown.

In the present study, we developed prostate cancer cell lines resistant to enzalutamide and found that intracrine androgen synthesis is activated in enzalutamide resistant prostate cancer cells. Activation of one of the important steroidogenic enzymes, AKR1C3, was identified as a critical mechanism that confers resistance to enzalutamide. Inhibition of AKR1C3 activity using either shRNA or indomethacin resensitized enzalutamide resistant prostate cancer cells to enzalutamide. Furthermore, the combination of indomethacin and enzalutamide resulted in

[1]Department of Urology, University of California, Davis, California. [2]Graduate Program in Pharmacology and Toxicology, University of California, Davis, Davis, California. [3]Departments of Nutrition and Environmental Toxicology, West Coast Metabolomics Center, University of California, Davis, Davis, California. [4]UC Davis Comprehensive Cancer Center, University of California, Davis, Davis, California.

Corresponding Author: Allen C. Gao, Department of Urology, University of California Davis Medical Center, 4645 2nd Avenue, Research III, Suite 1300, Sacramento, CA 95817. Phone: 916 734 8718; Fax: 916 734 8714; E mail: acgao@ucdavis.edu

doi: 10.1158/0008 5472.CAN 14 3080

Published OnlineFirst February 3, 2015; DOI: 10.1158/0008-5472.CAN-14-3080

significant inhibition of enzalutamide resistant prostate cancer xenograft tumor growth.

Materials and Methods

Reagents and cell culture

LNCaP, CWR22Rv1, VCaP, and HEK293T cells were obtained from the ATCC. All experiments with cell lines were performed within 6 months of receipt from the ATCC or resuscitation after cryopreservation. The ATCC uses short tandem repeat profiling for testing and authentication of cell lines. C4 2B cells were kindly provided and authenticated by Dr. Leland Chung, Cedars Sinai Medical Center (Los Angeles, CA). LN 95 cells were kindly provided and authenticated by Dr. Joel Nelson, University of Pittsburgh, Pittsburgh, PA. The cells were maintained in RPMI 1640 supplemented with 10% FBS, 100 U/mL penicillin, and 0.1 mg/mL streptomycin. LNCaP neo and LNCaP AKR1C3 cells were generated by stable transfection of LNCaP cells with either empty vector pcDNA3.1 or pcDNA3.1 encoding AKR1C3 and were maintained in RPMI 1640 medium containing 300 μg/mL G418. AKR1C3 shRNA (TRCN0000026561 and TRCN0000025694) were purchased from Sigma. Cells resistant to enzalutamide were referred to as C4 2B MDVR (C4 2B enzalutamide resistant) as described previously (2). All cells were maintained at 37°C in a humidified incubator with 5% carbon dioxide.

Sample preparation and analysis of steroids

The steroid extraction and analysis has been described previously (21). Briefly, 50 million C4 2B parental and C4 2B MDVR cells were cultured in serum and phenol red free RPMI 1640 medium for 5 days, then cells were suspended in 4 mL of a 1:1 water:methanol mixture. The suspension was homogenized, and the resulting homogenate was cooled on ice. The precipitated material was removed by centrifuging at high speed for 5 minutes, and the supernatant was removed and evaporated in a SpeedVac (Labconco Inc.) followed by lyophilizer (Labconco Inc.). The residue was suspended in 150 μL of CH3OH/H2O (1:1), filtered through a 0.2 μm ultracentrifuge filter (Millipore inc.) and subjected to UPLC/MS MS analysis. Samples were run in duplicate during UPLC/MS MS analysis. Samples were placed in an Acquity sample manager, which was cooled to 8°C to preserve the analytes. Pure standards were used to optimize the UPLC/MS MS conditions before sample analysis. Also, the standard mixture was run before the first sample to prevent errors due to matrix effect and day to day instrument variations. In addition, immediately after the initial standard and before the first sample, two spiked samples were run to calibrate for the drift in the retention time of all analytes due to the matrix effect. After standard and spiked sample runs, blank was injected to wash the injector and remove carry over effect.

UPLC/MS MS analysis of steroid metabolites

All experiments were performed on a Waters Xevo TQ triple quadruple mass spectrometer (Milford) and MS and MS MS spectra were recorded using Electro Spray Ionization (ESI) in positive ion (PI) and negative ion (NI) mode, capillary voltage of 3.0 kV, extractor cone voltage of 3 V, and detector voltage of 650 V. Cone gas flow was set at 50 L/h and desolvation gas flow was maintained at 600 L/h. Source temperature and desolvation temperatures were set at 150°C and 350°C, respectively. The collision energy was varied to optimize daughter ions. The acquisition range was 20 to 500 Da. Analytic separations were conducted on the UPLC system using an Acquity UPLC HSS T3 1.8 μm 1 × 150 mm analytic column kept at 50°C and at a flow rate of 0.15 mL/min. The gradient started with 100% A (0.1% formic acid in H2O) and 0% B (0.1% formic acid in CH3CN), after 2 minutes, changed to 80% A over 2 minutes, then 45% A over 5 minutes, followed by 20% A in 2 minutes. Finally, it was changed over 1 minute to original 100% A, resulting in a total separation time of 15 minutes. The elutions from the UPLC column were introduced to the mass spectrometer and resulting data were analyzed and processed using MassLynx 4.1 software.

cDNA microarray analysis

The microarray analysis has been described previously (22). Briefly, 24 hours after plating of 5×10^5 C4 2B parental and C4 2B MDVR cells, total RNA was isolated using TRIzol Reagent (Invitrogen) and purified with Eppendorf phase lock gel tube. RNA quality of all samples was tested by RNA electrophoresis to ensure RNA integrity. Samples were analyzed by the Genomics Shared Resource (UC Davis Medical Center, Sacramento, CA) using the Affymetrix Human Gene 1.0 ST array. The data were analyzed by *Subio* platform and Gene Set Enrichment Analysis (23). Microarray data have been deposited in GEO with the accession number GSE64143.

Western blot analysis

Cellular protein extracts were resolved on SDSPAGE and proteins were transferred to nitrocellulose membranes. After blocking for 1 hour at room temperature in 5% milk in PBS/0.1% Tween 20, membranes were incubated overnight at 4°C with the indicated primary antibodies [AKR1C3 (A6229, Sigma); CYP17A1 (SC 66849, Santa Cruz Biotechnology); HSD3B (SC 28206, Santa Cruz Biotechnology); AR (SC 815, Santa Cruz Biotechnology); Tubulin (T5168, Sigma Aldrich)]. Tubulin was used as loading control. Following secondary antibody incubation, immunoreactive proteins were visualized with an enhanced chemiluminescence detection system (Millipore).

Cell growth assay

C4 2B MDVR, CWR22Rv1 cells were seeded on 12 well plates at a density of 0.5×10^5 cells per well in RPMI 1640 media containing 10% FBS and transiently transfected with AKR1C3 shRNA or control shRNA following treatment with 20 μmol/L enzalutamide. Total cell numbers were counted after 3 or 5 days. LNCaP neo, LNCaP AKR1C3, or LN 95 cells were treated with different concentrations of enzalutamide for 48 hours. Total cell numbers were counted or the cell survival rate (%) was calculated. Cell survival rate (%) (treatment group cell number/control group cell number) × 100%.

Clonogenic assay

C4 2 parental or C4 2B MDVR cells were treated with DMSO, 10 μmol/L or 20 μmol/L enzalutamide in media containing 10% FBS. CWR22Rv1 cells or C4 2B MDVR cells were treated with 10 or 20 μmol/L indomethacin with or without 20 μmol/L enzalutamide, cells were plated at equal density (1500 cells/dish) in 100 mm dishes for 14 days, the medium was changed every 3 days; LNCaP neo or LNCaP AKR1C3 cells were treated with DMSO or 10 μmol/L enzalutamide in media containing 10% complete FBS, cells were plated at equal density (10,000 cells/dish) in 100 mm

Published OnlineFirst February 3, 2015; DOI: 10.1158/0008-5472.CAN-14-3080

dishes for 28 days, the colonies were rinsed with PBS before staining with 0.5% crystal violet/4% formaldehyde for 30 minutes, and the numbers of colonies were counted.

Real time quantitative RT PCR

Total RNAs were extracted using TRIzol reagent (Invitrogen). cDNAs were prepared after digestion with RNase free RQ1 DNase (Promega). The cDNAs were subjected to real time RT PCR using Sso Fast Eva Green Supermix (Bio Rad) according to the manufacturer's instructions and as described previously (24). Each reaction was normalized by coamplification of actin. Triplicates of samples were run on default settings of Bio Rad CFX 96 real time cycler. Primers used for Real time PCR are: AKR1C3, 5′ gagaagtaaagctttggaggtcaca 3′ (forward) and 5′ caacctgctcctcat tattgtataaatga 3′ (reverse); AKR1C1/2, 5′ ggtcacttcatgcctgtcct 3′ (forward) and 5′ actctggtcgatgggaattg 3′ (reverse); HSD3B1, 5′ agaatctagaccactcttctgtccagcttt 3′ (forward) and 5′ ctttgaattcaac tatgtgaaggaatggaa 3′ (reverse); HSD3B2, 5′ cgggcccaactcctacaag 3′ (forward) and 5′ ttttccagaggctcttcttcgt 3′ (reverse); CYP17A1, 5′ gggcggcctcaaatgg 3′ (forward) and 5′ cagcgaaggcgaaggcga tacccttа 3′ (reverse); HSD17B3, 5′ tgggacagtgggcagtga 3′ (forward) and 5′ cgagtacgctttcccaattcc 3′ (reverse); SRD5A1, 5′ acggg catcggtgcttaat 3′ (forward) and 5′ ccaacagtggcataggctttc 3′ (reverse); and Actin, 5′ agaactggcccttcttggagg 3′ (forward) and 5′ gtttttatgttcctctatggg 3′ (reverse).

Measurement of PSA

PSA levels were measured in sera from C4 2B parental or C4 2B MDVR tumor bearing mice using the PSA ELISA Kit (KA0208, Abnova, Inc.) according to the manufacturer's instructions.

In vivo tumorigenesis assay

C4 2B parental or C4 2B MDVR cells (4 million) were mixed with Matrigel (1:1) and injected into the prostates of 6 to 7 week old male SCID mice. When the serum PSA level reached 5 ng/mL, mice were randomized into two groups (4 mice in each group) and treated as follows: (i) vehicle control (0.5% weight/volume (w/v) Methocel A4M orally), (ii) enzalutamide (25 mg/kg, orally). Tumors were monitored by PSA level. All tumor tissues were harvested after 3 weeks of treatment.

CWR22Rv1 cells (4 million) were mixed with Matrigel (1:1) and injected s.c. into the flanks of 6 to 7 week old male SCID mice. Tumor bearing mice (tumor volume around 50 100 mm^3) were randomized into four groups (5 mice in each group) and treated as follows: (i) vehicle control (5% Tween 80 and 5% ethanol in PBS, i.p.), (ii) enzalutamide (25 mg/kg, orally), (iii) indomethacin (3 mg/kg, i.p.), and (iv) enzalutamide (25 mg/kg, orally) + indomethacin (3 mg/kg, i.p.). Tumors were measured using calipers twice a week and tumor volumes were calculated using length × width2/2. Tumor tissues were harvested after 3 weeks of treatment.

Immunohistochemistry

Tumors were fixed by formalin and paraffin embedded tissue blocks were dewaxed, rehydrated, and blocked for endogenous peroxidase activity. Antigen retrieving was performed in sodium citrate buffer (0.01 mol/L, pH 6.0) in a microwave oven at 1,000 W for 3 minutes and then at 100 W for 20 minutes. Nonspecific antibody binding was blocked by incubating with 10% FBS in PBS for 30 minutes at room temperature. Slides were then incubated with anti Ki 67 (at 1:500; NeoMarker), anti AKR1C3 (at 1:100; Sigma) at 4°C overnight. Slides were then washed and incubated with biotin conjugated secondary antibodies for 30 minutes, followed by incubation with avidin DH biotinylated horseradish peroxidase complex for 30 minutes (Vectastain ABC Elite Kit; Vector Laboratories). The sections were developed with the Diaminobenzidine Substrate Kit (Vector Laboratories) and counterstained with hematoxylin. Nuclear staining cells was scored and counted in five different vision areas. Images were taken with an Olympus BX51 microscope equipped with DP72 camera.

Statistical analysis

All data are presented as means ± SD of the mean. Statistical analyses were performed with Microsoft Excel analysis tools. Differences between individual groups were analyzed by one way ANOVA followed by the Scheffé procedure for comparison of means. A P value of <0.05 was considered statistically significant.

Results

Identification of AKR1C3 activation in enzalutamide resistant prostate cancer cells

In our previous study, we generated enzalutamide resistant prostate cancer cells, named C4 2B MDVR, by chronic culture of C4 2B cells in media containing enzalutamide (2). As shown in Fig. 1A and B, enzalutamide significantly inhibited proliferation and clonogenic ability of C4 2B parental cells, but had little effect on C4 2B MDVR cells. We also examined the effects of enzalutamide treatment on C4 2B MDVR cells *in vivo*. As shown in Fig. 1C, C4 2B MDVR xenografts were resistant to enzalutamide. Tumor weights of C4 2B xenograft were significantly inhibited by enzalutamide after 3 weeks treatment with enzalutamide, whereas tumor weights of treated C4 2B MDVR group were comparable with those of the nontreated control group. These results suggest that C4 2B MDVR cells are resistant to enzalutamide both *in vitro* and *in vivo*. We also characterized several other prostate cancer cell lines in response to enzalutamide treatment. As shown in Fig. 1D, LNCaP cells are sensitive to enzalutamide, whereas CWR22Rv1 and LN 95 cells are resistant to enzalutamide treatment, consistent with previously published studies (25 27).

Intratumoral androgen biosynthesis has been well characterized as a mechanism of CRPC (9 12, 28), but its role in enzalutamide resistance remains unknown. To further understand potential mechanisms that underlie enzalutamide resistance, we performed microarray analysis of the enzalutamide resistant C4 2B MDVR versus C4 2B parental cells. Expression of transcripts encoding for steroid hormone biosynthesis was analyzed by gene set enrichment. Among 45 genes involved in hormone biosynthesis, 31 genes were upregulated whereas 14 genes were downregulated in C4 2B MDVR cells. As shown in Fig. 2A, we found increased expression of AKR1C3, AKR1C1, AKR1C2, HSD3B1, CYP17A1, and SRD5A3, and decreased expression of UGT2B15, UGT2B17, CYP39A1, HSD17B6, and SRD5A1 in C4 2B MDVR cells compared with C4 2B parental cells. To verify the gene expression data, CYP17A1, HSD3B1, HSD3B2, HSD17B3, SRD5A1, AKR1C1/2, and AKR1C3 mRNA levels were measured using specific primers by qRT PCR. As shown in Fig. 2B left, the levels of mRNA expression were consistent with the microarray data. We also confirmed the results by Western blot analysis, as shown in Fig. 2B right, C4 2B MDVR cells express significantly higher levels of AKR1C3, HSD3B, and CYP17A1 proteins compared with C4 2B parental cells. These results suggested that

Published OnlineFirst February 3, 2015; DOI: 10.1158/0008-5472.CAN-14-3080

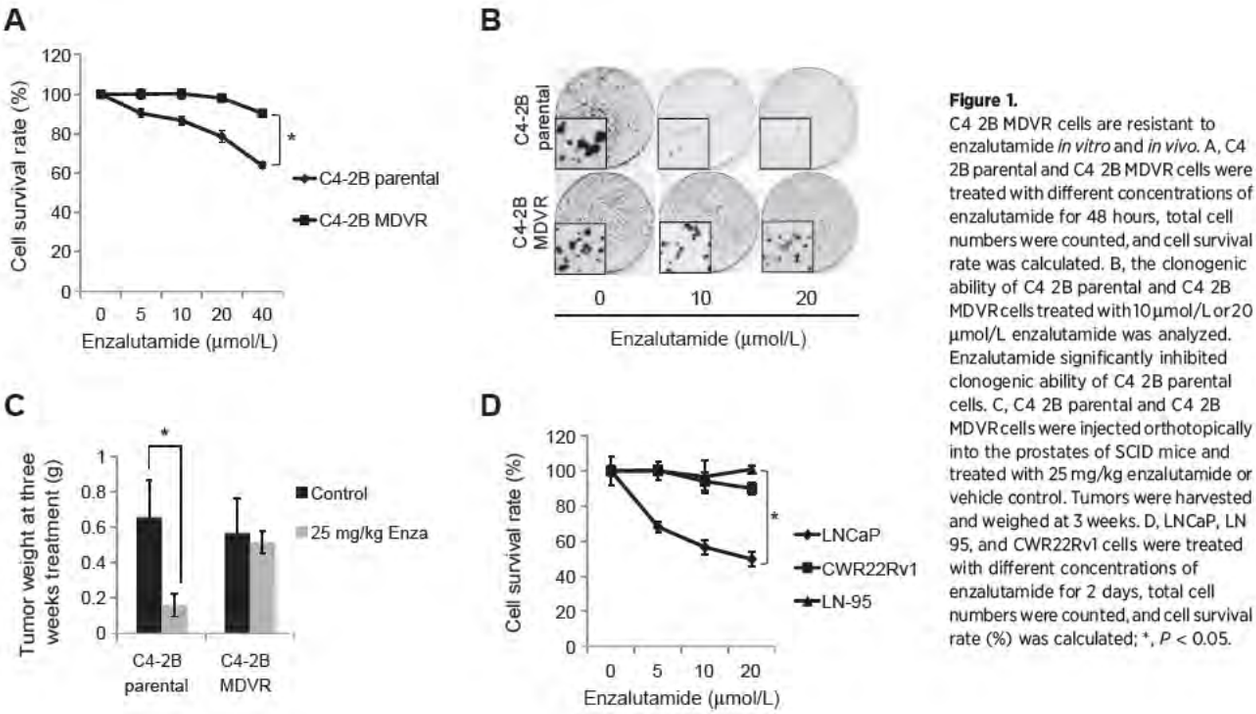

Figure 1.
C4 2B MDVR cells are resistant to enzalutamide *in vitro* and *in vivo*. A, C4 2B parental and C4 2B MDVR cells were treated with different concentrations of enzalutamide for 48 hours, total cell numbers were counted, and cell survival rate was calculated. B, the clonogenic ability of C4 2B parental and C4 2B MDVR cells treated with 10 μmol/L or 20 μmol/L enzalutamide was analyzed. Enzalutamide significantly inhibited clonogenic ability of C4 2B parental cells. C, C4 2B parental and C4 2B MDVR cells were injected orthotopically into the prostates of SCID mice and treated with 25 mg/kg enzalutamide or vehicle control. Tumors were harvested and weighed at 3 weeks. D, LNCaP, LN 95, and CWR22Rv1 cells were treated with different concentrations of enzalutamide for 2 days, total cell numbers were counted, and cell survival rate (%) was calculated; *, $P < 0.05$.

acquired androgen synthesis signaling was upregulated in enza lutamide resistant prostate cancer cells.

AKR1C3 is highly expressed in metastatic and recurrent prostate cancer and enzalutamide resistant prostate xenograft tumors

We found that AKR1C3 was upregulated by more than 16 fold in enzalutamide resistant C4 2B MDVR cells compared with the C4 2B parental cells. We examined AKR1C3 expression in differ ent prostate cancer cell lines, including VCaP, CWR22Rv1, LNCaP, LN 95, C4 2B, and C4 2B MDVR cells. C4 2B MDVR, CWR22Rv1, and LN 95 cells are resistant to enzalutamide, whereas C4 2B and LNCaP cells are sensitive to enzalutamide. As shown in Fig. 3A, C4 2B MDVR, VCaP, CWR22Rv1, and LN 95 cells, all express significantly higher levels of AKR1C3; C4 2B MDVR, CWR22Rv1, and LN 95 cells express higher levels of HSD3B; C4 2B MDVR and LN 95 cells also expressed higher levels of CYP17A1. We also examined AKR1C3 expression in tumor xenografts by IHC, as shown in Fig. 3B, C4 2B MDVR and CWR22Rv1 tumors express higher levels of AKR1C3 compared with C4 2B parental tumors.

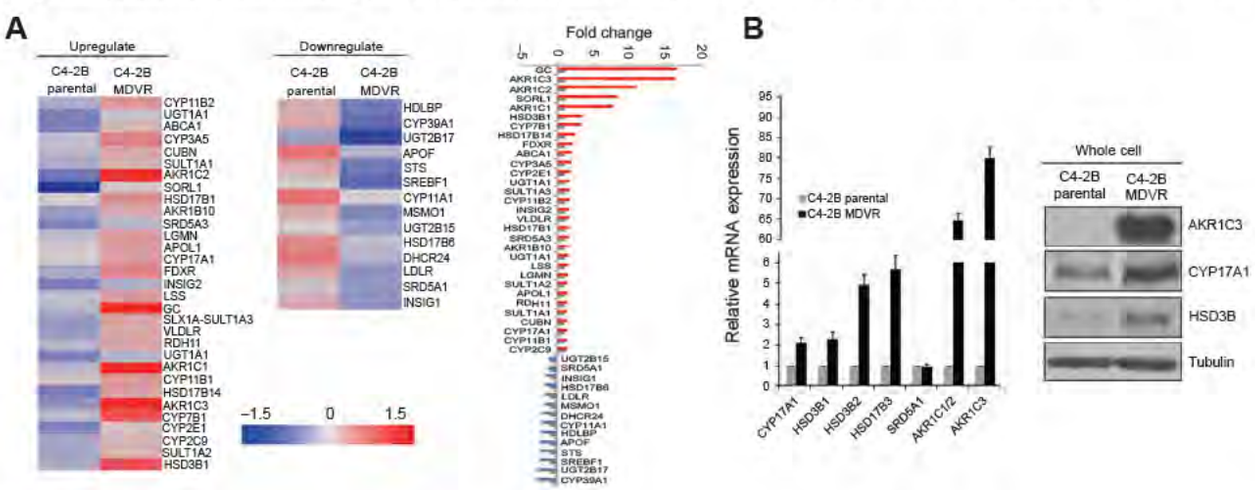

Figure 2.
The intracrine androgen synthesis pathway activated in enzalutamide resistant prostate cancer cells. A, expression of transcripts encoding genes involved in steroid hormone biosynthesis was analyzed by gene set enrichment. Genes that were regulated 1.3 fold between C4 2B parental cells and C4 2B MDVR cells were enriched and heatmap was generated by *Subio* platform. B, C4 2B parental cells and C4 2B MDVR cells were cultured in RPMI 1640 media containing 10% FBS for 3 days, total RNAs were extracted, and CYP17A1, HSD3B1, HSD3B2, HSD17B3, SRD5A1, AKR1C1/2 or AKR1C3 mRNA levels were analyzed by qRT PCR. AKR1C3, HSD3B, and CYP17A1 protein levels were examined by Western blot analysis (right).

Published OnlineFirst February 3, 2015; DOI: 10.1158/0008-5472.CAN-14-3080

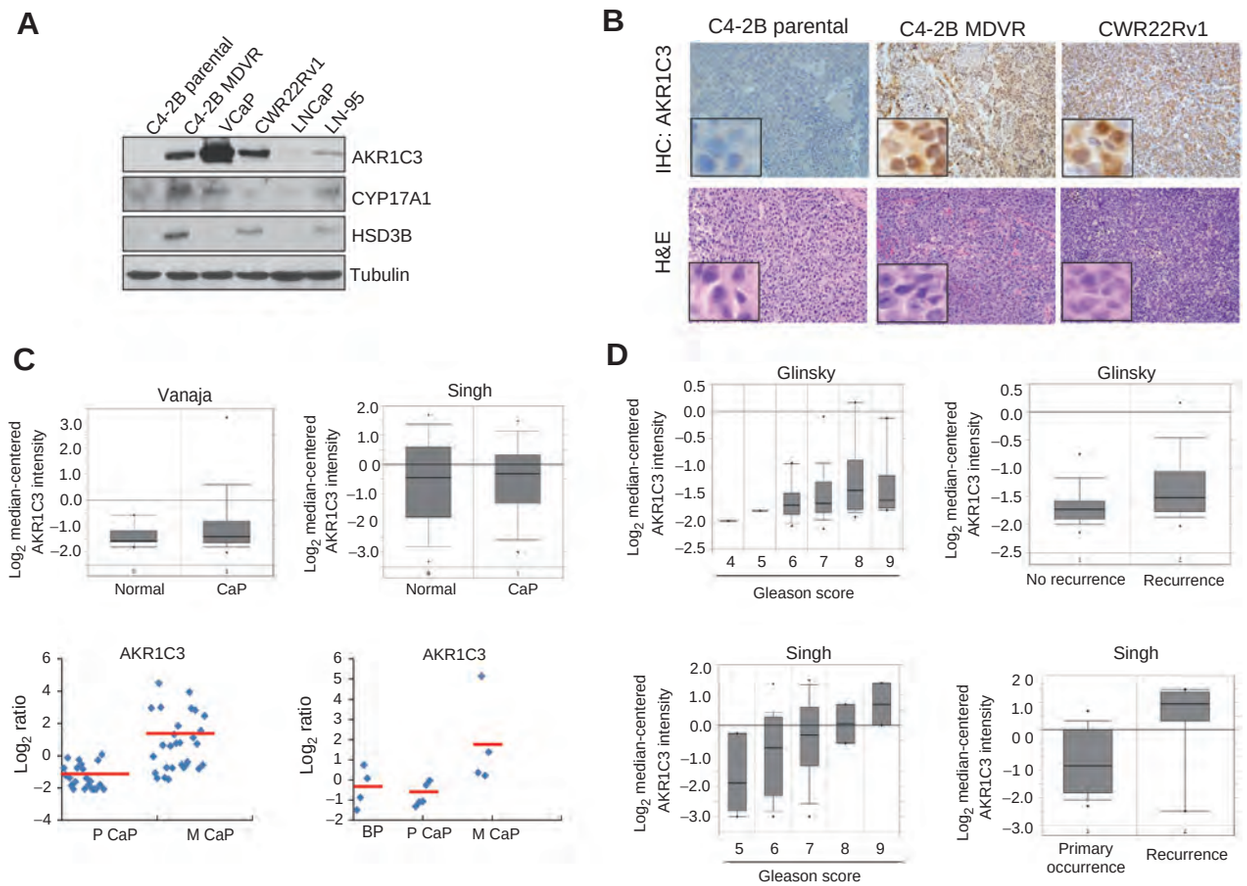

Figure 3.

AKR1C3 is highly expressed in metastatic prostate tumors and enzalutamide resistant xenografts. A, C4 2B parental, C4 2B MDVR, VCaP, CWR22Rv1, LNCaP, and LN 95 cells were harvested and whole lysates were subjected to Western blotting. B, AKR1C3 expression level was analyzed by IHC staining in C4 2B parental, C4 2B MDVR, and CWR22Rv1 xenografts. C, gene expression analysis using the Oncomine database showing the relative expression levels of AKR1C3 in two datasets comparing normal prostate tissue and prostate cancer. Vanaja, normal, $n = 8$; cancer, $n = 32$. Singh, normal, $n = 50$; cancer, $n = 52$. Data, mean ± SE of normalized expression units according to Oncomine output (top). AKR1C3 gene expression analysis using the GEO database in two datasets comparing benign, primary, or metastatic prostate cancer. GSE27616: benign, $n = 4$; primary prostate cancer, $n = 5$; and metastatic prostate cancer, $n = 4$; GSE32269: primary prostate cancer, $n = 22$; and metastatic prostate cancer, $n = 29$. Data were extracted and analyzed by *Subio* platform (bottom). D, gene expression analysis using the Oncomine database showed that AKR1C3 expression was correlated with prostate cancer progression and recurrence in two independent datasets (Glinsky and Singh prostate).

We performed data mining using the Oncomine and GEO data bases to compare the expression of AKR1C3 in normal prostate and prostate cancer. Primary prostate cancer and normal prostate express similar AKR1C3 levels in two independent prostate data sets, whereas AKR1C3 was significantly elevated in metastatic prostate cancer in GEO datasets (Fig. 3C), which is consistent with the previous reports (29, 30). We further examined the correlation between AKR1C3 and prostate cancer disease progres sion. As shown in Fig. 3D, AKR1C3 was significantly correlated with Gleason score and recurrence status in prostate cancer patients in two independent prostate datasets in Oncomine. Collectively, these results demonstrate that AKR1C3 is highly expressed in late stage prostate cancer.

Intracrine androgens are elevated in enzalutamide resistant prostate cancer cells

AKR1C3 (also named 17βHSD5) is one of the most important genes involved in androgen synthesis and metabolism. AKR1C3 facilitates the conversion of weak androgens A′ dione and 5α dione to the more active androgens, testosterone, and DHT, respectively. To further confirm that intracellular androgen syn thesis was acquired by C4 2B MDVR cells, steroid metabolism in C4 2B parental and C4 2B MDVR cells was analyzed by LC/MS. C4 2B parental and C4 2B MDVR cells were cultured in serum free and phenol red free medium for 5 days, and steroid metabolites were extracted from 50×10^6 cells and subjected to LC/MS analysis. As shown in Fig. 4A C, C4 2B MDVR cells synthesize extremely high levels of testosterone (131.025 vs. 0.15 pg/50 million cells), dihydrotestosterone (17.55 vs. 0 pg/50 million cells), and DHEA (72.075 vs. 0 pg/50 million cells), compared with C4 2B parental cells. Intriguingly, the active estrogen metab olite estradiol was significantly reduced (82.725 vs. 207.3 pg/50 million cells) in C4 2B MDVR cells, suggesting that the biosyn thesis of androgens was activated whereas transformation of estrogen from androgens was suppressed in C4 2B MDVR cells. Of note, the precursors involved in intracrine androgen synthesis such as cholesterol, DHEA, and progesterone are also elevated in C4 2B MDVR cells compared with C4 2B parental cells (Fig. 4C).

Published OnlineFirst February 3, 2015; DOI: 10.1158/0008-5472.CAN-14-3080

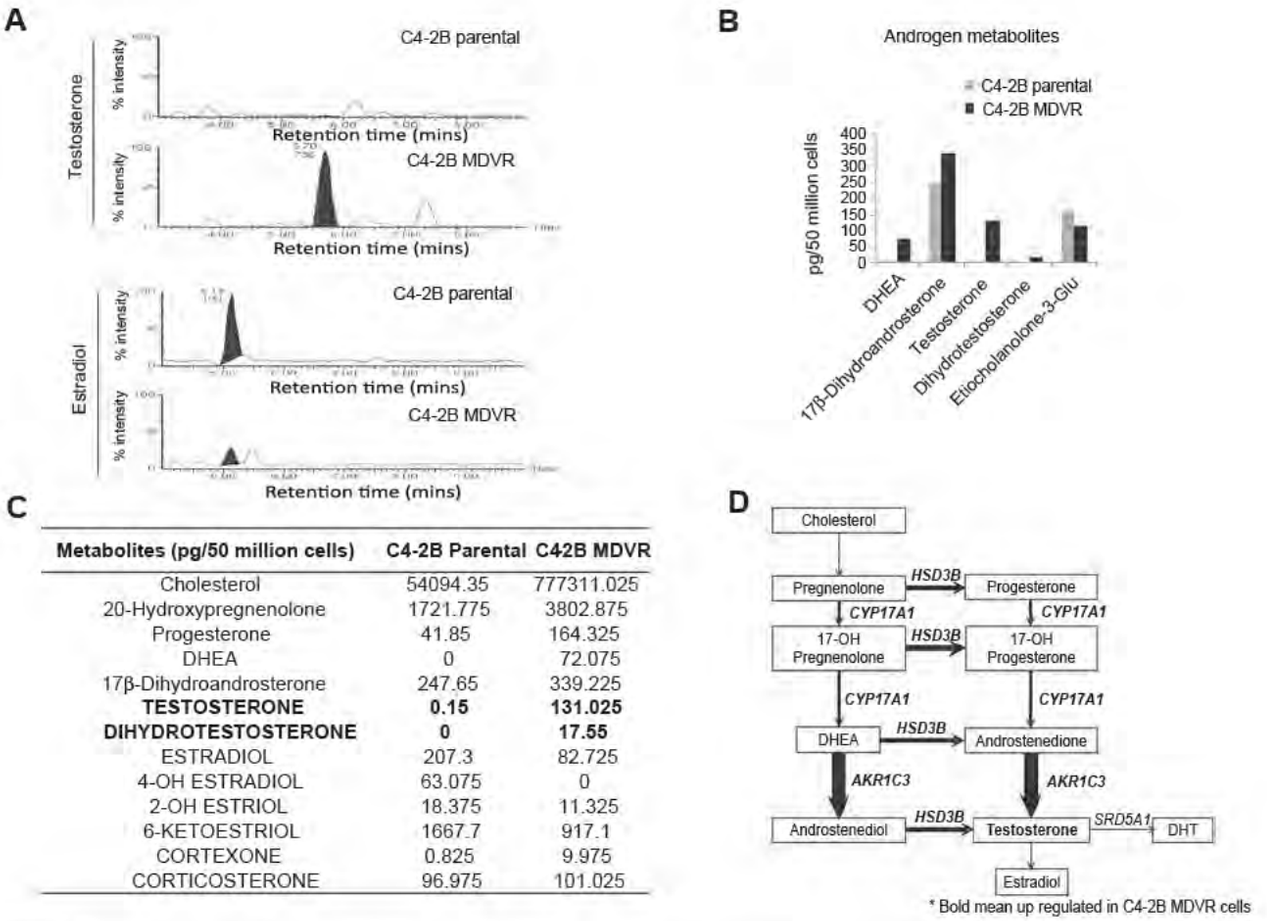

Metabolites (pg/50 million cells)	C4-2B Parental	C42B MDVR
Cholesterol	54094.35	777311.025
20-Hydroxypregnenolone	1721.775	3802.875
Progesterone	41.85	164.325
DHEA	0	72.075
17β-Dihydroandrosterone	247.65	339.225
TESTOSTERONE	**0.15**	**131.025**
DIHYDROTESTOSTERONE	**0**	**17.55**
ESTRADIOL	207.3	82.725
4-OH ESTRADIOL	63.075	0
2-OH ESTRIOL	18.375	11.325
6-KETOESTRIOL	1667.7	917.1
CORTEXONE	0.825	9.975
CORTICOSTERONE	96.975	101.025

Figure 4.
Intracrine androgens were upregulated in enzalutamide resistant prostate cancer cells. A, C4 2B parental and C4 2B MDVR cells were cultured in serum free and phenol red free RPMI 1640 medium for 5 days, and levels of steroids in the cell extracts were analyzed by LC/MS. Representative testosterone and estradiol chromatograms generated by MassLynx 4.1 software are shown. B, the difference between levels of androgen metabolites in C4 2B parental and C4 2B MDVR cells was analyzed and quantified. C, the represented steroid metabolites between C4 2B parental and C4 2B MDVR cells were quantified. D, the androgen metabolism pathway was upregulated in enzalutamide resistant prostate cancer cells.

The steroidogenic enzymes involved in androgen synthesis and metabolism are illustrated in Fig. 4D; bold arrows and bold font indicate upregulation in enzalutamide resistant prostate cancer cells compared with C4 2B parental cells (Fig. 4D). Collectively, these results suggest that intracrine acquired androgen synthesis was elevated in prostate cancer cells resistant to enzalutamide.

AKR1C3 confers resistance to enzalutamide in prostate cancer cells

Having demonstrated that AKR1C3 is upregulated in enzalutamide resistant prostate cancer cells and in late stage prostate cancer patients, we next examined whether AKR1C3 could confer resistance to enzalutamide. We found that AKR1C3 was sufficient to confer resistance to enzalutamide in prostate cancer cells. CWR22Rv1 or C4 2B MDVR cells were transiently transfected with control shRNA or AKR1C3 shRNA following treatment with enzalutamide for 3 days. As shown in Fig. 5A and B, CWR22Rv1 and C4 2B MDVR cells are resistant to enzalutamide, whereas knockdown of AKR1C3 expression by two independent shRNAs (#561 and #694) restored their sensitivity to enzalutamide. The downregulation of AKR1C3 by shRNA was confirmed by Western blot analysis (Fig. 5C). We also generated LNCaP cells stably expressing AKR1C3 (LNCaP AKR1C3) to test whether exogenous expression of AKR1C3 induces enzalutamide resistance. LNCaP AKR1C3 and LNCaP neo vector control cells were treated with different concentrations of enzalutamide for 48 hours and cell numbers were counted. As shown in Fig. 5D, LNCaP AKR1C3 cells exhibited greater resistance to enzalutamide than LNCaP neo cells. These results were also confirmed by clonogenic ability assay. LNCaP AKR1C3 cells showed significantly more clonogenic ability than the control LNCaP neo cells in response to enzalutamide treatment (Fig. 5E and F). Collectively, these results demonstrate that overexpression of AKR1C3 confers resistance to enzalutamide, whereas downregulation of AKR1C3 resensitizes enzalutamide resistant prostate cancer cells to enzalutamide treatment.

Indomethacin, an inhibitor of AKR1C3 activity, overcomes enzalutamide resistance

Indomethacin, an NSAID used for reducing fever, pain, and inflammation, has been shown to be able to inhibit AKR1C3 activity (9, 31, 32). To further examine the role of AKR1C3 in

Published OnlineFirst February 3, 2015; DOI: 10.1158/0008-5472.CAN-14-3080

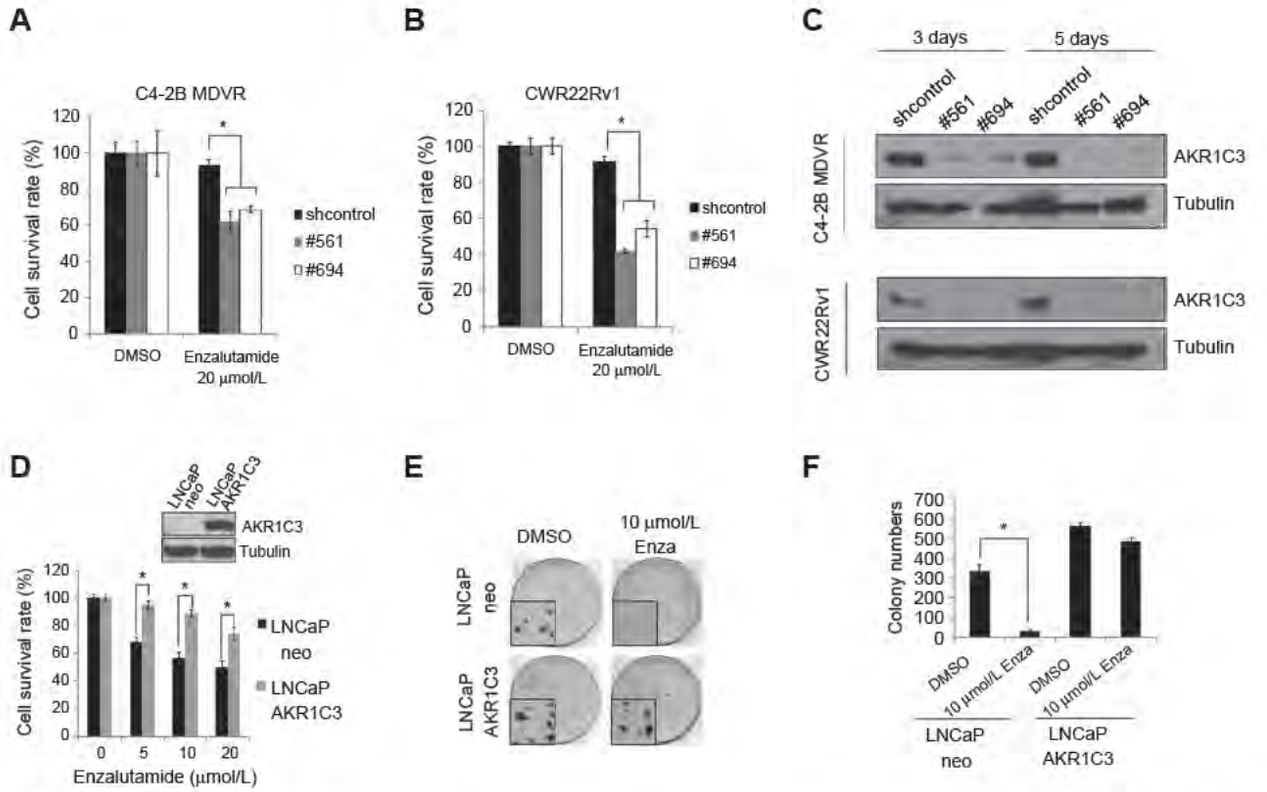

Figure 5.

AKR1C3 confers resistance to enzalutamide in prostate cancer cells. A, CWR22Rv1 cells were transiently transfected with control shRNA or AKR1C3 shRNA (#561 and #694) following treatment with 20 μmol/L enzalutamide, and cell numbers were determined after 3 days. B, C4 2B MDVR cells were transiently transfected with control shRNA or AKR1C3 shRNA (#561 and #694) following treatment with 20 μmol/L enzalutamide, and cell numbers were determined on day 3. C, CWR22Rv1 or C4 2B MDVR cells were transiently transfected with control shRNA or AKR1C3 shRNA (#561 and #694), cells were collected on day 3 or 5, and whole cell lysates were subjected to Western blotting. D, LNCaP neo or LNCaP AKR1C3 cells were treated with different concentrations of enzalutamide for 2 days, total cell numbers were counted, and cell survival rate (%) was calculated. E, LNCaP neo or LNCaP AKR1C3 cells were treated with 10 μmol/L enzalutamide and clonogenic assay was performed; the colony size pictures were taken under a microscope. F, colonies were counted and results are presented as means ± SD of two experiments performed in duplicate; *, $P < 0.05$. Enza, enzalutamide.

enzalutamide resistance, we used indomethacin to hinder AKR1C3 activation and examined the effects on the response of prostate cancer cells to enzalutamide treatment *in vitro* and *in vivo*. As shown in Fig. 6A left, indomethacin did not have an effect on CWR22Rv1 cell growth at 10 μmol/L, but inhibited cell growth marginally at 20 μmol/L. However, combination of indomethacin with enzalutamide significantly inhibited the growth of enzalutamide resistant CWR22Rv1 cells. The results were also confirmed by clonogenic assay. As shown in Fig. 6A right, combination of indomethacin with enzalutamide significantly inhibited colony numbers and reduced colony size in CWR22Rv1 cells. Similar results were also obtained in C4 2B MDVR cells (Fig. 6B). To test whether inhibition of AKR1C3 by indomethacin overcomes resistance to enzalutamide treatment *in vivo*, CWR22Rv1 xenograft model was used. As shown in Fig. 6C, although CWR22Rv1 tumors were resistant to enzalutamide treatment, indomethacin significantly inhibited tumor growth. Combination of indomethacin with enzalutamide further inhibited tumor growth of CWR22Rv1 xenografts. Immunohistochemical staining of Ki 67 showed that cell proliferation was significantly inhibited by indomethacin, and further inhibited by the combination treatment (Fig. 6D). Collectively, these results suggest that inhibition of AKR1C3 by indomethacin reduced enzalutamide resistant tumor growth, and that combination of enzalutamide with indomethacin further reduced the tumor growth of enzalutamide resistant prostate cancer. These results indicate that inhibition of AKR1C3 by indomethacin potentiates the cell killing effect of enzalutamide.

Discussion

The second generation androgen antagonist enzalutamide represents an improvement in therapy options for late stage metastatic CRPC (33, 34). However, the initial responders develop resistance inevitably. The potential mechanisms associated with enzalutamide resistance have been the focus of intense investigation. We previously identified several novel mechanisms involved in enzalutamide resistance, including activation of NFκB2/p52 (27, 35), AR V7 (2, 27), Stat3 (4), and induction of autophagy (36). In this study, we have identified AKR1C3 activation and elevated intracrine androgens as potential mechanisms contributing to enzalutamide resistance. We demonstrate that AKR1C3 is overexpressed in enzalutamide resistant prostate cancer cells. Overexpression of AKR1C3 confers resistance to

Published OnlineFirst February 3, 2015; DOI: 10.1158/0008-5472.CAN-14-3080

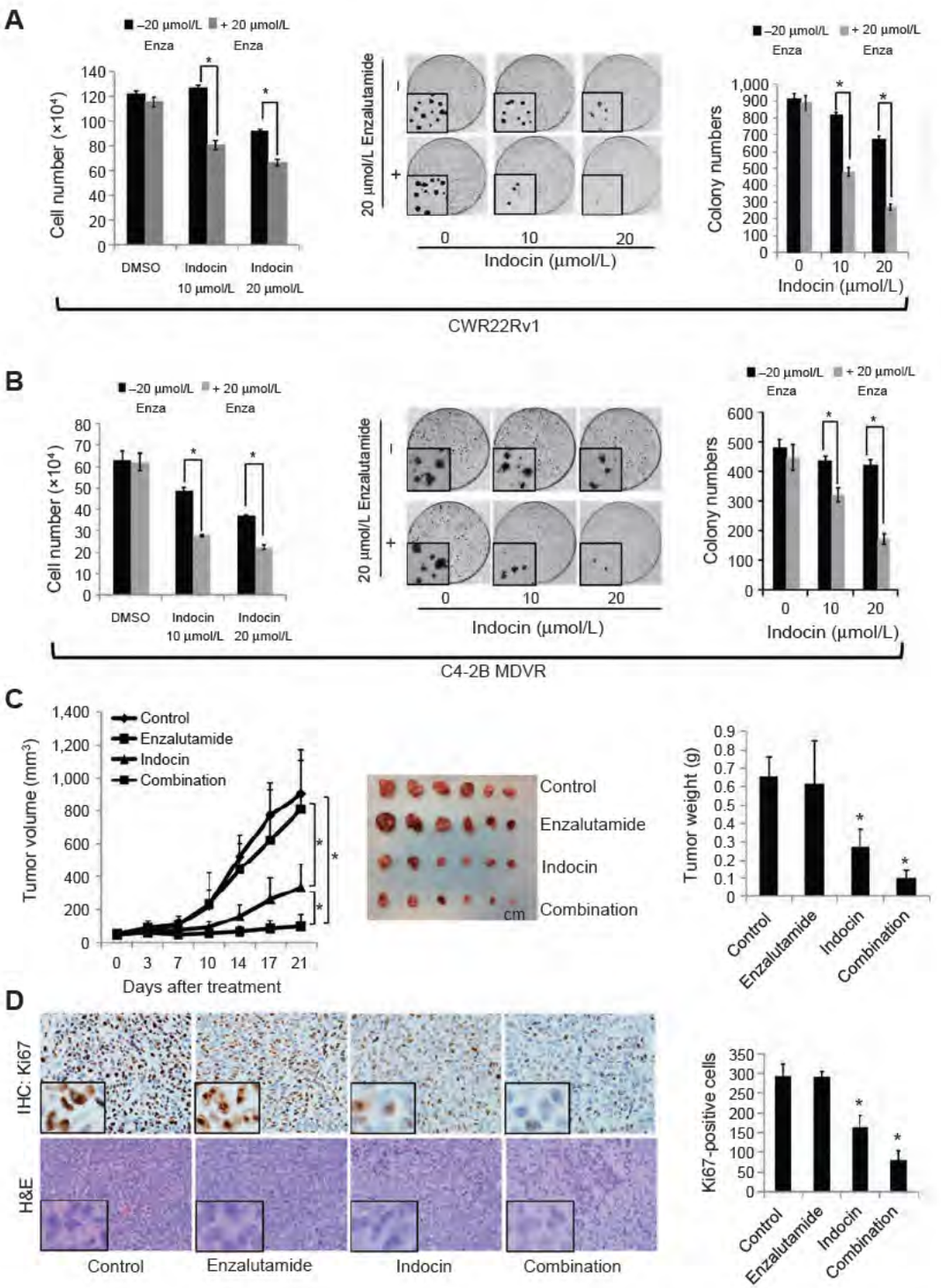

Figure 6.
Indomethacin, an inhibitor of AKR1C3activity, overcomes enzalutamide resistance. A, CWR22Rv1 cells were treated with 10 or 20 μmol/L indomethacin with or without 20 μmol/L enzalutamide for 2 days, total cell numbers were counted (left), and clonogenic assay was performed; the colony size pictures were taken under a microscope (middle). Colonies were counted and results are presented as means ± SD of two experiments performed in duplicate (right). B, C4 2B MDVR cells were treated with 10 or 20 μmol/L indomethacin with or without 20 μmol/L enzalutamide for 2 days, total cell numbers were counted (left), and clonogenic assay was performed; the colony size pictures were taken under a microscope (middle). Colonies were counted and results are presented as means ± SD of two experiments performed in duplicate (right). C, mice bearing CWR22Rv1 xenografts were treated with vehicle control, enzalutamide (25 mg/kg orally), indomethacin (3 mg/kg i.p), or their combination for 3 weeks, tumor volumes were measured twice weekly, and the tumors were collected and weighed. D, IHC staining of Ki 67 and hematoxylin and eosin (H&E) staining in each group was performed and quantified as described in Materials and Methods. *, $P < 0.05$. Enza, enzalutamide; indocin, indomethacin.

enzalutamide, whereas downregulation of AKR1C3 sensitizes prostate cancer cells to enzalutamide treatment. In addition, overexpression of AKR1C3 has been demonstrated in clinical metastatic prostate cancer and correlated with disease progression. We also demonstrated that intracrine steroids, including androgens are elevated in enzalutamide resistant cells, possibly through increased expression of steroidogenic enzymes such as AKR1C3. We further demonstrated that indomethacin, a potent inhibitor of AKR1C3, could be used to overcome enzalutamide resistance. The discovery of elevated intracrine androgen synthesis and enhanced AKR1C3 activation in enzalutamide resistant cells reveal a novel mechanism for the development and progression of resistant CRPC. Cotargeting AKR1C3 will provide proof of concept experiments to overcome resistance and achieve durable responses in men with second generation antiandrogen treatment.

Intracrine androgen biosynthesis has been well characterized as a mechanism of CRPC (9 12, 28). Many enzymes are involved in androgen synthesis, including CYP17A1, AKR1C3, and HSD3B. CYP17A1 can be inhibited by abiraterone in clinical treatments (37, 38). AKR1C3 is a steroidogenic enzyme involved in steroid biosynthesis and mediates the last step of testosterone biosynthesis from A′ dione. It catalyzes conversion of steroids and modulates transactivation of steroid receptors. Elevated expression of AKR1C3 has been associated with prostate cancer progression and aggressiveness (19, 20). AKR1C3 has also been identified as an AR coactivator (39). In this study, we used gene enrichment analysis to compare enzalutamide resistant cells with enzalutamide sensitive cells, and found that the steroid biosynthesis genes were highly enriched in C4 2B MDVR cells, and several important genes involved in androgen synthesis, such as AKR1C3, HSD3B, and CYP17A1 were upregulated in enzalutamide resistant cells. In another *de novo* enzalutamide resistant cell line CWR22Rv1, AKR1C3 was highly expressed compared with C4 2B or LNCaP cells, suggesting that AKR1C3 might play a pivotal role in enzalutamide resistance. To further confirm that intracrine androgen synthesis was acquired by C4 2B MDVR cells, steroid levels in C4 2B parental and C4 2B MDVR cells were determined by LC/MS. In addition to the higher levels of testosterone and DHT in enzalutamide resistant cells, the levels of the precursors of testosterone such as cholesterol, DHEA, and progesterone were all elevated in C4 2B MDVR cells compared with C4 2B parental cells. These results demonstrate that AKR1C3 was significantly elevated in enzalutamide resistant prostate cancer cells, which potentially resulted in higher levels of testosterone and DHT in enzalutamide resistant cells. The *de novo* intratumoral steroid synthesis has also been shown as a potential mechanism contributing to abiraterone resistance (9). Long term treatment of abiraterone in patients resulted in an increase in steroids biosynthesis through deregulated steroid enzymes, such as AKR1C3 (40).

Several inhibitors have been developed to target AKR1C3 activation, including indomethacin (32). Indomethacin is an NSAID used for reducing fever, pain, and inflammation. Several studies revealed that indomethacin might have the potential to increase the sensitivity of cancer cells to anticancer agents, such as that of human melanoma cells to TRAIL induced apoptosis (41), and of colon cancer cells to cisplatin (42). Indomethacin also has the ability to inhibit PSA and ERG protein expression and decreased testosterone and DHT levels in relapsed VCaP xenograft tumors (9). In the present study, we showed that inhibition of AKR1C3 enzyme activity by indomethacin restored enzalutamide sensitivity in enzalutamide resistant prostate cancer cells both *in vitro* and *in vivo*. Furthermore, the combination of indomethacin and enzalutamide resulted in significantly greater inhibition of enzalutamide resistant tumor growth. Our data suggest that inhibition of AKR1C3 holds promise as a sensitizing strategy to restore antitumor effects in patients resistant to enzalutamide.

Taken together, we found that AKR1C3 activation and the resultant intracrine androgen synthesis confers resistance to enzalutamide in prostate cancer cells. Inhibition of AKR1C3 by shRNA or indomethacin overcomes resistance to enzalutamide. Furthermore, the combination of indomethacin and enzalutamide resulted in significant inhibition of enzalutamide resistant tumor growth. Targeting AKR1C3 may provide an effective treatment strategy for patients resistant to enzalutamide.

Disclosure of Potential Conflicts of Interest

C. Liu has ownership interest (including patents) in patent application covering the use of indomethacin. W. Lou and A.C. Gao have ownership interest (including patents) in patent application. No potential conflicts of interest were disclosed by the other authors.

Authors' Contributions

Conception and design: C. Liu, W. Lou, A.C. Gao
Development of methodology: C. Liu, W. Lou, N.W. Gaikwad, A.C. Gao
Acquisition of data (provided animals, acquired and managed patients, provided facilities, etc.): C. Liu, W. Lou, Y. Zhu, J.C. Yang, A.C. Gao
Analysis and interpretation of data (e.g., statistical analysis, biostatistics, computational analysis): C. Liu, N.W. Gaikwad, C.P. Evans, A.C. Gao
Writing, review, and/or revision of the manuscript: C. Liu, C.P. Evans, A.C. Gao
Administrative, technical, or material support (i.e., reporting or organizing data, constructing databases): C. Liu, W. Lou, Y. Zhu, J.C. Yang, N. Nadiminty, C.P. Evans, A.C. Gao
Study supervision: C. Liu, A.C. Gao

Grant Support

This work was supported in part by grants NIH/NCI CA140468, CA168601, and CA179970.

The costs of publication of this article were defrayed in part by the payment of page charges. This article must therefore be hereby marked *advertisement* in accordance with 18 U.S.C. Section 1734 solely to indicate this fact.

Received October 17, 2014; revised December 19, 2014; accepted January 12, 2015; published OnlineFirst February 3, 2015.

References

1. Li Y, Chan SC, Brand LJ, Hwang TH, Silverstein KA, Dehm SM. Androgen receptor splice variants mediate enzalutamide resistance in castration-resistant prostate cancer cell lines. Cancer Res 2013;73:483–9.
2. Liu C, Lou W, Zhu Y, Nadiminty N, Schwartz CT, Evans CP, et al. Niclosamide inhibits androgen receptor variants expression and overcomes enzalutamide resistance in castration-resistant prostate cancer. Clin Cancer Res 2014;20:3198–210.
3. Antonarakis ES, Lu C, Wang H, Luber B, Nakazawa M, Roeser JC, et al. AR-V7 and resistance to enzalutamide and abiraterone in prostate cancer. N Engl J Med 2014;371:1028–38.

4. Liu C, Zhu Y, Lou W, Cui Y, Evans CP, Gao AC. Inhibition of constitutively active Stat3 reverses enzalutamide resistance in LNCaP derivative prostate cancer cells. Prostate 2014;74:201–9.
5. Korpal M, Korn JM, Gao X, Rakiec DP, Ruddy DA, Doshi S, et al. An F876L mutation in androgen receptor confers genetic and phenotypic resistance to MDV3100 (enzalutamide). Cancer Discov 2013;3:1030–43.
6. Joseph JD, Lu N, Qian J, Sensintaffar J, Shao G, Brigham D, et al. A clinically relevant androgen receptor mutation confers resistance to second-generation antiandrogens enzalutamide and ARN-509. Cancer Discov 2013; 3:1020–9.
7. Arora VK, Schenkein E, Murali R, Subudhi SK, Wongvipat J, Balbas MD, et al. Glucocorticoid receptor confers resistance to antiandrogens by bypassing androgen receptor blockade. Cell 2013;155:1309–22.
8. Isikbay M, Otto K, Kregel S, Kach J, Cai Y, Vander Griend DJ, et al. Glucocorticoid receptor activity contributes to resistance to androgen-targeted therapy in prostate cancer. Horm Cancer 2014;5:72–89.
9. Cai C, Chen S, Ng P, Bubley GJ, Nelson PS, Mostaghel EA, et al. Intratumoral *de novo* steroid synthesis activates androgen receptor in castration-resistant prostate cancer and is upregulated by treatment with CYP17A1 inhibitors. Cancer Res 2011;71:6503–13.
10. Ishizaki F, Nishiyama T, Kawasaki T, Miyashiro Y, Hara N, Takizawa I, et al. Androgen deprivation promotes intratumoral synthesis of dihydrotestosterone from androgen metabolites in prostate cancer. Sci Rep 2013;3:1528.
11. Locke JA, Guns ES, Lubik AA, Adomat HH, Hendy SC, Wood CA, et al. Androgen levels increase by intratumoral *de novo* steroidogenesis during progression of castration-resistant prostate cancer. Cancer Res 2008; 68:6407–15.
12. Mohler JL, Titus MA, Bai S, Kennerley BJ, Lih FB, Tomer KB, et al. Activation of the androgen receptor by intratumoral bioconversion of androstanediol to dihydrotestosterone in prostate cancer. Cancer Res 2011;71:1486–96.
13. Efstathiou E Titus MA,Tsavachidou D, Hoang A, Karlou M, Wen S, et al. MDV3100 effects on androgen receptor (AR) signaling and bone marrow testosterone concentration modulation: a preliminary report. ASCO Meeting Abstracts 2011;29:4501.
14. Efstathiou E, Titus M, Wen S, Hoang A, Karlou M, Ashe R, et al. Molecular characterization of enzalutamide-treated bone metastatic castration-resistant prostate cancer. Eur Urol 2014;67(1):53–60.
15. Chang KH, Li R, Kuri B, Lotan Y, Roehrborn CG, Liu J, et al. A gain-of-function mutation in DHT synthesis in castration-resistant prostate cancer. Cell 2013;154:1074–84.
16. Chang KH, Ercole CE, Sharifi N. Androgen metabolism in prostate cancer: from molecular mechanisms to clinical consequences. Br J Cancer 2014;111:1249–54.
17. Labrie F, Luu-The V, Lin SX, Labrie C, Simard J, Breton R, et al. The key role of 17 beta-hydroxysteroid dehydrogenases in sex steroid biology. Steroids 1997;62:148–58.
18. Bauman DR, Steckelbroeck S, Williams MV, Peehl DM, Penning TM. Identification of the major oxidative 3alpha-hydroxysteroid dehydrogenase in human prostate that converts 5alpha-androstane-3alpha,17beta-diol to 5alpha-dihydrotestosterone: a potential therapeutic target for androgen-dependent disease. Mol Endocrinol 2006; 20:444–58.
19. Stanbrough M, Bubley GJ, Ross K, Golub TR, Rubin MA, Penning TM, et al. Increased expression of genes converting adrenal androgens to testosterone in androgen-independent prostate cancer. Cancer Res 2006;66:2815–25.
20. Wako K, Kawasaki T, Yamana K, Suzuki K, Jiang S, Umezu H, et al. Expression of androgen receptor through androgen-converting enzymes is associated with biological aggressiveness in prostate cancer. J Clin Pathol 2008;61:448–54.
21. Gaikwad NW. Ultra performance liquid chromatography-tandem mass spectrometry method for profiling of steroid metabolome in human tissue. Anal Chem 2013;85:4951–60.
22. Zhu Y, Liu C, Nadiminty N, Lou W, Tummala R, Evans CP, et al. Inhibition of ABCB1 expression overcomes acquired docetaxel resistance in prostate cancer. Mol Cancer Ther 2013;12:1829–36.
23. Subramanian A, Tamayo P, Mootha VK, Mukherjee S, Ebert BL, Gillette MA, et al. Gene set enrichment analysis: a knowledge-based approach for interpreting genome-wide expression profiles. Proc Natl Acad Sci U S A 2005;102:15545–50.
24. Liu C, Nadiminty N, Tummala R, Chun JY, Lou W, Zhu Y, et al. Andrographolide targets androgen receptor pathway in castration-resistant prostate cancer. Genes Cancer 2011;2:151–9.
25. Hu R, Lu C, Mostaghel EA, Yegnasubramanian S, Gurel M, Tannahill C, et al. Distinct transcriptional programs mediated by the ligand-dependent full-length androgen receptor and its splice variants in castration-resistant prostate cancer. Cancer Res 2013;72:3457–62.
26. Dehm SM, Schmidt LJ, Heemers HV, Vessella RL, Tindall DJ. Splicing of a novel androgen receptor exon generates a constitutively active androgen receptor that mediates prostate cancer therapy resistance. Cancer Res 2008;68:5469–77.
27. Nadiminty N, Tummala R, Liu C, Yang J, Lou W, Evans CP, et al. NF-kappaB2/p52 induces resistance to enzalutamide in prostate cancer: role of androgen receptor and its variants. Mol Cancer Ther 2013;12:1629–37.
28. Fankhauser M, Tan Y, Macintyre G, Haviv I, Hong MK, Nguyen T, et al. Canonical androstenedione reduction is the predominant source of signalling androgens in hormone refractory prostate cancer. Clin Cancer Res 2014;20:5547–57.
29. Mitsiades N, Sung CC, Schultz N, Danila DC, He B, Eedunuri VK, et al. Distinct patterns of dysregulated expression of enzymes involved in androgen synthesis and metabolism in metastatic prostate cancer tumors. Cancer Res 2012;72:6142–52.
30. Montgomery RB, Mostaghel EA, Vessella R, Hess DL, Kalhorn TF, Higano CS, et al. Maintenance of intratumoral androgens in metastatic prostate cancer: a mechanism for castration-resistant tumor growth. Cancer Res 2008;68:4447–54.
31. Liedtke AJ, Adeniji AO, Chen M, Byrns MC, Jin Y, Christianson DW, et al. Development of potent and selective indomethacin analogues for the inhibition of AKR1C3 (Type 5 17beta-hydroxysteroid dehydrogenase/prostaglandin F synthase) in castrate-resistant prostate cancer. J Med Chem 2013;56:2429–46.
32. Flanagan JU, Yosaatmadja Y, Teague RM, Chai MZ, Turnbull AP, Squire CJ. Crystal structures of three classes of non-steroidal anti-inflammatory drugs in complex with aldo-keto reductase 1C3. PLoS ONE 2012;7:e43965.
33. Scher HI, Beer TM, Higano CS, Anand A, Taplin ME, Efstathiou E, et al. Antitumour activity of MDV3100 in castration-resistant prostate cancer: a phase 1-2 study. Lancet 2010;375:1437–46.
34. Scher HI, Fizazi K, Saad F, Taplin ME, Sternberg CN, Miller K, et al. Increased survival with enzalutamide in prostate cancer after chemotherapy. N Engl J Med 2012;367:1187–97.
35. Cui Y, Nadiminty N, Liu C, Lou W, Schwartz CT, Gao AC. Upregulation of glucose metabolism by NF-kappaB2/p52 mediates enzalutamide resistance in castration-resistant prostate cancer cells. Endocr Relat Cancer 2014;21:435–42.
36. Nguyen HG, Yang JC, Kung HJ, Shi XB, Tilki D, Lara PN Jr, et al. Targeting autophagy overcomes Enzalutamide resistance in castration-resistant prostate cancer cells and improves therapeutic response in a xenograft model. Oncogene 2014;33:4521–30.
37. de Bono JS, Logothetis CJ, Molina A, Fizazi K, North S, Chu L, et al. Abiraterone and increased survival in metastatic prostate cancer. N Engl J Med 2011;364:1995–2005.
38. Ryan CJ, Smith MR, de Bono JS, Molina A, Logothetis CJ, de Souza P, et al. Abiraterone in metastatic prostate cancer without previous chemotherapy. N Engl J Med 2013;368:138–48.
39. Yepuru M, Wu Z, Kulkarni A, Yin F, Barrett CM, Kim J, et al. Steroidogenic enzyme AKR1C3 is a novel androgen receptor-selective coactivator that promotes prostate cancer growth. Clin Cancer Res 2013;19:5613–25.
40. Mostaghel EA, Marck BT, Plymate SR, Vessella RL, Balk S, Matsumoto AM, et al. Resistance to CYP17A1 inhibition with abiraterone in castration-resistant prostate cancer: induction of steroidogenesis and androgen receptor splice variants. Clin Cancer Res 2011;17:5913–25.
41. Tse AK, Cao HH, Cheng CY, Kwan HY, Yu H, Fong WF, et al. Indomethacin sensitizes TRAIL-resistant melanoma cells to TRAIL-induced apoptosis through ROS-mediated upregulation of death receptor 5 and downregulation of survivin. J Invest Dermatol 2013;134:1397–407.
42. Brunelli C, Amici C, Angelini M, Fracassi C, Belardo G, Santoro MG. The non-steroidal anti-inflammatory drug indomethacin activates the eIF2alpha kinase PKR, causing a translational block in human colorectal cancer cells. Biochem J 2012;443:379–86.

Cancer Research
The Journal of Cancer Research (1916–1930) | The American Journal of Cancer (1931–1940)

AACR American Association for Cancer Research

Intracrine Androgens and AKR1C3 Activation Confer Resistance to Enzalutamide in Prostate Cancer

Chengfei Liu, Wei Lou, Yezi Zhu, et al.

Cancer Res 2015;75:1413-1422. Published OnlineFirst February 3, 2015.

Published OnlineFirst April 16, 2014; DOI: 10.1158/1078-0432.CCR-13-3296

Cancer Therapy: Preclinical

Clinical Cancer Research

Niclosamide Inhibits Androgen Receptor Variants Expression and Overcomes Enzalutamide Resistance in Castration-Resistant Prostate Cancer

Chengfei Liu[1], Wei Lou[1], Yezi Zhu[1,2], Nagalakshmi Nadiminty[1], Chad T. Schwartz[1], Christopher P. Evans[1,3], and Allen C. Gao[1,2,3]

Abstract

Purpose: Enzalutamide, a second generation antiandrogen, was recently approved for the treatment of castration resistant prostate cancer (CRPC) in patients who no longer respond to docetaxel. Despite these advances that provide temporary respite, resistance to enzalutamide occurs frequently. Androgen receptor (AR) splice variants such as AR V7 have recently been shown to drive castration resistant growth and resistance to enzalutamide. This study was designed to identify inhibitors of AR variants and test its ability to overcome resistance to enzalutamide.

Experimental Design: The drug screening was conducted using luciferase activity assay to determine the activity of AR V7 after treatment with the compounds in the Prestwick Chemical Library, which contains about 1,120 FDA approved drugs. The effects of the identified inhibitors on AR V7 activity and enzalu tamide sensitivity were characterized in CRPC and enzalutamide resistant prostate cancer cells *in vitro* and *in vivo*.

Results: Niclosamide, an FDA approved antihelminthic drug, was identified as a potent AR V7 inhibitor in prostate cancer cells. Niclosamide significantly downregulated AR V7 protein expression by protein degradation through a proteasome dependent pathway. Niclosamide also inhibited AR V7 transcription activity and reduced the recruitment of AR V7 to the PSA promoter. Niclosamide inhibited prostate cancer cell growth *in vitro* and tumor growth *in vivo*. Furthermore, the combination of niclosamide and enzalutamide resulted in significant inhibition of enzalutamide resistant tumor growth, suggesting that niclosamide enhances enzalutamide therapy and overcomes enzalutamide resistance in CRPC cells.

Conclusions: Niclosamide was identified as a novel inhibitor of AR variants. Our findings offer preclinical validation of niclosamide as a promising inhibitor of AR variants to treat, either alone or in combination with current antiandrogen therapies, patients with advanced prostate cancer, especially those resistant to enzalutamide. *Clin Cancer Res; 20(12); 3198 210. ©2014 AACR.*

Introduction

Next generation anti androgens such as enzalutamide and inhibitors of androgen synthesis such as abiraterone have improved the standard of care for patients with late stage prostate cancer (1, 2). Despite their successes and continuing wide spread use, development of resistance is inevitable (3, 4). Potential resistance mechanisms are emerging that per petuate disease progression during effective AR blockade. Alternative mRNA splicing generates truncated and consti tutively active AR variants that support the castration resis tant prostate cancer (CRPC) phenotype (5 8). The truncated androgen receptor (AR) variants that lack the ligand binding domain (LBD) naturally occur in both prostate cancer clinical samples and cell lines (5, 6, 9, 10). Several groups showed that AR variants are upregulated in CRPC patient samples compared with androgen sensitive patient samples and are associated with prostate cancer progression and resistance to AR targeted therapy (3, 11 13). AR variants have been shown to induce ligand independent activation of androgen responsive element (ARE) driven reporters in the absence of androgen, which indicates that those variants may have a distinct transcription program compared with the full length AR (9, 14), and the activity of AR variants is postulated to depend on the full length AR (15).

Authors' Affiliations: [1]Department of Urology; [2]Graduate Program in Pharmacology and Toxicology; and [3]UC Davis Comprehensive Cancer Center, University of California Davis, California

C. Liu and W. Lou contributed equally to this article.

Corresponding Author: Allen C. Gao, Department of Urology, University of California Davis Medical Center, 4645 2nd Avenue, Research III, Suite 1300, Sacramento, CA 95817. Phone: 916 734 8718; Fax: 916 734 8714; E mail: acgao@ucdavis.edu

doi: 10.1158/1078 0432.CCR 13 3296

Published OnlineFirst April 16, 2014; DOI: 10.1158/1078-0432.CCR-13-3296

Translational Relevance

Development of resistance to enzalutamide is eventually inevitable. Recent studies have linked androgen receptor (AR) alternative splicing, particularly AR V7, to the development of enzalutamide resistance. Targeting of AR signaling, especially AR variants, would improve current antiandrogen therapies for advanced prostate cancer. In this study, we identified niclosamide as a potent AR V7 inhibitor in prostate cancer cells. We found that niclosamide significantly inhibits AR V7 protein expression and AR V7 transcription activity and reduces AR V7 recruitment to the PSA promoter. Niclosamide inhibits prostate cancer cell growth *in vitro* and tumor growth *in vivo*. Furthermore, the combination of niclosamide and enzalutamide resulted in significant inhibition of enzalutamide resistant tumor growth, suggesting that niclosamide enhances enzalutamide therapy and overcomes enzalutamide resistance in castration resistant prostate cancer cells. These findings offer preclinical validation of niclosamide as a promising inhibitor of AR variants to treat, either alone or in combination with current antiandrogen therapies, patients with advanced prostate cancer, especially those resistant to enzalutamide.

Among the identified AR variants, AR V7, which is encoded by contiguous splicing of AR exons 1/2/3/CE3, has been well studied mainly because of its prevalence in prostate cancer samples (7, 12, 16). AR V7 functions as a constitutively active ligand independent transcription factor that can induce castration resistant cell growth *in vitro* and *in vivo* (7, 17). Recent studies have linked AR alternative splicing, particularly AR V7, to the development of enzalutamide resistance (18–21). Thus, targeting AR V7 would be a valuable strategy to treat patients with CRPC.

In this study, we screened the Prestwick Chemical Library and identified niclosamide, an FDA approved drug effective against human tapeworms, as a potent AR V7 inhibitor in prostate cancer cells. We found that niclosamide reduces AR V7 recruitment to the PSA promoter and significantly inhibits AR V7 protein expression by protein degradation via a proteasome dependent pathway. Niclosamide inhibits prostate cancer cell growth *in vitro* and tumor growth *in vivo*. Furthermore, niclosamide overcomes enzalutamide resistance and significantly enhances enzalutamide therapy in prostate cancer cells, suggesting that niclosamide can be used to treat, either alone or in combination with current antiandrogen therapies, patients with advanced prostate cancer, especially those resistant to enzalutamide.

Materials and Methods

Reagents and cell culture

LNCaP, VCaP, CWR22Rv1, PC3, and HEK293 cells were obtained from the American Type Culture Collection (ATCC). All experiments with cell lines were performed within 6 months of receipt from ATCC or resuscitation after cryopreservation. ATCC uses short tandem repeat (STR) profiling for testing and authentication of cell lines. C4-2 and C4-2B cells were kindly provided and authenticated by Dr. L. Chung, Cedars Sinai Medical Center (Los Angeles, CA). The cells were maintained in RPMI 1640 supplemented with 10% fetal bovine serum (FBS), 100 units/mL penicillin, and 0.1 mg/mL streptomycin. VCaP cells were maintained in DMEM supplemented with 10% FBS, 100 units/mL penicillin, and 0.1 mg/mL streptomycin. C4-2 neo and C4-2 AR V7 cells were generated by stable transfection of C4-2 cells with either empty vector pcDNA3.1 or pcDNA3.1 encoding AR V7 and were maintained in RPMI 1640 medium containing 300 μg/mL G418. HEK293 AR V7 PSA E/P LUC cells were generated by stable transfection of HEK293 cells with plasmids encoding AR V7 and PSA E/P LUC reporter and were maintained in RPMI 1640 medium containing 300 μg/mL G418. C4-2B cells were chronically exposed to increasing concentrations of enzalutamide (5–40 μmol/L) by passage in media containing enzalutamide for >12 months in complete FBS and stored for further analysis. Cells resistant to enzalutamide were referred to as C4-2B MR (C4-2B enzalutamide resistant; ref. 18). Parental C4-2B cells were passaged alongside the enzalutamide treated cells as an appropriate control. C4-2B MR cells were maintained in 20 μmol/L enzalutamide containing medium. All cells were maintained at 37°C in a humidified incubator with 5% carbon dioxide.

Cell transfection and luciferase assay

For small interfering RNA (siRNA) transfection, cells were seeded at a density of 1×10^5 cells per well in 12 well plates or 3×10^5 cells per well in 6 well plates and transfected with siRNA (Dharmacon) targeting the AR exon 7 sequence (UCAAGGAACUCGAUCGUAU; ref. 22) or AR V7 sequence (GUAGUUGUAAGUAUCAUGA; ref. 22) or a control siRNA targeting the luciferase (Luc) gene, sicontrol (CTTACGCTGAGTACTTCGA), using lipofectamine RNAiMAX (Invitrogen). Cells were transiently transfected with plasmids expressing wild type (WT) AR, AR V7, or pcDNA3.1 using Attractene transfection reagent (Qiagen). For luciferase assay, LNCaP or PC3 cells (1×10^5 cells per well of 12 well plate) were transfected with 0.5 μg of pGL3 PSA6.0 Luc reporter plasmid or the control plasmid along with WT AR or AR V7. The luciferase activity was determined 24 to 48 hours after transfection using a dual luciferase reporter assay system as described previously (Promega; ref. 23), the signal was normalized to *Renilla* luciferase control as relative luciferase units.

Chromatin immunoprecipitation assay

C4-2 neo and C4-2 AR V7 cells were cultured in CS FBS condition for 3 days. DNA–AR protein complexes were cross linked inside the cells by the addition of 1% formaldehyde. Whole cell extracts were prepared by sonication, and an aliquot of the cross linked DNA–protein complexes was immunoprecipitated by incubation with the

Published OnlineFirst April 16, 2014; DOI: 10.1158/1078-0432.CCR-13-3296

AR specific antibody (AR 441; Santa Cruz Biotechnology) overnight at 4°C with rotation. Chromatin antibody complexes were isolated from solution by incubation with protein A/G agarose beads for 1 hour at 4°C with rotation. The bound DNA protein complexes were washed and eluted from beads with elution buffer (1% SDS and 0.1 mol/L $NaHCO_3$), crosslinking was reversed, and DNA was extracted. The resulting chromatin preparations were analyzed by PCR using primers spanning AREs of the PSA promoter as described previously (24). Isotype matched IgG was used as control.

Preparation of nuclear and cytosolic extracts

C4 2B parental and C4 2B MR cells were cultured in media containing charcoal stripped FBS (CS FBS) for 4 days. Cells were harvested, washed with PBS twice, and resuspended in a low salt buffer [10 mmol/L HEPES KOH (pH 7.9), 1.5 mmol/L $MgCl_2$, 10 mmol/L KCl, and 0.1% NP40] and incubated on ice for 30 minutes. Nuclei were precipitated by centrifugation at 3,000 × *g* at 4°C for 10 minutes. The supernatants were collected as the cytosolic fraction. After washing once with the low salt buffer, the nuclei were lysed in a high salt lysis buffer [50 mmol/L Tris HCl (pH 8), 150 mmol/L NaCl, 1% Triton X 100] with vigorous shaking at 4°C for 30 minutes. The nuclear lysates were precleared by centrifugation at 10,000 rpm at 4°C for 15 minutes. Protein concentration was determined using the Coomassie Plus Protein Assay Kit (Pierce).

Western blot analysis

Cellular protein extracts were resolved on SDS PAGE and proteins were transferred to nitrocellulose membranes. After blocking for 1 hour at room temperature in 5% milk in PBS/0.1% Tween 20, membranes were incubated overnight at 4°C with the indicated primary antibodies [AR441 (SC 7305, Santa Cruz Biotechnology); AR V7 (AG10008; Precision antibody); PSA (SC 7316, Santa Cruz Biotechnology); Tubulin (T5168, Sigma Aldrich)]. Tubulin was used as loading control. Following secondary antibody incubation, immunoreactive proteins were visualized with an enhanced chemiluminescence detection system (Millipore).

Cell growth assay

C4 2 neo, C4 2 AR V7, CWR22Rv1, or PZ HPV 7 cells were seeded on 12 well plates at a density of 1×10^5 cells/well in RPMI 1640 media containing 10% FBS and treated with 0.5 μmol/L niclosamide for 48 hours. Total cell numbers were counted and the cell survival rate (%) was calculated. Cell survival rate (%) = (Treatment group cell number/Control group cell number) × 100%. CWR22Rv1 cells were transiently transfected with AR exon 7 siRNA or AR V7 siRNA in CS FBS condition, cell numbers were counted on different days. C4 2B or C4 2B MR cells were seeded on 12 well plates at a density of 0.5×10^5 cells/well in RPMI 1640 media containing 10% FBS and treated with 20 μmol/L enzalutamide. Total cell numbers were counted after 3 and 5 days. CWR22Rv1 cells or C4 2B MR cells were seeded on 12 well plates at a density of 0.5×10^5 cells/well in RPMI 1640 media containing 10% FBS and cotreated with 0.25 μmol/L niclosamide and 20 μmol/L enzalutamide in media containing FBS. Total cell numbers were counted after 3 and 5 days.

Clonogenic assay

C4 2 neo, C4 2 AR V7, CWR22Rv1, or C4 2B MR cells were treated with DMSO, 0.5 or 1.0 μmol/L niclosamide in media containing 10% complete FBS. CWR22Rv1 cells or C4 2B MR cells were treated with 0.25 μmol/L niclosamide with or without 20 μmol/L enzalutamide. Cells were plated at equal density (1,500 cells/dish) in 100 mm dishes for 14 days; the medium was changed every 7 days. The colonies were rinsed with PBS before staining with 0.5% crystal violet/4% formaldehyde for 30 minutes and the numbers of colonies were counted.

Cell death ELISA

C4 2 neo, C4 2 AR V7, CWR22Rv1, or PZ HPV 7 cells were seeded on 12 well plates (1×10^5 cells/well) in RPMI 1640 media containing 10% FBS and treated with DMSO or 0.5 μmol/L niclosamide for 48 hours. Mono and oligonucleosomes in the cytoplasmic fraction were measured by the Cell Death Detection ELISA Kit (Roche, Catalog No. 11544675001) according to the manufacturer's instructions. Briefly, floating and attached cells were collected and homogenized in 400 μL of incubation buffer. The wells were coated with antihistone antibodies and incubated with the lysates, horseradish peroxidase conjugated anti DNA antibodies, and the substrate, in that sequence. Absorbance was measured at 405 nm.

Real time quantitative reverse transcription PCR

Total RNAs were extracted using TRizol reagent (Invitrogen). cDNAs were prepared after digestion with RNase free RQ1 DNase (Promega). The cDNAs were subjected to real time reverse transcription PCR (RT PCR) using Sso Fast EvaGreen Supermix (Bio Rad) according to the manufacturer's instructions and as described previously (25). Each reaction was normalized by co amplification of actin. Triplicates of samples were run on default settings of Bio Rad CFX 96 real time cycler. Primers used for real time PCR were: AR full length: 5′ AAG CCA GAG CTG TGC AGA TGA, 3′ TGT CCT GCA GCC ACT GGT TC; AR V1: 5′ AAC AGA AGT ACC TGT GCG CC, 3′ TGA GAC TCC AAA CAC CCT CA; AR V7: 5′ AAC AGA AGT ACC TGT GCG CC, 3′ TCA GGG TCT GGT CAT TTT GA; AR V1/2/2b: 5′ TGG ATG GAT AGC TAC TCC GG, 3′ GTT CAT TCT GAA AAA TCC TTC AGC; AR1/2/3/2b: 5′ AAC AGA AGT ACC TGT GCG CC, 3′ TTC TGT CAG TCC CAT TGG TG; Actin: 5′ AGA ACT GGC CCT TCT TGG AGG, 3′ GTT TTT ATG TTC CTC TAT GGG.

Measurement of PSA

PSA levels were measured in the culture supernatants using PSA ELISA Kit (United Biotech, Inc.) according to the manufacturer's instructions.

Published OnlineFirst April 16, 2014; DOI: 10.1158/1078-0432.CCR-13-3296

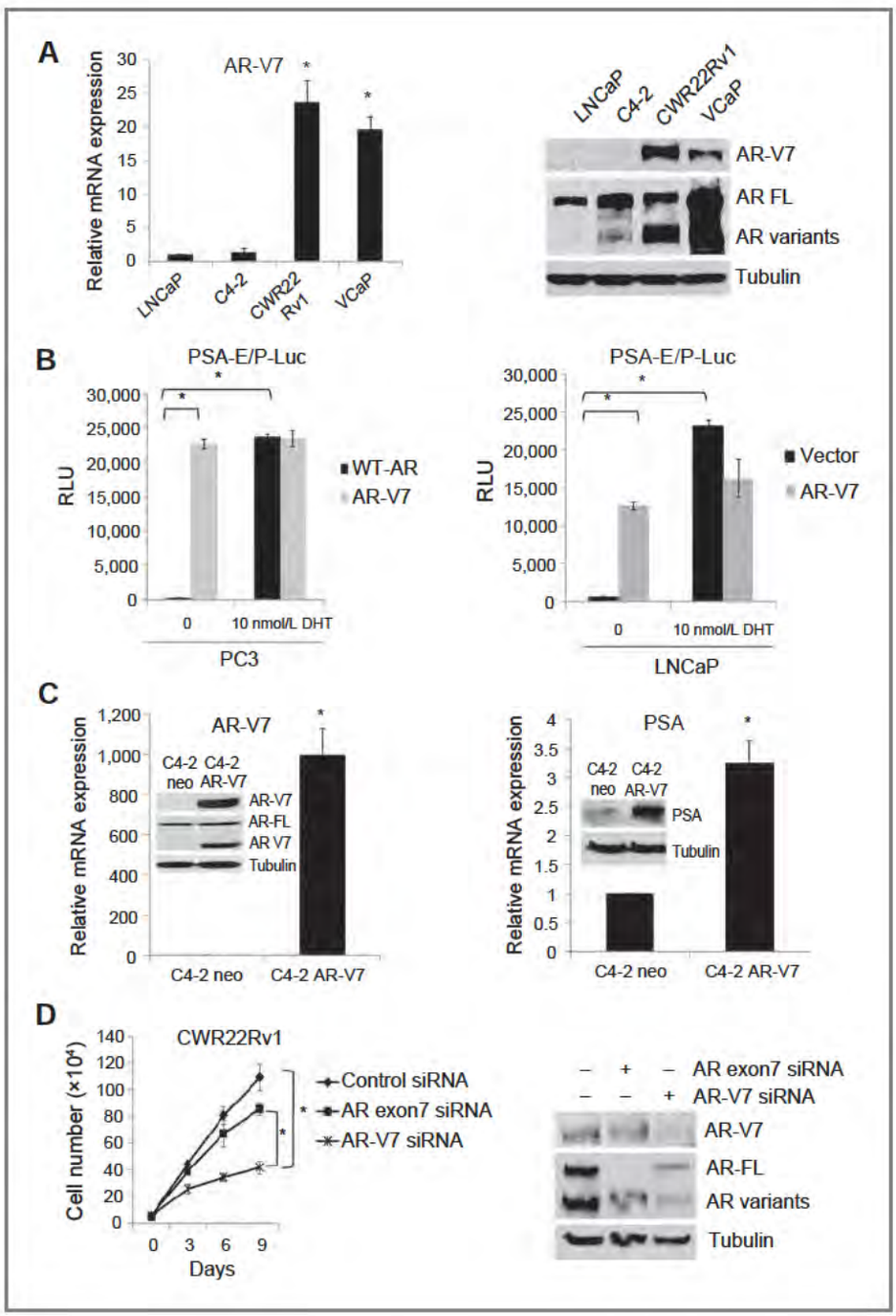

Figure 1. AR V7 is constitutively active in prostate cancer cells. A, LNCaP, C4 2, CWR22Rv1, and VCaP cells were cultured in CS FBS condition for 3 days. AR V7 mRNA levels were analyzed by qRT PCR, whole cell protein was extracted and immunoblotted with indicated antibodies. Results are presented as means ± SD of 3 experiments performed in duplicate. B, PC 3 cells and LNCaP cells were cultured in CS FBS condition and transiently transfected with WT AR or AR V7 plasmid for 3 days followed by treatment with 10 nmol/L DHT for another 24 hours and whole cell lysates were subjected to luciferase assay. C, C4 2 neo and C4 2 AR V7 stable clone were cultured in CS FBS condition, AR V7 and PSA mRNA level was determined by qRT PCR, the AR V7 and PSA protein expression was detected by Western blot analysis (insert). D, CWR22Rv1 cells were transiently transfected with control siRNA, AR exon 7 siRNA, or AR V7 siRNA in CS FBS condition, cell numbers were counted on different days and the knock down efficiency was examined by Western blot analysis. Results are presented as means ± SD of 3 experiments performed in duplicate. *, $P < 0.05$

In vivo tumorigenesis assay

CWR22Rv1 cells (3 million) were mixed with matrigel (1:1) and injected subcutaneously into the flanks of 6 to 7 week male SCID mice. Tumor bearing mice (tumor volume around 50 100 mm^3) were randomized into 4 groups (with 10 tumors in each group) and treated as follows: (i) vehicle control (5% Tween 80 and 5% ethanol in PBS, i.p.; ref. 2), (ii) enzalutamide (25 mg/kg, p.o.; ref. 3), (iii) niclosamide (25 mg/kg, i.p.; ref. 4), and (iv) enzalutamide (25 mg/kg, p.o.) + niclosamide (25 mg/kg, i.p.). Tumors were measured using calipers twice a week and tumor volumes were calculated using length × $width^2/2$. Tumor tissues were harvested after 3 weeks of treatment.

Immunohistochemistry

Tumors were fixed by formalin and paraffin embedded tissue blocks were dewaxed, rehydrated, and blocked for

Published OnlineFirst April 16, 2014; DOI: 10.1158/1078-0432.CCR-13-3296

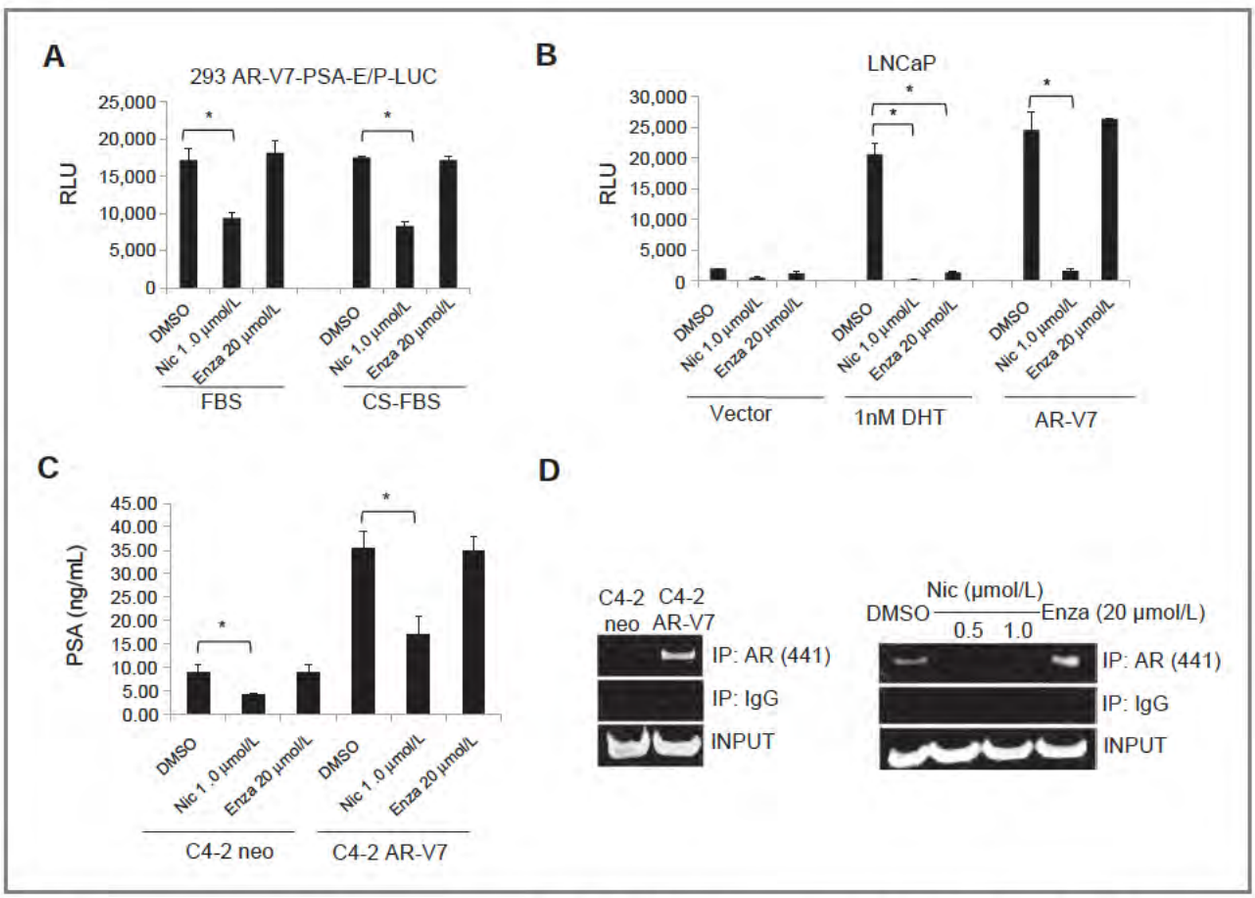

Figure 2. Niclosamide inhibited AR V7 transcription activity. A, 293 AR V7 PSA luciferase promoter stable clone was treated with 1.0 μmol/L niclosamide or 20 μmol/L enzalutamide overnight in media containing 10% FBS or 10% CS FBS and whole cell lysates were subjected to luciferase assay. B, LNCaP cells were cotransfected with PSA luciferase promoter and AR V7 in CS FBS condition for 24 hours, followed by treatment with 1.0 μmol/L niclosamide or 20 μmol/L enzalutamide overnight and whole cell lysates were subjected to luciferase assay. C, C4 2 neo and C4 2 AR V7 cells were cultured in CS FBS condition for 3 days, followed by treatment with 1.0 μmol/L niclosamide or 20 μmol/L enzalutamide overnight and the supernatants were subjected to PSA ELISA. D, C4 2 neo and C4 2 AR V7 cells were cultured in CS FBS condition for 3 days, whole cell lysates were subjected to ChIP assay (left). C4 2 AR V7 cells were treated with 0.5 μmol/L, 1.0 μmol/L niclosamide, or 20 μmol/L enzalutamide overnight and whole cell lysates were subjected to ChIP assay (right). Results are presented as means ± SD of 3 experiments performed in duplicate. *, $P < 0.05$. Enza, enzalutamide; Nic,niclosamide; RLU, relative luciferase unit.

endogenous peroxidase activity. Antigen retrieving was performed in sodium citrate buffer (0.01 mol/L, pH 6.0) in a microwave oven at 1,000 W for 3 minutes and then at 100 W for 20 minutes. Nonspecific antibody binding was blocked by incubating with 10% FBS in PBS for 30 minutes at room temperature. Slides were then incubated with anti Ki67 (at 1:500; NeoMarker) at room tempera ture for 30 minutes. Slides were then washed and incu bated with biotin conjugated secondary antibodies for 30 minutes, followed by incubation with avidin DH bioti nylated horseradish peroxidase complex for 30 minutes (Vectastain ABC Elite Kit; Vector Laboratories). The sec tions were developed with the Diaminobenzidine Sub strate Kit (Vector Laboratories) and counterstained with hematoxylin. Nuclear staining cells was scored and counted in 5 different vision areas. Images were taken with an Olympus BX51 microscope equipped with DP72 camera.

Statistical analysis

All data are presented as means ± standard deviation (SD) of the mean. Statistical analyses were performed with Microsoft Excel analysis tools. Differences between individ ual groups were analyzed by one way analysis of variance (ANOVA) followed by the Scheffé procedure for compar ison of means. $P < 0.05$ was considered statistically significant.

Results

AR V7 is constitutively activated in prostate cancer cells

The deletion of LBD results in constitutive activation of the AR (26, 27). AR V7, a C terminally truncated AR splice variant, has been linked to CRPC and enzalutamide resis tance (5, 7, 18). We detected AR V7 mRNA in different prostate cancer cell lines, as shown in Fig. 1A (left). CWR22Rv1 and VCaP cells expressed significantly higher

Published OnlineFirst April 16, 2014; DOI: 10.1158/1078-0432.CCR-13-3296

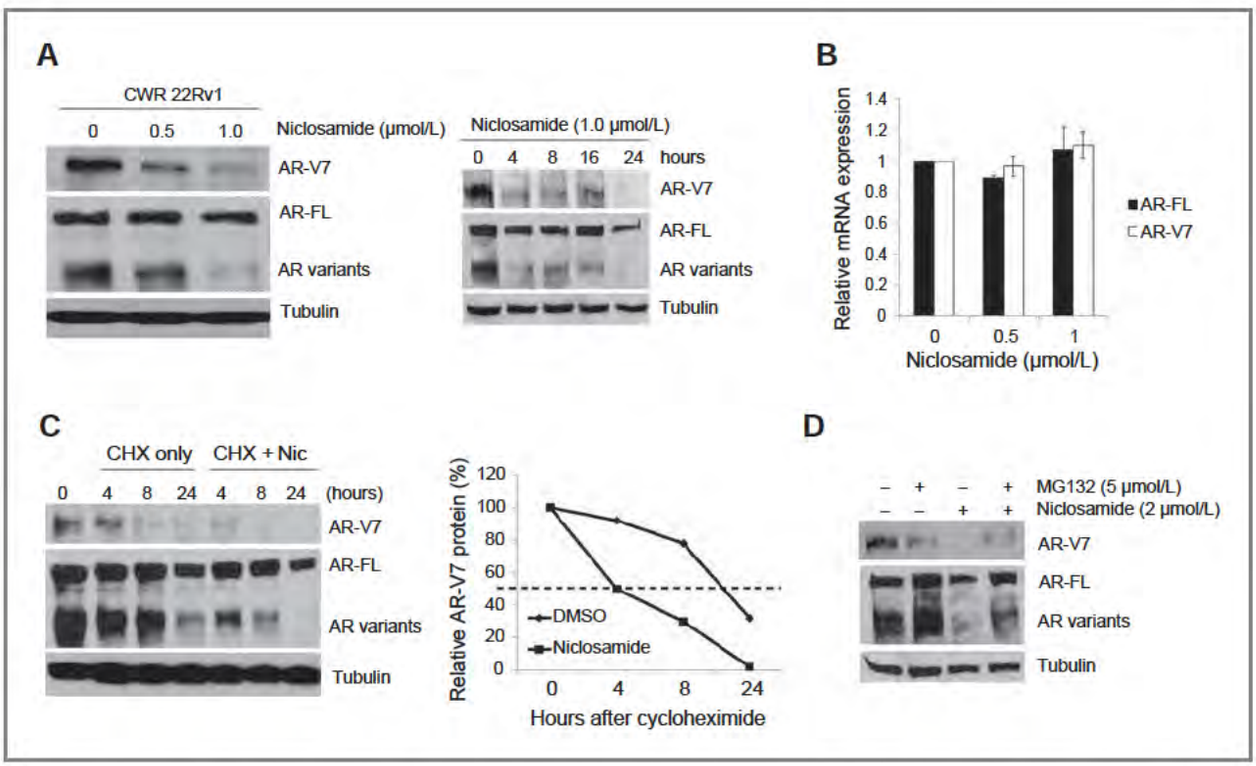

Figure 3. Niclosamide inhibited AR V7 protein expression through enhancing protein degradation. A, CWR22Rv1 cells were treated with 0, 0.5, or 1.0 μmol/L niclosamide in RPMI 1640 media containing 10% FBS overnight and the whole cell lysates were immunoblotted with the indicated antibodies (left). CWR22Rv1 cells were treated with 1.0 μmol/L niclosamide in RPMI 1640 media containing 10% FBS, whole cell lysates were extracted at different time points and immunoblotted with the indicated antibodies (right). B, CWR22Rv1 cells were treated with 0, 0.5, or 1.0 μmol/L niclosamide in RPMI 1640 media containing 10% FBS overnight, total RNAs were extracted and AR or AR V7 mRNA levels were analyzed by qRT PCR. C, 50 μg/mL CHX was added with or without 2 μmol/L niclosamide (Nic) at time 0 hour. At specified time points, cells were harvested, and the levels of AR V7 protein were measured by Western blot analysis using antibodies specific against AR V7. Plotted on semilog scale relative to respective time 0 AR V7 value as 100%, dashed line indicates 50% half life. D, effect of MG132 on niclosamide induced AR protein degradation. MG132 (5 μmol/L) was added to CWR22Rv1 cells together with CHX (50 μg/mL) in the presence or absence of 2 μmol/L niclosamide. The cell lysates were prepared at 8 hours. AR V7 protein levels were determined by Western blot analysis using antibodies specifically against AR V7 and tubulin as a control. Nic, niclosamide.

AR V7 than LNCaP and C4 2 cells. The results were also confirmed by Western blot analysis, as shown in Fig. 1A (right), in which CWR22Rv1 and VCaP cells expressed higher protein expression levels of AR variants, including AR V7, than LNCaP and C4 2 cells. To examine the tran scriptional activity of AR V7 in PC 3 and LNCaP cells, we transiently transfected WT AR, AR V7, or pcDNA3.1 along with PGL3 PSA 6.0 luciferase reporter plasmids. As shown in Fig. 1B, expression of AR V7 was able to activate PSA promoter in both PC 3 and LNCaP cells in the absence of DHT; whereas expression of WT AR could not activate PSA promoter in PC 3 cells in the absence of DHT, consistent with reports that AR V7 is constitutively activated in the absence of ligand (6). To further understand the function of AR V7 in prostate cancer cells, we stably transfected AR V7 into C4 2 cells, as shown in Fig. 1C(left). C4 2 AR V7 stable clone expressed significantly higher AR V7 mRNA and protein level compared with C4 2 neo cells. Furthermore, AR V7 functionally increased PSA mRNA and protein expression in C4 2 cells cultured in media containing androgen deprived charcoal stripped FBS (Fig. 1C, right). To examine the effect of AR V7 on cell growth in prostate cancer cells, CWR22Rv1 cells were transiently transfected with AR exon 7 siRNA (which targets full length AR, but not AR variants) or AR V7 siRNA in CS FBS condition, cell numbers were determined on different days. As shown in Fig. 1D(left), knocked down full length AR had moderate growth inhibition on CWR22Rv1 cells, whereas knocked down AR V7 significantly inhibited cell growth, consistent with previous reports that AR V7 but not full length AR plays dominant role in growth of CWR22Rv1 cells (19, 22). The knocked down efficiency was confirmed by Western blot analysis (Fig. 1D, right). Collectively, these data sug gested that AR V7 is constitutively activated in prostate cancer cells and targeting AR V7 could inhibit cell growth.

Identification of niclosamide as a novel inhibitor of AR V7

To identify potential inhibitors of AR V7, we generated an AR V7 expression cell system and used it to screen the Prestwick Chemical Library, which contains about 1,120 small molecules and approved drugs (FDA, EMEA, and other agencies). The drug screening was conducted using luciferase activity assay to determine the activity of AR V7

Published OnlineFirst April 16, 2014; DOI: 10.1158/1078-0432.CCR-13-3296

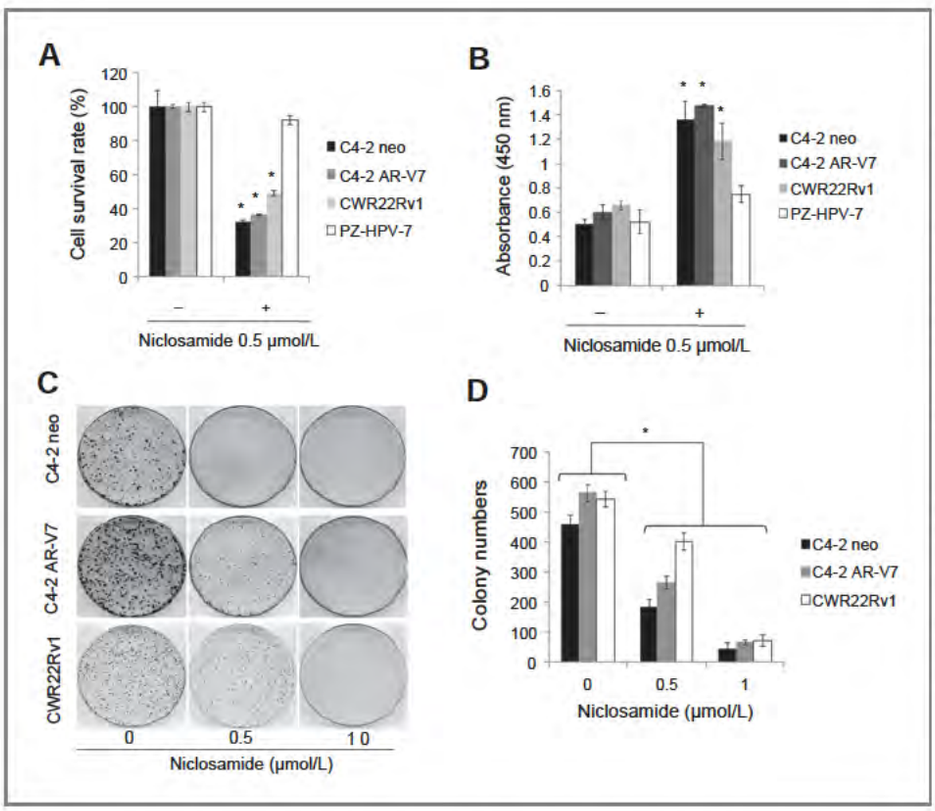

Figure 4. Niclosamide inhibited prostate cancer cell growth and induced cell apoptosis. A, C4 2 neo, C4 2 AR V7, CWR22Rv1, and PZ HPV 7 cells were treated with 0.5 μmol/L niclosamide in media containing FBS, cell numbers were counted, and cell survival rate was calculated after 48 hours. B, C4 2 neo, C4 2 AR V7, CWR22Rv1, and PZ HPV 7 cells were treated with 0.5 μmol/L niclosamide in media containing FBS, and apoptosis was analyzed by cell death ELISA after 48 hours. C, C4 2 neo, C4 2 AR V7, or CWR22Rv1 cells were treated with 0, 0.5, or 1.0 μmol/L niclosamide and clonogenic assays were performed. D, colonies were counted and results are presented as means ± SD of 2 experiments performed in duplicate. Niclosamide inhibited colony formation in a dose dependent manner. *, $P < 0.05$

after treatment with the compounds in the library. To avoid interference from expression of the full length AR, we used the HEK293 cell line that lacks the AR. The HEK293 cells were stably cotransfected with AR V7 plasmid and PGL3 PSA6.0 luciferase reporter plasmid, and stable clones were selected using G418. To perform compound screening, HEK293 AR V7 PSA luc stable clones were seeded in 96 well plates following treatment with each compound in the library for 24 hours and luciferase activities were measured. Niclosamide, an FDA approved antihelminthic drug, was identified as being able to inhibit AR V7 mediated lucifer ase activity. Niclosamide has been used to treat human tapeworm infections for around 50 years.

Niclosamide inhibited AR V7 transcriptional activity and reduced recruitment of AR V7 to PSA promoter

To further examine whether niclosamide inhibits AR V7 transcriptional activity, we first validated in HEK293 AR V7 PSA E/P LUC cell systems. As shown in Fig. 2A, niclosamide significantly inhibited AR V7 transcriptional activity where as enzalutamide had no effect. To examine whether the effects could be reproduced in a prostate cancer cell system, LNCaP cells were transiently transfected with AR V7, fol lowed by treatment with niclosamide or enzalutamide with or without DHT overnight. As shown in Fig. 2B, both niclosamide and enzalutamide dramatically inhibited DHT induced AR transcriptional activity, but only niclosa mide inhibited AR V7 transcriptional activity. To further determine whether the inhibition of luciferase activity could be translated to inhibition of protein expression, PSA ELISA was performed, as shown in Fig. 2C. C4 2 AR V7 cells were cultured in CS FBS condition and shown to express higher PSA levels than C4 2 neo cells. Niclosamide signif icantly inhibited PSA levels in C4 2 AR V7 cells. To further dissect the mechanism of AR V7 inhibition by niclosamide, a ChIP assay was performed. C4 2 neo and C4 2 AR V7 cells were cultured in CS FBS condition for 3 days and whole cell lysates were subjected to ChIP assay, as shown in Fig. 2D(left), AR V7 was recruited to the PSA promoter. Next, we cultured C4 2 AR V7 cells in CS FBS condition followed by treatment with niclosamide (0.5 and 1 μmol/L) or 20 μmol/L enzalutamide overnight and whole cell lysates was subjected to ChIP assay. As shown in Fig. 2D(right), niclosamide significantly reduced recruitment of AR V7 to PSA promoter whereas enzalutamide had no effect. Collec tively, these results demonstrate that niclosamide but not enzalutamide was able to inhibit AR V7 transactivation.

Niclosamide inhibits AR V7 protein expression through enhancing protein degradation

To determine whether niclosamide inhibits AR V7 expression, CWR22Rv1 cells, which express endogenous AR V7, were treated with different concentrations of niclo samide. As shown in Fig. 3A(left), niclosamide inhibited endogenous AR V7 protein in a dose dependent manner. A total of 0.5 μmol/L niclosamide significantly inhibited AR V7 expression but had little effect on full length AR (AR FL) expression, which suggested that niclosamide is more

Published OnlineFirst April 16, 2014; DOI: 10.1158/1078-0432.CCR-13-3296

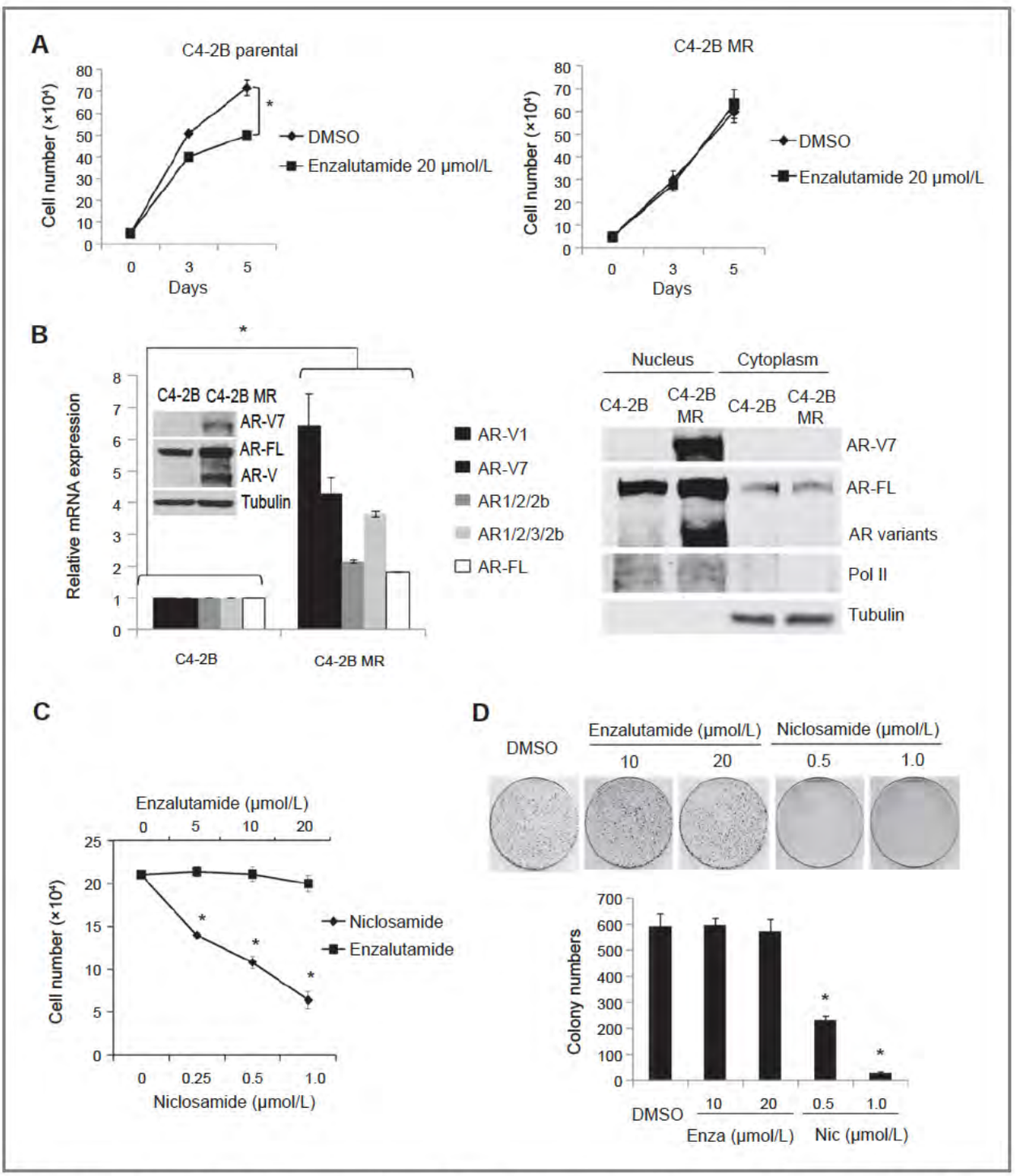

Figure 5. C4 2B cells chronically treated with enzalutamide express AR variants and are sensitive to Niclosamide. A, C4 2B parental or C4 2B MR cells were treated with 20 μmol/L enzalutamide in RPMI 1640 media containing 10% FBS and total cell numbers were counted at different time points as indicated. B, C4 2B parental cells and C4 2B MR cells were cultured in RPMI 1640 media containing 10% FBS for 3 days, total RNAs were extracted and AR V1, AR V7, AR1/2/2b, AR1/2/3/2b, or AR full length mRNA levels were analyzed by qRT PCR. AR V7 protein level was examined by Western blot analysis (inside).C4 2B parental cells and C4 2B MR cells were cultured in media containing 10% CS FBS for 3 days, the cells were harvested for preparation of cytosolic and nuclear fractions and analyzed by Western blotting using antibodies against AR V7, AR, RNA polymerase II, or Tubulin (right). The expression of RNA polymerase II and tubulin were used as markers for the integrity of the nuclear and cytosolic fractions, respectively. C, C4 2B MR cells were cultured in media containing 10% FBS and treated with different concentrations of enzalutamide or niclosamide as indicated and total cell numbers were counted after 48 hours. D, C4 2B MR cells were treated with DMSO, 10 or 20 μmol/L enzalutamide, 0.5 or 1.0 μmol/L niclosamide and clonogenic assays were performed. Colonies were counted and results are presented as means ± SD of 2 experiments performed in duplicate. *, $P < 0.05$. Enza, enzalutamide, Nic, niclosamide.

Published OnlineFirst April 16, 2014; DOI: 10.1158/1078-0432.CCR-13-3296

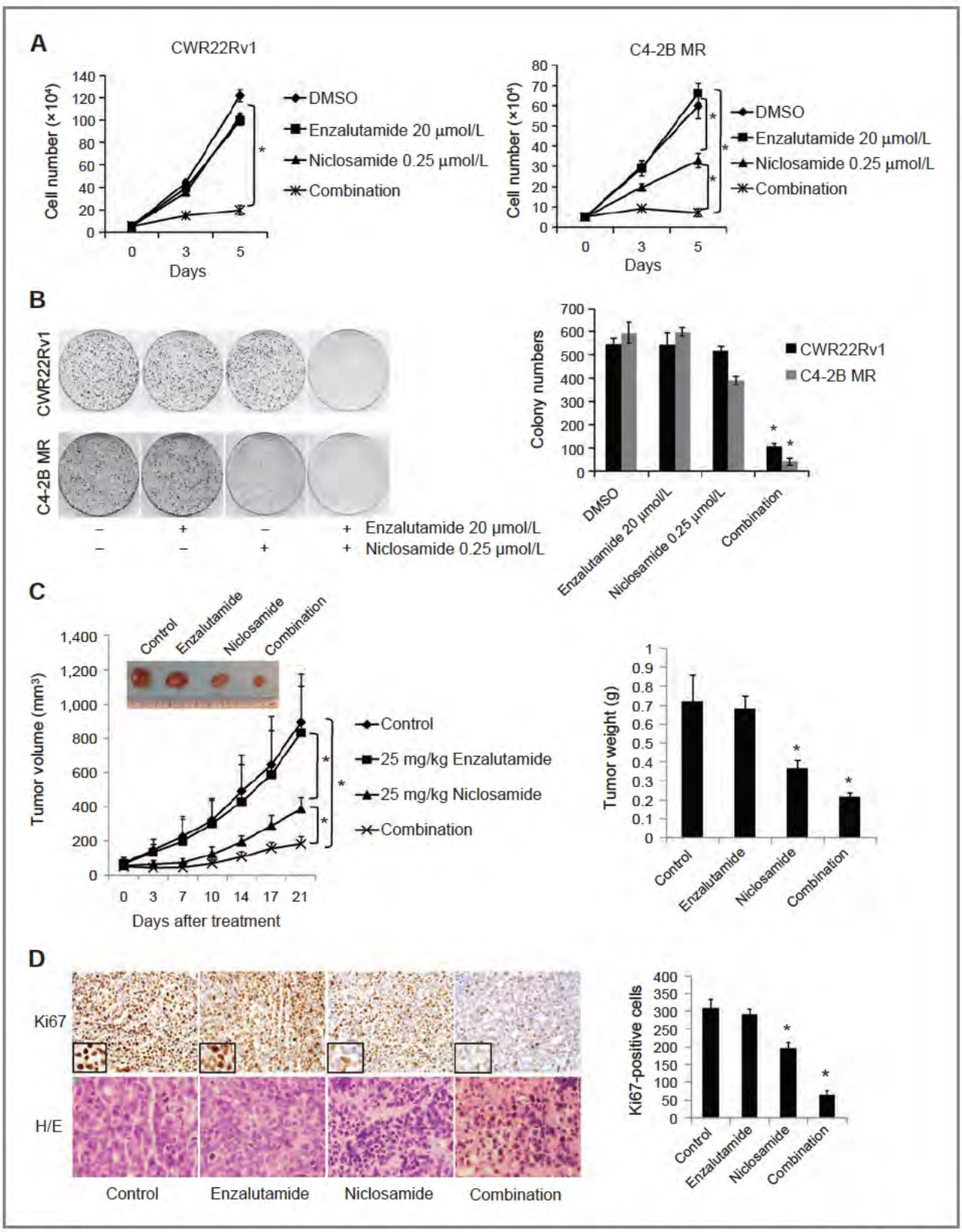

Figure 6. Niclosamide enhances enzalutamide effects both *in vitro* and *in vivo*. A, CWR22Rv1 cells or C4 2B MR cells were treated with 0.25 μmol/L niclosamide with or without 20 μmol/L enzalutamide in media containing FBS and cell numbers were counted after 3 and 5 days. Results are presented as means ± SD of 3 experiments performed in duplicate. (*Continued on the following page.*)

Published OnlineFirst April 16, 2014; DOI: 10.1158/1078-0432.CCR-13-3296

potent in inhibition of the truncated AR. Niclosamide inhibited AR V7 protein expression starting at 4 hours treatment (Fig. 3A, right). To further clarify how niclosamide decreases AR V7 protein expression, we first determined the effects of niclosamide on AR V7 expression at the transcriptional level. As shown in Fig. 3B, niclosamide did not affect AR V7 or full length AR mRNA level, suggesting that niclosamide did not affect AR V7 expression at the transcriptional level. Next, we examined the effect of niclosamide on AR V7 protein degradation after new protein synthesis was blocked by cycloheximide (CHX). The protein synthesis inhibitor CHX (50 μg/mL) was added with or without 2 μmol/L niclosamide at time 0 hour. At specified time points, cells were harvested, and the levels of AR V7 protein were measured by Western blot analysis using antibodies specific against AR V7. As shown in Fig. 3C, niclosamide increased AR V7 protein degradation compared with the untreated control cells. To examine whether niclosamide induced AR V7 protein degradation via the ubiquitin proteasome system, the 26S proteasome inhibitor MG132 (5 μmol/L) was added to the cells treated with niclosamide. MG132 was able to reduce the niclosamide mediated inhibition of AR V7 protein expression (Fig. 3D), suggesting that niclosamide induced AR V7 degradation via a proteasome dependent pathway.

Niclosamide inhibited prostate cancer cell growth and induced cell apoptosis

To examine whether niclosamide affects prostate cancer cell growth, C4 2 neo, C4 2 AR V7, CWR22Rv1, and PZ HPV 7 cells were treated with DMSO or 0.5 μmol/L niclosamide for 48 hours and cell numbers were determined. As shown in Fig. 4A, 0.5 μmol/L niclosamide significantly inhibited cell growth in prostate cancer cells, with little effect on PZ HPV 7 normal prostate epithelial cells. To further examine the anticancer effects of niclosamide, cell death ELISA was performed. As shown in Fig. 4B, 0.5 μmol/L niclosamide significantly induced cell apoptosis in prostate cancer cells, but had little effect on PZ HPV 7 cells. We also examined the effect of niclosamide on clonogenic ability. As shown in Fig. 4C and D, niclosamide significantly inhibited clonogenic ability of prostate cancer cells in a dose dependent manner. Collectively, these results revealed that niclosamide inhibited prostate cancer cell growth and induced cell apoptosis with minimal effects on normal prostate epithelial cells.

C4 2B cells chronically treated with enzalutamide express AR variants and are sensitive to niclosamide

We generated an enzalutamide resistant prostate cancer cell line by continuous culture of C4 2B cells in media containing enzalutamide. As shown in Fig. 5A, after 12 months of being cultured in media containing enzalutamide, C4 2B MR (C4 2B enzalutamide resistant) cells exhibited more resistance to enzalutamide treatment than C4 2B parental cells. Next, we examined the expression levels of AR variants in C4 2B parental and C4 2B MR cells. As shown in Fig. 5B(left), C4 2B MR cells express higher levels of AR variant mRNAs and protein than C4 2B parental cells, including AR V1, AR V7, AR1/2/2b, and AR1/2/3/2b. Furthermore, AR V7 was constitutively expressed in the nucleus but not in cytoplasm (Fig. 5B, right). Because niclosamide can inhibit AR V7 expression, we examined whether niclosamide inhibits C4 2B MR cell growth. As shown in Fig. 5C, C4 2B MR cells were resistant to enzalutamide but significantly inhibited by niclosamide in a dose dependent manner. The results were also confirmed by clonogenic assay. As shown in Fig. 5D, niclosamide but not enzalutamide significantly inhibited colony formation in C4 2B MR cells.

Niclosamide enhances enzalutamide treatment

To examine whether niclosamide could enhance enzalutamide therapy in prostate cancer cells, CWR22Rv1 cells were treated with niclosamide in combination with or without enzalutamide for 48 hours. As shown in Fig. 6A (left), single agent treatments with low dose of niclosamide or enzalutamide had moderate effects on CWR22Rv1 cells whereas combination treatments significantly inhibited cell growth in a time dependent manner. We also tested the effects in enzalutamide resistant cell line (C4 2B MR). Combination therapy of niclosamide with enzalutamide significantly inhibited C4 2B MR cell growth compared with single agent treatments (Fig. 6A, right). The synergistic effects were also confirmed by clonogenic assay (Fig. 6B).

To test whether niclosamide overcomes enzalutamide resistance of prostate cancer *in vivo*, xenografts generated from CWR22Rv1 cells were treated with vehicle, enzalutamide, niclosamide, or their combination for 3 weeks as described in Materials and Methods. As shown in Fig. 6C, CWR22Rv1 cells were resistant to enzalutamide treatment with tumor volumes comparable to those in the vehicle treated control group. Niclosamide alone decreased the tumor volume whereas combination of niclosamide and enzalutamide synergistically decreased CWR22Rv1 tumors, indicating that niclosamide could overcome enzalutamide resistance and restore sensitivity of CWR22Rv1 xenografts to enzalutamide *in vivo*. Representative tumor samples were analyzed by IHC for Ki67. As shown in Fig. 6D, niclosamide inhibited Ki67 expression whereas combination treatment further decreased Ki67 expression. In summary, these results suggested that niclosamide can improve enzalutamide treatment and overcome enzalutamide resistance.

(*Continued.*) B, CWR22Rv1 cells or C4 2B MR cells were treated with 0.25 μmol/L niclosamide with or without 20 μmol/L enzalutamide in media containing FBS and clonogenic assays were performed. Colony numbers were counted and results are presented as means ± SD of 2 experiments performed in duplicate. C, mice bearing CWR22Rv1 xenografts were treated with vehicle control, enzalutamide, niclosamide, or their combination for 3 weeks, tumor volumes were measured twice every week and the tumors were collected and weighed. D, Ki67 was analyzed in tumor tissues by IHC staining and quantified as described in Materials and Methods. *, $P < 0.05$.

Published OnlineFirst April 16, 2014; DOI: 10.1158/1078-0432.CCR-13-3296

Discussion

Development of resistance to enzalutamide is eventually inevitable with the development of several potential pathways of resistance (4, 28). Recent studies have linked AR alternative splicing, particularly AR V7, to the development of enzalutamide resistance (18, 20, 21, 29). Targeting of AR signaling, especially AR variants, would improve current antiandrogen therapies for advanced prostate cancer. In this study, we identified niclosamide as a potent AR V7 inhibitor in prostate cancer cells. We found that niclosamide significantly inhibits AR V7 protein expression and AR V7 transcription activity and reduces AR V7 recruitment to the PSA promoter. Niclosamide inhibits prostate cancer cell growth *in vitro* and tumor growth *in vivo*. Furthermore, niclosamide significantly enhanced enzalutamide therapy in prostate cancer cells, suggesting that niclosamide can be used to treat, either alone or in combination with current antiandrogen therapies, patients with advanced prostate cancer, especially those resistant to enzalutamide.

The potential molecular mechanisms underlying the development of resistance to enzalutamide are under intensive investigation. A recent report showed that increased expression of glucocorticoid receptor (GR) can bypass AR signaling and induces resistance to enzalutamide (30). A novel F876L mutation in AR was also identified as a potent driver of resistance to enzalutamide, and AR variants such as AR V7 induced by NF κB/p52 can drive prostate cancer cells to develop enzalutamide resistance (18 21). We confirmed increased expression of AR V7 in both CWR22Rv1 and VCaP cells but not in LNCaP and C4 2 cells. We demonstrated that overexpressing AR V7 in C4 2 cells significantly enhanced the expression level of PSA. In addition, C4 2B cells chronically treated with enzalutamide exhibited significantly higher levels of full length AR and AR variants, suggesting that persistent activation of signaling by AR variants is important during the development of enzalutamide resistance. Therefore, targeting both full length AR and AR variants may prove to be an effective strategy to treat advanced prostate cancer. Several compounds have been recently found to be able to affect AR variants. The analogs of EPI 001 were developed to treat CRPC, including those driven by AR variants expression (31, 32). Methylselenol prodrug methylseleninic acid (MSA) can down regulate both full length AR and AR variants expression (33). A protein kinase C (PKC) inhibitor Ro31 8220 was also shown to be able to down regulate both full length AR and AR variants (34). In this study, we identified niclosamide as a novel inhibitor of AR V7 and found that niclosamide reversed enzalutamide resistance in prostate cancer cells through inhibition of AR variants. Niclosamide significantly downregulates AR V7 protein expression in a dose and time dependent manner by protein degradation through a proteasome dependent pathway. Niclosamide also inhibits AR V7 transcriptional activity and reduces the recruitment of AR V7 to the PSA promoter. Enzalutamide effectively blocks the recruitment of AR but not of AR V7 to the PSA promoter, indicating that enzalutamide cannot inhibit AR V7 mediated transcriptional activity. A combination of niclosamide to target AR V7 and enzalutamide to target AR could provide an ideal strategy to treat advanced prostate cancer and prevent the development of resistance to enzalutamide driven by AR variants. This combination strategy was validated in this study in an animal model to show that niclosamide inhibits CWR22Rv1 tumor growth and enhances enzalutamide therapy. These results may warrant a combination treatment strategy using niclosamide to improve the efficacy of enzalutamide therapy.

Niclosamide is a FDA approved anthelminthic drug to treat tapeworm infection in humans for about 50 years, and has rich repository of pharmacokinetic data accumulated *in vivo*. It has low toxicity in mammals, with the oral median lethal dose calculated to be above 5,000 mg/kg (35). A single oral dose of 5 mg/kg niclosamide in rats generates a maximum plasma concentration of 1.08 μmol/mL (36). Niclosamide has been recently demonstrated to exhibit antitumor activity in several cancers such as colorectal cancer (37 39), ovarian cancer (40), acute myeloid leukemia (AML; ref. 41), breast cancer, and prostate cancer (20). Niclosamide has been shown to promote Fzd1 endocytosis, downregulate Dvl2 protein, and inhibit Wnt3A stimulated β catenin stabilization and downstream β catenin signaling (38). Niclosamide can also block TNFα induced IκBα phosphorylation, translocation of p65, and the expression of NF κB regulated genes (41). Niclosamide is a selective inhibitor of Stat3 and can overcome acquired resistance to erlotinib through suppression of Stat3 in non small cell lung cancer and head neck cancer (42, 43). Niclosamide can also induce autophagy and inhibit mTROC1 (44 46). Niclosamide treatment in colon cancer cells inhibited S100A4 induced metastasis *in vivo* (37). In this study we showed that niclosamide exhibits anti androgenic activity by inhibition of AR transcriptional activity and AR V7 expression.

In summary, our study identified niclosamide, as a novel AR V7 inhibitor that inhibits prostate cancer cell growth and induces apoptosis. Niclosamide can inhibit enzalutamide resistant prostate cancer cell growth and tumor growth. Furthermore, niclosamide exhibits a synergistic effect with enzalutamide and resensitizes treatment resistant prostate cancer cells to enzalutamide therapy. Our studies suggest that niclosamide has great potential as an effective and orally bioavailable drug candidate either as monotherapy or in combination with current antiandrogen therapies for the treatment of advanced metastatic prostate cancer.

Disclosure of Potential Conflicts of Interest

C. Liu, W. Lou, and A.C. Gao are co-inventors of a patent application covering the use of niclosamide. C.P. Evans is a consultant/advisory board member for and reports receiving speakers bureau honoraria from Astellas/Medivation and Janssen; a commercial research grant from Astellas/Medivation; and has ownership interest (including patents) in

Astellas/Medivation and Oncogenix. No potential conflicts of interest were disclosed by the other authors.

Authors' Contributions

Conception and design: C. Liu, W. Lou, A.C. Gao
Development of methodology: C. Liu, W. Lou, A.C. Gao
Acquisition of data (provided animals, acquired and managed patients, provided facilities, etc.): C. Liu, W. Lou, Y. Zhu
Analysis and interpretation of data (e.g., statistical analysis, biostatistics, computational analysis): C. Liu, W. Lou, C.P. Evans, A.C. Gao
Writing, review, and/or revision of the manuscript: C. Liu, W. Lou, N. Nadiminty, C.T. Schwartz, C.P. Evans, A.C. Gao
Administrative, technical, or material support (i.e., reporting or organizing data, constructing databases): C. Liu, W. Lou, Y. Zhu, C.P. Evans, A.C. Gao
Study supervision: C. Liu, W. Lou, A.C. Gao

Acknowledgments

The authors thank Dr. J. Luo (John Hopkins University, Baltimore, MD) for providing the AR-V7 plasmid, and Dr. J.C. Yang, Dr. H. Chen, and Z. Duan (University of California, Davis, CA) for technical assistance.

Grant Support

This work was supported in part by grants NIH/NCI CA140468, CA168601, and CA179970.

The costs of publication of this article were defrayed in part by the payment of page charges. This article must therefore be hereby marked *advertisement* in accordance with 18 U.S.C. Section 1734 solely to indicate this fact.

Received December 11, 2013; revised April 1, 2014; accepted April 4, 2014; published OnlineFirst April 16, 2014.

References

1. Scher HI, Fizazi K, Saad F, Taplin ME, Sternberg CN, Miller K, et al. Increased survival with enzalutamide in prostate cancer after chemo therapy. N Engl J Med 2012;367:1187 97.
2. de Bono JS, Logothetis CJ, Molina A, Fizazi K, North S, Chu L, et al. Abiraterone and increased survival in metastatic prostate cancer. N Engl J Med 2011;364:1995 2005.
3. Mostaghel EA, Marck BT, Plymate SR, Vessella RL, Balk S, Matsumoto AM, et al. Resistance to CYP17A1 inhibition with abiraterone in castration resistant prostate cancer: induction of steroidogenesis and androgen receptor splice variants. Clin Cancer Res 2011;17:5913 25.
4. Kim W, Ryan CJ. Androgen receptor directed therapies in castration resistant metastatic prostate cancer. Curr Treat Options Oncol 2012; 13:189 200.
5. Dehm SM, Schmidt LJ, Heemers HV, Vessella RL, Tindall DJ. Splicing of a novel androgen receptor exon generates a constitutively active androgen receptor that mediates prostate cancer therapy resistance. Cancer Res 2008;68:5469 77.
6. Hu R, Dunn TA, Wei S, Isharwal S, Veltri RW, Humphreys E, et al. Ligand independent androgen receptor variants derived from splicing of cryptic exons signify hormone refractory prostate cancer. Cancer Res 2009;69:16 22.
7. Guo Z, Yang X, Sun F, Jiang R, Linn DE, Chen H, et al. A novel androgen receptor splice variant is up regulated during prostate cancer pro gression and promotes androgen depletion resistant growth. Cancer Res 2009;69:2305 13.
8. Li Y, Alsagabi M, Fan D, Bova GS, Tewfik AH, Dehm SM. Intragenic rearrangement and altered RNA splicing of the androgen receptor in a cell based model of prostate cancer progression. Cancer Res 2011; 71:2108 17.
9. Hu R, Isaacs WB, Luo J. A snapshot of the expression signature of androgen receptor splicing variants and their distinctive transcriptional activities. Prostate 2011;71:1656 67.
10. Li Y, Hwang TH, Oseth LA, Hauge A, Vessella RL, Schmechel SC, et al. AR intragenic deletions linked to androgen receptor splice variant expression and activity in models of prostate cancer progression. Oncogene 2012;31:4759 67.
11. Schrader AJ, Schrader MG, Cronauer MV. Re: androgen receptor splice variants mediate enzalutamide resistance in castration resistant prostate cancer cell lines. Eur Urol 2013;64:169 70.
12. Zhang X, Morrissey C, Sun S, Ketchandji M, Nelson PS, True LD, et al. Androgen receptor variants occur frequently in castration resistant prostate cancer metastases. PLoS One 2011;6:e27970.
13. Sun S, Sprenger CC, Vessella RL, Haugk K, Soriano K, Mostaghel EA, et al. Castration resistance in human prostate cancer is conferred by a frequently occurring androgen receptor splice variant. J Clin Invest 2010;120:2715 30.
14. Cronauer MV, Hittmair A, Eder IE, Hobisch A, Culig Z, Ramoner R, et al. Basic fibroblast growth factor levels in cancer cells and in sera of patients suffering from proliferative disorders of the prostate. Prostate 1997;31:223 33.
15. Watson PA, Chen YF, Balbas MD, Wongvipat J, Socci ND, Viale A, et al. Constitutively active androgen receptor splice variants expressed in castration resistant prostate cancer require full length androgen receptor. Proc Natl Acad Sci U S A 2010;107: 16759 65.
16. Hornberg E, Ylitalo EB, Crnalic S, Antti H, Stattin P, Widmark A, et al. Expression of androgen receptor splice variants in prostate cancer bone metastases is associated with castration resistance and short survival. PLoS One 2011;6:e19059.
17. Chan SC, Li Y, Dehm SM. Androgen receptor splice variants activate androgen receptor target genes and support aberrant prostate cancer cell growth independent of canonical androgen receptor nuclear localization signal. J Biol Chem 2012;287:19736 49.
18. Nadiminty N, Tummala R, Liu C, Yang J, Lou W, Evans CP, et al. NF κB2/p52 induces resistance to enzalutamide in prostate cancer: role of androgen receptor and its variants. Mol Cancer Ther 2013;12: 1629 37.
19. Li Y, Chan SC, Brand LJ, Hwang TH, Silverstein KA, Dehm SM. Androgen receptor splice variants mediate enzalutamide resistance in castration resistant prostate cancer cell lines. Cancer Res 2013; 73:483 9.
20. Joseph JD, Lu N, Qian J, Sensintaffar J, Shao G, Brigham D, et al. A clinically relevant androgen receptor mutation confers resistance to 2nd generation anti androgens enzalutamide and ARN 509. Cancer Discov 2013;3:1020 9.
21. Korpal M, Korn JM, Gao X, Rakiec DP, Ruddy DA, Doshi S, et al. An F876L mutation in androgen receptor confers genetic and pheno typic resistance to MDV3100 (Enzalutamide). Cancer Discov 2013; 3:1030 43.
22. Hu R, Lu C, Mostaghel EA, Yegnasubramanian S, Gurel M, Tannahill C, et al. Distinct transcriptional programs mediated by the ligand depen dent full length androgen receptor and its splice variants in castration resistant prostate cancer. Cancer Res 2013;72:3457 62.
23. Chun JY, Nadiminty N, Dutt S, Lou W, Yang JC, Kung HJ, et al. Interleukin 6 regulates androgen synthesis in prostate cancer cells. Clin Cancer Res 2009;15:4815 22.
24. Liu C, Zhu Y, Lou W, Cui Y, Evans CP, Gao AC. Inhibition of consti tutively active Stat3 reverses enzalutamide resistance in LNCaP deriv ative prostate cancer cells. Prostate 2014;74:201 9.
25. Liu C, Nadiminty N, Tummala R, Chun JY, Lou W, Zhu Y, et al. Andrographolide targets androgen receptor pathway in castration resistant prostate cancer. Genes Cancer 2011;2:151 9.
26. Jenster G, van der Korput HA, van Vroonhoven C, van der Kwast TH, Trapman J, Brinkmann AO. Domains of the human androgen receptor involved in steroid binding, transcriptional activation, and subcellular localization. Mol Endocrinol 1991;5:1396 404.
27. Tepper CG, Boucher DL, Ryan PE, Ma AH, Xia L, Lee LF, et al. Characterization of a novel androgen receptor mutation in a relapsed CWR22 prostate cancer xenograft and cell line. Cancer Res 2002; 62:6606 14.

Published OnlineFirst April 16, 2014; DOI: 10.1158/1078-0432.CCR-13-3296

28. Scher HI, Beer TM, Higano CS, Anand A, Taplin ME, Efstathiou E, et al. Antitumour activity of MDV3100 in castration resistant prostate cancer: a phase 1 2 study. Lancet 2010;375:1437 46.
29. Nyquist MD, Li Y, Hwang TH, Manlove LS, Vessella RL, Silverstein KA, et al. TALEN engineered AR gene rearrangements reveal endocrine uncoupling of androgen receptor in prostate cancer. Proc Natl Acad Sci U S A 2013;110:17492 7.
30. Arora VK, Schenkein E, Murali R, Subudhi SK, Wongvipat J, Balbas MD, et al. Glucocorticoid receptor confers resistance to antiandrogens by bypassing androgen receptor blockade. Cell 2013;155:1309 22.
31. Myung JK, Banuelos CA, Fernandez JG, Mawji NR, Wang J, Tien AH, et al. An androgen receptor N terminal domain antagonist for treating prostate cancer. J Clin Invest 2013;123:2948 60.
32. Mostaghel EA, Plymate SR, Montgomery B. Molecular pathways: targeting resistance in the androgen receptor for therapeutic benefit. Clin Cancer Res 2014;20:791 8.
33. Zhan Y, Cao B, Qi Y, Liu S, Zhang Q, Zhou W, et al. Methylselenol prodrug enhances MDV3100 efficacy for treatment of castration resistant prostate cancer. Int J Cancer 2013;133:2225 33.
34. Shiota M, Yokomizo A, Takeuchi A, Imada K, Kashiwagi E, Song Y, et al. Inhibition of protein kinase C/Twist1 signaling augments anti cancer effects of androgen deprivation and enzalutamide in prostate cancer. Clin Cancer Res 2014;20:951 61.
35. Merschjohann K, Steverding D. *In vitro* trypanocidal activity of the anti helminthic drug niclosamide. Exp Parasitol 2008;118:637 40.
36. Mercer Haines N, Fioravanti CF. *Hymenolepis diminuta*: mitochondrial transhydrogenase as an additional site for anaerobic phosphorylation. Exp Parasitol 2008;119:24 9.
37. Sack U, Walther W, Scudiero D, Selby M, Kobelt D, Lemm M, et al. Novel effect of antihelminthic Niclosamide on S100A4 mediated metastatic progression in colon cancer. J Natl Cancer Inst 2011; 103:1018 36.
38. Osada T, Chen M, Yang XY, Spasojevic I, Vandeusen JB, Hsu D, et al. Antihelminth compound niclosamide downregulates Wnt signaling and elicits antitumor responses in tumors with activating APC mutations. Cancer Res 2011;71:4172 82.
39. Mook RAJr., Chen M, Lu J, Barak LS, Lyerly HK, Chen W. Small molecule modulators of Wnt/β catenin signaling. Bioorg Med Chem Lett 2013;23:2187 91.
40. Yo YT, Lin YW, Wang YC, Balch C, Huang RL, Chan MW, et al. Growth inhibition of ovarian tumor initiating cells by niclosamide. Mol Cancer ther 2012;11:1703 12.
41. Jin Y, Lu Z, Ding K, Li J, Du X, Chen C, et al. Antineoplastic mechanisms of niclosamide in acute myelogenous leukemia stem cells: inactivation of the NF κB pathway and generation of reactive oxygen species. Cancer Res 2010;70:2516 27.
42. Li R, Hu Z, Sun SY, Chen ZG, Owonikoko TK, Sica GL, et al. Niclosamide overcomes acquired resistance to erlotinib through suppression of STAT3 in non small cell lung cancer. Mol Cancer ther 2013; 12:2200 12.
43. Li R, You S, Hu Z, Chen ZG, Sica GL, Khuri FR, et al. Inhibition of STAT3 by niclosamide synergizes with erlotinib against head and neck cancer. PLoS One 2013;8:e74670.
44. Balgi AD, Fonseca BD, Donohue E, Tsang TC, Lajoie P, Proud CG, et al. Screen for chemical modulators of autophagy reveals novel therapeutic inhibitors of mTORC1 signaling. PLoS One 2009;4: e7124.
45. Fonseca BD, Diering GH, Bidinosti MA, Dalal K, Alain T, Balgi AD, et al. Structure activity analysis of niclosamide reveals potential role for cytoplasmic pH in control of mammalian target of rapamycin complex 1 (mTORC1) signaling. J Biol Chem 2012;287:17530 45.
46. Li M, Khambu B, Zhang H, Kang JH, Chen X, Chen D, et al. Suppression of lysosome function induces autophagy via a feedback downregulation of MTORC1 activity. J Biol Chem 2013;288:35769 80.

Published OnlineFirst April 16, 2014; DOI: 10.1158/1078-0432.CCR-13-3296

Clinical Cancer Research

Niclosamide Inhibits Androgen Receptor Variants Expression and Overcomes Enzalutamide Resistance in Castration-Resistant Prostate Cancer

Chengfei Liu, Wei Lou, Yezi Zhu, et al.

Clin Cancer Res 2014;20:3198-3210. Published OnlineFirst April 16, 2014.

Interleukin-6 Induces Neuroendocrine Differentiation (NED) Through Suppression of RE-1 Silencing Transcription Factor (REST)

Yezi Zhu,[1,2] Chengfei Liu,[1] Yuanyuan Cui,[1] Nagalakshmi Nadiminty,[1] Wei Lou,[1] and Allen C. Gao[1,2,3]*

[1]Department of Urology, University of California Davis, Sacramento, California
[2]Graduate Program in Pharmacology and Toxicology, University of California Davis, Sacramento, California
[3]Comprehensive Cancer Center, University of California Davis, Sacramento, California

BACKGROUND. Paracrine interleukin-6 (IL-6) can mediate neuroendocrine (NE) features, including the acquisition of a neurite-like phenotype and growth arrest in prostate cancer cells. However, little is known about the mechanisms underlying neuroendocrine differentiation induced by IL-6.

METHODS. Immunoblotting was performed to determine the status of RE1-silencing transcription factor (REST) and of neuroendocrine markers such as Neuron-specific Enolase (NSE), chromogranin A and synaptophysin in LNCaP cells treated with IL-6. To further study the impact of REST-mediated repression on neuroendocrine differentiation (NED) in LNCaP cells, either wild-type REST or a dominant-positive form of REST, REST-VP16, in which both repressor domains of REST were replaced with the activation domain of the herpes simplex virus protein VP16, was introduced into LNCaP cells.

RESULTS. In this study, we show that REST is suppressed in IL-6-induced neuroendocrine differentiation in LNCaP cells. Overexpression of exogenous REST abrogated IL-6-induced NED in prostate cancer cells. Expression of the recombinant REST-VP16 fusion protein activated REST target genes and other neuronal differentiation genes and produced neuronal physiological properties. In addition, REST protein turnover was accelerated in IL-6 induced NE differentiated LNCaP cells via the ubiquitin-proteasome pathway, accompanied by a decrease in the expression of the deubiquitylase HAUSP, indicating that pathway(s) priming REST degradation may be involved in IL-6 induced NE differentiation.

CONCLUSIONS. These results demonstrate that REST functions as a major switch of IL-6 induced neuroendocrine differentiation in LNCaP cells. *Prostate 74:1086–1094, 2014.*

KEY WORDS: **prostate cancer; interleukin-6; REST; neuroendocrine**

INTRODUCTION

Neuroendocrine (NE) cells represent a small proportion of the cell population in the developing and mature prostate gland epithelium in addition to basal and secretory epithelial cells [1]. NE cells are characterized morphologically by their neurosecretory granules and the expression of NE markers such as neuron-specific-enolase (NSE), chromogranin A (ChgA), synaptophysin (SYP) and tubulin, beta 3 class III (TUBB3) [1–3]. NE cells express and secrete a variety of neuropeptides such as bombesin/gastrin-releasing peptides (GRP), somatostatin, calcitonin, and parathyroid hormone-

Grant sponsor: NIH/NCI; Grant numbers: CA140468; CA168601; CA179970; Grant sponsor: US Department of Veterans Affairs; Grant sponsor: Office of Research and Development VA Merits; Grant number: I01 BX000526.

*Correspondence to: Allen C. Gao, Department of Urology, University of California Davis Medical Center, 4645 2nd Ave, Research III, Suite 1300, Sacramento, CA 95817. E mail: acgao@ucdavis.edu
Received 28 February 2014; Accepted 14 April 2014
DOI 10.1002/pros.22819
Published online 12 May 2014 in Wiley Online Library (wileyonlinelibrary.com).

related peptides [2]. These neuropeptides have mitogenic effects which sustain the growth and survival of adjacent cancer cells and thus contribute to prostate cancer cell proliferation. Although NE features are only detected in approximately 4–10% of prostate cancer patients at initial diagnosis, 40–100% of castration resistant prostate cancer (CRPC) have an acquired NE phenotype eventually [4,5]. The NE phenotype is associated with clinical aggressiveness and resistance to androgen deprivation therapy; therefore, neuroendocrine differentiation (NED) has been suggested as a marker of poor prognosis for prostate cancer.

Interleukin-6 (IL-6) has been shown to play a role in modulating growth and differentiation in many cancer types including prostate cancer [6,7]. The constitutive expression of IL-6 and its receptor has been demonstrated in human prostate cancer cell lines as well as clinical prostate cancer specimens [8]. Many studies have demonstrated that IL-6 is elevated in sera of patients with castration resistant prostate cancer compared to normal controls, benign prostatic hyperplasia, and localized prostate cancer [9,10]. IL-6 activates AR target genes through activation of the STAT3 pathway [11,12]. IL-6 can also function as a paracrine growth factor in androgen-sensitive LNCaP cells, inducing growth arrest and neuroendocrine differentiation (NED) [6]. However, little is known about the mechanisms underlying IL-6-induced neuroendocrine differentiation in prostate cancer cells.

RE1-silencing transcription factor (REST) is a main negative regulator of neurogenesis which binds to conserved DNA sequences, RE1 sites, to repress expression of neuroendocrine genes [13]. REST is expressed largely in non-neuronal cells to block the expression of neuronal genes. However, recently, reduced levels of REST activity were found in human small cell lung cancer (SCLC) samples as well as established SCLC cells expressing neuroendocrine markers [14]. Blockade of REST using RNAi in human mammary epithelial cells was found to result in a transformation phenotype, and growth in an anchorage-independent manner [15]. In a recent study investigating the molecular signature of castration-resistant neuroendocrine prostate cancer, reduced expression of REST was found to be associated with up-regulation of a neuronal signature in clinical NE prostate cancer samples [16]. In the current study, we demonstrate that REST functions as a critical regulator of IL-6-induced NE differentiation in LNCaP cells.

MATERIALS AND METHODS

Cell Culture and Reagents

LNCaP cells were cultured in RPMI-1640 medium containing 10% complete fetal bovine serum (FBS) and penicillin/streptomycin. All the experiments in this study were performed in FBS condition. Cells were maintained at 37°C in a humidified incubator with 5% CO_2. LNCaP passage numbers <30 were used throughout the study. rhIL-6 was purchased from R&D Systems (Minneapolis, MN).

Plasmids and Cell Transfection

The pcDNA3.1-REST and pcDNA3.1-REST-VP16 plasmids were kind gifts from Dr. Hsing-Jien Kung (UC Davis, CA). For transfection studies, cells were transiently transfected with expression plasmids using Attractene transfection reagent according to the manufacturer's procedure (QIAGEN).

Preparation of Whole-Cell Extracts

Wells were harvested, washed with cold PBS twice, and lysed in high-salt buffer 10 mM HEPES (pH 7.9), 250 mM NaCl, 1% NP-40, 1 mM EDTA with protease inhibitors (Roche, Basel, Switzerland). Total protein concentrations in the lysates were determined with the Coomassie Plus Protein Assay Reagent (Pierce, Rockford, IL).

Western Blot Analysis

Anti-REST (Cat#07-579, Millipore, 1:1,000), anti-HAUSP (ab4080, Abcam, 1:1,000), anti-NSE (MAB324, Millipore, 1:1,000), anti-synaptophysin (sc-9116; Santa Cruz; 1:1,000), anti-chromogranin A (sc-13090; Santa Cruz; 1:1,000), β-TrCP(H-300) (sc-15354; Santa Cruz; 1:1,000), anti-α-Tubulin (T5168; Sigma-Aldrich; 1:5,000) were used as primary antibodies in western blot analysis. Equal amounts of cell protein extracts were loaded on 8% or 10% SDS–PAGE, and proteins were transferred to nitrocellulose membranes. After blocking in 5% non-fat milk in 1 × PBS/0.1% Tween-20 at room temperature for 1 hr, membranes were washed three times with 1 × PBS/0.1% Tween-20. The membranes were incubated overnight with primary antibodies at 4°C. Proteins were visualized using the enhanced chemi-luminescence kit (Millipore) after incubation with the appropriate horseradish peroxidase-conjugated secondary antibodies.

Real-Time Quantitative RT-PCR

Total RNA was extracted using TRIzol (Invitrogen, Carlsbad, CA) reagent. One microgram RNA was digested by RQ1 DNase (Promega, Madison, WI). The resulting product was reverse transcribed with random primers by Im-Prom^{II} Reverse transcriptase (Promega). The newly synthesized cDNA was used to

perform real-time PCR. The reaction mixture contained 4 μl cDNA template and 0.5 μM specific primers for REST (Forward: 5′-CGC CAT GCA AGA CAG GTT CAC AAT-3′; Reverse: 5′-AGCTGC ATAGTC ACA TAC AGG GCA-3′), HAUSP(Forward: 5′-ACT TTG AGC CAC AGC CCG GTA ATA-3′; Reverse: 5′-GCC TTG AAC ACA CCA GCT TGG AAA-3′) and TUBB3 (Forward: 5′-ATC AGC AAG GTG CGTGAGGAGTAT-3′; Reverse: 5′-TCG TTG TCG ATG CAG TAG GTC TCA-3′). GAPDH primers were used as an internal control. The expression levels of REST, HAUSP, and TUBB3 were normalized to GAPDH. The experiments were repeated three times with triplicates.

REST Protein Stability Assay

Equal numbers of LNCaP cells were plated in six-well plates and treated with or without 20 ng/ml IL-6 for 3 days. Cells were then treated with 50 μg/ml cycloheximide for 0, 20, 40, 60, 120, and 270 min. Whole cell proteins were collected in high salt buffer containing 10 mM HEPES (pH 7.9), 250 mM NaCl, 1% NP-40, 1 mM EDTA with the addition of protease inhibitors (Roche). Equal amounts of protein were run on 8% SDS–PAGE and probed with anti-REST antibody (Cat#07-579, Millipore, 1:1,000) or anti-tubulin antibody (Sigma) as internal control.

Ubiquitination Assay

MG132 was used to block proteasome-mediated degradation of ubiquitin-conjugated proteins. LNCaP cells were treated with or without 20 ng/ml IL-6 for 3 days and then with 5 μM MG132 for another 4 hr. Cells were lysed in a buffer containing 10 mM HEPES (pH 7.9), 250 mM NaCl, 1% NP-40, 1 mM EDTA with the addition of protease inhibitors (Roche). The whole-cell lysates (200 μg total protein) were incubated overnight with 2 μg antibodies against REST (Cat#07-579, Milipore) or normal rabbit IgG (sc-2072; Santa Cruz), with constant rotation at 4°C. The immunoprecipitates were collected by incubation with 30 μl protein A/G-agarose for 3 hr at 4°C, washed with high-salt buffer, eluted with SDS sample buffer by boiling for 10 min, resolved on SDS–PAGE, and transferred to nitrocellulose membranes. Ubiquitin-conjugated REST was visualized by blotting the membranes with anti-ubiquitin antibodies (sc-8017; Santa Cruz; 1:1,000).

Statistical Analyses

All data are shown as means ± SD. Differences between multiple groups were analyzed by one-way ANOVA followed by the Scheffe procedure for comparison of means. $P < 0.05$ was considered significant.

RESULTS

Interleukin-6 Induces NE Differentiation in LNCaP Cells

IL-6 has been shown to be a paracrine factor that inhibits the growth of LNCaP cells and induces neuroendocrine differentiation [6]. To further examine this effect, LNCaP cells were treated with or without 20 ng/ml IL-6 for 7 days. During the course of the IL-6 treatment, we observed a significant acquisition of neuroendocrine morphological changes in LNCaP cells, including irregular dendrite-like phenotype and neuritic branching and extension (Fig. 1A). The protein levels of neuroendocrine markers NSE and synaptophysin were increased in IL-6 treated LNCaP cells compared with control (Fig. 1B). These results confirmed that paracrine IL-6 induces neuroendocrine differentiation in LNCaP cells, featuring neuroendocrine morphological characteristics and higher levels of neuroendocrine markers.

REST Is Down-Regulated in Neuroendocrine Differentiation

RE1-silencing transcription factor (REST)/neuron-restrictive silencing factor (NRSF) is a DNA-binding protein and has been found to be responsible for silencing the transcription of most neuronal differentiation

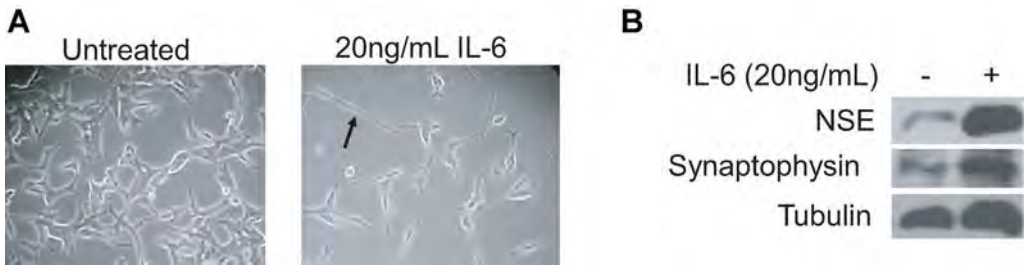

Fig. 1. IL 6 induced neuronal like morphology and neuroendocrine differentiation in LNCaP cells. **A**: LNCaP cells were incubated with or without 20 ng/ml IL 6 for 7 days. Arrows show neuritic branching and extension. **B**: Cell lysates were resolved by SDS–PAGE and probed with anti NSE, anti synaptophysin, or anti tubulin antibodies.

genes by binding to a 21-bp consensus sequence (RE1 binding site), which is present at the upstream promoter-enhancer region of these genes [13]. Recently, reduced expression of REST and associated up-regulation of a neuronal signature was observed in 50% of tumors with a NED component, including prostate cancer [4,17]. In order to examine the role of REST in IL-6 induced NED, whole cell extracts were collected from LNCaP cells treated with or without 20 ng/ml IL-6 at different time points and the protein expression of REST was analyzed by Western blotting. The levels of REST expression were significantly downregulated in IL-6 treated LNCaP cells in a time-dependent manner (Fig. 2A). The loss of REST expression was correlated with loss of AR expression (Fig. 2A), consistent with earlier reports which showed that loss of AR expression was accompanied with the acquisition of a NE phenotype [16,18]. To further confirm this result, LNCaP cells were treated with different concentrations of IL-6 for 4 days and the protein expression of REST was analyzed. As shown in Figure 2B, REST expression was significantly suppressed by IL-6 in a dose-dependent manner.

REST Is the Major Switch of IL6-Induced NED in LNCaP Cells

Having identified the downregulation of REST in IL-6-induced NE differentiation in LNCaP cells, we next examined whether REST functionally mediates IL-6-induced NE differentiation. We expressed either a wild-type REST or a dominant-positive recombinant transcription factor REST-VP16, in which both repressor domains of REST were replaced with the activation domains of herpes simplex virus protein VP16, in LNCaP cells (Fig. 3A). REST-VP16 has been shown to cause activation of REST target genes instead of repressing [13,19]. As shown in Figure 3B, IL-6 induced NE phenotype in LNCaP cells, while overexpression of the wild-type REST protein abolished the neuronal morphological changes induced by IL-6. Furthermore, elevated levels of NED markers such as NSE and synaptophysin induced by IL-6 were also inhibited by REST overexpression, indicating that expression of exogenous REST abrogated IL-6 induced NED in LNCaP cells. In contrast, overexpression of the dominant positive REST-VP16 in LNCaP cells induced NED and further enhanced IL-6 induced NED (Fig. 3C, left panel). REST-VP16 overexpression also increases the expression of synaptophysin and ChgA in either the presence or absence of IL-6 (Fig. 3C, right panel). These results demonstrated that REST functions as a major switch of IL-6-induced neuroendocrine differentiation.

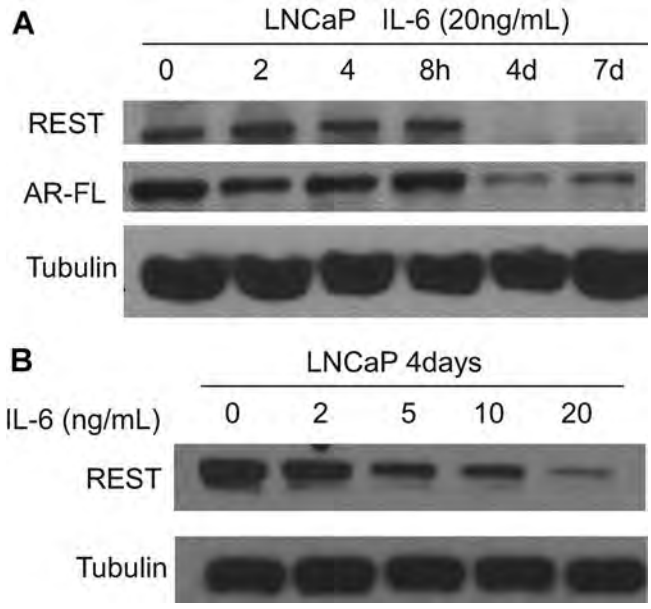

Fig. 2. REST level is downregulated in LNCaP cells treated with IL 6. **A**: LNCaP cells were treated with 20 ng/ml IL 6 for different time points as indicated. **B**: LNCaP cells were treated with IL 6 at different concentrations as indicated for 4 days. Cell lysates were resolved on SDS–PAGE and probed with antibodies as indicated.

IL-6 Decreases REST Protein Stability by Enhancing Protein Degradation

To determine the mechanism through which IL-6 regulates REST expression, we determined the REST messenger RNA levels in LNCaP cells treated with 20 ng/ml IL-6 for 7 days. Compared to a significant reduction of protein levels, the REST mRNA levels did not exhibit any downregulation in response to IL-6 treatment (Fig. 4A). This indicated that IL-6 may regulate REST expression at the post-transcriptional level. We next examined the effect of IL-6 on REST protein degradation after new protein synthesis was blocked by cycloheximide (50 μg/ml). Protein extracts were collected at different time points, and the protein levels of REST were analyzed by Western blot (Fig. 4B). As shown in Figure 4C, the half-life of REST protein in LNCaP cells was reduced from 120 to <40 min compared to the control cells after 3 days treatment with IL-6, suggesting that degradation of REST protein was greatly enhanced by IL-6 treatment.

IL-6 Enhances REST Protein DegradationThrough the Ubiquitin-Proteasome Pathway

Since REST protein degradation was accelerated by IL-6, we examined whether IL-6 induced REST protein degradation is associated with ubiquitination. We treated LNCaP cells with 20 ng/ml IL-6 for 3 days

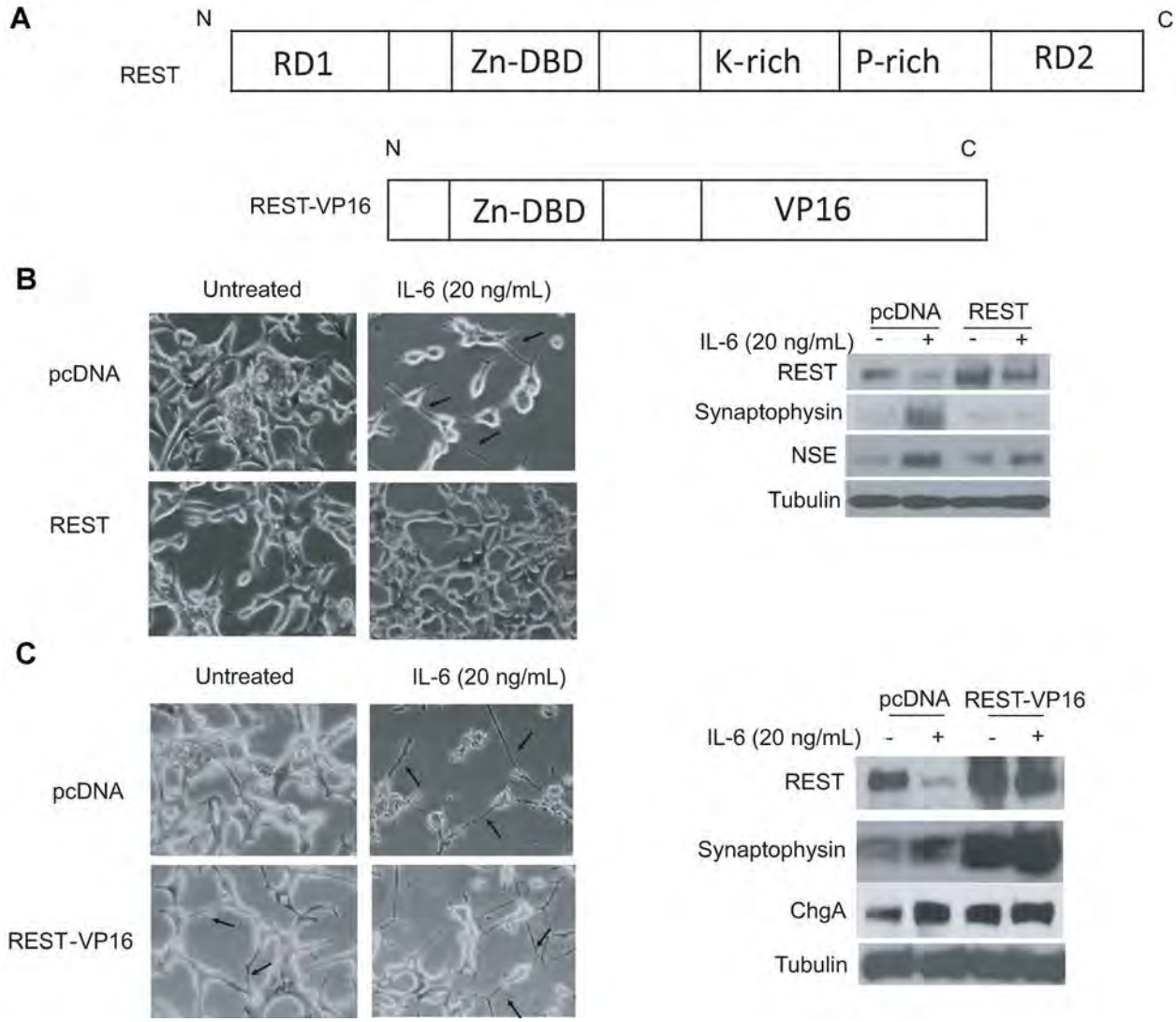

Fig. 3. REST regulates IL 6 induced NE differentiation. **A**: Schematic structures of wild type REST (upper) and REST VPI6 (bottom). LNCaP cells were transfected with pcDNA3.I REST (**B**) or pcDNA3.I REST VPI6 (**C**) for 48 hr and were treated with or without 20 ng/ml IL 6 for another 6 days. Arrows show neuritic branching and extensions. Cell lysates were resolved by SDS–PAGE and probed with antibodies against NSE, synaptophysin, REST, ChgA, and tubulin.

followed by the proteasome inhibitor MG132 (10 μM) for 4 hr. As shown in Figure 5A, the ubiquitination of REST was increased in cells treated with IL-6. These data suggest that REST protein degradation induced by IL-6 is mediated by the ubiquitin-proteasome mechanism.

As a critical transcription factor in regulating neuronal differentiation, REST protein is regulated in a "Ying-Yang" control model by both deubiquitylation and ubiquitylation systems [20]. The E3 ubiquitin ligase complex SCF-β-TrCP is the key player in post-translational regulation of REST protein [21]. However, IL-6 treatment failed to change the protein levels of SCF-β-TrCP in IL-6 induced NED in LNCaP cells, even though the levels of REST protein were significantly reduced (Fig. 5B), indicating that SCF-β-TrCP was not the critical regulator associated with IL-6 induced NED. Recently, Huang et al. [20] have demonstrated that the deubiquitylase HAUSP counter balances REST ubiquitylation and that downregulation of HAUSP decreases REST expression and induces neuronal differentiation. Therefore, we examined the mRNA levels of HAUSP in IL-6 treated LNCaP cells. Although the mRNA levels of REST did not change, the mRNA levels of HAUSP were significantly reduced by IL-6 treatment (Fig. 5C), in accordance with the elevated levels of TUBB3 mRNA, another neuroendocrine marker. In addition, the protein levels of

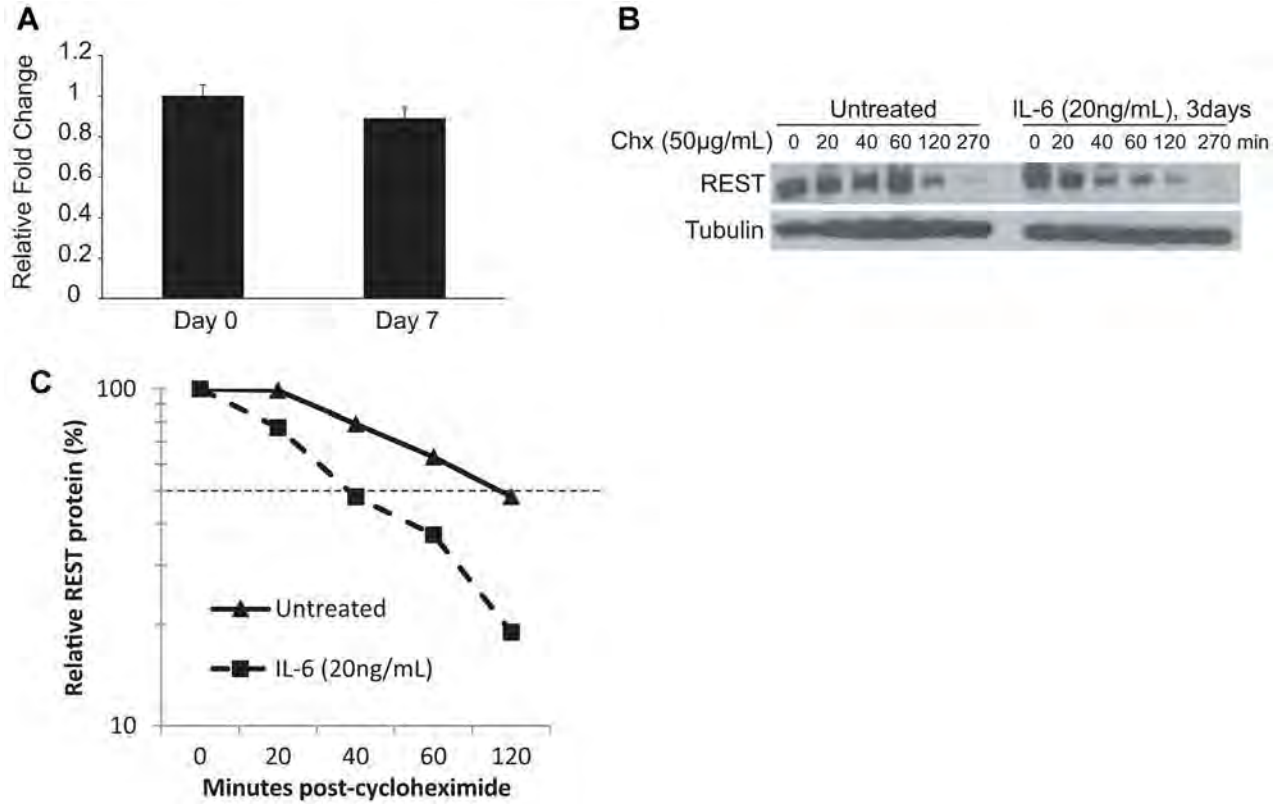

Fig. 4. REST protein turnover is accelerated in IL 6 induced NE differentiation. LNCaP cells were treated with or without 20 ng/ml IL 6 for 7 days. **A**: REST mRNA level was quantified relative to GAPDH by real time RT PCR. **B**: The protein synthesis inhibitor cycloheximide (50 μg/ml) was added at time 0. At specific time points, cells were harvested, and cell lysates were prepared. REST protein levels were deter mined by Western blot analysis using antibody specifically against REST and normalized to tubulin control. **C**: The levels of REST protein were quantified and normalized to the amount of tubulin. REST protein turnover was determined by comparing REST protein levels over time in cells treated with or without IL 6.

HAUSP in IL-6 treated LNCaP cells were also analyzed by Western blotting. IL-6 treatment significantly downregulated HAUSP protein expression (Fig. 5D). Collectively, these data suggest that IL-6 enhances REST protein degradation through a ubiquitin-proteasome-mediated mechanism accompanied by a decrease in the expression of the deubiquitylase HAUSP.

DISCUSSION

Neuroendocrine prostate cancer (NEPC) is an aggressive type of prostate cancer and is associated with disease progression and resistance to androgen deprivation therapy [1,4,5]. Multiple pathways involved in NE differentiation of prostate cancer cells have been elucidated. Androgen depletion [1,2], cAMP and its agonists [22], cytokines such as IL-1β and IL-6 treatment [7,22,23] are all shown to be able to induce NE differentiation in prostate cancer cells through different cell signaling pathways. IL-6 can function as a paracrine factor to induce NE differentiation and growth arrest in LNCaP cells. However, the underlying molecular mechanism is not fully elucidated although STAT3 is proposed as the mediator within this process [23]. In this study, we demonstrated that REST, which is responsible for silencing the transcription of many NE differentiation genes, is suppressed in IL-6-induced NE differentiation. In addition, we demonstrated that suppression of REST by IL-6 is through the ubiquitin-proteasome pathway accompanied by a decrease in deubiquitylase HAUSP gene expression, indicating that pathway(s) priming REST degradation may be involved in IL-6 induced NE differentiation.

REST, also known as NRSF (neural-restrictive silencing factor), binds to a 21-bp DNA element (RE1) within the promoter region of target genes. Genes (>1,300) containing the RE1 sequence have been identified which encode proteins playing crucial roles in cellular functions [17]. Abnormal expression of REST has been reported to correlate with several forms of cancer. REST has been attributed a tumor

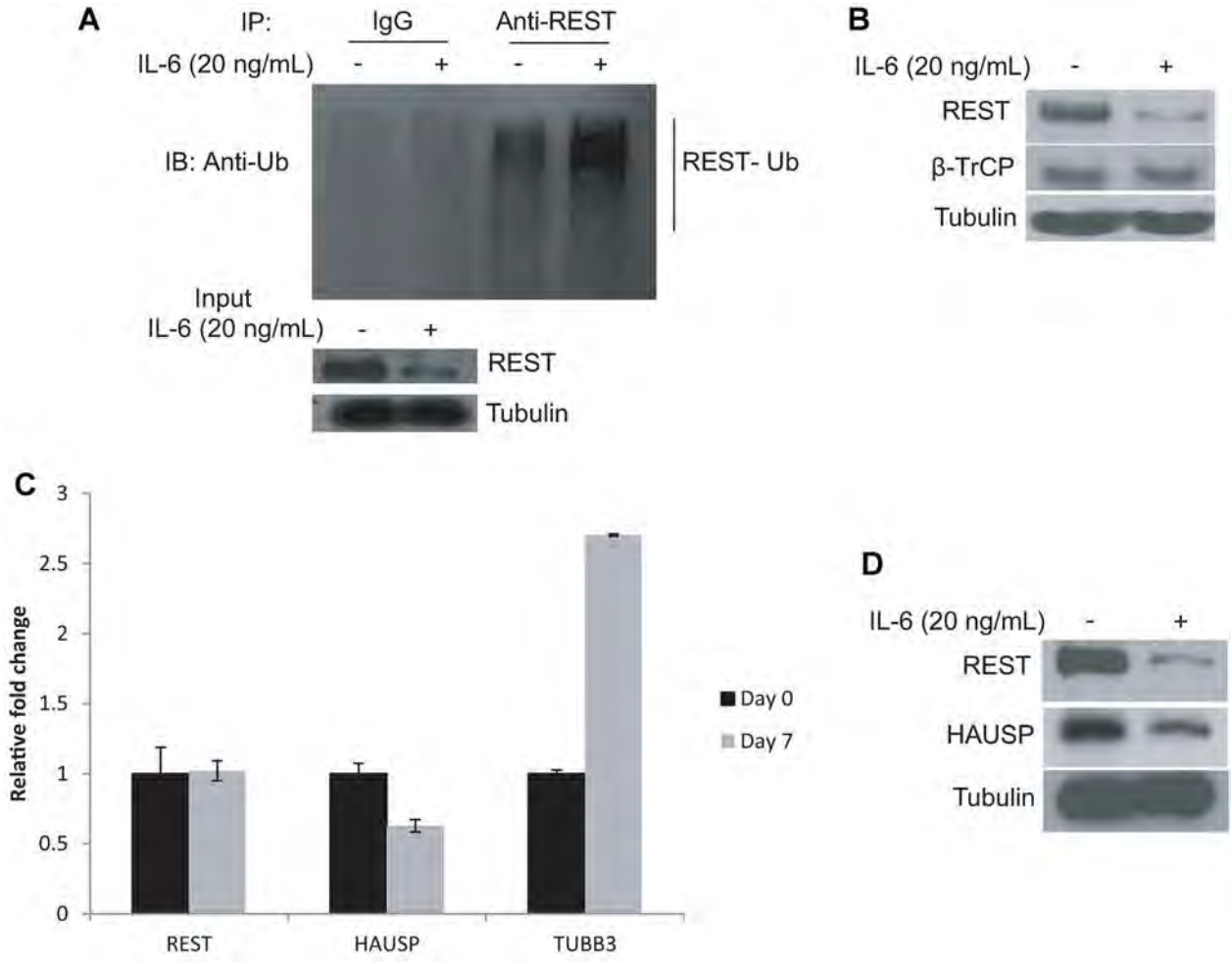

Fig. 5. IL 6 enhances REST degradation through the ubiquitin proteasome pathway. **A**: LNCaP cells were treated with or without 20 ng/ml IL 6 for 3 days and then treated with or without 5 μM MG 132 for 4 hr. Whole cell lysates were precipitated with antibodies against REST or normal rabbit IgG. The resulting eluates were blotted with antibodies specifically against ubiquitin. **B**: LNCaP cells were treated with or without 20 ng/ml IL 6 for 7 days, and the protein levels of REST and β TrCP were analyzed using specific antibodies. LNCaP cells were treated with 20 ng/ml IL 6 0 and 7 days, (**C**) and the mRNA levels of REST, HAUSP and TUBB3 were measured by real time RT PCR, (**D**) and the protein levels of REST, HAUSP were analyzed by Western blot analysis using specific antibodies.

suppressor function in breast cancer, and its expression is reduced with aggressiveness in breast cancer [15]. Interestingly, a SCLC-specific isoform of REST, which antagonizes REST-mediated neuroendocrine gene expression, promoted tumor aggressiveness and neuronal phenotype in SCLCs [14]. In colon cancer, the loss of REST expression confers a survival benefit during the progression of tumor cells [24]. A recent molecular sequence study of neuroendocrine prostate cancer revealed the downregulation of REST and upregulation of REST-repressed genes within the neuroendocrine prostate cancer component in patient samples [16]. REST inactivation regulates androgen deprivation- or enzalutamide-induced, as well as hypoxia-induced neuroendocrine differentiation in prostate cancer cells [25,26]. These reports are consistent with our results showing that REST is downregulated in IL-6 induced NE differentiation, and overexpression of REST abolishes such effects. S17 is the LNCaP cell line stably expressing IL-6. We also tested the REST levels upon IL-6 treatment, however, exogenous IL-6 did not affect REST protein expression in S17 cells (unpublished data). These results agree with a previous study [7] that S17 cells are resistant to exogenous IL-6-induced NE differentiation due to increased CIS/SOCS7 that blocks activation of JAK2/STAT3 pathway. Together, these results suggest that REST functions as the major switch of IL-6 induced NE differentiation in prostate cancer cells.

Our results showed that although REST mRNA levels were unchanged, protein levels were reduced by IL-6 treatment in prostate cancer cells possibly

through a ubiquitin-proteasome mechanism. REST protein level is delicately regulated by a "Ying-Yang" control model at the post-transcriptional level by both deubiquitylation and ubiquitylation as proposed by Huang et al. [20]. The herpes simplex virus associated ubiquitin-specific protease (HAUSP), also known as the ubiquitin-specific protease 7 (USP7) is the key deubiquitylase responsible for stabilization of REST [20]. We showed that HAUSP levels were down-regulated by IL-6, suggesting that the increase in REST degradation in IL-6-induced NED may be through loss of HAUSP, which destabilizes REST protein leading to degradation.

In conclusion, we described REST loss as a novel mechanism responsible for IL-6 induced NE differentiation in LNCaP cells. In addition, REST downregulation is regulated at post-transcriptional level by IL-6 through ubiquitin-proteasome mechanisms, probably through loss of HAUSP.

ACKNOWLEDGEMENTS

This work was supported in part by grants NIH/NCI CA140468, CA168601, CA179970, and US Department of Veterans Affairs, Office of Research and Development VA Merits I01 BX000526, and by resources from the VA Northern California Health Care System, Sacramento, California.

REFERENCES

1. Komiya A, Suzuki H, Imamoto T, Kamiya N, Nihei N, Naya Y, Ichikawa T, Fuse H. Neuroendocrine differentiation in the progression of prostate cancer. Int J Urol 2009;16(1):37 44.
2. Yang JC, Ok J H, Busby JE, Borowsky AD, Kung HJ, Evans CP. Aberrant activation of androgen receptor in a new neuropep tide autocrine model of androgen insensitive prostate cancer. Cancer Res 2009;69(1):151 160.
3. Yuan T C, Veeramani S, Lin M F. Neuroendocrine like prostate cancer cells: Neuroendocrine transdifferentiation of prostate adenocarcinoma cells. Endocr Relat Cancer 2007;14(3):531 547.
4. Dutt SS, Gao AC. Molecular mechanisms of castration resis tant prostate cancer progression. Future Oncol 2009;5(9): 1403 1413.
5. Beltran H, Rickman DS, Park K, Chae SS, Sboner A, MacDonald TY, Wang Y, Sheikh KL, Terry S, Tagawa ST, Dhir R, Nelson JB, de la Taille A, Allory Y, Gerstein MB, Perner S, Pienta KJ, Chinnaiyan AM, Wang Y, Collins CC, Gleave ME, Demichelis F, Nanus DM, Rubin MA. Molecular characterization of neuroen docrine prostate cancer and identification of new drug targets. Cancer Discov 2011;1(6):487 495.
6. Lee SO, Chun JY, Nadiminty N, Lou W, Gao AC. Interleukin 6 undergoes transition from growth inhibitor associated with neuroendocrine differentiation to stimulator accompanied by androgen receptor activation during LNCaP prostate cancer cell progression. Prostate 2007;67(7):764 773.
7. Ge D, Gao AC, Zhang Q, Liu S, Xue Y, You Z. LNCaP prostate cancer cells with autocrine interleukin 6 expression are resistant to IL 6 induced neuroendocrine differentiation due to increased expression of suppressors of cytokine signaling. Prostate 2012;72(12):1306 1316.
8. Hobisch A, Rogatsch H, Hittmair A, Fuchs D, Bartsch G Jr, Klocker H, Bartsch G, Culig Z. Immunohistochemical localiza tion of interleukin 6 and its receptor in benign, premalignant and malignant prostate tissue. J Pathol 2000;191(3):239 244.
9. Adler HL, McCurdy MA, Kattan MW, Timme TL, Scardino PT, Thompson TC. Elevated levels of circulating interleukin 6 and transforming growth factor beta 1 in patients with metastatic prostatic carcinoma. J Urol 1999;161(1):182 187.
10. Drachenberg DE, Elgamal A AA, Rowbotham R, Peterson M, Murphy GP. Circulating levels of interleukin 6 in patients with hormone refractory prostate cancer. Prostate 1999;41(2): 127 133.
11. Lou W, Ni Z, Dyer K, Tweardy DJ, Gao AC. Interleukin 6 induces prostate cancer cell growth accompanied by activation of Stat3 signaling pathway. Prostate 2000;42(3):239 242.
12. Zhu Y, Tummala R, Liu C, Nadiminty N, Lou W, Gao AC. RhoGDIα suppresses growth and survival of prostate cancer cells. Prostate 2012;72(4):392 398.
13. Majumader S. REST in good times and bad: Roles in tumor suppressor and oncogenic activities. Cell Cycle 2006;5(17):1929 1935.
14. Shimojo M, Shudo Y, Ikeda M, Kobashi T, Ito S. The small cell lung cancer specific isoform of RE1 silencing transcription factor (REST) is regulated by neural specific Ser/Arg repeat related protein of 100 kDa (nSR100). Mol Cancer Res 2013;11(10):1258 1268.
15. Reddy BY, Greco SJ, Patel PS, Trzaska KA, Rameshwar P. RE 1 silencing transcription factor shows tumor suppressor functions and negatively regulates the oncogenic TAC1 in breast cancer cells. Proc Natl Acad Sci USA 2009;106(11):4408 4413.
16. Lapuk AV, Wu C, Wyatt AW, McPherson A, McConeghy BJ, Brahmbhatt S, Mo F, Zoubeidi A, Anderson S, Bell RH, Haegert A, Shukin R, Wang Y, Fazli L, Hurtado Coll A, Jones EC, Hach F, Hormozdiari F, Hajirasouliha I, Boutros PC, Bristow RG, Zhao Y, Marra MA, Fanjul A, Maher CA, Chinnaiyan AM, Rubin MA, Beltran H, Sahinalp SC, Gleave ME, Volik SV, Collins CC. From sequence to molecular pathology, and a mechanism driving the neuroendocrine phenotype in prostate cancer. J Pathol 2012;227(3):286 297.
17. Negrini S, Prada I, D'Alessandro R, Meldolesi J. REST: An oncogene or a tumor suppressor? Trends Cell Biol 2013;23(6): 289 295.
18. Huang J, Wu C, di Sant'Agnese PA, Yao JL, Cheng L, Na Y. Function and molecular mechanisms of neuroendocrine cells in prostate cancer. Anal Quant Cytol Histol 2007;29(3):128 138.
19. Immaneni A, Lawinger P, Zhao Z, Lu W, Rastelli L, Morris JH, Majumder S. REST VP16 activates multiple neuronal differentia tion genes in human NT2 cells. Nucleic Acids Res 2000;28(17): 3403 3410.
20. Huang Z, Wu Q, Guryanova OA, Cheng L, Shou W, Rich JN, Bao S. Deubiquitylase HAUSP stabilizes REST and promotes maintenance of neural progenitor cells. Nat Cell Biol 2011;13(2): 142 152.
21. Westbrook TF, Hu G, Ang XL, Mulligan P, Pavlova NN, Liang A, Leng Y, Maehr R, Shi Y, Harper JW, Elledge SJ. SCFbeta TRCP controls oncogenic transformation and neural differentiation through REST degradation. Nature 2008; 452(7183):370 374.

22. Deeble PD, Marphy DJ, Parsons SJ, Cox ME. Interleukin 6 and cyclic AMP mediated signaling potentiates neuroendocrine dif ferentiation of LNCaP prostate tumor cells. Mol Cell Biol 2001;21(24):8471 8482.

23. Spiotto MT, Chung TDK. STAT3 mediates IL 6 induced neuroen docrine differentiation in prostate cancer cells. Prostate 2000; 42(3):186 195.

24. Westbrook TF, Martin ES, Schlabach MR, Leng Y, Liang AC, Feng B, Zhao JJ, Roberts TM, Mandel G, Hannon GJ, Depinho RA, Chin L, Elledge SJ. A genetic screen for candidate tumor suppressors identifies REST. Cell 2005;121(6):837 848.

25. Svensson C, Ceder J, Iglesias Gato D, Chuan YC, Pang ST, Bjartell A, Martinez RM, Bott L, Helczynski L, Ulmert D, Wang Y, Niu Y, Collins C, Flores Morales A. REST mediates androgen receptor actions on gene repression and predicts early recurrence of prostate cancer. Nucleic Acids Res 2014;42(2):999 1015.

26. Liang H, Studach L, Hullinger RL, Xie J, Andrisani OM. Down regulation of RE 1 silencing transcription factor (REST) in advanced prostate cancer by hypoxia induced miR 106b~25. Exp Cell Res 2014;320(2):188 199.

Upregulation of glucose metabolism by NF-κB2/p52 mediates enzalutamide resistance in castration-resistant prostate cancer cells

Yuanyuan Cui[1], Nagalakshmi Nadiminty[1], Chengfei Liu[1], Wei Lou[1], Chad T Schwartz[1] and Allen C Gao[1,2]

[1]Department of Urology, University of California Davis Medical Center, 4645 2nd Avenue, Research, III, Suite 1300, Sacramento, California 95817, USA
[2]UC Davis Comprehensive Cancer Center, University of California Davis, California, USA

Correspondence should be addressed to A C Gao
Email
acgao@ucdavis.edu

Abstract

Cancer cells reprogram their metabolic pathways to facilitate fast proliferation. Previous studies have shown that overexpression of NF-κB2/p52 (p52) in prostate cancer cells promotes cell growth and leads to castration resistance through aberrant activation of androgen receptor (AR). In addition, these cells become resistant to enzalutamide. In this study, we investigated the effects of p52 activation on glucose metabolism and on response to enzalutamide therapy. Data analysis of gene expression arrays showed that genes including *GLUT1* (*SLC2A1*), *PKM2*, *G6PD*, and *ME1* involved in the regulation of glucose metabolism were altered in LNCaP cells overexpressing p52 compared with the parental LNCaP cells. We demonstrated an increased amount of glucose flux in the glycolysis pathway, as well as the pentose phosphate pathway (PPP) upon p52 activation. The p52-overexpressing cells increase glucose uptake and are capable of higher ATP and lactate production compared with the parental LNCaP cells. The growth of p52-overexpressing cells depends on glucose in the culture media and is sensitive to glucose deprivation compared with the parental LNCaP cells. Targeting glucose metabolism by the glucose analog 2-deoxy-D-glucose synergistically inhibits cell growth when combined with enzalutamide, and resensitizes p52-overexpressing cells to enzalutamide treatment. These results suggest that p52 modulates glucose metabolism, enhances glucose flux to glycolysis and PPPs, thus facilitating fast proliferation of the cells. Co-targeting glucose metabolism together with AR axis synergistically inhibits cell growth and restores enzalutamide-resistant cells to enzalutamide treatment.

Key Words
- prostate cancer
- glucose metabolism
- NF κB2/p52
- enzalutamide

Endocrine Related Cancer
(2014) 21, 435 442

Introduction

As the second leading cause of cancer-related death among men in the United States, prostate tumors respond to androgen deprivation therapy initially; however, after time, relapse occurs and develops into a lethal form of disease, termed castration-resistance prostate cancer (CRPC; Chen *et al.* 2004, Harris *et al.* 2009). The NF-κB

http://erc.endocrinology-journals.org
DOI: 10.1530/ERC-14-0107

Published by Bioscientifica Ltd.

family has been identified as an important mediator in many cancer-causing processes. The family consists of five members: RelA/p65, NF-κB1/p50, c-Rel, RelB, and NF-κB2/p52, in which p65/p50 heterodimer and RelB/p52 heterodimer are involved in the canonical and non-canonical NF-κB pathways respectively (Fan & Maniatis 1991, Betts & Nabel 1996, Lin *et al*. 1998, Karin & Greten 2005). The non-canonical pathway that involves the processing of NF-κB2 p100 to p52 is inducible and tightly regulated (Xiao *et al*. 2001*a*,*b*, Xiao *et al*. 2004, Nadiminty *et al*. 2006). Overproduction of p52 from p100 causes hyperplastic growth in the liver, lymphocytes, and mammary glands of mice (Ishikawa *et al*. 1997, Connelly *et al*. 2007). In several solid tumors, including breast and prostate, overproduction of p52 has been observed (Cogswell *et al*. 2000, Lessard *et al*. 2006). In previous studies, we have shown that NF-κB2/p52 induces castration-resistant growth in prostate cancer cells through aberrant activation of androgen receptor (AR) (Nadiminty *et al*. 2008, 2010*a*). In addition, p52-overexpressing cells are resistant to enzalutamide, a newly approved anti-androgen drug for CRPC patients (Tran *et al*. 2009, Nadiminty *et al*. 2013). Yet, the effect of p52 on cellular metabolism has not previously been studied.

Different from highly differentiated normal cells, cancer cells reprogram their metabolism to facilitate fast proliferation. One typical feature is known as the 'Warburg effect', also called aerobic glycolysis, where cancer cells mainly depend on glycolysis for their energy production in the presence of oxygen (Warburg 1956). This process produces far less energy than that oxidative phosphorylation exhibited in normal cells; however, it produces more intermediate products for anabolic building blocks and much less oxidative stress to keep the redox balance (Cairns *et al*. 2011, Vander Heiden 2011, DeBerardinis & Thompson 2012, Teicher *et al*. 2012). It has been reported that metabolic enzymes such as pyruvate kinase can be alternatively spliced to isoform M2, which supports anabolic growth and promotes tumorigenesis (Christofk *et al*. 2008*a*, Sun *et al*. 2011). Activation of many oncogenes, such as *PI3K* (*PIK3CA*), *AKT*, *mTORC1*, and *MYC*, can also impact metabolism of mitochondria (Berwick *et al*. 2002, Buzzai *et al*. 2005, Hatzivassiliou *et al*. 2005, Cunningham *et al*. 2007).

In this study, we demonstrated through gene expression array data analysis that genes involved in glucose metabolic pathways in p52-overexpressing LNCaP cells were upregulated. Further analysis on glucose metabolism revealed enhancements in both the glycolysis and pentose phosphate pathways (PPPs) accompanied by higher glucose consumption and lactate production. Moreover, targeting glucose metabolism by glucose analog 2-deoxy-D-glucose (2-DG) resensitized p52-overexpressing prostate cancer cells' response to enzalutamide.

Materials and methods

Cell culture and reagents

LNCaP and C4-2B cells were cultured in RPMI-1640 medium supplemented with 10% fetal bovine serum (FBS), 100 units/ml penicillin, and 0.1 mg/ml streptomycin and maintained at 37 °C in a humidified incubator with 5% CO_2. LNCaP-neo and LNCaP-p52 stable cells are generated as described previously (Nadiminty *et al*. 2010*b*). C4-2B MDVR cells were generated by culturing C4-2B cells in media containing 20 μM enzalutamide until the cells became resistant to enzalutamide as described previously (Nadiminty *et al*. 2013). The cells were seeded in 24-well plates and treated with 20 μM enzalutamide and/or 1 mM/2 mM 2-DG after 24 h. After 48 72 h of treatment, they were counted and harvested; medium was collected for glucose consumption, lactate production, and PSA concentration assays. 2-DG was purchased from Sigma Aldrich. ATP assay kit was purchased from PerkinElmer (Santa Clara, CA, USA). Glucose consumption, lactate production, pyruvate kinase activity, and NADPH/NADP assay kits were all purchased from Biovision (Milpitas, CA, USA). PSA ELISA kit was purchased from Abnova (Walnut, CA, USA).

Microarray pathway analysis

Metabolic pathways of NF-κB2/p52 were analyzed using Ingenuity Pathway Analysis Software (Ingenuity). This method uses gene identities in conjunction with controlled, vocabulary-based data mining of literature associations, protein protein interaction databases, and a metabolism pathway database.

Preparation of whole-cell extracts

Cells were washed twice with PBS and lysed for 20 min on ice with cell lysis buffer containing 10 mM HEPES, pH 7.9, 250 mM NaCl, 1 mM EDTA, 1% NP-40, supplemented with 1 mM dithiothreitol, 1 mM phenylmethylsulphonyl fluoride, 5 mM NaF, 1 mM Na_3VO_4, and protease inhibitors (Roche).

http://erc.endocrinology-journals.org
DOI: 10.1530/ERC-14-0107

Published by Bioscientifica Ltd.

Western blot analysis

The cell extracts were obtained and separated by SDS PAGE and the proteins transferred onto nitrocellulose membranes. The membranes were blocked by 5% non-fat milk in PBS/0.05%Tween-20, followed by probing with appropriate primary and secondary antibodies.

Cell transfection

CWR22Rv1 cells were transiently transfected with HA tag-labeled p52 plasmid. The cells were plated at density of 1×10^5/ml 1 day before transfection, which was done by Attractene (Qiagen) following the manufacturer's instruction.

Measurement of ATP production, glucose consumption, and lactate production

ATP levels in the cell lysate were determined by luminescence-based assay kit (ATPlite; PerkinElmer) according to the manufacturer's instruction. The cells were seeded in the culture dishes and the medium was changed after 12 h. The culture medium was collected for the measurement of glucose and lactate concentration after 24 48 h. Glucose levels were determined by comparing difference in the collected medium and fresh medium using a glucose assay kit (Biovision). Lactate levels were measured by lactate assay kit (Biovision). ATP production, glucose consumption, and lactate production levels were normalized to cell number.

NADPH/NADP assay

The cells were harvested after 48 h of culture. NADP total (NADPH and NADP) levels and NADPH levels were determined by a commercially available assay kit (Biovision). NADP levels were determined by the difference between NADP total and NADPH levels. The ratio was calculated thereafter.

Glucose deprivation assay

The cells were seeded into 12-well plates 1 day before switching to an RPMI-1640 glucose-free medium containing 10% dialyzed FBS. The cells were counted 3 days after changing the medium.

PSA ELISA assay

Culture medium was collected 2 days after seeding cells or drug treatment. PSA levels in the medium were measured by a commercially available kit, following the manufacturer's instruction. Data are expressed as mean ± S.D. from three independent experiments.

Statistical analysis

All data presented are shown as mean ± S.D. Student's *t*-test was used to compare differences between two groups. $P<0.05$ was considered significant.

Results

Alteration of glucose pathways by p52

Our previous studies have demonstrated that p52-overexpressing LNCaP prostate cancer cells are more aggressive in terms of tumour growth, resistance to androgen deprivation, and enzalutamide treatment (Nadiminty *et al.* 2006, 2008, 2010*a*,*b*, 2013). As it is well documented that cancer cells reprogram their metabolism to facilitate fast proliferation, we examined the metabolic pathways in p52-overexpressing LNCaP cells by analyzing the gene expression microarray data generated from p52 retrovirus-infected cells (Nadiminty *et al.* 2010*b*).

Of the top 30 altered pathways by overexpression of p52 in LNCaP cells compared with the parental LNCaP cells, the intermediate or final products of 11 pathways, including the top 2 pathways, are involved in sugar metabolism, fatty acid synthesis, and/or lipid biosynthesis and degradation. Five pathways are correlated to amines, polyamines, amino acids biosynthesis, and degradation. In addition, pathways involved in the biosynthesis and degradation of nucleoside and nucleotide as well as biosynthesis of vitamin, NAD, and polysaccharides are all significantly enhanced. The most altered metabolic pathways are listed in Fig. 1A. These findings suggest that in p52 cells, anabolic metabolism pathways are enhanced, providing additional byproducts necessary for cell division, thus facilitating quicker cell proliferation.

In correspondence with the enhanced macromolecular biosynthesis, glycolysis processes including fermentation of pyruvate to lactate are at top of the list. Many key enzymes within glycolysis, such as PFKP, GAPDHS, PGK1, ENO1, ENO3, PKM2, and LDHA, have elevated expression levels in LNCaP-p52 cells compared with the parental LNCaP cells (Fig. 1B). In addition to the upregulated genes in glycolysis, genes within the PPP, such as *G6PD*, *PGD*, *TALDO1*, and *TKT*, are also upregulated (Fig. 1B).

http://erc.endocrinology-journals.org
DOI: 10.1530/ERC-14-0107

Published by Bioscientifica Ltd.

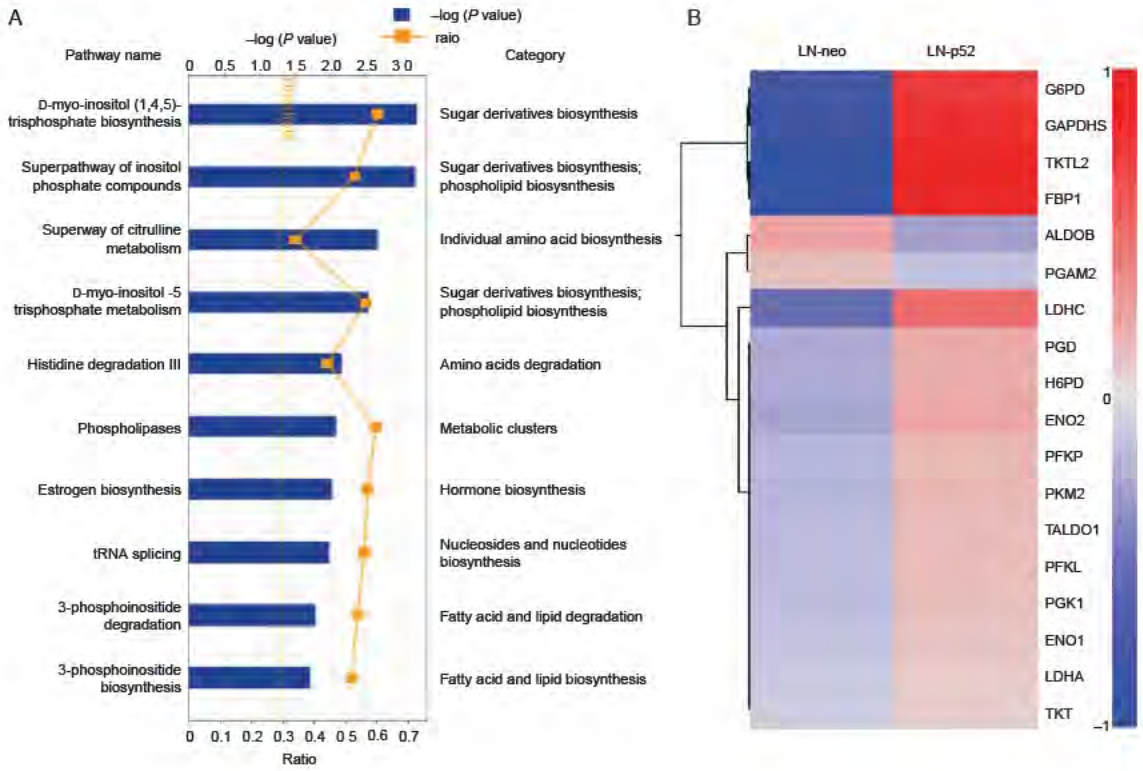

Figure 1

Metabolic pathways and genes altered in LNCaP p52 cells. (A) Top 10 altered metabolic pathways are listed. Blue boxes show log (*P* value). Yellow dots show in $\log_2$ (fold change). Fold change threshold is set as 1.2. (B) Heat map of gene expression within glycolysis and pentose phosphate pathways. All genes of the glycolysis and pentose phosphate pathways with a > 1.2 fold change are included in the heat map. Color scale shows the format of $\log_2$ (fold change).

p52 enhances glucose metabolism

Gene expression array data suggest the alteration of glucose metabolic pathway by p52 in LNCaP cells. To further understand reprogramed glucose metabolism by p52, we assayed several indicators within the glucose metabolic pathways. Glucose uptake is the first step in glucose metabolism, which can be measured by the expression levels of glucose transporter, GLUT1, and by glucose consumption assays. LNCaP-p52 cells expressed GLUT1 at higher levels compared with the control (Fig. 2A), consistent with higher glucose consumption in p52 overexpression cells compared with the control (Fig. 2B). These data suggest an increased glucose uptake and consumption by the cells overexpressing p52. As a rate-limiting final step of glycolysis, catalysis of PEP to pyruvate by PKM2, a splice isoform of pyruvate kinase, plays important roles in cancer metabolism. Expression of PKM2 has a growth advantage for tumor cells *in vivo* (Christofk *et al.* 2008*a*,*b*). Our gene expression array data indicated an increased expression of *PKM2* mRNA by overexpression of p52. To confirm whether p52 enhances PKM2 protein expression, we analyzed the expression of PKM2 and phosphorylated PKM2. As shown in Fig. 2A, the protein levels of both PKM2 and phosphorylated PKM2 were upregulated in LNCaP-p52 cells compared with the control. As cancer cells mainly generate energy from aerobic glycolysis of glucose, we measured ATP production as an indicator of aerobic glycolysis. The p52-overexpressing LNCaP cells are capable of generation of higher ATP production compared with the parental LNCaP cells (Fig. 2C). In addition to ATP production, lactate production was also increased in LNCaP-p52 cells compared with the parental LNCaP cells (Fig. 2D).

PPP is a branch shunt from glycolysis, which provides intermediate products for nucleoside synthesis, and more importantly provides reductants such as NADPH to maintain the redox balance of fast proliferating cells. The enzyme involved in the first step of PPP flux, G6PD, was upregulated in LNCaP-p52 cells (Fig. 3A). In addition, the NADPH:NADP ratio was also much higher in LNCaP-p52 cells than control cells (Fig. 3B), suggesting an overall

http://erc.endocrinology-journals.org
DOI: 10.1530/ERC-14-0107

Published by Bioscientifica Ltd.

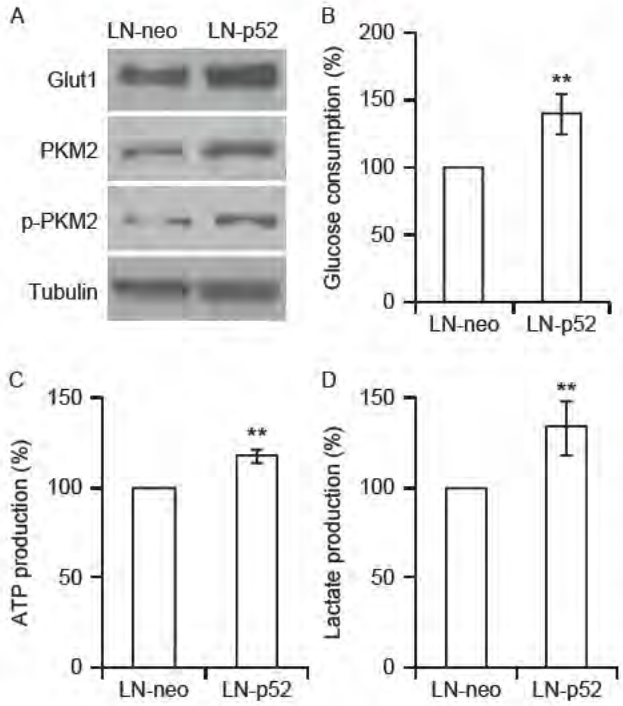

Figure 2
p52 increases LNCaP cells' glucose uptake and aerobic glycolysis. (A) Western blots for glucose transporter 1 (GLUT1), PKM2, phospho PKM2. Tubulin was used as a loading control. Glucose consumption (B), ATP production (C), lactate production (D) of LNCaP p52 cells compared with LNCaP neo cells. Data are presented as mean ± s.d. of at least three independent experiments. $^{**}P<0.01$.

enhanced PPP in LNCaP-p52 cells. To test whether p52-mediated glucose metabolism is not LNCaP cell specific, CWR22Rv1 cells were transiently transfected with p52. As shown in Fig. 3C, transient transfection of p52 increased PKM2 expression and glucose consumption in CWR22Rv1 cells (Fig. 3C). Collectively, these data suggest that overexpression of p52 enhances glucose metabolism in LNCaP cells.

Overexpression of p52 increases cell sensitivity to glucose deprivation and 2-DG treatment

As LNCaP-p52 cells have higher glucose uptake and rate of glucose metabolism, we hypothesized that p52-overexpressing LNCaP cells might be dependent on glucose for survival, and were more sensitive to glucose deprivation than parental LNCaP cells. To test that, we monitored cell growth in the absence of glucose. As shown in Fig. 4A, more cells were dead among p52-overexpressing LNCaP cells compared with the parental LNCaP cells when they grew in the media deprived of glucose. To further confirm this observation, we treated the cells with an analog of glucose, 2-DG, an inhibitor of glucose metabolism. As shown in Fig. 4B, p52-overexpressing LNCaP cells were more sensitive to 2-DG treatment than parental LNCaP cells. These results suggest that p52-overexpressing LNCaP cells are more sensitive to glucose deprivation than parental LNCaP cells.

Targeting glucose metabolism by 2-DG resensitizes LNCaP-p52 cells to enzalutamide treatment

Our previous studies have shown that LNCaP-p52 cells were resistant to enzalutamide treatment (Nadiminty *et al.* 2013). As LNCaP-p52 cells exhibit enhanced glucose consumption and are more sensitive to glucose deprivation and 2-DG treatment, we combined 2-DG with enzalutamide to examine whether the combination treatment could restore the cells' sensitivity to enzalutamide. As shown in Fig. 5A, a low dose of 2-DG (1 mM) combined with 20 μM enzalutamide dramatically reduced LNCaP-p52 cell number.

We previously generated enzalutamide-resistant C4-2B MDVR cells (Nadiminty *et al.* 2013). Similar to

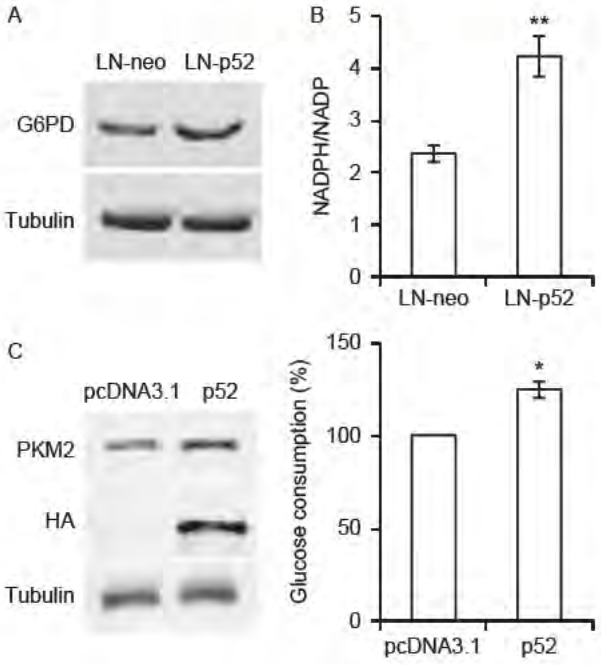

Figure 3
(A) Western blots for G6PD of LNCaP neo and LNCaP p52 cells. Tubulin was used as a loading control. (B) NADPH:NADP ratio of LNCaP p52 cells compared with LNCaP neo cells. (C) Transient transfection of p52 enhances glucose metabolism in CWR22Rv1 cells. Immunoblots of HA tagged p52, PKM2, and tubulin in transiently transfected LNCaP cells (left). Glucose consumption assay in transient vehicle and p52 transfected CWR22Rv1 cells (right). Data was presented as mean ± s.d. of three independent experiments. $^{*}P<0.05$, $^{**}P<0.01$.

http://erc.endocrinology-journals.org
DOI: 10.1530/ERC-14-0107

Published by Bioscientifica Ltd.

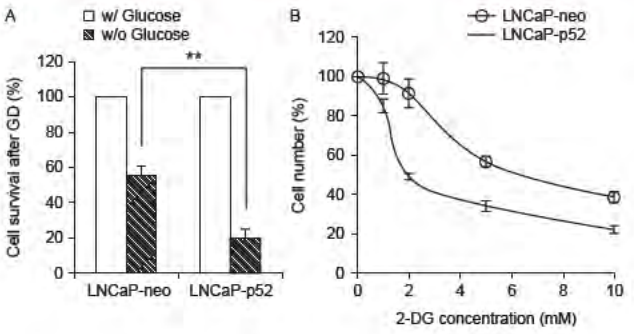

Figure 4
LNCaP p52 cells are more sensitive to glucose deprivation and 2 DG treatment. (A) Cell growth comparison after 3 days of glucose deprivation. Cell numbers of LNCaP neo and LNCaP p52 cells in absence of glucose are normalized to the ones with glucose respectively. (B) Cell growth of LNCaP p52 and LNCaP neo at different concentrations of 2 DG. Data are presented as mean ± s.d. in three independent experiments. $^{**}P<0.01$.

LNCaP-p52 cells, C4-2B MDVR cells have enhanced glucose consumption and ATP and lactate production (Fig. 5B). As 2-DG can greatly resensitize the response of LNCaP-p52 cells to enzalutamide, we tested whether 2-DG would have a similar effect to MDV-resistant cells. Combination treatment with 2-DG and enzalutamide significantly decreased cell number in C4-2B MDVR cells (Fig. 5C and D). Collectively, these data suggest that targeting glucose metabolism can resensitize enzalutamide treatment in enzalutamide-resistant prostate cancer cells.

Discussion

Our previous studies have demonstrated that p52-overexpressing LNCaP cells grew significantly larger tumors *in vivo*, became castration-resistant through aberrant AR activation and resistant to enzalutamide treatment. Cancer cells have reprogramed metabolism to facilitate fast proliferation. In the present study, we analyzed glucose metabolism in p52-overexpressing prostate cancer cells, and found that glycolysis and PPP are both upregulated, indicating upregulation of glucose metabolism and ATP production by p52. Targeting glucose metabolism by 2-DG resensitizes the cell's response to enzalutamide of not only LNCaP-p52 cells, but also other enzalutamide-resistant cells, like C4-2B MDVR cells.

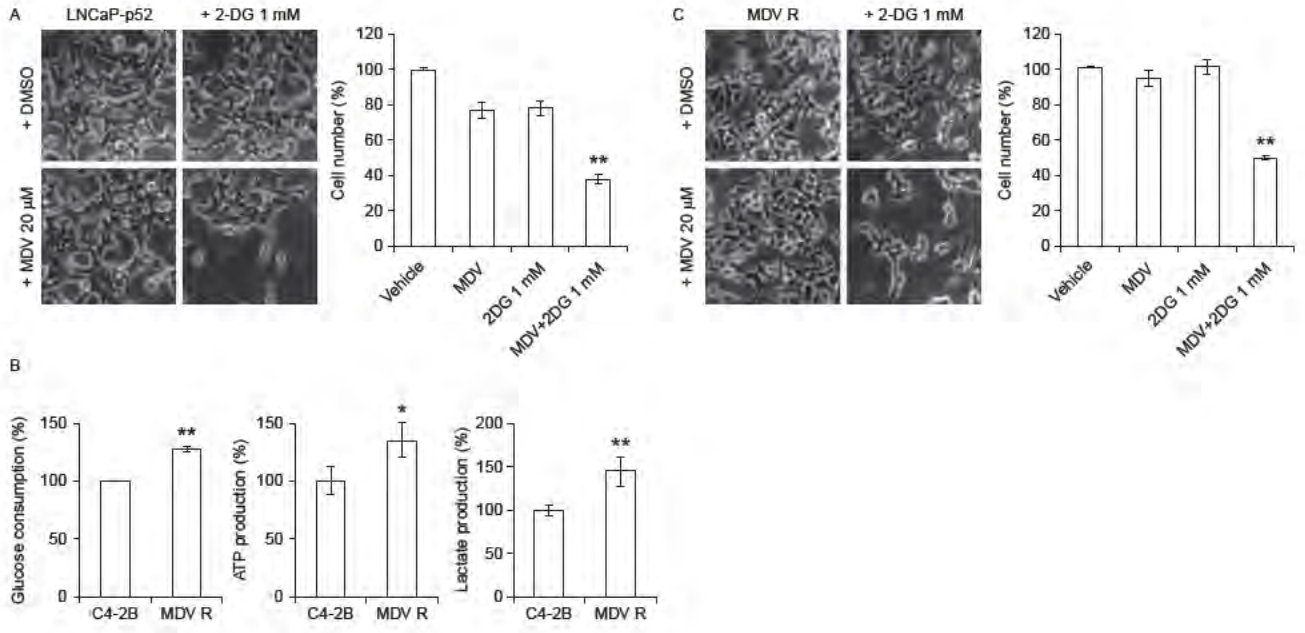

Figure 5
2 DG resensitizes cells to enzalutamide treatment. (A) Cell morphology of LNCaP p52 cells was shown after 2 days treatment with 2 DG in combination with or without enzalutamide. Vehicle control and 2 DG treatment were shown in top panel. Enzalutamide and combination treatment with 1 mM 2 DG were shown in bottom panel. (Right panel) Cell growth after 2 days of treatment. All numbers were normalized to vehicle group. Data were presented as mean ± s.d. in at least three independent experiments. (B) Glucose consumption (left), ATP production (middle), and lactate production (right) in C4 2B MDVR enzalutamide resistant cells compared with parental C4 2B enzalutamide sensitive cells. (C) 2 DG resensitizes C4 2B MDVR enzalutamide resistant cells' response to enzalutamide treatment. Cell numbers were normalized to vehicle group. Data were presented as mean ± s.d. in three independent experiments; $^{*}P<0.05$, $^{**}P<0.01$.

http://erc.endocrinology-journals.org
DOI: 10.1530/ERC-14-0107

Published by Bioscientifica Ltd.

The Warburg effect is a widely observed feature in tumors with elevated glucose uptake, glucose consumption, and lactate production. Several enzymes including GLUT1, PKM2, and LDHA are critically involved in glucose metabolism. We have shown that the levels of GLUT1 (*SLC2A1*), PKM2, and LDHA gene expression were upregulated in p52-overexpressing LNCaP cells, which correlated with higher glucose metabolism. The upregulation of these rate-limiting glucose metabolic enzymes may play a critical role in the p52-induced Warburg effect, featuring elevated glucose consumption and higher lactate production. One typical feature of cancer cells is switching energy production from oxidative phosphorylation to glycolysis to generate additional precursors for macromolecular biosynthesis. Gene expression microarray data analysis showed an enhanced macromolecular biosynthesis in p52-overexpressing LNCaP cells compared with the parental LNCaP cells, suggesting an enhanced production of building blocks for these macromolecules derived from glucose metabolites. This is in consistence with the upregulated glucose metabolism pathways observed in p52-overexpressing LNCaP cells.

Due to an altered glucose metabolism that cancer cells usually have, targeting glucose metabolism to inhibit cancer progression is an attractive approach for cancer therapy. 2-DG, a glucose analog, is the most widely investigated drug in experimental and clinical oncology (Dwarakanath & Jain 2009). 2-DG is competitively taken up by cells through the same transporter as glucose and transformed by hexokinase to 2-DG-6-phosphate which cannot be metabolized further, therefore decreasing the glucose flux to glycolysis and PPPs. However, as a single therapeutic agent, the clinical trial of 2-DG has been discontinued due to persistent side effects such as diaphoresis and disturbance of the CNS (Dwarakanath *et al*. 2009, Gupta *et al*. 2009). A potential promising approach is to combine 2-DG therapy with radiation or chemotherapy drugs (Gupta *et al*. 2009). Enzalutamide, a newly approved anti-androgen drug, can effectively inhibit CRPC cell growth *in vivo* (Tran *et al*. 2009). Despite its successes and continuing widespread use, development of resistance is inevitable. Our previous studies have demonstrated that p52-overexpressing LNCaP cells were resistant to enzalutamide (Nadiminty *et al*. 2013). In the present study, we combined 2-DG and enzalutamide and found that a low dose of 2-DG resensitized the response of p52-overexpressing LNCaP cells to enzalutamide treatment. The combination of these two drugs has profound synergistic effects on the inhibition of cell growth. We further validated the synergistic effects of combination treatment of 2-DG with enzalutamide in another enzalutamide-resistant C4-2B-MDVR cells.

In summary, these results suggest that p52 modulates glucose metabolism and enhances glucose flux to glycolysis and PPPs, thus facilitating fast proliferation of the cells. Targeting glucose metabolism by deprivation of glucose or using glucose analog, such as 2-DG, inhibits cell growth. We found that combination treatment of 2-DG with enzalutamide could resensitize enzalutamide-resistant prostate cancer cells to enzalutamide treatment, suggesting a potential therapeutic approach for CRPC patients, by co-targeting glucose metabolism and AR pathways.

Declaration of interest

The authors declare that there is no conflict of interest that could be perceived as prejudicing the impartiality of the research reported.

Funding

This work is supported in part by grants NIH/NCI CA140468, CA168601, CA179970, and US Department of Veterans Affairs, Office of Research and Development VA Merits I01 BX000526 (A C Gao), and by resources from the VA Northern California Health Care System, Sacramento, California.

References

Berwick DC, Hers I, Heesom KJ, Moule SK & Tavare JM 2002 The identification of ATP-citrate lyase as a protein kinase B (Akt) substrate in primary adipocytes. *Journal of Biological Chemistry* **277** 33895–33900. (doi:10.1074/jbc.M204681200)

Betts JC & Nabel GJ 1996 Differential regulation of NF-κB2(p100) processing and control by amino-terminal sequences. *Molecular and Cellular Biology* **16** 6363–6371.

Buzzai M, Bauer DE, Jones RG, Deberardinis RJ, Hatzivassiliou G, Elstrom RL & Thompson CB 2005 The glucose dependence of Akt-transformed cells can be reversed by pharmacologic activation of fatty acid β-oxidation. *Oncogene* **24** 4165–4173. (doi:10.1038/sj.onc.1208622)

Cairns RA, Harris IS & Mak TW 2011 Regulation of cancer cell metabolism. *Nature Reviews. Cancer* **11** 85–95. (doi:10.1038/nrc2981)

Chen CD, Welsbie DS, Tran C, Baek SH, Chen R, Vessella R, Rosenfeld MG & Sawyers CL 2004 Molecular determinants of resistance to anti-androgen therapy. *Nature Medicine* **10** 33–39. (doi:10.1038/nm972)

Christofk HR, Vander Heiden MG, Harris MH, Ramanathan A, Gerszten RE, Wei R, Fleming MD, Schreiber SL & Cantley LC 2008*a* The M2 splice isoform of pyruvate kinase is important for cancer metabolism and tumour growth. *Nature* **452** 230–233. (doi:10.1038/nature06734)

Christofk HR, Vander Heiden MG, Wu N, Asara JM & Cantley LC 2008*b* Pyruvate kinase M2 is a phosphotyrosine-binding protein. *Nature* **452** 181–186. (doi:10.1038/nature06667)

Cogswell PC, Guttridge DC, Funkhouser WK & Baldwin AS Jr 2000 Selective activation of NF-κB subunits in human breast cancer: potential roles for NF-κB2/p52 and for Bcl-3. *Oncogene* **19** 1123–1131. (doi:10.1038/sj.onc.1203412)

Connelly L, Robinson-Benion C, Chont M, Saint-Jean L, Li H, Polosukhin VV, Blackwell TS & Yull FE 2007 A transgenic model reveals

Published by Bioscientifica Ltd.

important roles for the NF-κB alternative pathway (p100/p52) in mammary development and links to tumorigenesis. *Journal of Biological Chemistry* **282** 10028–10035. (doi:10.1074/jbc.M611300200)

Cunningham JT, Rodgers JT, Arlow DH, Vazquez F, Mootha VK & Puigserver P 2007 mTOR controls mitochondrial oxidative function through a YY1-PGC-1α transcriptional complex. *Nature* **450** 736–740. (doi:10.1038/nature06322)

DeBerardinis RJ & Thompson CB 2012 Cellular metabolism and disease: what do metabolic outliers teach us? *Cell* **148** 1132–1144. (doi:10.1016/j.cell.2012.02.032)

Dwarakanath B & Jain V 2009 Targeting glucose metabolism with 2-deoxy-D-glucose for improving cancer therapy. *Future Oncology* **5** 581–585. (doi:10.2217/fon.09.44)

Dwarakanath BS, Singh D, Banerji AK, Sarin R, Venkataramana NK, Jalali R, Vishwanath PN, Mohanti BK, Tripathi RP, Kalia VK *et al.* 2009 Clinical studies for improving radiotherapy with 2-deoxy-D-glucose: present status and future prospects. *Journal of Cancer Research and Therapeutics* **5** (Suppl 1) S21–S26. (doi:10.4103/0973-1482.55136)

Fan CM & Maniatis T 1991 Generation of p50 subunit of NF-κB by processing of p105 through an ATP-dependent pathway. *Nature* **354** 395–398. (doi:10.1038/354395a0)

Gupta S, Farooque A, Adhikari JS, Singh S & Dwarakanath BS 2009 Enhancement of radiation and chemotherapeutic drug responses by 2-deoxy-D-glucose in animal tumors. *Journal of Cancer Research and Therapeutics* **5** (Suppl 1) S16–S20. (doi:10.4103/0973-1482.55135)

Harris WP, Mostaghel EA, Nelson PS & Montgomery B 2009 Androgen deprivation therapy: progress in understanding mechanisms of resistance and optimizing androgen depletion. *Nature Clinical Practice Urology* **6** 76–85. (doi:10.1038/ncpuro1296)

Hatzivassiliou G, Zhao F, Bauer DE, Andreadis C, Shaw AN, Dhanak D, Hingorani SR, Tuveson DA & Thompson CB 2005 ATP citrate lyase inhibition can suppress tumor cell growth. *Cancer Cell* **8** 311–321. (doi:10.1016/j.ccr.2005.09.008)

Ishikawa H, Carrasco D, Claudio E, Ryseck RP & Bravo R 1997 Gastric hyperplasia and increased proliferative responses of lymphocytes in mice lacking the COOH-terminal ankyrin domain of NF-κB2. *Journal of Experimental Medicine* **186** 999–1014. (doi:10.1084/jem.186.7.999)

Karin M & Greten FR 2005 NF-κB: linking inflammation and immunity to cancer development and progression. *Nature Reviews. Immunology* **5** 749–759. (doi:10.1038/nri1703)

Lessard L, Karakiewicz PI, Bellon-Gagnon P, Alam-Fahmy M, Ismail HA, Mes-Masson AM & Saad F 2006 Nuclear localization of nuclear factor-κB p65 in primary prostate tumors is highly predictive of pelvic lymph node metastases. *Clinical Cancer Research* **12** 5741–5745. (doi:10.1158/1078-0432.CCR-06-0330)

Lin X, Mu Y, Cunningham ET Jr, Marcu KB, Geleziunas R & Greene WC 1998 Molecular determinants of NF-κB-inducing kinase action. *Molecular and Cellular Biology* **18** 5899–5907.

Nadiminty N, Lou W, Lee SO, Lin X, Trump DL & Gao AC 2006 Stat3 activation of NF-κB p100 processing involves CBP/p300-mediated acetylation. *PNAS* **103** 7264–7269. (doi:10.1073/pnas.0509808103)

Nadiminty N, Chun JY, Lou W, Lin X & Gao AC 2008 NF-κB2/p52 enhances androgen-independent growth of human LNCaP cells via protection from apoptotic cell death and cell cycle arrest induced by androgen-deprivation. *Prostate* **68** 1725–1733. (doi:10.1002/pros.20839)

Nadiminty N, Lou W, Sun M, Chen J, Yue J, Kung HJ, Evans CP, Zhou Q & Gao AC 2010*a* Aberrant activation of the androgen receptor by NF-κB2/p52 in prostate cancer cells. *Cancer Research* **70** 3309–3319. (doi:10.1158/0008-5472.CAN-09-3703)

Nadiminty N, Dutt S, Tepper C & Gao AC 2010*b* Microarray analysis reveals potential target genes of NF-κB2/p52 in LNCaP prostate cancer cells. *Prostate* **70** 276–287. (doi:10.1002/pros.21062)

Nadiminty N, Tummala R, Liu C, Yang J, Lou W, Evans CP & Gao AC 2013 NF-κB2/p52 induces resistance to enzalutamide in prostate cancer: role of androgen receptor and its variants. *Molecular Cancer Therapeutics* **12** 1629–1637. (doi:10.1158/1535-7163.MCT-13-0027)

Sun Q, Chen X, Ma J, Peng H, Wang F, Zha X, Wang Y, Jing Y, Yang H, Chen R *et al.* 2011 Mammalian target of rapamycin up-regulation of pyruvate kinase isoenzyme type M2 is critical for aerobic glycolysis and tumor growth. *PNAS* **108** 4129–4134. (doi:10.1073/pnas.1014769108)

Teicher BA, Linehan WM & Helman LJ 2012 Targeting cancer metabolism. *Clinical Cancer Research* **18** 5537–5545. (doi:10.1158/1078-0432.CCR-12-2587)

Tran C, Ouk S, Clegg NJ, Chen Y, Watson PA, Arora V, Wongvipat J, Smith-Jones PM, Yoo D, Kwon A *et al.* 2009 Development of a second-generation antiandrogen for treatment of advanced prostate cancer. *Science* **324** 787–790. (doi:10.1126/science.1168175)

Vander Heiden MG 2011 Targeting cancer metabolism: a therapeutic window opens. *Nature Reviews. Drug Discovery* **10** 671–684. (doi:10.1038/nrd3504)

Warburg O 1956 On the origin of cancer cells. *Science* **123** 309–314. (doi:10.1126/science.123.3191.309)

Xiao G, Cvijic ME, Fong A, Harhaj EW, Uhlik MT, Waterfield M & Sun SC 2001*a* Retroviral oncoprotein Tax induces processing of NF-κB2/p100 in T cells: evidence for the involvement of IKKα. *EMBO Journal* **20** 6805–6815. (doi:10.1093/emboj/20.23.6805)

Xiao G, Harhaj EW & Sun SC 2001*b* NF-κB-inducing kinase regulates the processing of NF-κB2 p100. *Molecular Cell* **7** 401–409. (doi:10.1016/S1097-2765(01)00187-3)

Xiao G, Fong A & Sun SC 2004 Induction of p100 processing by NF-κB-inducing kinase involves docking IκB kinase α (IKKα) to p100 and IKKα-mediated phosphorylation. *Journal of Biological Chemistry* **279** 30099–30105. (doi:10.1074/jbc.M401428200)

Received in final form 19 March 2014
Accepted 21 March 2014
Made available online as an Accepted Preprint
21 March 2014

Published by Bioscientifica Ltd.

RhoGDIα Suppresses Growth and Survival of Prostate Cancer Cells

Yezi Zhu,[1,2] Ramakumar Tummala,[1] Chengfei Liu,[1,3] Nagalakshmi Nadiminty,[1] Wei Lou,[1] Christopher P. Evans,[1] Qinghua Zhou,[3] and Allen C. Gao[1,2]*

[1]*Department of Urology, University of California at Davis, Sacramento, California*
[2]*Graduate Program of Pharmacology and Toxicology and Cancer Center, University of California at Davis, Sacramento, California*
[3]*Tianjin Lung Cancer Institute, Tianjin Medical University General Hospital, Tianjin, China*

BACKGROUND. Treatment for primary prostate cancer (CaP) is the withdrawal of androgens. However, CaP eventually progresses to grow in a castration-resistant state. The mechanisms involved in the development and progression of castration-resistant prostate cancer (CRPC) remain unknown. We have previously generated LNCaP-IL6+ cells by treating LNCaP cells chronically with interleukin-6 (IL-6), which have acquired the ability to grow in androgen-deprived conditions.

METHODS. We compared the protein expression profile of LNCaP and LNCaP-IL6+ cells using two-dimensional gel electrophoresis. The gels were then silver stained in order to visualize proteins and the differentially expressed spots were identified and characterized by micro sequencing using MALDI-PMF mass spectrometry.

RESULTS. In this study, we have identified RhoGDIα (GDIα) as a suppressor of CaP growth. Expression of GDIα was reduced in LNCaP-IL6+ cells and was down-regulated in more aggressive CaP cells compared to LNCaP cells. Over expression of GDIα inhibited the growth of CaP cells and caused LNCaP-IL6+ cells reversal to androgen-sensitive state, while down-regulation of GDIα enhanced growth of androgen-sensitive LNCaP CaP cells in androgen-deprived conditions. In addition, GDIα suppressed the tumorigenic ability of prostate tumor xenografts in vivo.

CONCLUSIONS. These results demonstrate that loss of GDIα expression promotes the development and progression of prostate cancer. *Prostate 72: 392 398, 2012.*

KEY WORDS: **prostate cancer; RhoGDIα; IL-6**

INTRODUCTION

Prostate cancer (CaP) is the most common type of cancer in American men and ranks second to lung cancer in cancer-related deaths. One of the important challenges facing CaP is its evolution to castration resistance, for which no effective treatment has been developed. Understanding the molecular mechanisms leading to castration resistance is the key to developing successful therapies to combat this lethal response. IL-6 has been implicated in the modulation of growth and differentiation in many cancers and is associated with poor prognosis in renal cell carcinoma, ovarian cancer, lymphoma, and melanoma [1]. Elevated expression of IL-6 and its receptor have been consistently demonstrated in human CaP cell lines and clinical specimens of CaP and benign prostate hyperplasia [2–4]. Multiple studies have demonstrated that IL-6 is elevated in the sera of patients with

Grant sponsor: VA Merit award; Grant number: I01 BX000526; Grant sponsor: NIH; Grant numbers: CA 109441. CA 140468.

Yezi Zhu and Ramakumar Tummala contributed equally to this work.

*Correspondence to: Allen C. Gao, Department of Urology and Cancer Center, University of California Davis Medical Center, 4645 2nd Ave, Research III, Suite 1300, Sacramento, CA 95817, USA.
E mail: acgao@ucdavis.edu
Received 31 March 2011; Accepted 23 May 2011
DOI 10.1002/pros.21441
Published online 16 June 2011 in Wiley Online Library (wileyonlinelibrary.com).

metastatic CaP and the levels of IL-6 correlate with tumor burden, serum PSA, and clinically evident metastases [5,6]. In addition, serum IL-6 levels are elevated in men with castration-resistant prostate cancer (CRPC) compared to normal controls, benign prostatic hyperplasia, prostatitis, and localized CaP [5]. Collectively, these data suggest that elevated IL-6 levels are associated with the lethal phenotype of CaP.

IL-6 functions as a paracrine growth factor for the human LNCaP androgen-sensitive CaP cells and as an autocrine growth factor for the human DU145 and PC3 androgen-insensitive CaP cells [7]. It has also been reported that IL-6 mediates LNCaP cell growth arrest and induces neuroendocrine differentiation [8–10]. Targeting IL-6 signaling using an anti-IL-6 monoclonal antibody induces regression of human CaP xenografts in nude mice [11], while inhibition of IL-6 with CNT0328, an anti-IL-6 monoclonal antibody inhibits the conversion of an androgen-dependent to independent phenotype in a CaP xenograft in vivo model [12]. These studies suggest that IL-6 promotes CRPC progression.

RhoGDI (GDI) is a cellular regulatory protein that acts primarily by controlling the cellular distribution and activity of Rho GTPases [13]. GDI family comprises three mammalian members: GDIα, which is ubiquitously expressed; GDIβ which has hematopoietic tissue-specific expression, and GDIγ which is membrane-anchored through an amphipathic helix and is preferentially expressed in brain, pancreas, lung, kidney, and testis [14]. GDIα binds to and negatively regulates most Rho GTPases including RhoA, Rac1, and Cdc42 [14]. It has been shown that overexpression of GDI in various cell lines induces disruption of the actin cytoskeleton and loss of substratum adherence and microinjection of GDIα into fibroblasts inhibits cell motility [15,16]. GDIα mRNA level was found to be lower in the metastatic lineage (T24T) of a human bladder cancer cell line (T24) suggesting that Rho activation plays a role in the control of progression to metastasis [17]. Although GDIα is aberrantly expressed in several tumor tissues, its role in cancer progression remains to be unraveled. In this study, we show that GDIα suppresses CaP cell growth, and down-regulation of GDIα promotes the progression of androgen-sensitive cells to a castration-resistant state.

MATERIALS AND METHODS

Cell Culture and Transfections

LNCaP, LAPC-4, PC3, C4-2, and DU145 CaP cells were cultured in RPMI-1640 medium containing either 10% complete fetal bovine serum (FBS) or 10% charcoal-dextran-stripped FBS and penicillin/streptomycin as described previously (29). LNCaP passage numbers <30 were used throughout the study. IL-6-overexpressing LNCaP-IL6+ cells were cultured in RPMI 1640 containing 10% FBS as described previously [18]. For transfection studies, cells were transiently transfected with expressing plasmids using Lipofectamine 2000 (Invitrogen).

Preparation of Whole Cell Extracts

Cells were lysed in a high-salt buffer containing 10 mM Hepes (pH 7.9), 0.25 M NaCl, 1% Nonidet P-40, and 1 mM EDTA with protease inhibitors, and total protein in the lysates was determined with the Coomassie Plus Protein Assay Reagent (Pierce, Rockford, IL).

Cytosolic and Nuclear Protein Preparation

Cells were harvested, washed with PBS twice, and resuspended in a hypotonic buffer [10 mmol/L HEPES-KOH (pH 7.9), 1.5 mmol/L MgCl2, 10 mmol/L KCl, and 0.1% NP40] and incubated on ice for 10 min. Nuclei were precipitated by 3,000 × *g* centrifugation at 4°C for 10 min. The supernatant was collected as the cytosolic fraction. After washing once with the hypotonic buffer, the nuclei were lysed in a lysis buffer [50 mmol/L Tris–HCl (pH 8), 150 mmol/L NaCl, 1% TritonX-100] by mechanical disruption for 30 min at 4°C. The nuclear lysate was precleared by centrifugation at 4°C for 15 min. Protein concentration was determined using the Coomassie Plus protein assay kit (Pierce).

Proteomic Analysis UsingTwo-Dimensional Electrophoresis

Prior to two-dimensional electrophoresis, the protein samples were purified using a 2D Clean-Up kit (GE health care) according to the manufacturer's instructions. Differentially expressed proteins were identified using two-dimensional gel electrophoresis and mass spectrometry. Two-dimensional gel electrophoresis was performed using immobiline strips (pI range, 3–10; GE Healthcare, Piscataway, NJ) with proteins being separated according to charge and subsequently molecular weight. The gels were then silver stained in order to visualize proteins and the differentially expressed spots were identified by MALDI-PMF mass spectrometry.

Western Blot Analysis

Equal amounts of protein were loaded on 10% SDS–PAGE and transferred to nitrocellulose membranes. The membranes were blocked with 5% nonfat

milk in 1× PBS + 0.1% Tween 20 and probed with the indicated primary antibodies. The chemiluminescent signal was detected by enhanced chemiluminescence kit (Amersham) after incubation with the appropriate horseradish peroxidase-conjugated secondary antibodies.

Measurement of PSA

PSA levels were measured in the culture supernatants using ELISA (United Biotech, Inc.) according to the manufacturer's instructions and as described previously [19].

In Vitro Cell Proliferation

Cells (10^4 cells/well) were plated in 12-well plates in RPMI containing 10% FBS. After 2 or 3 days in regular culture medium with 10% FBS, cells were switched into phenol red-free RPMI containing either 10% FBS or 10% charcoal-stripped FBS (Hyclone, UT). Two days later, cell numbers were counted using Coulter counter.

Apoptosis Assays and Cell Death Detection ELISA

Cells were cultured under androgen-depleted conditions (10% charcoal-stripped serum) for 3–7 days after transfection with the indicated plasmids. The degree of apoptosis was measured by cell death detection ELISA according to the manufacturer's instructions. Briefly, floating and attached cells were collected and homogenized in 400 μl of incubation buffer. Five microliters of the supernatant diluted in 95 μl of incubation buffer was used in the ELISA. The wells were coated with anti-histone antibodies and then incubated with the lysates, horseradish peroxidase-conjugated anti-DNA antibodies, and the substrate subsequently, and absorbance was read at 620 nm.

In Vivo Tumor Growth

Four- to six-week-old athymic male nude mice (Harlan, Indianapolis, IN) were injected s.c. in both the flanks with 2×10^6 cells (LNCaP-IL6+/neo and LNCaP-IL6+/GDI) resuspended 1:1 in Matrigel (BD Biosciences, Bedford, MA) and complete culture medium. The volume of the growing tumors was estimated by measuring their three dimensions (Length × Width × Depth) with calipers (23).

Statistical Analysis

All data are presented as mean ± standard deviation (SD). Statistical analyses were performed with Microsoft Excel analysis tools, differences between individual groups were analyzed by paired *t*-test. $P < 0.05$ was considered statistically significant.

RESULTS

GDIα was Identified by Down-Regulated Expression in LNCaP-IL-6+ Cells Compared to LNCaP Cells

We previously generated a subline of LNCaP cells, LNCaP-IL6+, by chronically treating LNCaP cells with 5 ng/ml IL-6 [18]. LNCaP-IL6+ cells were found to have acquired the ability to secrete IL-6 and to grow in castration-resistant conditions in vitro and in vivo [18]. To identify factors that potentially mediate CaP cell growth induced by IL-6, the protein expression profile in LNCaP and LNCaP-IL-6+ cells was analyzed by 2-D gel electrophoresis (Fig. 1A). The differentially expressed spots were isolated from the 2-D gels and micro sequenced by MALDI-PMF. One of the spots that were present in parental LNCaP cells was lost in LNCaP-IL-6+ cells. The spot was identified as GDIα by MALDI-PMF micro sequencing mass spectrometry.

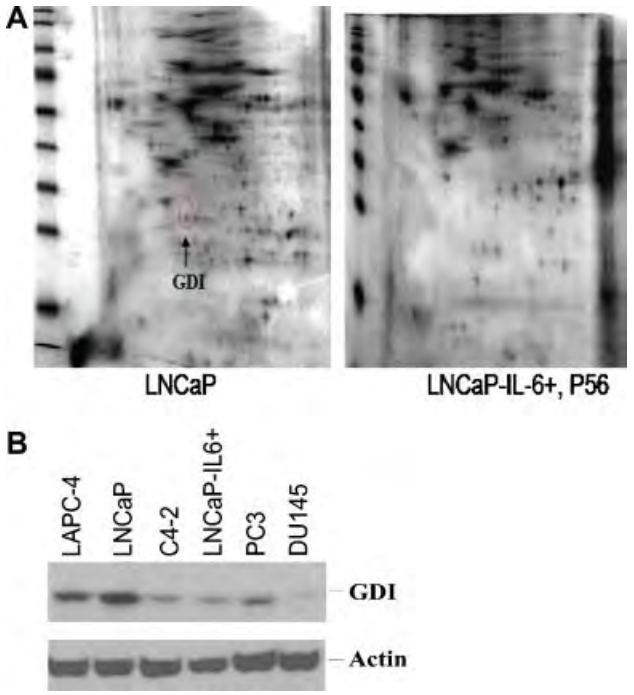

Fig. 1. Identification and characterization of GDIα. **A**: Identification of GDIα protein that is down regulated in LNCaP IL6+ cells compared to LNCaP cells. 2 D gel analysis of LNCaP and LNCaP IL 6+ cells. Arrow indicates GDIα. **B**: GDIα expression is decreased in androgen insensitive cells versus androgen sensitive cells. GDIα expression was analyzed by Western blot using whole cell lysates of androgen sensitive LNCaP, LAPC 4 cells and androgen insenistive C4 2, LNCap IL6+, PC3, and DUI45 cells using antibodies specifically against GDIα. Actin was used as loading control.

GDIα Expression is Decreased in Androgen-Insensitive Cells Versus Androgen-Sensitive Cells

To test whether down-regulation of GDIα expression is associated with the progression of CRPC, we analyzed the expression levels of GDIα in androgen-sensitive LNCaP, LAPC-4 cells, and androgen-insensitive C4-2, LNCaP-IL-6+, PC-3, and DU145 cells by Western blot analysis using antibodies against GDIα. The levels of GDIα protein were decreased in the androgen-insensitive cells compared to those in androgen-sensitive cells. These results suggest that androgen-insensitive growth is associated with decreased levels of GDIα protein (Fig. 1B).

GDIα Inhibits Cell Growth and Induces Apoptotic Cell Death

To examine the effects of GDIα on cell growth in vitro, LNCaP-IL-6+ and DU145 cells that express low levels of GDIα protein were transfected with different concentrations of expression plasmids encoding GDIα and cell numbers were determined. Overexpresion of GDIα inhibited the growth of LNCaP-IL-6+ and DU145 cells in vitro (Fig. 2A). Apoptosis was measured by analyzing the degree of DNA fragmentation with the Cell Death Detection ELISA kit (Roche). Over expression of GDIα-induced significant levels of apoptotic cell death compared to the vector control ($P < 0.01$, Fig. 2B). These data suggest that overexpression of GDIα inhibits the growth of CaP cells via induction of apoptotic cell death.

RhoGDIα Inhibits LNCaP-IL-6+ Cell Growth in Androgen-Deprived Conditions

To determine the potential significance of over expression of GDIα in CaP cells, LNCaP-IL-6+ were transfected with plasmids expressing control or GDIα. After transfection, cells were switched to media containing either FBS or charcoal-stripped FBS (CS-FBS) and allowed to grow for 3 more days and cell numbers were determined. The growth of LNCaP-IL-6+ cells transfected with vector control grown in CS-FBS was reduced ~5–10% compared to those grown in FBS. The growth of LNCaP-IL-6+ cells transfected with GDIα grown in similar conditions showed reduction by 40–50% (Fig. 3). These results suggest that over expression of GDIα can reduce the growth of LNCaP-IL-6+ cells in androgen-deprived conditions in vitro.

Down-Regulation of GDIα Promotes Growth of LNCaP Cells in Androgen-Deprived Conditions

LNCaP cells express higher levels of GDIα protein and do not grow well in CS-FBS condition. To test

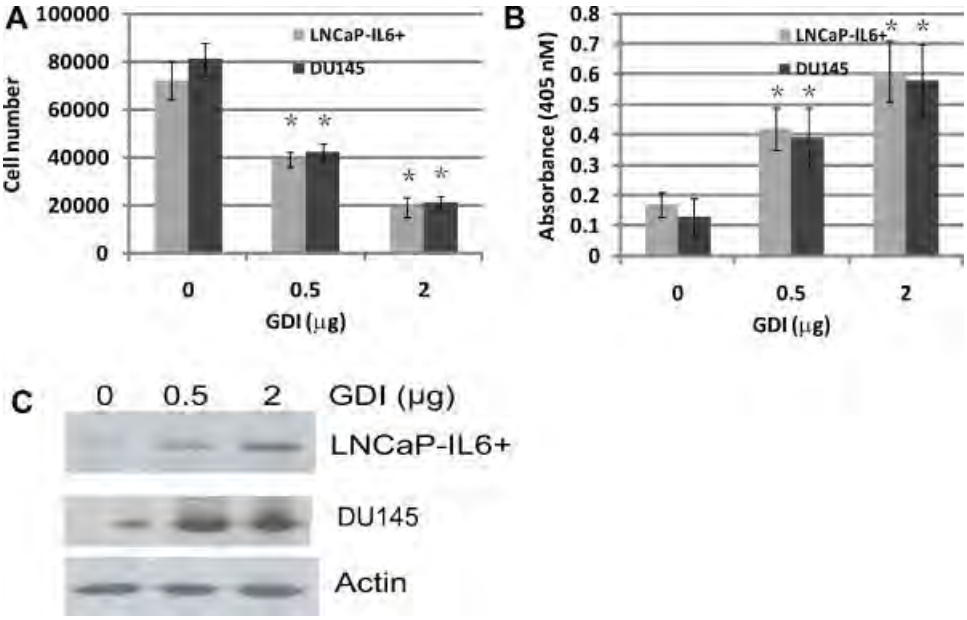

Fig. 2. Expression of GDIα inhibited growth and induced apoptotic cell death in vitro. **A**: Over expression of GDIα inhibits LNCaP IL6+ and DUI45 cells growth in vitro. LNCaP IL6+ and DUI45 cells were transfected with different doses of plasmids containing GDIα cDNA. The cell number was determined 3 days after transfection. **B**: Overexpression of GDIα induces apoptotic cell death. LNCaP IL6+ and DUI45 cells were transfected with different doses of expression plasmids containing GDIα cDNA. Apoptotic cell death was determined 3 days after transfection. **C**: GDIα expression by Western blot analysis using antibody specific against GDIα. *Statistical significance compared to controls.

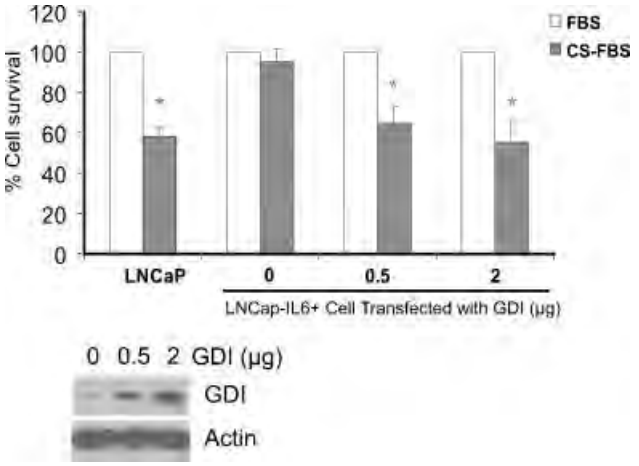

Fig. 3. Effect of over expression of GDIα on LNCaP IL6+ cell growth in the presence and absence of androgen in vitro. LNCaP IL6+ cells were cultured in RPMI 1640 supplemented with 10% FBS or 10% charcoal stripped FBS (CS FBS) and cultured for 72 hr. MTT values for the complete FBS were expressed as 100% and MTT values for charcoal stripped FBS were expressed as % relative to complete FBS. *Statistical significance compared to the value of FBS conditions. The bottom panel shows GDIα protein expression by Western blot analysis using antibody against GDIα.

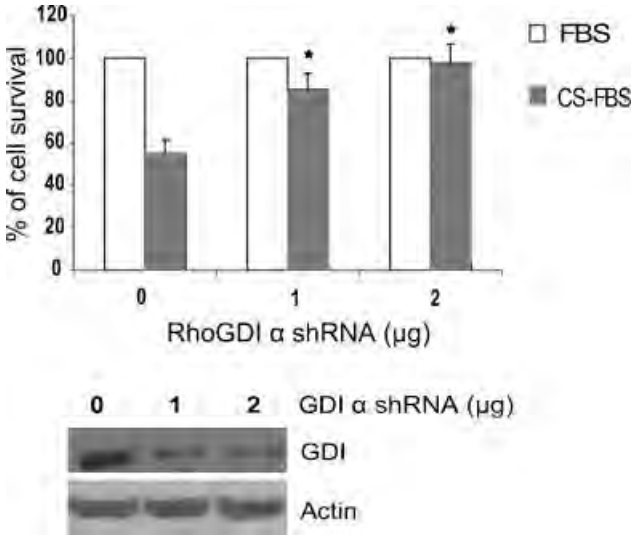

Fig. 4. Knockdown of RhoGDIa expression promotes LNCaP cell growth in androgen deprived conditions in vitro. Effect of knockdown of RhoGDIα expression on LNCaP cell growth in the presence and absence of androgen in vitro. LNCaP cells were cul tured in RPMI 1640 supplemented with 10% FBS. After 24 hr, the cells were transfected with GDIα shRNA as indicated. GFP shRNA was used as control. After transfection, the cells were switched to either 10% FBS or 10% charcoal stripped FBS (CS FBS) and cultured for 72 hr. MTT values for cell grown in complete FBS were expressed as 100% and MTT values for cell grown in charcoal stripped FBS were expressed as % relative to complete FBS. Bot tom panel shows GDIα protein expression by Western blot analysis using antibody against GDIα. *Statistical significance compared to the value of GFP shRNA in CS FBS conditions.

whether knockdown of GDIα expression stimulates androgen-independent growth of androgen-sensitive LNCaP cells, LNCaP cells were transfected with shRNA specifically for GDIα and GFP shRNA as control. Cells were cultured in the presence and absence of androgen and cell growth was determined. The growth of androgen-sensitive LNCaP transfected with GFP control was reduced by approximately 50% after 72 hr in CS-FBS compared to that in regular FBS. In cells transfected with GDIα shRNA there was only 5–15% reduction in growth in CS-FBS compared to FBS indicating that knockdown of GDIα protein expression can enhance the growth of LNCaP cells in androgen-deprived conditions in vitro (Fig. 4).

RhoGDIα Suppresses LNCaP-IL-6+ Tumor Growth

To test the effect of GDIα on tumor formation in vivo, 8-week-old male nude mice were inoculated s.c. with 2×10^6 LNCaP-IL6+ cells stably transfected with GDIα or vector control. The mice developed tumors 2 weeks after injection with LNCaP-IL6+/neo cells, and 5 weeks after injection with LNCaP-IL6+/GDIα cells (Fig. 5). Tumor volumes were measured twice a week. At the end of 9 weeks, blood and tumor tissues were collected and serum levels of PSA were determined by ELISA. The over expression of GDIα suppressed tumor growth of LNCaP-IL6+ cells. All the tumors produced PSA and the levels of PSA were 25.4 ± 6.5 ng/ml in mice-bearing LNCaP-IL6+/neo tumors and 5.1 ± 2.8 ng/ml in mice-bearing LNCaP-Il6+/GDIα tumors. These results demonstrate that GDIα expression suppresses prostate tumor growth in vivo.

DISCUSSION

IL-6 has been implicated in growth and differentiation and is associated with poor prognosis in many cancers including CaP. Multiple studies have demonstrated that IL-6 is elevated in the sera of patients with metastatic CaP and correlates with tumor burden and clinically evident metastases [1,3–5]. An interesting observation is the dynamic nature of CaP cells such as LNCaP in response to IL-6. IL-6 exerts its effects in both paracrine and autocrine manner [18]. Prolonged passage of LNCaP cells in the presence of IL-6 generated a subline, LNCaP-IL6+, which is adapted to IL-6 and grows in a castration-resistant manner [18,20]. In the present study, we analyzed protein expression profiles of parental LNCaP and LNCaP-IL-6+ cells, and identified that GDIα is

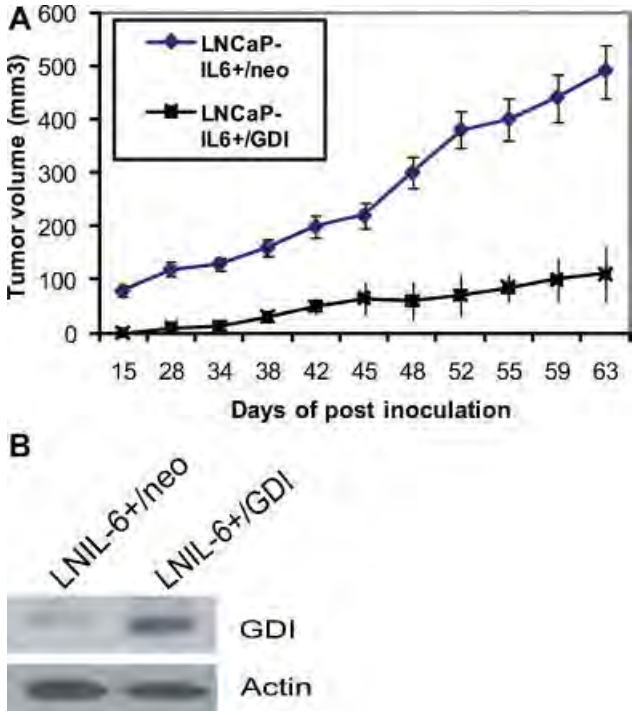

Fig. 5. Effects of overexpression of GDIα on tumor growth. **A**: Over expression of GDIα suppresses LNCaP IL6+ cell tumor growth in vivo. LNCaP IL6+ cells/neo and LNCaP IL6+/GDIα cells were injected into intact male nude mice (N = 8). Tumor volumes were measured. **B**: Levels of GDIα protein in tumors originating from LNCaP IL6+/neo and LNCaP IL6+/GDIα cells analyzed by Western blot using antibody against GDIα. [Color figure can be viewed in the online issue, which is available at wileyonlinelibrary.com.]

down-regulated in CaP and its down-regulation plays a critical role during CaP progression to CRPC.

GDIα was identified by comparison of the protein expression profiles of LNCaP and LNCaP-IL6+ cells. GDIα is down-regulated in LNCaP-IL6+ cells which exhibit higher levels of IL-6 compared to LNCaP cells. The levels of expression of GDIα are higher in androgen-sensitive LNCaP and LAPC-4 cells compared to more aggressive and androgen-insensitive C4-2, PC3, DU145, and LNCaP-IL6+ cells, suggesting that down-regulation of GDIα expression may participate in the progression of CaP cells to androgen-insensitive state. It should be noted that the data is obtained from CaP cell lines derived from human CaP. It would be interesting to examine the levels of GDIα expression in specimens directly derived from patients representing different stages of CaP.

Our study shows a novel role of GDIα in CaP. Overexpression of GDIα helps check uncontrolled proliferation of LNCaP-IL-6+ cells in vitro and in vivo. In addition to LNCaP-IL6+ cells, GDIα also inhibits the proliferation of DU145 CaP cells at least in vitro. We have previously showed that LNCaP-IL6+ cells have the ability to grow in androgen-deprived charcoal-stripped FBS conditions in cell culture [18], which was hampered by overexpression of GDIα in LNCaP-IL6+ cells. Conversely, down-regulation of GDIα expression in LNCaP cells enhanced the growth of these cells in androgen-deprived charcoal-stripped FBS conditions in vitro. These results suggest that decreased expression of GDIα facilitates the progression of castration-resistance from androgen-sensitive CaP. The possible involvement of GDIα in CRPC progression is suggested by a recent publication in which loss of GDIα expression promotes MCF-7 breast cancer cells resistant to tamoxifen treatment [21].

In conclusion, we have identified GDIα as a suppressor of CaP growth through comparison of the protein expression profiles of LNCaP and LNCaP-IL6+ cells. Overexpression of GDIα inhibits the growth of CaP cells, while down-regulation of GDIα enhances the growth of androgen-sensitive CaP cells in androgen-deprived conditions. The mechanisms of GDIα-mediated cellular signaling involved in promoting CaP cell progression are currently under investigation.

REFERENCES

1. Simpson RJ, Hammacher A, Smith DK, Matthews JM, Ward LD. Interleukin 6: Structure function relationships. Protein Sci 1997;6(5):929 955.
2. Siegall CB, Schwab G, Nordan RP, FitzGerald DJ, Pastan I. Expression of the interleukin 6 receptor and interleukin 6 in prostate carcinoma cells. Cancer Res 1990;50(24):7786 7788.
3. Siegsmund MJ, Yamazaki H, Pastan I. Interleukin 6 receptor mRNA in prostate carcinomas and benign prostate hyperplasia. J Urol 1994;151(5):1396 1399.
4. Hobisch A, Rogatsch H, Hittmair A, Fuchs D, Bartsch G Jr, Klocker H, Bartsch G, Culig Z. Immunohistochemical localization of interleukin 6 and its receptor in benign, premalignant and malignant prostate tissue. J Pathol 2000;191(3):239 244.
5. Drachenberg DE, Elgamal AA, Rowbotham R, Peterson M, Murphy GP. Circulating levels of interleukin 6 in patients with hormone refractory prostate cancer. Prostate 1999;41(2):127 133.
6. Adler HL, McCurdy MA, Kattan MW, Timme TL, Scardino PT, Thompson TC. Elevated levels of circulating interleukin 6 and transforming growth factor beta1 in patients with metastatic prostatic carcinoma. J Urol 1999;161(1):182 187.
7. Okamoto M, Lee C, Oyasu R. Interleukin 6 as a paracrine and autocrine growth factor in human prostatic carcinoma cells in vitro. Cancer Res 1997;57(1):141 146.
8. Qiu Y, Robinson D, Pretlow TG, Kung HJ. Etk/Bmx, a tyrosine kinase with a pleckstrin homology domain, is an effector of phosphatidylinositol 3′ kinase and is involved in interleukin 6 induced neuroendocrine differentiation of prostate cancer cells. Proc Natl Acad Sci USA 1998;95(7):3644 3649.
9. Spiotto MT, Chung TD. STAT3 mediates IL 6 induced neuro endocrine differentiation in prostate cancer cells. Prostate 2000; 42(3):186 195.

10. Deeble PD, Murphy DJ, Parsons SJ, Cox ME. Interleukin 6 and cyclic AMP mediated signaling potentiates neuroendocrine differentiation of LNCaP prostate tumor cells. Mol Cell Biol 2001;21(24):8471 8482.
11. Smith PC, Keller ET. Anti interleukin 6 monoclonal antibody induces regression of human prostate cancer xenografts in nude mice. Prostate 2001;48(1):47 53.
12. Wallner L, Dai J, Escara Wilke J, Zhang J, Yao Z, Lu Y, Trikha M, Nemeth JA, Zaki MH, Keller ET. Inhibition of interleukin 6 with CNTO328, an anti interleukin 6 monoclonal antibody, inhibits conversion of androgen dependent prostate cancer to an androgen independent phenotype in orchiectomized mice. Cancer Res 2006;66(6):3087 3095.
13. Olofsson B. Rho guanine dissociation inhibitors: Pivotal mole cules in cellular signalling. Cell Sig 1999;11(8):545 554.
14. Dovas A, Couchman JR, Rho GDI. multiple functions in the regulation of Rho family GTPase activities. Biochem J 2005; 390(1):1 9.
15. Takaishi KKA, Kuroda S, Sasaki T, Takai Y. Involvement of rho p21 and its inhibitory GDP/GTP exchange protein (rho GDI) in cell motility. Mol Cell Biol 1999;13(1):545 554.
16. Togawa AMJ, Ishizaki H, et al. Progressive impairment of kid neys and reproductive organs in mice lacking Rho GDIαλπηα. Oncogene 1999;18(39):5373 5380.
17. Seraj M, Harding M, Gildea J, Welch D, Theodorescu D. The relationship of BRMS1 and RhoGDI2 gene expression to metastatic potential in lineage related human bladder cancer cell lines. Clin Exp Metastasis 2000;18(6):519 525.
18. Lee SO, Chun JY, Nadiminty N, Lou W, Gao AC. Interleukin 6 undergoes transition from growth inhibitor associated with neuroendocrine differentiation to stimulator accompanied by androgen receptor activation during LNCaP prostate cancer cell progression. Prostate 2007;67(7):764 773.
19. Lou W, Ni Z, Dyer K, Tweardy DJ, Gao AC. Interleukin 6 induces prostate cancer cell growth accompanied by activa tion of stat3 signaling pathway. Prostate 2000;42(3):239 242.
20. Hobisch A, Ramoner R, Fuchs D, Godoy Tundidor S, Bartsch G, Klocker H, Culig Z. Prostate cancer cells (LNCaP) generated after long term interleukin 6 (IL 6) treatment express IL 6 and acquire an IL 6 partially resistant phenotype. Clin Cancer Res 2001;7(9):2941 2948.
21. Barone I, Brusco L, Gu G, Selever J, Beyer A, Covington KR, Tsimelzon A, Wang T, Hilsenbeck SG, Chamness GC, Ando S, Fuqua SA. Loss of Rho GDI{alpha} and resistance to tamoxifen via effects on estrogen receptor {alpha}. J Natl Cancer Inst 103(7):538 552.

The American Journal of Pathology, Vol. 183, No. 1, July 2013

The American Journal of
PATHOLOGY
ajp.amjpathol.org

TUMORIGENESIS AND NEOPLASTIC PROGRESSION

Lin28 Promotes Growth of Prostate Cancer Cells and Activates the Androgen Receptor

Ramakumar Tummala,* Nagalakshmi Nadiminty,*† Wei Lou,* Yezi Zhu,*‡ Regina Gandour-Edwards,†§ Hong-Wu Chen,†¶ Christopher P. Evans,*† and Allen C. Gao*†‡

From the Departments of Urology, Pathology,§ and Biochemistry and Molecular Medicine,¶ the Comprehensive Cancer Center,† and the Graduate Program in Pharmacology and Toxicology,‡ University of California at Davis, Sacramento, California*

Accepted for publication March 19, 2013.

Address correspondence to Nagalakshmi Nadiminty, Ph.D., or Allen C. Gao, M.D., Ph.D., Department of Urology, University of California at Davis, 4645 2nd Ave, Research III, Suite 1300, Sacramento, CA 95817. E mail: nnadiminty@ucdavis.edu or acgao@ucdavis.edu.

Prostate cancer (CaP) progresses to a castration-resistant state assisted by multifold molecular changes, most of which involve activation of the androgen receptor (AR). Having previously demonstrated the importance of the Lin28/let-7/Myc axis in CaP, we tested the hypothesis that Lin28 is overexpressed in CaP and that it activates AR and promotes growth of CaP cells. We analyzed human clinical CaP samples for the expression of Lin28 by quantitative real-time RT-PCR, Western blot analysis, and IHC. Growth characteristics of CaP cell lines transiently and stably expressing Lin28 were examined. The clonogenic ability of CaP cells expressing Lin28 was determined by colony formation and soft agar assays. Increase in expression of AR and subsequent increase in transcription of AR-target genes were analyzed by quantitative real-time RT-PCR, luciferase assays, and ELISA. LNCaP cells stably expressing Lin28 were injected into nude mice, and tumorigenesis was monitored. We found that Lin28 is overexpressed in clinical CaP compared to benign prostates. Overexpression of Lin28 enhanced, while down-regulation reduced, growth of CaP cells. Lin28 enhanced the ability of CaP cells to form colonies in anchorage-dependent and anchorage-independent conditions. LNCaP cells stably expressing Lin28 exhibited significantly higher tumorigenic ability *in vivo*. Lin28 induced expression of the AR and its target genes such as *PSA* and *NKX3.1*. Collectively, our findings demonstrate a novel role for Lin28 in CaP development and activation of the AR axis. *(Am J Pathol 2013, 183: 288–295; http://dx.doi.org/10.1016/j.ajpath.2013.03.011)*

Prostate cancer (CaP) remains one of the cancers with high incidence and mortality rates among men in the United States. Progression of CaP to castration resistance is the major challenge facing efforts to develop effective therapies against CaP. Castration-resistant prostate cancer evades androgen ablation by activating androgen receptor (AR) dependent signaling through alternative mechanisms. Previous reports have shown that castration-resistant prostate cancer may evolve by suppression of tumor-suppressor genes and miRNAs, activation of potential oncogenes, overexpression of the AR, and activation of other signaling cascades.[1] miRNAs are small RNAs that regulate gene expression by binding to the untranslated regions of target mRNAs and inhibiting their translation. The let-7 family of miRNAs is regulated by Lin28 and Lin28B, two homologues of the heterochronic gene *lin-28* in *Caenorhabditis elegans*.[2] The let-7 family miRNAs are tumor suppressors and are implicated as prognostic factors in a multitude of cancers.[3–5] Hence, Lin28/Lin28B, which inhibit maturation of let-7 miRNAs, may be potential oncogenes in several malignancies. Our previous studies indicated that the Lin28/let-7 double-negative feedback loop regulates AR-dependent signaling in human CaP and that let-7 miRNA expression is suppressed in most cases of primary and castration-resistant CaP.[6,7]

Lin28, a highly conserved RNA-binding protein and a master regulator of let-7 miRNA processing, is overexpressed in primary human tumors[8,9] and is postulated to be one of the embryonic stem cell factors that promote oncogenesis and proliferation of cancer cells.[10] Lin28 binds to

Supported, in part, by NIH/National Cancer Institute grants CA140468, CA118887, and Department of Defense grant PCRP PC080538, the US Department of Veterans Affairs, the Office of Research and Development (Veteran Affairs Merits I01 BX000526), and resources from the Veteran Affairs Northern California Health Care System (Sacramento) (to A.C.G.), and Department of Defense grant PCRP PC100502 (N.N.).

http://dx.doi.org/10.1016/j.ajpath.2013.03.011

the terminal loops of the precursors of let-7 family miRNAs and blocks their processing into mature miRNAs.[11,12] Lin28 also derepresses c-Myc by repressing let-7, and c-Myc activates transcription of *Lin28*.[13,14] This Lin28/let-7/c-Myc loop may play an important role in the deregulated miRNA expression signature observed in many cancers.[15]

In this study, we hypothesized that Lin28 may function as a prosurvival factor in CaP. To test this hypothesis, we analyzed expression levels of Lin28 in human CaP samples and found that Lin28 levels are up-regulated in CaP. We expressed Lin28 transiently and constitutively in LNCaP human CaP cells and found that Lin28 enhances growth, invasion, and soft agar colony formation. Expression of Lin28 also led to up-regulation of expression of AR and its target genes. Constitutive expression of Lin28 also promoted tumorigenicity of LNCaP cells in nude mice. Knockdown of endogenous Lin28 inhibited expression of the AR and led to reduced levels of cell growth. Taken together, these data demonstrate the functional importance of Lin28 in human CaP.

Materials and Methods

Cell Lines, Antibodies, and Other Reagents

LNCaP, C4-2B, and DU145 prostate cancer cell lines and the PZ-HPV7 normal prostate epithelial cell line were purchased from ATCC (Manassas, VA). LNCaP-S17 and LNCaP-IL6 cell lines were described previously.[16] LNCaP cells stably expressing Lin28 (LN-Lin28) were generated by transfection of pLKO.1-Lin28 (Open Biosystems, Pittsburgh, PA) into LNCaP cells. Expression of Lin28 in the stable transfectants was confirmed by Western blot analysis. LNCaP cells expressing Tet-inducible Lin28 (LN/TR/Lin28) were generated according to the manufacturer's instructions using the ViraPower Lentiviral Transduction System (Invitrogen, Grand Island, NY). Inducible expression of Lin28 was confirmed by Western blot analysis after induction with 0.5 μg/mL doxycycline (Sigma, St. Louis, MO). Antibodies against AR and tubulin (AR-441 and T5168) were from Santa Cruz Biotechnologies (Santa Cruz, CA), and Lin28 antibodies (Ab-71415) were from Abcam (San Francisco, CA).

Western Blot Analysis

Cells were lysed in high salt buffer containing 50 mmol/L HEPES (pH 7.9), 250 mmol/L NaCl, 1 mmol/L EDTA, 1% NP-40, 1 mmol/L phenylmethylsulfonyl fluoride, 1 mmol/L Na vanadate, 1 mmol/L NaF, and protease inhibitors (Roche, Indianapolis, IN), as previously described.[6] Total protein was estimated using the Coomassie Protein Assay Reagent (Pierce, Rockford, IL). Equal amounts of protein were loaded onto 10% SDS-PAGE and transferred to nitrocellulose membranes. The membranes were blocked with 5% nonfat milk in PBST (1× PBS + 0.1% Tween-20) and probed with primary antibodies in 1% bovine serum albumin. The signal was detected by enhanced chemiluminescence (GE Healthcare, Waukesha, WI) after incubation with the appropriate horseradish peroxidase conjugated secondary antibodies.

Real-Time RT-qPCR

Total RNAs were extracted using TRIzol (Invitrogen) and were subjected to digestion with RNase-free RQ1 DNase (Promega, Madison, WI) before reverse transcription. The resultant cDNAs were subjected to real-time quantitative RT-PCR (RT-qPCR) using SsoFast Eva Green supermix (Bio-Rad, Hercules, CA), as described previously.[7] Each reaction was normalized by coamplification of actin. Triplicates of samples were run on default settings of a Bio-Rad CFX-96 real-time cycler. Sequences of primers used have been published previously.[6,7,17]

Clonogenic Assays

Anchorage-dependent clonogenic ability assays were performed as described previously.[18] At the end of the experiment, colonies were fixed with methanol, stained with crystal violet, and counted.

Soft-Agar Colony Formation Assays

Anchorage-independent colony formation assays were performed as described previously.[7] At the end of the experiment, colonies were stained with 0.005% crystal violet and counted.

Cell Growth Assays

PZ-HPV7, LNCaP, C4-2B, DU145, LNCaP-S17, LN-Lin28, and LN/TR/Lin28 cells were plated in 12-well plates in triplicate, and viable cell numbers were determined at 0, 24, and 48 hours using a Coulter cell counter (Beckman Coulter, Brea, CA).

Invasion Assays

Boyden chamber invasion assays were performed as described previously.[19] Briefly, 1×10^5 cells were plated in defined medium on Matrigel-coated cell culture inserts (BD Biosciences, San Jose, CA), with complete medium in the lower chamber. After incubation at 37°C for 48 hours, uninvaded cells were scraped off, the membrane inserts were washed and stained, and invaded cells on the lower surface were counted.

Animals

Male nude mice (aged 6 to 8 weeks) were maintained in the Animal Facility at University of California (UC) Davis Medical Center (Sacramento). All experimental procedures using animals were approved by the Institutional Animal Care and Use Committee of UC Davis. Cells (2×10^6 per flank) were injected s.c. into both flanks, and tumors were allowed to grow.

Tumors were measured twice weekly. At the end of the experiments, tumors were excised and sera were collected for measurement of prostate-specific antigen (PSA).

Measurement of PSA

PSA levels were measured in the culture supernatants and mouse sera using enzyme-linked immunosorbent assay (ELISA; United Biotech Inc., Mountain View, CA), according to the manufacturer's instructions.

Human CaP Specimens

The paired benign and tumor prostate tissues used for RT-qPCR of Lin28 were previously described.[20] The protein extracts from human prostate specimens used for Western blot analysis of Lin28 were previously described.[21,22] Immunohistochemical (IHC) staining of Lin28 was performed using a TMA PROS-006 obtained from UC Davis Comprehensive Cancer Center Biorepository. Staining was performed by the pathology core facility, and staining intensity was scored on a scale of 0 to 3 (0, negative; 1, weak; 2, strong; and 3, very strong). Brown color was considered positive staining for Lin28, and nuclear staining was denoted by blue color.

Statistical Analysis

Data are shown as means ± SD. Multiple-group comparison was performed by one-way analysis of variance. $P \leq 0.05$ was considered significant.

Results

Lin28 Is Overexpressed in Clinical Prostate Cancer Specimens

To determine the relative levels of expression of Lin28 in human CaP compared to benign prostates, we examined RNAs from 10 paired benign and tumor human CaP samples by RT-qPCR. Expression levels of Lin28 were found to be significantly elevated in 9 of 10 pairs of matched benign and tumor prostate specimens (Figure 1A). Extracts from archived human clinical prostatectomy specimens were also examined for expression of Lin28 by Western blot analysis. The data set contains 42 matched benign and cancer specimens, and expression levels of Lin28 were higher in cancer tissues (86% positive and 14% negative) compared to matched benign prostate tissues (47% positive and 53% negative) (Figure 1B). IHC was performed in formalin-fixed, paraffin-embedded prostate clinical specimens in a TMA PROS-006 (UC Davis Cancer Center Biorepository) with Lin28 antibody (Ab-71415[23]), and staining intensity was scored over a scale of 0 to 3 (0, negative; 1, weak; 2, strong; and 3, very strong). Lin28 was expressed in both nuclear and cytoplasmic compartments, with no significant differences in the pattern of expression with increasing Gleason grade (Figure 1C). We observed strong nuclear staining of Lin28 in benign prostate tissues almost exclusively in the basal cell layer, with no staining in the luminal epithelial compartment. In contrast, an apparent shift from mostly nuclear localization in benign prostate to a nuclear + cytoplasmic or mostly cytoplasmic localization appeared to occur in CaP (Table 1). Documentation of staining specificity for IHC is presented in Supplemental Figure S1.

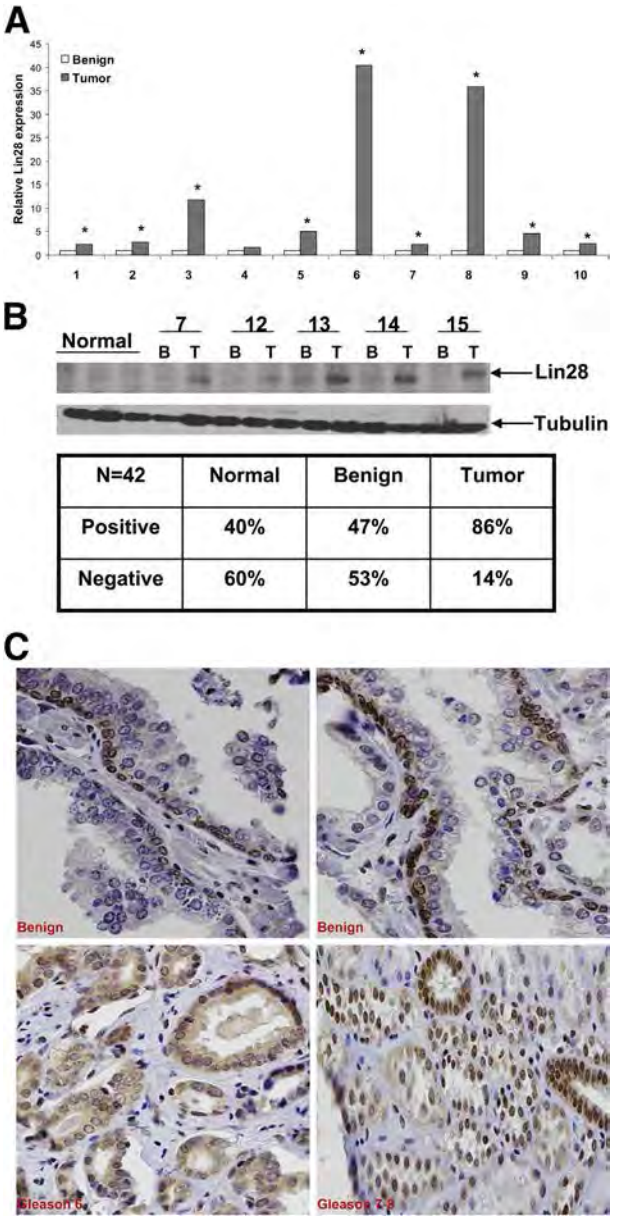

N=42	Normal	Benign	Tumor
Positive	40%	47%	86%
Negative	60%	53%	14%

Figure 1 Lin28 is overexpressed in human prostate cancer. **A**: RT qPCR analysis of Lin28 expression in 10 paired benign and tumor CaP tissues. Data are presented as means ± SD of two experiments performed in triplicate. *$P \leq 0.05$. Lin28 mRNA expression levels were higher in cancer tissues compared to matched benign tissues. **B**: Western blot analysis of Lin28 expression in 42 paired benign (B) and tumor (T) samples. Representative Western blot analysis is shown. The table summarizes the results of Lin28 protein expression levels in the data set. **C**: IHC analysis of Lin28 expression in benign and cancer CaP tissues. Brown staining represents positive staining for expression of Lin28. Original magnification, ×200.

Table 1 Summary of IHC Results for Lin28 in TMA PROS-006

No. of cores	Benign (n = 19)	Gleason 6 (n = 29)	Gleason 7-8 (n = 26)
Nuclear alone	12 (63)	1 (3)	0 (0)
Nuclear + cytoplasmic	4 (21)	17 (58)	11 (42)
Cytoplasmic alone	3 (15)	11 (38)	15 (57)

Data are given as number (percentage).

Lin28 Enhances Growth of Prostate Cancer Cells

To test whether Lin28 activates a prosurvival mechanism in CaP cells, we transfected Lin28 into a panel of CaP cell lines (LNCaP, C4-2B, DU145, LNCaP-S17, and LNCaP-IL6) and a nontumorigenic prostate epithelial cell line (PZ-HPV7). Lin28 enhanced the growth rate of all CaP cell lines tested (Figure 2A). To confirm these results, LNCaP and C4-2B cells stably expressing Lin28 (LN-Lin28 and C4-2B-Lin28) were generated, and growth characteristics were examined. Compared to control LNCaP cells expressing the empty vector (LN-neo and C4-2B-neo), LN-Lin28 and C4-2B-Lin28 cells exhibited faster growth rates (Figure 2, B and C), suggesting that Lin28 promotes growth of prostate cancer cells *in vitro*.

To examine the effects of down-regulation of Lin28 on CaP growth, lentiviral vector-driven shRNA against Lin28 (Open Biosystems) was transfected into C4-2B cells, and cell growth was monitored. C4-2B cells transfected with Lin28 shRNA exhibited lower rates of growth, compared to cells transfected with shRNA against enhanced green fluorescent protein (EGFP) (Figure 3). Down-regulation of Lin28 was confirmed by Western blot analysis (Figure 3). These data demonstrated that down-regulation of Lin28 reduces proliferation of CaP cells.

Lin28 Increases Clonogenic Ability of LNCaP Cells

To test whether Lin28 influences the ability of CaP cells to form colonies in anchorage-dependent and anchorage-independent conditions, we performed clonogenic assays by transiently transfecting Lin28 into C4-2B and LNCaP-S17 cells. The results showed that the number of colonies formed by C4-2B cells expressing Lin28 was 356 ± 14, whereas the number of colonies formed by control C4-2B cells was 182 ± 10 (Figure 4A). Similarly, the number of colonies formed by LNCaP-S17 cells expressing Lin28 was 392 ± 19, whereas the number of colonies formed by control LNCaP-S17 cells was 212 ± 15 (Figure 4A). These experiments were confirmed using LN-Lin28 cells (LNCaP cells stably expressing Lin28), which exhibited a 3.4-fold increase in colony-forming ability compared to LN-neo cells (228 ± 21 versus 67 ± 13 colonies) (Figure 4B). These results were also confirmed using LN/TR/Lin28 cells (LNCaP cells expressing tet-inducible Lin28), which exhibited higher clonogenic ability compared to control LN/TR/Con cells upon doxycycline induction (Figure 4B). Collectively, these findings suggest that Lin28 enhances the ability of prostate cancer cells to form colonies in anchorage-dependent conditions.

To further test whether Lin28 regulates anchorage-independent growth of CaP cells, we performed soft agar colony formation assays with C4-2B and LNCaP-S17 cells transfected with Lin28, as described in *Materials and Methods*. The results showed that Lin28 promoted the growth of both C4-2B (Figure 3C) and LNCaP-S17 (Figure 4C) cells in soft agar, compared to control C4-2B or LNCaP-S17 cells transfected with the empty vector. Similarly, LN-Lin28 cells exhibited significantly better ability to grow in soft agar, whereas control LN-neo cells failed to

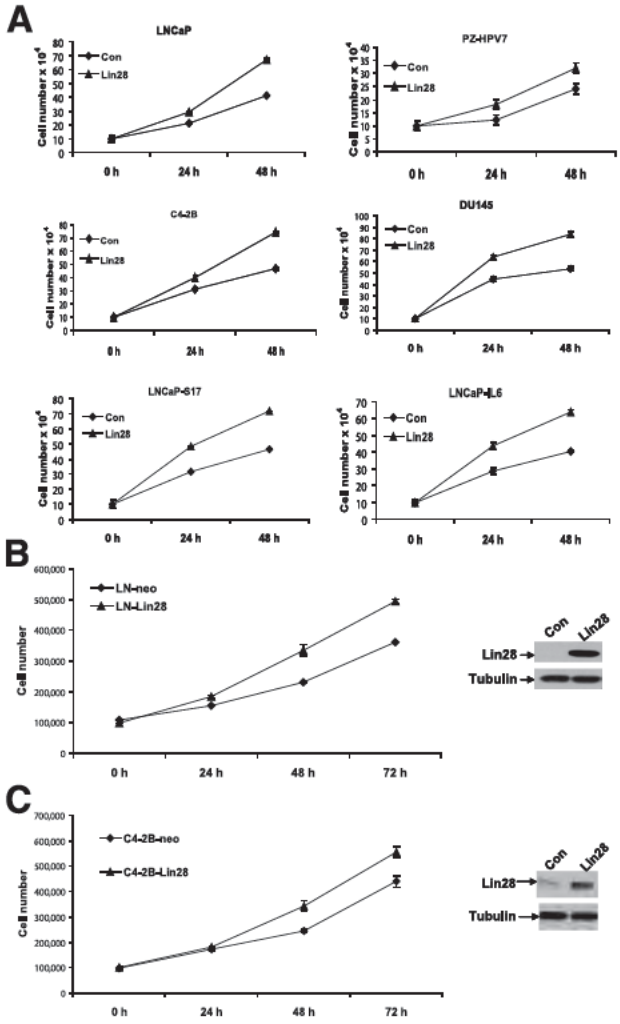

Figure 2 Lin28 promotes growth of CaP cells. **A:** LNCaP, PZ HPV7, C4 2B, DU145, LNCaP S17, and LNCaP IL6 cells were transfected with empty vector or pLKO.1 Lin28, and growth was monitored at 0, 24, and 48 hours. Lin28 enhanced growth rates of all cell lines tested. **B:** LNCaP cells stably expressing Lin28 (LN Lin28), and control (Con) LN neo cells were plated in media containing complete FBS and growth was monitored at 0, 24, 48, and 72 hours. **Left panel:** Lin28 enhanced the growth of LNCaP cells. **Right panel:** The expression levels of Lin28 in LN Lin28 and LN neo cells. **C: Left panel:** C4 2B cells stably expressing Lin28 (C4 2B Lin28), and control C4 2B neo cells were plated in media containing complete FBS and growth was monitored at 0, 24, 48, and 72 hours. **Right panel:** The expression levels of Lin28 in C4 2B Lin28 and C4 2B neo cells. Data are presented as means ± SD of three experiments performed in triplicate.

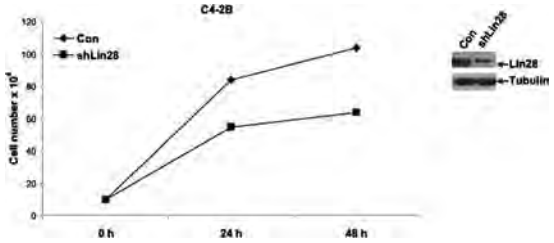

Figure 3 Down regulation of endogenous Lin28 suppresses CaP cell growth. C4 2B cells were transfected with shRNA against Lin28, and growth was measured in media containing complete FBS. **Left panel:** Growth of C4 2B cells was abrogated with down regulation of Lin28. **Right panel:** Reduced expression of Lin28 protein after transfection with shRNA. Data are presented as means ± SD of three experiments performed in triplicate.

grow in soft agar (Figure 4D), demonstrating that Lin28 confers soft agar colony-forming ability on CaP cells.

Lin28 Increases Invasiveness of LNCaP Cells

To test whether Lin28 regulates the ability of CaP cells to invade through Matrigel *in vitro*, we performed Boyden chamber invasion assays using LN-Lin28 and control LN-neo cells. Cells were plated on Matrigel in the upper compartment of the Boyden chamber and allowed to invade toward the lower compartment filled with complete medium containing complete fetal bovine serum (FBS) or charcoal dextran-stripped FBS (CS-FBS). The number of LN-Lin28 cells invading through Matrigel in FBS-containing medium was 118 ± 10, whereas the number of control cells invading through Matrigel was 60 ± 5 (Figure 4D). Similarly, the number of LN-Lin28 cells invading through Matrigel in CS-FBS containing medium was 54 ± 6, whereas the number of control cells was 4 ± 2 (Figure 4D), indicating that Lin28 induces invasion of CaP cells through basement membrane *in vitro*.

Lin28 Promotes Tumorigenicity of CaP Cells *in Vivo*

To test whether the growth-promoting effect of Lin28 can be recapitulated *in vivo*, we injected 2×10^6 LN-Lin28 cells or control LN-neo cells s.c. into each flank of male nude mice and monitored their tumorigenic ability. Tumors were measured twice weekly, and serum samples were collected at the end of the experiment to confirm that the tumor cells secreted PSA. We found that mice injected with LN-Lin28 cells exhibited significantly higher rates of incidence and growth of tumors compared to control LN-neo cells, which formed slow-growing tumors (Figure 5A). Higher levels of secretion of PSA were observed in mice bearing tumors expressing Lin28 compared to mice bearing control tumors (Figure 5B). Total RNA and protein extracts from the tumors were examined for expression levels of Lin28 and AR. Lin28 was highly expressed in the tumors, which was correlated positively with expression levels of AR (Figure 5C), indicating that higher expression of Lin28 enhances expression of AR and promotes tumor growth of LNCaP human CaP cells *in vivo*.

Lin28 Activates Androgen Receptor Signaling Axis

As we previously reported that hsa-let-7c, an miRNA regulated by Lin28, suppressed expression of the AR,[6] we examined whether Lin28 regulates expression of the AR. We transfected a luciferase reporter vector driven by the full-length promoter of AR (pGL4-AR-Prom-Luc) into LN-neo and LN-Lin28 cells and performed luciferase assays. LN-Lin28 cells exhibited higher levels of activation of AR promoter compared to control cells (Figure 6A), indicating that Lin28 may activate transcription of the AR gene. Next, we analyzed the mRNA levels of AR in LN-neo and LN-Lin28 cells and found that LN-Lin28 cells exhibited significantly higher levels of AR mRNA (Figure 6A).

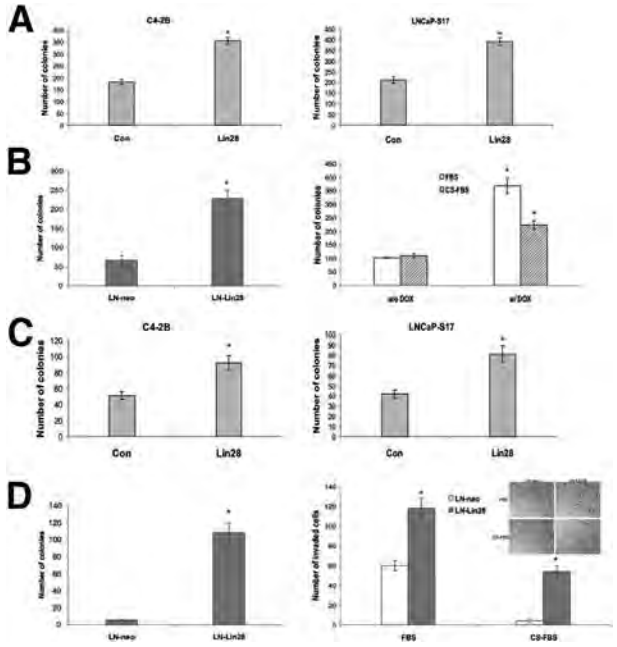

Figure 4 Lin28 promotes clonogenic ability of CaP cells. **A:** C4 2B and LNCaP S17 cells were transfected with empty vector or pLKO.1 Lin28, and anchorage dependent clonogenic assays were performed. Lin28 enhanced the colony forming ability of both C4 2B and LNCaP S17 cells. **B:** LN Lin28 and control (Con) LN neo cells were subjected to clonogenic assays. Lin28 expressing LNCaP cells exhibited higher clonogenic ability compared to control cells. LN/TR/Lin28 (LNCaP cells expressing Lin28 under a Tet inducible promoter) and LN/TR/Con cells were subjected to clonogenic assays in media containing either complete FBS or CS FBS. Induction of Lin28 expression by doxycycline (DOX) enhanced colony formation of LN/TR/Lin28 cells compared to control cells. **C:** C4 2B and LNCaP S17 cells were transfected with empty vector or pLKO.1 Lin28 and subjected to anchorage independent soft agar colony formation assays. Lin28 expression increased the number of colonies formed in soft agar by both cell lines. **D: Left panel:** LN Lin28 and control LN neo cells were subjected to soft agar assays. LN Lin28 cells were able to form more colonies in soft agar compared to LN neo cells. **Right panel:** Lin28 increases invasiveness of CaP cells. LN Lin28 and LN neo cells were subjected to Boyden chamber invasion assays. **Inset:** Representative images of invading cells. Data are presented as means ± SD of three exper iments performed in triplicate. $^*P \leq 0.05$.

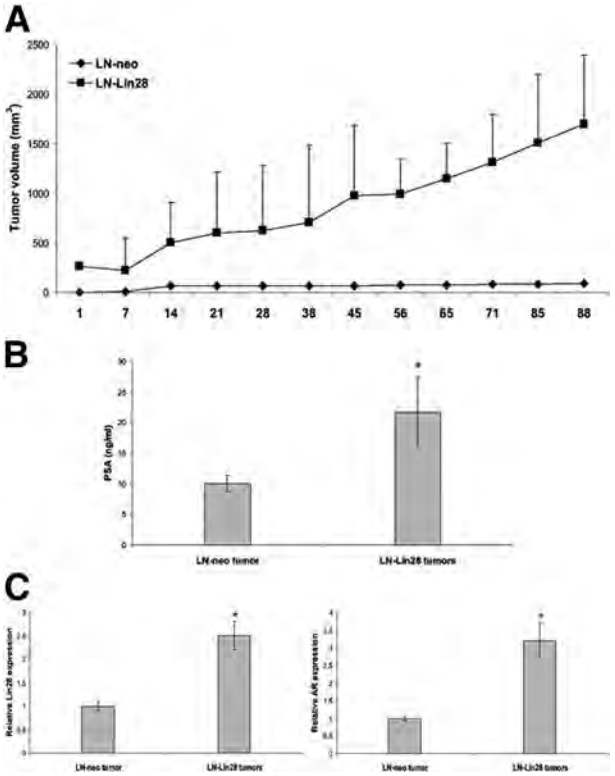

Figure 5 Lin28 promotes tumor growth of CaP xenografts. **A**: Cells (2×10^6 per flank of LN Lin28 or LN neo) were injected s.c. into both flanks of male nude mice, and tumor growth was monitored. **B**: Secretion of PSA by the CaP xenografts was measured in the mouse serum samples. Tumors expressing Lin28 secreted more PSA compared to the control tumors. **C**: Higher expression levels of Lin28 (**left panel**) and AR (**right panel**) were confirmed by RT qPCR in total RNAs from xenograft tissues. $^*P \leq 0.05$.

These results were confirmed by Western blot analysis (Figure 6B). To determine whether down-regulation of Lin28 affects the expression of AR, we transfected shRNA against Lin28 into C4-2B cells and analyzed the protein levels of AR by Western blot analysis. The results showed that down-regulation of Lin28 led to a decrease in protein levels of AR (Figure 6B), suggesting that Lin28 expression is necessary for maintenance of AR expression in CaP cells.

To determine whether Lin28 regulates AR-dependent signaling, we analyzed the expression levels of *PSA* and *NKX3.1*, two typical AR target genes, in LN-neo and LN-Lin28 cells by RT-qPCR. The results showed that expression levels of *PSA* and *NKX3.1* were enhanced in LN-Lin28 cells (Figure 6C). We analyzed the effect of Lin28 on the transactivating ability of AR using luciferase assays. A luciferase reporter vector driven by the full-length promoter of PSA (PSA-E/P-Luc) was transfected into LN-neo and LN-Lin28 cells, and luciferase assays were performed. The results showed that Lin28 induced the activity of PSA promoter (Figure 6D), indicating that Lin28 may contribute to increased transcription of AR-dependent genes by activating the AR. To confirm these findings, we analyzed levels of PSA in supernatants of LN-neo and LN-Lin28 cells by ELISA and found that secretion of PSA by LN-Lin28 cells was higher compared to LN-neo cells (Figure 6D). We also examined the effect of Lin28 on recruitment of AR to the promoters of *PSA* and *NKX3.1* genes by chromatin immunoprecipitation assays. The results showed that recruitment of AR to AR-responsive element (ARE) I/II and ARE III regions in *PSA* (Figure 6E), and ARE in *NKX3.1* (Figure 6E) promoters, was enhanced

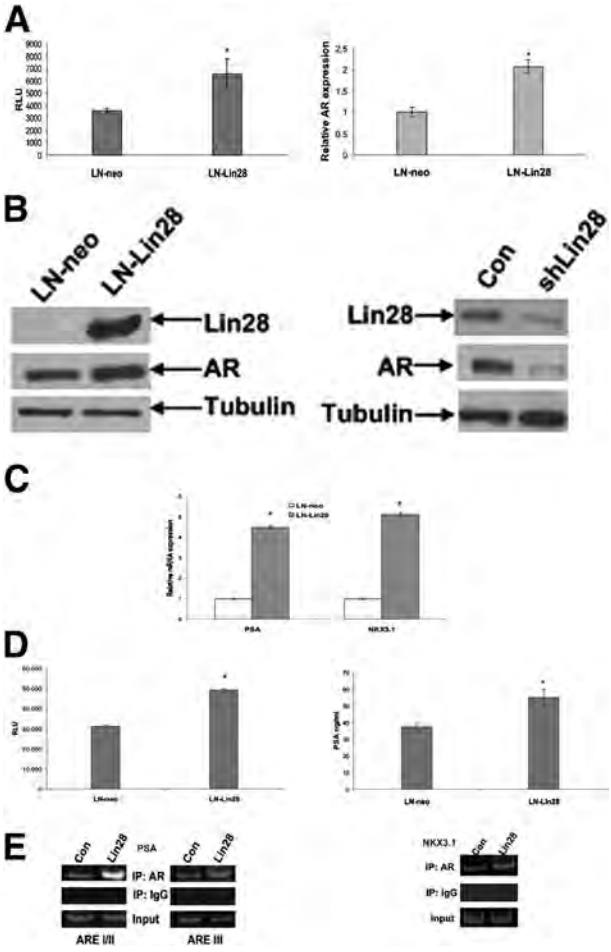

Figure 6 Lin28 enhances expression and activation of the AR. **A**: LN Lin28 and LN neo cells were transfected with pGL4 AR Prom Luc, and luciferase activities were measured. Activity of the full length promoter of AR was increased in Lin28 expressing cells. RT qPCR assays showing the increase in AR mRNA expression in Lin28 expressing LNCaP cells. **B**: Western blot analysis showing the increase in AR protein expression in LN Lin28 cells compared to LN neo cells. C4 2B cells were transfected with shRNA against Lin28, and protein expression of AR was analyzed. Down regulation of Lin28 by shRNA reduced the expression of AR. **C**: Expression levels of AR target genes, *PSA* and *NKX3.1*, were measured by RT qPCR in LN neo and LN Lin28 cells. mRNA levels of both genes were increased in Lin28 expressing cells compared to control (Con) cells. **D**: LN Lin28 and LN neo cells were transfected with PSA E/P Luc, and luciferase activities were measured. **Left panel**: Activation of *PSA* promoter was enhanced in Lin28 expressing cells compared to control cells. **Right panel**: Secretion of PSA by LN Lin28 and LN neo cells with measured by ELISA. Levels of PSA secreted by Lin28 expressing cells were higher than control cells. Data are presented as means ± SD of three experiments performed in triplicate. $^*P \leq 0.05$. **E**: Recruitment of AR to the ARE I/II and ARE III regions of *PSA* promoter and ARE in *NKX3.1* promoter was analyzed by chromatin immunoprecipitation assays. Expression of Lin28 enhanced recruitment of AR to AREs in target gene promoters. IP, immunoprecipitation; RLU, relative light units.

in Lin28-expressing cells compared to controls. Taken together, these results demonstrate that Lin28 activates the AR signaling axis.

Discussion

Lin28 is an RNA-binding protein postulated to be overexpressed in several malignancies.[8,23] [26] Lin28 controls the biogenesis of let-7 miRNAs[27,28] and is one of the pluripotency factors that are responsible for the reprogramming of differentiated cells to stem cell like.[29] In this study, we showed that Lin28 is overexpressed in human CaP compared to benign tissues, promotes growth of human CaP cells *in vitro*, and enhances growth of CaP xenografts. To our knowledge, this is the first report demonstrating the role of Lin28 in CaP cell proliferation and the ability of Lin28 to promote prostate tumor growth.

Lin28 was originally identified as a key regulator of developmental timing in *C. elegans*.[30] It is a conserved cytoplasmic protein, but on export to the nucleus, regulates the translation or stability of mRNAs.[31] In mammals, Lin28 is widely expressed in early development and in stem cells, but its expression is down-regulated with differentiation and is absent in most adult tissues.[2,32] On the other hand, Lin28 is up-regulated in human tumors and promotes transformation and tumor progression.[8] Depletion of Lin28 and expression of let-7 suppress bone metastasis.[14] Lin28B, a homologue of Lin28, is overexpressed in hepatocellular carcinoma, and exogenous Lin28B promotes cancer cell proliferation.[33] Lin28B plays an important role in Myc-dependent cellular proliferation.[34] Several recent reports demonstrated that Lin28 expression correlates with survival of patients with malignant diseases.[33] In ovarian cancer, patients with high Lin28B expression had shorter progression-free and overall survival times than those with low Lin28B expression.[35] High Lin28B staining intensity in stage I/II colon cancers correlated with reduced survival and increased probability of tumor recurrence.[25] A correlation between high expression of Lin28 and Lin28B and poor prognosis of patients with esophageal cancers was reported.[23] Collectively, these reports emphasize the importance of Lin28 in development and cellular transformation and as a potential oncogene. Our current findings that Lin28 promotes CaP growth *in vitro* and *in vivo* are in accordance with the studies described herein and provide novel evidence for the role of Lin28 in prostate cancer.

We observed strong nuclear staining of Lin28 in benign prostate tissues almost exclusively in the basal cell layer, with no staining in the luminal epithelial compartment. This can be explained by the following: Lin28 is highly expressed in progenitor cells, and the basal cell compartment is generally considered to harbor putative prostate stem cells. Thus, it is conceivable that the benign prostate gland exhibits high expression of Lin28 in the basal cell layer. An apparent shift from mostly nuclear localization in benign prostate to a nuclear + cytoplasmic or mostly cytoplasmic localization appears to occur in CaP, which would have to be confirmed by further studies with a larger sample size.

We have demonstrated increased levels of Lin28 in human prostate tumors, which may likely result from the activation of c-Myc.[36] c-Myc is a known target of let-7 miRNAs and also a transcriptional target of STAT3 and NF-κB2/p52, which we have already shown to be constitutively activated in prostate tumors.[22,37] Alternatively, up-regulation of Lin28 in human CaP may occur due to stabilization of its mRNA owing to suppression of let-7 miRNAs. Our earlier studies showed that the double-negative feedback loop between let-7 and Lin28, encompassing c-Myc, likely plays a major role in prostate carcinogenesis.[6,7] Recent evidence suggests that Lin28 does not rely solely on its regulation of let-7 miRNA biogenesis, but also modulates gene expression by altering translation[38,39] and by modulating levels of splicing factors involved in alternative splicing of mature transcripts.[40] Lin28 may regulate expression of prosurvival genes in CaP via one of these mechanisms. As Lin28 is being increasingly implicated in critical cellular processes, including development, transformation, and maintenance of stem cell signatures, the need to fully elucidate its multiple mechanisms of action becomes urgent to exploit its potential as a therapeutic target in human CaP.

In summary, we have shown that Lin28 is overexpressed in prostate carcinomas and promotes prostate tumor growth. Lin28 also activates AR-dependent signaling and enhances growth of human CaP cells. These findings underline the multifactorial nature of Lin28 and present it as an attractive target for therapeutic intervention in CaP.

Acknowledgments

We thank Drs. Leland W.K. Chung and Wen-Chin Huang (Cedars-Sinai Medical Center, Los Angeles, CA) and Dr. Donald Tindall (Mayo Clinic, Rochester, MN) for the pGL4-AR-Prom-Luc plasmid.

Supplemental Data

Supplemental material for this article can be found at *http://dx.doi.org/10.1016/j.ajpath.2013.03.011*.

References

1. Nadiminty N, Gao AC: Mechanisms of persistent activation of the androgen receptor in CRPC: recent advances and future perspectives. World J Urol 2012, 30:287–295
2. Moss EG, Tang L: Conservation of the heterochronic regulator Lin 28, its developmental expression and microRNA complementary sites. Dev Biol 2003, 258:432–442
3. Takamizawa J, Konishi H, Yanagisawa K, Tomida S, Osada H, Endoh H, Harano T, Yatabe Y, Nagino M, Nimura Y, Mitsudomi T, Takahashi T: Reduced expression of the let 7 microRNAs in human lung cancers in association with shortened postoperative survival. Cancer Res 2004, 64:3753–3756

4. Shell S, Park SM, Radjabi AR, Schickel R, Kistner EO, Jewell DA, Feig C, Lengyel E, Peter ME: Let 7 expression defines two differentiation stages of cancer. Proc Natl Acad Sci U S A 2007, 104: 11400–11405
5. Akao Y, Nakagawa Y, Naoe T: let 7 microRNA functions as a potential growth suppressor in human colon cancer cells. Biol Pharm Bull 2006, 29:903–906
6. Nadiminty N, Tummala R, Lou W, Zhu Y, Zhang J, Chen X, DeVere White RW, Kung H J, Evans CP, Gao AC: MicroRNA let 7c suppresses androgen receptor expression and activity via regulation of Myc expression in prostate cancer cells. J Biol Chem 2012, 287: 1527–1537
7. Nadiminty N, Tummala R, Lou W, Zhu Y, Shi X B, Zou JX, Chen H, Zhang J, Chen X, Luo J, DeVere White RW, Kung H J, Evans CP, Gao AC: MicroRNA let 7c is downregulated in prostate cancer and suppresses prostate cancer growth. PLoS One 2012, 7:e32832
8. Viswanathan SR, Powers JT, Einhorn W, Hoshida Y, Ng TL, Toffanin S, O'Sullivan M, Lu J, Phillips LA, Lockhart VL, Shah SP, Tanwar PS, Mermel CH, Beroukhim R, Azam M, Teixeira J, Meyerson M, Hughes TP, Llovet JM, Radich J, Mullighan CG, Golub TR, Sorensen PH, Daley GQ: Lin28 promotes transformation and is associated with advanced human malignancies. Nat Genet 2009, 41:843–848
9. Iliopoulos D, Hirsch H, Struhl K: An epigenetic switch involving NF kappaB, Lin28, Let 7 microRNA and IL6 links inflammation to cell transformation. Cell 2009, 139:693–706
10. Peng S, Maihle N, Huang Y: Pluripotency factors Lin28 and Oct4 identify a sub population of stem cell like cells in ovarian cancer. Oncogene 2010, 29:2153–2159
11. Viswanathan SR, Daley GQ, Gregory RI: Selective blockade of microRNA processing by Lin28. Science 2008, 320:97–100
12. Viswanathan SR, Daley GQ: Lin28: a microRNA regulator with a macro role. Cell 2010, 140:445–449
13. Chang T C, Zeitels LR, Hwang H W, Chivukula RR, Wentzel EA, Dews M, Jung J, Gao P, Dang CV, Beer MA, Thomas Tikhonenko A, Mendell JT: Lin 28B transactivation is necessary for Myc mediated let 7 repression and proliferation. Proc Natl Acad Sci U S A 2009, 106:3384–3389
14. Dangi Garimella S, Yun J, Eves EM, Newman M, Erkeland SJ, Hammond SM, Minn AJ, Rosner MR: Raf kinase inhibitory protein suppresses a metastasis signalling cascade involving LIN28 and let 7. EMBO J 2009, 28:347–358
15. Lu J, Getz G, Miska EA, Alvarez Saavedra E, Lamb J, Peck D, Sweet Cordero A, Ebert BL, Mak RH, Ferrando AA, Downing JR, Jacks T, Horvitz HR, Golub TR: MicroRNA expression profiles classify human cancers. Nature 2005, 435:834–838
16. Chun JY, Nadiminty N, Dutt S, Lou W, Yang JC, Kung H J, Evans CP, Gao AC: Interleukin 6 regulates androgen synthesis in prostate cancer cells. Clin Cancer Res 2009, 15:4815–4822
17. Nadiminty N, Lou W, Sun M, Chen J, Yue J, Kung H J, Evans CP, Zhou Q, Gao AC: Aberrant activation of the androgen receptor by NF κB2/p52 in prostate cancer cells. Cancer Res 2010, 70: 3309–3319
18. Nadiminty N, Chun JY, Lou W, Lin X, Gao AC: NF κB2/p52 enhances androgen independent growth of human LNCaP cells via protection from apoptotic cell death and cell cycle arrest induced by androgen deprivation. Prostate 2008, 68:1725–1733
19. Yang JC, Ok JH, Busby JE, Borowsky AD, Kung HJ, Evans CP: Aberrant activation of androgen receptor in a new neuropeptide autocrine model of androgen insensitive prostate cancer. Cancer Res 2009, 69:151–160
20. Dunn TA, Chen S, Faith DA, Hicks JL, Platz EA, Chen Y, Ewing CM, Sauvageot J, Isaacs WB, De Marzo AM, Luo J: A novel role of myosin VI in human prostate cancer. Am J Pathol 2006, 169: 1843–1854
21. Ni Z, Lou W, Lee SOK, Dhir R, De Miguel F, Grandis JR, Gao AC: Selective activation of members of the signal transducers and activators of transcription family in prostate carcinoma. J Urol 2002, 167: 1859–1862
22. Dhir R, Ni Z, Lou W, DeMiguel F, Grandis JR, Gao AC: Stat3 activation in prostatic carcinomas. Prostate 2002, 51:241–246
23. Hamano R, Miyata H, Yamasaki M, Sugimura K, Tanaka K, Kurokawa Y, Nakajima K, Takiguchi S, Fujiwara Y, Mori M, Doki Y: High expression of Lin28 is associated with tumour aggressiveness and poor prognosis of patients in oesophagus cancer. Br J Cancer 2012, 106:1415–1423
24. Helland Ã, Anglesio MS, George J, Cowin PA, Johnstone CN, House CM, Sheppard KE, Etemadmoghadam D, Melnyk N, Rustgi AK, Phillips WA, Johnsen H, Holm R, Kristensen GB, Birrer MJ, Pearson RB, Børresen Dale AL, Huntsman DG, deFazio A, Creighton CJ, Smyth GK, Bowtell DD; Australian Ovarian Cancer Study Group: Deregulation of MYCN, LIN28B and LET7 in a molecular subtype of aggressive high grade serous ovarian cancers. PLoS One 2011, 6:e18064
25. King CE, Cuatrecasas M, Castells A, Sepulveda AR, Lee J S, Rustgi AK: LIN28B promotes colon cancer progression and metastasis. Cancer Res 2011, 71:4260–4268
26. King CE, Wang L, Winograd R, Madison BB, Mongroo PS, Johnstone CN, Rustgi AK: LIN28B fosters colon cancer migration, invasion and transformation through let 7 dependent and independent mechanisms. Oncogene 2011, 30:4185–4193
27. Heo I, Joo C, Kim Y K, Ha M, Yoon M J, Cho J, Yeom K H, Han J, Kim VN: TUT4 in concert with Lin28 suppresses microRNA biogenesis through pre microRNA uridylation. Cell 2009, 138:696–708
28. Lehrbach NJ, Miska EA: Regulation of pre miRNA processing. Adv Exp Med Biol 2010, 700:67–75
29. Vêncio EF, Nelson AM, Cavanaugh C, Ware CB, Miller DG, Garcia JC, Vêncio RZ, Loprieno MA, Liu AY: Reprogramming of prostate cancer associated stromal cells to embryonic stem like. Prostate 2012, 72:1453–1463
30. Moss EG, Lee RC, Ambros V: The cold shock domain protein LIN 28 controls developmental timing in C. elegans and is regulated by the lin 4 RNA. Cell 1997, 88:637–646
31. Balzer E, Moss EG: Localization of the developmental timing regulator Lin28 to mRNP complexes, P bodies and stress granules. RNA Biol 2007, 4:16–25
32. Yang D H, Moss EG: Temporally regulated expression of Lin 28 in diverse tissues of the developing mouse. Gene Expression Patterns 2003, 3:719–726
33. Guo Y, Chen Y, Ito H, Watanabe A, Ge X, Kodama T, Aburatani H: Identification and characterization of lin 28 homolog B (LIN28B) in human hepatocellular carcinoma. Gene 2006, 384:51–61
34. Shyh Chang N, Daley GQ: Lin28: primal regulator of growth and metabolism in stem cells. Cell Stem Cell 2013, 12:395–406
35. Lu L, Katsaros D, Shaverdashvili K, Qian B, Wu Y, de la Longrais IAR, Preti M, Menato G, Yu H: Pluripotent factor lin 28 and its homologue lin 28b in epithelial ovarian cancer and their associations with disease outcomes and expression of let 7a and IGF II. Eur J Cancer 2009, 45:2212–2218
36. Iliopoulos D, Hirsch HA, Struhl K: An epigenetic switch involving NF κB, Lin28, Let 7 microRNA, and IL6 links inflammation to cell transformation. Cell 2009, 139:693–706
37. Nadiminty N, Dutt S, Tepper C, Gao AC: Microarray analysis reveals potential target genes of NF κB2/p52 in LNCaP prostate cancer cells. Prostate 2010, 70:276–287
38. Huang Y: A mirror of two faces: Lin28 as a master regulator of both miRNA and mRNA. Wiley Interdiscip Rev RNA 2012, 3:483–494
39. Lei XX, Xu J, Ma W, Qiao C, Newman MA, Hammond SM, Huang Y: Determinants of mRNA recognition and translation regulation by Lin28. Nucleic Acids Res 2012, 40:3574–3584
40. Wilbert ML, Huelga SC, Kapeli K, Stark TJ, Liang TY, Chen SX, Yan BY, Nathanson JL, Hutt KR, Lovci MT, Kazan H, Vu AQ, Massirer KB, Morris Q, Hoon S, Yeo GW: LIN28 binds messenger RNAs at GGAGA motifs and regulates splicing factor abundance. Mol Cell 2012, 48:195–206

Molecular Cancer Therapeutics

NF-κB2/p52 Induces Resistance to Enzalutamide in Prostate Cancer: Role of Androgen Receptor and Its Variants

Nagalakshmi Nadiminty[1], Ramakumar Tummala[1], Chengfei Liu[1], Joy Yang[1], Wei Lou[1], Christopher P. Evans[1,2], and Allen C. Gao[1,2]

Abstract

Resistance of prostate cancer cells to the next generation antiandrogen enzalutamide may be mediated by a multitude of survival signaling pathways. In this study, we tested whether increased expression of NF κB2/p52 induces prostate cancer cell resistance to enzalutamide and whether this response is mediated by aberrant androgen receptor (AR) activation and AR splice variant production. LNCaP cells stably expressing NF κB2/p52 exhibited higher survival rates than controls when treated with enzalutamide. C4 2B and CWR22Rv1 cells chronically treated with enzalutamide were found to express higher levels of NF κB2/p52. Downregulation of NF κB2/p52 in CWR22Rv1 cells chronically treated with enzalutamide rendered them more sensitive to cell growth inhibition by enzalutamide. Analysis of the expression levels of AR splice variants by quantitative reverse transcription PCR and Western blotting revealed that LNCaP cells expressing p52 exhibit higher expression of AR splice variants. Downregulation of expression of NF κB2/p52 in VCaP and CWR22Rv1 cells by short hairpin RNA abolished expression of splice variants. Downregulation of expression of either full length AR or the splice variant AR V7 led to an increase in sensitivity of prostate cancer cells to enzalutamide. These results collectively demonstrate that resistance to enzalutamide may be mediated by NF κB2/p52 via activation of AR and its splice variants. *Mol Cancer Ther; 12(8); 1629 37. ©2013 AACR.*

Introduction

Localized prostate cancer is dependent on androgens, and the majority of patients respond to androgen ablation. However, virtually every patient will develop castration-resistant prostate cancer (CRPC) and no longer respond to androgen deprivation therapy (ADT). Persistent androgen receptor (AR) activation remains an important player in CRPC progression. CRPC cells often continue to express AR and AR axis genes (1, 2), implying that the AR is active in AR-positive CRPC cells. Such observations form the basis for continued attempts to target the AR axis and for the development of next-generation antiandrogens such as enzalutamide (formerly MDV3100). Enzalutamide binds to the AR with greater affinity than bicalutamide and inhibits its nuclear translocation and expression of its target genes (3). Despite initial success, development of resistance is a contraindication for its use in many patients, and as demographics change, an increasing number of patients are likely to develop resistance to enzalutamide. The mechanisms leading to resistance have been poorly understood, even though a recent report showed that AR splice variants play a major role in development of resistance (4). AR splice variants lack the ligand-binding domain targeted by enzalutamide and variants such as AR-V7 are postulated to be constitutively active. The mechanistic aspects of regulation of variant expression leading to resistance against enzalutamide are unknown. Therefore, an urgent need exists to fully understand the mechanisms of resistance and to devise ways to overcome them.

The classical NF-κB pathway involving the p65/p50 heterodimer has been shown to be constitutively activated in several cancers including prostate cancer (5). The non-canonical NF-κB pathway involves the processing of p100 to NF-κB2/p52 via the recruitment of NF-κB inducing kinase (NIK) and subsequent activation of IκB kinase α (IKKα). The processing of p100 to p52 is a tightly controlled event in many cells and tissues (6 9). The functional significance of p100 processing has been confirmed by genetic evidence from humans and mice (10). Overproduction of p52 has been observed in several solid tumors including breast and prostate cancers (11, 12). Our previous studies showed that NF-κB2/p52 induces castration-resistant growth in LNCaP cells (13), that several genes involved in processes such as cell growth,

Authors' Affiliations: [1]Department of Urology and [2]Comprehensive Cancer Center, University of California at Davis, Sacramento, California

Note: Supplementary data for this article are available at Molecular Cancer Therapeutics Online (http://mct.aacrjournals.org/).

Corresponding Authors: Allen C. Gao and Nagalakshmi Nadiminty, Department of Urology, University of California Davis Medical Center, 4645 2nd Ave, Research III, Suite 1300, Sacramento, CA 95817. Phone: 916 734 8718; Fax: 916 734 8714; E mail: acgao@ucdavis.edu and nnadiminty@ucdavis.edu

doi: 10.1158/1535 7163.MCT 13 0027

proliferation, cell movement are potential targets of NF-κB2/p52 (14), and that NF-κB2/p52 induces aberrant activation of the AR in a ligand-independent manner and thus promotes castration resistance (15).

In this study, we report that NF-κB2/p52 promotes resistance of prostate cancer cells to enzalutamide. We show that increased resistance of prostate cancer cells expressing p52 to enzalutamide may be mediated by induction of AR splice variants (such as AR-V7) and by activation of the AR axis by p52.

Materials and Methods

Cell lines and reagents

LNCaP, CWR22Rv1, and VCaP cells were obtained from the American Type Culture Collection (ATCC). All experiments with cell lines were performed within 6 months of receipt from ATCC or resuscitation after cryopreservation. ATCC uses short tandem repeat (STR) profiling for testing and authentication of cell lines. C4-2B cells were kindly provided and authenticated by Dr. Leland Chung, Cedars-Sinai Medical Center, Los Angeles, CA. Cells were cultured in RPMI containing either 10% complete FBS or 10% charcoal/dextran-stripped FBS (CS-FBS) and penicillin/streptomycin. LNCaP passage numbers less than 20 were used throughout the study. VCaP cells were cultured in Dulbecco's Modified Eagle Medium (DMEM) supplemented with 10% FBS. NF-κB2/p52 (K-27), AR (441; mouse monoclonal), hemagglutinin (HA), and tubulin antibodies were purchased from Santa Cruz Biotechnologies. Antibodies against AR-V7 splice variant were kindly provided by Dr. Jun Luo (Department of Urology, Johns Hopkins University, Baltimore, MD). All other reagents were of analytical grade and obtained from local suppliers. Sso Fast Eva Green qPCR Supermix was from Bio-Rad.

Generation of stable cell lines

Stable cell lines of LNCaP expressing NF-κB2/p52 (LN-p52) were generated by transfection of plasmids containing the cDNA and selection of clones after application of selective pressure with appropriate antibiotics. LNCaP cells expressing p52 under the control of a tetracycline-inducible cassette (LN/TR/p52) were generated using the ViraPower lentiviral transduction system (Invitrogen).

Cell growth assays

Cells were transfected with plasmids or treated with the indicated reagents, and viable cell numbers were determined at various time points using a Coulter cell counter.

Western blot analysis

Cells were lysed in high-salt buffer containing 50 mmol/L HEPES, pH 7.9, 250 mmol/L NaCl, 1 mmol/L EDTA, 1% NP-40, 1 mmol/L phenylmethylsulfonylfluoride (PMSF), 1 mmol/L Na vanadate, 1 mmol/L NaF, and protease inhibitor cocktail (Roche) as described earlier (16). Total protein was estimated using the Coomassie Protein Assay Reagent (Pierce). Equal amounts of protein were loaded on 10% SDS-PAGE and transferred to nitrocellulose membranes. The membranes were blocked with 5% nonfat milk in PBST (1× PBS + 0.1% Tween-20) and probed with primary antibodies in 1% bovine serum albumin (BSA). The signal was detected by ECL (GE Healthcare) after incubation with the appropriate horseradish peroxidase (HRP)-conjugated secondary antibodies.

Real-time quantitative reverse transcription PCR

Total RNAs were extracted using TRIzol reagent (Invitrogen). cDNAs were prepared after digestion with RNase-free RQ1 DNase (Promega). The cDNAs were subjected to real-time reverse transcription PCR (RT-PCR) using Sso Fast Eva Green Supermix (Bio-Rad) according to the manufacturer's instructions and as described previously (15). Each reaction was normalized by coamplification of actin. Triplicates of samples were run on default settings of Bio-Rad CFX-96 real-time cycler.

Clonogenic assays

Anchorage-dependent clonogenic ability assays were performed as described previously (13). Briefly, cells were seeded at low densities (400 cells/dish) in 10-cm culture plates. The plates were incubated at 37°C in media containing either 10% FBS or 10% charcoal-stripped FBS (CS-FBS) and were left undisturbed for 14 days. At the end of the experiment, cells were fixed with methanol, stained with crystal violet, and the numbers of colonies were counted.

Luciferase assays

Cells were transfected with reporters along with plasmids and AR and AR-V7 siRNAs as indicated in the figures. Cell lysates were subjected to luciferase assays with the Luciferase Assay System (Promega).

Statistical analyses

Data are shown as means ± SD. Multiple group comparison was performed by one-way ANOVA followed by the Scheffe procedure for comparison of means. $P \leq 0.05$ was considered significant.

Results

Prostate cancer cells expressing NF-κB2/p52 are resistant to enzalutamide and bicalutamide

LN-neo (LNCaP cells expressing the empty vector) and LN-p52 cells (LNCaP cells stably expressing p52) were treated with 0 and 20 μmol/L enzalutamide or bicalutamide in media containing either complete FBS or charcoal-stripped FBS, and cell growth was examined after 48 hours. Dimethyl sulfoxide (DMSO) was used as the vehicle control. As shown in Fig. 1A, cells stably expressing p52 exhibited better cell survival ability when exposed to enzalutamide or bicalutamide compared to control LN-neo cells. To confirm these experiments, we treated LN-neo or LN-p52 cells with 0, 20, and 40 μ mol/L enzalutamide or bicalutamide and performed clonogenic assays. As shown

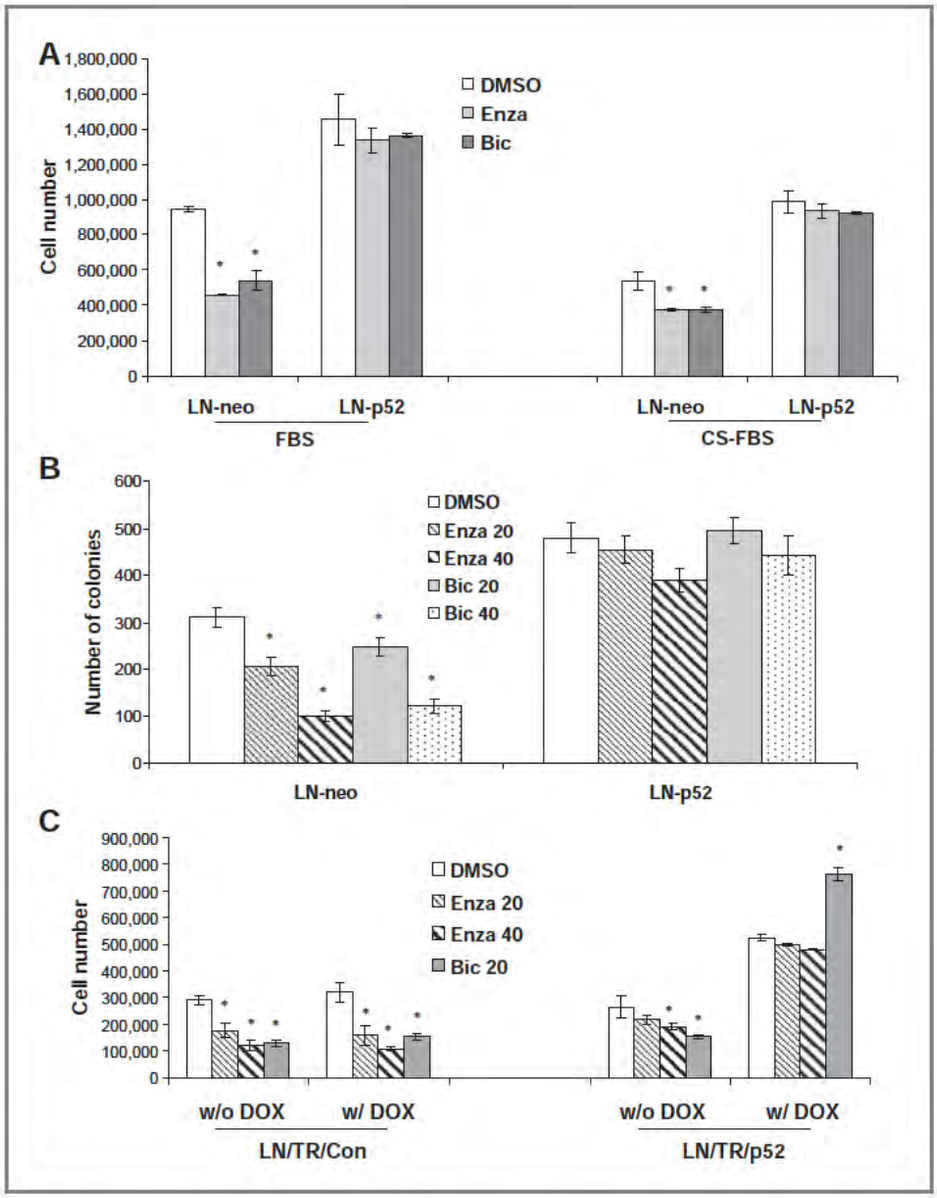

Figure 1. NF κB2/p52 expressing prostate cancer cells are resistant to enzalutamide. A, LNCaP cells stably expressing p52 (LN p52) and control LNCaP cells (LN neo) were treated with 0 and 20 μmol/L enzalutamide or bicalutamide in media containing either FBS or CS FBS, and cell numbers were counted after 48 hours. Results are presented as mean ± SD of 3 experiments performed in triplicate. LN p52 cells exhibited higher survival rates when treated with enzalutamide or bicalutamide than LN neo cells. B, LN neo and LN p52 cells were treated with 0, 20, or 40 μmol/L enzalutamide or bicalutamide, and clonogenic assays were performed. Results are presented as mean ± SD of 2 experiments performed in triplicate. LN p52 cells formed higher numbers of colonies than LN neo cells when treated with enzalutamide or bicalutamide. C, LN/TR/p52 cells [expressing p52 under the control of a tetracycline (tet) inducible promoter] and control LN/TR/Con cells were treated with 0, 20, or 40 μmol/L enzalutamide or 20 μmol/L bicalutamide in the presence or absence of 0.5 μmol/L doxycycline (DOX), and cell numbers were counted after 48 hours. Results are presented as mean ± SD of 3 experiments performed in triplicate. *, $P \leq 0.05$. LN/TR/p52 cells displayed higher survival rates when p52 expression was induced with DOX, compared to uninduced LN/TR/p52 cells as well as LN/TR/Con cells.

in Fig. 1B, LN-neo cells were highly sensitive to both enzalutamide and bicalutamide and formed fewer colonies, whereas the number of colonies formed by cells expressing p52 was significantly higher, indicating that NF-κB2/p52 may induce resistance to enzalutamide and bicalutamide in prostate cancer cells. To further confirm these results, we used the tetracycline-inducible system to induce p52 expression in LNCaP cells and tested enzalutamide and bicalutamide sensitivity. We treated LN/TR/Con and LN/TR/p52 cells with 0, 20, and 40 μ mol/L enzalutamide or bicalutamide and performed growth assays. As shown in Fig. 1C, induction of expression of p52 by doxycycline significantly enhanced the ability of LN/TR/p52 cells to survive in the presence of enzalutamide or bicalutamide compared to control LN/TR/Con cells. These results collectively demonstrate that prostate cancer cells expressing higher levels of NF-κB2/p52 are more resistant to enzalutamide and bicalutamide compared to cells which do not express p52.

Prostate cancer cells chronically treated with enzalutamide exhibit higher levels of NF-κB2/p52

Our previous studies showed that most androgen-dependent prostate cancer cell lines do not express detectable levels of endogenous NF-κB2/p52 (13). Hence, to test whether prostate cancer cells resistant to enzalutamide exhibit higher levels of p52, we treated CWR22Rv1 cells with 5 to 10 μ mol/L enzalutamide chronically for more than 10 months. The resultant cells showed higher cell survival rates when treated with enzalutamide. We examined the expression levels of NF-κB2/p52 in these cells by quantitative RT-PCR (qRT-PCR) and Western

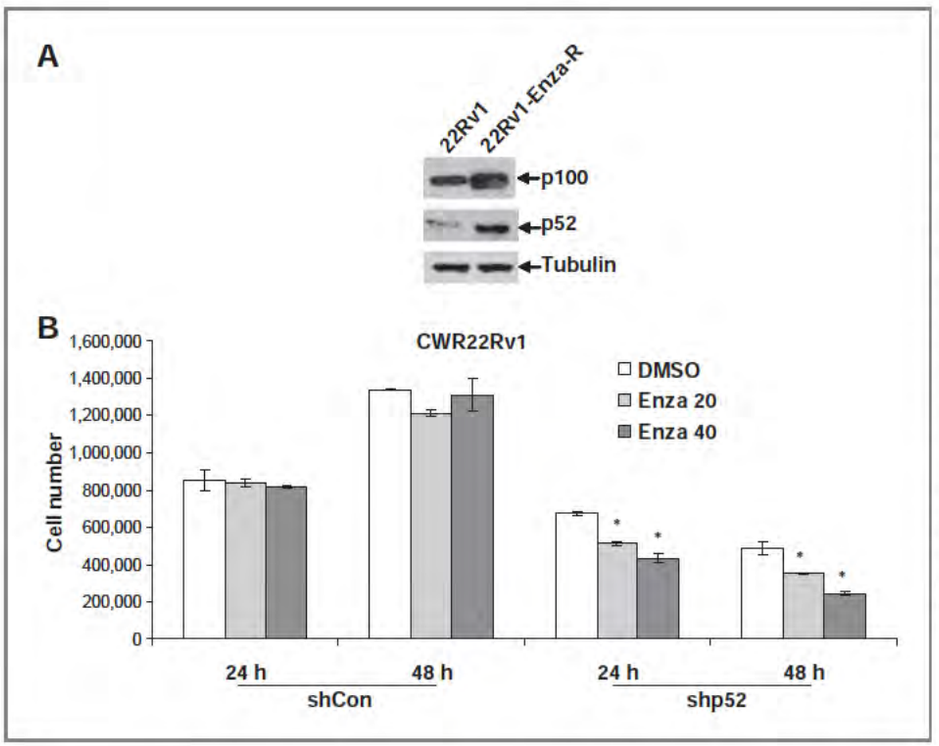

Figure 2. Prostate cancer cells treated chronically with enzalutamide upregulate the expression of NF κB2/p52. A, CWR22Rv1 cells treated chronically with enzalutamide exhibit higher endogenous levels of both p100 and p52. B, CWR22Rv1 cells treated chronically with enzalutamide were transfected with either control shRNAs or shRNAs against NF κB2/p52 and were treated with 0, 20, or 40 μmol/L enzalutamide. Cell numbers were counted after 24 and 48 hours. Results are presented as mean ± SD of 2 experiments performed in triplicate. *, $P \leq 0.05$. Cells transfected with shRNAs against p52 exhibited lower cell survival when treated with enzalutamide.

blotting. As shown in Fig. 2A, CWR22Rv1 cells treated chronically with enzalutamide exhibited higher levels of both precursor p100 as well as p52, indicating that prostate cancer cells resistant to enzalutamide may upregulate the endogenous levels of NF-κB2/p52. To test whether downregulation of p52 resensitizes these cells to enzalutamide, we transfected short hairpin RNAs (shRNA) specific to p52 into CWR22Rv1 cells treated chronically with enzalutamide (expressing higher levels of p52) and examined cell growth after 24 and 48 hours. Downregulation of p52 after transfection was confirmed by qRT-PCR. As shown in Fig. 2B, cells transfected with p52 shRNA were increasingly sensitive to enzalutamide compared to control CWR22Rv1-Enza-R cells, indicating that expression of p52 may be necessary for the survival of cells treated chronically with enzalutamide. These results collectively demonstrate that NF-κB2/p52 may regulate the induction of resistance to enzalutamide in prostate cancer cells.

NF-κB2/p52 enhances expression of AR splice variants

It has been shown that higher levels of AR splice variants may be responsible for the resistance to enzalutamide in prostate cancer (4), hence, we tested whether NF-κB2/p52 regulates the expression of AR splice variants. Total RNAs from LNCaP and C4-2B cells transfected with either empty vector or p52 in media containing either complete or charcoal-stripped FBS (CS-FBS) were analyzed by qRT-PCR for the expression levels of full-length (FL) AR as well as the major splice variant AR-V7. As shown in Fig. 3A, expression of p52 enhanced the expression levels of the splice variant AR-V7 in both FBS and CS-FBS, whereas expression of FL AR remained unchanged in LNCaP cells (left). These results were confirmed by Western blotting using antibodies specific for FL AR and AR-V7 (right). Similar results were observed in C4-2B cells, in which expression of p52 enhanced the expression levels of AR-V7, whereas expression levels of FL AR were unaffected (Fig. 3B). To substantiate these results, we examined expression levels of FL AR and AR-V7 in LN-neo and LN-p52 cells by qRT-PCR and Western blotting and found that expression levels of AR-V7 were elevated in LN-p52 cells compared to LN-neo cells (Fig. 3C). We also analyzed expression levels of AR-V7 in xenografts of LNCaP cells expressing p52 and found that xenografts expressing p52 exhibited significantly higher levels of AR-V7 mRNA compared to control LNCaP cell xenografts (Fig. 3D). These findings show that NF-κB2/p52 may induce upregulation of the expression of AR-V7.

Downregulation of NF-κB2/p52 abrogates expression of AR splice variants

Next, we tested whether NF-κB2/p52 was necessary for the enhanced expression of AR splice variants. VCaP and CWR22Rv1 prostate cancer cells express endogenous levels of AR splice variants AR-V1, AR-V5, AR-V7, AR-1/2/2b, and AR-1/2/3/2b. We transfected shRNA specific to p52 into VCaP and CWR22Rv1 cells and examined the expression levels of these splice variants by qRT-PCR using specific primers. As shown in Fig. 4A and B (left), downregulation of p52 reduced the expression levels of most of the splice variants significantly, whereas levels of

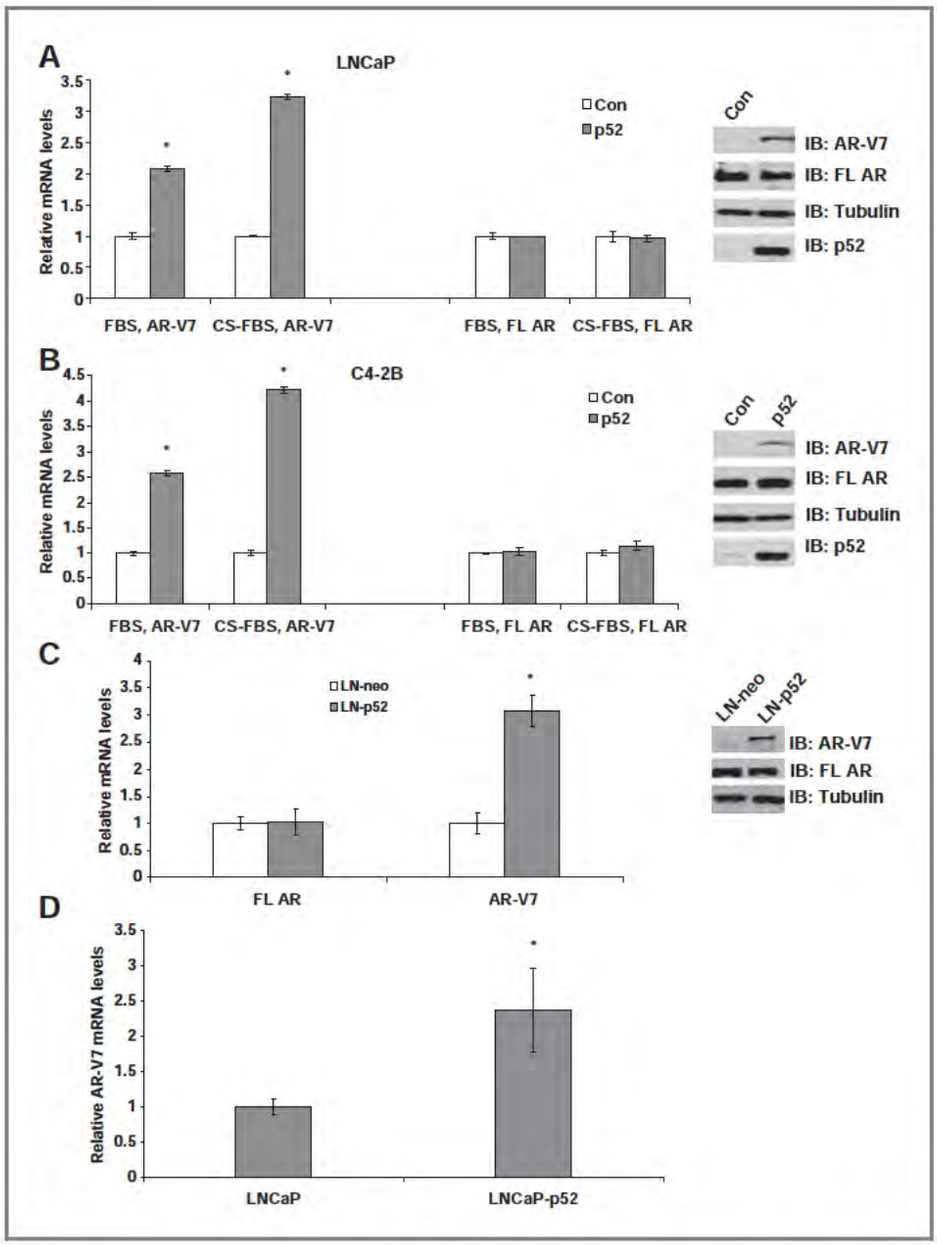

Figure 3. NF κB2/p52 induces higher expression of AR splice variants. Total RNAs from LNCaP (A) and C4 2B (B) cells transfected with empty vector or p52 were analyzed by qRT PCR for the expression of FL AR and AR V7 in media containing either FBS or CS FBS. Expression of p52 enhanced the levels of AR V7, whereas levels of FL AR remained unchanged. Right, immunoblotting of above lysates with antibodies specific against either FL AR or AR V7. C, total RNAs from LN p52 and LN neo cells were analyzed by qRT PCR for the expression levels of FL AR or AR V7. LN p52 cells showed higher levels of expression of AR V7 compared to LN neo cells, whereas FL AR levels were unaffected. Right, immunoblotting of above lysates with antibodies against FL AR or AR V7. D, expression levels of AR V7 were enhanced in xenografts from LNCaP cells expressing p52 compared to xenografts from parental LNCaP cells. Results are presented as mean ± SD of 2 experiments performed in triplicate. *, $P \leq 0.05$.

FL AR remained unaffected. These results were confirmed for AR-V7 expression by Western blotting using antibodies specific against AR-V7 and FL AR in VCaP and CWR22Rv1 cells (Fig. 4A and B, right), indicating that expression of p52 may be necessary for the synthesis of AR splice variants.

Downregulation of FL AR and AR-V7 increases sensitivity of p52-expressing prostate cancer cells to enzalutamide

LNCaP cells stably expressing p52 (LN-p52) exhibit higher levels of AR-V7. We also assessed expression levels of other members of the NF-κB family by Western blotting and found that their levels were not altered (Supplementary Fig. S1), indicating that the effect on AR-V7 expression was mainly due to the expression of NF-κB2/p52. Next, we analyzed expression levels of antiapoptotic proteins such as Bcl-xL, survivin, and cyclin D1 in LN-p52 cells compared to LN-neo cells and found that LN-p52 cells express higher levels of Bcl-xL, survivin, and cyclin D1 (Supplementary Fig. S2), indicating that activation of antiapoptotic genes may play an important role in resistance against enzalutamide. As reported previously, the cells also exhibit aberrant activation of AR in the absence of androgen and exhibit castration-resistant growth (15). In the current study, we also showed that LN-p52 cells are resistant to enzalutamide-induced growth inhibition compared to control LN-neo cells. Hence, to test whether

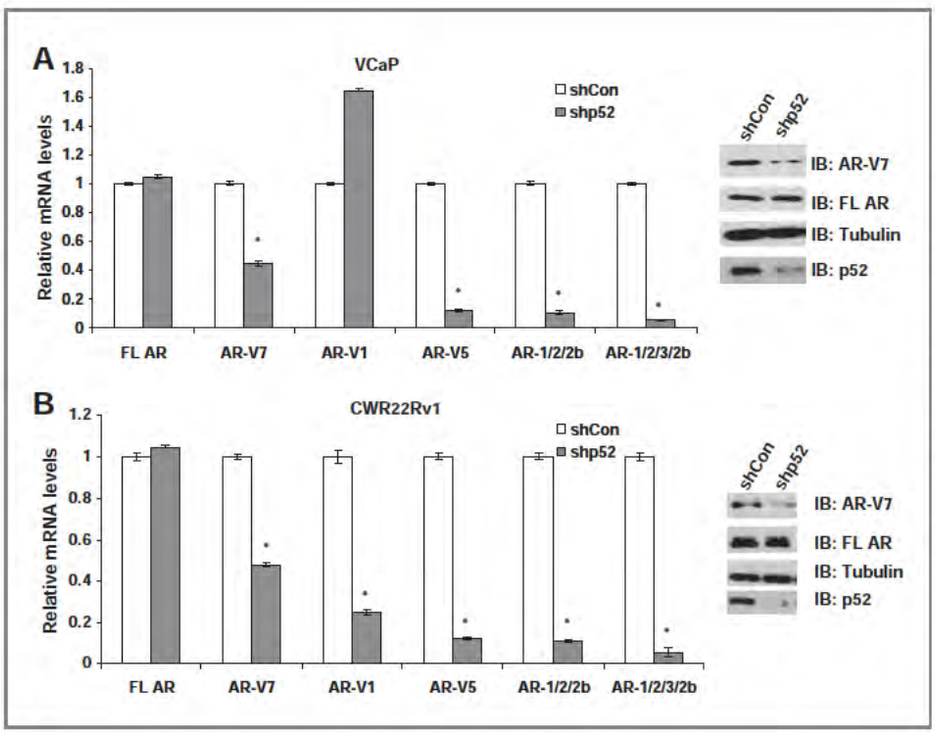

Figure 4. Downregulation of NF κB2/p52 in prostate cancer (CaP) cells reduces expression of AR splice variants. VCaP (A) and CWR22Rv1 (B) cells were transfected with either control shRNAs or shRNAs against p52 and expression levels of the indicated AR splice variants were analyzed by qRT PCR. Downregulation of p52 led to a decrease in synthesis of AR splice variants, whereas expression levels of FL AR remained unchanged. Right panels show immunoblots of above lysates with antibodies against FL AR or AR V7. Results are presented as mean ± SD of 3 experiments performed in triplicate. *, $P \leq 0.05$.

FL AR or AR-V7 plays a role in the p52-induced resistance to enzalutamide, we transfected siRNAs specific against either FL AR or AR-V7 into LN-neo and LN-p52 cells and monitored cell growth in response to enzalutamide. As shown in Fig. 5A, downregulation of either FL AR or AR-V7 reduced growth of control LN-neo cells by ~20%, and enzalutamide itself reduced growth of LN-neo cells by ~50%. No additional reduction of growth was observed in LN-neo cells when FL AR or AR-V7 was downregulated in the presence of enzalutamide, showing that inhibition of either FL AR or AR-V7 had no effect on the sensitivity of LN-neo cells to enzalutamide. In LN-p52 cells which express higher levels of AR-V7, downregulation of either FL AR or AR-V7 reduced growth by ~50% in the presence of enzalutamide, thus resensitizing LN-p52 cells to enzalutamide. In other words, LN-p52 cells are more sensitive to enzalutamide when expression of either FL AR or AR-V7 was inhibited. These results suggest that resistance of LN-p52 cells to enzalutamide is mediated by alterations in the AR signaling pathway and demonstrate that activation of the AR axis by p52 plays an important role in the p52-induced resistance to enzalutamide. To confirm these results and test whether downregulation of FL AR or AR-V7 modulates p52-induced AR activation, we co-transfected a luciferase reporter containing the enhancer and promoter regions of PSA (PSA-E/P-Luc) along with p52 and siRNAs against FL AR or AR-V7 into VCaP and CWR22Rv1 cells. The cells were treated with either vehicle or 20 μmol/L enzalutamide and luciferase assays performed. VCaP and CWR22Rv1 cells express higher endogenous levels of p52, and our previous studies show that p52 induces ligand-independent activation of AR (13, 15). As shown in Fig. 5B and as shown in our previous studies (15), p52 induces activation of AR-mediated target gene transcription, which was abolished by downregulation of either FL AR or AR-V7. p52-induced activation of AR was unaffected by enzalutamide treatment. Treatment with enzalutamide further enhanced the suppressive effect of siRNAs against FL AR or AR-V7 on p52-induced AR-mediated target gene transcription. These results demonstrate that activation of AR signaling is necessary for the p52-induced resistance against enzalutamide. Similar results were obtained in CWR22Rv1 cells (Fig. 5C), showing that the interplay between FL AR, AR-V7 and NF-κB2/p52 may be critical in the development of resistance to enzalutamide in prostate cancer cells. These results implicate the activation of the AR signaling axis by p52 via FL AR and its splice variants as being responsible for the induction of resistance against enzalutamide.

Discussion

Next-generation antiandrogens such as enzalutamide and inhibitors of androgen synthesis such as abiraterone have revolutionized the standard of care for patients with both early- and late-stage prostate cancer. Despite their successes and continuing widespread use, threat of development of resistance looms large (17, 18). The understanding of mechanisms by which resistance against these agents may develop in prostate cancer cells may be critical for early intervention strategies in the event of development of resistance. Enzalutamide binds to the ligand-binding domain of AR and inhibits its nuclear translocation, DNA binding, and transactivation of target

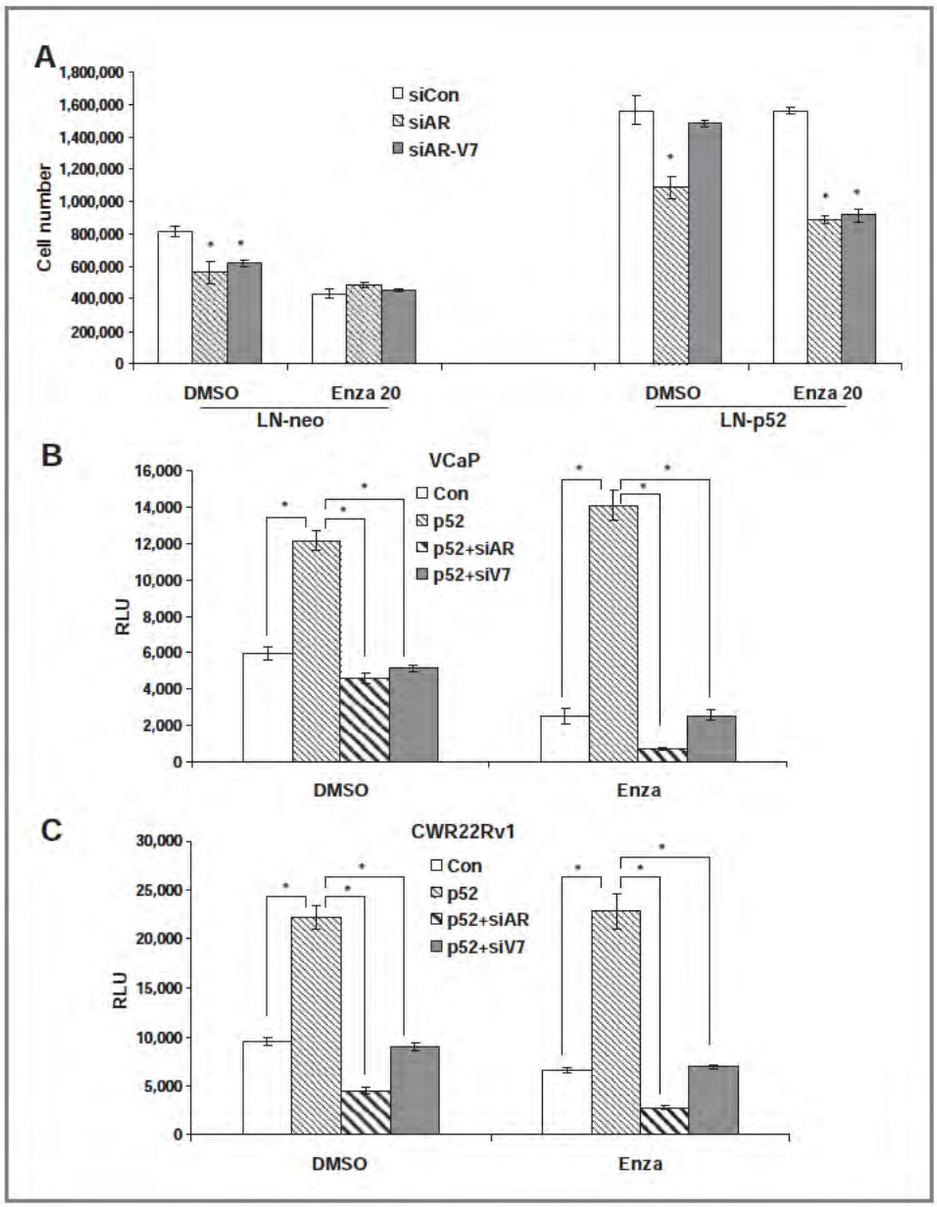

Figure 5. Downregulation of FL AR and AR V7 increases sensitivity of p52 expressing prostate cancer (CaP) cells to enzalutamide. A, LN p52 and LN neo cells were transfected with siRNAs specific to either FL AR or AR V7 and were treated with 0 or 20 μmol/L enzalutamide. Cell numbers were counted after 48 hours. Results are presented as mean ± SD of 3 experiments performed in triplicate. Downregulation of either FL AR or AR V7 increased sensitivity of LN p52 cells to enzalutamide. VCaP (B) and CWR22Rv1 (C) cells were transfected with PSA E/P Luc reporter, empty vector, or p52 together with siRNAs against FL AR or AR V7. Cells were treated with 0 or 40 μmol/L enzalutamide, and luciferase assays were performed after 48 hours. Results are presented as mean ± SD of 2 experiments performed in triplicate. *, $P \leq 0.05$. Downregulation of either FL AR or AR V7 suppressed p52 induced activation of AR in both VCaP and CWR22Rv1 cells.

genes (3). In the current study, we show that NF-κB2/p52 may play a crucial role in the development of resistance to enzalutamide and that the interplay between p52 and the AR signaling axis may be one of the underlying mechanisms. Even though enzalutamide and bicalutamide have similar mechanisms of action, clinically patients who progress on bicalutamide may respond to enzalutamide, indicating the existence of different mechanisms of resistance and that NF-κB2/p52 may be one of the many mediators of resistance. Our studies also show that prostate cancer cells treated chronically with enzalutamide may develop resistance against the agent via upregulation of expression of p52. These findings have important implications for therapeutic regimen in which patients are treated for long periods of time with enzalutamide. Further studies are warranted to test whether blocking of cellular signaling pathways in combination with antiandrogens may prove beneficial.

Our current data demonstrate that signaling networks such as p52 and AR interactions can mediate resistance to therapies targeting FL AR, including the next-generation antiandrogen, enzalutamide. The significance of these studies lies in the fact that resistance, either *de novo* or acquired, is one of the major clinical limitations for new AR inhibitors. The majority of patients who display disease progression on enzalutamide also display increasing prostate-specific antigen (PSA), indicating that enzalutamide-resistant tumors remain driven by persistent AR activity. AR variants are overexpressed in a subset of CRPC metastases and correlate with poor survival

(19, 20). As AR splice variants lack the ligand-binding domain, they may be insensitive to inhibition by both bicalutamide and enzalutamide. One of the pioneering studies about enzalutamide showed that it may be effective against cells expressing higher levels of AR splice variants, although this fact remains to be substantiated (21). Even though AR variants have been hypothesized to be independent mediators of castration resistance (4), FL AR may still be necessary and may augment the castration-resistant response (21). Conflicting results have been obtained about the distinct transcriptional programs activated by AR variants and FL AR in prostate cancer cells (4, 22). It is probable that such perceived differences are due to experimental platforms used and do not reflect physiologic deviations. It is also possible that AR variants execute a "tumor-specific" program, which is a part of the broader transcriptional program of the FL AR, and hence are enriched in tumors. This may not necessarily mean that the FL AR is no longer a player in the progression of prostate cancer. It would be more likely that co-operation between FL AR and its splice variants is the driver behind CRPC progression, rather than a distinct and dominant transcriptional program driven by the splice variants alone.

Our earlier studies showed that NF-κB2/p52 promotes castration-resistant progression of prostate cancer by activating the AR in conditions of androgen deprivation (13, 15). In this study, we showed that p52 also induces expression of AR splice variants. Since the mechanism of action of enzalutamide is the inhibition of AR activation, we hypothesized that prostate cancer cells expressing higher levels of p52 may be resistant to enzalutamide. Our current results confirm the hypothesis and point to the role of the interaction between AR and p52 as being one of the critical turns during the progression to castration resistance.

In summary, our study demonstrates a link between persistent activation of the AR by NF-κB2/p52 and development of resistance to enzalutamide in prostate cancer. Future points of interest would be whether overcoming these networks and improving the efficacy of currently available clinical agents represents a viable area of research.

Disclosure of Potential Conflicts of Interest

C.P. Evans has other commercial research support from, honoraria from speakers bureau from, and is a consultant/advisory board member for Medivation/Astellas. No potential conflicts of interest were disclosed by the other authors.

Authors' Contributions

Conception and design: N. Nadiminty, J. Yang, C.P. Evans, A.C. Gao
Development of methodology: N. Nadiminty, A.C. Gao
Acquisition of data (provided animals, acquired and managed patients, provided facilities, etc.): N. Nadiminty, R. Tummala, W. Lou, C.P. Evans, A.C. Gao
Analysis and interpretation of data (e.g., statistical analysis, biostatistics, computational analysis): N. Nadiminty, R. Tummala, C.P. Evans, A.C. Gao
Writing, review, and/or revision of the manuscript: N. Nadiminty, R. Tummala, C.P. Evans, A.C. Gao
Administrative, technical, or material support (i.e., reporting or organizing data, constructing databases): C. Liu, J. Yang, W. Lou, A.C. Gao
Study supervision: N. Nadiminty, C.P. Evans, A.C. Gao

Acknowledgments

The authors thank Dr. Jun Luo (Department of Urology, Johns Hopkins University) for the kind gift of AR-V7 specific antibody.

Grant Support

This work was supported in part by NIH CA140468, CA118887, CA109441, and DOD PC080538 (A.C. Gao) and by DOD PC100502 (N. Nadiminty).

The costs of publication of this article were defrayed in part by the payment of page charges. This article must therefore be hereby marked *advertisement* in accordance with 18 U.S.C. Section 1734 solely to indicate this fact.

Received January 10, 2013; revised April 12, 2013; accepted May 6, 2013; published OnlineFirst May 22, 2013.

References

1. Hobisch A, Culig Z, Radmayr C, Bartsch G, Klocker H, Hittmair A. Distant metastases from prostatic carcinoma express androgen receptor protein. Cancer Res 1995;55:3068 72.
2. van der Kwast TH, Schalken J, Ruizeveld de Winter JA, van Vroonho ven CC, Mulder E, Boersma W, et al. Androgen receptors in endocrine therapy resistant human prostate cancer. Int J Cancer 1991;48: 189 93.
3. Tran C, Ouk S, Clegg NJ, Chen Y, Watson PA, Arora V, et al. Devel opment of a second generation antiandrogen for treatment of advanced prostate cancer. Science 2009;324:787 90.
4. Li Y, Chan SC, Brand LJ, Hwang TH, Silverstein KA, Dehm SM. Androgen receptor splice variants mediate enzalutamide resistance in castration resistant prostate cancer cell lines. Cancer Res 2013;73: 483 9.
5. Karin M. NF κB as a critical link between inflammation and cancer. Cold Spring Harb Perspect Biol 2009;1:a000141.
6. Xiao G, Harhaj EW, Sun SC. NF kappaB inducing kinase regulates the processing of NF kappaB2 p100. Mol Cell 2001;7:401 9.
7. Xiao G, Fong A, Sun SC. Induction of p100 processing by NF kappaB inducing kinase involves docking IkappaB kinase alpha (IKKalpha) to p100 and IKKalpha mediated phosphorylation. J Biol Chem 2004; 279:30099 105.
8. Qing G, Xiao G. Essential role of IkappaB kinase alpha in the consti tutive processing of NF kappaB2 p100. J Biol Chem 2005;280: 9765 8.
9. Qing G, Qu Z, Xiao G. Regulation of NF kappa B2 p100 processing by its cis acting domain. J Biol Chem 2005;280:18 27.
10. Xiao G, Rabson AB, Young W, Qing G, Qu Z. Alternative pathways of NF kappaB activation: a double edged sword in health and disease. Cytokine Growth Factor Rev 2006;17:281 93.
11. Cogswell PC, Guttridge DC, Funkhouser WK, Baldwin AS Jr. Selective activation of NF kappa B subunits in human breast cancer: potential roles for NF kappa B2/p52 and for Bcl 3. Oncogene 2000;19:1123 31.
12. Lessard L, Karakiewicz PI, Bellon Gagnon P, Alam Fahmy M, Ismail HA, Mes Masson AM, et al. Nuclear localization of nuclear factor kappaB p65 in primary prostate tumors is highly predictive of pelvic lymph node metastases. Clin Cancer Res 2006;12:5741 5.
13. Nadiminty N, Chun JY, Lou W, Lin X, Gao AC. NF κB2/p52 enhances androgen independent growth of human LNCaP cells via protection from apoptotic cell death and cell cycle arrest induced by androgen deprivation. Prostate 2008;68:1725 33.
14. Nadiminty N, Dutt S, Tepper C, Gao AC. Microarray analysis reveals potential target genes of NF κ2/p52 in LNCaP prostate cancer cells. Prostate 2010;70:276 87.

15. Nadiminty N, Lou W, Sun M, Chen J, Yue J, Kung HJ, et al. Aberrant activation of the androgen receptor by NF κB2/p52 in prostate cancer cells. Cancer Res 2010;70:3309 19.
16. Nadiminty N, Lou W, Lee SO, Lin X, Trump DL, Gao AC. Stat3 activation of NF kappaB p100 processing involves CBP/p300 mediated acety lation. Proc Natl Acad Sci USA 2006;103:7264 9.
17. Dehm SM, Schmidt LJ, Heemers HV, Vessella RL, Tindall DJ. Splicing of a novel androgen receptor exon generates a constitutively active androgen receptor that mediates prostate cancer therapy resistance. Cancer Res 2008;68:5469 77.
18. Mostaghel EA, Marck BT, Plymate SR, Vessella RL, Balk S, Matsumoto AM, et al. Resistance to CYP17A1 inhibition with abiraterone in castration resistant prostate cancer: induction of steroidogenesis and androgen receptor splice variants. Clin Cancer Res 2011;17:5913 25.
19. Hornberg E, Ylitalo EB, Crnalic S, Antti H, Stattin P, Widmark A, et al. Expression of androgen receptor splice variants in prostate cancer bone metastases is associated with castration resistance and short survival. PLoS One 2011;6:e19059.
20. Hu R, Dunn TA, Wei S, Isharwal S, Veltri RW, Humphreys E, et al. Ligand independent androgen receptor variants derived from splicing of cryptic exons signify hormone refractory prostate cancer. Cancer Res 2009;69:16 22.
21. Watson PA, Chen YF, Balbas MD, Wongvipat J, Socci ND, Viale A, et al. Constitutively active androgen receptor splice variants expressed in castration resistant prostate cancer require full length androgen receptor. Proc Natl Acad Sci U S A 2010;107: 16759 65.
22. Hu R, Lu C, Mostaghel EA, Yegnasubramanian S, Gurel M, Tanna hill C, et al. Distinct transcriptional programs mediated by the ligand dependent full length androgen receptor and its splice var iants in castration resistant prostate cancer. Cancer Res 2012;72: 3457 62.

OPEN ACCESS Freely available online

PLoS one

MicroRNA let-7c Is Downregulated in Prostate Cancer and Suppresses Prostate Cancer Growth

Nagalakshmi Nadiminty[1]*, Ramakumar Tummala[1], Wei Lou[1], Yezi Zhu[1], Xu-Bao Shi[1], June X. Zou[2,3], Hongwu Chen[2,3], Jin Zhang[4], Xinbin Chen[3,4], Jun Luo[5], Ralph W. deVere White[1,3], Hsing-Jien Kung[2,3], Christopher P. Evans[1,3], Allen C. Gao[1,3]*

1 Department of Urology, University of California Davis, Sacramento, California, United States of America, **2** Department of Biochemistry and Molecular Medicine, University of California Davis, Sacramento, California, United States of America, **3** Cancer Center, University of California Davis, Sacramento, California, United States of America, **4** Comparative Oncology Laboratory, School of Veterinary Medicine, University of California Davis, Sacramento, California, United States of America, **5** Department of Urology, Johns Hopkins University, Baltimore, Maryland, United States of America

Abstract

Purpose: Prostate cancer (PCa) is characterized by deregulated expression of several tumor suppressor or oncogenic miRNAs. The objective of this study was the identification and characterization of miR-let-7c as a potential tumor suppressor in PCa.

Experimental Design: Levels of expression of miR-let-7c were examined in human PCa cell lines and tissues using qRT-PCR and *in situ* hybridization. Let-7c was overexpressed or suppressed to assess the effects on the growth of human PCa cell lines. Lentiviral-mediated re-expression of let-7c was utilized to assess the effects on human PCa xenografts.

Results: We identified miR-let-7c as a potential tumor suppressor in PCa. Expression of let-7c is downregulated in castration-resistant prostate cancer (CRPC) cells. Overexpression of let-7c decreased while downregulation of let-7c increased cell proliferation, clonogenicity and anchorage-independent growth of PCa cells *in vitro*. Suppression of let-7c expression enhanced the ability of androgen-sensitive PCa cells to grow in androgen-deprived conditions *in vitro*. Reconstitution of Let-7c by lentiviral-mediated intratumoral delivery significantly reduced tumor burden in xenografts of human PCa cells. Furthermore, let-7c expression is downregulated in clinical PCa specimens compared to their matched benign tissues, while the expression of Lin28, a master regulator of let-7 miRNA processing, is upregulated in clinical PCa specimens.

Conclusions: These results demonstrate that microRNA let-7c is downregulated in PCa and functions as a tumor suppressor, and is a potential therapeutic target for PCa.

Citation: Nadiminty N, Tummala R, Lou W, Zhu Y, Shi X B, et al. (2012) MicroRNA let 7c Is Downregulated in Prostate Cancer and Suppresses Prostate Cancer Growth. PLoS ONE 7(3): e32832. doi:10.1371/journal.pone.0032832

Editor: Gokul M. Das, Roswell Park Cancer Institute, United States of America

Received July 13, 2011; **Accepted** February 2, 2012; **Published** March 30, 2012

Funding: This work was supported in part by NIH CA140468, CA118887, CA109441, DOD PC080538 (AG) and DOD PC100502, American Cancer Society IRG (NN). The funders had no role in study design, data collection and analysis, decision to publish, or preparation of the manuscript.

Competing Interests: The authors have declared that no competing interests exist.

* E mail: acgao@ucdavis.edu (ACG); nnadiminty@ucdavis.edu (NN)

Introduction

Prostate cancer (PCa) is the most commonly occurring malignancy and the second most frequent cause of cancer related mortality in men in the US. The majority of patients with advanced PCa respond initially to androgen deprivation therapy, but relapse due to the growth of castration resistant prostate cancer (CRPC) cells. Significant efforts have been focused on understanding the mechanisms involved in the development and progression of CRPC. MicroRNAs (miRNAs) are endogenous small non coding RNAs that can interfere with protein expression either by inducing cleavage of their specific target mRNAs or by inhibiting their translation. Mature miRNAs are evolutionarily conserved ~22nt single stranded RNAs resulting from a multistep processing of larger precursor molecules via Drosha and Dicer. Eventually the mature miRNAs are incorporated into the RISC complex along with their target mRNAs which are recognized by sequence complementarity in the 3' UTR [1]. Each miRNA can target several different mRNAs and each mRNA can be targeted by multiple miRNAs, generating an intricate network of gene expression regulation. MiRNAs have been shown to regulate a rapidly increasing list of complex biological processes including differentiation, cell cycle, apoptosis and metabolism [2]. An overwhelming amount of new evidence points to their roles as tumor suppressors or oncogenes which presents a whole spectrum of novel diagnostic and therapeutic opportunities [1,3].

Let 7 encodes an evolutionarily conserved family of 13 homologous miRNAs located in genomic locations frequently deleted in human cancers [4]. Expression of let 7 in lung cancer cell lines reduced cell proliferation [5] and inhibited tumorigenesis of breast cancer cells while also reducing metastases [6]. Overexpression of let 7 also decreased lung cancer cell resistance to radiation therapy [7]. Reduced expression of let 7 in human lung cancers has been associated with shortened post operative

survival, suggesting that let 7 may be an important prognostic marker in lung cancer [8]. Similarly, 5 year progression free survival rate was found to be higher in ovarian cancer patients with lower HMGA2/let 7 ratios compared to those with higher HMGA2/let 7 ratios [9]. There is an evident link between loss of let 7 expression and development of poorly differentiated and aggressive cancers [10]. Let 7 expression was found to be downregulated in localized PCa tissues relative to benign peripheral zone tissue [11,12]. Let 7 members have been shown to regulate expression levels of oncogenes like HMGA2 [5], RAS [13] and Myc [14] along with genes involved in cell cycle and cell division regulation. Therapeutic strategies are being developed targeting let 7, using either lenti or adeno viral encoded overexpression of let 7 or transient transfection of double stranded precursors of let 7 [15,16]. Thus, let 7 shows promise as a molecular marker in certain cancers and as a potential therapeutic in cancer treatment.

Lin28, a highly conserved RNA binding protein and a master regulator of let 7 miRNA processing, is overexpressed in primary human tumors [17,18] and is postulated to be one of the embryonic stem cell factors that promote oncogenesis and proliferation of cancer cells, by repression of the let 7 family of tumor suppressors [19]. Lin28 binds to the terminal loops of the precursors of let 7 family miRNAs and blocks their processing into mature miRNAs [20,21]. Lin28 also derepresses c Myc by repressing let 7 and c Myc transcriptionally activates Lin28 [22,23]. This Lin28/let 7/c Myc loop may play an important role in the deregulated miRNA expression signature observed in many cancers [24].

In this study, we demonstrate that let 7c, one of the members of the let 7 family, suppresses PCa growth *in vitro* and *in vivo*. Overexpression of let 7c led to inhibition of anchorage dependent as well as anchorage independent growth of PCa cells. Reexpression of let 7c in xenografts of human PCa cells using lentivirally encoded let 7c inhibited tumor growth significantly. In addition, let 7c expression is downregulated in clinical PCa specimens. Our results imply that prostate tumor growth is regulated by let 7c and that reconstitution of let 7 may have beneficial effects in PCa by decreasing survival and proliferation of tumor cells.

Materials and Methods

Cell lines and Reagents

LNCaP, C4 2B, PC 346C and DU145 cells were obtained from the American Type Culture Collection (ATCC, Manassas, VA). LNCaP, C4 2B and PC346C cells are androgen receptor (AR) positive and respond to androgen supplementation, while DU145 cells are AR negative and are androgen insensitive. LNCaP S17 and LNCaP IL6+ cell lines were generated in our laboratory by stable transfection of full length IL 6 cDNA into LNCaP cells and by chronic treatment of LNCaP cells with 5 ng/ml recombinant IL 6 respectively. Both cell lines exhibit autocrine IL 6 signaling. Antibodies against Actin and Tubulin were purchased from Santa Cruz Biotechnologies (Santa Cruz, CA). Lin28 antibodies were obtained from Abcam (San Francisco, CA). SYBR Green iQ Supermix was from Bio Rad. Lentivector based let 7c construct was obtained from System Biosciences and Lin28 ORF and shRNA constructs were obtained from Open Biosystems.

Western Blot Analysis

Cells were lysed in high salt buffer containing 50 mM Hepes pH 7.9, 250 mM NaCl, 1 mM EDTA, 1% NP 40, 1 mM PMSF, 1 mM Na Vanadate, 1 mM NaF and protease inhibitor cocktail (Roche) as described earlier [25]. Total protein was estimated using the Coomassie Protein Assay Reagent (Pierce, Rockford, IL). Equal amounts of protein were loaded on 10% SDS PAGE and transferred to nitrocellulose membranes. The membranes were blocked with 5% nonfat milk in PBST (1x PBS+0.1% Tween 20) and probed with primary antibodies in 1% BSA. The signal was detected by ECL (GE Healthcare) after incubation with the appropriate HRP conjugated secondary antibodies.

Measurement of PSA

PSA levels were measured in the culture supernatants using ELISA (United Biotech Inc, Mountain View, CA) according to the manufacturer's instructions.

Real-Time Quantitative RT-PCR

LNCaP cells were transfected with the indicated plasmids or oligonucleotides and total RNAs were extracted using Trizol reagent (Invitrogen). cDNAs were prepared after digestion with RNase free RQ1 DNase (Promega). The cDNAs were subjected to real time reverse transcription PCR (RT PCR) using SYBR Green iQ Supermix (Bio Rad) according to the manufacturer's instructions and as described previously [26,27]. Reactions were performed with 1 μL RT PCR cDNA, 0.5 μL each of forward and reverse primers (10 μmol/L), 10.5 μL double distilled water, and 12.5 μL iQ SYBR Green supermix. Each reaction was normalized by coamplification of actin. Triplicates of samples were run on default settings of Bio Rad CFX 96 real time cycler. Primers used for quantification of Lin28 were: Forward 5′ GCCCCTTGGATATTCCAGTC 3′ and Reverse 5′ AATGT GAATTCCACTGGTTCTCCT 3′. miRNA qPCR was performed with the use of miRCURY LNA Universal RT microRNA PCR kit and LNA conjugated miRNA primers (Exiqon) according to manufacturer's instructions.

Northern Blotting

20 μg each of total RNAs from LNCaP, PC 3, DU145, LNCaP S17 and LNCaP IL6+ cells were run on 15% Urea PAGE gels and transferred to nylon membranes. After UV cross linking, membranes were hybridized to a probe recognizing the mature sequence of let 7c. U6 snRNA was used as loading control.

miRNA in Situ Hybridization

In situ hybridization (ISH) was performed to determine the patterns of expression of let 7c in human clinical PCa tissue microarray containing 160 cores each from unmatched benign and cancerous prostates. ISH was performed using the locked nucleic acid (LNA) conjugated let 7c specific probe from Exiqon according to manufacturer's instructions.

Clonogenic Assays

Anchorage dependent clonogenic ability assays were performed as described previously [28]. Briefly, LNCaP cells transfected with either empty vector or let 7c were seeded at low densities (400 cells/dish) in 10 cm culture plates. The plates were incubated at 37°C in media containing either 10% FBS or 10% charcoal stripped FBS (CS FBS) and were left undisturbed for 14 days. At the end of the experiment, cells were fixed with methanol, stained with crystal violet and the numbers of colonies were counted.

Soft-agar Colony Formation Assays

Anchorage independent colony formation assays were performed using C4 2B and LNCaP S17 cells transfected with the indicated plasmids. After transfection, cells were plated in 0.35% agarose overlying a 1.2% agar layer. Cells were fed twice a week

with complete RPMI1640 and were incubated at 37^{0}C for 2 weeks. At the end of the experiment, colonies were stained with 0.005% Crystal Violet and counted.

Cell Growth Assays

LNCaP, C4 2B, DU145, LNCaP S17 and LN IL6+ cells were transfected with plasmids expressing let 7c and viable cell numbers were determined at 0, 24 and 48 h using a Coulter cell counter.

Apoptosis Assays using Cell Death Detection ELISA

DNA fragmentation in LNCaP, DU145, LNCaP S17 and LN IL6+ cells transfected with plasmids as indicated in figures was assessed by the Cell death detection ELISA kit (Roche, Indianapolis, IN) according to the manufacturer's instructions.

Generation of Stable Cell Lines

Stable cell lines of LNCaP and C4 2B expressing let 7c were generated by transfection of plasmids containing the cDNAs and selection of clones after application of selective pressure with appropriate antibiotics.

Animals

6 8 week old male nude mice were maintained in the Animal Facility at the UC Davis Medical Center. All experimental

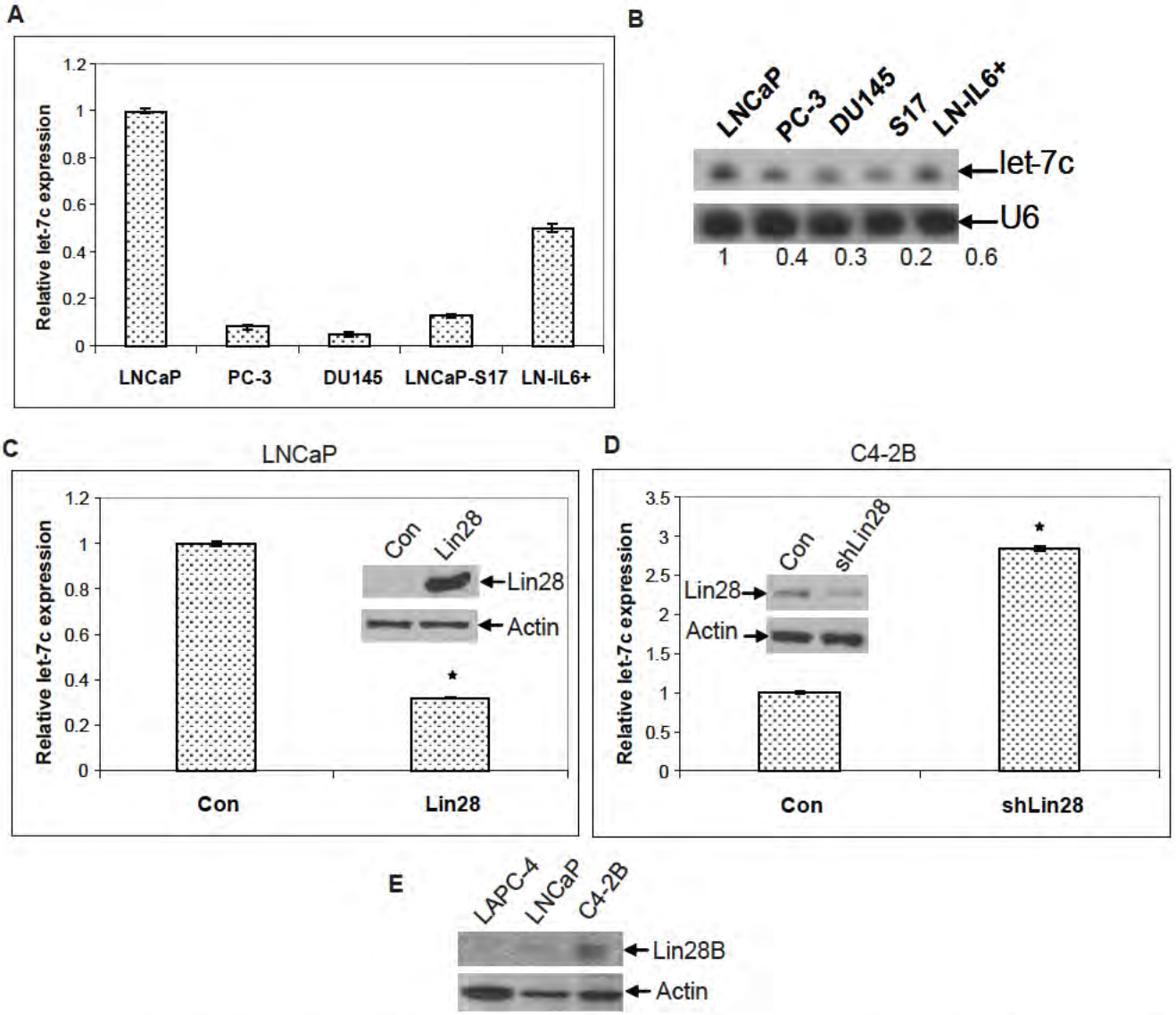

Figure 1. Let 7c is expressed in PCa cells. A) Total RNAs from LNCaP, PC 3, DU145, LNCaP S17 and LN IL6+ cells were analyzed by qRT PCR. Results are presented as relative fold change compared to expression levels in LNCaP. Data points represent mean ± SD of triplicate samples from two independent experiments. **B**) 20 µg each of the above RNAs were also analyzed by northern blotting. U6 snRNA was used as the loading control. **C**) qRT PCR showing the decrease in let 7c expression in LNCaP cells expressing Lin28 compared to LNCaP cells transfected with the empty vector (Con). Inset Western blot shows expression of Lin28. **D**) qRT PCR showing the increase in let 7c expression in C4 2B cells transfected with shRNA against Lin28 compared to C4 2B cells transfected with control GFP shRNA. Inset Western blot shows downregulation of Lin28. Data points represent mean ± SD of triplicate samples from two independent experiments. Error bars denote ± SD (*$p < 0.05$). **E**) Western blot showing the expression levels of Lin28 in PCa cells. Actin is used as a loading control.
doi:10.1371/journal.pone.0032832.g001

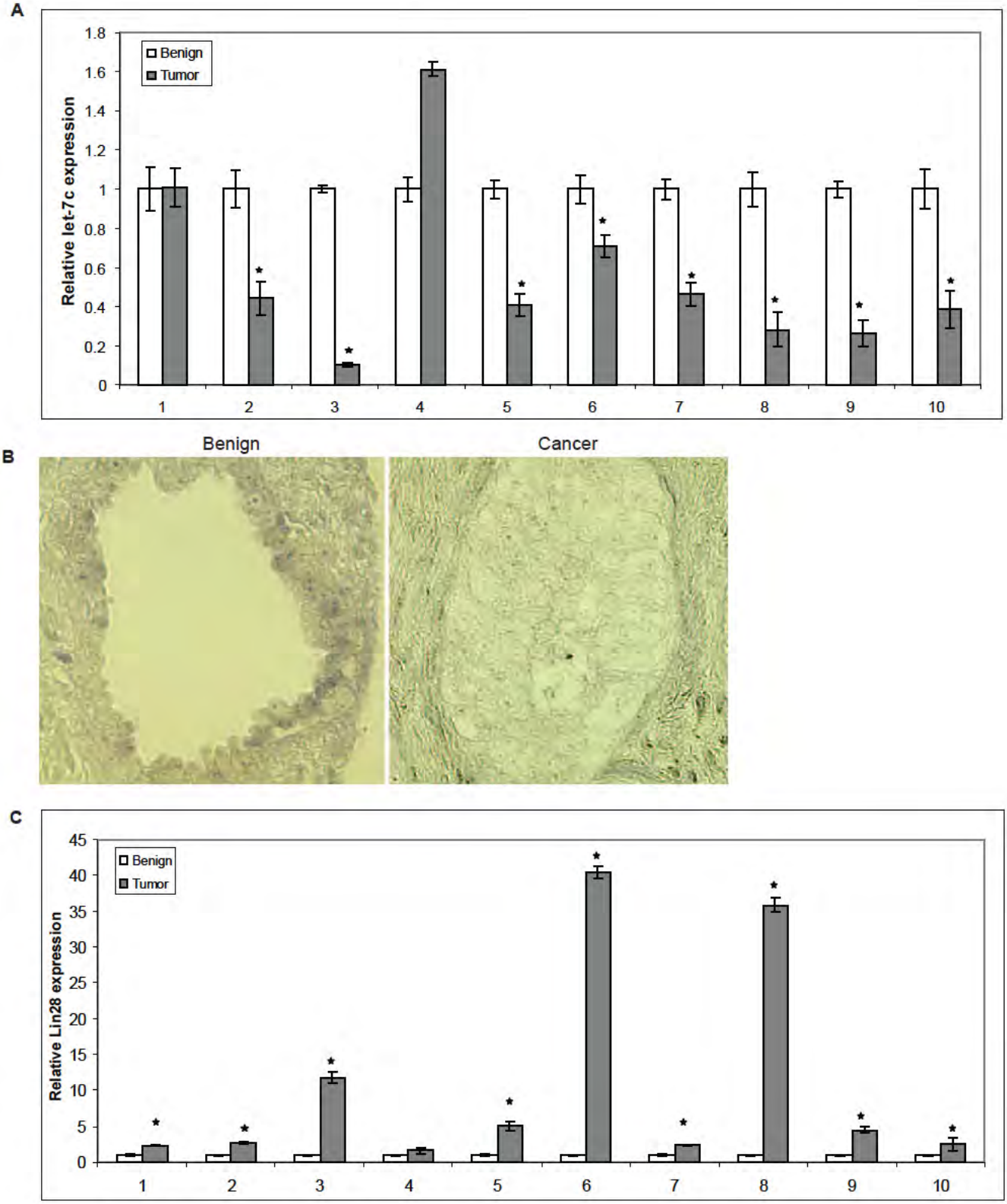

Figure 2. Let 7c expression is downregulated in human PCa. A) Relative expression levels of let 7c were measured by qRT PCR in total RNAs extracted from 10 paired benign and tumor human prostate samples. **B**) Let 7c levels were measured using *in situ* hybridization in TMAs containing 160 cores each from unmatched benign and cancerous prostate biopsies. Representative images are shown for benign and cancer cores. Expression of let 7c was higher in benign prostates compared to cancerous prostates. **C**) Relative expression levels of Lin28 in the 10 paired benign and tumor human prostate samples. Expression levels of Lin28 were correlated inversely with those of let 7c. Error bars denote ± SD (*$p < 0.05$).
doi:10.1371/journal.pone.0032832.g002

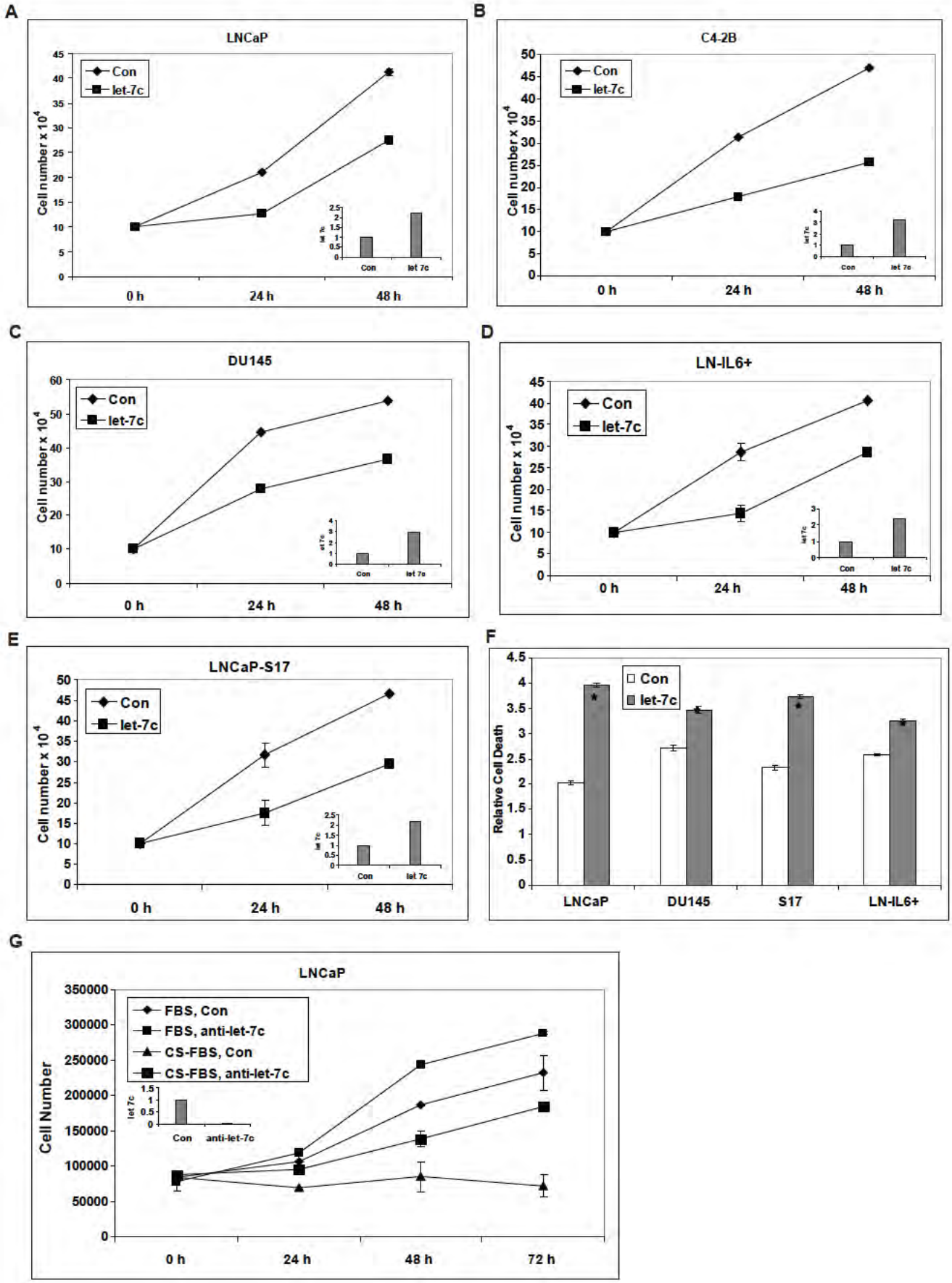
A
LNCaP
Con
let-7c
Cell number x 10^4
0 h
24 h
48 h
let 7c
Con
let 7c
B
C4-2B
C
DU145
D
LN-IL6+
E
LNCaP-S17
F
Relative Cell Death
LNCaP
DU145
S17
LN-IL6+
G
LNCaP
FBS, Con
FBS, anti-let-7c
CS-FBS, Con
CS-FBS, anti-let-7c
Cell Number
anti-let-7c
72 h

Figure 3. Let 7c inhibits growth of human PCa cells *in vitro*. LNCaP (**A**), C4 2B (**B**), DU145 (**C**), LN IL6+ (**D**) and LNCaP S17 (**E**) cells were transfected with let 7c or empty vector (Con) and cell numbers were determined after 24 and 48 h. Growth of PCa cells was suppressed by let 7c. Insets show the levels of expression of let 7c plasmid. **F**) Cell death was analyzed in LNCaP, DU145, LNCaP S17 and LN IL6+ cells transfected with let 7c or empty vector (Con). Let 7c induced apoptotic cell death of prostate cancer cells. **G**) LNCaP cells transfected with anti sense oligos against let 7c or scrambled oligos (Con) were grown in FBS and CS FBS and cell numbers determined. Inset shows the downregulation of expression of let 7c by anti sense oligos. LNCaP cells with downregulated expression of let 7c exhibited faster growth in CS FBS compared to controls. Data points represent mean ± SD of triplicate samples from two independent experiments. Error bars denote ± SD (*$p < 0.05$).
doi:10.1371/journal.pone.0032832.g003

procedures using animals were approved by the Institutional Animal Care and Use Committee of UC Davis. 1 2×10^6 cells/flank were injected s.c. into both flanks and tumors were allowed to grow. Once the tumors reached 0.5 cm^3, $1x10^7$ ifu (infectious units) of lentiviruses containing either empty vector with GFP or let 7c precursor were injected intratumorally. At the end of the experiments, mice were sacrificed and tumors were excised. Sera were collected for measurement of PSA.

Human PCa Specimens

Paired benign and tumor prostate tissues were prepared as described previously [29]. Surgical specimens used in this study were radical prostatectomy specimens (one from robotic surgery) collected at the Johns Hopkins University from 2002 to 2007. Specimens were selected from the frozen prostate tumor bank if paired frozen blocks enriched for histologically normal and tumor areas were available. Frozen blocks were manually trimmed to further enrich the histology of interest. Cryosections (7 μm) were prepared from each block before RNA extraction. The tumor content in the tumor specimens was greater than 80%, whereas normal samples had at least 60% epithelium content and no evidence of tumor present. The first and last sections for each block were H&E stained and used for % epithelium calculation. The use of de identified surgical specimens for molecular analysis was approved by the IRB.

Statistical Analyses

Data are shown as means ± SD. Multiple group comparison was performed by one way ANOVA followed by the Scheffe procedure for comparison of means. $P<0.05$ was considered significant.

Results

Let-7c is Expressed in PCa Cells

Our previous studies using miRNA microarrays showed that let 7c was among the most commonly modulated miRNAs in PCa cells (unpublished data). To determine the relative levels of expression of let 7c in PCa cells, we isolated total RNAs from LNCaP (androgen dependent, AR positive), PC 3, DU145 (cas tration resistant, AR negative) cells as well as LNCaP S17 cells expressing IL 6 [30] and LN IL6+ cells chronically treated with IL 6 [31]. cDNAs were analyzed by quantitative RT PCR using primers amplifying the mature form of let 7c (Exiqon) specifically. Our results showed that let 7c is expressed at high levels in LNCaP cells compared to the hormone refractory PC 3 and DU145 cells (Fig. 1A). Earlier reports showed that IL 6 and let 7 exhibit reciprocal regulation of expression. LNCaP IL6+ and LNCaP S17 cells (autocrine IL 6 signaling) showed reduction in let 7c levels, consistent with the report that IL 6 reduces let 7 expression in PCa cells and that let 7 regulates IL 6 expression [18]. These results were also confirmed by northern blotting using a probe against the mature let 7c sequence (Fig. 1B), suggesting that let 7c levels are reduced in more aggressive and castration resistant PCa cells.

Recent reports showed that expression of let 7 family of miRNAs is regulated by Lin28, a master regulator of miRNA processing [18,20]. Consistent with the finding, we found that overexpression of Lin28 led to a reduction in let 7c levels in LNCaP cells (Fig. 1C), while downregulation of Lin28 using Lin28 shRNA led to an increase in let 7c levels (Fig. 1D) in C4 2B cells which express endogenous Lin28 (Fig. 1E). Downregulation or overexpression of Lin28 was confirmed by Western blotting (Inset Fig. 1C&D). These results show that Lin28 plays a critical role in regulation of let 7c expression in PCa cells.

Let-7c Expression is Downregulated in Human PCa

To determine whether the levels of let 7c expression are downregulated in clinical PCa, we analyzed RNAs from 10 paired benign and tumor human PCa specimens by quantitative RT PCR. RNAs were isolated from human tissues, reverse transcribed and subjected to qRT PCR using LNA conjugated let 7c primers (Exiqon). The levels of let 7c were significantly decreased in 8/10 tumors compared to their matched benign prostate tissues (Fig. 2A). We also analyzed two tissue microarrays containing benign and cancerous prostate biopsies respectively by *in situ* hybridization using LNA conjugated mature let 7c specific probe (Exiqon). The images were analyzed using an Olympus IX81 microscope and DP Controller Software. Our results showed that let 7c was highly expressed in benign PCa, while its expression was downregulated in the cancerous prostate (Fig. 2B). Collectively, these results suggest that loss of let 7c expression may be associated with prostate tumorigenesis.

Since Lin28 is a key regulator of let 7c expression, we examined Lin28 expression in the 10 paired benign and tumor prostate samples by qRT PCR using primers which amplify Lin28 mRNA specifically. Expression levels of Lin28 were found to be significantly elevated in 9/10 pairs of matched benign and tumor prostate specimens (Fig. 2C). Expression of Lin28 was correlated inversely with expression of let 7c with a correlation coefficient of 0.4, suggesting that let 7c expression is regulated primarily by Lin28 in human PCa.

Let-7c Decreases the Growth of PCa Cells in Vitro

To determine whether let 7c affects the growth of PCa cells, LNCaP, C4 2B, DU145, LNCaP S17 and LN IL6+ cells were transfected with plasmids encoding let 7c or empty vector and cell numbers were counted after 24 and 48 h. Cell numbers of all PCa cell lines overexpressing let 7c were reduced by ~40% at 48 h (Fig. 3A E). Insets show the levels of expression of let 7c plasmid in these cells. To determine whether the observed decrease in cell growth was due to apoptotic cell death, DNA fragmentation was analyzed by Cell Death Detection ELISA. As shown in Fig. 3F, apoptosis in cells overexpressing let 7c was enhanced compared to the controls, suggesting that the inhibition in cell growth induced by let 7c is partly due to increased apoptotic cell death.

In addition, we tested whether downregulation of let 7c would enhance the ability of androgen sensitive PCa cells to grow in androgen deprived conditions. We transfected anti sense oligos

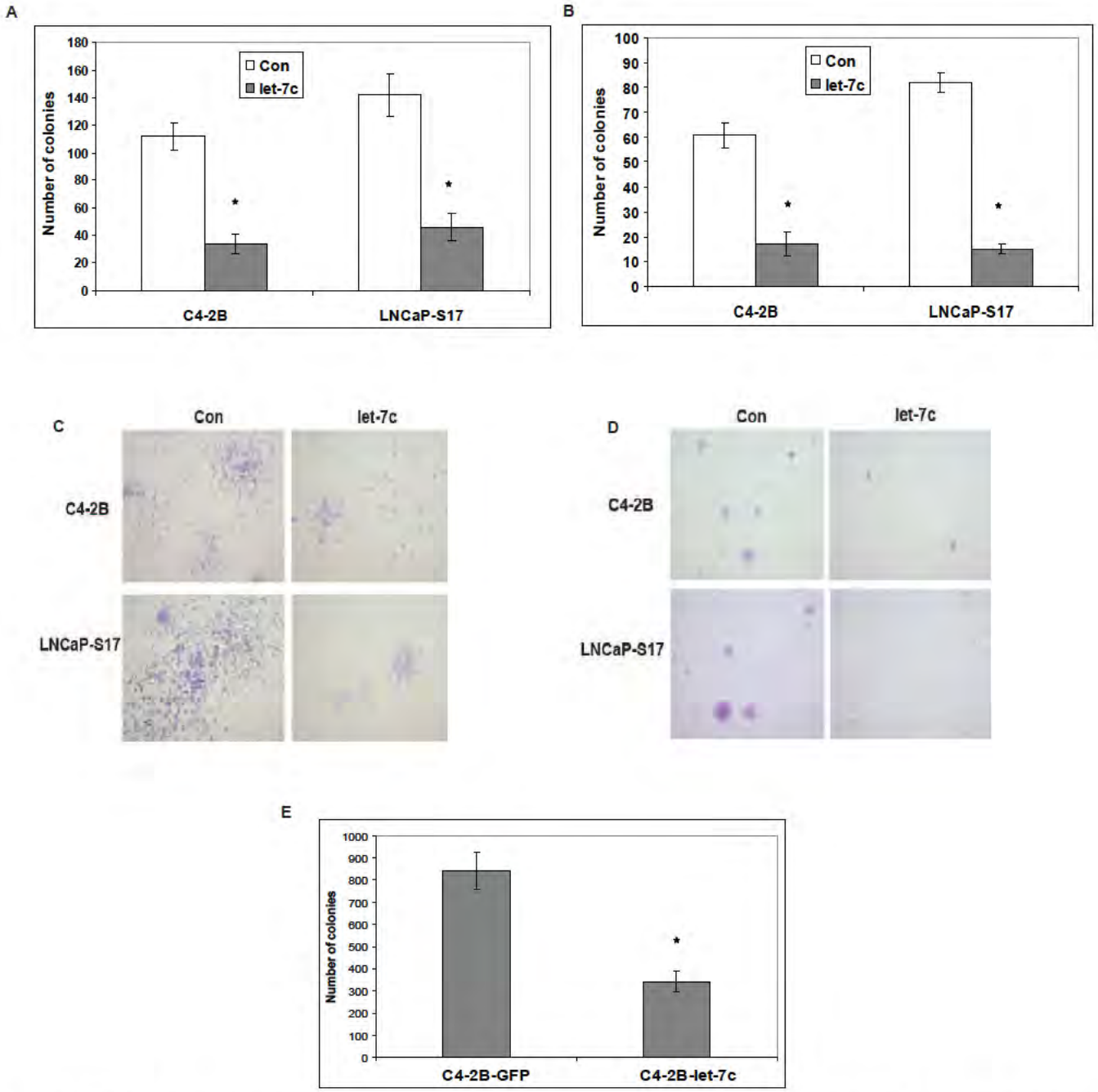

Figure 4. Let 7c inhibits colony forming abilities of human PCa cells. Clonogenic (**A**) and soft agar colony forming (**B**) abilities of LNCaP S17 and C4 2B cells transfected with let 7c or empty vector (Con) were assayed. Let 7c inhibited cell growth and survival in anchorage dependent and independent conditions. **C**) Clonogenic assay Upper and lower panels represent colony sizes of C4 2B and LNCaP S17 cells expressing control (empty vector) or let 7c respectively. **D**) Soft agar assay Upper and lower panels represent colony sizes of C4 2B and LNCaP S17 cells expressing control (empty vector) or let 7c respectively. **E**) Number of colonies formed in clonogenic assay by C4 2B cells stably expressing let 7c. Let 7c decreased the number of colonies formed by the PCa cells. Data points represent mean ± SD of triplicate samples from two independent experiments. Error bars denote ± SD (*$p < 0.05$).
doi:10.1371/journal.pone.0032832.g004

against let 7c or control scrambled oligos into LNCaP cells supplemented with either FBS or charcoal stripped FBS (CS FBS) and monitored cell growth. The results demonstrated that downregulation of let 7c by anti sense promoted androgen dependent LNCaP cell growth in conditions of androgen deprivation (Fig. 3G). Downregulation of let 7c by the anti sense oligos was confirmed using qRT PCR (Fig. 3G, inset). These findings suggested that castration resistant growth of PCa may be characterized by downregulation of let 7c expression.

We also analyzed clonogenic ability of PCa cells expressing let 7c in both anchorage dependent and anchorage independent conditions. LNCaP S17 and C4 2B cells were transfected with let 7c or empty vector and colony formation assays were performed. Both clonogenic (Fig. 4A) and soft agar colony

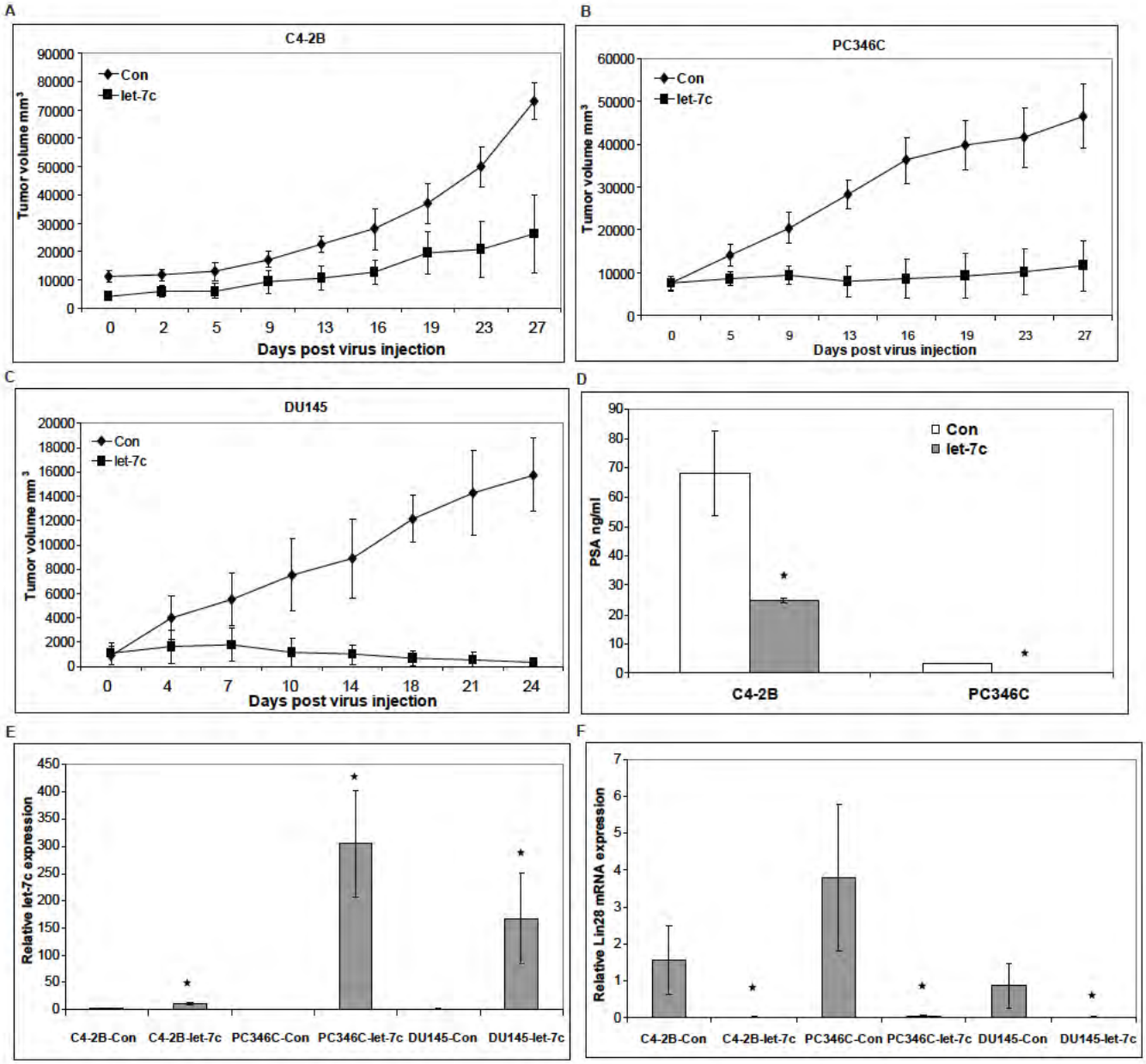

Figure 5. Let 7c suppresses tumor growth of human PCa xenografts *in vivo*. C4 2B (**A**), PC346C (**B**) and DU145 (**C**) cells were injected into both flanks of nude mice and the tumors received a single intratumoral injection of lentiviruses expressing either GFP (control) or let 7c. Tumor growth was monitored twice weekly over 3 weeks. Data points represent mean ± SD of tumor volume (mm^3) of all mice at the indicated time points. **D**) Secretion of PSA by C4 2B and PC346C xenografts was measured in mouse sera by ELISA. Reconstitution of let 7c in the tumors reduced secretion of PSA by the xenografts. At the end of the experiments, tumor tissues were excised, total RNAs prepared and subjected to qRT PCR to assess mRNA levels of let 7c (**E**) and Lin28 (**F**). Error bars denote ± SD (*$p < 0.05$).
doi:10.1371/journal.pone.0032832.g005

(Fig. 4B) formation abilities of LNCaP S17 and C4 2B cells were suppressed by overexpression of let 7c. The number of colonies formed on substrata by LNCaP S17 cells was reduced from 142±15 to 46±10 and the number of colonies formed by C4 2B cells was reduced from 122±10 to 34±7 (Fig. 4A). Similarly, the number of colonies formed in soft agar by LNCaP S17 cells was reduced from 82±4 to 15±2 and the number of colonies formed by C4 2B cells was reduced from 61±5 to 21±5 (Fig. 4B) by overexpression of let 7c. Furthermore, the size of colonies formed by control transfected cells was larger compared to the colonies formed by let 7c transfected cells (Fig. 4C&D). These results suggest that let 7c may inhibit PCa cell growth in anchorage dependent as well as independent conditions. These findings were also confirmed with clonogenic assay in C4 2B cells stably expressing let 7c (Fig. 4E).

Let-7c Inhibits Tumor Growth of Human PCa Cell Xenografts

We generated lentiviruses encoding GFP tagged let 7c precursor using the Lentivector Expression System (System Biosciences). To determine whether let 7c exhibits anti proliferative effects on PCa xenografts *in vivo*, we injected $2x10^6$ C4 2B or PC346C (both

cell lines are AR positive) cells s.c. into both flanks of male nude mice and monitored tumor development. Once tumors reached the size of 0.5 cm^3, mice were randomized into two groups. The experimental mice received a single intratumoral injection of lentivirally encoded let 7c, while control mice received lentiviruses expressing GFP. Tumor growth was monitored over 3 weeks, with tumor measurements twice weekly. At the end of 3 weeks, tumors were excised, RNAs prepared and qRT PCR performed to assess levels of let 7c in the xenografts. The results showed that tumor growth of C4 2B (Fig. 5A) and PC346C (Fig. 5B) xenografts was inhibited significantly in mice injected with let 7c containing lentiviruses compared to mice injected with control lentiviruses. In addition, we also tested whether let 7c can suppress tumor growth of AR negative xenografts. We injected $1x10^6$ DU145 cells/flank s.c. into male nude mice and performed similar experiments with half the mice receiving a single intratumoral injection of lentiviruses encoding let 7c and the other half receiving lentivi ruses encoding the empty vector. The results showed that let 7c was successful in suppressing tumor growth of DU145 xenografts similar to C4 2B or PC346C xenografts (Fig. 5C). Levels of PSA, a classic target gene of AR, secreted by the AR positive xenografts were measured in the mouse sera using a human specific PSA ELISA kit and were normalized to tumor weights. Results showed that injection of let 7c expressing lentiviruses reduced the secretion of PSA by the tumor xenografts of C4 2B and PC346C compared to control lentiviruses (Fig. 5D). qRT PCR showed that let 7c levels were enhanced in the tumors injected with let 7c encoding lentiviruses, while levels of Lin28 were reduced (Fig. 5E&F). These findings suggest that overexpression of let 7c suppresses prostate tumor growth, and that reconstitution of let 7c levels may present an attractive therapeutic strategy against human PCa.

Discussion

In this study, we found that let 7c expression is downregulated in castration resistant PCa cells and clinical specimens. Transfec tion of lentiviral encoded let 7c inhibited the growth and clonogenicity of PCa cells while enhancing apoptotic cell death. Conversely, downregulation of let 7c by anti sense oligonucleo tides conferred a survival advantage on PCa cells in androgen replete as well as androgen depleted environments. Intratumoral injection of lentivirally encoded let 7c inhibited PCa xenograft tumor growth, demonstrating that let 7c functions as a tumor suppressor that inhibits prostate tumor growth. These results suggest that miRNA let 7c plays an important role in PCa cell proliferation and may be exploited for therapeutic applications.

The mechanisms of suppression of prostate tumor growth by let 7c may include direct or indirect regulation of expression levels of oncogenes such as Myc and Lin28. In a recent report, we showed that let 7c targets the expression of the AR via targeting the expression of Myc [32]. The AR is a key survival factor for prostate tumor cells and reduction of its expression has been demonstrated to suppress prostate tumor growth [33]. In confirmation of these findings, expression of PSA, one of the classic target genes of the AR, was found to be suppressed by let 7c in xenografts of C4 2B and PC346C cells in this study.

It is well documented that Lin28 plays a major role in regulation of let 7c expression [18,21]. This is consistent with our studies showing that Lin28 suppresses let 7c expression in PCa cells. Overexpression of Lin28 inhibited let 7c expression in LNCaP cells, while knockdown of Lin28 expression increased let 7c in C4 2B cells. In addition, we demonstrated that overexpression of let 7c reduced the levels of Lin28 expression in the tumors of PCa xenograft models (Fig. 5F), indicating that a negative feedback loop exists between Lin28 and let 7c.

Several reports have established the important role of let 7, showing that members of the let 7 family are downregulated in lung cancers and that this downregulation is correlated with poor survival [8]. A tumor suppressor role has been attributed to the let 7 family of miRNAs and appears to be undisputed except in rare cases, such as let 7a, which has been reported to target caspase 3 in human cancers [34], thus suppressing susceptibility of cancer cells to chemotherapeutic induced cell death. In malignant mesothelioma, let 7b* was found to be highly expressed [35] and the upregulation of let 7b and let 7i was associated with high grade transformation in lymphoma [36]. These conflicting data on deregulation of let 7 in various human cancers show that individual let 7 family members may have distinct and varying activities in different cells and do not simply exhibit redundant functions.

An earlier study by Dong et al. [37] reported that let 7a suppresses prostate tumor growth by targeting E2F2 and CCND2. Our studies suggest that let 7c suppresses prostate tumor growth by several pathways including regulation of IL 6, Myc, Lin28 and the AR [32]. In addition, direct reconstitution of let 7c by injection of lentivirally encoded let 7c into established xenograft tumors marks an important step in the direction of prospective therapeutic strategies using let 7c. Even though members of the let 7 family may exhibit some redundant functions, individual components may be subject to differential and tissue specific regulation in different cell types. Our results with lentivirally encoded let 7c show that, if feasible strategies to reconstitute let 7c in prostate tumors can be developed, reconstitution of let 7c may represent a potential therapeutic agent for PCa treatment.

In summary, our study demonstrates that the miRNA let 7c plays an important role in inhibition of PCa cell proliferation and castration resistant progression. Downregulation of expression of Let 7c and the let 7c/Lin28 feedback loop may facilitate prostate tumor growth. Targeting this novel pathway may pave the way for effective therapeutic strategies in PCa therapy.

Author Contributions

Conceived and designed the experiments: NN HC XC JL RDVW HJK CPE AG. Performed the experiments: NN RT WL YZ XS JXZ JZ. Analyzed the data: NN CPE AG. Contributed reagents/materials/analysis tools: XB RDVW XC. Wrote the paper: NN AG.

References

1. Shi X-B, Tepper CG, deVere White RW (2008) Cancerous miRNAs and their regulation Cell Cycle 7: 1529 1538.
2. Coppola V, de Maria R, Bonci D (2009) MicroRNAs and prostate cancer. Endocr Relat Cancer: ERC-09 0172.
3. Gandellini P, Folini M, Zaffaroni N (2009) Towards the definition of prostate cancer-related microRNAs: where are we now? Trends in Molecular Medicine 15: 381 390.
4. Calin GA, Sevignani C, Dumitru CD, Hyslop T, Noch E, et al. (2004) Human microRNA genes are frequently located at fragile sites and genomic regions involved in cancers. Proc Natl Acad Sci USA 101: 2999 3004.
5. Lee YS, Dutta A (2007) The tumor suppressor microRNA let-7 represses the HMGA2 oncogene. Genes & Development 21: 1025 1030.
6. Yu F, Yao H, Zhu P, Zhang Z, Pan Q, et al. (2007) let-7 regulates self-renewal and tumorigenicity of breast cancer cells Cell 131: 1109 1123.
7. Weidhaas JB, Babar I, Nallur SM, Trang P, Roush S, et al. (2007) MicroRNAs as Potential Agents to Alter Resistance to Cytotoxic Anticancer Therapy. Cancer Res 67: 11111 11116.
8. Takamizawa J, Konishi H, Yanagisawa K, Tomida S, Osada H, et al. (2004) Reduced Expression of the let-7 MicroRNAs in Human Lung Cancers in Association with Shortened Postoperative Survival. Cancer Res 64: 3753 3756.

9. Shell S, Park S-M, Radjabi AR, Schickel R, Kistner EO, et al. (2007) Let-7 expression defines two differentiation stages of cancer. Proc Natl Acad Sci USA 104: 11400 11405.
10. Boyerinas B, Park S-M, Hau A, Murmann AE, Peter ME (2010) The role of let-7 in cell differentiation and cancer. Endocr Relat Cancer 17: F19 36.
11. Ozen M, Creighton C, Ozdemir M, Ittmann M (2007) Widespread deregulation of microRNA expression in human prostate cancer. Oncogene 27: 1788 1793.
12. Jiang J, Lee EJ, Gusev Y, Schmittgen TD (2005) Real-time expression profiling of microRNA precursors in human cancer cell lines. Nucl Acids Res 33: 5394 5403.
13. Johnson S, Grosshans H, Shingara J, Byrom M, Jarvis R, et al. (2005) RAS is regulated by the let-7 microRNA family Cell 120: 635 647.
14. Kumar MS, Lu J, Mercer KL, Golub TR, Jacks T (2007) Impaired microRNA processing enhances cellular transformation and tumorigenesis. Nat Genet 39: 673 677.
15. Barh D, Malhotra R, Ravi B, Sindhurani P (2010) MicroRNA let-7: an emerging next-generation cancer therapeutic. Current Oncology 17(1): 70 80.
16. Esquela-Kerscher A, Trang P, Wiggins J, Patrawala L, Cheng A, et al. (2008) The let-7 microRNA reduces tumor growth in mouse models of lung cancer Cell Cycle 7: 759 764.
17. Viswanathan SR, Powers JT, Einhorn W, Hoshida Y, Ng TL, et al. (2009) Lin28 promotes transformation and is associated with advanced human malignancies. Nat Genet 41: 843 848.
18. Iliopoulos D, Hirsch H, Struhl K (2009) An epigenetic switch involving NF-kappaB, Lin28, Let-7 microRNA and IL6 links inflammation to cell transformation Cell 139: 693 706.
19. Peng S, Maihle N, Huang Y (2010) Pluripotency factors Lin28 and Oct4 identify a sub-population of stem cell-like cells in ovarian cancer. Oncogene 29: 2153 2159.
20. Viswanathan SR, Daley GQ, Gregory RI (2008) Selective Blockade of MicroRNA Processing by Lin28. Science 320: 97 100.
21. Viswanathan SR, Daley GQ (2010) Lin28: A microRNA regulator with a macro role Cell 140: 445 449.
22. Chang T-C, Zeitels LR, Hwang H-W, Chivukula RR, Wentzel EA, et al. (2009) Lin-28B transactivation is necessary for Myc-mediated let-7 repression and proliferation. Proc Natl Acad Sci USA 106: 3384 3389.
23. Dangi-Garimella S, Yun J, Eves EM, Newman M, Erkeland SJ, et al. (2009) Raf kinase inhibitory protein suppresses a metastasis signalling cascade involving LIN28 and let-7. EMBO J 28: 347 358.
24. Lu J, Getz G, Miska EA, Alvarez-Saavedra E, Lamb J, et al. (2005) MicroRNA expression profiles classify human cancers. Nature 435: 834 838.
25. Nadiminty N, Lou W, Lee SO, Lin X, Trump DL, et al. (2006) Stat3 activation of NF-kappaB p100 processing involves CBP/p300-mediated acetylation. Proc Natl Acad Sci USA 103: 7264 7269.
26. Nadiminty N, Dutt S, Tepper C, Gao AC (2009) Microarray analysis reveals potential target genes of NF-kappaB2/p52 in LNCaP prostate cancer cells. Prostate 70: 276 287.
27. Nadiminty N, Lou W, Sun M, Chen J, Yue J, et al. (2010) Aberrant Activation of the Androgen Receptor by NF-kappaB2/p52 in Prostate Cancer Cells. Cancer Research 70: 3309 3319.
28. Nadiminty N, Chun JY, Lou W, Lin X, Gao AC (2008) NF-kappaB2/p52 enhances androgen-independent growth of human LNCaP cells via protection from apoptotic cell death and cell cycle arrest induced by androgen-deprivation. Prostate 68: 1725 1733.
29. Dunn TA, Chen S, Faith DA, Hicks JL, Platz EA, et al. (2006) A novel role of myosin VI in human prostate cancer. Am J Pathol 169: 1843 1854.
30. Lee SO, Lou W, Hou M, de Miguel F, Gerber L, et al. (2003) Interleukin-6 promotes androgen-independent growth in LNCaP human prostate cancer cells. Clin Cancer Res 9: 370 376.
31. Lee SO, Chun JY, Nadiminty N, Lou W, Gao AC (2007) Interleukin-6 undergoes transition from growth inhibitor associated with neuroendocrine differentiation to stimulator accompanied by androgen receptor activation during LNCaP prostate cancer cell progression. The Prostate 67: 764 773.
32. Nadiminty N, Tummala R, Lou W, Zhu Y, Zhang J, et al. (2011) MicroRNA let-7c suppresses androgen receptor expression and activity via regulation of Myc expression in prostate cancer cells. Journal of Biological Chemistry [Epub ahead of print].
33. Andersen RJ, Mawji NR, Wang J, Wang G, Haile S, et al. (2010) Regression of Castrate-Recurrent Prostate Cancer by a Small-Molecule Inhibitor of the Amino-Terminus Domain of the Androgen Receptor. Cancer Cell 17: 535 546.
34. Tsang W, Kwok T (2008) Let-7a microRNA suppresses therapeutics-induced cancer cell death by targeting caspase-3. Apoptosis 13: 1215 1222.
35. Guled M, Lahti L, Lindholm PM, Salmenkivi K, Bagwan I, et al. (2009) CDKN2A, NF2, and JUN are dysregulated among other genes by miRNAs in malignant mesothelioma - A miRNA microarray analysis. Genes, Chromosomes and Cancer 48: 615 623.
36. Lawrie CH, Chi J, Taylor S, Tramonti D, Ballabio E, et al. (2009) Expression of microRNAs in diffuse large B cell lymphoma is associated with immunophenotype, survival and transformation from follicular lymphoma. J Cell Mol Med 13: 1248 1260.
37. Dong Q, Meng P, Wang T, Qin W, Qin W, et al. (2010) MicroRNA Let-7a Inhibits Proliferation of Human Prostate Cancer Cells *In Vitro* and *In Vivo* by Targeting E2F2 and CCND2. PLoS ONE 5: e10147.

THE JOURNAL OF BIOLOGICAL CHEMISTRY VOL. 287, NO. 2, pp. 1527–1537, January 6, 2012

MicroRNA let-7c Suppresses Androgen Receptor Expression and Activity via Regulation of Myc Expression in Prostate Cancer Cells*[S]

Received for publication, July 1, 2011, and in revised form, November 10, 2011 Published, JBC Papers in Press, November 28, 2011, DOI 10.1074/jbc.M111.278705

Nagalakshmi Nadiminty[‡1], Ramakumar Tummala[‡], Wei Lou[‡], Yezi Zhu[‡], Jin Zhang[§], Xinbin Chen[§¶], Ralph W. deVere White[‡¶], Hsing-Jien Kung[¶‖], Christopher P. Evans[‡¶], and Allen C. Gao[‡¶2]

From the [‡]Department of Urology, [¶]Cancer Center, [§]Comparative Oncology Laboratory, School of Veterinary Medicine, and [‖]Department of Biochemistry and Molecular Medicine, University of California at Davis, Sacramento, California 95817

Background: Let-7c is a microRNA down-regulated in prostate cancer.
Results: Let-7c suppresses androgen receptor expression by targeting its transcription via c-Myc. Suppression of AR by let-7c leads to decreased cell proliferation and tumor growth.
Conclusion: Let-7c suppresses androgen receptor expression.
Significance: Our study demonstrates that let-7c plays an important role in regulation of androgen signaling and prostate cancer proliferation.

Castration-resistant prostate cancer continues to rely on androgen receptor (AR) expression. AR plays a central role in the development of prostate cancer and progression to castration resistance during and after androgen deprivation therapy. Here, we identified miR-let-7c as a key regulator of expression of AR. miR-let-7c suppresses AR expression and activity in human prostate cancer cells by targeting its transcription via c-Myc. Suppression of AR by let-7c leads to decreased cell proliferation of human prostate cancer cells. Down-regulation of Let-7c in prostate cancer specimens is inversely correlated with AR expression, whereas the expression of Lin28 (a repressor of let-7) is correlated positively with AR expression. Our study demonstrates that the miRNA let-7c plays an important role in the regulation of androgen signaling in prostate cancer by down-regulating AR expression. These results suggest that reconstitution of miR-let-7c may aid in targeting enhanced and hypersensitive AR in advanced prostate cancer.

Prostate cancer (PCa)[3] is the most commonly occurring malignancy and the second highest cause of cancer-related mortality in men in the United States. The majority of patients with advanced PCa respond initially to androgen deprivation therapy, but relapse because of the growth of castration-resistant prostate cancer (CRPC) cells. Significant efforts have been focused on understanding the mechanisms involved in the development and progression of CRPC. Although the levels of androgen are reduced to castration levels, the AR is still expressed, and AR target genes such as prostate-specific antigen (PSA) are activated. AR activation in CRPC may occur by a variety of mechanisms that alter the sensitivity or specificity of AR, including AR mutations, alternative splicing, amplification, alterations of coregulators, sensitization by growth factors and cytokines, and response to intracrine androgens (1, 2). The study of factors that regulate expression and activation of the AR will enhance our understanding of the mechanisms leading to castration resistance and will play a key role in devising therapeutic strategies to combat this lethal cancer.

MicroRNAs (miRNAs) are endogenous, small, non-coding RNAs that interfere with protein expression either by inducing cleavage of their specific target mRNAs or by inhibiting their translation. MiRNAs have been shown to regulate a rapidly increasing list of complex biological processes, including differentiation, cell cycle, apoptosis, and metabolism (3). Their emerging roles as tumor suppressors or oncogenes present novel diagnostic and therapeutic opportunities (4, 5). Let-7 encodes an evolutionarily conserved family of 13 homologous miRNAs located in genomic locations frequently deleted in human cancers (6). Let-7 expression was observed to be down-regulated in localized PCa tissues relative to benign peripheral zone tissue (7, 8). There is a significant association between loss of let-7 expression and development of poorly differentiated and aggressive cancers (9). Let-7 members have been shown to regulate expression levels of oncogenes like HMGA2 (10), RAS (11), and Myc (12), along with genes involved in cell cycle and cell division regulation. Thus, let-7 shows promise as a molecular marker in certain cancers and as a potential therapeutic agent in cancer treatment. Lin28, a highly conserved RNA-binding protein and a master regulator of let-7 miRNA processing, binds to the terminal loops of the precursors of let-7 family miRNAs and blocks their processing into mature miRNAs (13, 14). Lin28 also derepresses c-Myc by repressing let-7, and c-Myc transcriptionally activates Lin28 (15, 16). This Lin28/let-7/c-Myc loop may play an important role in the deregulated miRNA expression signature observed in many cancers (17).

* This work was supported, in whole or in part, by National Institutes of Health Grants CA140468, CA118887, CA109441, and DOD PC080538.
[S] This article contains supplemental Figs. 1–4 and experimental procedures.
[1] To whom correspondence may be addressed: Department of Urology, University of California Davis Medical Center, 4645 2nd Ave., Research III, Suite 1300, Sacramento, CA 95817. E-mail: nnadiminty@ucdavis.edu.
[2] To whom correspondence may be addressed: Department of Urology, University of California Davis Medical Center, 4645 2nd Ave., Research III, Suite 1300, Sacramento, CA 95817. E-mail: acgao@ucdavis.edu.
[3] The abbreviations used are: PCa, prostate cancer; CRPC, castration-resistant prostate cancer; AR, androgen receptor; PSA, prostate-specific antigen; miRNA, microRNA; qRT-PCR, quantitative RT-PCR.

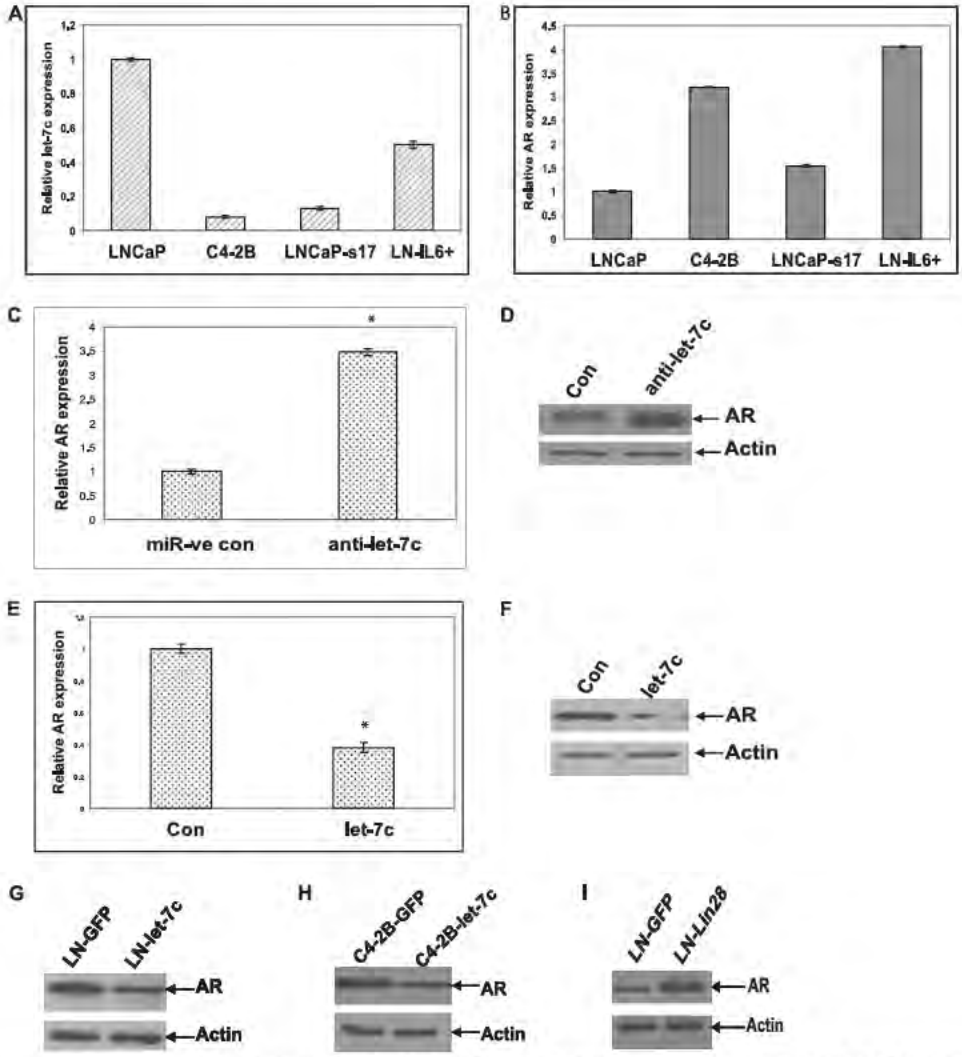

FIGURE 1. **Let-7c suppresses AR expression.** Relative expression levels of let-7c (*A*) and AR (*B*) were determined in LNCaP, C4-2B, LNCaP-s17, and LN-IL6+ cells by qRT-PCR. Results are presented as relative fold change compared to expression levels in LNCaP cells. *C*, LNCaP cells were transfected with let-7c antisense oligonucleotides, and AR mRNA levels were analyzed by qRT-PCR. Results are presented as relative fold change compared to expression levels in LNCaP cells transfected with control oligonucleotides. Data points represent mean ± S.D. of triplicate samples from two independent experiments. *Error bars* denote mean ± S.D. * denotes $p \leq 0.05$. AR expression was increased when let-7c expression was down-regulated. *D*, Western blot analysis showing the increase in AR expression in LNCaP cells transfected with let-7c antisense. Actin is shown as loading control. *E*, LN-IL6+ cells were transfected with let-7c, and AR mRNA levels were analyzed by qRT-PCR. AR expression was reduced when let-7c was overexpressed. *Con*, control. * denotes $p \leq 0.05$. *F*, Western blot analysis showing the down-regulation of AR expression in LN-IL6+ cells transfected with let-7c. *G* and *H*, AR levels were analyzed in LNCaP and C4-2B cells stably expressing let-7c by Western blotting. AR protein levels were reduced when let-7c was expressed. *I*, protein levels of AR were analyzed in LNCaP cells stably expressing Lin28 by Western blotting. AR expression was enhanced in cells expressing Lin28.

In this study, we show that let-7c, one of the members of the let-7 family, antagonizes AR expression by degradation of c-Myc. Let-7c-mediated decrease in AR expression and activation led to inhibition of proliferation of PCa cells. Down-regulation of Let-7c expression in prostate cancer clinical specimens is inversely correlated, whereas expression of Lin28 is positively correlated, with AR expression. Our results imply that AR signaling can be regulated by let-7c in PCa by decreasing survival and proliferation of tumor cells.

EXPERIMENTAL PROCEDURES

Cell Lines and Reagents—Human prostate cancer cell lines were obtained from the ATCC. Antibodies against c-Myc, AR (441) and actin were purchased from Santa Cruz Biotechnology, Inc. (Santa Cruz, CA). Lin28 antibodies were obtained from Abcam (San Francisco, CA). SYBR Green iQ Supermix was from Bio-Rad.

Western Blot Analysis—Cells were lysed in high-salt buffer as described earlier (18). Western blots were probed with the indicated primary antibodies, and the chemiluminescence was detected by ECL (GE Healthcare).

Measurement of PSA—PSA levels were measured in the culture supernatants using ELISA (United Biotech, Inc., Mountain View, CA) according to the manufacturer's instructions.

Luciferase Assays—LNCaP cells were transfected with pGL3-PSA6.0-Luc or pGL4-AR-prom-Luc (~6 kb) reporters along with plasmids as indicated in the figures. Cell lysates were subjected to luciferase assays with the luciferase assay system (Promega).

Real-time Quantitative RT-PCR—LNCaP cells were transfected with the indicated plasmids or oligonucleotides, and

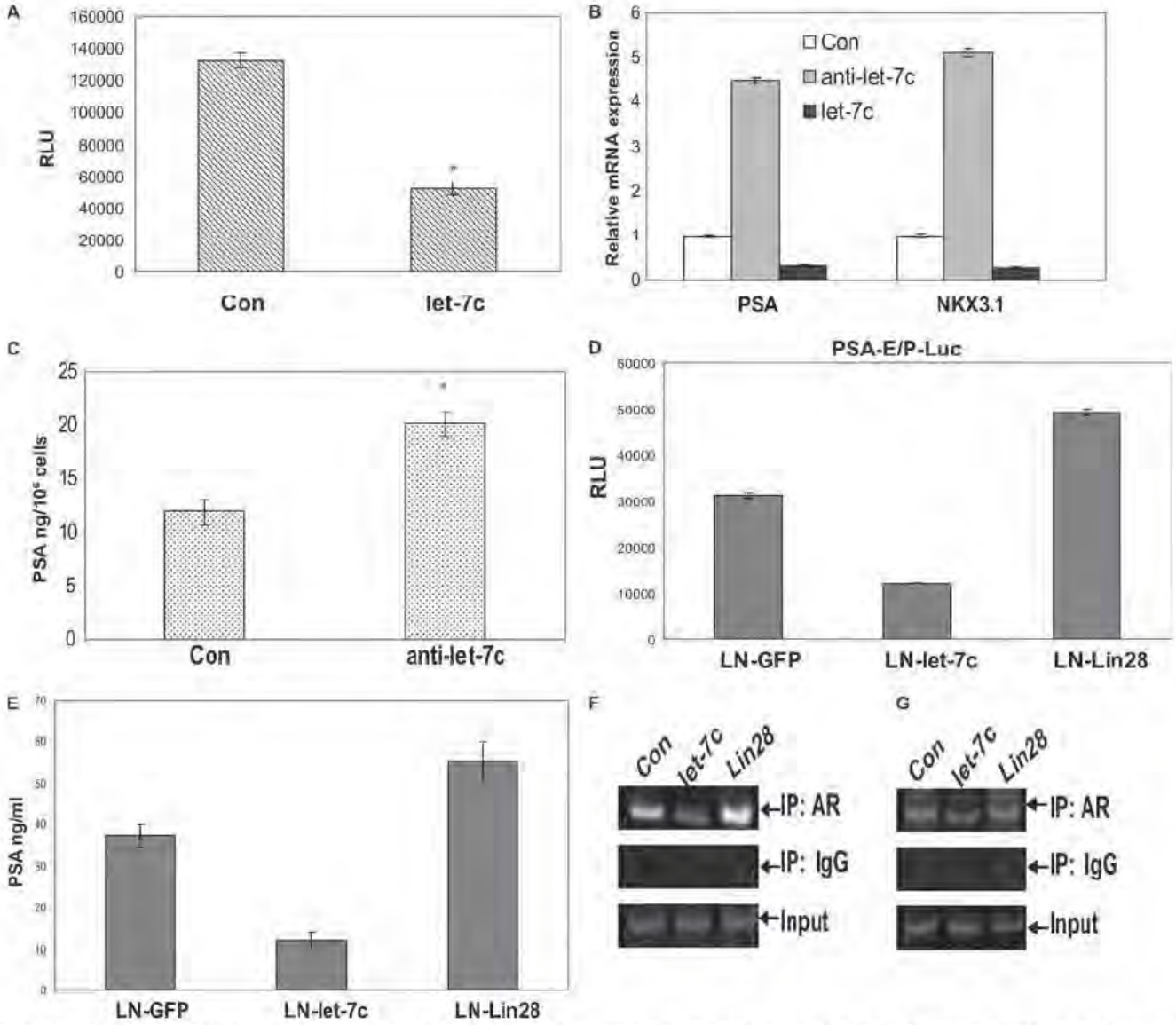

FIGURE 2. **Let-7c inhibits AR activity and transcription of AR target genes.** *A*, LNCaP cells were cotransfected with let-7c and pGL3-PSA6.0-Luc reporter. Data points represent mean ± S.D. of triplicate samples from two independent experiments. *Error bars* denote mean ± S.D. * denotes $p \leq 0.05$. Transactivation of the PSA promoter by AR was reduced with let-7c overexpression. *B*, LNCaP cells were transfected with control or let-7c or let-7c antisense, and levels of PSA and NKX3.1 mRNAs were analyzed by qRT-PCR. Results are presented as relative fold change compared with expression levels in LNCaP cells transfected with control oligonucleotides. Down-regulation of let-7c enhanced the levels of PSA and NKX3.1 mRNAs, whereas overexpression of let-7c reduced their expression. *Con*, control. *C*, PSA secretion in LNCaP cells was enhanced when let-7c expression was down-regulated. * denotes $p \leq 0.05$. *D*, LNCaP cells stably expressing control, let-7c, or Lin28 were transfected with pGL3-PSA6.0-Luc reporter, and luciferase activities were assayed. Transactivation of the reporter by AR was reduced in cells expressing let-7c, whereas it was increased in cells expressing Lin28. *RLU*, Relative Luciferase Units. *E*, secretion of PSA by LNCaP cells stably expressing let-7c or Lin28 was analyzed by ELISA. PSA secretion was reduced in cells expressing let-7c and increased in cells expressing Lin28. Recruitment of AR to AREs in PSA (*F*) and NKX3.1 (*G*) promoters was analyzed by ChIP assays in LNCaP cells transfected with let-7c or Lin28. Recruitment of AR to the AREs was reduced in cells overexpressing let-7c and was enhanced in cells expressing Lin28. *IP*, immunoprecipitation.

qRT-PCR analyses were performed as described previously (19, 20). (Sequences of primers are listed in the supplemental methods.)

ChIP Assays—LNCaP cells were transfected with the indicated plasmids, and DNA-protein complexes were isolated after cross-linking with 1% formaldehyde. ChIP assays were performed as described previously (20) using primers spanning androgen responsive elements (AREs) in PSA and NKX3.1 promoters or Myc-binding sites in the AR promoter. Isotype-matched IgG was used as a control. (Primer sequences are listed in the supplemental methods.)

Human PCa Specimens—The human prostate cancer specimens were obtained with consent from patients who underwent radical prostatectomies at University of California Davis Medical Center. The protein extracts from human prostate specimens used for the analysis of Lin28 expression were described previously (21, 22).

Gene Expression Omnibus Analysis—Two separate datasets from the Gene Expression Omnibus National Center for Biotechnology Information gene expression and hybridization array data repository were screened independently for expression levels of Lin28, AR, and Myc. The first data set (GDS1439)

(23) compared specimens of benign prostatic hyperplasia with clinically localized primary prostate cancer and with metastatic prostate cancer. The second dataset (GDS2547) (24) compared normal prostate specimens without any pathology, normal prostate adjacent to tumor, primary prostate tumor, and metastatic prostate cancer. Relative levels of expression of Lin28, AR, and Myc were determined by comparison of single channel counts and expressed as a percentage of the highest count in the data set (25). Significant differences between groups were determined by Microsoft Excel Tools.

Oncomine Analysis—A gene search of the Oncomine database for expression levels of Lin28, AR, and Myc was performed at a significance threshold of $p \leq 0.001$ and data sets generated from three comparisons of normal prostate tissue with prostate carcinoma: Wallace_prostate (26), Yu_prostate (27), and Vanaja_prostate (28) were analyzed by the differential expression function of Oncomine.

Statistical Analyses—Data are shown as means ± S.D. Multiple group comparison was performed using Microsoft Excel Tools. $p \leq 0.05$ was considered significant.

RESULTS

Let-7c Decreases Expression of AR—We initially determined let-7c expression in several prostate cancer cell lines, including androgen-sensitive and castration-resistant prostate cancer cells. Our data showed that the levels of let-7c were lower in the castration-resistant cell lines C4-2B, LNCaP-s17 (overexpressing IL-6), and LN-IL6+ (LNCaP chronically treated with IL-6), which express higher levels of AR compared with parental LNCaP cells that express lower levels of AR (Fig. 1, *A* and *B*) (29, 30), indicating an inverse relationship between AR and let-7c. Hence, we tested whether let-7c affects AR expression in PCa cells. Antisense oligonucleotides against let-7c (Ambion) were transfected into LNCaP cells, which express high levels of let-7c, and the expression level of AR was analyzed by qRT-PCR. Down-regulation of let-7c enhanced AR mRNA level ~3.5-fold (Fig. 1*C*). Down-regulation of let-7c was confirmed by qRT-PCR (supplemental Fig. 1*A*). To confirm that the increase in AR mRNA results in an increase in AR protein, we analyzed whole cell lysates from LNCaP cells transfected with let-7c antisense oligos by Western blotting. The AR protein level was increased ~70% when let-7c was down-regulated (Fig. 1*D*). These findings were further confirmed in LN-IL6+ cells, which express higher levels of AR but lower levels of let-7c compared with LNCaP cells. Overexpression of let-7c in LNCaP-IL6+ cells reduced the levels of AR mRNA (Fig. 1*E*) and protein expression (*F*). Overexpression of let-7c was confirmed by qRT-PCR (supplemental Fig. 1*B*). These results suggested that let-7c inhibits AR expression in PCa cells. Because the above results were obtained by transient overexpression of let-7c and to test whether stable expression of let-7c would exhibit similar effects, we generated LNCaP and C4-2B cells stably expressing let-7c and LNCaP cells stably expressing Lin28. Western blotting was performed to analyze protein levels of AR and Lin28. The results demonstrated that levels of AR were down-regulated in both LNCaP and C4-2B cells stably expressing let-7c, whereas AR expression was enhanced in LNCaP cells expressing Lin28 (Fig. 1, *G*, *H*, and *I*). Higher levels of expression of

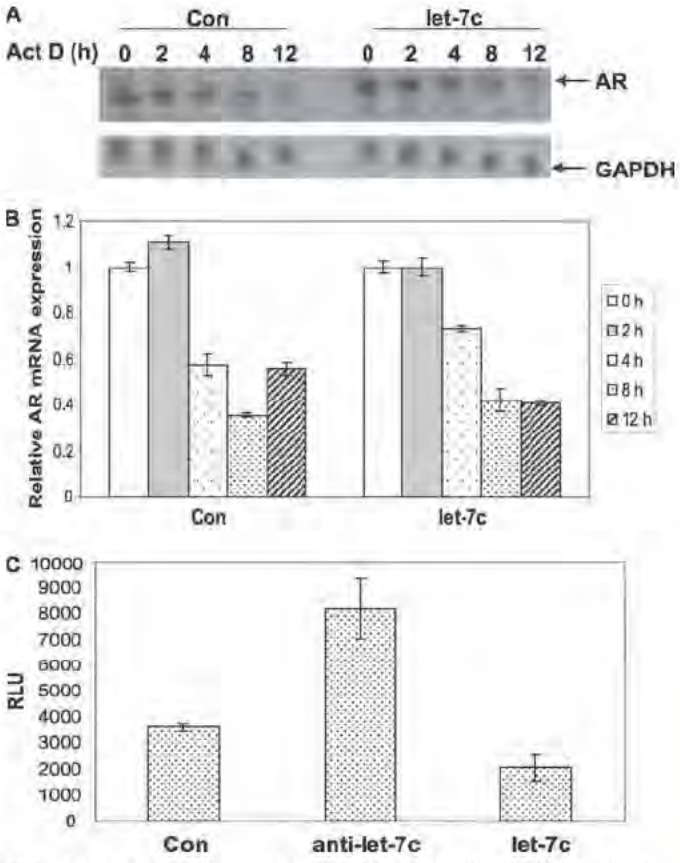

FIGURE 3. **Let-7c regulates AR expression at the level of transcription.** LNCaP cells were transfected with a control (*Con*) or let-7c plasmid in the presence or absence of actinomycin D, and AR mRNA levels were analyzed by Northern blotting (*A*) or qRT-PCR (*B*). Half-life of AR mRNA was not altered in the presence of let-7c. *C*, LNCaP cells were cotransfected with control or let-7c or with let-7c antisense oligos along with the pGL4-AR-Prom-Luc reporter. Data points represent the mean ± S.D. of triplicate samples from two independent experiments. AR promoter activity was repressed in let-7c-overexpressing cells and was enhanced when let-7c was down-regulated. *RLU*, Relative Luciferase Units.

let-7c in C4-2B cells stably expressing let-7c were confirmed by qRT-PCR (supplemental Fig. 1*C*). Collectively, these data demonstrate that let-7c represses AR expression in prostate cancer cells.

Let-7c Reduces AR Activity—We next examined whether the reduction in expression of AR by let-7c results in inhibition of transcriptional activity of AR. LNCaP cells were cotransfected with the pGL3-PSA6.0-Luc reporter containing the enhancer and promoter regions of the PSA gene and plasmids expressing let-7c. As shown in Fig. 2*A*, transcriptional activity of the AR in activating reporter gene expression was reduced by ~60% in the presence of let-7c. These results were confirmed by analysis of PSA mRNA and protein expression by qRT-PCR and ELISA, respectively. LNCaP cells were transfected with let-7c or let-7c antisense oligonucleotides, and PSA mRNA levels were analyzed. Down-regulation of let-7c expression by let-7c antisense oligonucleotides led to a > 4-fold increase in PSA expression, whereas overexpression of let-7c reduced PSA expression by ~50% (Fig. 2*B*). In addition to PSA, down-regulation of let-7c expression by let-7c antisense increased, whereas overexpression of let-7c reduced, NKX3.1 (another typical androgen-regulated gene) mRNA expression (Fig. 2*B*). Similarly, PSA levels

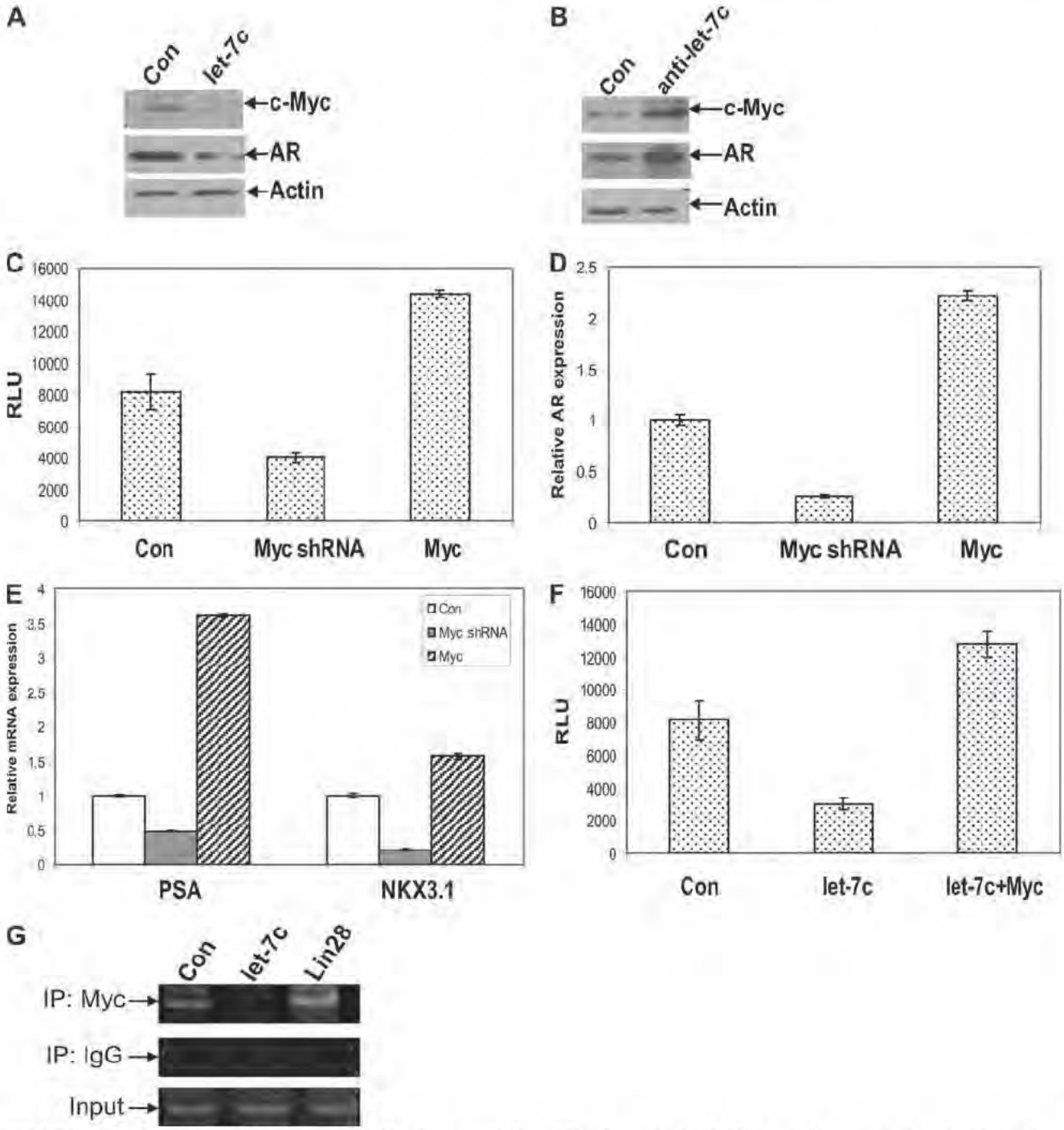

FIGURE 4. **Down-regulation of AR by let-7c is mediated by down-regulation of Myc.** Expression levels of AR and c-Myc were analyzed by Western blotting in LNCaP cells transfected with let-7c (*A*) or let-7c antisense oligos (*B*). Protein levels of AR and c-Myc were reduced in let-7c-overexpressing cells and were increased when let-7c was down-regulated. *Con*, control. *C*, LNCaP cells were transfected with plasmids expressing Myc or shRNA against Myc along with the pGL4-AR prom-Luc reporter. Luciferase assays showed that down-regulation of Myc reduced transactivation of the AR promoter, whereas overexpression of Myc enhanced reporter activity. *RLU*, Relative Luciferase Units. *D* and *E*, mRNA levels of AR, PSA, and NKX3.1 were measured by qRT-PCR in LNCaP cells transfected with Myc or shRNA against Myc. Expression levels of all three genes were decreased when Myc was down-regulated and were enhanced when Myc was overexpressed. *F*, LNCaP cells were transfected with let-7c and Myc alone or together along with the pGL4-AR prom-Luc reporter. Overexpression of Myc could overcome the repression of AR promoter activity by let-7c. *G*, recruitment of Myc to the Myc binding site in the AR promoter was analyzed by ChIP assays. Overexpression of let-7c reduced and expression of Lin28 enhanced the recruitment of Myc to the AR promoter. *IP*, immunoprecipitation.

in the supernatants of LNCaP cells transfected with let-7c antisense were found to be up-regulated by ~40% (Fig. 2*C*). These results were also confirmed in LNCaP and C4-2B cells stably expressing let-7c. Stable expression of let-7c decreased, whereas stable expression of Lin28 increased, transactivation of reporter activity by AR (Fig. 2*D*) and secretion of PSA by LNCaP cells (*E*). To determine whether expression of let-7c affects the recruitment of AR to PSA and NKX3.1 promoters, ChIP assays were performed. Overexpression of let-7c in LNCaP cells reduced binding of AR to PSA (Fig. 2*F*) and

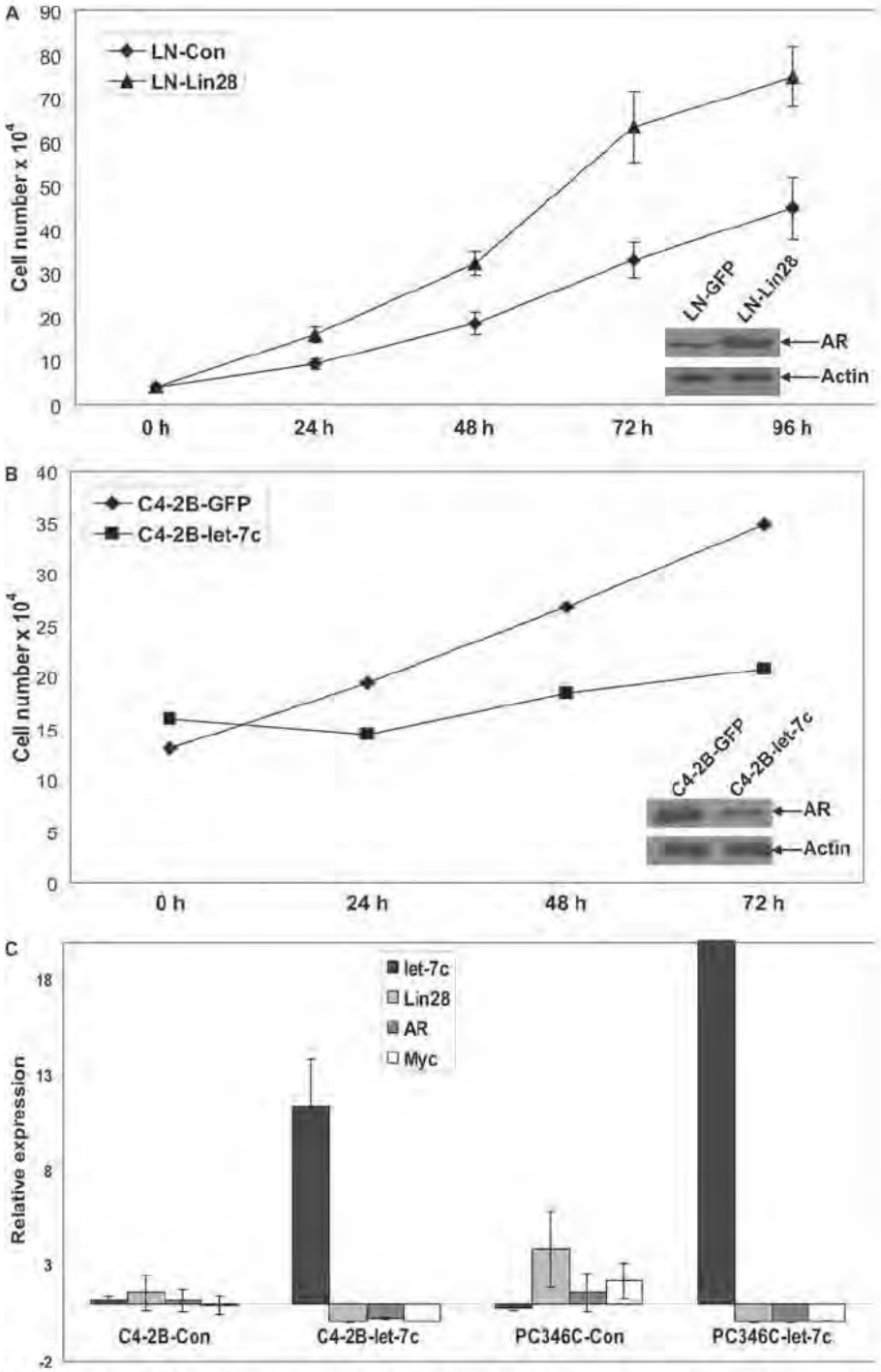

FIGURE 5. **Let-7c reduces proliferation of PCa cells.** *A*, cell growth of LNCaP cells stably expressing Lin28 was determined by cell counting up to 96 h. Expression of Lin28 enhanced the growth rate of LNCaP cells. The *inset* (Western blot analysis) shows the increase in expression of AR with increased expression of Lin28. *B*, cell growth of C4-2B cells stably expressing let-7c was analyzed up to 72 h. Expression of let-7c decreased the growth rate of C4-2B cells. The *inset* (Western blot analysis) shows the reduction in AR protein levels with expression of let-7c. *C*, relative expression levels of let-7c, AR, Lin28, and Myc were analyzed by qRT-PCR in PCa xenografts injected intratumorally with let-7c expressing lentiviruses. Enhanced expression of let-7c suppressed expression of AR, Lin28, and Myc. Data points represent mean ± S.D. of triplicate samples from two independent experiments. *Error bars* denote mean ± S.D. $p \leq 0.05$.

NKX3.1 (*G*) promoters, whereas expression of Lin28, a repressor of let-7c, increased AR binding to these promoters. Collectively, these results demonstrate that the suppression of AR expression by let-7c leads to decrease in the transactivation potential of AR, whereas increased AR expression by let-7c antisense or Lin28 leads to an increase in the transactivation potential of AR and expression of its target genes.

Repression of AR by let-7c Is Mediated by Myc—MiRNAs target several genes by binding to consensus binding sites in the 3′ untranslated region of the transcript, leading to degradation of the mRNA via the RISC complex. Therefore, we analyzed whether let-7c binding sites exist in the 3′ untranslated region of the AR mRNA using algorithms from miRBase, TargetScan, PictarVert, and Microcosm. Analysis of the 3′ untranslated

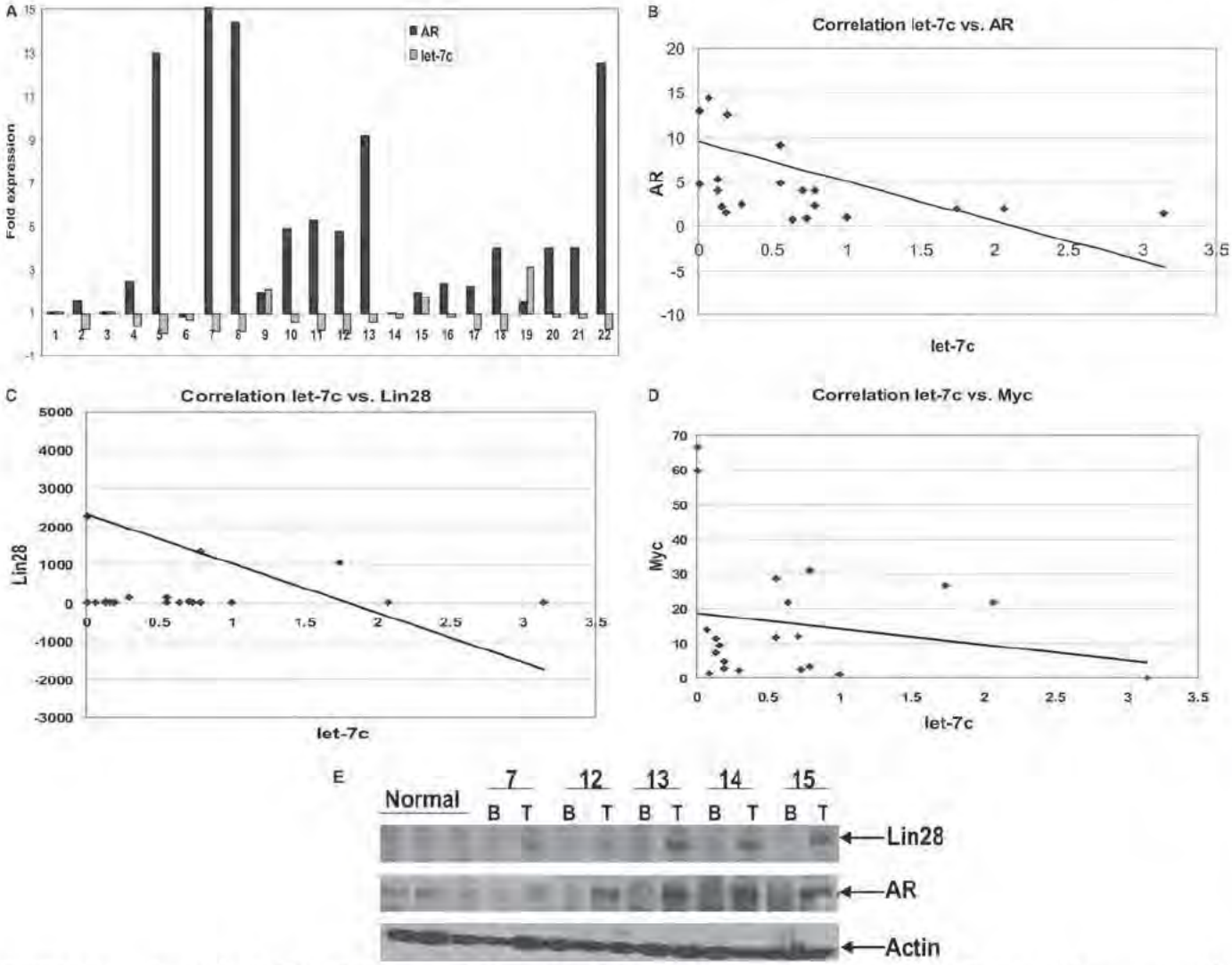

FIGURE 6. **Expression levels of let-7c and AR are negatively correlated in human PCa.** *A*, relative expression levels of let-7c and AR were measured by qRT-PCR in total RNAs extracted from 22 human prostate cancer samples. Levels of let-7c and AR were correlated negatively with each other. $p = 0.015$ by two-tailed Student's *t* test. *B*, plot showing the negative correlation between levels of let-7c and AR mRNAs in the above samples. The correlation coefficient (*R*) was found to be −0.5135. *C* and *D*, plots showing negative correlation between relative expression levels of let-7c and Lin28 and let-7c and Myc, respectively, in the above samples. $r = -0.1765$ (Lin28) and $r = -0.3354$ (Myc). *E*, representative Western blot analysis showing protein levels of Lin28 and AR in extracts from normal, benign (*B*), and adjacent tumor (*T*) containing human prostate samples. Actin is shown as a loading control. The levels of Lin28 and AR are positively correlated with each other.

region of AR failed to detect the presence of let-7c binding sites. To confirm whether let-7c leads to degradation of the AR mRNA, we analyzed the stability of AR mRNA in LNCaP cells expressing high levels of let-7c. LNCaP cells were transfected with plasmids expressing let-7c, were treated with vehicle or 50 μM actinomycin D (to inhibit *de novo* RNA synthesis), and total RNAs were isolated. Northern blotting (Fig. 3*A*) and qRT-PCR (*B*) were performed with a probe specifically against AR mRNA and primers amplifying AR mRNA, respectively. As shown in Fig. 3, *A* and *B*, the half-life of AR mRNA in LNCaP cells was ~3.5 h in the presence of androgen, which was not altered when let-7c was overexpressed in LNCaP cells. These results suggest that let-7c does not enhance the degradation of AR mRNA, implying that a mechanism other than direct mRNA degradation may be involved in let-7c-mediated AR inhibition. Next, we examined whether let-7c affects transcription of AR. Let-7c or let-7c antisense oligos were cotransfected with a luciferase reporter driven by the full-length (~6 kb) promoter of the AR gene into LNCaP cells, and luciferase assays were performed. Down-regulation of let-7c expression by let-7c antisense increased, whereas overexpression of let-7 decreased, the activation of the AR promoter (Fig. 3*C*), suggesting that suppression of AR expression by let-7c may be at the level of transcription.

Because our results showed that suppression of AR expression and activity by let-7c is not through typical miRNA-mediated mRNA degradation but at the level of transcription, we hypothesized that a let-7c target gene may function as a transcriptional regulator of AR. We analyzed whether any of the transcription factors binding to the AR promoter was a target of let-7c using MatInspector and miRBase and found that Myc, which activates AR transcription by binding to a consensus element in the AR promoter (12), was one of the targets of let-7c. LNCaP cells overexpressing let-7c were analyzed by Western

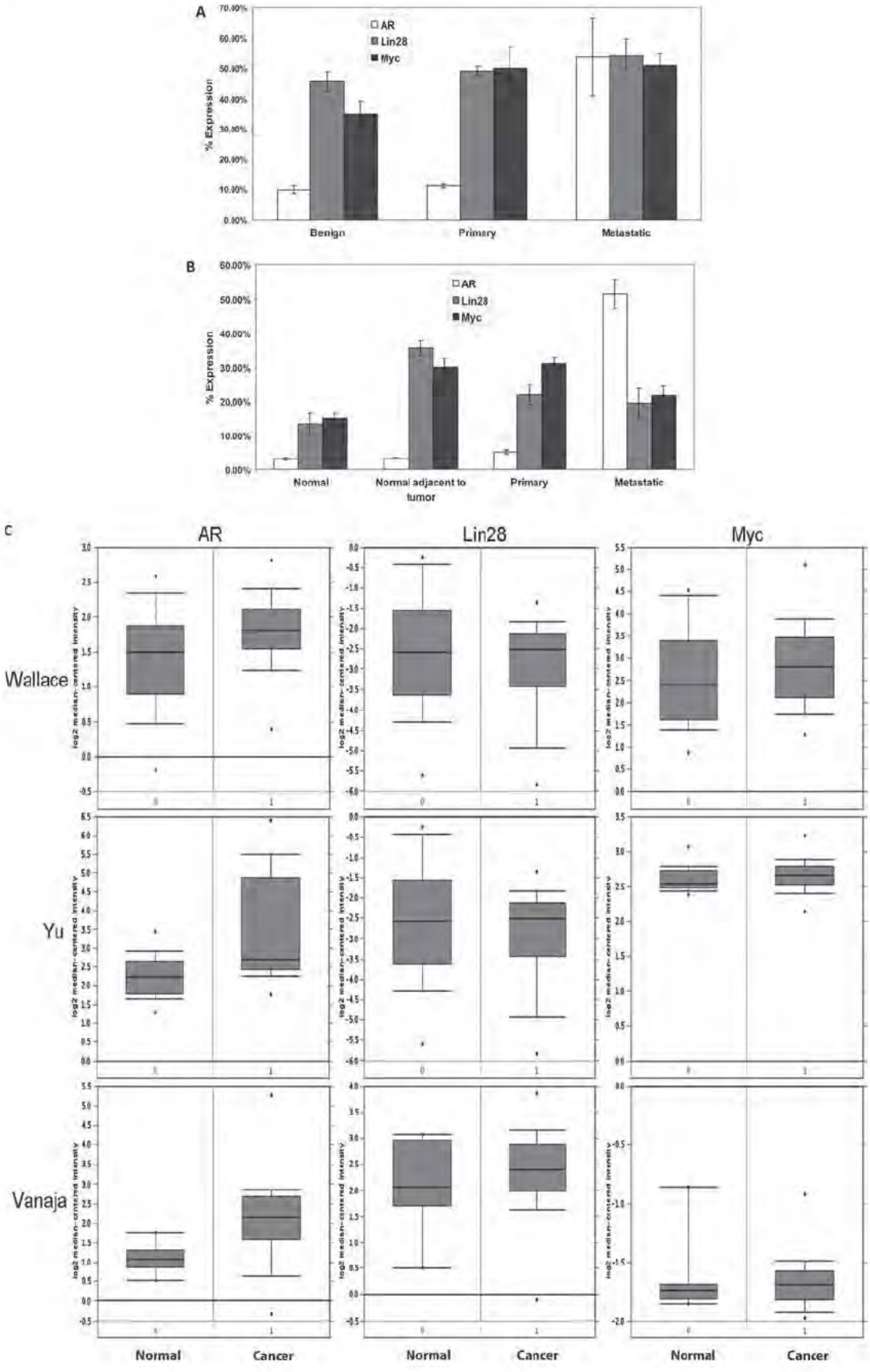

blotting to confirm whether let-7c reduces Myc expression. Results showed that Myc expression was down-regulated in LNCaP cells expressing let-7c (Fig. 4*A*). Similarly, we found an increase in Myc expression in LNCaP cells transfected with let-7c antisense oligos (Fig. 4*B*). In addition, the levels of Myc are correlated with AR expression (Fig. 4*B*). These results were confirmed in LNCaP and C4-2B cells stably expressing let-7c (supplemental Fig. 2, *A* and *B*). Down-regulation of Myc by Myc shRNA reduced AR promoter activity (Fig. 4*C*) and AR mRNA expression (*D*), whereas overexpression of Myc enhanced AR promoter activity (*C*) and AR mRNA expression (*D*). Down-regulation of Myc also reduced the levels of PSA and NKX3.1 mRNA, whereas overexpression of Myc enhanced the levels of PSA and NKX3.1 mRNA (*E*).

To determine whether reduced expression of Myc is responsible for let-7c-mediated AR suppression, we cotransfected let-7c with Myc in LNCaP cells expressing a luciferase reporter driven by the full-length AR promoter. The results showed that let-7c suppressed AR promoter activity, which was reversed by overexpression of Myc (Fig. 4*F*). ChIP assays were performed using primers spanning the consensus binding site for Myc in the AR promoter to determine whether let-7c affects the recruitment of Myc to the promoter of the AR gene. Overexpression of let-7c reduced, whereas overexpression of Lin28 increased the recruitment of Myc to the AR promoter (Fig. 4*G*). To confirm that Myc mediates regulation of AR by let-7c, we transfected Myc along with the pGL4-AR prom-Luc reporter into LNCaP and C4-2B cells stably expressing let-7c and performed luciferase assays. AR promoter activity was lower in cells stably expressing let-7c, which was reversed by overexpression of Myc (supplemental Fig. 3, *A* and *B*). Previous studies have shown that Myc is a direct target of let-7c (31). Conserved let-7c binding sites exist in the 3′ untranslated region of Myc that are conserved across several vertebrate classes (supplemental Fig. 4, *A* and *B*). Collectively, these results demonstrate that AR suppression by let-7c is mediated by direct down-regulation of Myc.

To test whether reduction of AR expression by let-7c affects proliferation of PCa cells *in vitro*, we analyzed cell growth of LNCaP and C4-2B cells stably expressing Lin28 or let-7c, respectively. As shown in Fig. 5, *A* and *B*, expression of Lin28 enhanced growth of LNCaP cells, indicating that increased expression of AR due to Lin28 leads to increased growth of PCa cells. Similarly, C4-2B cells stably expressing let-7c exhibited a lower rate of growth compared with controls, indicating that suppression of AR expression by let-7c leads to reduced survival of PCa cells. Expression levels of AR in these cell lines were confirmed by Western blotting (Fig. 5, *A* and *B*, *insets*).

Expression of let-7c Suppresses AR, Lin28, and Myc in PCa Xenografts—To determine whether let-7c suppresses AR expression in xenografts of PCa cells *in vivo*, we generated xenografts of AR-positive C4-2B and PC346C human PCa cells in nude mice. After the tumors reached 0.5 cm^3, the control mice were injected with control lentiviruses, whereas experimental mice were injected intratumorally with lentiviruses expressing let-7c. At the end of 3 weeks, the tumors were excised, RNAs prepared, and levels of let-7c, AR, Lin28, and Myc were analyzed by qRT-PCR. As shown in Fig. 5*C*, expression of let-7c suppressed AR, Lin28, and Myc levels in the xenograft tissues.

Let-7c and AR Are Negatively Correlated in Human PCa—We have demonstrated that let-7c represses AR expression and that the levels of let-7c are inversely correlated with AR in cell culture and xenografts of PCa mouse models. To determine whether a correlation exists between expression levels of let-7c and AR in clinical PCa, we analyzed RNAs from 22 human PCa specimens by quantitative RT-PCR. RNAs were isolated from human tissues, reverse-transcribed, and subjected to qRT-PCR using LNA-conjugated let-7c primers (Exiqon). This was followed by measurement of expression levels of AR using primers specifically amplifying AR mRNA. The levels of let-7c and AR were negatively correlated, with a correlation coefficient of −0.52 using a two tailed Student's *t* test in Microsoft Excel Tools (Fig. 6, *A* and *B*). Expression levels of Lin28 and Myc were also examined in these specimens and were correlated negatively with expression levels of let-7c with correlation coefficients of −0.1765 and −0.3354, respectively, using a two-tailed Student's *t* test in Microsoft Excel Tools (Fig. 6, *C* and *D*). The correlation coefficients do not show a perfect negative correlation between expression levels of the respective genes but demonstrate a trend toward negative correlation, which should be validated with larger numbers of samples.

As Lin28 is a key regulator of let-7c expression, we examined Lin28 expression in 42 archival matched pairs of benign and cancerous human prostate samples and 20 samples of normal prostate by Western blotting using an antibody specifically against Lin28 (Abcam). The levels of Lin28 protein expression were higher in most of the tumors compared with the matched benign prostates (Fig. 6*E*). We found that 86% of tumor tissues were positive for Lin28, whereas only 47% of benign and 40% of normal tissues exhibited Lin28 expression. We also analyzed expression levels of AR in these samples by Western blotting, and the results show that AR levels correlate with Lin28 levels (Fig. 6*E*). Collectively, these data suggest that expression levels of let-7c and AR are negatively correlated with each other and that Lin28 is overexpressed in prostate cancer *versus* benign prostate and is correlated positively with AR.

Expression Levels of AR, Lin28, and Myc Are Increased in Human PCa—To validate our above results from clinical PCa specimens, gene expression analysis was performed using public domain data sets deposited in the Gene Expression Omnibus of the National Center for Biotechnology Informa-

FIGURE 7. **Expression levels of AR, Lin28 and Myc are correlated with each other in human PCa.** *A*, comparison of AR, Lin28, and Myc expression in the dataset GDS1439 (23). Benign, $n = 6$; primary prostate cancer, $n = 7$; and metastatic prostate cancer, $n = 6$. *B*, comparison of AR, Lin28, and Myc levels in GDS2547 (24). Normal prostate tissue, $n = 18$; normal tissue adjacent to tumor, $n = 16$; primary prostate cancer, $n = 65$; and metastatic prostate cancer, $n = 25$. Data are expressed as mean ±S.E. (in percentages) of the maximum single channel count determined in each data set. *C*, gene expression analysis using the Oncomine database showing the relative expression levels of AR, Lin28, and Myc in three datasets comparing normal prostate tissue and prostate cancer. Wallace_prostate: normal, $n = 20$; cancer, $n = 69$. Yu_prostate: normal, $n = 23$; cancer, $n = 64$. Vanaja_prostate: normal, $n = 8$; cancer, $n = 32$. Data are presented as mean ± S.E. of normalized expression units according to Oncomine output.

tion and in Oncomine. The former utilized data sets generated by Affymetrix human genome microarrays of well described human tissues, whereas the latter utilized the Oncomine cancer transcriptome data. Analysis of Affymetrix human gene arrays demonstrated that expression levels of AR, Lin28, and Myc were enhanced ($p \leq 0.05$) in primary and metastatic prostate cancer specimens compared with benign prostate specimens (Fig. 7, *A* and *B*). Similarly, significant ($p \leq 0.001$) increases were observed in expression levels of AR, Lin28, and Myc in prostate cancer specimens compared with their normal counterparts and were positively correlated with each other (Fig. 7*C*). These results imply that Lin28 and Myc play important roles in the regulation of AR expression in human PCa. Down-regulation of expression of let-7c in human PCa may lead to higher levels of expression of Lin28 and Myc, which in turn enhance the expression of AR, which is an important survival factor for PCa cells.

DISCUSSION

In this study, we found that let-7c suppresses AR expression via a transcriptional mechanism involving Myc. Down-regulation of let-7c by antisense oligonucleotides increased AR expression, thereby conferring a survival advantage on PCa cells. We also found that down-regulation of Lin28 in PCa cells led to an up-regulation of let-7c expression and inhibited cell growth. These results suggest that this novel pathway by which miRNA let-7c regulates AR expression and PCa cell proliferation may be exploited for therapeutic applications.

A tumor suppressor role has been attributed to the let-7 family of miRNAs in several human cancers. Here, we demonstrate that let-7c functions as a tumor suppressor that inhibits prostate tumor growth by regulating AR expression. The most important and well studied targets of let-7 are the oncogenes: HMGA2, RAS, and Myc. Each of these proteins is an important transcription factor, and it is conceivable that by repressing their expression directly, let-7 may influence cancer cell proliferation in a cell type- and target-specific manner. In our study, we show that by targeting Myc, which is a pivotal transcription factor regulating the expression of AR in PCa cells, let-7c suppresses AR expression and plays an important tumor suppressor role in PCa. Our results also indicate that, if feasible strategies to reconstitute let-7c in prostate tumors can be developed, reconstitution of let-7c may become a potential therapeutic agent for prostate cancer treatment. The down-regulation of potential oncogenic and survival factors by let-7c may represent an attractive therapeutic opportunity in human PCa.

It is well documented that Lin28 plays a major role in regulation of let-7c expression (14, 32). Overexpression of Lin28 inhibited let-7c expression in LNCaP cells, whereas knockdown of Lin28 expression increased let-7c in C4-2B cells. In addition, we showed that expression levels of let-7c and Lin28 are correlated inversely with each other in the tumors of prostate cancer xenograft models as well as in prostate cancer clinical specimens, indicating that a negative feedback loop exists between Lin28 and let-7c. Since overexpression of Lin28 enhanced AR expression and increased cell growth in prostate cancer cells, it is possible that overexpression of let-7c suppresses AR expression on one hand while negatively regulating Lin28 expression on the other hand, leading to further inhibition of prostate tumor growth.

The AR is an important survival factor in prostate cells and tumors. Up-regulation of AR expression has been recognized as a major determinant in the pathogenesis of PCa. Up-regulation of AR expression has been shown to be sufficient for conversion of a castration-sensitive phenotype to a castration-resistant phenotype (33). CRPC tissues expressing higher levels of the AR require 80% lower concentrations of androgens to maintain androgen signaling (34). High levels of AR expression also convert AR antagonists like bicalutamide and flutamide into agonists and confer promiscuity to ligands like estrogens (33). Recent data also indicate that elevated expression of the AR detected in biopsy specimen predicts response or resistance to therapy (35). Silencing AR signaling by down-regulating its expression has been the focus of research efforts in the recent past. Use of synthetic siRNA, AR antisense, geldanamycin analogs, and selective AR modulators (SARMs) has demonstrated that down-regulation of AR expression is sufficient to slow prostate tumor growth and induce apoptosis (36–39). In view of the above studies and the importance of the AR in PCa pathogenesis, our study, which shows a novel way of antagonizing AR expression and thereby CRPC progression by let-7c, may have important translational implications.

In summary, we show that the miRNA let-7c plays an important role in regulation of androgen signaling by down-regulating AR expression and thereby inhibits PCa cell proliferation. Our results suggest that re-expression of the miRNA let-7c may help target enhanced and hypersensitive AR in advanced PCa.

Acknowledgments—We thank Drs. Leland W. K. Chung and Wen-Chin Huang (Cedars-Sinai Medical Center, Los Angeles, CA) and Dr. Donald Tindall (Mayo Clinic, Rochester, MN) for the pGL4-AR-Prom-Luc plasmid.

REFERENCES

1. Chen, Y., Sawyers, C. L., and Scher, H. I. (2008) Targeting the androgen receptor pathway in prostate cancer. *Curr. Opin. Pharmacol.* **8,** 440–448
2. Lamont, K. R., and Tindall, D. J. (2010) Androgen regulation of gene expression. *Adv. Cancer Res.* **107,** 137–162
3. Coppola, V., de Maria, R., and Bonci, D. (2010) *Endocr. Relat. Cancer* **17,** F1–F17
4. Shi, X. B., Tepper, C. G., and deVere White, R. W. (2008) Cancerous miRNAs and their regulation. *Cell Cycle* **7,** 1529–1538
5. Gandellini, P., Folini, M., and Zaffaroni, N. (2009) Towards the definition of prostate cancer-related microRNAs. Where are we now? *Trends Mol. Med.* **15,** 381–390
6. Calin, G. A., Sevignani, C., Dumitru, C. D., Hyslop, T., Noch, E., Yendamuri, S., Shimizu, M., Rattan, S., Bullrich, F., Negrini, M., and Croce, C. M. (2004) Human microRNA genes are frequently located at fragile sites and genomic regions involved in cancers. *Proc. Natl. Acad. Sci. U.S.A.* **101,** 2999–3004
7. Ozen, M., Creighton, C. J., Ozdemir, M., and Ittmann, M. (2008) Widespread deregulation of microRNA expression in human prostate cancer. *Oncogene* **27,** 1788–1793
8. Jiang, J., Lee, E. J., Gusev, Y., and Schmittgen, T. D. (2005) Real-time expression profiling of microRNA precursors in human cancer cell lines. *Nucleic Acids Res.* **33,** 5394–5403
9. Boyerinas, B., Park, S. M., Hau, A., Murmann, A. E., and Peter, M. E. (2010) The role of let-7 in cell differentiation and cancer. *Endocr. Relat. Cancer* **17,** F19–36

10. Lee, Y. S., and Dutta, A. (2007) The tumor suppressor microRNA let-7 represses the HMGA2 oncogene. *Genes Dev.* **21,** 1025–1030
11. Johnson, S. M., Grosshans, H., Shingara, J., Byrom, M., Jarvis, R., Cheng, A., Labourier, E., Reinert, K. L., Brown, D., and Slack, F. J. (2005) RAS is regulated by the let-7 microRNA family. *Cell* **120,** 635–647
12. Kumar, M. S., Lu, J., Mercer, K. L., Golub, T. R., and Jacks, T. (2007) Impaired microRNA processing enhances cellular transformation and tumorigenesis. *Nat. Genet.* **39,** 673–677
13. Viswanathan, S. R., Daley, G. Q., and Gregory, R. I. (2008) Selective blockade of microRNA processing by Lin28. *Science* **320,** 97–100
14. Viswanathan, S. R., and Daley, G. Q. (2010) Lin28. A microRNA regulator with a macro role. *Cell* **140,** 445–449
15. Chang, T. C., Zeitels, L. R., Hwang, H. W., Chivukula, R. R., Wentzel, E. A., Dews, M., Jung, J., Gao, P., Dang, C. V., Beer, M. A., Thomas-Tikhonenko, A., and Mendell, J. T. (2009) Lin-28B transactivation is necessary for Myc-mediated let-7 repression and proliferation. *Proc. Natl. Acad. Sci. U.S.A.* **106,** 3384–3389
16. Dangi-Garimella, S., Yun, J., Eves, E. M., Newman, M., Erkeland, S. J., Hammond, S. M., Minn, A. J., and Rosner, M. R. (2009) Raf kinase inhibitory protein suppresses a metastasis signalling cascade involving LIN28 and let-7. *EMBO J.* **28,** 347–358
17. Lu, J., Getz, G., Miska, E. A., Alvarez-Saavedra, E., Lamb, J., Peck, D., Sweet-Cordero, A., Ebert, B. L., Mak, R. H., Ferrando, A. A., Downing, J. R., Jacks, T., Horvitz, H. R., and Golub, T. R. (2005) MicroRNA expression profiles classify human cancers. *Nature* **435,** 834–838
18. Nadiminty, N., Lou, W., Lee, S. O., Lin, X., Trump, D. L., and Gao, A. C. (2006) Stat3 activation of NF-κB p100 processing involves CBP/p300-mediated acetylation. *Proc. Natl. Acad. Sci. U.S.A.* **103,** 7264–7269
19. Nadiminty, N., Dutt, S., Tepper, C., and Gao, A. C. (2010) Microarray analysis reveals potential target genes of NF-κB2/p52 in LNCaP prostate cancer cells. *Prostate* **70,** 276–287
20. Nadiminty, N., Lou, W., Sun, M., Chen, J., Yue, J., Kung, H. J., Evans, C. P., Zhou, Q., and Gao, A. C. (2010) Aberrant activation of the androgen receptor by NF-κB2/p52 in prostate cancer cells. *Cancer Res.* **70,** 3309–3319
21. Dhir, R., Ni, Z., Lou, W., DeMiguel, F., Grandis, J. R., and Gao, A. C. (2002) Stat3 activation in prostatic carcinomas. *Prostate* **51,** 241–246
22. Ni, Z., Lou, W., Lee, S. O., Dhir, R., DeMiguel, F., Grandis, J. R., and Gao, A. C. (2002) Selective activation of members of the signal transducers and activators of transcription family in prostate carcinoma. *J. Urol.* **167,** 1859–1862
23. Varambally, S., Yu, J., Laxman, B., Rhodes, D. R., Mehra, R., Tomlins, S. A., Shah, R. B., Chandran, U., Monzon, F. A., Becich, M. J., Wei, J. T., Pienta, K. J., Ghosh, D., Rubin, M. A., and Chinnaiyan, A. M. (2005) Integrative genomic and proteomic analysis of prostate cancer reveals signatures of metastatic progression. *Cancer Cell* **8,** 393–406
24. Chandran, U. R., Ma, C., Dhir, R., Bisceglia, M., Lyons-Weiler, M., Liang, W., Michalopoulos, G., Becich, M., and Monzon, F. A. (2007) Gene expression profiles of prostate cancer reveal involvement of multiple molecular pathways in the metastatic process. *BMC Cancer* **7,** 64
25. Prasad, P. D., Stanton, J. A., and Assinder, S. J. (2010) Expression of the actin-associated protein transgelin (SM22) is decreased in prostate cancer. *Cell Tissue Res.* **339,** 337–347
26. Wallace, T. A., Prueitt, R. L., Yi, M., Howe, T. M., Gillespie, J. W., Yfantis, H. G., Stephens, R. M., Caporaso, N. E., Loffredo, C. A., and Ambs, S. (2008) Tumor immunobiological differences in prostate cancer between African-American and European-American men. *Cancer Res.* **68,** 927–936
27. Yu, Y. P., Landsittel, D., Jing, L., Nelson, J., Ren, B., Liu, L., McDonald, C., Thomas, R., Dhir, R., Finkelstein, S., Michalopoulos, G., Becich, M., and Luo, J. H. (2004) Gene expression alterations in prostate cancer predicting tumor aggression and preceding development of malignancy. *J. Clin. Oncology* **22,** 2790–2799
28. Vanaja, D. K., Cheville, J. C., Iturria, S. J., and Young, C. Y. (2003) Transcriptional silencing of zinc finger protein 185 identified by expression profiling is associated with prostate cancer progression. *Cancer Res.* **63,** 3877–3882
29. Lee, S. O., Lou, W., Hou, M., de Miguel, F., Gerber, L., and Gao, A. C. (2003) Interleukin-6 promotes androgen-independent growth in LNCaP human prostate cancer cells. *Clin. Cancer Res.* **9,** 370–376
30. Lee, S. O., Chun, J. Y., Nadiminty, N., Lou, W., and Gao, A. C. (2007) Interleukin-6 undergoes transition from growth inhibitor associated with neuroendocrine differentiation to stimulator accompanied by androgen receptor activation during LNCaP prostate cancer cell progression. *Prostate* **67,** 764–773
31. Koscianska, E., Baev, V., Skreka, K., Oikonomaki, K., Rusinov, V., Tabler, M., and Kalantidis, K. (2007) Prediction and preliminary validation of oncogene regulation by miRNAs. *BMC Mol. Biol.* **8,** 79
32. Iliopoulos, D., Hirsch, H. A., and Struhl, K. (2009) An epigenetic switch involving NF-κB, Lin28, Let-7 MicroRNA, and IL6 links inflammation to cell transformation. *Cell* **139,** 693–706
33. Chen, C. D., Welsbie, D. S., Tran, C., Baek, S. H., Chen, R., Vessella, R., Rosenfeld, M. G., and Sawyers, C. L. (2004) Molecular determinants of resistance to antiandrogen therapy. *Nat. Med.* **10,** 33–39
34. Bonkhoff, H., and Berges, R. (2010) From pathogenesis to prevention of castration-resistant prostate cancer. *Prostate* **70,** 100–112
35. Donovan, M. J., Khan, F. M., Fernandez, G., Mesa-Tejada, R., Sapir, M., Zubek, V. B., Powell, D., Fogarasi, S., Vengrenyuk, Y., Teverovskiy, M., Segal, M. R., Karnes, R. J., Gaffey, T. A., Busch, C., Haggman, M., Hlavcak, P., Freedland, S. J., Vollmer, R. T., Albertsen, P., Costa, J., and Cordon-Cardo, C. (2009) Personalized prediction of tumor response and cancer progression on prostate needle biopsy. *J. Urol.* **182,** 125–132
36. Heinlein, C. A., and Chang, C. (2004) Androgen receptor in prostate cancer. *Endocr. Rev.* **25,** 276–308
37. Singh, P., Uzgare, A., Litvinov, I., Denmeade, S. R., and Isaacs, J. T. (2006) Combinatorial androgen receptor-targeted therapy for prostate cancer. *Endocr. Relat. Cancer* **13,** 653–666
38. Pienta, K. J., and Bradley, D. (2006) Mechanisms underlying the development of androgen-independent prostate cancer. *Clin. Cancer Res.* **12,** 1665–1671
39. Tran, C., Ouk, S., Clegg, N. J., Chen, Y., Watson, P. A., Arora, V., Wongvipat, J., Smith-Jones, P. M., Yoo, D., Kwon, A., Wasielewska, T., Welsbie, D., Chen, C. D., Higano, C. S., Beer, T. M., Hung, D. T., Scher, H. I., Jung, M. E., and Sawyers, C. L. (2009) Development of a second-generation antiandrogen for treatment of advanced prostate cancer. *Science* **324,** 787–790

Signal Transduction:

MicroRNA let-7c Suppresses Androgen Receptor Expression and Activity via Regulation of Myc Expression in Prostate Cancer Cells

Nagalakshmi Nadiminty, Ramakumar Tummala, Wei Lou, Yezi Zhu, Jin Zhang, Xinbin Chen, Ralph W. deVere White, Hsing-Jien Kung, Christopher P. Evans and Allen C. Gao

J. Biol. Chem. 2012, 287:1527-1537.
doi: 10.1074/jbc.M111.278705 originally published online November 28, 2011

World J Urol (2012) 30:287–295
DOI 10.1007/s00345-011-0771-3

TOPIC PAPER

Mechanisms of persistent activation of the androgen receptor in CRPC: recent advances and future perspectives

Nagalakshmi Nadiminty · Allen C. Gao

Received: 29 June 2011 / Accepted: 20 September 2011 / Published online: 19 October 2011

Abstract
Background The emergence of castration resistance has remained the primary obstacle in prostate cancer therapy for several decades. Mechanisms likely to be involved in castration-resistant progression have been studied extensively, but have failed to yield many meaningful and effective targets. The re-activation of the androgen receptor (AR) in castration-resistant prostate cancer (CRPC) is now recognized as the central event in this process, and therapeutic modalities are being devised to combat it.
Methods A review of literature was performed to highlight the important factors that play a role in the aberrant activation of the AR in CRPC.
Results Seminal and exciting advances made in the past few years in the discovery of the roles of new intrinsic factors such as intracrine androgens, gene fusions involving the ETS oncogenes, and splice variants of the AR are reviewed. New and emerging hypotheses about the involvement of factors such as cytokines and other signaling pathways are discussed.
Conclusions This review summarizes the most recent advances in the persistent activation of the androgen receptor signaling pathway and provides a perspective about their significance in CRPC progression.

N. Nadiminty · A. C. Gao (✉)
Department of Urology and Cancer Center,
University of California Davis Medical Center,
4645 2nd Ave, Research III, Suite 1300,
Sacramento, CA 95817, USA
e-mail: acgao@ucdavis.edu

Keywords Androgen receptor · Castration-resistant prostate cancer · Cytokines · Intracrine androgens · Splice variants

Introduction

Prostate cancer (CaP) has emerged as one of the leading causes of cancer-related mortality among men in the Western World, accounting for 94,000 deaths in Europe in 2008 and 32,050 deaths in the United States in 2010 [1]. Androgen ablation therapy is the treatment of choice for androgen-dependent prostate cancer, but most patients eventually progress to a castration-resistant stage at which therapeutic choices are limited. Castration-resistant prostate cancer (CRPC) is often characterized by overexpression or hyperactivation of the androgen receptor (AR) despite availability of only castrate levels of androgens. Several mechanisms including amplification of the AR gene, mutations, overexpression of co-activators, activation by growth factors or cytokine signaling, cross-talk with other transcription factors, synthesis of intracrine androgens by the prostate tumors, and synthesis of constitutively active splice variants have been implicated in the persistent activation of the AR in CRPC. Pre-clinical studies have validated these concepts, and there has been a considerable paradigm shift in recent years regarding the role of the AR and androgens in CaP, which is reflected by the recognition that targeting functional AR in CRPC is essential for the success of any therapy. shRNA-mediated knockdown of AR attenuated ligand-independent activation and delayed tumor progression [2]. This has encouraged the development of several inhibitors of AR transcriptional activity targeting different domains that are currently in clinical trials. This review will focus on the knowledge gained in the past

few years about the aberrant activation of the AR by some of the factors outlined above.

Amplification of the AR gene

Amplification of the AR gene has been suggested as one of the mechanisms of hormone-refractory CaP. Comparative genome hybridization showed the amplification of AR gene in 30% of recurrent prostate tumors after failure of androgen deprivation therapy [3]. Expression profiling by microarray showed increased AR mRNA in hormone-refractory prostate tumor xenografts compared to their hormone-sensitive parental cells [4]. The study also showed that hormone-refractory tumor growth mediated by AR amplification is still dependent on androgens and that higher levels of the AR convert antagonists to agonists and alter co-activator assemblies [4]. An association between AR gene amplification and therapy response has been demonstrated in patients who underwent combined androgen blockade after initial androgen deprivation [5]. Some studies have found that increase in AR mRNA and as a result AR protein level occurs in CRPC, irrespective of AR gene copy number [6], suggesting that other mechanisms that enhance the expression of the AR play critical roles in castration-recurrent progression.

AR mutations

AR is the most mutated one among the steroid hormone receptors, with >660 mutations being reported to date. Great variability has been found in the frequency of somatic AR mutations in CaP, with 25% frequency in androgen-dependent CaP, and up to 50% in hormone-refractory and metastatic CaP. The gain-of-function AR mutations in CaP are detected in different functional domains but rarely in the 5′- and 3′-untranslated regions of the transcript. Most of the mutations are single base substitutions that affect AR function either directly or indirectly. The LBD harbors ~40% of these mutations, while the NTD and the DBD harbor ~37 and ~9%, respectively [7]. Mutations in the LBD may alter the sensitivity of AR to weak ligands such as adrenal androgens or even antagonists such as bicalutamide or flutamide. Activating mutations of the AR may also alter interactions with co-regulators and impair intramolecular interactions [8]. Polyglutamine tract and CAG repeat mutations have been shown to produce a more active and stable receptor [9]. Mutations that disrupt the inhibitory hinge region thus leading to enhanced activity of the AF-2 domain have also been described [10]. A recent study reported that the frequency of mutations in the AR is higher in metastatic and hormone-refractory CaP compared to localized untreated disease [11]. Another study showed that AR mutations and mutation frequencies can be detected in circulating tumor cells from the blood of CaP patients [12], suggesting that these approaches may compensate for the difficulties in obtaining metastatic tissue from CaP patients. It has been suggested that AR mutants may exploit several mechanisms to evade therapy including altered stability, promoter preference, or ligand specificity [13]. Hence, the development and validation of reliable protocols for the accurate assessment of the functional status, frequency, and functional relevance of mutations in the AR may be critical for the successful development and clinical implementation of novel targeted therapies for progressive CRPC.

Gene fusions

Gene fusions or chromosomal rearrangements include chromosome translocations or deletions that result in fusion of two distinct genes. Recently, gene fusions involving the prostate specific gene transmembrane protease, serine 2 (TMPRSS2), and members of the erythroblastosis virus E26 transforming sequence (ETS) family of transcription factors were identified in human prostate cancers. TMPRSS2/ERG is detected in about 50% of PSA-screened localized prostate cancers [14]. The androgen-regulated TMPRSS2 gene and the transcription factor ERG (the most common ETS gene in the fusion events) are located about 3 Mb apart on chromosome 21q22 [15]. In a report that summarized 15 studies containing 1,051 cases, 477 samples (45%) were positive for TMPRSS2/ERG rearrangements [16]. Fusion of the two genes results in the androgen-regulated expression of the truncated ERG gene, which may have a possible causal role in the prostate cancer–specific death of TMPRSS2/ERG-positive patients [17]. It has been suggested that TMPRSS2/ERG fusion is an early event in the initiation of prostate cancer that drives the transformation of the prostate epithelium [15, 18]. Studies have shown that expression of the TMPRSS2/ERG fusion transcript in luminal prostate led to precancerous prostate intraepithelial neoplasia (PIN) but not prostate cancer [19]. The rearrangement was found to be homologous in the circulating tumor cells (CTCs) from 49 patients, and the expression of the fusion gene did not change with the development of castration resistance [18]. Androgen induces expression of the fusion transcript in non-malignant prostate epithelial cells [20]. TMPRSS2/ERG gene fusion was found to be associated with lower core-specific and overall Gleason scores and not with high-grade morphologies. Conversely, TMPRSS2/ERG copy number increase, with or without rearrangement, was associated with higher Gleason score [21]. ERG disrupts androgen receptor (AR) signaling by

inhibiting AR expression, binding to and inhibiting AR activity at gene-specific loci, and inducing repressive epigenetic programs via direct activation of the H3K27 methyltransferase EZH2, a Polycomb group protein. These findings provide a working model in which TMPRSS2/ERG plays a critical role in cancer progression by disrupting lineage-specific differentiation of the prostate and potentiating the EZH2-mediated dedifferentiation program [22]. Transgenic overexpression of ERG in a PTEN haploinsufficient background promotes proliferation and progression of prostatic adenocarcinoma in a mouse model [23]. In addition, it was reported that CaP specimens harboring the TMPRSS2/ERG fusion were significantly enriched for the loss of the tumor suppressor PTEN [23]. Another study showed that TMPRSS2/ERG fusions and loss of PTEN together are a predictor of earlier biochemical recurrence of CaP [24]. These findings show that aberrant expression of ERG is a progression event in prostate tumorigenesis.

A number of strategies targeting the TMPRSS2/ERG fusions have been developed [14]. It is likely that the current therapies that target androgen signaling have at least a partial effect on the fusion transcript, since TMPRSS2 is an androgen-regulated gene. Urinary detection of the TMPRSS2/ERG fusion transcript has been suggested to be able to predict prostate cancer prognosis when combined with serum PSA [25]. Targeting Poly (ADP-Ribose) Polymerase1 (PARP1) was recently shown to be beneficial in ETS-fusion-positive prostate cancers [26]. The prognostic or diagnostic value of the detection of gene fusions in CRPC remains to be determined in clinical studies.

Chromosomal rearrangement and activation of androgen-regulated genes

The spatial and temporal spacing and restructuring of AR binding sites and components of AR transcriptional complexes that control different target genes have long remained elusive. A few recent studies shed some light on these aspects. Wang et al. [27] showed that in contrast to other nuclear receptor-driven transcriptional complexes, the levels of regulatory regions bound by AR transcriptional complexes rise over a period of 16 h and then decline slowly. Three models have been proposed to explain how a distal enhancer communicates with a proximal promoter. The looping model proposes that proteins bound to enhancers directly interact with the proteins bound to promoters with the intervening DNA looped out; the tracking model suggests signals recruited by enhancers slide through the DNA to promoters; the linking model proposes that the looped enhancer–promoter communication involves propagation of nucleoprotein structures along the intervening DNA [28, 29]. The regulation of PSA promoter by AR has been shown to involve chromosomal looping that regulates the tracking of RNA polymerase II from the enhancer to the proximal promoter AREs [27]. The current model proposes that unlike other nuclear receptors, AR activity involves sustained chromatin association and transcriptional activation of target genes for more than 96 h. This activity of AR is dependent on phosphorylated Pol II tracking from the PSA enhancer to the promoter through looped DNA [27]. This group also showed that AR collaborates with other transcription factors such as FOXA1, GATA2, and Oct1 in regulating promoters of target genes such as PSA and TMPRSS2 [30]. These authors demonstrated that the AR executes a distinct transcriptional program with regulation of M-phase genes such as UBE2C (ubiquitin-conjugating enzyme 2C) in CRPC cells as opposed to androgen-dependent CaP and that it cooperates with other transcription factors in this process [31]. These findings reveal the complexity of the transcriptional network regulated by the AR in CRPC.

Intrinsic factors

The most exciting recent findings in the field of CaP research have been the identification of steroidogenic ability of CaP cells and the discovery of truncated forms of the AR encoded by splice variants. We will summarize the salient findings below as pertinent to this review.

AR variants

The AR is a 110-kDa protein composed of an N-terminal ligand-independent transactivation domain (NTD), a central DNA-binding domain (DBD), a short hinge region, and a C-terminal region composed of a ligand-binding domain (LBD), a ligand-dependent activation function-2 (AF-2), and a bipartite nuclear localization sequence (NLS). The human AR gene contains 8 exons (with the recent identification of another exon downstream of exon 8, named exon 9 [32]). The earliest reports of the presence of AR splice variants have been sporadic and identified two constitutively active variants in the CWR22Rv1 cell line and postulated that these are the result of proteolytic cleavage [33]. But several groups have recently identified a multitude of other variants that appear to be products of insertion of a premature stop codon generated due to the duplication and insertion of exons 2 and 3. The first variants identified in the CWR22Rv1 cell line contained a duplicated 17-bp portion of exon 2 after exons 2 or 3 [34]. The AR variants described to date have been shown to promote castration-resistant progression in in vitro and in vivo models of CaP, and suppression of their expression resulted in decreased

Table 1 List of AR variants

Name	Splice junction	Alternative names	Transcriptional activity
AR-V1	3/CE1	AR4	Conditional
AR-V2	3/3/CE1	N/A	Unknown
AR-V3	2/CE4	AR 1/2/2b	Constitutive
AR-V4	3/CE4	AR 1/2/3/2b; AR5	Constitutive
AR-V5	3/CE2	N/A	Unknown
AR-V6	3/CE2	N/A	Unknown
AR-V7	3/CE3	AR3	Constitutive
AR-V8	3/intron 3	N/A	Unknown
AR-V9	3/CE 5	N/A	Conditional
AR-V10	3/intron 3	N/A	Unknown
AR-V11	3/intron 3	N/A	Unknown
AR-V12	4/8/9	ARv567es	Constitutive
AR-V13	6/9	N/A	Unknown
AR-V14	7/9	N/A	Unknown

proliferation of CaP cell lines [35]. Gene expression analyses indicated that these variants are functionally different from the full-length AR and regulate a distinct spectrum of target genes [35, 36].

To date, up to 14 splice variants of AR have been described, named from AR-V1 to AR-V14 (summarized in Table 1, refer to [32] for individual articles). All constitutively active AR variants are characterized by nuclear localization in the absence of ligand, while all inactive forms are localized in the cytoplasm. Some controversy exists regarding the requirement of full-length AR for the activity of these variants with some arguing that full-length AR is required [37], while others suggest that full-length AR may not be required for full transcriptional activity of the constitutively active variants [32]. Although expression levels of the splice variants are elevated in CRPC specimens, the absolute abundance of individual variants is ~2 orders of magnitude lower than that of full-length AR [37]. Expression of the variants was suggested to likely be an acute response to castration, rather than a driver of castration-resistant progression [37]. Expression of AR splice variants has also been detected in CaP bone metastases and is associated with castration recurrence and shorter survival [38]. Taken together, these studies demonstrate the complexity of the AR signaling pathway and attest to the importance of identifying AR splice variants in patient samples to help in prognosis.

Intracrine androgens

Prostate cells are not only dependent on the supply of circulating testicular androgens but can also survive with adrenal androgens. Even though androgen ablation reduces the levels of circulating androgens to castrate levels [39], persistent activation of the AR has been observed in CRPC and metastatic tissues [40]. The expression of in situ androgen-producing enzymes in CaP cells was reported several years ago [41], but its significance in CRPC has only recently come to light. It has been postulated that the continued activation of the AR in CRPC is partly due to the ability of CaP cells to synthesize intracellular androgens from other precursors. Intraprostatic androgen levels persist at ~20–30% of pre-castration levels after medical castration in healthy men [42]. CRPC cells acquire the full steroidogenic potential to synthesize intracrine androgens from cholesterol by upregulation of steroidogenic enzymes [43]. The AR can also be activated by the intratumoral bioconversion of androstanediol to DHT in CaP, bypassing the synthesis of testosterone. The steroidogenic potential of CRPC cells and tissues and the elevated expression levels of androgen biosynthetic enzymes in CRPC predict that androgen deprivation therapies are destined to fail in the majority of patients [44]. Recent studies also show that alterations in cholesterol regulation may contribute to the steroidogenic potential of CaP cells [45] and that steroidogenic enzymes and stem cell markers are upregulated in CRPC [46]. The interest generated by this phenomenon has resulted in the general acceptance of intracrine androgen synthesis as one of the mechanisms of continued AR activation in CRPC [47], even though one study showed only limited contributions to CRPC progression by intratumoral androgen-synthesizing enzymes [48]. Targeting intracrine androgen biosynthesis is currently being pursued as a potential therapeutic strategy for CRPC [49].

Extrinsic factors

Pro-inflammatory cytokines

The significance of interleukins-4, 6, and 8 has been investigated extensively in the past few years. They play pivotal roles in cell cycle progression, apoptosis, angiogenesis, migration, and invasion of cancer cells. IL-6 is a pleiotropic pro-inflammatory cytokine that binds the IL-6 receptor on the cell surface and signals through Janus kinases and downstream effector STAT3 (signal transducer and activator of transcription 3). Elevated levels of serum IL-6 and of soluble IL-6 receptor have been associated with CRPC progression and are predictive of recurrence after treatment of localized cancer [50, 51]. IL-6 exhibits multifaceted effects in human prostate cancer cells used in many studies. In LAPC-4 and MDA-PCa-2b cells, the effects of IL-6 treatment are agonistic, while in LNCaP cells derived from a lymph node metastasis, short-term treatment with IL-6

inhibits proliferation with induction of STAT3 phosphorylation and induces neuroendocrine differentiation [52]. After prolonged treatment with IL-6, LNCaP cells acquire an IL-6 autocrine loop, in which they are growth stimulated by IL-6 and exhibit castration-resistant growth [53]. These differential effects are also reflected on the expression of the AR with its expression being reduced with short treatments and chronic treatments leading to overexpression. In addition, IL-6 has been shown to enhance the resistance of prostate cancer cells to the anti-androgen bicalutamide by enhanced recruitment of the co-activator TIF-2/GRIP-1 [54] and to induce ligand-independent activation of the AR through another co-activator SRC-1 [55]. IL-6 also induces the expression of several steroidogenic enzymes including AKR1C3 and HSD3B2, leading to enhanced synthesis of intracellular androgens by prostate cancer cells and tissues [56]. In AR-negative prostate cancer cells such as PC-3 and DU145, IL-6 acts as an autocrine growth factor and an inhibitor of apoptosis [57]. IL-6 exhibits trans-signaling via the soluble IL-6 receptor and plays important roles in regulation of invasion and metastasis [58]. IL-6 is also synthesized by osteoblasts and promotes osteoblastogenesis [59]. Interactions between metastatic prostate cancer cells and osteoblasts increase the local concentrations of IL-6 in the bone microenvironment [60]. These results suggest that IL-6 may promote the incidence of bone metastases through the activation of AR in the bone microenvironment, thereby conferring a survival advantage on the metastatic cells.

Paracrine factors such as IL-6 have long been strong candidates for therapeutic intervention. Several pre-clinical studies targeting IL-6 activity with neutralizing antibodies [61, 62] have resulted in the development of the first humanized anti-IL-6 antibody, siltuximab, which is being evaluated in clinical trials. Although initial results as monotherapy are not promising [63], it shows potential as a sensitizing agent to chemotherapeutic drugs like docetaxel and may be considered for combination strategies. In a recently reported phase I study, siltuximab succeeded in reducing phosphorylation of STAT3 and MAPK, while downregulating genes immediately downstream of IL-6 in the IL-6 pathway such as GRB2, SHC, SOS-1, and JAK3. Interestingly, in this study, siltuximab also downregulated the expression levels of key enzymes such as HSD17B1 and HSD3B1 in the androgen biosynthetic pathway [64]. These findings suggest that IL-6 plays a major role in CRPC progression and targeting it may confer therapeutic benefit.

IL-4 is another pro-inflammatory cytokine that signals through its receptor and downstream effector STAT6. Levels of IL-4 are elevated in sera of CaP patients [65], and IL-4 activates the AR and induces expression of its target genes mediated by the Akt pathway [66]. Activation of AR by IL-4 occurs via recruitment of the co-activator CBP/p300 to the AR transcriptional complex [67]. Activation of AR by IL-4 requires the NF-κB pathway that culminates in the activation of STAT6 [68]. IL-4 has been shown to stimulate castration-resistant growth of the androgen-dependent LNCaP human CaP cells [69]. These studies suggest that similar to IL-6, IL-4 functions as an anti-apoptotic and pro-survival cytokine in the progression of CRPC.

IL-8 belongs to the pro-inflammatory chemokine family, which is regulated by the NF-κB pathway. Levels of IL-8 and its receptors are also elevated in CRPC [70] and can be used to distinguish between benign and malignant tumors [71]. IL-8 induces the expression and activation of the AR [72] in castrate conditions and leads to castration-resistant progression by signaling through Src and FAK tyrosine kinases [73]. IL-8 is also a strong inducer of pro-angiogenic and pro-metastatic molecules in CRPC [74]. IL-8 exerts its effects through modulation of the levels of cyclin D1 and by antagonizing the pro-apoptotic effects of TRAIL [75, 76]. Chemotherapeutic drugs induce signaling through IL-8 and other chemokines leading to activation of the NF-κB pathway and evasion of apoptosis and confer resistance to oxaliplatin in metastatic prostate carcinoma cells [77]. Downregulation of IL-8 by siRNA has shown promising results in CaP cells by enhancing apoptosis and sensitivity to docetaxel [78]. Based on these findings, IL-8 may be considered a potential therapeutic target in CRPC.

Transcription factors

Constitutive activation of STAT3 is a hallmark of CRPC and has been observed downstream of elevated levels of IL-6 signaling in CRPC tissues and cells [79]. Phosphorylation of STAT3 as a result of IL-6 signaling leads to the expression of several genes associated with progression and metastasis. Constitutive activation of STAT3 has been observed in CRPC cells and tissues [79]. Suppression of STAT3 expression and constitutive activation using either siRNA or dominant negative mutant approach induced apoptosis and abolished growth of CaP cells [80]. STAT3 interacts physically with amino acids 234–558 of the AR leading to its ligand-independent activation [81]. This interaction is dependent upon phosphorylation of STAT3 at Ser722. STAT3 also enhances transactivation of target genes by other steroid hormone receptors [82] and promotes castration-resistant growth of LNCaP cells in vitro and in vivo [83]. Stable expression of constitutively active STAT3 has also been shown to change the phenotype of benign prostate epithelial cells to one resembling malignant cells [84]. STAT3 also plays a key role in signaling downstream from B-cell-derived lymphotoxin, independent of IL-6 signaling, and promotes castration-resistant progression and metastasis of CaP [85].

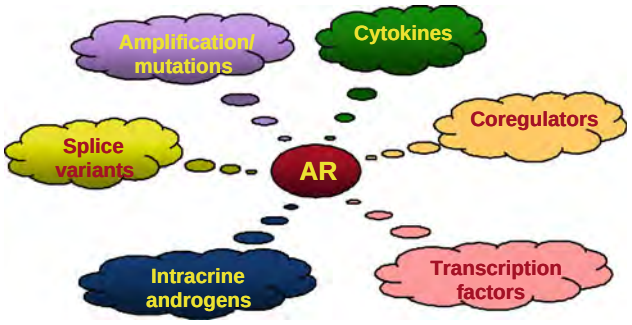

Fig. 1 Schematic diagram of AR function

NF-κB signaling is involved in the processes of survival, proliferation, evasion of apoptosis, and metastasis in CRPC. The canonical NF-κB pathway that involves the heterodimerization of p65 and p50 subunits of NF-κB is constitutively active in CRPC cells and tissues. A few of the earliest reports about the interaction of NF-κB and the AR have shown that the RelA [p65) subunit of NF-κB and the AR exhibit mutual transcriptional antagonism [86] and that activation of NF-κB negatively regulates transcription of the AR-responsive gene PSA through a negative regulatory element in the PSA promoter–enhancer [87]. But more recent reports have demonstrated that constitutive NF-κB activity maintains higher levels of nuclear AR that promotes transcription of pro-proliferative and pro-survival genes [88] and that CRPC progression is dependent on constitutive NF-κB activity [89]. Canonical NF-κB also regulates the expression of inflammatory cytokines such as IL-6 and thereby plays an important role in CRPC [90]. It has recently been reported that tumor-initiating prostate cancer stem-like cells exhibit increased NF-κB activity [91]. NF-κB is also activated by the TMPRSS2/ERG fusion genes found in CRPC [92]. Downregulation of the constitutive activation of NF-κB abolished castration-resistant prostate tumor growth [89].

The non-canonical pathway that involves the tightly regulated proteolytic processing of NF-κB2/p100 leading to the production of p52 has also been shown to be active in CRPC cells. Levels of nuclear p52 are enhanced in CRPC tissues [93, 94], and androgen stimulates production of p52 [95]. NF-κB2/p52 interacts with the NTD of AR and induces ligand-independent activation in prostate cancer cells, which is mediated by enhanced recruitment of the co-activator p300 to the AR transcriptional complex. Aberrant activation of AR by p52 induces expression of AR-responsive genes and castration-resistant growth of androgen-dependent LNCaP prostate cancer cells [96]. In addition, NF-κB2/p52 also modulates expression levels of several metastasis- and invasion-related genes when overexpressed in LNCaP cells [97]. Downregulation of NF-κB2/p100 using shRNA resulted in reduced production of p52 and decreased AR transactivation ability and castration-resistant growth in C4-2 CaP cells [96]. Cross-talk between the STAT3 and alternative NF-kB pathways has also been observed. STAT3 is activated by LIGHT, a stimulator of the alternative pathway [98], and in turn induces the processing of NF-κB2/p100 to p52 [99]. These findings support the feasibility of targeting both the canonical and alternative pathways of NF-κB as a means of controlling CRPC progression.

Summary and future perspectives

The seminal advances made in the past few years have demonstrated the importance of activation of the AR in CRPC. These mechanisms, summarized in Fig. 1, are likely to act in concert with each other to culminate in the progression of CaP. New AR-targeted therapies for CRPC including hormonal, targeted, immune, and cytotoxic therapies are emerging. Chemotherapeutic agents such as estramustine, mitoxantrone, docetaxel, and cabazitaxel; hormonal agents such as CYP17 inhibitors (ketoconazole, abiraterone, TAK-700, and TOK-001) and AR antagonists (MDV-3100, ARN-509); small molecule inhibitors of protein–protein interactions (EPI-001); and decoy oligonucleotides are all being tested as novel therapeutic agents. The challenge remains the identification of right amalgam of therapeutic targets, and a patient-customized approach is warranted. This would involve interfering with specific pathways active in a particular patient's tumor combined with inhibition of the AR transcriptional activity. The new generation of anti-androgens, inhibitors of steroid synthesis, and other small molecule inhibitors raise the hope that longer and more effective remission of CRPC can be achieved in the not too distant future.

Acknowledgments This work was supported in part by NIH CA140468, CA118887, CA109441, DOD PC080538 (Gao, AC), and DOD PC100502 (Nadiminty N).

Conflict of interest None.

References

1. Jemal A, Siegel R, Xu J, Ward E (2010) Cancer statistics. CA Cancer J Clin 60:277–300
2. Cheng H, Snoek R, Ghaidi F, Cox ME, Rennie PS (2006) Short hairpin RNA knockdown of the androgen receptor attenuates ligand-independent activation and delays tumor progression. Cancer Res 66:10613–10620
3. Visakorpi T, Hyytinen E, Koivisto P et al (1995) In vivo amplification of the androgen receptor gene and progression of human prostate cancer. Nat Genet 9:401–406
4. Chen CD, Welsbie DS, Tran C et al (2004) Molecular determinants of resistance to antiandrogen therapy. Nat Med 10:33–39
5. Palmberg C, Koivisto P, Kakkola L, Tammela TLJ, Kallioniemi OP, Visakorpi T (2000) Androgen receptor gene amplification at primary progression predicts response to combined androgen

blockade as second line therapy for advanced prostate cancer. J Urol 164:1992–1995
6. Scher HI, Sawyers CL (2005) Biology of progressive, castration-resistant prostate cancer: directed therapies targeting the androgen-receptor signaling axis. J Clin Oncol 23:8253–8261
7. Koochekpour S (2010) Androgen receptor signaling and mutations in prostate cancer. Asian J Androl 12:639–657
8. Brooke GN, Bevan CL (2009) The role of androgen receptor mutations in prostate cancer progression. Curr Genomics 10:18–25
9. Buchanan G, Yang M, Cheong A et al (2004) Structural and functional consequences of glutamine tract variation in the androgen receptor. Hum Mol Genet 13:1677–1692
10. Buchanan G, Yang M, Harris JM et al (2001) Mutations at the boundary of the hinge and ligand binding domain of the androgen receptor confer increased transactivation function. Mol Endocrinol 15:46–56
11. Taylor BS, Schultz N, Hieronymus H et al (2010) Integrative genomic profiling of human prostate cancer. Cancer Cell 18:11–22
12. Jiang Y, Palma JF, Agus DB, Wang Y, Gross ME (2010) Detection of androgen receptor mutations in circulating tumor cells in castration-resistant prostate cancer. Clin Chem 56:1492–1495
13. Steinkamp MP, O'Mahony OA, Brogley M et al (2009) Treatment-dependent androgen receptor mutations in prostate cancer exploit multiple mechanisms to evade Therapy. Cancer Res 69:4434–4442
14. Tomlins SA, Bjartell A, Chinnaiyan AM et al (2009) ETS gene fusions in prostate cancer: from discovery to daily clinical practice. Eur Urol 56:275–286
15. Tomlins SA, Mehra R, Rhodes DR et al (2006) TMPRSS2:ETV4 gene fusions define a third molecular subtype of prostate cancer. Cancer Res 66:3396–3400
16. Morris DS, Tomlins SA, Montie JE, Chinnaiyan AM (2008) The discovery and application of gene fusions in prostate cancer. BJU Int 102:276–282
17. Demichelis F, Fall K, Perner S et al (2007) TMPRSS2:ERG gene fusion associated with lethal prostate cancer in a watchful waiting cohort. Oncogene 26:4596–4599
18. Attard G, Swennenhuis JF, Olmos D et al (2009) Characterization of ERG, AR and PTEN gene status in circulating tumor cells from patients with castration-resistant prostate cancer. Cancer Res 69:2912–2918
19. Klezovitch O, Risk M, Coleman I et al (2008) A causal role for ERG in neoplastic transformation of prostate epithelium. Proc Natl Acad Sci USA 105:2105–2110
20. Bastus NC, Boyd LK, Mao X et al (2010) Androgen-induced TMPRSS2:ERG fusion in nonmalignant prostate epithelial cells. Cancer Res 70:9544–9548
21. Fine SW, Gopalan A, Leversha MA et al (2010) TMPRSS2-ERG gene fusion is associated with low Gleason scores and not with high-grade morphological features. Mod Pathol 23:1325–1333
22. Yu J, Yu J, Mani R-S et al (2010) An integrated network of androgen receptor, polycomb, and TMPRSS2-ERG gene fusions in prostate cancer progression. Cancer Cell 17:443–454
23. Carver BS, Tran J, Gopalan A et al (2009) Aberrant ERG expression cooperates with loss of PTEN to promote cancer progression in the prostate. Nat Genet 41:619–624
24. Yoshimoto M, Joshua AM, Cunha IW et al (2008) Absence of TMPRSS2:ERG fusions and PTEN losses in prostate cancer is associated with a favorable outcome. Mod Pathol 21:1451–1460
25. Salami SS, Schmidt F, Laxman B et al Combining urinary detection of TMPRSS2:ERG and CaP3 with serum PSA to predict diagnosis of prostate cancer. Urologic oncology: seminars and original investigations. (in press, corrected proof)
26. Brenner JC, Ateeq B, Li Y et al (2011) Mechanistic rationale for inhibition of poly (ADP-Ribose) polymerase in ETS gene fusion-positive prostate cancer. Cancer Cell 19:664–678
27. Wang Q, Carroll JS, Brown M (2005) Spatial and temporal recruitment of androgen receptor and its coactivators involves chromosomal looping and polymerase tracking. Mol Cell 19:631–642
28. Bulger M, Groudine M (1999) Looping versus linking: toward a model for long-distance gene activation. Genes Dev 13:2465–2477
29. Blackwood EM, Kadonaga JT (1998) Going the distance: the current view of enhancer action. Science 281:60–63
30. Wang Q, Li W, Liu XS et al (2007) A hierarchical network of transcription factors governs androgen receptor-dependent prostate cancer growth. Mol Cell 27:380–392
31. Wang Q, Li W, Zhang Y et al (2009) Androgen receptor regulates a distinct transcription program in androgen-independent prostate cancer. Cell 138:245–256
32. Hu R, Isaacs WB, Luo J (2011) A snapshot of the expression signature of androgen receptor splicing variants and their distinctive transcriptional activities. Prostate: n/a-n/a
33. Tepper CG, Boucher DL, Ryan PE et al (2002) Characterization of a novel androgen receptor mutation in a relapsed CWR22 prostate cancer xenograft and cell line. Cancer Res 62:6606–6614
34. Dehm SM, Schmidt LJ, Heemers HV, Vessella RL, Tindall DJ (2008) Splicing of a novel androgen receptor exon generates a constitutively active androgen receptor that mediates prostate cancer therapy resistance. Cancer Res 68:5469–5477
35. Guo Z, Yang X, Sun F et al (2009) A novel androgen receptor splice variant is up-regulated during prostate cancer progression and promotes androgen depletion-resistant growth. Cancer Res 69:2305–2313
36. Hu R, Dunn TA, Wei S et al (2009) Ligand-independent androgen receptor variants derived from splicing of cryptic exons signify hormone-refractory prostate cancer. Cancer Res 69:16–22
37. Watson PA, Chen YF, Balbas MD et al Constitutively active androgen receptor splice variants expressed in castration-resistant prostate cancer require full-length androgen receptor. In: Proceedings of the national academy of sciences 107:16759–16765
38. Hornberg E, Ylitalo EB, Crnalic S et al (2011) Expression of androgen receptor splice variants in prostate cancer bone metastases is associated with castration-resistance and short survival. PLoS One 6:e19059
39. Nishiyama T, Hashimoto Y, Takahashi K (2004) The influence of androgen deprivation therapy on dihydrotestosterone levels in the prostatic tissue of patients with prostate cancer. Clin Cancer Res 10:7121–7126
40. Titus MA, Schell MJ, Lih FB, Tomer KB, Mohler JL (2005) Testosterone and dihydrotestosterone tissue levels in recurrent prostate cancer. Clin Cancer Res 11:4653–4657
41. Nakamura Y, Suzuki T, Nakabayashi M et al (2005) In situ androgen producing enzymes in human prostate cancer. Endocr Relat Cancer 12:101–107
42. Page ST, Lin DW, Mostaghel EA et al (2006) Persistent intraprostatic androgen concentrations after medical castration in healthy men. Clin Endocrinol Metab 91:3850–3856
43. Dillard PR, Lin M-F, Khan SA (2008) Androgen-independent prostate cancer cells acquire the complete steroidogenic potential of synthesizing testosterone from cholesterol. Mol Cell Endocrinol 295:115–120
44. Mostaghel EA, Page ST, Lin DW et al (2007) Intraprostatic androgens and androgen-regulated gene expression persist after testosterone suppression: therapeutic implications for castration-resistant prostate cancer. Cancer Res 67:5033–5041
45. Leon CG, Locke JA, Adomat HH et al (2010) Alterations in cholesterol regulation contribute to the production of intratumoral androgens during progression to castration-resistant prostate cancer in a mouse xenograft model. Prostate 70:390–400
46. Pfeiffer MJ, Smit FP, Sedelaar JP, Schalken JA (2011) Steroidogenic enzymes and stem cell markers are upregulated during

androgen deprivation in prostate cancer. Mol Med. doi:10.2119/molmed.2010.00143
47. Mostaghel EA, Nelson PS (2008) Intracrine androgen metabolism in prostate cancer progression: mechanisms of castration resistance and therapeutic implications. Best Pract Res Clin Endocrinol Metab 22:243–258
48. Hofland J, van Weerden WM, Dits NFJ et al (1999) Evidence of limited contributions for intratumoral steroidogenesis in prostate cancer. Cancer Res 70:1256–1264
49. Mostaghel EA, Montgomery B, Nelson PS (2009) Castration-resistant prostate cancer: targeting androgen metabolic pathways in recurrent disease. Urol Oncol Semin Orig Investig 27:251–257
50. George DJ, Halabi S, Shepard TF et al (2005) The prognostic significance of plasma interleukin-6 levels in patients with metastatic hormone-refractory prostate cancer: results from cancer and leukemia group B 9480. Clin Cancer Res 11:1815–1820
51. Shariat SF, Andrews B, Kattan MW, Kim J, Wheeler TM, Slawin KM (2001) Plasma levels of interleukin-6 and its soluble receptor are associated with prostate cancer progression and metastasis. Urology 58:1008–1015
52. Corcoran NM, Costello AJ (2003) Interleukin-6: minor player or starring role in the development of hormone-refractory prostate cancer? BJU Int 91:545–553
53. Lee SO, Chun JY, Nadiminty N, Lou W, Gao AC (2007) Interleukin-6 undergoes transition from growth inhibitor associated with neuroendocrine differentiation to stimulator accompanied by androgen receptor activation during LNCaP prostate cancer cell progression. Prostate 67:764–773
54. Feng S, Tang Q, Sun M, Chun JY, Evans CP, Gao AC (2009) Interleukin-6 increases prostate cancer cells resistance to bicalutamide via TIF2. Mol Cancer Ther 8:665–671
55. Ueda T, Mawji NR, Bruchovsky N, Sadar MD (2002) Ligand-independent activation of the androgen receptor by interleukin-6 and the role of steroid receptor coactivator-1 in prostate cancer cells. J Chem Biol 277:38087–38094
56. Chun JY, Nadiminty N, Dutt S et al (2009) Interleukin-6 regulates androgen synthesis in prostate cancer cells. Clin Cancer Res 15:4815–4822
57. Culig Z Cytokine disbalance in common human cancers. Biochimica et Biophysica Acta (BBA). Mole Cell Res 1813:308–314
58. Santer FdrR, Malinowska K, Culig Z, Cavarretta IT (2010) Interleukin-6 trans-signalling differentially regulates proliferation, migration, adhesion and maspin expression in human prostate cancer cells. Endocr Relat Cancer 17:241–253
59. Taguchi Y, Yamamoto M, Yamate T et al (1998) Interleukin-6-type cytokines stimulate mesenchymal progenitor differentiation toward the osteoblastic lineage. Proc Assoc Am Physicians 110:559–574
60. García-Moreno C, Méndez-Dávila C, de la Piedra C, Castro-Errecaborde NA, Traba ML (2002) Human prostatic carcinoma cells produce an increase in the synthesis of interleukin-6 by human osteoblasts. Prostate 50:241–246
61. Smith PC, Keller ET (2001) Anti-interleukin-6 monoclonal antibody induces regression of human prostate cancer xenografts in nude mice. Prostate 48:47–53
62. Wallner L, Dai J, Escara-Wilke J et al (2006) Inhibition of interleukin-6 with CNTO328, an anti-interleukin-6 monoclonal antibody, inhibits conversion of androgen-dependent prostate cancer to an androgen-independent phenotype in orchiectomized mice. Cancer Res 66:3087–3095
63. Dorff TB, Goldman B, Pinski JK et al (2010) Clinical and correlative results of SWOG S0354: a phase II trial of CNTO328 (Siltuximab), a monoclonal antibody against interleukin-6, in chemotherapy-pretreated patients with castration-resistant prostate cancer. Clin Cancer Res 16:3028–3034
64. Karkera J, Steiner H, Li W et al (2011) The anti-interleukin-6 antibody siltuximab down-regulates genes implicated in tumorigenesis in prostate cancer patients from a phase I study. Prostate (Epub ahead of print)
65. Takeshi U, Sadar MD, Suzuki H et al (2005) Interleukin-4 in patients with prostate cancer. Anticancer Res 25:4595–4598
66. Lee SO, Lou W, Hou M, Onate SA, Gao AC (2003) Interleukin-4 enhances prostate-specific antigen expression by activation of the androgen receptor and Akt pathway. Oncogene 22:7981–7988
67. Lee SO, Chun JY, Nadiminty N, Lou W, Feng S, Gao AC (2009) Interleukin-4 activates androgen receptor through CBP/p300. Prostate 69:126–132
68. Lee SO, Lou W, Nadiminty N, Lin X, Gao AC (2005) Requirement for NF-κB in interleukin-4-induced androgen receptor activation in prostate cancer cells. Prostate 64:160–167
69. Lee SO, Pinder E, Chun JY, Lou W, Sun M, Gao AC (2008) Interleukin-4 stimulates androgen-independent growth in LNCaP human prostate cancer cells. Prostate 68:85–91
70. Huang J, Yao JL, Zhang L et al (2005) Differential expression of interleukin-8 and Its receptors in the neuroendocrine and non-neuroendocrine compartments of prostate can./cer. Am J Pathol 166:1807–1815
71. Veltri RW, Miller MC, Zhao G et al (1999) Interleukin-8 serum levels in patients with benign prostatic hyperplasia and prostate cancer. Urology 53:139–147
72. Seaton A, Scullin P, Maxwell PJ et al (2008) Interleukin-8 signaling promotes androgen-independent proliferation of prostate cancer cells via induction of androgen receptor expression and activation. Carcinogenesis 29:1148–1156
73. Lee L-F, Louie MC, Desai SJ et al (2004) Interleukin-8 confers androgen-independent growth and migration of LNCaP: differential effects of tyrosine kinases Src and FAK. Oncogene 23:2197–2205
74. Waugh DJJ, Wilson C (2008) The interleukin-8 pathway in cancer. Clin Cancer Res 14:6735–6741
75. MacManus CF, Pettigrew J, Seaton A et al (2007) Interleukin-8 signaling promotes translational regulation of cyclin D in androgen-independent prostate cancer cells. Mol Cancer Res 5:737–748
76. Wilson C, Wilson T, Johnston PG, Longley DB, Waugh DJJ (2008) Interleukin-8 signaling attenuates TRAIL- and chemotherapy-induced apoptosis through transcriptional regulation of c-FLIP in prostate cancer cells. Mol Cancer Ther 7:2649–2661
77. Wilson C, Purcell C, Seaton A et al (2008) Chemotherapy-induced CXC-Chemokine/CXC-Chemokine receptor signaling in Metastatic prostate cancer cells confers resistance to oxaliplatin through potentiation of nuclear factor-Î B transcription and evasion of apoptosis. J Pharmacol Exp Ther 327:746–759
78. Singh R, Lokeshwar B (2009) Depletion of intrinsic expression of Interleukin-8 in prostate cancer cells causes cell cycle arrest, spontaneous apoptosis and increases the efficacy of chemotherapeutic drugs. Mol Cancer 8:57
79. Dhir R, Ni Z, Lou W, DeMiguel F, Grandis JR, Gao AC (2002) Stat3 activation in prostatic carcinomas. Prostate 51:241–246
80. Ok Lee S, Lou W, Qureshi KM, Mehraein-Ghomi F, Trump DL, Gao AC (2004) RNA interference targeting Stat3 inhibits growth and induces apoptosis of human prostate cancer cells. Prostate 60:303–309
81. Matsuda T, Junicho A, Yamamoto T et al (2001) Cross-talk between signal transducer and activator of transcription 3 and androgen receptor signaling in prostate carcinoma cells. Biochem Biophys Res Commun 283:179–187
82. De Miguel F, Lee S, Onate S, Gao A (2003) Stat3 enhances transactivation of steroid hormone receptors. Nucl Recept 1:3
83. De Miguel F, Lee SO, Lou W et al (2002) Stat3 enhances the growth of LNCaP human prostate cancer cells in intact and castrated male nude mice. Prostate 52:123–129

84. Huang H, Murphy T, Shu P, Barton A, Barton B (2005) Stable expression of constitutively-activated STAT3 in benign prostatic epithelial cells changes their phenotype to that resembling malignant cells. Mol Cancer 4:2
85. Ammirante M, Luo J-L, Grivennikov S, Nedospasov S, Karin M (2010) B-cell-derived lymphotoxin promotes castration-resistant prostate cancer. Nature 464:302–305
86. Palvimo JJ, Reinikainen P, Ikonen T, Kallio PJ, Moilanen A, Jänne OA (1996) Mutual transcriptional interference between RelA and androgen receptor. J Biol Chem 271:24151–24156
87. Cinar B, Yeung F, Konaka H et al (2004) Identification of a negative regulatory cis-element in the enhancer core region of the prostate-specific antigen promoter: implications for intersection of androgen receptor and nuclear factor-kappaB signalling in prostate cancer cells. Biochem J 379:421–431
88. Zhang L, Altuwaijri S, Deng F et al (2009) NF-[kappa]B regulates androgen receptor expression and prostate cancer growth. Am J Pathol 175:489–499
89. Jin RJ, Lho Y, Connelly L et al (2008) The nuclear factor-kappaB pathway controls the progression of prostate cancer to androgen-independent growth. Cancer Res 68:6762–6769
90. Ishiguro H, Akimoto K, Nagashima Y et al (2009) aPKCε promotes growth of prostate cancer cells in an autocrine manner through transcriptional activation of interleukin-6. Proc Natl Acad Sci 106:16369–16374
91. Rajasekhar VK, Studer L, Gerald W, Socci ND, Scher HI (2011) Tumour-initiating stem-like cells in human prostate cancer exhibit increased NF-[kappa]B signalling. Nat Commun 2:162
92. Wang J, Cai Y, Shao L-j et al (2010) Activation of NF-Î B by TMPRSS2/ERG fusion isoforms through toll-like receptor-4. Cancer Res 71:1325–1333
93. Lessard L, Begin LR, Gleave ME, Mes-Masson AM, Saad F (2005) Nuclear localisation of nuclear factor-kappaB transcription factors in prostate cancer: an immunohistochemical study. Br J Cancer 93:1019–1023
94. Nadiminty N, Chun JY, Lou W, Lin X, Gao AC (2008) NF-κB2/p52 enhances androgen-independent growth of human LNCaP cells via protection from apoptotic cell death and cell cycle arrest induced by androgen-deprivation. Prostate 68:1725–1733
95. Lessard L, Saad F, Le Page C et al (2007) NF-[kappa]B2 processing and p52 nuclear accumulation after androgenic stimulation of LNCaP prostate cancer cells. Cell Signal 19:1093–1100
96. Nadiminty N, Lou W, Sun M et al (2010) Aberrant activation of the androgen receptor by NF-kappaB2/p52 in prostate cancer cells. Cancer Res 70:3309–3319
97. Nadiminty N, Dutt S, Tepper C, Gao AC (2010) Microarray analysis reveals potential target genes of NF-κB2/p52 in LNCaP prostate cancer cells. prostate 70:276–287
98. Nadiminty N, Chun JY, Hu Y, Dutt S, Lin X, Gao AC (2007) LIGHT, a member of the TNF superfamily, activates Stat3 mediated by NIK pathway. Biochem Biophys Res Commun 359:379–384
99. Nadiminty N, Lou W, Lee SO, Lin X, Trump DL, Gao AC (2006) Stat3 activation of NF-Î B p100 processing involves CBP/p300-mediated acetylation. Proc Natl Acad Sci 103:7264–7269

RhoGDIα Suppresses Growth and Survival of Prostate Cancer Cells

Yezi Zhu,[1,2] Ramakumar Tummala,[1] Chengfei Liu,[1,3] Nagalakshmi Nadiminty,[1] Wei Lou,[1] Christopher P. Evans,[1] Qinghua Zhou,[3] and Allen C. Gao[1,2]*

[1]*Department of Urology, University of California at Davis, Sacramento, California*
[2]*Graduate Program of Pharmacology and Toxicology and Cancer Center, University of California at Davis, Sacramento, California*
[3]*Tianjin Lung Cancer Institute, Tianjin Medical University General Hospital, Tianjin, China*

BACKGROUND. Treatment for primary prostate cancer (CaP) is the withdrawal of androgens. However, CaP eventually progresses to grow in a castration-resistant state. The mechanisms involved in the development and progression of castration-resistant prostate cancer (CRPC) remain unknown. We have previously generated LNCaP-IL6+ cells by treating LNCaP cells chronically with interleukin-6 (IL-6), which have acquired the ability to grow in androgen-deprived conditions.

METHODS. We compared the protein expression profile of LNCaP and LNCaP-IL6+ cells using two-dimensional gel electrophoresis. The gels were then silver stained in order to visualize proteins and the differentially expressed spots were identified and characterized by micro sequencing using MALDI-PMF mass spectrometry.

RESULTS. In this study, we have identified RhoGDIα (GDIα) as a suppressor of CaP growth. Expression of GDIα was reduced in LNCaP-IL6+ cells and was down-regulated in more aggressive CaP cells compared to LNCaP cells. Over expression of GDIα inhibited the growth of CaP cells and caused LNCaP-IL6+ cells reversal to androgen-sensitive state, while down-regulation of GDIα enhanced growth of androgen-sensitive LNCaP CaP cells in androgen-deprived conditions. In addition, GDIα suppressed the tumorigenic ability of prostate tumor xenografts in vivo.

CONCLUSIONS. These results demonstrate that loss of GDIα expression promotes the development and progression of prostate cancer. *Prostate 72: 392 398, 2012.*

KEY WORDS: **prostate cancer; RhoGDIα; IL-6**

INTRODUCTION

Prostate cancer (CaP) is the most common type of cancer in American men and ranks second to lung cancer in cancer-related deaths. One of the important challenges facing CaP is its evolution to castration resistance, for which no effective treatment has been developed. Understanding the molecular mechanisms leading to castration resistance is the key to developing successful therapies to combat this lethal response. IL-6 has been implicated in the modulation of growth and differentiation in many cancers and is associated with poor prognosis in renal cell carcinoma, ovarian cancer, lymphoma, and melanoma [1]. Elevated expression of IL-6 and its receptor have been consistently demonstrated in human CaP cell lines and clinical specimens of CaP and benign prostate hyperplasia [2–4]. Multiple studies have demonstrated that IL-6 is elevated in the sera of patients with

Grant sponsor: VA Merit award; Grant number: I01 BX000526; Grant sponsor: NIH; Grant numbers: CA 109441. CA 140468.

Yezi Zhu and Ramakumar Tummala contributed equally to this work.

*Correspondence to: Allen C. Gao, Department of Urology and Cancer Center, University of California Davis Medical Center, 4645 2nd Ave, Research III, Suite 1300, Sacramento, CA 95817, USA.
E mail: acgao@ucdavis.edu
Received 31 March 2011; Accepted 23 May 2011
DOI 10.1002/pros.21441
Published online 16 June 2011 in Wiley Online Library (wileyonlinelibrary.com).

metastatic CaP and the levels of IL-6 correlate with tumor burden, serum PSA, and clinically evident metastases [5,6]. In addition, serum IL-6 levels are elevated in men with castration-resistant prostate cancer (CRPC) compared to normal controls, benign prostatic hyperplasia, prostatitis, and localized CaP [5]. Collectively, these data suggest that elevated IL-6 levels are associated with the lethal phenotype of CaP.

IL-6 functions as a paracrine growth factor for the human LNCaP androgen-sensitive CaP cells and as an autocrine growth factor for the human DU145 and PC3 androgen-insensitive CaP cells [7]. It has also been reported that IL-6 mediates LNCaP cell growth arrest and induces neuroendocrine differentiation [8–10]. Targeting IL-6 signaling using an anti-IL-6 monoclonal antibody induces regression of human CaP xenografts in nude mice [11], while inhibition of IL-6 with CNT0328, an anti-IL-6 monoclonal antibody inhibits the conversion of an androgen-dependent to independent phenotype in a CaP xenograft in vivo model [12]. These studies suggest that IL-6 promotes CRPC progression.

RhoGDI (GDI) is a cellular regulatory protein that acts primarily by controlling the cellular distribution and activity of Rho GTPases [13]. GDI family comprises three mammalian members: GDIα, which is ubiquitously expressed; GDIβ which has hematopoietic tissue-specific expression, and GDIγ which is membrane-anchored through an amphipathic helix and is preferentially expressed in brain, pancreas, lung, kidney, and testis [14]. GDIα binds to and negatively regulates most Rho GTPases including RhoA, Rac1, and Cdc42 [14]. It has been shown that overexpression of GDI in various cell lines induces disruption of the actin cytoskeleton and loss of substratum adherence and microinjection of GDIα into fibroblasts inhibits cell motility [15,16]. GDIα mRNA level was found to be lower in the metastatic lineage (T24T) of a human bladder cancer cell line (T24) suggesting that Rho activation plays a role in the control of progression to metastasis [17]. Although GDIα is aberrantly expressed in several tumor tissues, its role in cancer progression remains to be unraveled. In this study, we show that GDIα suppresses CaP cell growth, and down-regulation of GDIα promotes the progression of androgen-sensitive cells to a castration-resistant state.

MATERIALS AND METHODS

Cell Culture and Transfections

LNCaP, LAPC-4, PC3, C4-2, and DU145 CaP cells were cultured in RPMI-1640 medium containing either 10% complete fetal bovine serum (FBS) or 10% charcoal-dextran-stripped FBS and penicillin/streptomycin as described previously (29). LNCaP passage numbers <30 were used throughout the study. IL-6-overexpressing LNCaP-IL6+ cells were cultured in RPMI 1640 containing 10% FBS as described previously [18]. For transfection studies, cells were transiently transfected with expressing plasmids using Lipofectamine 2000 (Invitrogen).

Preparation of Whole Cell Extracts

Cells were lysed in a high-salt buffer containing 10 mM Hepes (pH 7.9), 0.25 M NaCl, 1% Nonidet P-40, and 1 mM EDTA with protease inhibitors, and total protein in the lysates was determined with the Coomassie Plus Protein Assay Reagent (Pierce, Rockford, IL).

Cytosolic and Nuclear Protein Preparation

Cells were harvested, washed with PBS twice, and resuspended in a hypotonic buffer [10 mmol/L HEPES-KOH (pH 7.9), 1.5 mmol/L MgCl2, 10 mmol/L KCl, and 0.1% NP40] and incubated on ice for 10 min. Nuclei were precipitated by 3,000 × *g* centrifugation at 4°C for 10 min. The supernatant was collected as the cytosolic fraction. After washing once with the hypotonic buffer, the nuclei were lysed in a lysis buffer [50 mmol/L Tris–HCl (pH 8), 150 mmol/L NaCl, 1% TritonX-100] by mechanical disruption for 30 min at 4°C. The nuclear lysate was precleared by centrifugation at 4°C for 15 min. Protein concentration was determined using the Coomassie Plus protein assay kit (Pierce).

Proteomic Analysis UsingTwo-Dimensional Electrophoresis

Prior to two-dimensional electrophoresis, the protein samples were purified using a 2D Clean-Up kit (GE health care) according to the manufacturer's instructions. Differentially expressed proteins were identified using two-dimensional gel electrophoresis and mass spectrometry. Two-dimensional gel electrophoresis was performed using immobiline strips (pI range, 3–10; GE Healthcare, Piscataway, NJ) with proteins being separated according to charge and subsequently molecular weight. The gels were then silver stained in order to visualize proteins and the differentially expressed spots were identified by MALDI-PMF mass spectrometry.

Western Blot Analysis

Equal amounts of protein were loaded on 10% SDS–PAGE and transferred to nitrocellulose membranes. The membranes were blocked with 5% nonfat

milk in 1× PBS + 0.1% Tween 20 and probed with the indicated primary antibodies. The chemiluminescent signal was detected by enhanced chemiluminescence kit (Amersham) after incubation with the appropriate horseradish peroxidase-conjugated secondary antibodies.

Measurement of PSA

PSA levels were measured in the culture supernatants using ELISA (United Biotech, Inc.) according to the manufacturer's instructions and as described previously [19].

In Vitro Cell Proliferation

Cells (10^4 cells/well) were plated in 12-well plates in RPMI containing 10% FBS. After 2 or 3 days in regular culture medium with 10% FBS, cells were switched into phenol red-free RPMI containing either 10% FBS or 10% charcoal-stripped FBS (Hyclone, UT). Two days later, cell numbers were counted using Coulter counter.

Apoptosis Assays and Cell Death Detection ELISA

Cells were cultured under androgen-depleted conditions (10% charcoal-stripped serum) for 3–7 days after transfection with the indicated plasmids. The degree of apoptosis was measured by cell death detection ELISA according to the manufacturer's instructions. Briefly, floating and attached cells were collected and homogenized in 400 μl of incubation buffer. Five microliters of the supernatant diluted in 95 μl of incubation buffer was used in the ELISA. The wells were coated with anti-histone antibodies and then incubated with the lysates, horseradish peroxidase-conjugated anti-DNA antibodies, and the substrate subsequently, and absorbance was read at 620 nm.

In Vivo Tumor Growth

Four- to six-week-old athymic male nude mice (Harlan, Indianapolis, IN) were injected s.c. in both the flanks with 2×10^6 cells (LNCaP-IL6+/neo and LNCaP-IL6+/GDI) resuspended 1:1 in Matrigel (BD Biosciences, Bedford, MA) and complete culture medium. The volume of the growing tumors was estimated by measuring their three dimensions (Length × Width × Depth) with calipers (23).

Statistical Analysis

All data are presented as mean ± standard deviation (SD). Statistical analyses were performed with Microsoft Excel analysis tools, differences between individual groups were analyzed by paired *t*-test. $P < 0.05$ was considered statistically significant.

RESULTS

GDIα was Identified by Down-Regulated Expression in LNCaP-IL-6+ Cells Compared to LNCaP Cells

We previously generated a subline of LNCaP cells, LNCaP-IL6+, by chronically treating LNCaP cells with 5 ng/ml IL-6 [18]. LNCaP-IL6+ cells were found to have acquired the ability to secrete IL-6 and to grow in castration-resistant conditions in vitro and in vivo [18]. To identify factors that potentially mediate CaP cell growth induced by IL-6, the protein expression profile in LNCaP and LNCaP-IL-6+ cells was analyzed by 2-D gel electrophoresis (Fig. 1A). The differentially expressed spots were isolated from the 2-D gels and micro sequenced by MALDI-PMF. One of the spots that were present in parental LNCaP cells was lost in LNCaP-IL-6+ cells. The spot was identified as GDIα by MALDI-PMF micro sequencing mass spectrometry.

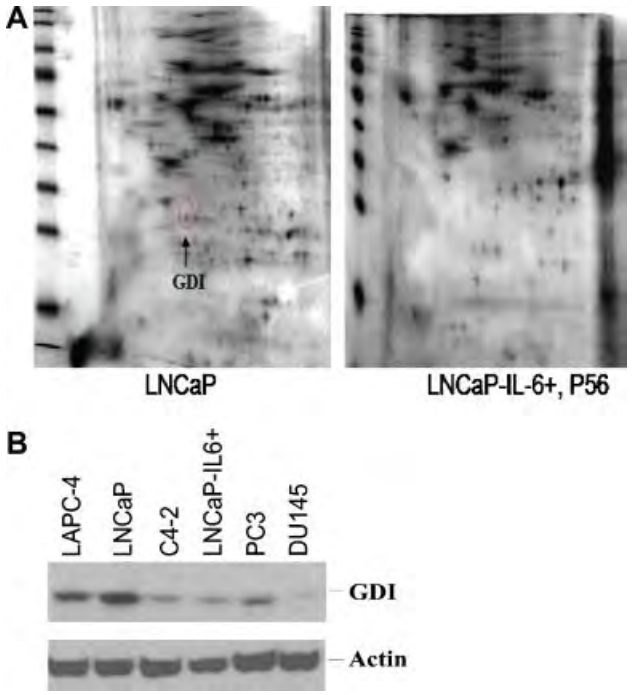

Fig. 1. Identification and characterization of GDIα. **A**: Identification of GDIα protein that is down regulated in LNCaP IL6+ cells compared to LNCaP cells. 2 D gel analysis of LNCaP and LNCaP IL 6+ cells. Arrow indicates GDIα. **B**: GDIα expression is decreased in androgen insensitive cells versus androgen sensitive cells. GDIα expression was analyzed by Western blot using whole cell lysates of androgen sensitive LNCaP, LAPC 4 cells and androgen insenistive C4 2, LNCap IL6+, PC3, and DUI45 cells using antibodies specifically against GDIα. Actin was used as loading control.

GDIα Expression is Decreased in Androgen-Insensitive Cells Versus Androgen-Sensitive Cells

To test whether down-regulation of GDIα expression is associated with the progression of CRPC, we analyzed the expression levels of GDIα in androgen-sensitive LNCaP, LAPC-4 cells, and androgen-insensitive C4-2, LNCaP-IL-6+, PC-3, and DU145 cells by Western blot analysis using antibodies against GDIα. The levels of GDIα protein were decreased in the androgen-insensitive cells compared to those in androgen-sensitive cells. These results suggest that androgen-insensitive growth is associated with decreased levels of GDIα protein (Fig. 1B).

GDIα Inhibits Cell Growth and Induces Apoptotic Cell Death

To examine the effects of GDIα on cell growth in vitro, LNCaP-IL-6+ and DU145 cells that express low levels of GDIα protein were transfected with different concentrations of expression plasmids encoding GDIα and cell numbers were determined. Overexpresion of GDIα inhibited the growth of LNCaP-IL-6+ and DU145 cells in vitro (Fig. 2A). Apoptosis was measured by analyzing the degree of DNA fragmentation with the Cell Death Detection ELISA kit (Roche). Over expression of GDIα-induced significant levels of apoptotic cell death compared to the vector control ($P < 0.01$, Fig. 2B). These data suggest that overexpression of GDIα inhibits the growth of CaP cells via induction of apoptotic cell death.

RhoGDIα Inhibits LNCaP-IL-6+ Cell Growth in Androgen-Deprived Conditions

To determine the potential significance of over expression of GDIα in CaP cells, LNCaP-IL-6+ were transfected with plasmids expressing control or GDIα. After transfection, cells were switched to media containing either FBS or charcoal-stripped FBS (CS-FBS) and allowed to grow for 3 more days and cell numbers were determined. The growth of LNCaP-IL-6+ cells transfected with vector control grown in CS-FBS was reduced ~5–10% compared to those grown in FBS. The growth of LNCaP-IL-6+ cells transfected with GDIα grown in similar conditions showed reduction by 40–50% (Fig. 3). These results suggest that over expression of GDIα can reduce the growth of LNCaP-IL-6+ cells in androgen-deprived conditions in vitro.

Down-Regulation of GDIα Promotes Growth of LNCaP Cells in Androgen-Deprived Conditions

LNCaP cells express higher levels of GDIα protein and do not grow well in CS-FBS condition. To test

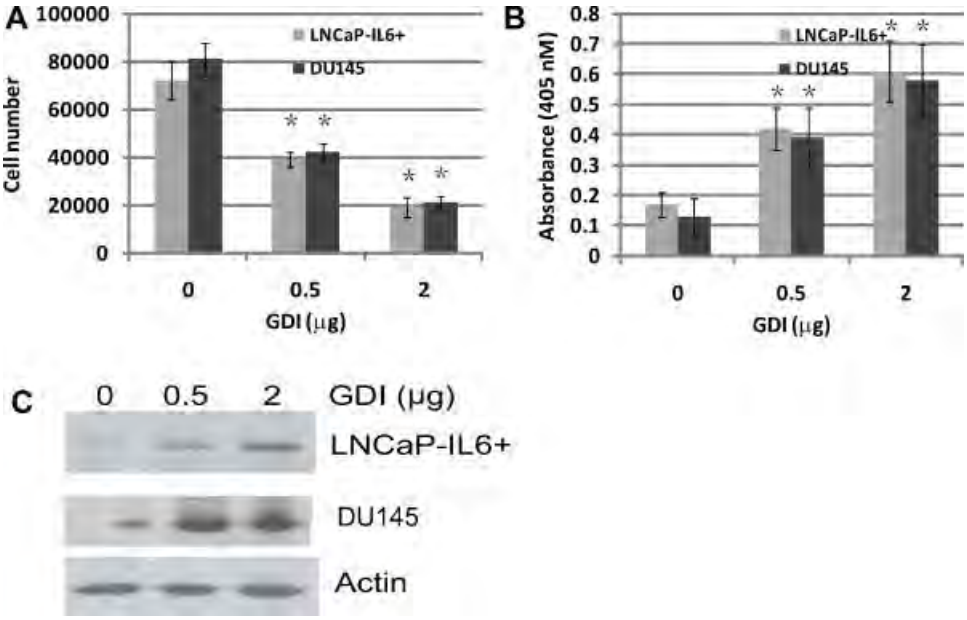

Fig. 2. Expression of GDIα inhibited growth and induced apoptotic cell death in vitro. **A**: Over expression of GDIα inhibits LNCaP IL6+ and DUI45 cells growth in vitro. LNCaP IL6+ and DUI45 cells were transfected with different doses of plasmids containing GDIα cDNA. The cell number was determined 3 days after transfection. **B**: Overexpression of GDIα induces apoptotic cell death. LNCaP IL6+ and DUI45 cells were transfected with different doses of expression plasmids containing GDIα cDNA. Apoptotic cell death was determined 3 days after transfection. **C**: GDIα expression by Western blot analysis using antibody specific against GDIα. *Statistical significance compared to controls.

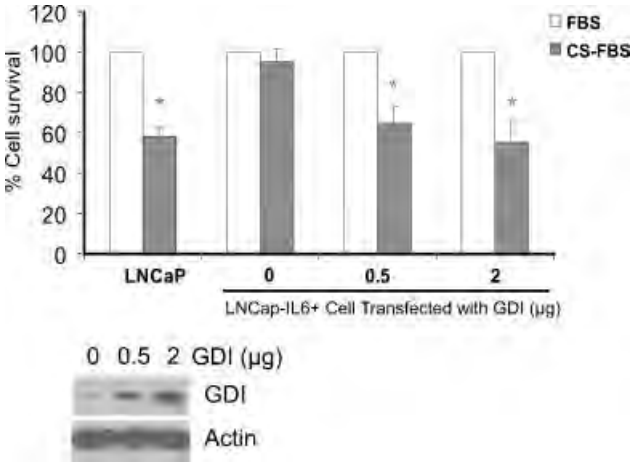

Fig. 3. Effect of over expression of GDIα on LNCaP IL6+ cell growth in the presence and absence of androgen in vitro. LNCaP IL6+ cells were cultured in RPMI 1640 supplemented with 10% FBS or 10% charcoal stripped FBS (CS FBS) and cultured for 72 hr. MTT values for the complete FBS were expressed as 100% and MTT values for charcoal stripped FBS were expressed as % relative to complete FBS. *Statistical significance compared to the value of FBS conditions. The bottom panel shows GDIα protein expression by Western blot analysis using antibody against GDIα.

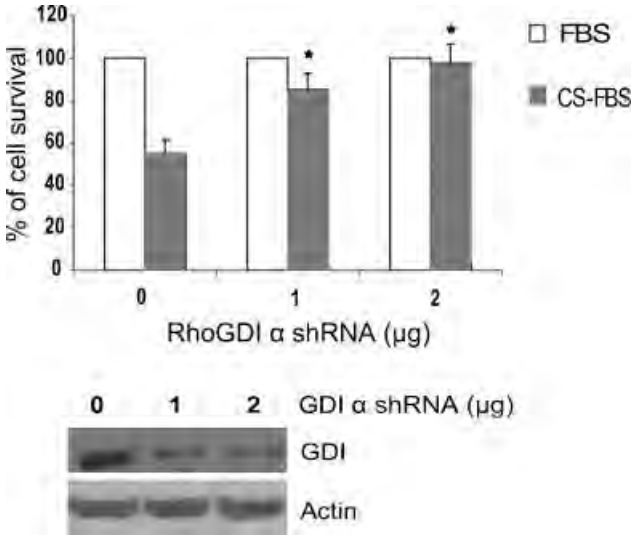

Fig. 4. Knockdown of RhoGDIa expression promotes LNCaP cell growth in androgen deprived conditions in vitro. Effect of knockdown of RhoGDIα expression on LNCaP cell growth in the presence and absence of androgen in vitro. LNCaP cells were cul tured in RPMI 1640 supplemented with 10% FBS. After 24 hr, the cells were transfected with GDIα shRNA as indicated. GFP shRNA was used as control. After transfection, the cells were switched to either 10% FBS or 10% charcoal stripped FBS (CS FBS) and cultured for 72 hr. MTT values for cell grown in complete FBS were expressed as 100% and MTT values for cell grown in charcoal stripped FBS were expressed as % relative to complete FBS. Bot tom panel shows GDIα protein expression by Western blot analysis using antibody against GDIα. *Statistical significance compared to the value of GFP shRNA in CS FBS conditions.

whether knockdown of GDIα expression stimulates androgen-independent growth of androgen-sensitive LNCaP cells, LNCaP cells were transfected with shRNA specifically for GDIα and GFP shRNA as control. Cells were cultured in the presence and absence of androgen and cell growth was determined. The growth of androgen-sensitive LNCaP transfected with GFP control was reduced by approximately 50% after 72 hr in CS-FBS compared to that in regular FBS. In cells transfected with GDIα shRNA there was only 5–15% reduction in growth in CS-FBS compared to FBS indicating that knockdown of GDIα protein expression can enhance the growth of LNCaP cells in androgen-deprived conditions in vitro (Fig. 4).

RhoGDIα Suppresses LNCaP-IL-6+ Tumor Growth

To test the effect of GDIα on tumor formation in vivo, 8-week-old male nude mice were inoculated s.c. with 2×10^6 LNCaP-IL6+ cells stably transfected with GDIα or vector control. The mice developed tumors 2 weeks after injection with LNCaP-IL6+/neo cells, and 5 weeks after injection with LNCaP-IL6+/GDIα cells (Fig. 5). Tumor volumes were measured twice a week. At the end of 9 weeks, blood and tumor tissues were collected and serum levels of PSA were determined by ELISA. The over expression of GDIα suppressed tumor growth of LNCaP-IL6+ cells. All the tumors produced PSA and the levels of PSA were 25.4 ± 6.5 ng/ml in mice-bearing LNCaP-IL6+/neo tumors and 5.1 ± 2.8 ng/ml in mice-bearing LNCaP-Il6+/GDIα tumors. These results demonstrate that GDIα expression suppresses prostate tumor growth in vivo.

DISCUSSION

IL-6 has been implicated in growth and differentiation and is associated with poor prognosis in many cancers including CaP. Multiple studies have demonstrated that IL-6 is elevated in the sera of patients with metastatic CaP and correlates with tumor burden and clinically evident metastases [1,3–5]. An interesting observation is the dynamic nature of CaP cells such as LNCaP in response to IL-6. IL-6 exerts its effects in both paracrine and autocrine manner [18]. Prolonged passage of LNCaP cells in the presence of IL-6 generated a subline, LNCaP-IL6+, which is adapted to IL-6 and grows in a castration-resistant manner [18,20]. In the present study, we analyzed protein expression profiles of parental LNCaP and LNCaP-IL-6+ cells, and identified that GDIα is

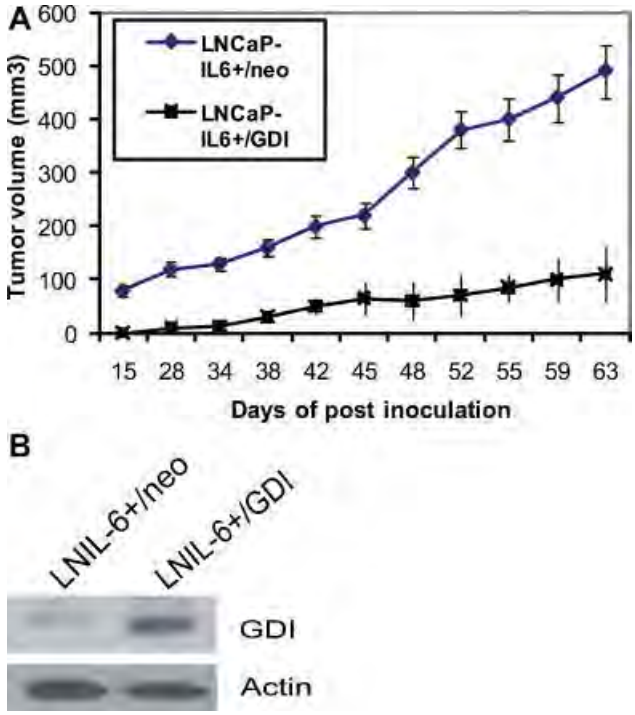

Fig. 5. Effects of overexpression of GDIα on tumor growth. **A**: Over expression of GDIα suppresses LNCaP IL6+ cell tumor growth in vivo. LNCaP IL6+ cells/neo and LNCaP IL6+/GDIα cells were injected into intact male nude mice (N = 8). Tumor volumes were measured. **B**: Levels of GDIα protein in tumors originating from LNCaP IL6+/neo and LNCaP IL6+/GDIα cells analyzed by Western blot using antibody against GDIα. [Color figure can be viewed in the online issue, which is available at wileyonlinelibrary.com.]

down-regulated in CaP and its down-regulation plays a critical role during CaP progression to CRPC.

GDIα was identified by comparison of the protein expression profiles of LNCaP and LNCaP-IL6+ cells. GDIα is down-regulated in LNCaP-IL6+ cells which exhibit higher levels of IL-6 compared to LNCaP cells. The levels of expression of GDIα are higher in androgen-sensitive LNCaP and LAPC-4 cells compared to more aggressive and androgen-insensitive C4-2, PC3, DU145, and LNCaP-IL6+ cells, suggesting that down-regulation of GDIα expression may participate in the progression of CaP cells to androgen-insensitive state. It should be noted that the data is obtained from CaP cell lines derived from human CaP. It would be interesting to examine the levels of GDIα expression in specimens directly derived from patients representing different stages of CaP.

Our study shows a novel role of GDIα in CaP. Overexpression of GDIα helps check uncontrolled proliferation of LNCaP-IL-6+ cells in vitro and in vivo. In addition to LNCaP-IL6+ cells, GDIα also inhibits the proliferation of DU145 CaP cells at least in vitro. We have previously showed that LNCaP-IL6+ cells have the ability to grow in androgen-deprived charcoal-stripped FBS conditions in cell culture [18], which was hampered by overexpression of GDIα in LNCaP-IL6+ cells. Conversely, down-regulation of GDIα expression in LNCaP cells enhanced the growth of these cells in androgen-deprived charcoal-stripped FBS conditions in vitro. These results suggest that decreased expression of GDIα facilitates the progression of castration-resistance from androgen-sensitive CaP. The possible involvement of GDIα in CRPC progression is suggested by a recent publication in which loss of GDIα expression promotes MCF-7 breast cancer cells resistant to tamoxifen treatment [21].

In conclusion, we have identified GDIα as a suppressor of CaP growth through comparison of the protein expression profiles of LNCaP and LNCaP-IL6+ cells. Overexpression of GDIα inhibits the growth of CaP cells, while down-regulation of GDIα enhances the growth of androgen-sensitive CaP cells in androgen-deprived conditions. The mechanisms of GDIα-mediated cellular signaling involved in promoting CaP cell progression are currently under investigation.

REFERENCES

1. Simpson RJ, Hammacher A, Smith DK, Matthews JM, Ward LD. Interleukin 6: Structure function relationships. Protein Sci 1997;6(5):929 955.
2. Siegall CB, Schwab G, Nordan RP, FitzGerald DJ, Pastan I. Expression of the interleukin 6 receptor and interleukin 6 in prostate carcinoma cells. Cancer Res 1990;50(24):7786 7788.
3. Siegsmund MJ, Yamazaki H, Pastan I. Interleukin 6 receptor mRNA in prostate carcinomas and benign prostate hyperplasia. J Urol 1994;151(5):1396 1399.
4. Hobisch A, Rogatsch H, Hittmair A, Fuchs D, Bartsch G Jr, Klocker H, Bartsch G, Culig Z. Immunohistochemical localization of interleukin 6 and its receptor in benign, premalignant and malignant prostate tissue. J Pathol 2000;191(3):239 244.
5. Drachenberg DE, Elgamal AA, Rowbotham R, Peterson M, Murphy GP. Circulating levels of interleukin 6 in patients with hormone refractory prostate cancer. Prostate 1999;41(2):127 133.
6. Adler HL, McCurdy MA, Kattan MW, Timme TL, Scardino PT, Thompson TC. Elevated levels of circulating interleukin 6 and transforming growth factor beta1 in patients with metastatic prostatic carcinoma. J Urol 1999;161(1):182 187.
7. Okamoto M, Lee C, Oyasu R. Interleukin 6 as a paracrine and autocrine growth factor in human prostatic carcinoma cells in vitro. Cancer Res 1997;57(1):141 146.
8. Qiu Y, Robinson D, Pretlow TG, Kung HJ. Etk/Bmx, a tyrosine kinase with a pleckstrin homology domain, is an effector of phosphatidylinositol 3′ kinase and is involved in interleukin 6 induced neuroendocrine differentiation of prostate cancer cells. Proc Natl Acad Sci USA 1998;95(7):3644 3649.
9. Spiotto MT, Chung TD. STAT3 mediates IL 6 induced neuro endocrine differentiation in prostate cancer cells. Prostate 2000; 42(3):186 195.

10. Deeble PD, Murphy DJ, Parsons SJ, Cox ME. Interleukin 6 and cyclic AMP mediated signaling potentiates neuroendocrine differentiation of LNCaP prostate tumor cells. Mol Cell Biol 2001;21(24):8471 8482.
11. Smith PC, Keller ET. Anti interleukin 6 monoclonal antibody induces regression of human prostate cancer xenografts in nude mice. Prostate 2001;48(1):47 53.
12. Wallner L, Dai J, Escara Wilke J, Zhang J, Yao Z, Lu Y, Trikha M, Nemeth JA, Zaki MH, Keller ET. Inhibition of interleukin 6 with CNTO328, an anti interleukin 6 monoclonal antibody, inhibits conversion of androgen dependent prostate cancer to an androgen independent phenotype in orchiectomized mice. Cancer Res 2006;66(6):3087 3095.
13. Olofsson B. Rho guanine dissociation inhibitors: Pivotal mole cules in cellular signalling. Cell Sig 1999;11(8):545 554.
14. Dovas A, Couchman JR, Rho GDI. multiple functions in the regulation of Rho family GTPase activities. Biochem J 2005; 390(1):1 9.
15. Takaishi KKA, Kuroda S, Sasaki T, Takai Y. Involvement of rho p21 and its inhibitory GDP/GTP exchange protein (rho GDI) in cell motility. Mol Cell Biol 1999;13(1):545 554.
16. Togawa AMJ, Ishizaki H, et al. Progressive impairment of kid neys and reproductive organs in mice lacking Rho GDIαλπηα. Oncogene 1999;18(39):5373 5380.
17. Seraj M, Harding M, Gildea J, Welch D, Theodorescu D. The relationship of BRMS1 and RhoGDI2 gene expression to metastatic potential in lineage related human bladder cancer cell lines. Clin Exp Metastasis 2000;18(6):519 525.
18. Lee SO, Chun JY, Nadiminty N, Lou W, Gao AC. Interleukin 6 undergoes transition from growth inhibitor associated with neuroendocrine differentiation to stimulator accompanied by androgen receptor activation during LNCaP prostate cancer cell progression. Prostate 2007;67(7):764 773.
19. Lou W, Ni Z, Dyer K, Tweardy DJ, Gao AC. Interleukin 6 induces prostate cancer cell growth accompanied by activa tion of stat3 signaling pathway. Prostate 2000;42(3):239 242.
20. Hobisch A, Ramoner R, Fuchs D, Godoy Tundidor S, Bartsch G, Klocker H, Culig Z. Prostate cancer cells (LNCaP) generated after long term interleukin 6 (IL 6) treatment express IL 6 and acquire an IL 6 partially resistant phenotype. Clin Cancer Res 2001;7(9):2941 2948.
21. Barone I, Brusco L, Gu G, Selever J, Beyer A, Covington KR, Tsimelzon A, Wang T, Hilsenbeck SG, Chamness GC, Ando S, Fuqua SA. Loss of Rho GDI{alpha} and resistance to tamoxifen via effects on estrogen receptor {alpha}. J Natl Cancer Inst 103(7):538 552.